Design and Development of Quinone Catalysts for Aerobic C–N Bond Dehydrogenation Reactions

By

Alison E. Wendlandt

A dissertation submitted in partial fulfillment of

the requirements for the degree of

Doctor of Philosophy

(Chemistry)

at the

UNIVERSITY OF WISCONSIN-MADISON

2015

Date of final oral examination: 05/18/2015

The dissertation is approved by the following members of the Final Oral Committee:
Shannon S. Stahl, Professor, Chemistry
Clark R. Landis, Professor, Chemistry
Tehshik P. Yoon, Professor, Chemistry
Laura L. Kiessling, Professor, Chemistry
Ive Hermans, Associate Professor, Chemistry

Design and Development of Quinone Catalysts for Aerobic C–N Bond Dehydrogenation Reactions

Alison E. Wendlandt

Under the supervision of Professor Shannon S. Stahl

At the University of Wisconsin – Madison

Abstract

The selective oxidation of organic compounds is a prominent challenge in organic chemistry. Towards this goal, molecular oxygen is an ideal oxidant. Uncatalyzed aerobic oxidation reactions have found important application in the commodity scale synthesis of certain compounds. However, such autoxidation reactions are intrinsically substrate-controlled. More frequently, selective aerobic oxidations are achieved by using a catalyst to promote the desired transformation. Under such a regime the identity of the catalyst – and therefore the reaction mechanism – dictates the chemical outcome of the reaction. The development of new catalysts which promote aerobic oxidation reactions is therefore of great significance.

This thesis highlights two classes of catalyst that promote selective aerobic oxidation reactions. Chapters 1-4 describe the development of a family of *o*-quinone catalysts based on *o*-quinone cofactors found in certain oxidase and dehydrogenase enzymes. Unlike the natural cofactors, which have limited substrate scope, we find evidence for an unnatural reaction pathway that broadens the synthetic utility of these reagents. This family of bioinspired *o*-quinone catalysts is particularly effective in the aerobic dehydrogenation of C—N bonds.

Subsequently, in chapters 5 and 6 I discuss the application of Cu-based catalysts to aerobic oxidation reactions, emphasizing an apparent mechanistic bifurcation between single electron transfer-based mechanisms and organometallic mechanisms within the published literature. Further work describes an application of Cu^{II} reagents in the aerobic oxidative cyclization of enamides to oxazoles.

Acknowledgements

This work would not have been possible without the help and support of many. First, I would like to thank my advisor, Professor Shannon Stahl. During my Ph.D. training Shannon provided me with freedom as well as opportunity, and challenged me to become a better scientist, mentor and communicator. Simultaneously a champion and a critic, his feedback never failed to elevate the level of scholarship of my research. I am deeply grateful for his support and for the opportunity to continue my training as a chemist in his laboratory.

I have also had the great privilege of working alongside many outstanding colleagues at UW Madison. Professor Jessica Hoover, Dr. Adam Weinstein and Dr. Paul White were, and continue to be, great scientific mentors. These people, as well as Dr. Alison Campbell, Dr. Bradford Ryland, Dr Joanne Harmata, Jamie Chen, Scott McCann, and Colin Anson are terrific colleagues and friends. I am humbled by their intelligence, inspired by their enthusiasm and deeply grateful for their friendship. I have also greatly enjoyed mentoring, and working with, Bao Li and Jun Chuang.

Finally, I wish to thank my family and friends for their love and support. I thank my parents for their wisdom, support and for setting such a high bar of academic achievement. I thank Sarah Jubinski and Eric Boyko for 10+ (!) years of friendship. And most of all I thank my partner, Laura Alex Frye-Levine, who has been a constant source of love and joy and surprise and adventure. In no uncertain terms, this work would not have been possible without her. Thank you, Laura Alex, for your patience and kindness and forgiveness. Thank you for believing in me so unequivocally. Thank you for so many great discussions about hexagons, the (de)construction of science, and for explaining Latour. Most of all, thank you for sharing your life with me: I can't wait to see what our future holds next!

Table of Contents

List of Schemes

List of Tables

List of Figures

Abbreviations and Acronyms

Ac	acetyl
Ar	aryl
atm	atmosphere
Bn	benzyl
Bu	butyl
CAO	copper amine oxidase
CAN	ceric ammonium nitrate
CDC	cross-dehydrogenative coupling
DCM	dichloromethane
DDQ	2,3-dichloro-5,6-dicyano-1,4-benzoquinone
DME	dimethoxyethane
DMF	*N*,*N*-dimethylformamide
DMSO	dimethylsulfoxide
Et	ethyl
ET	electron transfer
ETM	electron transfer mediator
EXSY	exchange spectroscopy
HAT	hydrogen atom transfer
HMBC	heteronuclear multiple-bond correlation
HSQC	heteronuclear single quantum coherence
KIE	kinetic isotope effect
LTQ	lysine tyrosylquinone

M.S.	molecular sieves
Me	methyl
MeSal	methyl salicylate
NHE	normal hydrogen electrode
NMR	nuclear magnetic resonance
NOESY	Nuclear Overhouser Effect spectroscopy
pc	phthalocyanine
Ph	phenyl
phd	1,10-phenanthroline-5,6-dione
PMB	p-methoxybenzyl
PPTS	pyridinium *p*-toluenesulfonic acid
PQQ	pyrroloquinoline quinone
rt	room temperature
salophen	*N*,*N*-salicylidenephenylenediamine
SCE	saturated calomel electrode
SET	single electron transfer
tpp	5,10,15,20-tetraphenylporphyrin
TBHBQ	5-*tert*-butyl-2-hydroxy-1,4-benzoquinone
THF	tetrahydrofuran
TPQ	topaquinone
Ts	*p*-toluenesulfonyl
TTQ	tryptophan tryptophylquinone

Chapter 1

Quinone-Catalyzed Oxidations of Organic Substrates

1.1. Abstract

Quinones are important reagents in organic synthesis. High potential quinones such as 2,3-dichloro-5,6-dicyano-1,4-benzoquinone (DDQ) and chloranil typically react via hydride abstraction mechanisms, and have found broad application as stoichiometric oxidants in oxidative functionalization and dehydrogenation reactions of organic molecules. Many of these transformations can be rendered catalytic in quinone by using transition metal salts, anodic oxidation or molecular oxygen to regenerate the catalyst *in situ*. Concurrently, numerous recent studies have led to the development of novel quinone catalysts that resemble Copper Amine Oxidase *o*-quinone cofactors. These bioinspired quinones are highly selective and efficient catalysts for aerobic and anodic dehydrogenation of amines, and likely proceed through electrophilic transamination and/or addition-elimination reaction mechanisms, rather than hydride abstraction pathways. These observations align with broader findings that quinone structure significantly influences reaction mechanism, and has important implications for the development of new quinone reagents and quinone-catalyzed transformations.

1.2 Introduction

The selective oxidation of organic compounds is a prominent chemical challenge. Transition metal catalysts are commonly employed to promote these reactions, and enormous progress has been made in this area.[1] Though used less frequently than transition metals, redox-active organic molecules are increasingly recognized as robust and efficient (co)catalysts in oxidative transformations. One of the most broadly used classes of organic catalyst is nitroxyl radicals. For example, 2,2,6,6-tetramethylpiperidine *N*-oxyl (TEMPO, Eq 1.1) and its derivatives promote a range of oxidative transformations, notably including alcohol oxidation reactions.[2] Additionally, pthalimide *N*-oxyl (PINO, Eq 1.2) – generated in situ from *N*-hydroxyphthalimide (NHPI) – is widely employed in aerobic autoxidation reactions.[3] Both reagents are amenable to industrial scale oxidation processes.[4] The use of organic catalysts and co-catalysts provides access to reaction mechanisms distinct from those mediated by transition metal catalysts, leading to complementary reactivity, enhanced selectivity, and often milder reaction conditions. Selective oxidation reactions promoted by organic catalysts and co-catalysts represent promising targets for future development.

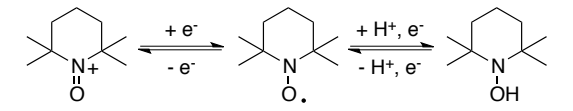

(1.1)

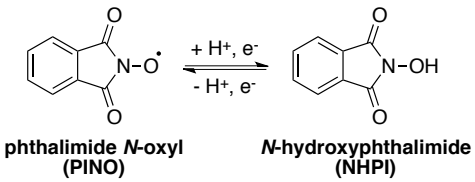

(1.2)

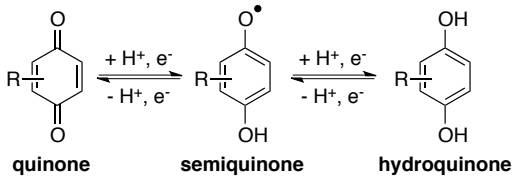

(1.3)

Quinones are important redox-active organic molecules with applications in diverse redox processes, including in the manufacture of industrial chemicals, in oxidation reactions for organic synthesis, and as electron carriers, antioxidants and cofactors in biological processes. Like nitroxyl radicals, quinones are capable of mediating both closed- and open-shell processes, via three oxidation states: fully-oxidized quinone, one electron-reduced semiquinone, and two electron-reduced hydroquinone (Eq 1.3). In contrast to nitroxyl radicals, however, quinones have been much less extensively developed as catalysts in the oxidation of organic compounds.

Cycling between oxidized and reduced quinone species forms the conceptual basis for the anthraquinone-mediated industrial synthesis of hydrogen peroxide.[5] Hydrogen peroxide is produced in near quantitative yields by the stoichiometric autoxidation of 2-alkyl-9,10-anthrahydroquinone (Scheme 1.1, *autoxidation step*). The resulting oxidized anthraquinone co-product is subsequently reduced in a separate step via catalytic hydrogenation (Scheme 1.1, *hydrogenation step*). This sequence affords the net conversion of molecular oxygen and hydrogen into hydrogen peroxide (Scheme 1.1, *net reaction*). Over 95% of the world supply of hydrogen peroxide is made using this quinone-mediated process. While the fundamental incompatibility of the oxidation and reduction steps requires the sequential operation of two stoichiometric half reactions in this case, the use of a quinone mediator common to both half reactions suggests broader potential for engaging quinones as catalysts in redox processes.

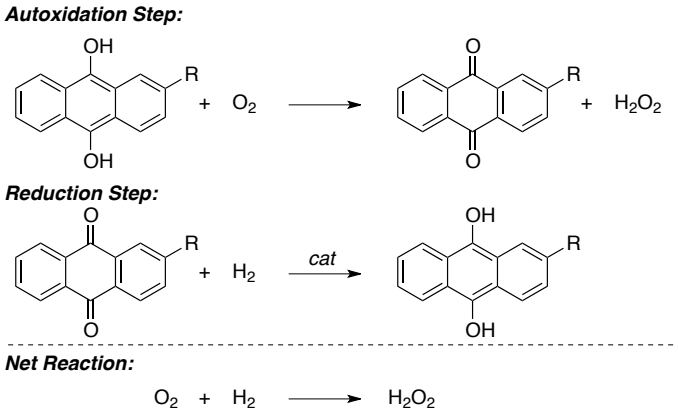

Scheme 1.1. The anthraquinone oxidation (AO) process for industrial synthesis of H_2O_2.

Nature provides a framework for the use of catalytic quinones as redox shuttles in oxidative transformations: plastoquinone and ubiqinone act as electron carriers in the photosynthetic and mitochondrial electron transport chains (ETC), respectively. In the mitochondrial ETC a series of cofactors shuttle electrons from a sacrificial reductant (NADH) to molecular oxygen. The reduction of molecular oxygen to water ultimately serves as the thermodynamic driving force for the synthesis of ATP via oxidative phosphorylation. Conceptually-related synthetic systems popularized by Bäckvall and others employ quinones as catalytic redox shuttles (also referred to as "electron transfer mediators" or ETMs) in the aerobic transition-metal catalyzed oxidation of organic molecules, such as the Pd-catalyzed aerobic allylic acetoxylation shown in Scheme 1.2.[6] Efficient reactivity is proposed to involve a series of "coupled catalytic cycles." Substrate oxidation first occurs via a transition metal-mediated step. A quinone (typically benzoquinone[7] or derivatives[8]) subsequently acts as a redox shuttle to transfer protons and electrons from the transition metal catalyst to a metal macrocycle co-catalyst, such as Co(salophen) (salophen = *N*,*N*-salicylidene phenylenediamine), Fe(pc) (pc = phthalocyanine), or Co(tpp) (tpp = 5,10,15,20-tetraphenylporphyrin). Finally, the metal macrocycle co-catalyst is re-oxidized by molecular oxygen, the terminal oxidant (Scheme 1.2). In addition to serving as a redox shuttle between Pd

and a metal macrocycle, benzoquinone additives may also promote oxidatively-induced reductive elimination of the substrate from Pd^{II}. Applications of quinones as redox shuttles/ETMs are the subject of a recent review, and will not be discussed here.[9] However, many of the fundamental principles established through the development of quinone-based coupled catalytic cycles for transition metal-catalyzed reactions have been leveraged in the quinone-catalyzed oxidation reactions found herein.

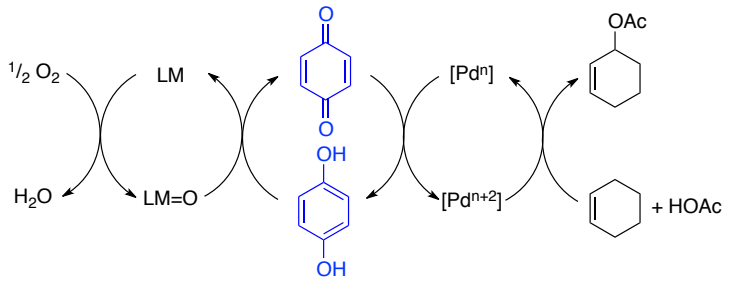

Scheme 1.2. Pd-catalyzed allylic acetoxylation reaction featuring Pd, quinone, and metal macrocycle coupled catalytic cycles.

The present review highlights recent progress in the development of quinone-catalyzed oxidations of organic substrates. We limit our discussion to examples involving direct oxidation of organic substrates by quinone catalysts, and to the reaction of quinones in their ground state.[10] These quinone catalysts can be divided into two families: high-potential quinones, such as 2,3-dichloro-5,6-dicyano-1,4-benzoquinone (DDQ) and chloranil; and *o*-quinone catalysts inspired from quinone cofactors found in Copper Amine Oxidases (CAOs) and other enzymes.

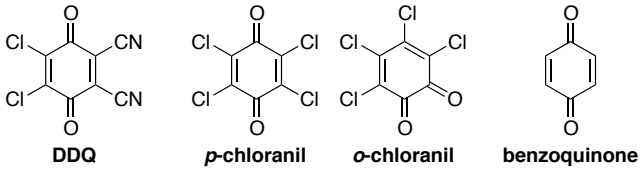

DDQ is the most prominently featured high potential quinone, and is typically thought to promote hydride abstraction mechanisms. DDQ has found broad application as a stoichiometric

oxidant in the functionalization of activated C-H bonds and the dehydrogenation of saturated C-C, C-O and C-N bonds, including in several process-scale pharmaceutical syntheses. In response to concerns over the cost and toxicity of DDQ, recent efforts have led to the development of strategies for employing catalytic quantities of DDQ in these transformations. In section 1.3 of this review we provide an overview of the types of reactions and the corresponding reaction mechanisms promoted by stoichiometric DDQ and chloranil oxidants. While not an exhaustive summary of DDQ-mediated transformations, this overview provides important context for the range of transformations accessible using this class of reagent. From this foundation, we then discuss strategies for using these quinones as catalysts, summarizing the examples of DDQ- and chloranil-catalyzed reactions, and highlighting the potential for future development in this area. In general, the types of reactions promoted by catalytic DDQ very closely parallel those achieved using the stoichiometric reagent, although in several instances we note reactions that can be achieved only using catalytic amounts of DDQ.

Concurrent with the development of DDQ-catalyzed transformations, has been the development of a second family of quinone catalysts inspired from the *o*-quinone cofactors found in oxidase and dehydrogenase enzymes. These bioinspired quinones have a more moderate thermodynamic potential than DDQ or chloranil, and react through distinct C-H bond cleavage mechanisms. Consequently, distinct reactivity and reaction scope is observed in comparison with DDQ. In section 1.4, we provide mechanistic context for copper amine oxidases and other quinoenzymes found in nature, highlighting the biochemical mechanisms proposed for enzymatic quinone-catalyzed oxidations of organic substrates. We subsequently describe the development of bioinspired *o*-quinone catalysts and their applications in aerobic and electrochemical C-N bond dehydrogenation reactions.

1.3. DDQ-Catalyzed Oxidations of Organic Substrates

1.3.1. Survey of DDQ-Mediated Transformations and Mechanistic Insights

High potential quinones – notably DDQ and chloranil – are important stoichiometric reagents for the oxidation of organic compounds.[11] As the literature in this area has not been comprehensively reviewed since 1967,[12] a brief summary of archetypal stoichiometric transformations – with an emphasis on reaction mechanism – is provided here. Careful consideration of reactivity trends and mechanistic pathways of DDQ-mediated substrate oxidation provides a lens through which to frame our subsequent discussion of quinone-catalyzed transformations.

The synthetic applications of DDQ fall neatly into several categories of reactions. These include: (a) C-O, C-N and C-C bond dehydrogenation reactions, such as *p*-methoxybenzyl (PMB) ether deprotections, the oxidation of benzylic and allylic alcohols, and the synthesis of unsaturated arenes and heteroarenes; (b) oxidative functionalization of activated C-H bonds; and (c) dehydrogenation of ketones to α,β-unsaturated ketones.

PMB Ether Deprotection

The oxidative cleavage of *p*-methoxybenzyl (PMB) and 3,4-dimethoxybenzyl (DMB) ether protecting groups is among the most broadly implemented application of DDQ in organic synthesis.[13] Selective deprotection is accomplished in the presence of other standard protecting groups (e.g. MOM, TBDPS, Ac, Bn, etc). For example, Yonemitsu reported the selective deprotection of a PMB ether in complex dihydropyran **1**, a synthetic intermediate en route to tylonolide (Scheme 1.3).[14]

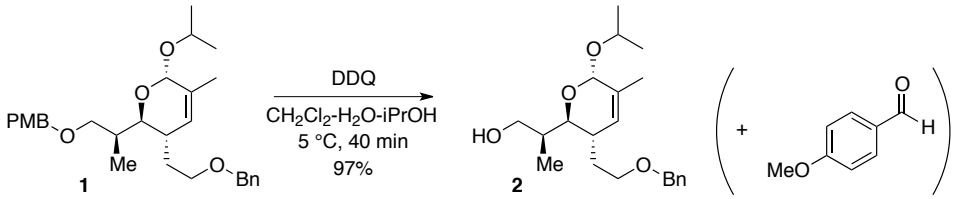

Scheme 1.3. Selective DDQ-mediated PMB ether deprotection.

The reaction of DDQ with electron-rich organic substrates, such as PMB ethers, is thought to proceed through the formation of a quinone-substrate π–π charge transfer complex, typically observed as a significant color change during the early stages of the reaction. This charge transfer complex is thought to be a true intermediate – rather than an off-cycle species – by the observation of negative reaction entropy.[15,16] Following formation of the charge transfer complex, substrate oxidation occurs via net hydride transfer from substrate to quinone, giving an ion-paired product.[17] In the case of PMB ether cleavage, hydrolysis of the oxocarbenium intermediate liberates deprotected alcohol with *p*-methoxybenzaldehyde and $DDQH_2$ as stoichiometric byproducts (Scheme 1.4).

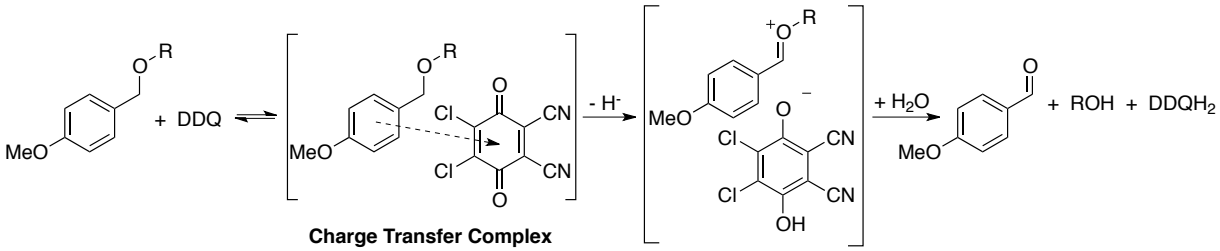

Scheme 1.4. Proposed mechanism for DDQ-mediated PMB ether deprotection.

DDQ and chloranil are considered to be hydride-abstracting reagents, although the specific mechanism of hydride abstraction has been the subject of some controversy. Depending on the specific substrate, several plausible reaction pathways have been suggested. These include (a) single electron transfer followed by hydrogen atom abstraction (SET-HAT, Scheme 1.5A);[18] (b)

hydrogen atom transfer followed by SET (HAT-SET, Scheme 1.5B);[19] or by (c) direct hydride transfer (polar pathway, Scheme 1.5C).[20] Polar reaction mechanisms are typically favored, and have gained increasing support. Recent mechanistic studies by Mayr have demonstrated the potential generality of polar reaction pathways in the reaction of diverse quinones with hydride donors.[21]

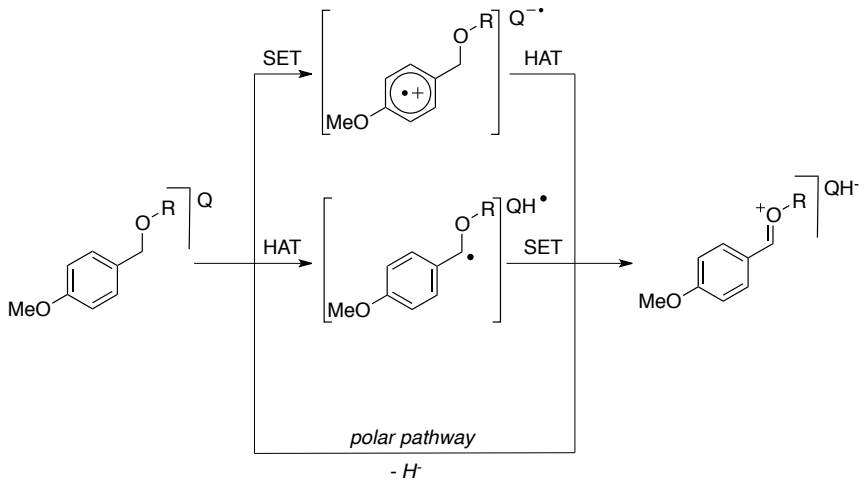

Scheme 1.5. Proposed reaction pathways for net hydride abstraction, including (A) SET-HAT, (B) HAT-SET, and (C) polar reaction pathways.

Oxidation of Allylic, Benzylic and Other Activated Alcohols

DDQ is also used to oxidize activated alcohols to aldehydes and ketones.[22] This reaction bears conceptual similarity to PMB ether deprotection (e.g. R=H in Schemes 1.4 and 1.5, with deprotonation by QH). The reactivity of DDQ with alcohol substrates follows the trend benzylic>allylic>>aliphatic. As a result, activated alcohols can be selectively oxidized in the presence of aliphatic alcohols. For example, Ganem reported the selective oxidation of the allylic alcohol of shikimic acid in 60% yield; no oxidation or epimerization of the remaining stereocenters is observed (Scheme 1.6).[23]

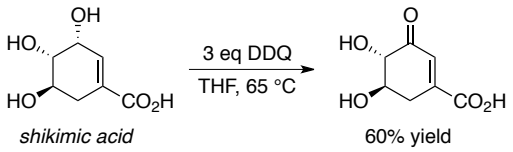

Scheme 1.6. Selective DDQ-mediated oxidation of allylic alcohols.

More contemporary applications of DDQ involve formation of new C-C and C-X bonds by intercepting the intermediate oxocarbenium or iminium species with a nucleophile.[24] For example, Li and coworkers have reported the cross-dehydrogenative coupling (CDC) of isochroman with various ketone coupling partners by employing a slight excess of DDQ under neat conditions at 100 °C (Scheme 1.7A).[25] Analogously, Todd has reported the CDC-type coupling of tetrahydroisoquinolines with nitronates, isolating intermediate iminium species, which precipitates during the course of the reaction (Scheme 1.7B).[26]

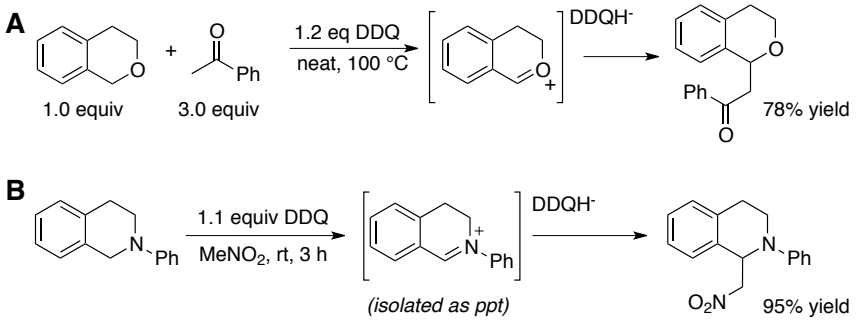

Scheme 1.7. DDQ-mediated cross-dehydrogenative coupling of (A) isochroman and (B) tetrahydroisoquinoline.

Floreancig and coworkers have presented several reports of DDQ-mediated synthesis of pyranones and piperidines via intramolecular oxidative cyclization reactions.[27,28] For example, allylic ether **3** undergoes oxidation by 2.0 equiv DDQ in the presence of 4.0 equiv 2,6-dichloropyridine and 0.1 equiv $LiClO_4$, at room temperature in DCE in the presence of 4Å molecular sieves. Interception of the oxocarbenium intermediate by pendant vinyl acetate gives desired 4-pyranone **4** in 81% yield (Scheme 1.8).

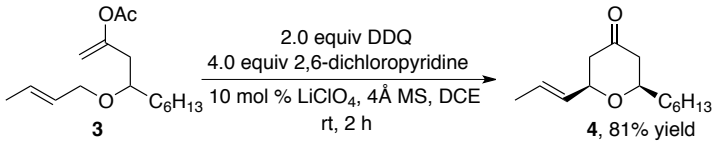

Scheme 1.8. DDQ-mediated intramolecular oxidative annulation reaction.

Dehydrogenation Leading to (Hetero)Arenes

DDQ has been used extensively in C-C and C-X dehydrogenation reactions for the synthesis of arenes and heteroarenes.[29,30] For example, Taylor has reported a synthetic route to furo[2,3-b]pyridine derivatives, employing 2.0 equiv DDQ in the final step of the synthesis (Scheme 1.9).[31]

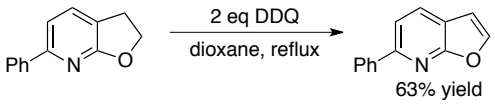

Scheme 1.9. DDQ-mediated C-C bond dehydrogenation

The mechanism of DDQ- and chloranil-mediated dehydrogenation of model hydroaromatic compounds (such as dihydroanthracene, acenaphthene, tetralin, etc) has been extensively studied by Linstead[32] and others.[33] Collectively, these studies establish a two step reaction mechanism consisting of rate limiting hydride abstraction to form a substrate cation/$DDQH^-$ ion pair, followed by deprotonation by $DDQH^-$ to afford the corresponding dehydrogenated product.[34] Subsequent studies by Trost, using 1,2-cis-dideuteroacenaphthene as a substrate, reported preferential formation of cis-elimination products and the observation that the ratio of cis/trans elimination products depends on reaction solvent polarity.[20] These findings support the two-step reaction mechanism initially proposed by Linstead, where deprotonation occurs directly from the initially-formed ion pair (preferential cis-elimination) unless reaction conditions favor separation of the ion pair (leading to both cis- and trans-elimination).[35]

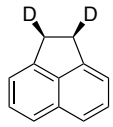

1,2-cis-dideutereo-acenaphthene

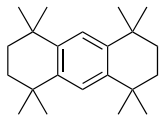

octahydro-octamethyl-anthracene

These mechanistic studies have several important implications for understanding the reactivity of high potential quinones and for subsequent reaction development. First, while DDQ is a strongly oxidizing reagent, the hydride abstraction mechanism limits dehydrogenation reactions to substrates containing activated (e.g. benzylic, allylic) C-H bonds. For example, no dehydrogenation is observed in the case of octahydro-octamethylanthracene, as the benzylic positions are blocked. Second, the formation of a carbocationic intermediate suggests the possibility of out-competing the elimination process (which leads to dehydrogenation) by intra- or intermolecular rearrangements and addition reactions. For example, Wagner-Meerwein rearrangement is observed in the DDQ-mediated oxidation of 1,1-dimethyltetralin (Scheme 1.10)[36] and the addition of nucleophiles to the cationic intermediate has been exploited to achieve oxidative C-H functionalization reactions.

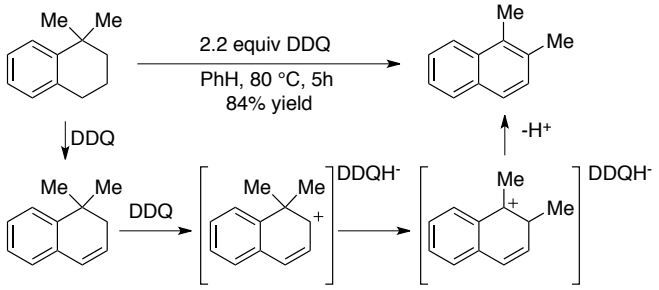

Scheme 1.10. Alkyl shift observed in the DDQ-mediated oxidation of 1,1-dimethyltetralin.

Functionalization of Activated Positions

In some cases dehydrogenation can be avoided by trapping the initially formed benzylic carbocation with a nucleophile. Typically solvent H_2O or AcOH is used as a nucleophile.[37] For

example, Yonemitsu has reported the selective oxygenation of tetrahydrocarbazole using 2.0 equiv DDQ in THF/H_2O mixture (Scheme 1.11A),[38] and Petrini and colleagues disclosed a benzylic acetoxylation in the course of their studies on podophyllotoxin analogs (Scheme 1.11B).[39] More recent applications have used this approach to generate new C-C bonds using non-solvent nucleophiles.[40]

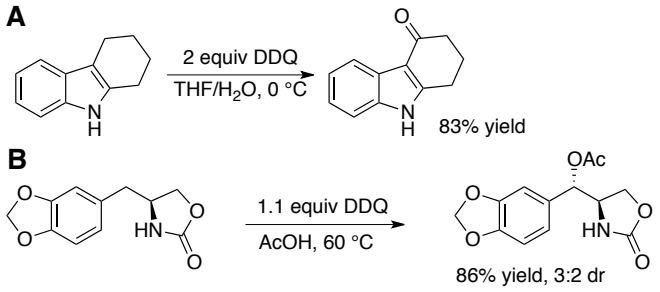

Scheme 1.11. Selective DDQ-mediated oxidative C-H bond (A) oxygenation and (B) acetoxylation.

In certain instances covalent quinone/substrate adducts are observed.[41] For example, Crabtree and Batista have reported the isolation of a quinol ether formed between DDQ and toluene (Scheme 1.12).[42] Treating the quinol ether with PPh_3 or triethyl phosphite led to the corresponding benzyl triphenylphosphonium salt or diethyl benzylphosphonate, respectively. These types of adducts may be formed by collapse of the ion paired intermediate, which may compete kinetically with dehydrogenation and/or nucleophilic addition steps. Other types of adducts, such as those resulting from Diels-Alder reactions of quinone and substrate, have also been observed.

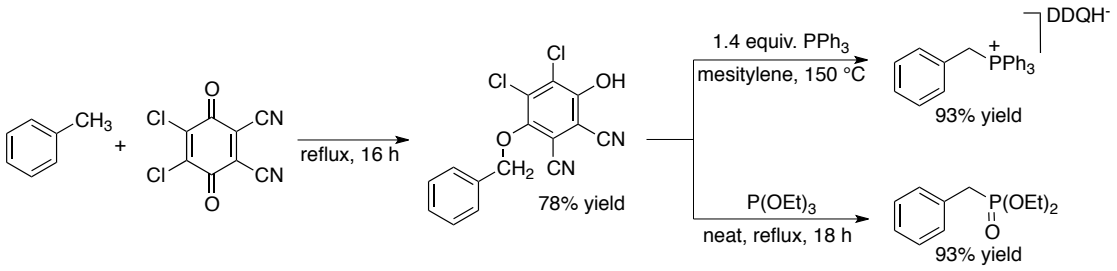

Scheme 1.12. Formation of DDQ benzyl quinol ether from reaction with toluene and subsequent transformations.

Dehydrogenation of ketones to α,β-unsaturated ketones

DDQ and chloranil have also been applied to the dehydrogenation of ketones and silyl enol ethers to α,β-unsaturated ketones.[43] Extensive historical effort was directed towards the dehydrogenation of steroids.[44] A notable example is the reaction of Δ^4-3-ketosteroids with stoichiometric DDQ or chloranil (Scheme 1.13). In reaction with DDQ, dehydrogenation gives $\Delta^{1,4}$-3-ketosteroid.[45] When treated with excess chloranil, the $\Delta^{4,6}$-3-keto product predominates.[46]

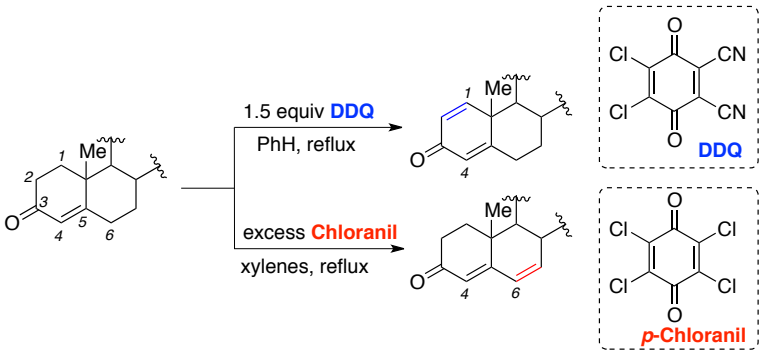

Scheme 1.13. Divergent reactivity of DDQ and chloranil with Δ^4-3-ketosteroids.

Divergent reactivity in this case highlights the differences between DDQ, chloranil and other high potential quinone reagents. The rationale in this case is thought to be the difference between the reaction with the kinetic and thermodynamic enolates. DDQ, a stronger oxidant than chloranil, reacts readily with the kinetic $\Delta^{2,4}$-enolate to abstract the C1 hydride. Chloranil, on the

other hand, reacts exclusively with the thermodynamic $\Delta^{3,5}$ -enolate by abstraction of C7 hydride. Indeed, reaction with DDQ in the presence of anhydrous HCl gives the $\Delta^{4,6}$-3-keto product, as the thermodynamic $\Delta^{3,5}$-enolate is readily established under these conditions.

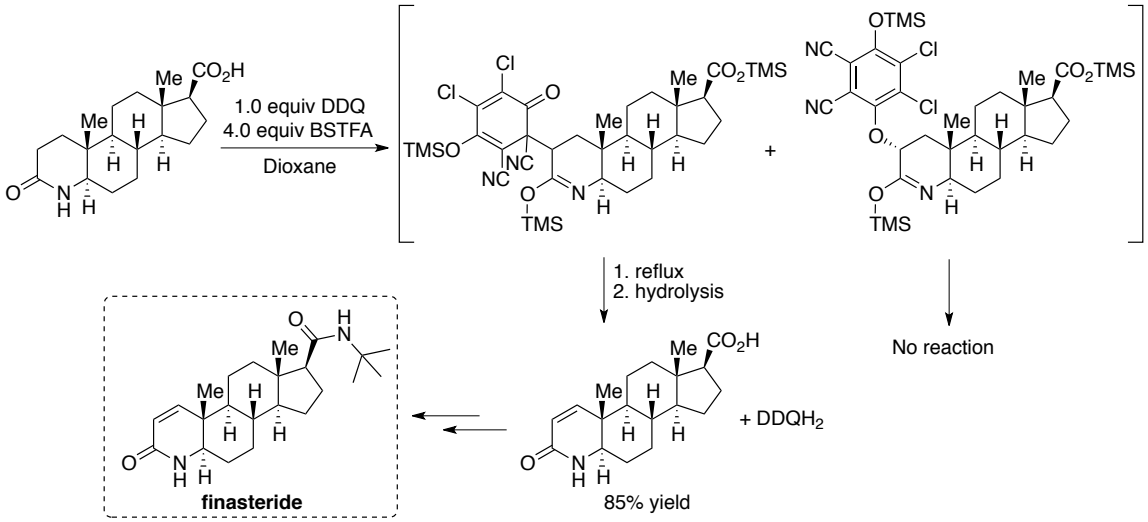

Scheme 1.14. DDQ-mediated dehydrogenation of azasteroid in the process scale synthesis of Finasteride.

A particularly fascinating example comes from the commercial synthesis of finasteride, where it was found that the dehydrogenation of azasteroid could be accomplished using 1.0 equiv DDQ and 4.0 equiv of the silylating agent *N*,*O*-bis(trimethylsilyl)-trifluoroacetamide (BSTFA) in refluxing dioxane (Scheme 1.14). Closer examination of the reaction revealed that at room temperature starting material was consumed to form covalent C-C and C-O adducts between substrate at quinone.[47] Dehydrogenation products were not observed until the reaction was heated to reflux, and were discovered to arise exclusively from C-C adducts; C-O adducts were found to be unreactive. Analogous C-C adduct formation was observed in the reaction of enol ethers with other quinones, such as *p*-chloranil and benzoquinone, however no elimination/dehydrogenation reaction occurs, even under forcing conditions with these reagents.

The discovery of these covalent intermediates proved to be critical to the development of the optimized process-scale route to finasteride.[48]

Mayr and coworkers carried out a comprehensive study on the reaction of various π-nucleophiles, including silyloxy alkenes and enamines, with several quinone derivatives.[49] In particular, they highlight the presence of competing polar and electron-transfer (ET) pathways in the reaction of DDQ with silyl enol ethers and silyl ketene acetals.[50] For example, in the stoichiometric reaction of DDQ with 1-trimethylsilyloxycyclohexene two adducts are observed: a C-C linked adduct resulting from reversible polar conjugate addition of silyl enol ether to quinone, and a C-O linked quinol ether resulting from irreversible single electron transfer and radical coupling (Scheme 1.15). The ratio of C-C and C-O products is a consequence of reaction conditions (solvent, temperature, concentration) as well as the nature of the quinone and reactants. Consistent with the findings of Grabowski and coworkers at Merck in the case of finasteride, decomposition of the C-C adducts formed from polar addition of nucleophile to quinone results in the dehydrogenation products, however the C-O products formed by ET pathways are not intermediates to dehydrogenation.

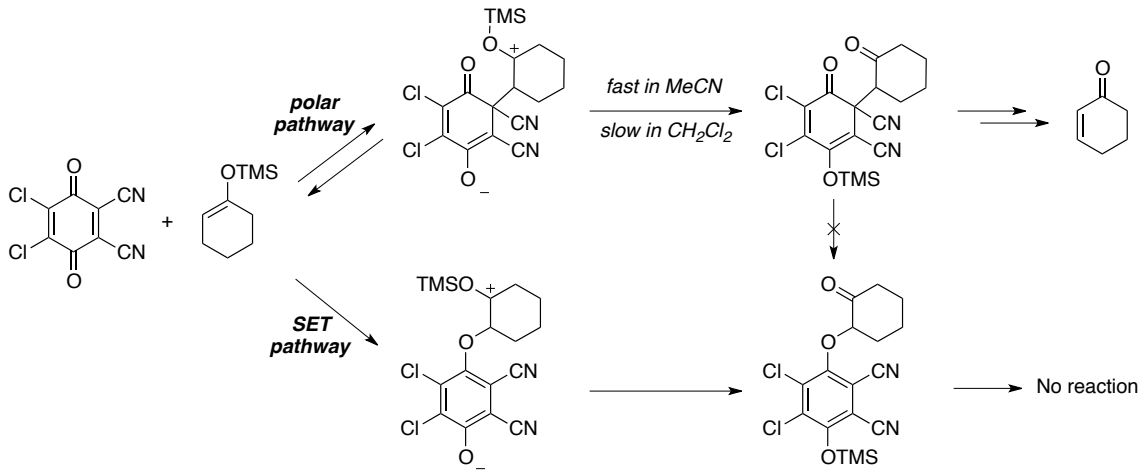

Scheme 1.15. Competing polar and SET pathways lead to C-C coupled and C-O coupled adducts, respectively.

The electrophilic (rather than oxidizing) character of DDQ clearly plays an important mechanistic role in some DDQ-mediated substrate oxidation reactions. Nonetheless, the generality of adduct-intermediates in DDQ-mediated dehydrogenation reactions more broadly has yet to be elucidated.

1.3.2 DDQ- and Chloranil-Catalyzed Reactions

Despite the versatility of DDQ as a stoichiometric reagent, there are numerous limitations to the use of DDQ on scale. These include: relatively high toxicity (LD_{50} 82 mg/kg rat); relatively high cost (>$500/mol); environmental hazard (i.e. H_2O-mediated liberation of HCN); and complicated reaction workup due to challenging removal of $DDQH_2$. Because of the differential reactivity of DDQ, chloranil and other quinones, the application of alternative, more-benign reagents is not always possible or desirable. Despite these limitations, DDQ has nonetheless proven to be an important reagent in the production-scale synthesis of several recent pharmaceutical drugs and drug candidates.[48,51,52] Citing the high cost of DDQ in the process scale synthesis of Finasteride, Merck isolates spent hydroquinone from the aqueous waste (96% recovery) and regenerates DDQ by HNO_3/AcOH (75% yield) in a subsequent step.[48,53]

Transition Metal Salts as Stoichiometric Terminal Oxidant

The development of strategies for the use of catalytic amounts of DDQ or choranil in otherwise quinone-mediated reactions is a subject of interest. Catalytic quantities of DDQ can be used by addition of an alternative stoichiometric terminal oxidant, such as $FeCl_3$, $MnOAc_3$, PbO_2, or MnO_2 (Scheme 1.16). Though these reactions are catalytic in DDQ, catalyst loadings

remain quite high (10-20 mol %), and a large excess of the terminal oxidant is typically employed.

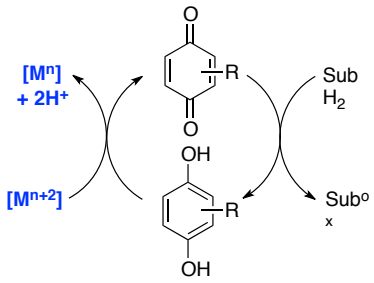

Scheme 1.16. Generic concept of using catalytic quinone for oxidation of organic substrate.

Cacchi and coworkers reported the first DDQ-catalyzed transformation in 1978, showing that the oxidation of allylic alcohols to α,β-unsaturated ketones could be accomplished using 10 mol % DDQ in the presence of 30 mol % periodic acid under slightly acidic,[54] biphasic conditions at room temperature (Scheme 17).[55] In the absence of periodic acid, only stoichiometric substrate oxidation (with respect to DDQ) was observed; no reaction was observed in the absence of DDQ.

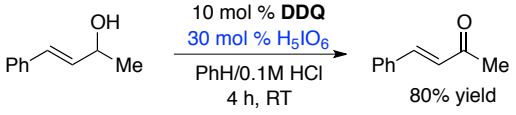

Scheme 1.17. Catalytic oxidation of activated alcohols using catalytic DDQ in combination with periodic acid under biphasic conditions.

Helquist and colleagues subsequently demonstrated similar reactivity employing $Mn(OAc)_3$ as the stoichiometric oxidant. Using 20 mol % DDQ and 6.0 equiv $Mn(OAc)_3$, allylic alcohols and electron-rich benzylic alcohols are oxidized to the corresponding aldehydes and ketones under mild conditions (Scheme 1.18A).[56] Good chemoselectivity for allylic alcohols over benzylic alcohols was observed (Scheme 1.18B). Again, no reaction was observed in the absence of DDQ.

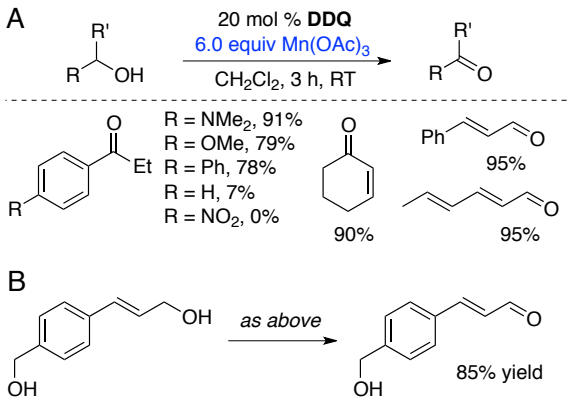

Scheme 1.18. (A) Catalytic oxidation of activated alcohols using catalytic DDQ with $Mn(OAc)_3$ as the terminal oxidant, and (B) selective oxidation of allylic alcohols.

Chandrasekhar demonstrated the deprotection of PMB (4-methoxybenzyl) and DMB (3,4-dimethoxybenzyl) ethers using 10 mol % DDQ in combination with 3.0 equiv $FeCl_3$ under biphasic conditions (Scheme 1.19A).[57] While the substrate scope is limited, these catalytic conditions allow for the selective removal of PMB ether protecting groups in the presence of Ac, THP, TBDPS, MOM, and Bn protecting groups (as with stoichiometric application of DDQ). To avoid incompatibility with acid-sensitive substrates, Sharma has subsequently reported neutral conditions for PMB ether deprotection using 10 mol % DDQ and 3.0 equiv $Mn(OAc)_3$ in CH_2Cl_2 at room temperature (Scheme 1.19B).[58]

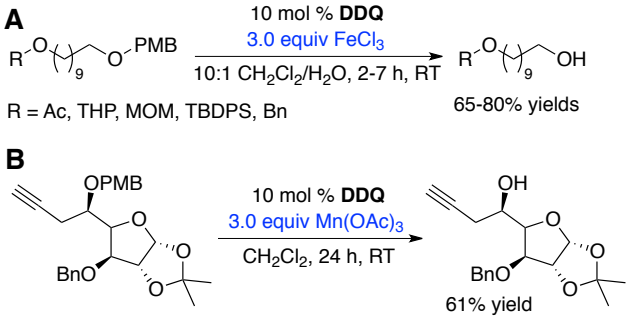

Scheme 1.19. Catalytic deprotection of PMB ethers using DDQ in combination with (A) 3.0 equiv $FeCl_3$, or (B) 3.0 equiv $Mn(OAc)_3$ as the (super)stoichiometric terminal oxidant.

Florenacig reported several examples of novel DDQ-mediated oxidative C-C bond forming reactions, including the intramolecular dehydrogenative-coupling of allylic ethers to form pyranone as well as piperidine-derivatives (cf, Scheme 1.8).[27] In conjunction with this broader program, Floreancig and Liu have reported conditions for carrying out some of these reactions catalytically, using 15-20 mol % DDQ with either PbO_2 or MnO_2 in superstoichiometric excess (Scheme 1.20).[59]

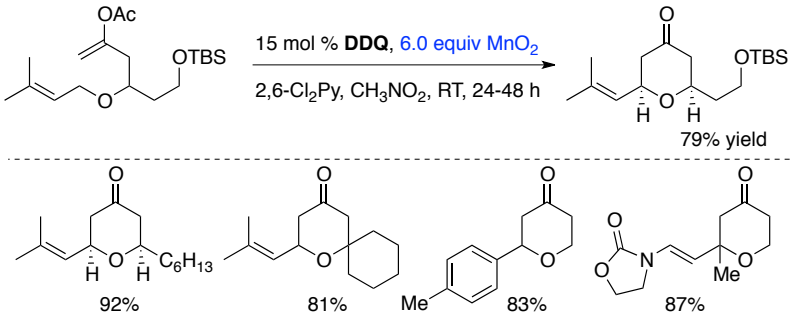

Scheme 1.20. Stoichometric DDQ-mediated oxidative intramolecular synthesis of pyranone derivatives, and subsequently-developed catalytic conditions.

Demonstrating the versatility of replacing stoichiometric DDQ-mediated transformations with catalytic conditions, the authors also demonstrated efficient PMB ether deprotection (Scheme 1.21A), arene and heteroarene dehydrogenation reactions (Scheme 1.21B and C, respectively), and a cross-dehydrogenative coupling type reaction of isochroman with acetophenone (Scheme 1.21D) originally developed as a stoichiometric DDQ-mediated reaction by Li (*vida supra*).[25]

Ghosh and coworkers reported a similar DDQ-catalyzed intramolecular C-C bond forming reaction for the synthesis of tetrahydropyran derivatives, based on a stoichiometric DDQ-mediated transformation developed in their efforts towards the natural product (-)-Zampanolide (Scheme 1.22A).[60] A variety of substituted tetrahydropyran derivatives were obtained using 20 mol % DDQ, 2.0 equiv PPTS, 2.0 equiv ceric ammonium nitrate (CAN), and 4Å MS in MeCN at -38 °C (Scheme 1.22B).[61]

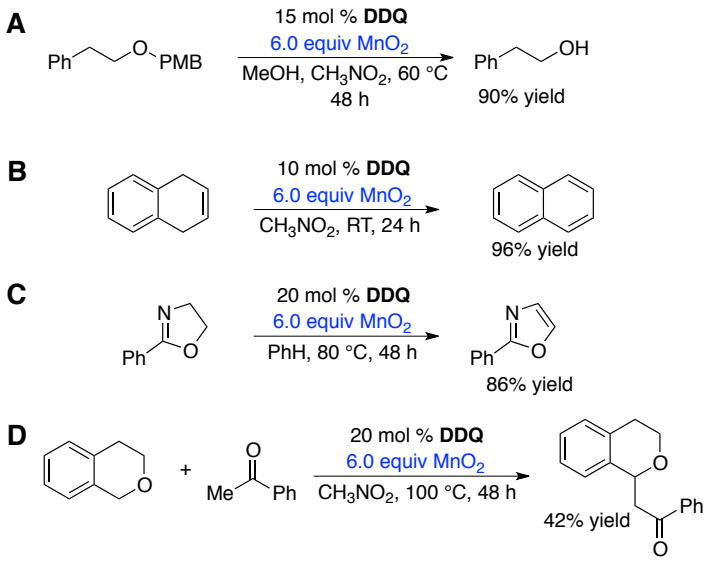

Scheme 1.21. Examples of DDQ-catalyzed transformations including (A) PMB deprotection, (B) arene and (C) heteroarene dehydrogenation reactions, as well as (D) CDC reaction of isochroman with acetophenone.

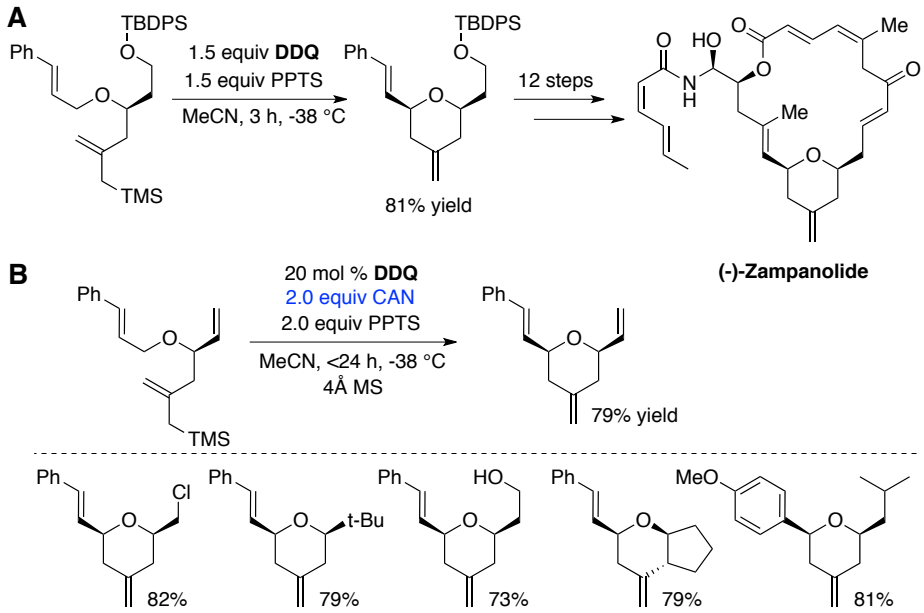

Scheme 1.22. (A) Stoichiometric DDQ-mediated oxidative cyclization reaction, and (B) subsequently developed DDQ-catalyzed conditions employing 2.0 equiv CAN as terminal oxidant.

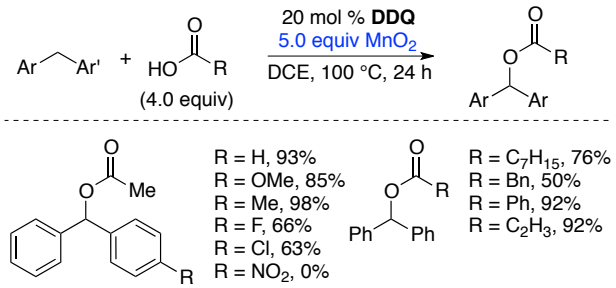

Scheme 1.23. DDQ-catalyzed oxidative C-O coupling employing MnO_2 as the terminal oxidant.

Lei and coworkers reported a DDQ-catalyzed oxidative C-O coupling of diaryl methane C-H bonds with carboxylic acids. Good yields of cross-coupled product could be obtained by using 20 mol % DDQ and 5.0 equiv MnO_2 in dichloroethane at 100 °C (Scheme 1.23). [62]

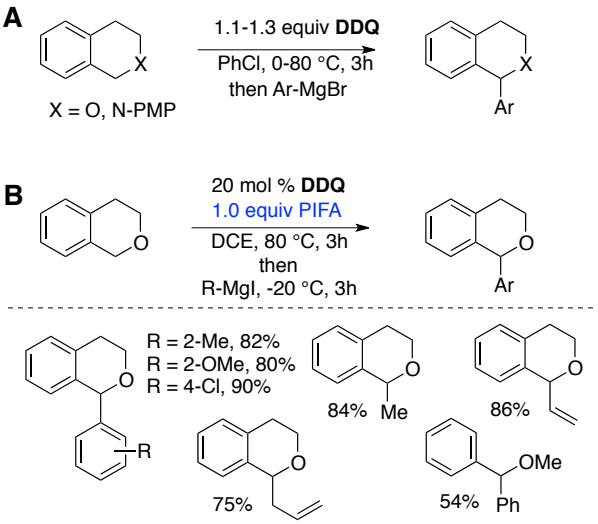

Scheme 1.24. Cross-dehydrogenative coupling of activated C-H bonds with aryl Grignard reagents using (A) stoichiometric DDQ or (B) catalytic DDQ with PIFA as stoichiometric oxidant.

Muramatsu and Nakano reported a DDQ-catalyzed cross-dehydrogenative coupling-type reaction based on an earlier transformation employing stoichiometric DDQ (Scheme 24A).[63] New C-C bonds are formed from oxidation of isochroman or tetrahydroisoquinoline substrates,

followed by addition of aryl Grignard reagents. Catalytic DDQ (20 mol %) can be employed with 1.0 equiv [bis(trifluoroacetoxy)iodo]-benzene (PIFA) as the stoichiometric oxidant (Scheme 1.24B).[64]

Electrochemical regeneration of DDQ/quinones

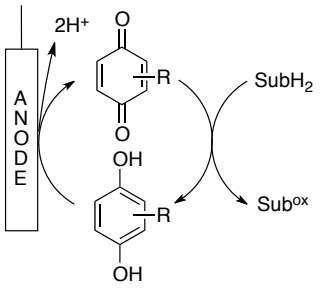

Scheme 1.25. Generic electrocatalytic quinone-mediated oxidation of organic substrates.

Authoritative previous reviews have discussed the use of redox mediators in the electrochemical oxidation of organic substrates, and quinones such as DDQ are among the mediators which have been employed (Scheme 1.25).[65] While the electrochemistry of quinones has been extensively studied, only a handful of examples of DDQ-catalyzed electrochemical reactions have been reported to date. In addition to stoichiometric chemical recycling of $DDQH_2$, the external electrochemical regeneration of DDQ has also been reported.[66,67]

In the course of their synthetic studies on the euglobal family of natural products, Chiba and colleages found that stoichiometric DDQ (2.0 equiv) could effect a desired Diels-Alder reaction between grandinol and pinene derivatives (Scheme 1.26A).[68] Under these stoichiometric conditions, however, the reaction of grandinol model compound **5** with α-phellandrene, lead to undesired Diels-Alder reaction of DDQ with α–phellandrene in quantitative yield and no formation of desired product (Scheme 1.26B). To solve this problem, Chiba subsequently developed an electrocatalytic, DDQ-catalyzed oxidation of **5** to an intermediate quinone methide

species at a polytetrafluoroethylene (PTFE)-fiber coated working electrode at 0.70 V (NHE) in Et_4NOTs (50 mM in $MeNO_2$). Subsequent Diels-Alder reaction with α-phellandrene or α- or β-pinene was used to generate a desired euglobal analogue (Scheme 1.26C).[69] An elegant demonstration of challenging stoichiometric transformations made plausible by catalytic conditions, six distict euglobal natural products could be obtained using this electrochemical approach.

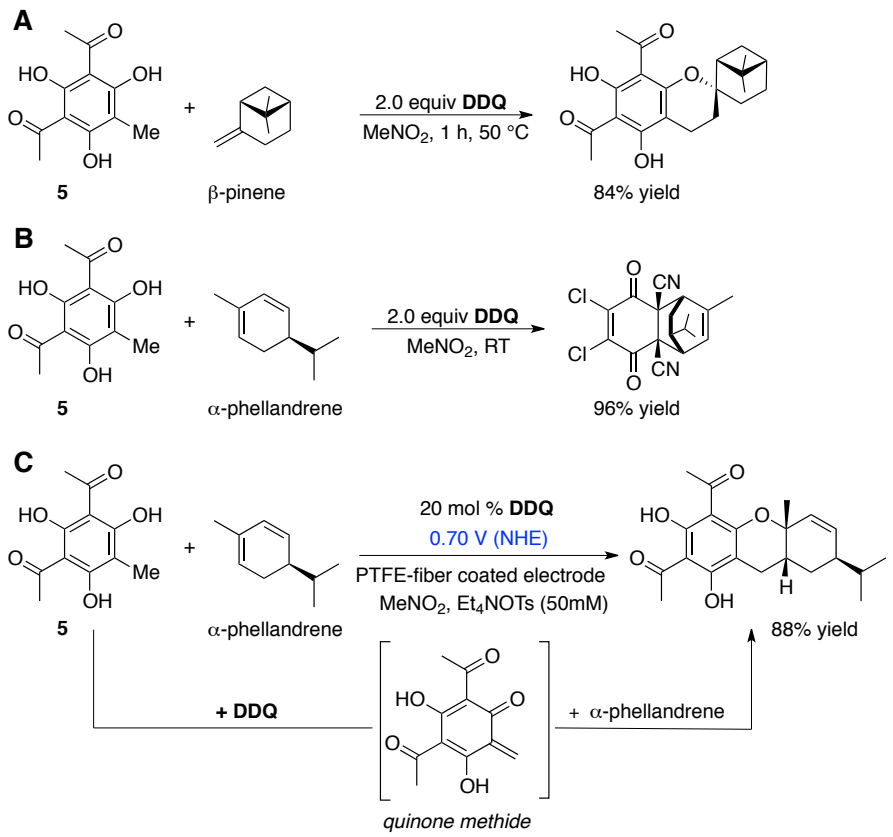

Scheme 1.26. Stoichiometric DDQ-promoted Diels-Alder reaction of compound 5 leads to desired product with (A) β-pinene, but not with (B) α-phellandrene. (C) Reaction with α-phellandrene is successful when electrochemical catalytic DDQ conditions are employed.

Utley and Rosenberg employed DDQ as an electrocatalyst for the benzylic oxidation of electron-rich 2-alkylnaphthalenes.[41f, 70] Crabtree reported conditions for electrochemical DDQ regeneration in the context of "virtual hydrogen storage" research. Using 15 mol % DDQ in

MeCN (0.5 M $NaClO_4$) at room temperature, *N*-phenylbenzylidine could be obtained from *N*-phenylbenzylamine in 95% yield (Scheme 1.127) after 6 hour controlled potential electrolysis at 0.964 V NHE.[71]

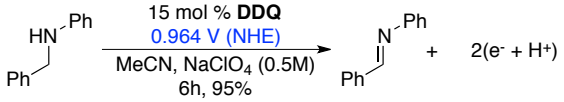

Scheme 1.27. Electrochemical DDQ-catalyzed dehydrogenation of C-N bonds.

Aerobic regeneration of DDQ/quinones

Molecular oxygen is an ideal terminal oxidant.[72] Accordingly, attempts to develop aerobic quinone-catalyzed methods for organic substrate oxidation reactions have been reported. While the direct aerobic oxidation of high potential hydroquinones is not typically feasible,[73] several strategies for mediating the aerobic re-oxidation of hydroquinone species have emerged, typically requiring co-catalytic amounts of an electron transfer mediator (ETM, Scheme 1.28A). A notable co-catalytic system enabling aerobic DDQ-catalyzed transformations involves the use of an NO/NO_2 redox cycle (Scheme 1.28B).

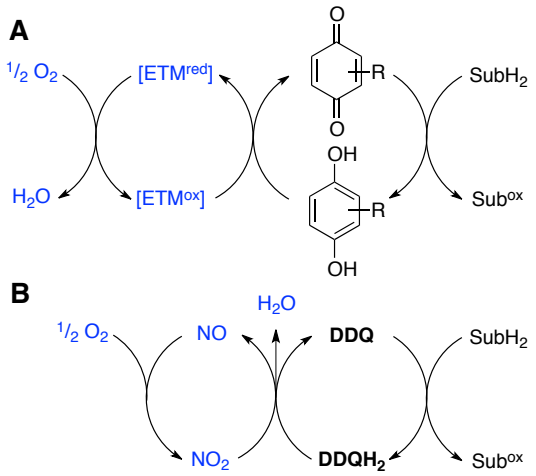

Scheme 1.28. A aerobic regeneration of hydroquinones employing (A) an electron transfer mediator (ETM) or (B) NO/NO_2 redox couple.

Extensive literature has also focused on the stoichiometric, aerobic oxidation of hydroquinones to quinones, either uncatalyzed (autoxidation) or using co-catalysts such as metal macrocycles[74] including catecholase mimics.[75] Examples employing high potential quinones, such as DDQ or chloranil, are rare. Miyamura, Kobayashi and coworkers reported the aerobic oxidation of a wide variety of hydroquinone derivatives with heterogeneous, styrene-based polymer-incarcerated Au[76] (PI Au) and Pt[77] (PI Pt) nanoclusters. Reaction conditions are mild, proceeding with very low catalyst loadings at room temperature in $CHCl_3/H_2O$ under 1 atm O_2 (Scheme 1.29). Remarkable substrate scope is demonstrated: tetrachlorohydroquinone can be oxidized to choranil in 99% yield at room temperature within 3 h using 1 mol % PI-Pt catalyst.

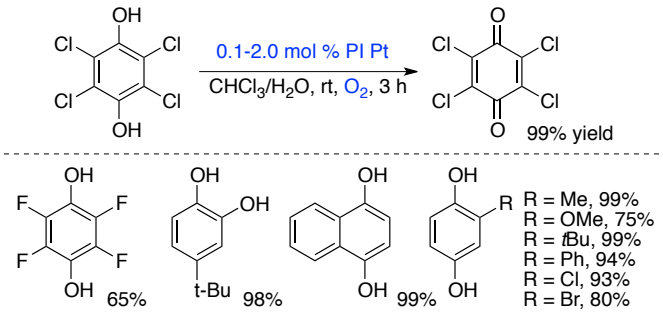

Scheme 1.29. Aerobic oxidation of *p*-chloranil-H_2 and other hydroquinone derivatives to corresponding quinones using polymer incarcerated Pt (PI Pt) nanoclusters.

In subsequent application of this concept, Miyamura, Kobayashi and coworkers demonstrated that a catalyst system composed of catalytic *o*-chloranil, and co-catalytic organic/inorganic hybrid platinum nanocluster catalyst (HB Pt) can be employed in the oxidation of organic substrates using molecular oxygen as the terminal oxidant. Efficient oxidation of Hantzsch-type dihydropyridines to substituted pyridines could be accomplished using 5-10 mol % *o*-chloranil in combination with 0.5-1.0 mol % HB Pt in CH_2Cl_2/H_2O solvent at room temperature under 1 atm O_2 (Scheme 1.30A).[78] Dehydrogenation of 2-methylindoline to the corresponding indole could also be accomplished using this catalyst system (Scheme 1.30B). Efficient PMB ether

deprotection could be accomplished as well, under modified reaction conditions consisting of 1 mol % oxidation-resistant polymer-incarcerated Pt catalyst (RPI Pt) and 10 mol % o-chloranil in DCE/H_2O at 100 °C, (Figure 1.30C).

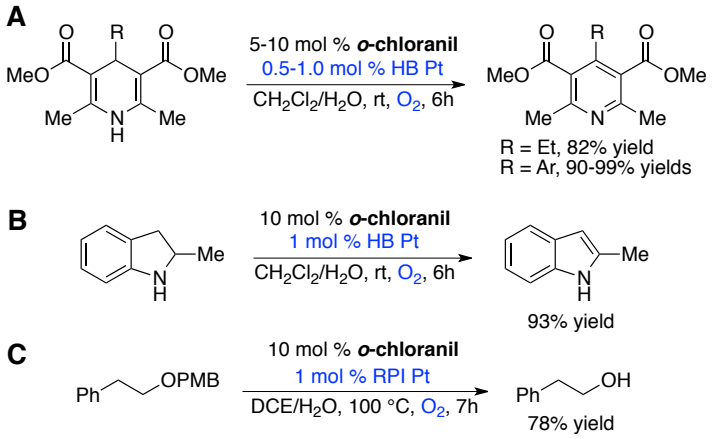

Scheme 1.30. Aerobic, *o*-chloranil-catalyzed dehydrogenation of (A) dihydropyridines to pyridines, (B) 2-methylindoline to 2-methylindole, and (C) a PMB ether.

When stoichiometric chloranil (3.0 equiv) was used in the oxidation of tetrahydroquinoline derivative **6**, substrate/chloranil ketal adduct **8** was obtained as the major product. Under catalytic conditions, on the other hand, the desired oxygenated compound, **7**, could be obtained in 88% yield (Scheme 1.31).

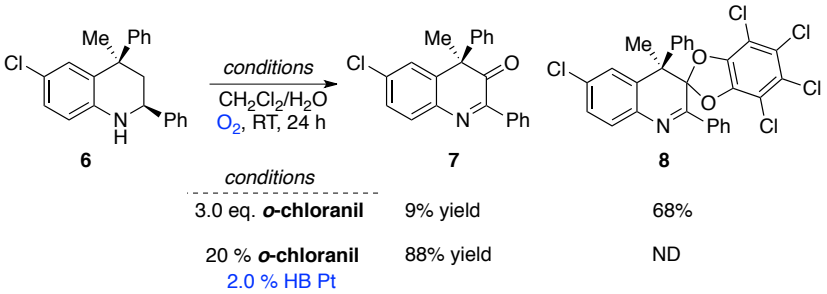

Scheme 1.31. An example of catalytic technology enabling a reaction that was not feasible under stoichiometric conditions.

Heteropolyacids are also effective co-catalysts in the aerobic regeneration of high potential quinones. For example, Neumann and coworkers reported an aerobic oxidation of allylic and benzylic alcohols using 5 mol % *o*-chloranil with 1.5 mol % $Na_5PV_2Mo_{10}O_{40}$ at 90 °C in H_2O/decalin under 1 atm O_2.[79]

Reports by Kochi and coworkers in 1994 demonstrated the quantitative aerobic oxidation of hydroquinone to benzoquinone using 1 mol % NO_2 in CH_2Cl_2 at -10 °C under 1 atm O_2 (Scheme 1.32).[80] A range of substituted quinone species could be generated in this way.[81]

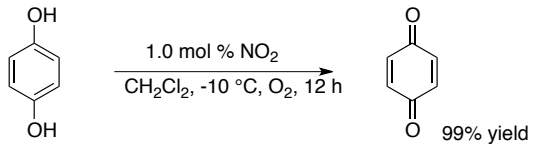

Scheme 1.32. NO_2-catalyzed aerobic oxidation of hydroquinones to quinones.

The observation that a NO/NO_2 redox couple could be employed to promote the aerobic oxidation of $DDQH_2$ to DDQ (cf Scheme 1.28B) was first reported by Xu and coworkers. Using a catalyst system consisting of 5 mol % DDQ and 5 mol % $NaNO_2$ under 1.3 MPa O_2 at 120 °C, dihydroanthracene could be dehydrogenated to anthracene in >99% yield after 8 h reaction time (Figure 1.33).[82]

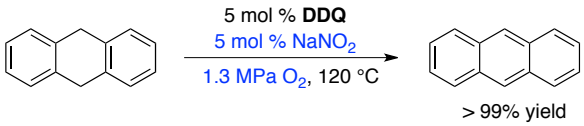

Scheme 1.33. DDQ-catalyzed aerobic dehydrogenation of dihydroanthracene employing co-catalytic $NaNO_2$.

The observation that a NO/NO_2 redox couple can enable an aerobic DDQ-catalyzed reaction is an important finding. Traditional electron transfer mediators (ETMs), which couple the oxidation of hydroquinone with the reduction of O_2 to H_2O_2 are not effective with DDQ, as the

thermodynamic potential of DDQ/$DDQH_2$ (E° = 0.750 V NHE) is greater than that of the 2e- reduction of O_2 to H_2O_2 (0.670 V NHE). Because of the unique mechanism of O_2 reduction by NO, which results in the net $4e^-$ reduction of O_2 to H_2O, more of the oxidizing potential of O_2 is utilized, thus enabling favorable thermodynamics for the oxidation of $DDQH_2$ to DDQ.

Mo, Hu and coworkers have reported a similar catalyst system for the oxidation of activated alcohols, using 5 mol % DDQ and 5 mol % $tBuNO_2$ in dichloroethane at 80 °C under 0.2 MPa O_2 pressure. Excellent yields of the corresponding aldehydes or ketones were obtained (Scheme 1.34A). [83] Under modified reaction conditions (ethylene glycol diethylether as solvent, 140 °C), the authors found that methyl aryl ethers could also be transformed to the corresponding benzylic aldehydes (Scheme 1.34B). Additionally, selective PMB ether deprotection could be accomplished under similar reaction conditions (Scheme 1.34C). As usual, aliphatic alcohols are inert under the reaction conditions; alcohol products were obtained from the deprotection of aliphatic PMB ethers in excellent yield.

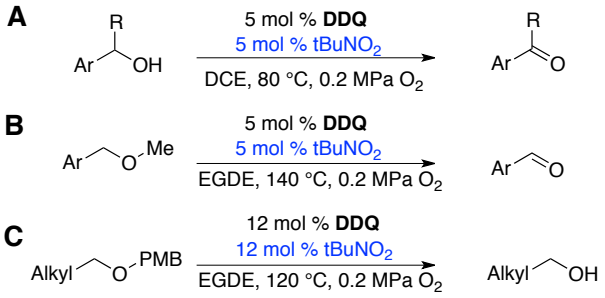

Scheme 1.34. DDQ-catalyzed aerobic oxidation of (A) alcohols and (B) ethers, and (C) selective deprotection of PMB.

Shortly thereafter, Gao and colleagues reported a DDQ-catalyzed (1-20 mol %) method for the aerobic oxidation of allylic and benzylic alcohols to corresponding aldehydes. [84] The reaction, which requires 10 mol % $NaNO_2$ to proceed, is carried out in a CH_2Cl_2/AcOH solvent

mixture at ambient temperatures under an O_2 balloon (Figure 1.35). Reactions could also be carried out under air in good yields.

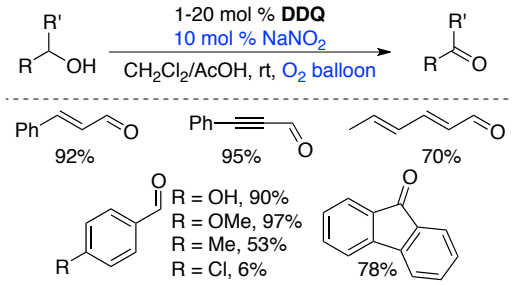

Scheme 1.35. DDQ-catalyzed aerobic oxidation of activated alcohols to aldehydes employing co-catalytic $NaNO_2$.

Following their initial report,[83] Shen, Hu and colleagues reported a milder aerobic DDQ-catalyzed deprotection of PMB ethers, affording the corresponding alcohol in excellent yield.[85] Conditions were similar to those employed by Gao (5 mol % DDQ, 5 mol % $NaNO_2$); however, reaction temperature was increased to 100 °C in chlorobenzene solvent. Moody has subsequently reported even milder conditions for PMB ether deprotection, employing 1.5-5 mol % DDQ, 3-10 mol % $NaNO_2$ in AcOH at room temperature under 1 atm O_2 (balloon)[86]

Yan and coworkers reported aerobic DDQ-catalyzed oxidative coupling of diarylpropenes with 1,3-diketones.[87] A range of new C-C coupled products could be obtained in good to excellent yields using 1 mol % DDQ and 10 mol % $NaNO_2$ in $MeNO_2/HCO_2H$ at room temperature under O_2 balloon (Scheme 1.36).

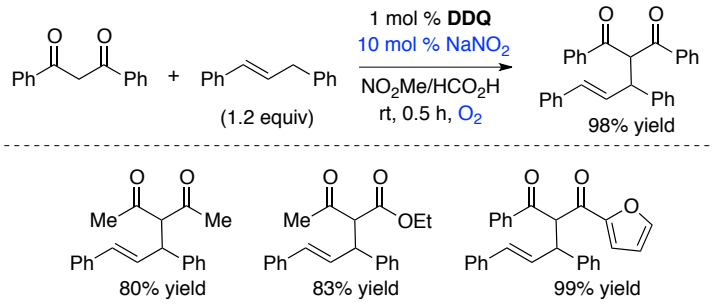

Scheme 1.36. DDQ-catalyzed aerobic C-C coupling of diarylpropenes and 1,3-dicarbonyls employing co-catalytic $NaNO_2$.

Finally, Westwood applied DDQ-catalyzed alcohol oxidation using O_2/NO_x co-catalyst system to lignin depolymerization applications,[88] and related systems have been reported for aerobic alcohol oxidation,[89] cross-dehydrogenative coupling-type reactions,[90] and porphyrin synthesis.[91]

1.4. Bioinspired *o*-Quinone Catalysts

1.4.1. Enzymatic Context

Quinones play an important role as cofactors in the enzymatic oxidation of organic substrates. Several families of so-called "quinoenzymes"[92] are known, and include: copper amine oxidases (containing active-site cofactors TPQ[93] and LTQ[94]), methylamine dehydrogenase (TTQ[95]), and methanol and glucose dehydrogenases (PQQ).

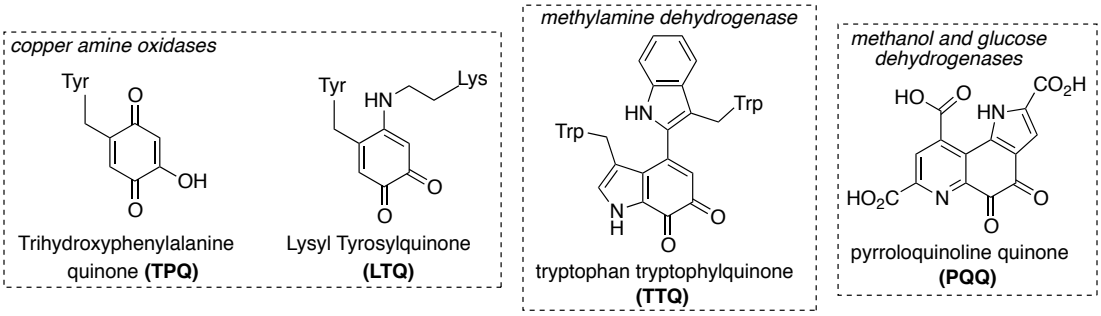

Copper amine oxidases (CAOs) convert primary amines to aldehydes using molecular oxygen (Scheme 1.37A).[96] While copper is present in the active site of these enzymes, substrate oxidation takes place exclusively at an *o*-quinone cofactor (eg TPQ and LTQ), which is formed by copper-mediated post-translational modification of an active-site tyrosine residue.[97] Substrate oxidation occurs through a transamination mechanism, which involves initial condensation of primary amine substrate with the quinone cofactor to give an imine adduct, **9**.[98] Imine **9**

undergoes a tautomerization (or net prototropic rearrangement) to give a second imine species, **10**. Hydrolysis liberates aldehyde product and reduced aminohydroquinone cofactor, **11**. Aerobic reoxidation to an iminoquinone species, **12**, followed by transamination with another equivalent of amine, closes the catalytic cycle (Figure 1.37B).

Klinman,[99] Sayre,[100] Itoh[101] and others developed biomimetic model quinone cofactors in connection with their fundamental biochemical mechanistic studies of CAO and methylamine dehydrogenase quinoenzymes (Figure 1.38). These model quinones carry out selective aerobic oxidation of primary amines to imines and aldehydes through a transamination mechanism akin to the enzymatic mechanism.

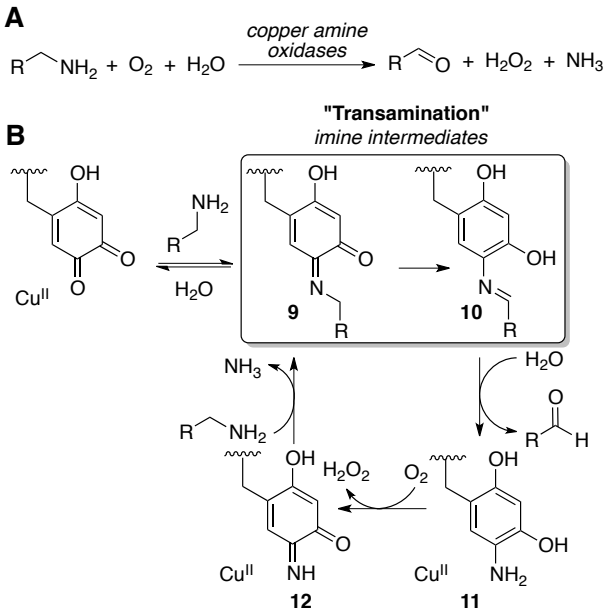

Scheme 1.37. Copper amine oxidases carry out (A) the aerobic oxidation of primary amines in vivo, via a (B) transamination mechanism.

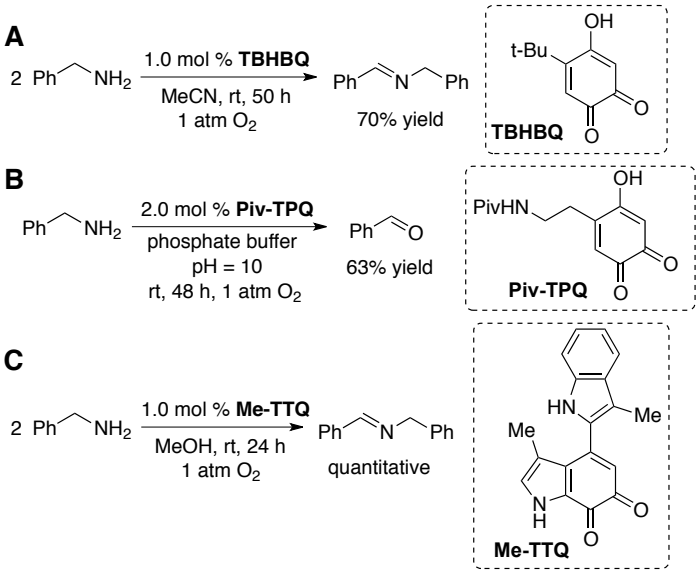

Scheme 1.38. Model quinone cofactors (a) TBHBQ, developed by Klinman, (b) Piv-TPQ, developed by Sayre, and (c)Me-TTQ, developed by Itoh.

In addition to model substrate oxidation, Itoh further examined mechanistic features of the C-H bond-cleaving step in tryptophan tryptophylquinone (TTQ) model quinone **Me-TTQ**.[101a] The authors carried out kinetic measurements, where k_{obs} was proposed to reflect imine rearrangement step on the basis of large KIE (7.8 – 9.2). They proposed that k_{obs} reflects two competing C-H bond cleavage processes: a slow "spontaneous" intramolecular prototropic rearrangement, k_1; and a faster bimolecular "base-catalyzed" rearrangement step, k_1' (Scheme 1.39). These findings suggest a distinction between these biomimetic *o*-quinone catalysts, which involve *deprotonative* C-H bond cleavage, and high potential quinones which involve *hydridic* C-H bond cleavage.

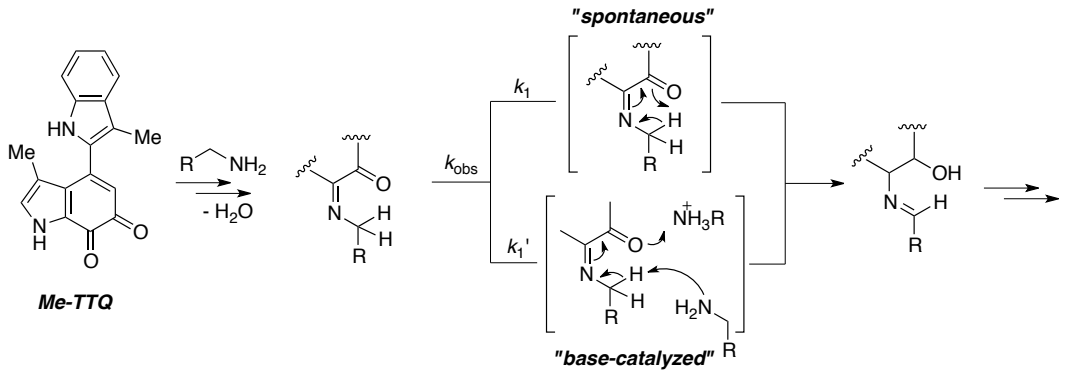

Scheme 1.39. Mechanistic proposal for C-H bond breaking step in biomimetic model quinone-catalyzed aerobic oxidation of primary amines to imines.

Pyrroloquinoline quinone (PQQ) is a quinone cofactor found in bacterial alcohol dehydrogenases, including methane dehydrogenase and glucose dehydrogenase. Biochemical studies of the PQQ cofactor established a complementary mechanism for substrate oxidation.[102] In this case an "addition-elimination" mechanism has been proposed, wherein substrate oxidation (typically an alcohol, such as methanol) occurs from a hemiacetal intermediate (Scheme 1.40).[103]

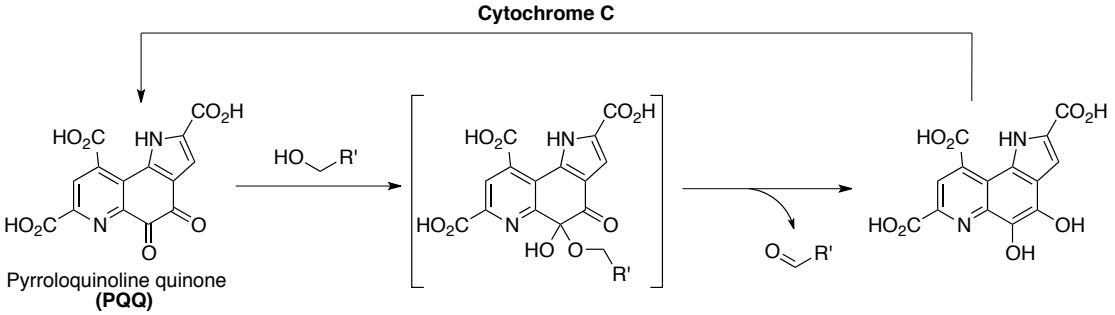

Scheme 1.40. Proposed mechanism of alcohol oxidation mediated by cofactor PQQ.

In model studies, Itoh, Fukuzumi and coworkers showed that the oxidation of low molecular weight alcohols such as ethanol and methanol are oxidized to the corresponding aldehydes using the tri-methyl ester of PQQ (Scheme 1.41).[104] PQQ is not an aerobic cofactor in nature, but this synthetic system employs molecular oxygen as the terminal oxidant. The thermodynamic potential of PQQ-3OMe is low, estimated at 0.05 V (NHE, MeCN; cf free PQQ -0.05 V NHE,

DMF).[111] DDQ, on the other hand, is a significantly stronger oxidant from a thermodynamic perspective (0.750 V NHE, MeCN).[105] Yet DDQ is not known to oxidize methanol; in fact, many DDQ-mediated substrate oxidations take place in methanol as solvent. That efficient methanol dehydrogenation is achieved by PQQ is an impressive example of the importance of reaction kinetics, and consequently catalyst design, in quinone-mediated transformations of organic substrates.

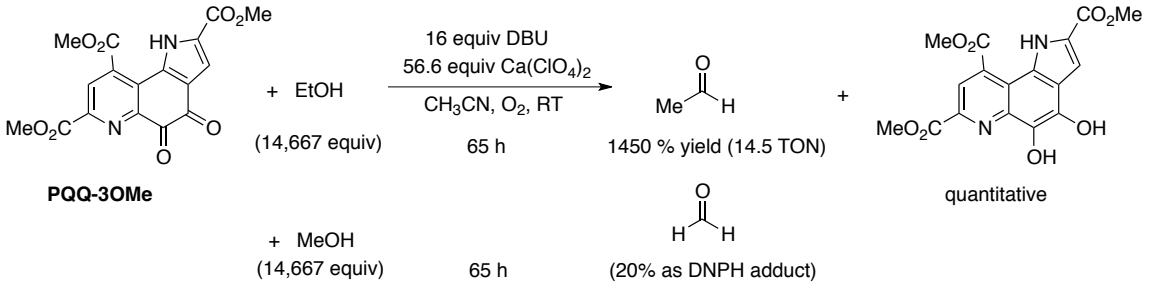

Scheme 1.41. Biomimetic **PQQ-3OMe**-catalyzed aerobic oxidation of methanol and ethanol.

Itoh, Ohshiro and coworkers additionally demonstrated the PQQ-mediated oxidation of simple sugars to the corresponding carboxylic acids (eg glucose to gluconic acid), modeling the activity of PQQ quinoenzyme glucose dehydrogenase. [106]

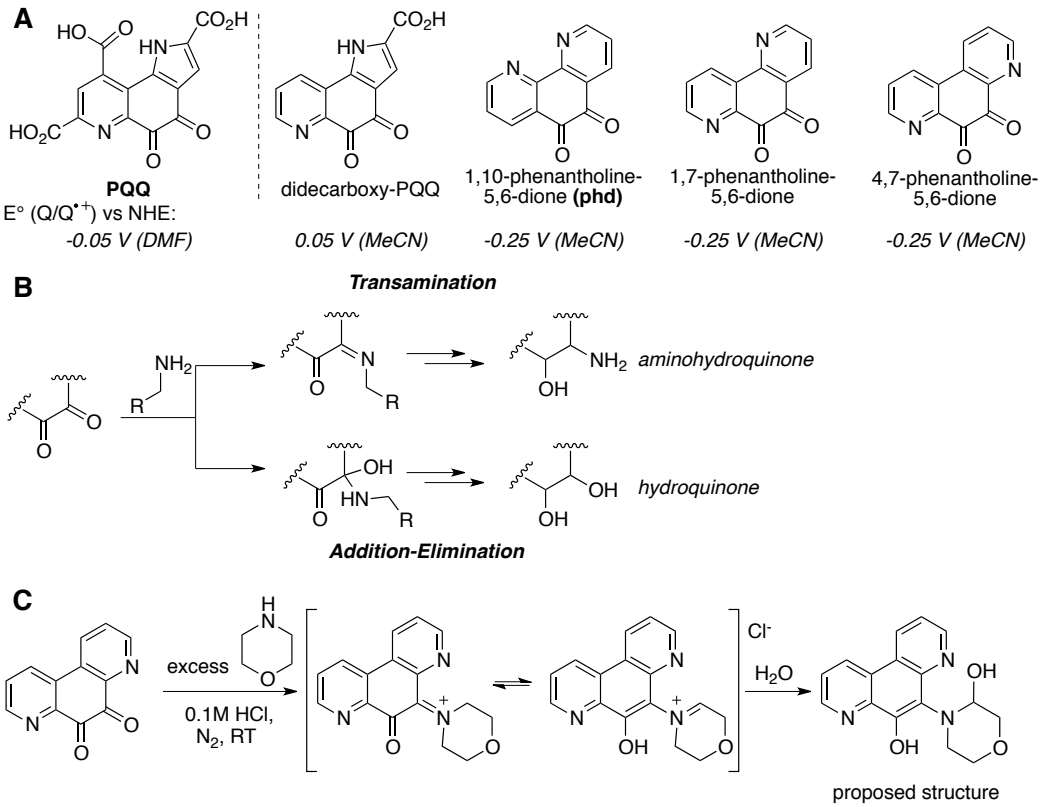

Scheme 1.42. (A) PQQ and PQQ model compounds, (B) different mechanism lead to different reduction products, and (C) adduct formation.

Unlike other quinone cofactors, PQQ is not covalently bound to the enzyme. In fact, glucose dehydrogenase can be reconsitituted with simplified derivatives (related to 1,7- and 4,7-phenanthroline quinones) to give an active, albeit attenuated, enzyme.[107] Bruice has carried out a series of mechanistic studies using PQQ, and simplified PQQ-like structures, such as di-decarboxy-PQQ and 1,10-, 1,7-, and 4,7-phenanthroline-derived quinones (Scheme 1.42A) on the oxidation of alcohols and amines.[108] Phenanthroline-derived quinones share a number of physical and chemical similarities with PQQ, including similar electrochemical potential (cf Scheme 1.42A), facile formation of covalent adducts with water, methanol, and acetone, and stoichiometric oxidation of simple organic substrates.[109,110,111]

In a series of mechanistic studies, Bruice showed that the stoichiometric reduction of PQQ phenanthroline-derived model quinones by primary amines (cyclohexylamine and glycine) results in the formation of aminohydroquinone products, consistent with a transamination mechanism.[112] In the presence of the secondary amine morpholine, a much slower reaction occurred, leading to the identification of substrate-quinone adduct as the predominant product (Scheme 1.42C), also suggesting a transamination-type mechanism. Oxidation of the tertiary amine *N*,*N*-dimethylbenzylamine was also significantly slower than primary amine oxidation, and led to the formation of hydroquinone as well as benzaldehyde and formaldehyde products. Bruice also tested the stoichiometric oxidation of *p*-methylbenzylalcohol with these phenanthroline-derived quinones. No reaction was observed after 7 days at 60 °C with 1,10- and 1,7-phenanthrolinedione, and only 6% yield was observed using 4,7-phenanthrolinedione. (In contrast 90% yield was obtained when DDQ was employed as the oxidant under otherwise identical conditions). Across each of these substrate classes Bruice found that quinones containing a nitrogen atom adjacent to the quinone carbonyls (eg, 1,7- and 4,7-phenanthrolinedione) were found to carry out substrate oxidation more rapidly that 1,10-phenanthrolinedione, despite nearly identical electrochemical potential.

In contrast to phenanthroline-derived quinones, secondary and tertiary amines are not substrates for the didecarboxy-PQQ model compound, and endproduct analysis of the reaction of didecarboxy-PQQ with primary amines reveals the formation of hydroquinone, rather than aminohydroquinone (cf Scheme 1.42B).[113] These findings are consistent with the work of Itoh, Ohshiro, and coworkers, who proposed that oxidation of primary amines by PQQ proceeds through an "addition-elimination"-like mechanism.[114] The authors provide some kinetic evidence for this pathway in addition to the observation of mixtures of aminohydroquinone

(transamination product) and hydroquinone (addition-elimination product) species isolated at the end of model reactions. Reaction endproduct analyses of this kind are complicated by redox scrambling of the quinone and hydroquinone species, and are therefore difficult to interpret. Interconversion of aminoquinol and quinol catalyzed by the presence of even a small amount of quinone occurs even under anaerobic conditions, and the ratios of products are found to depend significantly on reaction conditions.[115]

1.4.2 o-Quinone Catalyzed C-N Bond Dehydrogenation Reactions

Based on the fundamental mechanistic and model studies of enzyme quinone cofactors discusses above, a number of biomimetic quinone-mediated transformations have been developed. In particular, biomimetic *o*-quinones are recognized as selective and efficient catalysts for C-N bond dehydrogenation reactions. [116]

Prior to the elucidation of quinone cofactors in amine oxidase enzymes, Corey demonstrated that branched primary amines could be treated with stoichiometric 3,5-di-*tert*-butyl-*o*-quinone in MeOH to give a tautomeric imine adduct.[117] Upon hydrolysis, ketone products could be obtained in excellent yields (Figure 1.43). Unbranched primary amines were not effective substrates in this case, as benzoxazole products were obtained.[118]

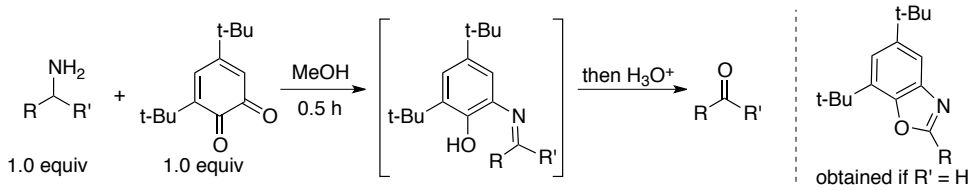

Scheme 1.43. Stoichiometric oxidation of branched primary amines to ketones.

Wanner and Koomen applied this methodology to the divergent synthesis of a variety of alkaloid natural products, including anabasine, lupinamine, and sparteine (Scheme 1.44).[119]

Instead of hydrolysis, the intermediate quinone-imine adduct undergoes intramolecular transamination with pendant secondary amine. Subsequent tautomerization affords enamine as a common intermediate.

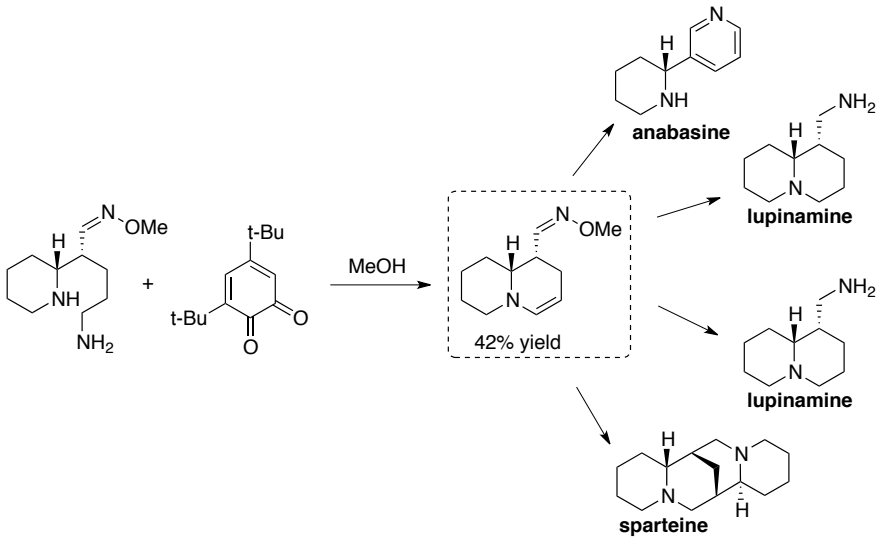

Scheme 1.44. Application of Corey's quinone to synthesis of alkaloid natural products.

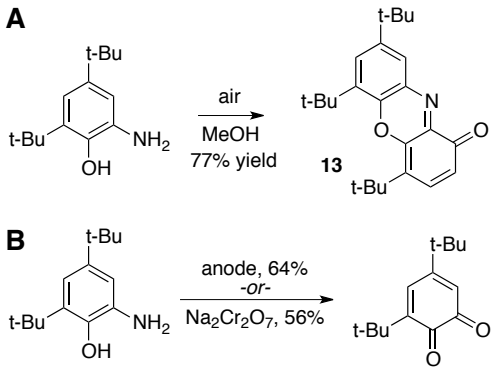

Scheme 1.45. (A) Aerobic oxidation of aminohydroquinone results in formation of dimeric species **13**, and (B) additional attempts at regeneration of quinone from reduced aminohydroquinone.

Independent attempts at regenerating the 3,5-di-*tert*-butylquinone from the reduced aminophenol by O_2 in neutral media led to dimeric compound **13** (Scheme 1.45A), while

electrochemical regeneration and chromate regeneration in acidic media gave quinone in 64% and 56% yields, respectively (Scheme 1.45B).[120]

The catalytic aerobic oxidation of primary amines to ketones and aldehydes was demonstrated by Itoh using PQQ as a catalyst under aqueous micellar conditions: 1 mol % of the quinone PQQ, 10 mol % hexadecyltrimethylammonium bromide (CTAB), in pH 9-10 aqueous solution under ambient air at room temperature (Scheme 1.46).[121] In subsequent report, Itoh and coworkers extended this reaction to the oxidative decarboxylation of amino acids, and oxidative dealdolation or β-hydroxy amino acids, to give aldehydes.[122,123] Aerobic PQQ-catalyzed oxidation of thiols to disulfide is also achieved under similar conditions.[124]

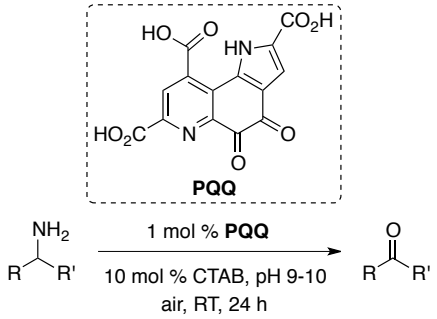

Scheme 1.46. Catalytic oxidation of primary amines to aldehydes and ketones.

Largeron and Fleury developed *o*-quinones **Q1**^{red} and **Q2**^{red} as catalysts for the electrochemical oxidation of primary amines to imines.[125] Controlled potential electrolysis of benzylic or aliphatic primary amines could be accomplished using only 2 mol % of precatalyst **Q1**^{red} or **Q2**^{red} at 0.60 V SCE with a Pt anode in MeOH at room temperature (Scheme 1.47A). While good catalyst turnover numbers could be obtained, products were isolated as dinitrophenylhydrazone adducts, limiting the synthetic value of this transformation. To address this limitation, Largeron and coworkers generated cross-coupled imine compounds by carrying out the oxidation of benzylamine in the presence of a second, less-readily oxidized amine.

Following electrolysis, the Pt anode is replaced with a Hg pool cathode. Electrolysis at -1.6 V for 1 h reduced the cross-coupled imine species to a secondary amine, which could be isolated after workup (Scheme 1.47B).[126] If this reaction was run in the presence of a Cu(I) co-catalyst, 0.2 mol % Cu^{I}(MeSal) (MeSal = methylsalicylate), **Q2^{red}** can also be employed as a catalyst in the aerobic oxidation of primary amines.[127] Under these ambient conditions, at room temperature under ambient air, dimeric and cross-coupled imine products could be directly obtained in excellent yields (Scheme 1.47C).

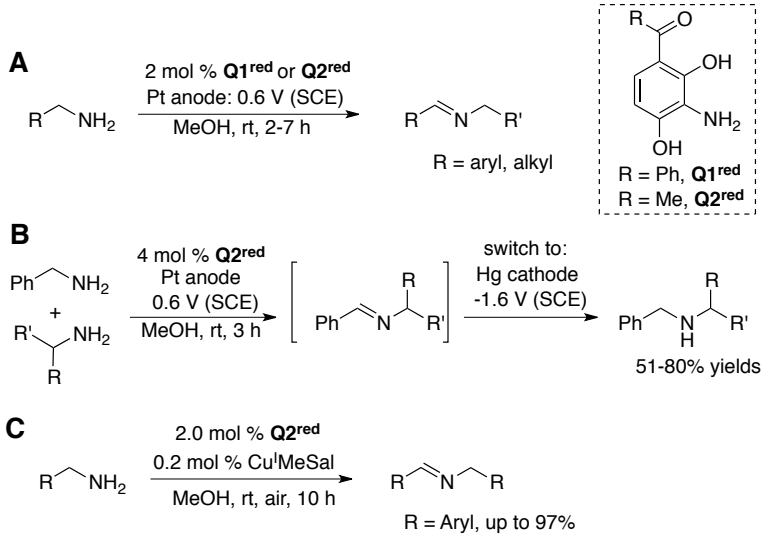

Scheme 1.47. (A) Electrochemical oxidation of amines to imines and (B) secondary amines, as well as (C) Cu^{I}-cocatalyzed aerobic oxidation of primary amines by CAO mimic **Q1^{red}** and **Q2^{red}**.

Wendlandt and Stahl subsequently demonstrated the aerobic oxidation of a diversity of benzylic amines to the corresponding secondary imines using TBHBQ, a model quinone initially developed by Mure and Klinman (Scheme 1.48).[128,129] Selective cross-coupling products could be obtained by running the reaction in the presence of a second, unactivated amine.

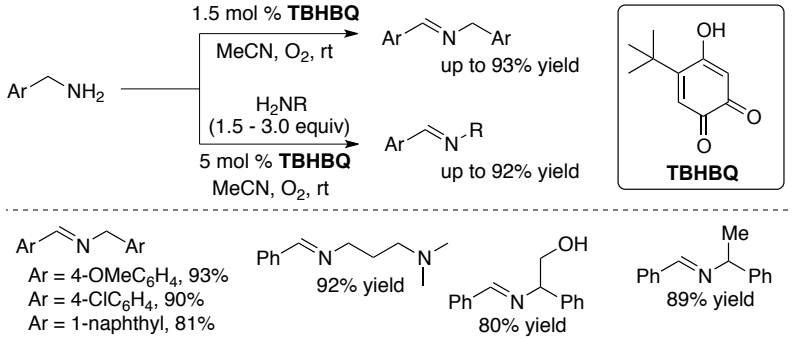

Scheme 1.48. Aerobic oxidation of primary amines to imines using biomimetic *o*-quinone catalyst TBHBQ.

While unbranched substrates are readily oxidized by these aerobic quinone catalysts, both the methods reported by Stahl and Largeron suffer limitation with respect to α-branched substrates. Luo and colleagues have recently reported that branched benzylic primary amines are readily dehydrogenated to imines by 4-methoxy-5-tert-butyl-o-quinone, **Q3**.[130] Excellent yields of dimeric imine products were obtained using 10 mol % **Q3** at room temperature under O_2 atmosphere (Scheme 1.49).

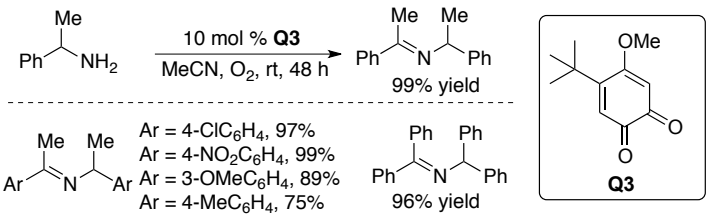

Scheme 1.49. Aerobic oxidation of α-branched primary amines to imines using a biomimetic *o*-quinone catalyst.

In the biomimetic systems developed by Largeron and Stahl, exceptional selectivity for primary amine oxidation is observed. Secondary and tertiary amines are not substrates for these quinone catalysts, and primary alcohols are not oxidized under these reaction conditions. This exquisite selectivity is likely a consequence of the transamination mechanism, which requires the formation of an imine adduct for substrate oxidation to occur. Secondary amines have been

shown to be mechanism-based inhibitors of quinones such as TBHBQ.[131] Formation of iminium adducts ultimately results in irreversible modification of the catalyst (Figure 1.50).

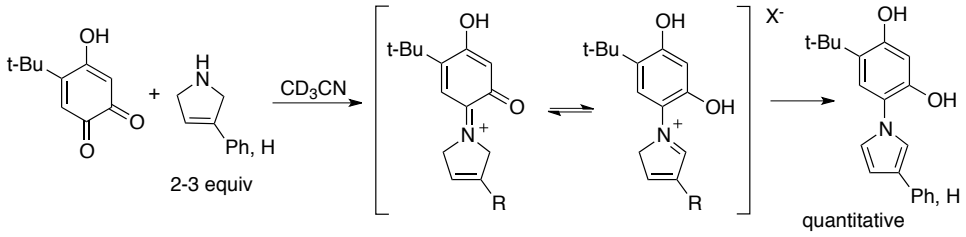

Scheme 1.50. Irreversible pyrrolation of TBHBQ catalyst via transamination-type mechanism.

While secondary and tertiary amines are not substrates for quinones that proceed via a transamination mechanism, the oxidation of these substrates should be possible using quinones which proceed via an addition-elimination mechanism. The shift between these two mechanistic paradigms, while subtle, has important implications for reaction scope.

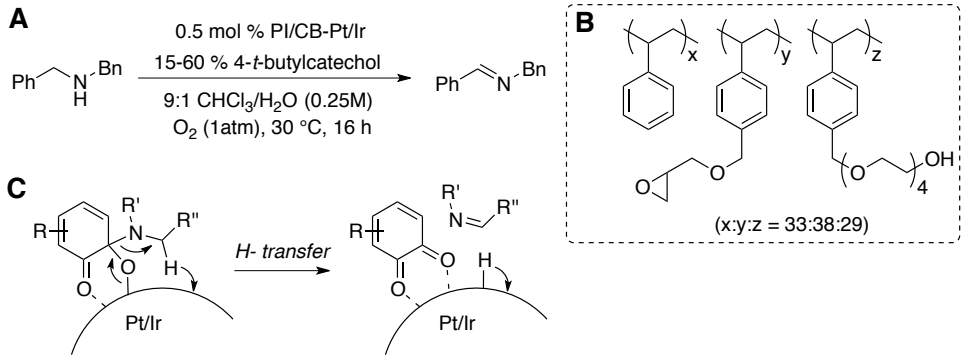

Scheme 1.51. (A) Dehydrogenation of C-N bonds using Pt/Ir alloy incarcerated (B) coblock polymer catalyst used in combination with co-catalytic catechol additives. (C) Proposed mechanism involving hemiaminal intermediates.

Kobayashi and coworkers reported a method for the aerobic dehydrogenation of C-N bonds, employing 0.5 mol % of a co-block polymer-incarcerated Pt/Ir alloy catalyst in combination with a 15-60 mol % catechol co-catalyst (Scheme 1.51A and B).[132] While C-H bond cleavage is proposed to occur at the Pt/Ir nanocluster, Kobayashi suggests a crucial role for substrate

activation at the quinone cofactor – implicating a hemiaminal intermediate reminiscent of the addition-elimination mechanism (Scheme 1.51C). Very recently, Doris and coworkers have reported that carbon nanotube-supported Rh nanoparticles (Rh-CNT) are efficient co-catalysts in 4-*tert*-butylquinone-catalyzed aerobic dehydrogenations of *N*-heterocycles as well.[133]

Using a PQQ model compound, 1,10-phenanthroline-5,6-dione (phd), Wendlandt and Stahl have demonstrated the aerobic quinone-catalyzed oxidation of secondary amines and *N*-heterocycles (Scheme 1.52A). Using 5 mol % phd, 2.5 mol % ZnI_2, and 15 mol % pyridinium p-toluenesulfonic acid (PPTS) in MeCN at room temperature under 1 atm O_2 (balloon), a diverse range of *N*-heterocyclic compounds are dehydrogenated (Scheme 1.52B).

Through spectroscopic studies, Stahl has shown that substrate oxidation proceeds via the addition-elimination, rather than transamination, mechanism (Scheme 1.52C). [134] The addition of ZnI_2 is proposed to play two roles. First, *N*–*N* coordination of Zn^{2+} to the phenanthroline-derived quinone enhances the rate of substrate oxidation. Second, I^- counterions promote aerobic catalyst turnover, and the authors suggest that iodide may play a redox role in hydroquinone oxidation (Scheme 1.52C). This subtle shift in transamination versus addition-elimination reaction mechanism results in a dramatically enhanced substrate scope for biomimetic *o*-quinone-catalyzed C–N bond dehydrogenation reactions.

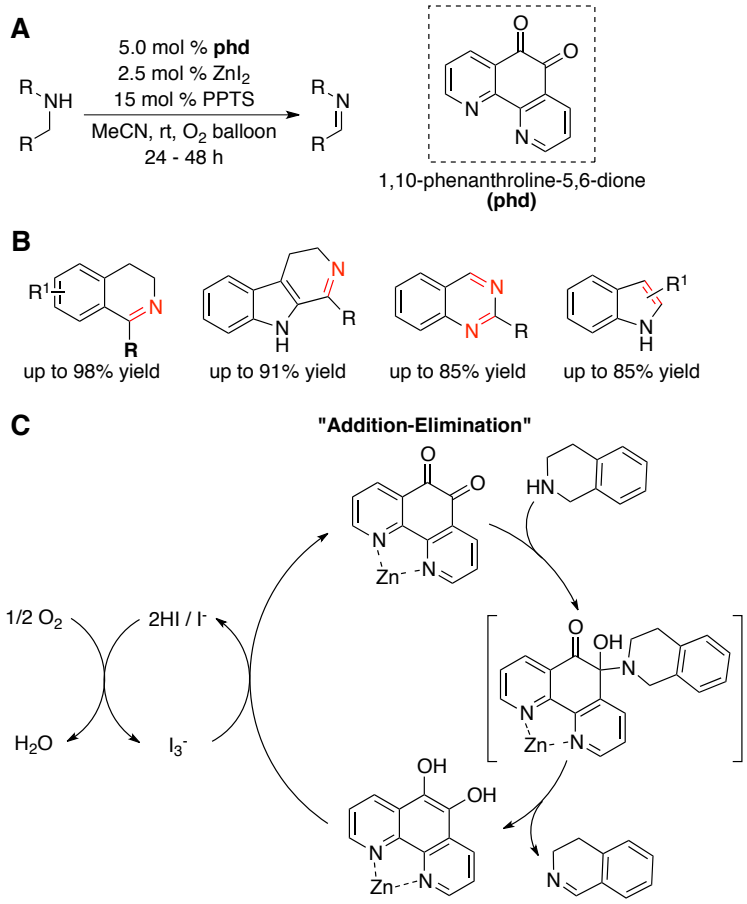

Scheme 1.52. (A) Aerobic phd-catalyzed oxidation of (B) a variety of secondary amines, and (C) proposed mechanism.

Subsequent work by Wendlandt and Stahl focused on leveraging catalyst system modularity to develop improved reaction conditions. Stahl examined the influence of transition metal/Lewis acid promoter on the reaction of 1,2,3,4-tetrahydroquinoline to quinoline. Homoleptic $Fe(phd)_3^{2+}$ and $Ru(phd)_3^{2+}$ complexes promoted enhanced reaction rate compared to the Zn^{2+}-promoted reaction, with Ru^{2+} affording the best results (Scheme 1.53, black versus blue trace). Changing the co-catalyst from I^-/I_3^- to Co(salophen) resulted in a marked improvement in reaction rate as well (Scheme 1.53, blue versus red trace), and allowed the reaction to be carried out using ambient air in place of an O_2 balloon. A broad range of quinoline products can be obtained using the optimized reactions conditions of 2.5 mol % $Ru(phd)_3(PF_6)_2$ and 5 mol % Co(salophen) in

MeCN under ambient air. Using these second generation conditions previously sluggish substrates can be obtained in good yields and with improved reaction rates.[135]

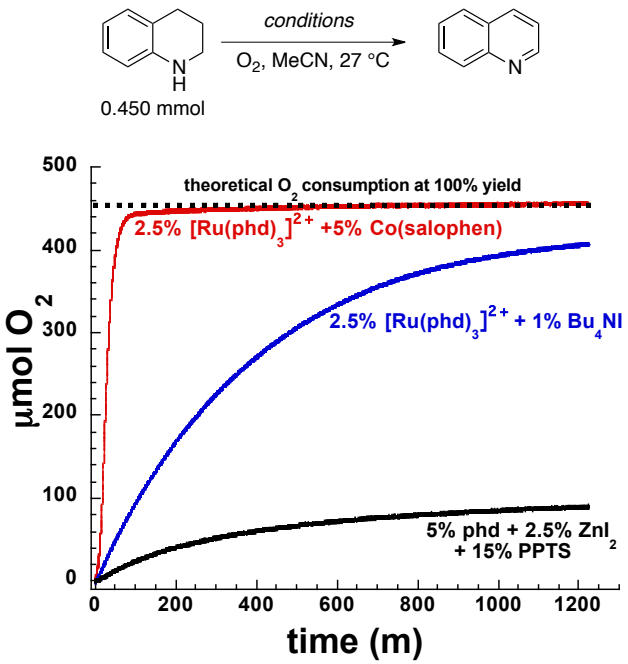

Scheme 1.53. Influence of different Lewis acid promoters and co-catalysts on the quinone-catalyzed aerobic dehydrogenation of tetrahydroquinoline to quinoline.

Finally, PQQ and related phenanthroline-derived quinones, including phd and metal-phd coordination complexes have seen extensive application in the aerobic and electrochemical oxidation of NADH to NAD+. [136 137] While thermodynamic potential of NADH is quite low (E° = -0.320 V NHE), uncatalyzed electrochemical NADH oxidation requires >1.0 V overpotential. Using quinone catalysts such as phd and related complexes, the catalytic oxidation takes place at ~0.25 NHE, reducing overpotential by ~0.5 V. Applications have included aerobic and electrochemical NADH regeneration for synthetic enzymatic transformations,[138] as well as in applications as biosensors.[139,140]

1.5 Summary and Outlook

This review has summarized the development of quinone-catalyzed oxidations of organic substrates, identifying two complementary approaches. On one hand we highlighted high potential quinones, such as DDQ and chloranil, which have traditionally been employed as stoichiometric reagents. These reagents are typically thought to operate via hydride-abstraction mechanisms, and consequently typically only react with electron rich substrates. Through the contributions of a number of different researchers new methodologies have been developed which enable these reagents to be used catalytically. These findings may have important implications for the development of DDQ-mediated transformations on scale.

On the other hand, we discussed the development of biomimetic *o*-quinone catalysts for C-N bond dehydrogenations. This family of quinones has been adapted from biological origins to electrochemical and aerobic oxidation reactions of synthetic value. Mechanistic studies have found that these quinones engage in electrophilic reaction pathways such as transamination and addition-elimination mechanisms. While these reagents have significantly lower thermodynamic potential than DDQ or chloranil, we highlight several cases in which they are kinetically more efficient oxidants.

By organizing this review in this way, we are able to contrast the types of reactions carried out using each class of reagent. Several important observations arise from this comparison, notably the importance of catalyst control over reaction mechanism – and consequently reaction scope. In the case of DDQ and chloranil, reactivity differences observed in the dehydrogenation of steroidal ketones (cf Scheme 1.13) have been justified on the basis of the differential electrochemical potential of the two reagents. However, a systematic examination of halogenated quinones by Mayr and coworkers suggests that structure/activity relationship in high-potential

quinones may be more complicated than just electrochemical potential.[49] This observation is more conspicuous in the case of bioinspired quinones. For example, phenanthroline-derived quinones, didecarboxy-PQQ have similar electrochemical potentials, however the former oxidize secondary and tertiary amines, while the latter only reacts with primary amines. Further, substantial differences in reaction scope arise from quinones which react via addition-elimination, rather than transamination reaction mechanisms, however the structural features which control the bifurcation between these two mechanisms remain to be elucidated.

These observations emphasize the importance of continued development of novel quinone catalysts, and the potential for the development of novel synthetic methodologies using such reagents.

1.6 References and Notes

1. For selected reviews on transition metal catalyzed oxidative transformations published in the last 5 years, see: T. W. Lyons, M. S. Sanford, *Chem. Rev.* **2010**, *110*, 1147-1169. J.-Q. Yu, R. Giri, X. Chen, *Org. Biomol. Chem.* **2006**, *4*, 4041-4047. S. E. Allen, R. R. Walvoord, R. Padilla-Salinas, M. C. Kozlowski, *Chem. Rev.* **2013**, *113*, 6234-6458. T. Punniyamurthy, L. Rout, *Coord. Chem. Rev.* **2008**, *252*, 134-154. G. Dyker, *Angew. Chem. Int. Ed.* **1999**, *38*, 1698-1712. T. Punniyamurthy, S. Velusamy, J. Iqbal, *Chem. Rev.* **2005**, *105*, 2329-2364.
2. For selected reviews on the applications of nitroxyl radicals with and without metal co-catalysts, see: a) A. E. J. d. Nooy, A. C. Besemer, H. v. Bekkum, *Synthesis* **1996**, *1996*, 1153-1176. b) Q. Cao, L. M. Dornan, L. Rogan, N. L. Hughes, M. J. Muldoon, *Chem. Commun.* **2014**, *50*, 4524-4543. c) S. Wertz, A. Studer, *Green Chemistry* **2013**, *15*, 3116-3134. d) L. Tebben, A. Studer, *Angew. Chem. Int. Ed.* **2011**, *50*, 5034-5068. e) R. A. Sheldon, I. W. C. E. Arends, *J. Mol. Cat. A: Chem.* **2006**, *251*, 200-214. f) R. A. Sheldon, I. W. C. E. Arends, *Adv. Synth. Catal.* **2004**, *346*, 1051-1071. g) R. Ciriminna, M. Pagliaro, *Org. Proc. Res. Dev.* **2010**, *14*, 245-251. h) J. M. Bobbitt, C. Brückner, N. Merbouh, *Org. React.* **2009**, *74,* 106–132. i) B. L. Ryland, S. S. Stahl, *Angew. Chem. Int. Ed.* **2014**, *53*, 8824-8838. j) Miles, K. C.; Stahl, S. S. *Aldrichimica Acta* **2015**, *48*, 8-10.
3. For reviews focusing on synthetic applications of *N*-hydroxyphthalimide (NHPI)/Phthalimide N-oxyl (PINO), see: a) F. Recupero, C. Punta, *Chem. Rev.* **2007**, *107*, 3800-3842. b) L. Melone, C. Punta, *Beilstein J. Org. Chem.* **2013**, *9*, 1296-1310. c) C. Galli, P. Gentili, O. Lanzalunga, *Angew. Chem. Int. Ed.* **2008**, *47*, 4790-4796. d) S.

Coseri, *Catalysis Reviews* **2009**, *51*, 218-292. d) Y. Ishii, S. Sakaguchi, *Catal. Today* **2006**, *117*, 105-113. e) Y. Ishii, S. Sakaguchi, T. Iwahama, *Adv. Synth. Catal.* **2001**, *343*, 393-427.

4. a) R. Ciriminna, M. Pagliaro, *Org. Process Res. Dev.* **2010**, *14*, 245-251. b) T. Iwahama, K. Syojyo, S. Sakaguchi, Y. Ishii, *Org. Process Res. Dev.* **1998**, *2*, 255-260. c) Y. Ishii, Y. Kajikawa, US Patent 7,015,356 (Daicel Chem. Ind), issued Mar 21, 2006.

5. a) G. Goor, J. Glenneberg, S. Jacobi. (2012) Hydrogen Peroxide, in *Ullmann's Encyclopedia of Industrial Chemistry*. Wiley-VCH Verlag GmbH & Co. KGaA, Weinheim. b) W. Eul, A. Moeller, N. Steiner. (2000) Hydrogen Peroxide, in *Kirk-Othmer Encyclopedia of Chemical Technology*. (eds Seidel, A., Bickford, M.) John Wiley & Sons, Inc. c) *Applications of Hydrogen Peroxide and Derivatives* (Eds.: C. W. Jones, J. H. Clark), The Royal Society of Chemistry, **1999**.

6. a) J. E. Bäckvall, A. K. Awasthi, Z. D. Renko, *J. Am. Chem. Soc.* **1987**, *109*, 4750-4752. b) Bäckvall, *J. Am. Chem. Soc.* **1990**, *112*, 5160-5166.

7. a) J. E. Bäckvall, A. K. Awasthi, Z. D. Renko, *J. Am. Chem. Soc.* **1987**, *109*, 4750-4752. b) J.-E. Bäckvall, R. B. Hopkins, *Tetrahedron Letters* **1988**, *29*, 2885-2888. c) J.-E. Baeckvall, R. B. Hopkins, H. Grennberg, M. Mader, A. K. Awasthi, *J. Am. Chem. Soc.* **1990**, *112*, 5160-5166. d) J.-E. Backvall, R. L. Chowdhury, U. Karlsson, *J. Chem. Soc., Chem. Commun.* **1991**, 473-475. e) T. Yokota, S. Fujibayashi, Y. Nishiyama, S. Sakaguchi, Y. Ishii, *J. Mol. Cat. A: Chem.* **1996**, *114*, 113-122. f) H. Grennberg, K. Bergstad, J.-E. Bäckvall, *J. Mol. Cat. A: Chem.* **1996**, *113*, 355-358. g) K. Bergstad, H. Grennberg, J.-E. Bäckvall, *Organometallics* **1998**, *17*, 45-50. h) J. Wöltinger, J.-E. Bäckvall, Á. Zsigmond, *Chem. – Eur. J.* **1999**, *5*, 1460-1467. i) J. Piera, K. Närhi, J.-E.

Bäckvall, *Angew. Chem. Int. Ed.* **2006**, *45*, 6914-6917. j) C. M. R. Volla, J.-E. Bäckvall, *Angew. Chem. Int. Ed.* **2013**, *52*, 14209-14213.

8. a) G.-Z. Wang, U. Andreasson, J.-E. Backvall, *J. Chem. Soc., Chem. Commun.* **1994**, 1037-1038. b) G. Csjernyik, A. H. Éll, L. Fadini, B. Pugin, J.-E. Bäckvall, *J. Org. Chem.* **2002**, *67*, 1657-1662. c) J. S. M. Samec, A. H. Éll, J.-E. Bäckvall, *Chem. –Eur. J.* **2005**, *11*, 2327-2334.

9. Piera, J.; Bäckvall, J.-E. *Angew. Chem. Int. Ed.* **2008**, *47*, 3506-3523.

10. Photoexcited quinones have unique and underexplored reactivity, a topic recently reviewed here: S. Lerch, L.-N. Unkel, P. Wienefeld, M. Brasholz, *Synlett* **2014**, *25*, 2673-2680.

11. The Chemistry of the Quinonoid Compounds, Wiley-Interscience, New York, 1974 and 1988; Buckle, D. R.; Collier, S. J.; McLaws, M. D. In *Encyclopedia of Reagents for Organic Synthesis*; John Wiley & Sons, Ltd: 2001.

12. D. Walker, J. D. Hiebert, *Chem. Rev.* **1967**, *67*, 153-195.

13. a) Y. Oikawa, T. Yoshioka, O. Yonemitsu, *Tetrahedron Lett.* **1982**, *23*, 885-888. For related transformations, see: b) Y. Oikawa, T. Tanaka, K. Horita, T. Yoshioka, O. Yonemitsu, *Tetrahedron Lett.* **1984**, *25*, 5393-5396. c) M. A. Rahim, S. Matsumura, K. Toshima, *Tetrahedron Lett.* **2005**, *46*, 7307-7309. d) J.-M. Vatèle, *Tetrahedron* **2002**, *58*, 5689-5698. e) G. V. M. Sharma, Rakesh, *Tetrahedron Lett.* **2001**, *42*, 5571-5573. f) J. S. Yadav, S. Chandrasekhar, G. Sumithra, R. Kache, *Tetrahedron Lett.* **1996**, *37*, 6603-6606. g) K. Jarowicki, P. Kocienski, *J. Chem. Soc., Perkin Trans. 1* **2001**, 2109-2135.

14. a) K. Horita, T. Yoshioka, T. Tanaka, Y. Oikawa, O. Yonemitsu, *Tetrahedron* **1986**, *42*, 3021-3028. b) Tanaka, Y. Oikawa, T. Hamada, O. Yonemitsu, *Chem. Pharm. Bull.* **1987**,

35, 2209-2218.

15. a) S. Yamamoto, T. Sakurai, L. Yingjin, Y. Sueishi, *Phys. Chem. Chem. Phys.* **1999**, *1*, 833-837. b) S. Fukuzumi, K. Ohkubo, Y. Tokuda, T. Suenobu, *J. Am. Chem. Soc.* **2000**, *122*, 4286-4294. See also: c) K. M. Zaman, S. Yamamoto, N. Nishimura, J. Maruta, S. Fukuzumi, *J. Am. Chem. Soc.* **1994**, *116*, 12099-12100.

16. Charge transfer complex formation is also supported by theoretical studies. For example: O. R. Luca, T. Wang, S. J. Konezny, V. S. Batista, R. H. Crabtree, *New Journal of Chemistry* **2011**, *35*, 998-999.

17. M. Lemaire, A. Guy, D. Imbert, J.-P. Guette, *J. Chem. Soc., Chem. Commun.* **1986**, 741-742.

18. H. H. Jung, P. E. Floreancig, *Tetrahedron* **2009**, *65*, 10830-10836.

19. For selected mechanistic studies proposing related HAT-based processes, see: a) C. Höfler, C. Rüchardt, *Liebigs Annalen* **1996**, *1996*, 183-188. b) C. Rüchardt, M. Gerst, J. Ebenhoch, *Angew. Chem. Int. Ed.* **1997**, *36*, 1406-1430.

20. B. M. Trost, *J. Am. Chem. Soc.* **1967**, *89*, 1847-1851.

21. Mayr has suggested that in the case of C-H hydride donors reaction occurs are the carbonyl oxygen of DDQ, forming a new O-H bond, while with Sn-H and B-H donors, a new C-H bond is formed by reaction at C5: X. Guo, H. Zipse, H. Mayr, *J. Am. Chem. Soc.* **2014**, *136*, 13863-13873.

22. For representative examples, see: a) K. Peng, F. Chen, X. She, C. Yang, Y. Cui, X. Pan, *Tetrahedron Lett.* **2005**, *46*, 1217-1220. b) J. A. Steenkamp, C. H. L. Mouton, D. Ferreira, *Tetrahedron* **1991**, *47*, 6705-6716. c) K. Mori, K. Koseki, *Tetrahedron* **1988**, *44*, 6013-6020. d) H. D. Becker, A. Bjoerk, E. Adler, *J. Org. Chem.* **1980**, *45*, 1596-1600.

e) A. Ohki, T. Nishiguchi, K. Fukuzumi, *Tetrahedron* **1979**, *35*, 1737-1743. f) D. R. Brown, A. B. Turner, *J. Chem. Soc., Perkin Trans. 2* **1975**, 1307-1309.

23. B. A. McKittrick, B. Ganem, *J. Org. Chem.* **1985**, *50*, 5897-5898.

24. For example: a) B.-P. Ying, B. G. Trogden, D. T. Kohlman, S. X. Liang, Y.-C. Xu, *Organic Letters* **2004**, *6*, 1523-1526. b) Z. Li, H. Li, X. Guo, L. Cao, R. Yu, H. Li, S. Pan, *Organic Letters* **2008**, *10*, 803-805.

25. a) Y. Zhang, C.-J. Li, *J. Am. Chem. Soc.* **2006**, *128*, 4242-4243. See also: b) Y. Zhang, C.-J. Li, *Angew. Chem. Int. Ed.* **2006**, *45*, 1949-1952.

26. a) A. S. K. Tsang, M. H. Todd, *Tetrahedron Letters* **2009**, *50*, 1199-1202. b) A. S. K. Tsang, P. Jensen, J. M. Hook, A. S. K. Hashmi, M. H. Todd, *Pure and Applied Chemistry* **2011**, *83*, 655-665.

27. a) L. Liu, P. E. Floreancig, *Angew. Chem. Int. Ed.* **2010**, *49*, 3069-3072. b) L. Liu, P. E. Floreancig, *Angew. Chem. Int. Ed.* **2010**, *49*, 5894-5897. c) G. Peh, P. E. Floreancig, *Org. Lett.* **2012**, *14*, 5614-5617. d) W. Tu, P. E. Floreancig, *Angew. Chem. Int. Ed.* **2009**, *48*, 4567-4571. e) W. Tu, L. Liu, P. E. Floreancig, *Angew. Chem. Int. Ed.* **2008**, *47*, 4184-4187. f) G. J. Brizgys, H. H. Jung, P. E. Floreancig, *Chem. Sci.* **2012**, *3*, 438-442. g) L. Liu, P. E. Floreancig, *Org. Lett.* **2009**, *11*, 3152-3155. h) Y. Cui, P. E. Floreancig, *Org. Lett.* **2012**, *14*, 1720-1723. i) X. Han, P. E. Floreancig, *Org. Lett.* **2012**, *14*, 3808-3811.

28. See also: B. Yu, T. Jiang, J. Li, Y. Su, X. Pan, X. She, *Org. Lett.* **2009**, *11*, 3442-3445.

29. a) G. Hilt, M. Danz, *Synthesis* **2008**, *2008*, 2257-2263. b) P. P. Fu, R. G. Harvey, *Chem. Rev.* **1978**, *78*, 317-361, and references therein.

30. For representative examples, see: a) D. Pla, A. Marchal, C. A. Olsen, F. Albericio, M. Álvarez, *J. Org. Chem.* **2005**, *70*, 8231-8234. b) T. Ohmura, K. Masuda, I. Takase, M.

Suginome, *J. Am. Chem. Soc.* **2009**, *131*, 16624-16625. c) P. Ploypradith, T. Petchmanee, P. Sahakitpichan, N. D. Litvinas, S. Ruchirawat, *J. Org. Chem.* **2006**, *71*, 9440-9448. d) J. R. Manning, H. M. L. Davies, *J. Am. Chem. Soc.* **2008**, *130*, 8602-8603. e) J. Sun, E.-Y. Xia, L.-L. Zhang, C.-G. Yan, *Eur. J. Org. Chem.* **2009**, *2009*, 5247-5254. f) R. P. Wurz, A. B. Charette, *Org. Lett.* **2005**, *7*, 2313-2316. g) M. Shimizu, A. Takahashi, S. Kawai, *Org. Lett.* **2006**, *8*, 3585-3587. h) P. Haldar, G. Barman, J. K. Ray, *Tetrahedron* **2007**, *63*, 3049-3056. i) E. Bellur, I. Freifeld, P. Langer, *Tetrahedron Lett.* **2005**, *46*, 2185-2187.

31. E. C. Taylor, J. E. Macor, *Tetrahedron Lett.* **1986**, *27*, 431-432.

32. a) E. A. Braude, L. M. Jackman, R. P. Linstead, *J. Chem. Soc.* **1954**, 3548-3563. b) E. A. Braude, L. M. Jackman, R. P. Linstead, *J. Chem. Soc.* **1954**, 3564-3568. c) E. A. Braude, A. G. Brook, R. P. Linstead, *J. Chem. Soc.* **1954**, 3569-3574. d) E. A. Braude, R. P. Linstead, K. R. Wooldridge, *J. Chem. Soc.* **1956**, 3070-3074. e) J. R. Barnard, L. M. Jackman, *J. Chem. Soc.* **1960**, 3110-3115. f) E. A. Braude, L. M. Jackman, R. P. Linstead, J. S. Shannon, *J. Chem. Soc.* **1960**, 3116-3122. g) E. A. Braude, L. M. Jackman, R. P. Linstead, G. Lowe, *J. Chem. Soc.* **1960**, 3133-3138.

33. a) R. Paukstat, M. Brock, A. Heesing, *Chem. Ber.* **1985**, *118*, 2579-2592. c) N. Dost, *Recl. Trav. Chim. Pays-Bas* **1952**, *71*, 857-868. d) P. Müller, D. Joly, *Helv. Chim. Acta* **1983**, *66*, 1110-1118.

34. For mechanistic studies which suggest that direct hydride abstraction is not feasible, see: a) P. Mueller, J. Rocek, *J. Am. Chem. Soc.* **1972**, *94*, 2716-2719. b) F. Stoos, J. Rocek, *J. Am. Chem. Soc.* **1972**, *94*, 2719-2723. c) F. Wurche, W. Sicking, R. Sustmann, F.-G. Klärner, C. Rüchardt, *Chem – Eur. J.* **2004**, *10*, 2707-2721.

35. For similar findings, and applications, see: a) M. Brock, H. Hintze, A. Heesing, *Chem. Ber.* **1986**, *119*, 3727-3736. b) P. Müller, D. Joly, F. Mermoud, *Helv. Chim. Acta* **1984**, *67*, 105-112. c) A. Guy, A. Lemor, D. Imbert, M. Lemaire, *Tetrahedron Lett.* **1989**, *30*, 327-330.

36. E. A. Braude, L. M. Jackman, R. P. Linstead, G. Lowe, *J. Chem. Soc.* **1960**, 3123-3132.

37. For representative examples, see: a) S. Aubry, S. Pellet-Rostaing, M. Lemaire, *Eur. J. Org. Chem.* **2007**, 5212-5225. b) E. Marcantoni, M. Petrini, R. Profeta, *Tetrahedron Lett.* **2004**, *45*, 2133-2136. c) R. E. Lehr, P. L. Kole, K. D. Tschappat, *Tetrahedron Lett.* **1986**, *27*, 1649-1652.

38. Y. Oikawa, O. Yonemitsu, *J. Org. Chem.* **1977**, *42*, 1213-1216.

39. a) E. Marcantoni, M. Petrini, R. Profeta, *Tetrahedron Lett.* **2004**, *45*, 2133-2136. See also: b) K. Tomioka, Y. Kubota, K. Koga, *J. Chem. Soc., Chem. Commun.* **1989**, 1622-1624. c) K. Tomioka, Y. Kubota, K. Koga, *Tetrahedron* **1993**, *49*, 1891-1900.

40. For selected examples, see: a) D. Cheng, W. Bao, *J. Org. Chem.* **2008**, *73*, 6881-6883. b) D. Cheng, W. Bao, *Adv. Synth. Catal.* **2008**, *350*, 1263-1266. c) F. Benfatti, M. G. Capdevila, L. Zoli, E. Benedetto, P. G. Cozzi, *Chem. Commun.* **2009**, 5919-5921. d) Y. Li, W. Bao, *Adv. Synth. Catal.* **2009**, *351*, 865-868. e) J. Jin, Y. Li, Z.-j. Wang, W.-x. Qian, W.-l. Bao, *Eur. J. Org. Chem.* **2010**, *2010*, 1235-1238. f) G. L. V. Damu, J. Jon Paul Selvam, C. Venkata Rao, Y. Venkateswarlu, *Tetrahedron Lett.* **2009**, *50*, 6154-6158. g) D. Ramesh, U. Ramulu, S. Rajaram, P. Prabhakar, Y. Venkateswarlu, *Tetrahedron Lett.* **2010**, *51*, 4898-4903. g) C. Guo, J. Song, S.-W. Luo, L.-Z. Gong, *Angew. Chem. Int. Ed.* **2010**, *49*, 5558-5562.

41. For selected examples, see ref 36 and: a) E. F. Kiefer, F. E. Lutz, *J. Org. Chem.* **1972**, *37*, 1519-1522. b) R. Foster, I. Horman, *J. Chem. Soc. B: Phys. Org.* **1966**, 1049-1053. c) F. E. Lutz, E. F. Kiefer, *J. Chem. Soc. D: Chem, Commun.* **1970**, 1722b-1723. d) M. Lemaire, J. Doussot, euml, A. Guy, *Chemistry Lett.* **1988**, *17*, 1581-1584. e) D. J. Wallace, A. D. Gibb, I. F. Cottrell, D. J. Kennedy, K. M. J. Brands, U. H. Dolling, *Synthesis* **2001**, 1784-1789. f) J. H. P. Utley, G. G. Rozenberg, *J. Appl. Electrochem.* **2003**, *33*, 525-532.

42. V. S. Batista, R. H. Crabtree, S. J. Konezny, O. R. Luca, J. M. Praetorius, *New J. Chem.* **2012**, *36*, 1141-1144.

43. a) A. Bhattacharya, L. M. DiMichele, U. H. Dolling, E. J. J. Grabowski, V. J. Grenda, *J. Org. Chem.* **1989**, *54*, 6118-6120. b) S. Matsuura, M. Iinuma, K. Ishikawa, K. Kagei, *Chem. Pharm. Bull.* **1978**, *26*, 305-306. c) M. E. Jung, Y.-G. Pan, M. W. Rathke, D. F. Sullivan, R. P. Woodbury, *J. Org. Chem.* **1977**, *42*, 3961-3963. d) I. Ryu, S. Murai, Y. Hatayama, N. Sonoda, *Tetrahedron Lett.* **1978**, *19*, 3455-3458. e) T. L. Fevig, R. L. Elliott, D. P. Curran, *J. Am. Chem. Soc.* **1988**, *110*, 5064-5067. f) I. Fleming, I. Paterson, *Synthesis* **1979**, *1979*, 736-738. See related: g) C. H. Heathcock, C. Mahaim, M. F. Schlecht, T. Utawanit, *J. Org. Chem.* **1984**, *49*, 3264-3274.

44. See ref 12a and references therein. For selected examples, see: a) A. B. Turner, H. J. Ringold, *Journal of the Chemical Society C: Organic* **1967**, 1720-1730. b) P. Westerhof, J. Hartog, *Recueil des Travaux Chimiques des Pays-Bas* **1965**, *84*, 918-931. c) J. F. Bagli, P. F. Morand, K. Wiesner, R. Gaudry, *Tetrahedron Lett.* **1964**, *5*, 387-389. d) S. K. Pradhan, H. J. Ringold, *The Journal of Organic Chemistry* **1964**, *29*, 601-604. e) J. A. Edwards, M. C. Calzada, L. C. Ibáñez, M. E. C. Rivera, R. Urquiza, L. Cardona, J. C.

Orr, A. Bowers, *J. Org. Chem.* **1964**, *29*, 3481-3486. e) J. A. Edwards, C. Orr, A. Bowers, *J. Org. Chem.* **1962**, *27*, 3378-3384.

45. D. Burn, D. N. Kirk, V. Petrow, *Proc. Chem. Soc.* **1960**, 14.

46. a) E. J. Agnello, G. D. Laubach, *J. Am. Chem. Soc.* **1960**, *82*, 4293-4299. b) E. J. Agnello, G. D. Laubach, *J. Am. Chem. Soc.* **1957**, *79*, 1257-1258.

47. A. Bhattacharya, L. M. DiMichele, U. H. Dolling, A. W. Douglas, E. J. J. Grabowski, *J. Am. Chem. Soc.* **1988**, *110*, 3318-3319.

48. J. M. Williams, in *The Art of Process Chemistry*, Wiley-VCH Verlag GmbH & Co. KGaA, **2010**, pp. 77-115.

49. X. Guo, H. Mayr, *J. Am. Chem. Soc.* **2014**, *136*, 11499-11512.

50. X. Guo, H. Mayr, *J. Am. Chem. Soc.* **2013**, *135*, 12377-12387.

51. For selected examples involving the use of (super)-stoichiometric DDQ, see: a) A. Merschaert, P. Boquel, J.-P. Van Hoeck, H. Gorissen, A. Borghese, B. Bonnier, A. Mockel, F. Napora, *Org. Process Res. Dev.* **2006**, *10*, 776-783. b) P. K. Sharma, A. Kolchinski, H. A. Shea, J. J. Nair, Y. Gou, L. J. Romanczyk, H. H. Schmitz, *Org. Process Res. Dev.* **2007**, *11*, 422-430. c) S. J. Mickel, G. H. Sedelmeier, D. Niederer, F. Schuerch, M. Seger, K. Schreiner, R. Daeffler, A. Osmani, D. Bixel, O. Loiseleur, J. Cercus, H. Stettler, K. Schaer, R. Gamboni, A. Bach, G.-P. Chen, W. Chen, P. Geng, G. T. Lee, E. Loeser, J. McKenna, F. R. Kinder, K. Konigsberger, K. Prasad, T. M. Ramsey, N. Reel, O. Repič, L. Rogers, W.-C. Shieh, R.-M. Wang, L. Waykole, S. Xue, G. Florence, I. Paterson, *Org. Process Res. Dev.* **2003**, *8*, 113-121.

52. For an example involving the use of stoichiometric chloranil, see: M. Armitage, G. Bret, B. M. Choudary, M. Kingswood, M. Loft, S. Moore, S. Smith, M. W. J. Urquhart, *Org. Process Res. Dev.* **2012**, *16*, 1626-1634.

53. For selected examples of methods for the regeneration of DDQ from $DDQH_2$, see: a) D. Walker, T. D. Waugh, *J. Org. Chem.* **1965**, *30*, 3240-3240. b) M. S. Newman, V. K. Khanna, *Org. Prep. Proc. Int.* **1985**, *17*, 422-423. c) K. H. Kim, G. L. Grunewald, *Org. Prep. Proc. Int.* **1976**, *8*, 141-143. d) J. W. Scott, D. R. Parrish, F. T. Bizzarro, *Org. Prep. Proc. Int.* **1977**, *9*, 91-94.

54. While DDQ decomposes in water, it is stable in aqueous mineral acids: see ref 53a.

55. S. Cacchi, F. La Torre, G. Paolucci, *Synthesis* **1978**, *1978*, 848-849.

56. C. C. Cosner, P. J. Cabrera, K. M. Byrd, A. M. A. Thomas, P. Helquist, *Org. Lett.* **2011**, *13*, 2071-2073.

57. S. Chandrasekhar, G. Sumithra, J. S. Yadav, *Tetrahedron Lett.* **1996**, *37*, 1645-1646.

58. G. V. M. Sharma, B. Lavanya, A. K. Mahalingam, P. R. Krishna, *Tetrahedron Lett.* **2000**, *41*, 10323-10326.

59. L. Liu, P. E. Floreancig, *Org. Lett.* **2010**, *12*, 4686-4689.

60. A. K. Ghosh, X. Cheng, *Org. Lett.* **2011**, *13*, 4108-4111.

61. A. K. Ghosh, X. Cheng, *Tetrahedron Lett.* **2012**, *53*, 2568-2570.

62. H. Yi, Q. Liu, J. Liu, Z. Zeng, Y. Yang, A. Lei, *ChemSusChem* **2012**, *5*, 2143-2146.

63. W. Muramatsu, K. Nakano, C.-J. Li, *Org. Lett.* **2013**, *15*, 3650-3653.

64. W. Muramatsu, K. Nakano, *Org. Lett.* **2014**, *16*, 2042-2045.

65. a) R. Francke, R. D. Little, *Chem. Soc. Rev.* **2014**, *43*, 2492-2521. See also: b) E. Steckhan, *Angew. Chem. Int. Ed.* **1986**, *25*, 683-701. c) E. Steckhan, in *Electrochemistry*

I, Vol. 142 (Ed.: E. Steckhan), Springer Berlin Heidelberg, **1987**, pp. 1-69.

66. U. H. Brinker, M. Tyner III, W. M. Jones, *Synthesis* **1975**, *1975*, 671.

67. The electrochemical oxidation of numerous other hydroquinones to their corresponding quinones have been reported, however, fewer reports of the use of *these quinones* organic synthesis have been communicated. See: F. Bediouri, P.-L. Fabre, J. Devynck, *J. Chem. Soc., Chem. Commun.* **1982**, 290-291.

68. K. Chiba, T. Arakawa, M. Tada, *Chem. Commun.* **1996**, 1763-1764.

69. K. Chiba, T. Arakawa, M. Tada, *J. Chem. Soc., Perkin Trans. 1* **1998**, 2939-2942.

70. J. H. P. Utley, G. G. Rozenberg, *Tetrahedron* **2002**, *58*, 5251-5265.

71. O. R. Luca, T. Wang, S. J. Konezny, V. S. Batista, R. H. Crabtree, *New J. Chem.* **2011**, *35*, 998-999.

72. For selected recent reviews, see: a) S. S. Stahl, *Science* **2005**, *309*, 1824-1826. b) A. E. Wendlandt, A. M. Suess, S. S. Stahl, *Angew. Chem. Int. Ed.* **2011**, *50*, 11062-11087. c) T. Punniyamurthy, S. Velusamy, J. Iqbal, *Chem. Rev.* **2005**, *105*, 2329-2364. d) S. S. Stahl, *Angew. Chem. Int. Ed.* **2004**, *43*, 3400-3420. e) K. M. Gligorich, M. S. Sigman, *Chem. Commun.* **2009**, 3854-3867. f) B. M. Stoltz, *Chem. Lett.* **2004**, *33*, 362-367.

73. For an example proposing the direct aerobic re-oxidation of p-chloranil, see: Y. Fan, Z. An, X. Pan, X. Liu, X. Bao, *Chem. Commun.* **2009**, 7488-7490.

74. For selected examples, see: a) K. Sakata, T. Kikutake, Y. Shigaki, M. Hashimoto, H. Iyehara Ogawa, Y. Kato, *Inorg. Chim. Acta* **1988**, *144*, 1-3. b) T. Sakamoto, H. Yonehara, C. Pac, *J. Org. Chem.* **1997**, *62*, 3194-3199. c) B. Sain, P. S. Murthy, T. Venkateshwar Rao, T. S. R. Prasada Rao, G. C. Joshi, *Tetrahedron Lett.* **1994**, *35*, 5083-5084. d) K. Sakai, T. Tsubomura, K. Matsumoto, *Inorg. Chim. Acta* **1995**, *234*, 157-161.

e) D.-R. Hwang, D.-R. Hwang, C.-Y. Chu, S.-K. Wang, B.-J. Uang, *Synlett* **1999**, *1999*, 77-78. f) S. Fujibayashi, K. Nakayama, Y. Nishiyama, Y. Ishii, *Chemistry Lett*. **1994**, *23*, 1345-1348.

75. For selected examples, see: (a) H. Sakamoto, T. Funabiki, S. Yoshida, K. Tarama, *Bull. Chem. Soc. Jpn*. **1979**, *52*, 2760-2765. (b) S. Tsuruya, S. Yanai, M. Masai, *Inorg. Chem*. **1986**, *25*, 141-146. (c) K. Sakata, T. Kikutake, Y. Shigaki, M. Hashimoto, H. Iyehara Ogawa, Y. Kato, *Inorganica Chimica Acta* **1988**, *144*, 1-3. (d) L. I. Simándi, T. M. Simándi, Z. May, G. Besenyei, *Coord. Chem. Rev*. **2003**, *245*, 85-93.

76. H. Miyamura, M. Shiramizu, R. Matsubara, S. Kobayashi, *Chemistry Lett*. **2008**, *37*, 360-361.

77. H. Miyamura, M. Shiramizu, R. Matsubara, S. Kobayashi, *Angew. Chem. Int. Ed*. **2008**, *47*, 8093-8095.

78. H. Miyamura, K. Maehata, S. Kobayashi, *Chem. Commun*. **2010**, *46*, 8052-8054.

79. R. Neumann, A. M. Khenkin, I. Vigdergauz, *Chem. – Eur. J*. **2000**, *6*, 875-882.

80. a) E. Bosch, R. Rathore, J. K. Kochi, *J. Org. Chem*. **1994**, *59*, 2529-2536. b) R. Rathore, E. Bosch, J. K. Kochi, *Tetrahedron Lett*. **1994**, *35*, 1335-1338.

81. NO/NO_2 redox couples have also been used to promote the aerobic reoxidation of hydroquinones to quinones in Pd-catalyzed oxidation reactions. See: a) Z. An, X. Pan, X. Liu, X. Han, X. Bao, *J. Am. Chem. Soc*. **2006**, *128*, 16028-16029. b) G. Zhang, X. Xie, Y. Wang, X. Wen, Y. Zhao, C. Ding, *Org. Biomol. Chem*. **2013**, *11*, 2947-2950.

82. a) W. Zhang, H. Ma, L. Zhou, Z. Sun, Z. Du, H. Miao, J. Xu, *Molecules* **2008**, *13*, 3236-3245. b) W. Zhang, H. Ma, L. Zhou, H. Miao, J. Xu, *Chin. J. Catal*. **2009**, *30*, 86-88.

83. Z. Shen, J. Dai, J. Xiong, X. He, W. Mo, B. Hu, N. Sun, X. Hu, *Adv. Synth. Catal.* **2011**, *353*, 3031-3038.

84. L. Wang, J. Li, H. Yang, Y. Lv, S. Gao, *J. Org. Chem.* **2011**, *77*, 790-794.

85. Z. Shen, L. Sheng, X. Zhang, W. Mo, B. Hu, N. Sun, X. Hu, *Tetrahedron Letters* **2013**, *54*, 1579-1583.

86. K. Walsh, H. F. Sneddon, C. J. Moody, *Tetrahedron* **2014**, *70*, 7380-7387.

87. D. Cheng, K. Yuan, X. Xu, J. Yan, *Tetrahedron Lett.* **2015**, *56*, 1641-1644.

88. C. S. Lancefield, O. S. Ojo, F. Tran, N. J. Westwood, *Angew. Chem. Int. Ed.* **2015**, *54*, 258-262.

89. a) X. Tong, Y. Sun, Y. Yan, X. Luo, J. Liu, Z. Wu, *J. Mol. Catal. A: Chem.* **2014**, *391*, 1-6. b) C. Qiu, L. Jin, Z. Huang, Z. Tang, A. Lei, Z. Shen, N. Sun, W. Mo, B. Hu, X. Hu, *ChemCatChem* **2012**, *4*, 76-80.

90. K. Alagiri, P. Devadig, K. R. Prabhu, *Chem. – Eur. J.* **2012**, *18*, 5160-5164.

91. a) M. Ravikanth, C. Achim, J. S. Tyhonas, E. Münck, J. S. Lindsey, *J. Porphyrins Phthalocyanines* **1997**, *1*, 385-394. b) J. S. Lindsey, K. A. MacCrum, J. S. Tyhonas, Y. Y. Chuang, *J. Org. Chem.* **1994**, *59*, 579-587. c) S. H. H. Zaidi, R. M. Fico, J. S. Lindsey, *Org. Proc. Res. Dev.* **2006**, *10*, 118-134.

92. C. Anthony, *Biochem J.* **1996**, *320*, 697-711.

93. S. Janes, D. Mu, D. Wemmer, A. Smith, S. Kaur, D. Maltby, A. Burlingame, J. Klinman, *Science* **1990**, *248*, 981-987.

94. S. X. Wang, M. Mure, K. F. Medzihradszky, A. L. Burlingame, D. E. Brown, D. M. Dooley, A. J. Smith, H. M. Kagan, J. P. Klinman, *Science* **1996**, *273*, 1078-1084.

95. W. McIntire, D. Wemmer, A. Chistoserdov, M. Lidstrom, *Science* **1991**, *252*, 817-824.

96. In contrast to CAOs, which are aerobic enzymes in nature, TTQ and PQQ use the enzymes Amicyanin, Heme C, Cytochrome C and Ubiquinone as the terminal electron acceptors for substrate oxidation. a) K. A. Gray, V. L. Davidson, D. B. Knaff, *J. Biol Chem.* **1988**, *263*, 13987-13990. b) L. Chen, R. Durley, F. Mathews, V. Davidson, *Science* **1994**, *264*, 86-90.

97. For an authoritative review on *o*-quinone cofactor self-processing, see: J. P. Klinman, F. Bonnot, *Chemical Reviews* **2014**, *114*, 4343-4365.

98. a) M. Mure, S. A. Mills, J. P. Klinman, *Biochem.* **2002**, *41*, 9269-9278. b) M. Mure, *Acc. Chem. Res.*, **2004**, *37*, 131-139.

99. a) M. Mure, J. P. Klinman, *J. Am. Chem. Soc.* **1995**, *117*, 8698-8706. b) M. Mure, J. P. Klinman, *J. Am. Chem. Soc.* **1995**, *117*, 8707-8718.

100. a) Y. Lee, L. M. Sayre, *J. Am. Chem. Soc.* **1995**, *117*, 3096-3105. b) Y. Lee, L. M. Sayre, *J. Am. Chem. Soc.* **1995**, *117*, 11823-11828. c) K.-Q. Ling, J. Kim, L. M. Sayre, *J. Am. Chem. Soc.* **2001**, *123*, 9606-9611.

101. a) S. Itoh, N. Takada, S. Haranou, T. Ando, M. Komatsu, Y. Ohshiro, S. Fukuzumi, *J. Org. Chem.* **1996**, *61*, 8967-8974. b) S. Itoh, N. Takada, T. Ando, S. Haranou, X. Huang, Y. Uenoyama, Y. Ohshiro, M. Komatsu, S. Fukuzumi, *J. Org. Chem.* **1997**, *62*, 5898-5907. c) S. Itoh, M. Taniguchi, S. Fukuzumi, *Chem. Commun.* **2000**, 329-330. d) S. Itoh, M. Ogino, S. Haranou, T. Terasaka, T. Ando, M. Komatsu, Y. Ohshiro, S. Fukuzumi, K. Kano, *J. Am. Chem. Soc.* **1995**, *117*, 1485-1493.

102. a) Davidson, V. L. In *Advances in Protein Chemistry*; Judith P. Klinman, J. E. D., Ed.; Academic Press: 2001; Vol. Volume 58, p 95. b) C. Anthony, M. Ghosh, C. C. Blake, *Biochem. J.* **1994**, *304*, 665-674.

103. For selected mechanistic studies: a) H. S. Forrest, S. A. Salisbury, C. G. Kilty, *Biochemical and Biophysical Research Communications* **1980**, *97*, 248-251. b) S. Itoh, H. Kawakami, S. Fukuzumi, *Biochem.* **1998**, *37*, 6562-6571. c) J. Frank, S. H. van Krimpen, P. E. J. Verwiel, J. A. Jongejan, A. C. Mulder, J. A. Duine, *Eur. J. Biochem.* **1989**, *184*, 187-195. For computational studies: d) Y.-J. Zheng, T. C. Bruice, *Proc. Natl. Acad. Sci.* **1997**, *94*, 11881-11886. e) J. Andres, V. Moliner, L. R. Domingo, M. T. Picher, J. Krechl, *J. Am. Chem. Soc.* **1995**, *117*, 8807-8815. f) J. Andres, V. Moliner, J. Krechl, *Bioorg. Chem.* **1994**, *22*, 58-71. g) Oubrie, A. *Biochim. Biophys. Acta - Proteins and Proteomics* **2003**, *1647*, 143.

104. a) S. Itoh, H. Kawakami, S. Fukuzumi, *J. Am. Chem. Soc.* **1997**, *119*, 439-440. See also: b) S. Itoh, H. Kawakami, S. Fukuzumi, *Biochem.* **1998**, *37*, 6562-6571.

105. K. Sasaki, T. Kashimura, M. Ohura, Y. Ohsaki, N. Ohta, *J. Electrochem. Soc.* **1990**, *137*, 2437-2443.

106. S. Itoh, M. Mure, Y. Ohshiro, *J. Chem. Soc., Chem. Commun.* **1987**, 1580-1581.

107. J. A. Duine, J. Frank Jzn, P. E. J. Verwiel, *Eur. J. Biochem.* **1980**, *108*, 187-192.

108. Prior to the discovery of Topaquinone it was thought that PQQ was the cofactor associated with the copper amine oxidase family of enzymes. Accordingly PQQ was studied in the context of amine oxidation as well as for alcohol oxidation.

109. R. H. Dekker, J. A. Duine, J. Frank, J. P. E. J. Verwiel, J. Westerling, *Eur. J. Biochem.* **1982**, *125*, 69-73.

110. P. R. Sleath, J. B. Noar, G. A. Eberlein, T. C. Bruice, *J. Am. Chem. Soc.* **1985**, *107*, 3328-3338.

111. T. S. Eckert, T. C. Bruice, J. A. Gainor, S. M. Weinreb, *Proc. Natl. Acad. Sci.* **1982**, *79*, 2533-2536.

112. T. S. Eckert, T. C. Bruice, *J. Am. Chem. Soc.* **1983**, *105*, 4431-4441.

113. a) P. R. Sleath, J. B. Noar, G. A. Eberlein, T. C. Bruice, *J. Am. Chem. Soc.* **1985**, *107*, 3328-3338. b) E. J. Rodriguez, T. C. Bruice, *J. Am. Chem. Soc.* **1989**, *111*, 7947-7956.

114. a) S. Itoh, Y. Kitamura, Y. Ohshiro, T. Agawa, *Bull. Chem. Soc. Jpn.* **1986**, *59*, 1907-1910. b) Y. Ohshiro, S. Itoh, *Bioorg. Chem.* **1991**, *19*, 169-189.

115. For additional examples, see refs 100b, 113b, and 114b.

116. M. Largeron, M.-B. Fleury, *Science* **2013**, *339*, 43-44.

117. E. J. Corey, K. Achiwa, *J. Am. Chem. Soc.* **1969**, *91*, 1429-1432.

118. Similar benzoxazole adducts have been observed as decomposition products in enzymatic systems: Y. Lee, E. Shepard, J. Smith, D. M. Dooley, L. M. Sayre, *Biochem.* **2000**, *40*, 822-829.

119. M. J. Wanner, G.-J. Koomen, *J. Org. Chem.* **1996**, *61*, 5581-5586.

120. R. F. X. Klein, L. M. Bargas, V. Horak, *J. Org. Chem.* **1988**, *53*, 5994-5998.

121. Y. Ohshiro, S. Itoh, K. Kurokawa, J. Kato, T. Hirao, T. Agawa, *Tetrahedron Lett.* **1983**, *24*, 3465-3468.

122. S. Itoh, N. Kato, Y. Ohshiro, T. Agawa, *Tetrahedron Lett.* **1984**, *25*, 4753-4756.

123. M. Mure, A. Suzuki, S. Itoh, Y. Ohshiro, *J. Chem. Soc., Chem. Commun.* **1990**, 1608-1611.

124. S. Itoh, N. Kato, Y. Ohshiro, T. Agawa, *Chem. Lett.* **1985**, *14*, 135-136.

125. a) M. Largeron, M.-B. Fleury, *J Org. Chem.* **2000**, *65*, 8874-8881. b) M. Largeron, A. Neudorffer, M.-B. Fleury, *Angew. Chem. Int. Ed.* **2003**, *42*, 1026-1029. c) M. Largeron,

A. Chiaroni, M.-B. Fleury, *Chem. – Eur. J.* **2008**, *14*, 996-1003. d) M. Largeron, M.-B. Fleury, M. Strolin Benedetti, *Org. Biomol. Chem.* **2010**, *8*, 3796-3800.

126. a) M. Largeron, M.-B. Fleury, *Org. Lett.* **2009**, *11*, 883-886. b) M. Largeron, *Electrochimica Acta* **2009**, *54*, 5109-5115.

127. M. Largeron, M.-B. Fleury, *Angew. Chem. Int. Ed.* **2012**, *51*, 5409-5412.

128. A. E. Wendlandt, S. S. Stahl, *Org. Lett.* **2012**, *14*, 2850-2853.

129. K. Yamamoto, in *Encyclopedia of Reagents for Organic Synthesis*, John Wiley & Sons, Ltd, **2001**.

130. Y. Qin, L. Zhang, J. Lv, S. Luo, J.-P. Cheng, *Org. Lett.* **2015**, *17*, 1469-1472.

131. a) Y. Lee, H. Huang, L. M. Sayre, *J. Am. Chem. Soc.* **1996**, *118*, 7241-7242. b) Y. Lee, K.-Q. Ling, X. Lu, R. B. Silverman, E. M. Shepard, D. M. Dooley, L. M. Sayre, *J. Am. Chem. Soc.* **2002**, *124*, 12135-12143. c) Y. Zhang, C. Ran, G. Zhou, L. M. Sayre, *Bioorg. Med. Chem.* **2007**, *15*, 1868-1877. See also ref 112.

132. a) H. Yuan, W.-J. Yoo, H. Miyamura, S. Kobayashi, *J. Am. Chem. Soc.* **2012**, *134*, 13970-13973. b) H. Yuan, W.-J. Yoo, H. Miyamura, S. Kobayashi, *Adv. Synth. Catal.* **2012**, *354*, 2899-2904.

133. D. V. Jawale, E. Gravel, N. Shah, V. Dauvois, H. Li, I. N. N. Namboothiri, E. Doris, *Chem – Eur. J.* **2015**, *21*, 7039-7042.

134. A. E. Wendlandt, S. S. Stahl, *J. Am. Chem. Soc.* **2014**, *136*, 506-512.

135. A. E. Wendlandt, S. S. Stahl, *J. Am. Chem. Soc.* **2014**, *136*, 11910-11913.

136. For selected reports of NADH oxidation, see: a) C. A. Goss, H. D. Abruna, *Inorg. Chem.* **1985**, *24*, 4263-4267. b) Q. Wu, M. Maskus, F. Pariente, F. Tobalina, V. M. Fernández, E. Lorenzo, H. D. Abruña, *Anal. Chem.* **1996**, *68*, 3688-3696. c) G. Hilt, T. Jarbawi, W.

R. Heineman, E. Steckhan, *Chem. – Eur. J.* **1997**, *3*, 79-88. d) A. Pinczewska, M. Sosna, S. Bloodworth, J. D. Kilburn, P. N. Bartlett, *J. Am. Chem. Soc.* **2012**, *134*, 18022-18033. e) K. Yokoyama, Y. Ueda, N. Nakamura, H. Ohno, *Chemistry Lett.* **2005**, *34*, 1282-1283. f) I. Catalin Popescu, E. Domínguez, A. Narváez, V. Pavlov, I. Katakis, *J. Electroanal. Chem.* **1999**, *464*, 208-214.

137. *O*-quinones as a class have been recognized as particularly effective for electrocatalytic NADH oxidation. For examples, see: a) D. C.-S. Tse, T. Kuwana, *Anal. Chem.* **1978**, *50*, 1315-1318. b) H. Jaegfeldt, T. Kuwana, G. Johansson, *J. Am. Chem. Soc.* **1983**, *105*, 1805-1814. c) H. Jaegfeldt, A. B. C. Torstensson, L. G. O. Gorton, G. Johansson, *Anal. Chem.* **1981**, *53*, 1979-1982. d) H. Huck, H.-L. Schmidt, *Angew. Chem. Int. Ed.* **1981**, *20*, 402-403.

138. For selected examples, see: a) S. Itoh, M. Kinugawa, N. Mita, Y. Ohshiro, *J. Chem. Soc., Chem. Commun.* **1989**, 694-695. b) N. Rivera, Y. Colón, A. R. Guadalupe, *Bioelectrochem. Bioenergetics* **1994**, *34*, 169-175. c) S. Itoh, N. Mita, Y. Ohshiro, *Chemistry Letters* **1990**, *19*, 1949-1952. d) G. Hilt, B. Lewall, G. Montero, J. H. P. Utley, E. Steckhan, *Liebigs Annalen* **1997**, *1997*, 2289-2296. e) G. Hilt, E. Steckhan, *J. Chem. Soc., Chem. Commun.* **1993**, 1706-1707.

139. For a review of biosensors based on NAD(P)-dependent dehydrogenase enzymes: M. J. Lobo, A. J. Miranda, P. Tuñón, *Electroanalysis* **1997**, *9*, 191-202.

140. For selected examples, see: a) M. E. B. Santiago, G. A. Daniel, A. David, B. Casañas, G. Hernández, A. R. Guadalupe, J. L. Colón, *Electroanalysis* **2010**, *22*, 1097-1105. b) M. E. B. Santiago, M. M. Vélez, S. Borrero, A. Díaz, C. A. Casillas, C. Hofmann, A. R. Guadalupe, J. L. Colón, *Electroanalysis* **2006**, *18*, 559-572. c) E. Lorenzo, F. Pariente, L.

Hernàndez, F. Tobalina, M. Darder, Q. Wu, M. Maskus, H. D. Abruña, *Biosensors and Bioelectronics* **1998**, *13*, 319-332. d) F. Tobalina, F. Pariente, L. Hernández, H. D. Abruña, E. Lorenzo, *Analytica Chimica Acta* **1999**, *395*, 17-26. e) M. Hedenmo, A. Narvaez, E. Dominguez, I. Katakis, *Analyst* **1996**, *121*, 1891-1895.

Chapter 2

Chemoselective Organocatalytic Aerobic Oxidation of Primary Amines to Secondary Imines

This work has been published:

Wendlandt, A. E.; Stahl, S. S. *Org. Lett.* **2012**, *14*, 2850-2853.

2.1 Introduction

Imines are valuable synthetic intermediates,[1] and a range of methods for the preparation of secondary imines from primary or secondary amines is known.[2] Typical strategies employ transition-metal catalysts with a stoichiometric oxidant, and these include methods capable of using molecular oxygen as the terminal oxidant.[2a-c,e-h] In biology, copper amine oxidases mediate aerobic oxidation of primary amines to aldehydes using *ortho*-quinone cofactors, such as topaquinone (TPQ) and lysine tyrosylquinone (LTQ).[3] Biochemical studies suggest that copper is required for biosynthesis of the quinone cofactors, but it is not involved in amine oxidation. Indeed, model quinones have been shown to mediate amine oxidase activity *ex vivo* in the absence of metals, using simple amine substrates.[4] The synthetic scope of such reactions has received little attention, however, and, in connection with our broader interest in aerobic oxidation catalysis,[5] we sought to explore this class of reactions. In the present study, we report a highly chemoselective method for aerobic oxidative homo- and heterocoupling of benzylic amines to secondary imines using the TPQ analog, 4-*tert*-butyl-2-hydroxybenzoquinone (TBHBQ) as the catalyst.[6] Like the amine oxidases noted above, the reactions proceed effectively in the absence of Cu or another redox-active co-catalyst.

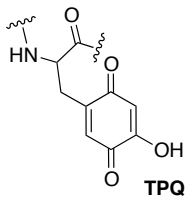

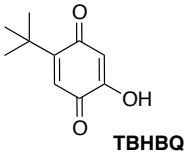

2.2 Results and Discussion

Important precedents to our work include the use of quinones as stoichiometric reagents[7] and catalysts[8] in the oxidation of primary amines to aldehydes and ketones, and as electrocatalysts for

the oxidation of primary amines to secondary imines[9] and amines.[10] And, during preparation of this manuscript, Largeron et al. reported a study very similar to the one presented here using an iminoquinone catalyst in combination with a copper co-catalyst, which facilitates aerobic reoxidation of the quinone.[11]

Building upon the work of Mure and Klinman,[4e,f] we evaluated the oxidation of benzylamine **1a** to *N*-benzylidenebenzylamine **1b** with TBHBQ. Efficient oxidation takes place with 1.5 mol % TBHBQ in a number of solvents, including 1,4-dioxane, THF, DMF, and MeCN (76%, 76%, 76% and 87% yields, respectively) at room temperature under 1 atm O_2. The reactions can be carried out with ambient air as the oxidant, but the reactions are slower. For example, 26% unreacted **1a** was observed after 24 h.

Under the optimized conditions, a range of *ortho- meta-*, and *para*-substituted benzylamines undergo oxidation to their secondary imine dimers under these conditions (Table 2.1). Electon-rich amines, such as *p*-methoxybenzylamine (93%, entry 3) and piperonylamine (91%, entry 12), and some electron-deficient amines, such as *p*-chlorobenzylamine (90%, entry 4) and *p*-fluorobenzylamine (91%, entry 5) are readily converted to the secondary imines in high yields. More electron-deficient benzylamines, such as *p*-trifluoromethylbenzylamine (78%, entry 6) and *m*-chlorobenzylamine (72%, entry 7) oxidize more slowly and require 48 h for complete conversion. The observation that electron-withdrawing substituents react more slowly is evident from an initial-rate study of substrates **1a**–**3a**, **5a**, and **6a**, from which a substantial negative Hammett correlation was determined ($\rho = -1.3$; see Supporting Information).

The free amino group of *p*-aminobenzylamine does not inhibit dimerization; however, the yield is slightly lower than some of the other derivatives (76%, entry 2). As noted above, halogen substituents, including *m*-iodobenzylamine, are well tolerated (entries 4, 5, 7 and 8, respectively).

Sterically bulky groups, such as 1-naphthyl (81%, entry 11) and *ortho* substitution on the aromatic ring (entries 9, 10) cause only a slight diminution in yield. The heterocycle furfurylamine (80%, entry 13) undergoes oxidative dimerization, but 2- and 4-(aminomethyl)-pyridines are not efficient substrates (not shown). The hydrochloride salt of benzylamine does not react, but good reactivity can be recovered upon addition of a Brønsted base, such as Et_3N (entry 14).

Table 2.1. Quinone-catalyzed aerobic oxidation of primary benzylic amines.[a]

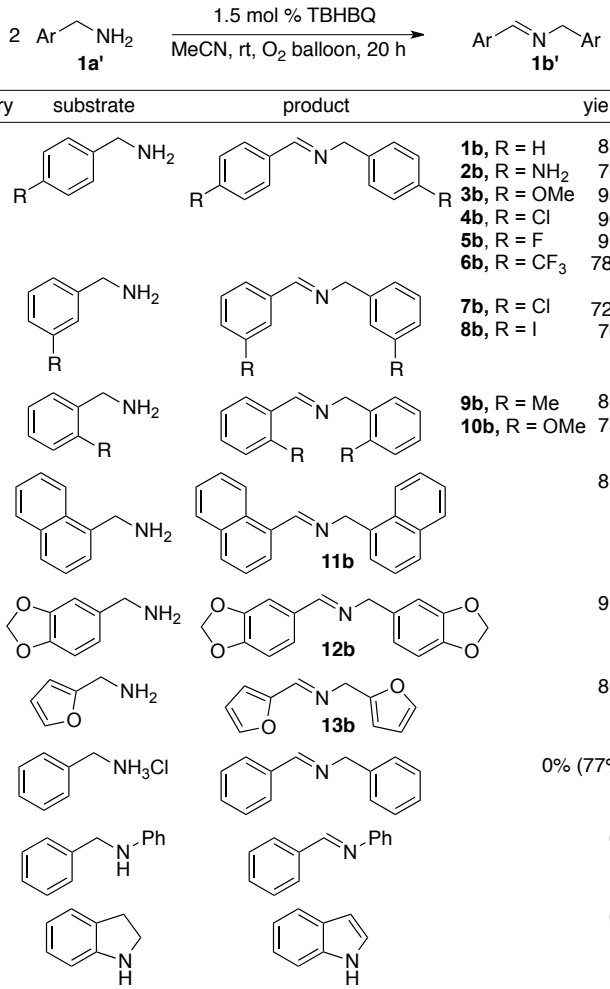

[a] Conditions: amine substrate (1.0 mmol), TBHBQ (0.015 mmol, 1.5 mol %), O_2 balloon, MeCN (3.5 mL), rt, 20 h. [b] Yield determined by ^{1}H NMR spectroscopy versus internal standard. [c] Reaction time was 48 h. [d] Carried out in the presence of 1.0 equiv Et_3N.

Secondary amines, such as *N*-phenylbenzylamine and indoline (Table 2.1, entries 15, 16), and tertiary amines, such as Et_3N and *N*,*N*-dimethybenzylamine (not shown), are not oxidized under the reaction conditions. This selectivity for primary amines is readily explained by the reaction mechanism (Scheme 2.1), which has been elucidated in previous biochemical model studies.[3] Condensation of the primary amine **1a** with TBHBQ leads to the iminoquinone intermediate **14**. Tautomerization of this species to form **15** results in net two-electron oxidation of the amine. Addition of a second equivalent of amine **1a** to imine **15** generates an aminal that can react further to liberate the product **1b** and reduced aminohydroquinone **17**. Aerobic oxidation of **17** generates iminoquinone **18**, which can undergo transimination with substrate **1a** to liberate NH_3 and close the catalytic cycle.

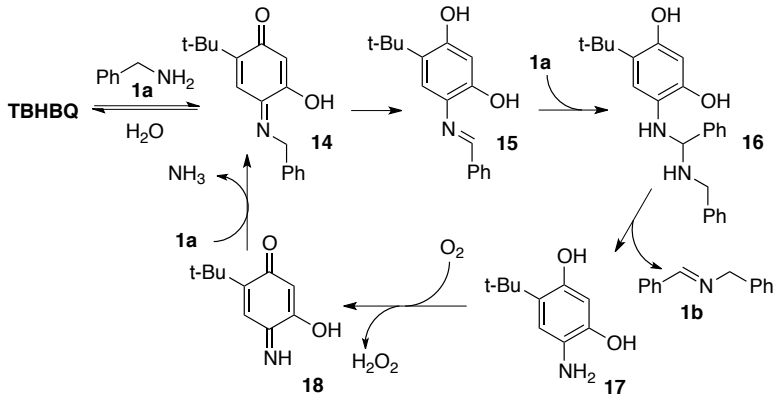

Scheme 2.1. Proposed Mechanism of Quinone-Catalyzed Aerobic Oxidation of Primary Amines

Aliphatic primary amines are not oxidized by TBHBQ under these reactions conditions, probably because this quinone is not sufficiently oxidizing to promote the reaction. The sec-primary amine α-methylbenzylamine is also not oxidized under these mild reaction conditions. In this case, the lack of reactivity must be a steric effect because the α-C–H bond should be weaker than that of the parent benzylamine. Reactivity is observed under more forcing

conditions, using 10 mol % TBHBQ and with 1.0 equiv sodium formate as a Brønsted base in DMF for 48 h, 69% of the imine dimer is obtained (eq 2.1).

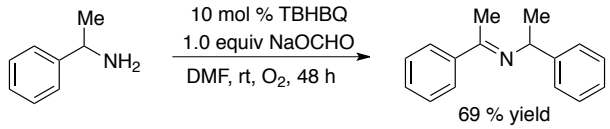

(2.1)

The exquisite selectivity for primary benzylic amines suggested that selective heterocoupling could be achieved by combining a benzylic amine with a less readily oxidized amine. Upon increasing the catalyst loading to 5 mol %, cross-coupled products were formed in very good yields, often with excellent selectivities (Table 2.2). The coupling of benzylamine and α-methylbenzylamine is facile (89%, entry 1), forming *N*-benzylidene-α-methylbenzylamine **19** as the exclusive product. Linear and branched aliphatic amines, such as cyclohexylamine (91%, entry 2), hexylamine (83%, entry 5) and 2-ethylhexylamine (85%, entry 6) are also good substrates for cross-product formation, though in the latter cases small amounts of *N*-benzylidenebenzylamine are also observed.

Primary amines that contain a tertiary amine (92%, entry 4) or primary alcohol (80%, entry 4) undergo effective heterocoupling with benzylamine, with no background oxidation of the tertiary amine or primary alcohol fragment. These observations highlight a potential advantage of the organocatalytic oxidation method described here, as transition-metal catalysts are unlikely to demonstrate comparable chemoselectivity. The sterically hindered tritylamine serves as an effective coupling partner (78%, entry 7), with the product crystallizing out of the reaction mixture. Aniline affords *N*-benzylidene aniline in good yield after 48 h (76%, entry 8), provided a second 5 mol % portion of the catalyst is added after 24 h.

Table 2.2. Quinone-catalyzed aerobic cross-coupling of primary amines.[a]

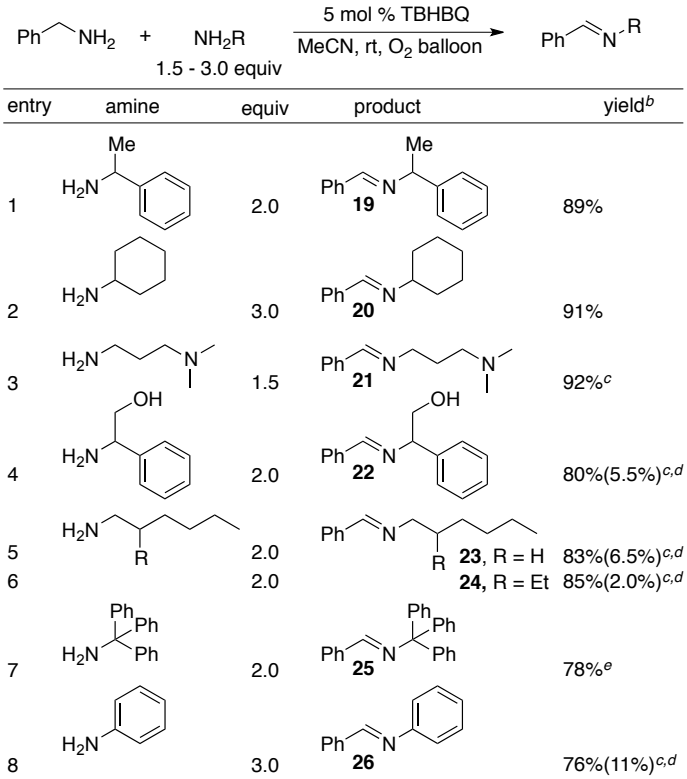

[a] Conditions: benzylamine (1.0 mmol), amine (1.5 – 3.0 mmol), TBHBQ (0.05 mmol), O_2 balloon, MeCN (3.5 mL), rt, 20-48 h. [b] Yield determined by ^{1}H NMR spectroscopy versus internal standard [c] After 24 h an additional aliquot of TBHBQ (5.0 mol %) was added and the reaction was run for a total of 48 h. [d] Number in parentheses indicates yield *N*-benzylidenebenzylamine also obtained.[e] Isolated yield.

In order to explore the origin of the excellent cross-product selectivity, two heterocoupling reactions were monitored by ^{1}H NMR spectroscopy (Figure 2.1). In the reaction of benzylamine with 2.0 equiv of α-methylbenzylamine (Figure 2.1A), the time course reveals parallel formation of homo- and heterocoupled products **1b** and **19** at early stages of the reaction. As the reaction progresses, the homocoupled product **1b** is progressively consumed, and the reaction converges to exclusive formation of **19** at the end of the reaction. A different profile is evident in the reaction of benzylamine and 2.0 equiv of aniline (Figure 2.1B). In this case, the time course

reveals that the homocoupled dimer **1b** is formed exclusively and accumulates in good yield at early stages of the reaction (t < 300 min). This observation is consistent with the tolerance of an aromatic amine in the oxidative homocoupling reactions noted above (cf. Table 2.1, entry 2). At longer reaction times, the homodimer **1b** is slowly converted into the cross-product **26**.

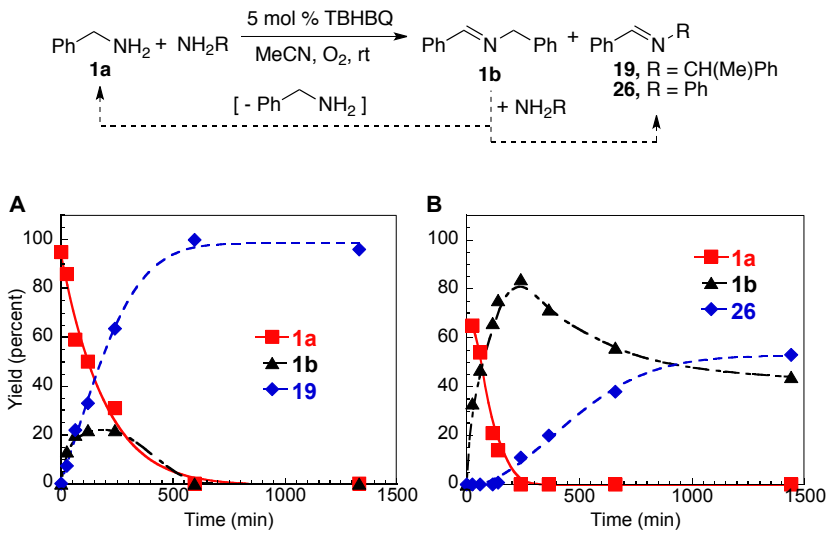

Figure 2.1. A ^{1}H NMR timecourse of the TBHBQ-catalyzed oxidation of (A) benzylamine and methylbenzylamine, and (B) benzylamine and aniline. Reaction conditions: benzylamine (0.28 M), α-methylbenzlamine (0.57 M), TBHBQ (0.014 M), trimethoxybenzene (internal standard, 0.078 M), MeCN-d_3, O_2 balloon, rt.

The cross-coupling results depicted in Figure 2.1 can be rationalized by three considerations: (1) the relative nucleophilicity of the two amines with the catalytic intermediate **15**, (2) equilibrium exchange of the amine substrates with the secondary imine products, and (3) the relative reactivity of the amine substrates toward oxidation.

The parallel formation of **1b** and **19** in Figure 2.1A suggests that benzylamine and α-methylbenzylamine can react with catalytic intermediate **15** to afford the homo- and heterocoupled dimers, respectively. Control experiments show that **1b** and **19** equilibrate readily

under the reaction conditions in the presence of the amine substrates (eq 2.2), and the equilbrium constant (K_{eq} ~ 0.7) shows a slight preference for **1b**. The substantially higher reactivity of benzylamine toward oxidation by TBHBQ (see above), however, causes the equilibrium mixture to be driven toward formation of the hetero-coupled product **19**.

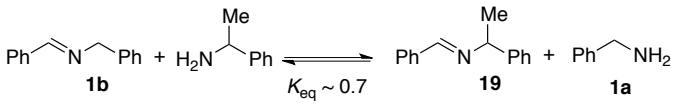

(2.2)

Similar considerations rationalize the reactivity observed with benzylamine and aniline in Figure 1B. Exclusive formation of homodimer **1b** early in the reaction is readily explained by the higher reactivity of benzylamine relative to aniline with imine-hydroquinone intermediate **15**. Formation of *N*-benzylidene aniline **26** at longer reaction times is relatively sluggish. Formation of **26** via condensation of aniline with **1b** is thermodynamically unfavorable (K_{eq} << 1; eq 2.3). Nevertheless, its formation can be driven by continuous oxidation of the benzylamine generated, albeit in small quantities, from this exchange reaction.

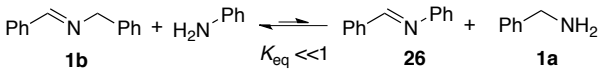

(2.3)

The ability of a dynamic equilibrium mixture of species to converge toward a single product by consumption of one of the species has been termed "self-sorting."[12] With the pair of substrates shown in Figure 2.1A, oxidatively promoted self-sorting overcomes the slight thermodynamic preference of **1b** over **19**, enabling exclusive formation of **19**. With the substrate pair in Figure 1B, the kinetically preferred product may be obtained in good yield at short reaction times, or oxidative self-sorting can be exploited to obtain the otherwise strongly disfavored product. This

oxidative strategy to achieve imine self-sorting is complementary to other approaches being pursued in the field of dynamic covalent chemistry[13-15] (e.g., through the use of templates) to promote selective product formation within an equilibrating mixture.

In summary, we have identified a highly chemoselective method for the aerobic oxidative coupling of primary benzylic amines to afford secondary imines, and dynamic self-sorting of the imine products enables selective formation of heterocoupled imines. The mild reaction conditions, the functional group compatibility, the use of O_2 as the oxidant, and the low catalyst loadings compare favorably with previously reported metal-catalyzed methods.

2.3 Acknowledgment

We thank the U.S. Department of Energy (DE-FG02-05ER15690) for financial support of this work. Analytical instrumentation was partially funded by the NSF (CHE-9208463, CHE-0342998, CHE-9629688, CHE-9974839).

2.4 Experimental Details and Supporting Information

2.4.1. General Considerations

All commercially available compounds were purchased from Sigma-Aldrich, and used as received unless otherwise indicated. Solvents were dried over alumina columns prior to use. ^{1}H and ^{13}C NMR spectra were recorded on Bruker AC-300 MHz or Varian Mercury-300 MHz spectrometers. Chemical shift values are given in parts per million relative to residual solvent peaks or TMS internal standard. High-resolution, exact mass measurements were obtained by the mass spectrometry facility at the University of Wisconsin. Melting points were taken on a Mel-Temp II melting point apparatus. Flash chromatography was performed using SilicaFlash® P60 (Silicycle, particle size 40-63 μm, 230-400 mesh) from Sigma Aldrich.

2.4.2. Synthesis of TBHBQ

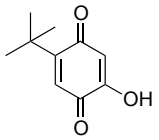

4-tert-butyl-2-hydroxy-p-benzoquinone, **TBHBQ**

The quinone catalyst, TBHBQ, was prepared in two steps from commercially available resorcinol. Resorcinol was alkylated to 4-*tert*-butylresorcinol according to the method of Sayre.[16] 4-*tert*-butylresorcinol was converted to TBHBQ according to the method of Klinman,[4e] with the following additional detail.

Without further purification, 4-*tert*-butylresorcinol (2.0 g, 12 mmol) was dissolved in a solution of water (30 mL) containing K_2HPO_4 (2.1 g, 9.2 mmol). This mixture was added over the course of 5 min to a solution of water (240 mL) containing K_2HPO_4 (2.1 g, 9.2 mmol) and Fremy's salt

(8.0 g, 30 mmol) at room temperature. The purple solution of Fremy's salt turns dark red upon addition of the *t*-butylresorcinol, and is stirred at rt for an additional 5 min. Concentrated sulfuric acid (3 M) is added dropwise (to quench any remaining Fremy's salt) until a yellow suspension appears and the yellow color of the solution persists. The aqueous mixture is then extracted into Et_2O, dried over $MgSO_4$, and concentrated to give dark yellow solids. TBHBQ can be dissolved in hot cyclohexanes, and separated from a red-brown residue. Concentration of the cyclohexanes (or recrystallization) affords pure TBHBQ as a yellow solid (1.45 g, 67% yield). We recommend storing TBHBQ in the dark, as slow discoloration (to red/brown) is observed when the catalyst is left exposed to ambient light for prolonged periods. Control experiments carried out in both the light and the dark have confirmed that catalyst efficiency and stability is not influenced by running amine oxidation reactions in the light. TBHBQ can be stored on the bench for long periods if protected from the light. Characterization data matched those previously reported.[2] ^{1}H NMR (300 MHz, $CDCl_3$) δ 6.97 (br s, 1H), 6.62 (s, 1H), 6.03 (s, 1H), 1.29 (s, 9H); ^{13}C NMR (75 MHz, $CDCl_3$) δ 188.06, 184.58, 159.80, 153.61, 127.48, 110.25, 36.04, 29.71; EMM (ESI) Calc for $C_{10}H_{12}O_3$ (M+H): 180.0781, found 180.0778.

Fremy's salt can be prepared from $NaNO_2$ according to the procedure of Cram.[17] However authentic material was highly unstable in our hands and could not be dried and stored without decomposition. We found that the most reliable results were obtained by using commercially obtained (Sigma Aldrich) Fremy's salt, which can be stored for long periods without apparent deleterious effect.

2.4.3. Procedures for Amine Oxidation

Typical procedure for the oxidation of homo-coupled amines is as follows. A flame-dried 25 mL flask was flushed with O_2 and equipped with an O_2 balloon. Benzylamine (110 uL, 1.0 mmol) was added to the flask followed by a solution of TBHBQ (2.7 mg, 0.015 mmol) in anhydrous MeCN (3.5 mL). The yellow solution immediately became intensely red, which faded to a lighter orange color over the first 20 min of the reaction. The reaction was stirred at room temperature for 20 h or until TLC indicated completion. (At this point internal standard was added, for yield determination). The reaction mixture was then concentrated by rotary evaporation. In cases where purification was necessary, the reaction crude was plugged though a pipette containing Et_3N-washed silica gel using hexanes or 1:10 EtOAc/Hexanes.

Typical procedure for the oxidation of cross-coupled amines is as follows. A flame-dried 25 mL flask was flushed with O_2 and equipped with an O_2 balloon. Benzylamine (110 uL, 1.0 mmol) and methylbenzylamine (260 uL, 2.0 mmol) was added to the flask followed by a solution of TBHBQ (9.0 mg, 0.05 mmol) in anhydrous MeCN (3.5 mL). The yellow solution immediately became intensely red, which either faded or persisted during the course of the reaction depending on the substrates. The reaction was stirred at room temperature for 24 h, at which point the reaction was either concentrated as above, or a second aliquot (9.0 mg, 0.05 mmol) or TBHBQ was added to the reaction mixture and the reaction allowed to stir for an additional 24 h. In cases where purification was necessary, the reaction crude could be (A) plugged though a pipette containing Et_3N-washed silica gel using hexanes or EtOAc/Hexanes, (B) rapidly chromatographed by Et_3N-washed silica column, or (C) purified by preparative TLC on plates which had been previously run with Hexanes/Et_3N.

Procedure for the oxidation of methylbenzylamine to N-(1-phenylethyl-1-phenylethanimine):

A flame-dried 25 mL flask was flushed with O_2 and equipped with an O_2 balloon. NaOCHO (65 mg, 1.0 mmol) and TBHBQ (18.0 mg, 0.10 mmol) were dissolved in anhydrous DMF (0.5 mL). Methylbenzylamine was added (130 uL, 1.0 mmol) and the reaction was stirred at RT for 48 h. DMF was removed by vacuum and the material re-suspended in chloroform and the precipitates were removed by filtration. The crude filtrate was concentrated, suspended in chloroform, and pushed through a short pipette containing Et_3N-washed Silica gel using 1:10 EtOAc/Hexanes to give *N*-(1-phenylethyl-1-phenylethanimine) in high purity; characterization data matched those previously reported.[18]

2.4.4. Hammett Correlation Studies

Gas Uptake Kinetic Studies:

A standard procedure was as follows: A series of volume-calibrated 25mL round bottom flasks equipped with stirbars were attached to a gas-uptake apparatus. The flasks were alternately evacuated and then re-filled with O_2 (to 500 Torr) 5 times, and then final pressure was set to 550 Torr. A solution of amine in MeCN (0.3 M, 1.0 mmol, 3.25 mL) was added by syringe into each flask, and the pressure was allowed to equilibrate at 27 °C for 3-4 h. The reactions were initiated by the addition of TBHBQ in MeCN (0.015 mmol, 0.25 mL), and the instantaneous pressure of each flask was collected using a LabVIEW software program for 16 h. Initial rates were measured in Excel.

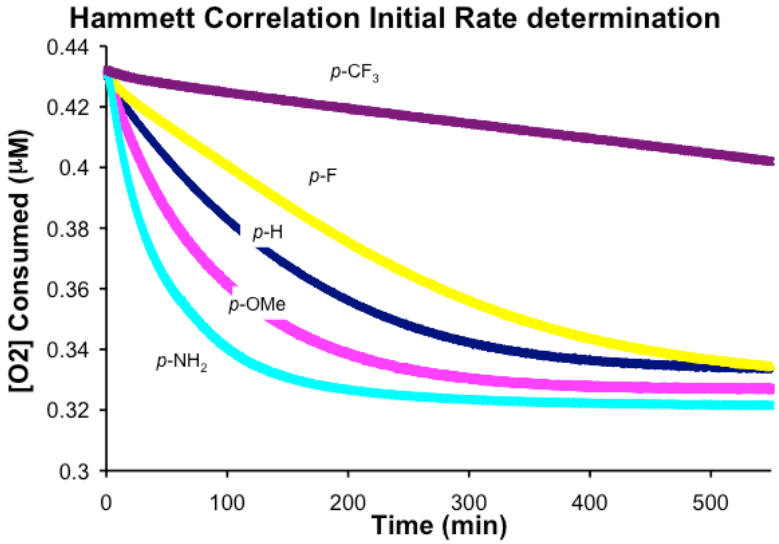

Figure 2.2. Measurement of O_2 consumption in the oxidation of electronically substituted benzylic amines by TBHBQ.

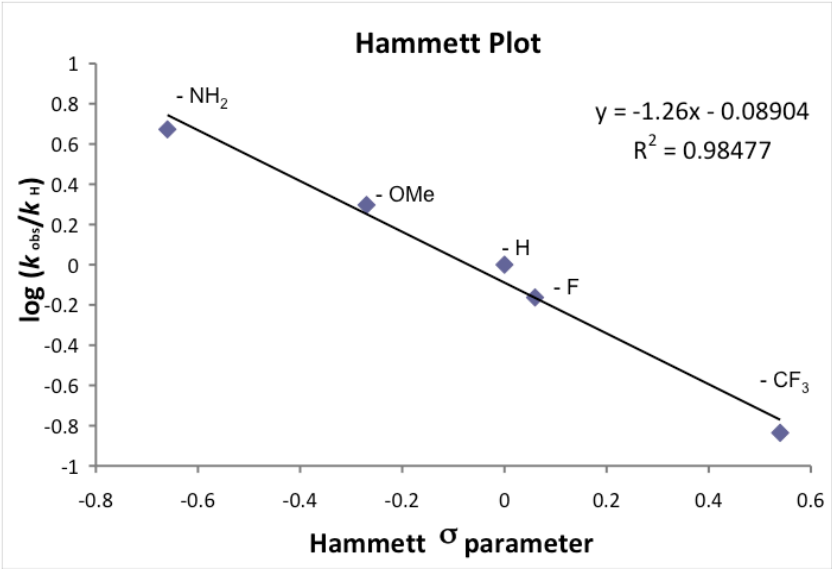

Figure 2.3. Linear free energy relationship (Hammett Plot) between the initial rates of oxidation of electronically substituted benzylic amines by TBHBQ versus Hammett sigma parameter.

2.4.5. Synthesis and Characterization of Homo-coupled imine products

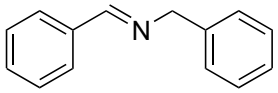

N-benzylidenebenzylamine, **1b**

Spectroscopic data match those previously reported.[19] ^{1}H NMR (300 MHz, $CDCl_3$) δ 8.37 (s, 1H), 7.78 (m, 2H), 7.21-7.41 (m, 8H), 4.81 (s, 2H); ^{13}C NMR (75 MHz, $CDCl_3$) δ 162.21, 139.56, 136.42, 131.00, 128.83, 128.73, 128.52, 128.22, 127.22, 65.29; EMM (ESI) Calc for $C_{14}H_{13}N$ (M+H): 196.1121, found 196.1111.

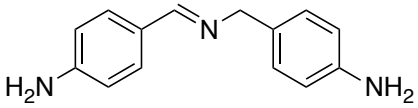

N-(4-aminobenzylidene)-4-aminobenzylamine, **2b**

Isolated as a white solid mp: 185-188 °C; ^{1}H NMR (300 MHz, DMSO-d_6) δ 8.11 (s, 1H), 7.37 (d, 2H, J = 8.4 Hz), 6.89 (d, 2H, J = 8.1 Hz), 6.52 (m, 4H), 5.53 (br s, 2H) 4.88 (br s, 2H), 4.43 (s, 2H); ^{13}C NMR (75 MHz, DMSO-d_6) δ 160.82, 151.87, 147.97, 130.06, 129.34, 127.89, 124.81, 114.44, 113.95, 64.64; EMM (ESI) Calc for $C_{14}H_{15}N_3$ (M+H): 226.1339, found 226.1333.

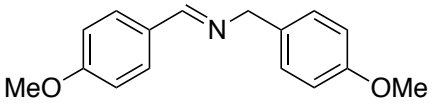

N-(4-methoxybenzylidene)-4-methoxybenzylamine, **3b**

Spectroscopic data match those previously reported.[19] ^{1}H NMR (300 MHz, $CDCl_3$) δ 8.30 (s, 1H), 7.73 (d, 2H, J = 8.4 Hz), 7.25 (d, 2H, J = 8.4 Hz), 6.8-6.9 (m, 4H), 4.73 (s, 2H) 3.83 (s, 3H), 3.79 (s, 3H); ^{13}C NMR (75 MHz, $CDCl_3$) δ 161.90, 161.12, 158.87, 131.92 130.02, 129.39,

114.19, 114.12, 64.62, 55.56, 55.51; EMM (ESI) Calc for $C_{16}H_{17}NO_2$ (M+H): 256.1333, found 256.1323.

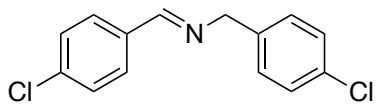

N-(4-chlorobenzylidene)-4-chlorobenzylamine, **4b**

Spectroscopic data match those previously reported.[19] ^{1}H NMR (300 MHz, $CDCl_3$) δ 8.33 (s, 1H), 7.71 (m, 2H), 7.2-7.4 (m, 6H), 4.76 (s, 2H); ^{13}C NMR (75 MHz, $CDCl_3$) δ 161.16, 137.78, 137.15, 134.62, 133.08, 129.70, 129.50, 120.17, 128.87, 64.36; EMM (ESI) Calc for $C_{14}H_{11}Cl_2N$ (M+H): 264.0342, found 264.0344.

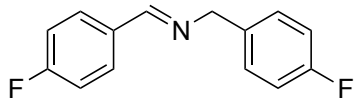

N-(4-fluorobenzylidene)-4-fluorobenzylamine, **5b**

Spectroscopic data match those previously reported.[19] ^{1}H NMR (300 MHz, $CDCl_3$) δ 8.32 (s, 1H), 7.75 (m, 2H), 7.27 (m, 2H), 7.01-7.11 (m, 2H), 4.74 (s, 2H); ^{13}C NMR (75 MHz, $CDCl_3$) δ 165.07 (d, $J_{C,F}$ = 185 Hz), 161.77 (d, $J_{C,F}$ = 178 Hz) 163.83, 162.96, 160.73, 160.58, 135.20 (d, $J_{C,F}$ = 2.5 Hz) 132.59 (d, $J_{C,F}$ = 2.7 Hz), 130.39 (d, $J_{C,F}$ = 8.8 Hz) 129.69 (d, $J_{C,F}$ = 7.7 Hz), 115.95 (d, $J_{C,F}$ = 21.9 Hz) 115.50 (d, $J_{C,F}$ = 21.7 Hz), 64.36; EMM (ESI) Calc for $C_{14}H_{11}F_2N$ (M+H): 232.0933, found 232.0939.

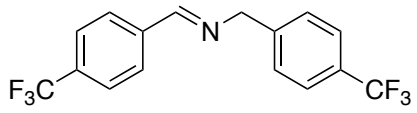

N-(4-trifluoromethylbenzylidene)-4-trifluoromethylbenzylamine, **6b**

Spectroscopic data match those previously reported.[20] ^{1}H NMR (300 MHz, $CDCl_3$) δ 8.47 (s, 1H), 7.91 (d, 2H, J = 8.1 Hz) 7.69 (d, 2H, J = 8.4 Hz), 7.62 (d, 2H, J = 8.4 Hz), 7.48 (d, 2H, J = 7.8 Hz), 4.90 (s, 2H); ^{13}C NMR (75 MHz, $CDCl_3$) δ 161.42, 143.25, 139.21, 132.75 (q, 32.5 Hz), 129.6 (q, $J_{C,F}$ = 32.1 Hz), 128.75, 128.34, 125. 83 (q, $J_{C,F}$ = 3.8 Hz), 125.68 (q, $J_{C,F}$ = 3.9 Hz), 124.5 (q, $J_{C,F}$ = 270 Hz) 124.14 (q, J = 270 Hz), 64.53; EMM (ESI) Calc for $C_{16}H_{11}F_6N$ (M+H): 332.0869, found 332.0857.

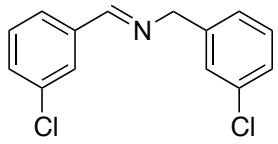

*N-(3-chlorobenzylidene)-3-chlorobenzylamine,***7b**

Spectroscopic data match those previously reported.[21] ^{1}H NMR (300 MHz, $CDCl_3$) δ 8.32 (s, 1H), 7.80 (s, 1H), 7.62 (m, 1H), 7.2-7.5 (m, 6H), 4.77 (s, 2H); ^{13}C NMR (75 MHz, $CDCl_3$) δ 161.23, 141.20, 137.86, 135.10, 134.62, 131.15, 130.13, 130.01, 128.26, 128.21, 127.49, 126.88, 126.27, 64.45; EMM (ESI) Calc for $C_{14}HCl_2N$ (M+H): 264.0342, found 264.0348.

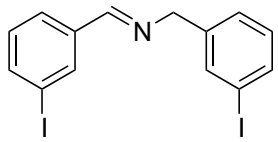

N-(3-iodobenzylidene)-3-iodobenzylamine, **8b**

Spectroscopic data match those previously reported.[21] ^{1}H NMR (300 MHz, $CDCl_3$) δ 8.26 (s, 1H), 8.15 (s, 1H), 7.6-7.7 (m, 3H), 7.59 (d, 1H, J = 7.8 Hz), 7.29 (d, 1H, J = 7.5 Hz), 7.123 (t, 1H, J = 7.8 Hz) 7.07 (t, 1H, J = 7.8 Hz); ^{13}C NMR (75 MHz, $CDCl_3$) δ 160.89, 141.56, 139.97,

138.13, 137.12, 137.09, 136.42, 130.53, 130.51, 127.95, 127.46, 94.80, 64.40; EMM (ESI) Calc for $C_{14}H_{11}I_2N$ (M+H): 447.9054, found 447.9068.

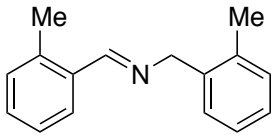

N-(2-methylbenzylidene)-2-methylbenzylamine, **9b**

Spectroscopic data match those previously reported.[19] ^{1}H NMR (300 MHz, $CDCl_3$) δ 8.65 (s, 1H), 7.90 (d, 1H, J = 7.5 Hz), 7.1-7.3 (m, 7H), 4.81 (s, 2H), 2.48 (s, 3H), 2.37 (s, 3H); ^{13}C NMR (75 MHz, $CDCl_3$) δ 160.97, 137.89, 137.85, 136.37, 134.41, 131.05, 130.57, 130.38, 128.58, 127.92, 127.34, 126.45, 126.33, 63.43, 19.59, 19.52; EMM (ESI) Calc for $C_{16}H_{17}N$ (M+H): 224.1434, found 224.1431.

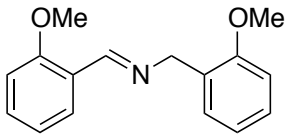

N-(2-methoxybenzylidene)-2-methoxybenzylamine, **10b**

Spectroscopic data match those previously reported.[22] ^{1}H NMR (300 MHz, $CDCl_3$) δ 8.87 (s, 1H), 8.06 (d, 1H, J = 7.5 Hz), 7.2-7.4 (m, 3H), 6.8-7.0 (m, 4H), 4.86 (s, 2H), 3.87 (s, 3H), 3.86 (s, 3H); ^{13}C NMR (75 MHz, $CDCl_3$) δ 159.02, 158.53, 157.30, 132.00, 129.37, 128.44, 128.15, 127.74, 125.18, 120.99, 120.76, 11.24, 110.43, 59.90, 55.76, 55.59; EMM (ESI) Calc for $C_{16}H_{17}NO_2$ (M+H): 256.1333, found 256.1337.

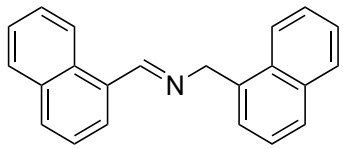

N-(1-naphthalenylmethylene)-1-naphthalenemethanamine, **11b**

Spectroscopic data match those previously reported.[19] ^{1}H NMR (300 MHz, $CDCl_3$) δ 9.09 (s, 1H), 8.89 (d, 1H, J = 8.1 Hz), 8.24 (d, 1H, J = 8.4 Hz); 7.8-7.9 (m, 5H), 7.4-7.6 (m, 7H), 5.42 (s, 2H); ^{13}C NMR (75 MHz, $CDCl_3$) δ 161.94, 135.49, 133.83, 133.78, 131.64, 131.32, 131.12, 129.16, 128.67, 128.59, 127.78, 127.18, 126.10, 126.01, 125.84, 125.68, 125.60, 125.20, 124.43, 123.94, 63.24; EMM (ESI) Calc for $C_{22}H_{17}N$ (M+H): 296.1434, found 296.1427.

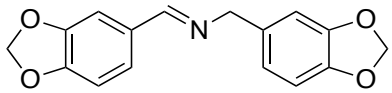

N-(1,3-benzodioxol-5-ylmethylene)-1,3-benzodioxole-5-methanamine, **12b**

Spectroscopic data match those previously reported.[2a] ^{1}H NMR (300 MHz, $CDCl_3$) δ 8.24 (s, 1H), 7.37 (s, 1H), 7.14 (dd, 1H, J = 8.4, 1.8 Hz), 6.7-6.8 (m, 4H), 5.99 (s, 2H), 5.93 (s, 2H), 4.67 (s, 2H); ^{13}C NMR (75 MHz, $CDCl_3$) δ 160.96, 150.04, 148.35, 147.81, 146.59, 133.46, 131.04, 124.67, 131.09, 108.66, 108.27, 108.13, 106.67, 101.55, 100.98, 64.52; EMM (ESI) Calc for $C_{16}H_{13}NO_4$ (M+H): 284.0918, found 284.0907.

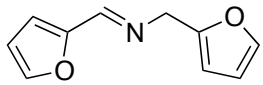

N-(2-furanylmethylene)-2-furanylmethanamine, **13b**

Spectroscopic data match those previously reported.[2a] ^{1}H NMR (300 MHz, $CDCl_3$) δ 8.11 (s, 1H), 7.51 (s, 1H), 7.37 (s, 1H), 6.78 (d, 1H, J = 3.3 Hz), 6.47 (m, 1H), 6.33 (d, 1H, J = 1.8 Hz) 6.26 (d, J = 1.5 Hz), 4.75 (s, 2H); ^{13}C NMR (75 MHz, $CDCl_3$) δ 152.02, 151.64, 151.51, 145.17, 142.52, 114.77, 111.89, 110.59, 108.15, 56.99; EMM (ESI) Calc for $C_{10}H_9NO_2$ (M+H): 176.0707, found 176.0709.

2.4.6. Synthesis and Characterization of Cross-coupled Imines.

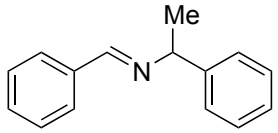

N-benzylidenemethylbenzylamine, **19**

Spectroscopic data match those previously reported.[2d] ^{1}H NMR (300 MHz, $CDCl_3$) δ 8.34 (s, 1H), 7.77 (m, 2H), 7.2-7.4 (m, 8H), 4.51 (q, 1H, J = 6.6 Hz), 1.58 (d, 3H, J = 6.9 Hz); ^{13}C NMR (75 MHz, $CDCl_3$) δ 159.37, 145.18, 136.40, 130.52, 128.49, 128.22, 126.78, 126.59, 69.69, 24.86; EMM (ESI) Calc for $C_{15}H_{15}N$ (M+H): 209.1199, found 209.1194.

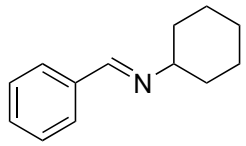

N-benzylidenecyclohexanamine, **20**

Spectroscopic data match those previously reported.[23] ^{1}H NMR (300 MHz, $CDCl_3$) δ 8.31 (s, 1H), 7.72 (m, 2H), 7.38 (m, 3H), 3.19 (m, 1H), 1.2-1.8 (m, 10H); ^{13}C NMR (75 MHz, $CDCl_3$) δ 158.55, 136.64, 130.29, 128.50, 128.04, 69.99, 34.37, 25.65, 24.81; EMM (ESI) Calc for $C_{13}H_{17}N$ (M+H): 188.1444, found 188.1442.

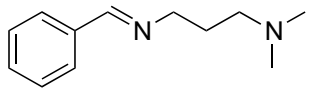

N-benzylidene-N',N'-dimethyl-1,3-propanediamine, **21**

Spectroscopic data match those previously reported.[24] ^{1}H NMR (300 MHz, $CDCl_3$) δ 8.29 (s, 1H), 7.72 (m, 2H), 7.40 (m, 3H), 3.64 (t, 2H, J = 7.2 Hz), 2.35 (t, 2H, J = 7.2 Hz), 2.23 (s, 6H), 1.87 (pent, 2H, J = 7.2 Hz); ^{13}C NMR (75 MHz, $CDCl_3$) δ 161.30, 136.53, 130.70, 128.78, 128.24, 59.85, 57.79, 45.74, 29.18; EMM (ESI) Calc for $C_{12}H_{18}N_2$ (M+H): 191.1543, found 191.1542.

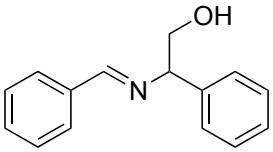

β-(phenylmethylene)amino]-benzeneethanol, **22**

Spectroscopic data match those previously reported.[22] ^{1}H NMR (300 MHz, $CDCl_3$) δ 8.23 (s, 1H), 6.64 (m, 2H), 7.16-7.37 (m, 8H), 4.42 (dd, 1H, J = 8.7, 4.5 Hz), 3.95 (dd, 1H, J = 11.4, 8.7 Hz) 3.82 (dd, 1H, J = 11.4, 3.9 Hz), 3.11 (br s, 1H); ^{13}C NMR (75 MHz, $CDCl_3$) d 162.99, 140.89, 136.13, 131.21, 128.92, 128.81, 128.68, 127.71, 127.61, 76.91, 67.96; EMM (ESI) Calc for $C_{15}H_{15}NO$ (M+H): 226.1227, found 226.1221.

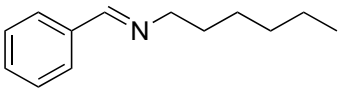

N-benzylidene-1-hexanamine, **23**

Spectroscopic data match those previously reported.[19] ^{1}H NMR (300 MHz, $CDCl_3$) δ 8.27 (s, 1H), 7.73 (m, 2H), 7.40 (m, 3H), 3.61 (td, 2H, J = 6.9, 1.2 Hz), 1.70 (m, 2H), 1.2-1.4 (m, 6H), 0.89 (br t, 3H, J = 6.9 Hz); ^{13}C NMR (75 MHz, $CDCl_3$) δ 160.87, 136.63, 130.62, 128.77, 128.22, 62.05, 31.90, 31.12, 27.26, 22.84, 14.29; EMM (ESI) Calc for $C_{13}H_{19}N$ (M+H): 190.1591, found 190.1591.

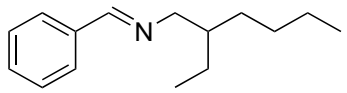

N-benzylidene-2-ethyl-1-hexanamine, **24**

Spectroscopic data match those previously reported.[25] ^{1}H NMR (300 MHz, $CDCl_3$) δ 8.26 (s, 1H), 7.74 (m, 2H), 7.40 (m, 3H), 3.54 (m, 2H), 1.70 (m, 1H), 1.2-1.4 (m, 8H), 0.8-0.9 (m, 6H); ^{13}C NMR (75 MHz, $CDCl_3$) δ 160.92, 136.74, 130.54, 128.75, 128.21, 65.38, 40.75, 31.60, 29.20, 24.79, 23.28, 14.33, 11.20; EMM (ESI) Calc for $C_{15}H_{23}N$ (M+H): 218.1904, found 218.1908.

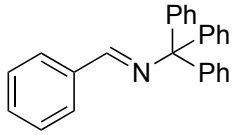

N-benzylidene-α,α-diphenylbenzylamine, **25**

Spectroscopic data match those previously reported.[26] Highly crystalline white solid, mp: 147-150 °C (lit. 153-159 °C); ^{1}H NMR (300 MHz, $CDCl_3$) δ 7.85 (m, 3H), 7.43 (m, 3H), 7.2-7.3 (m, 15H); ^{13}C NMR (75 MHz, $CDCl_3$) δ 159.87, 146.07, 137.00, 130.97, 130.04, 128.85, 128.80, 128.37, 128.14, 127.98, 127.01, 78.52; EMM (ESI) Calc for $C_{16}H_{13}NO_4$ (M+H): 348.1747, found348.1748.

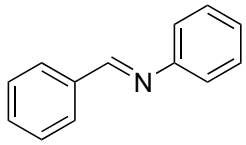

N-benzylideneaniline, **26**

Spectroscopic data match those previously reported.[19] ^{1}H NMR (300 MHz, $CDCl_3$) δ 8.46 (s, 1H), 7.92 (m, 2H), 7.26-7.5 (m, 5H), 7.23 (m, 3H); ^{13}C NMR (75 MHz, $CDCl_3$) δ 160.62, 152.34, 136.47, 131.60, 129.37, 12905, 129.00, 126.16, 121.10; EMM (ESI) Calc for $C_{13}H_{11}N$ (M+H): 182.0965, found 182.0964.

2.5 References and Notes

(1) For a recent review highlighting the versatility of imine electrophiles, see: Kobayashi, S.; Mori, Y.; Fossey, J. S.; Salter, M. M., *Chem. Rev.* **2011,** 111, 2626-2704.

(2) For several recent examples, see: (a) Lang, X.; Ji, H.; Chen, C.; Ma, W.; Zhao, J., *Angew. Chem. Int. Ed.* **2011**, *50*, 3934-3937. (b) Murahashi, S.-I.; Okano, Y.; Sato, H.; Nakae, T.; Komiya, N., *Synlett*, **2007**, 1675-1678. (c) Zhu, B.; Angelici, R. J., *Chem. Commun.* **2007**, 2157-2159. (d) Choi, H.; Doyle, M. P., *Chem. Commun.* **2007**, 745-747. (e) Wang, J.-R.; Fu, Y.; Zhang, B.-B.; Cui, X.; Liu, L.; Guo, Q.-X., *Tetrahedron Lett.* **2006,** 47, 8293-8297. (f) Samec, J. S. M.; Éll, A. H.; Bäckvall, J.-E., *Chem. Eur. J.* **2005,** *11*, 2327-2334. (g) Maeda, Y.; Nishimura, T.; Uemura, S., *Bull. Chem. Soc. Jpn.* **2003,** 76, 2399-2403. (h) Yamaguchi, K.; Mizuno, N. *Angew. Chem. Int. Ed.* **2003**, *42*, 1480-1483. (i) Nicolaou, K. C.; Mathison, C. J. N.; Montagnon, T., *J. Am. Chem. Soc.* **2004**, *126*, 5192-5201.

(3) For reviews, see: (a) Mure, M., *Acc. Chem. Res.* **2004,** *37*, 131-139. (b) Mure, M.; Mills, S.A.; Klinman, J. P. *Biochem.* **2002**, *41*, 9269-9278.

(4) For selected examples, see: (a) Eckert, T. S.; Bruice, T. C., *J. Am. Chem. Soc.* **1983**, *105*, 4431-4441. (b) Itoh, S.; Mure, M.; Ogino, M.; Ohshiro, Y. *J. Org. Chem.* **1991**, *56*, 6857-6865. (c) Ohshiro, Y.; Itoh, S., *Bioorg. Chem.* **1991,** *19*, 169-189. (d) Lee, Y.; Sayre, L. M., *J. Am. Chem. Soc.* **1995**, *117*, 3096-3105. (e) Mure, M.; Klinman, J. P., *J. Am. Chem. Soc.* **1995,** *117*, 8698-8706. (f) Mure, M.; Klinman, J. P., *J. Am. Chem. Soc.* **1995,** *117*, 8707-8718. (g) Itoh, S.; Takada, N.; Haranou, S.; Ando, T.; Komatsu, M.; Ohshiro, Y.; Fukuzumi, S.; *J. Org. Chem.* **1996**, *61*, 8967-8974. (h) Itoh, S.; Takada, N.; Ando, T.;

Haranou, S.; Huang, X.; Uenoyama, Y.; Ohshiro, Y.; Komatsu, M.; Fukuzumi, S., *J. Org. Chem.* **1997**, *62*, 5898-5907. (i) Ling, K.-Q.; Kim, J.; Sayre, L. M. *J. Am. Chem. Soc.* **2001**, *123*, 9606-9611. (j) Mure, M.; Wang, S. X.; Klinman, J. P. *J. Am. Chem. Soc.* **2003**, *125*, 6113-6125. (k) Murakami, Y.; Yoshimoto, N.; Fujieda, N.; Ohkubo, K.; Hasegawa, T.; Kano, K.; Fukuzumi, S.; Itoh, S., *J. Org. Chem.* **2007,** *72*, 3369-3380.

(5) (a) Stahl, S. S. *Angew. Chem. Int. Ed.,* **2004**, 43, 3400-3420. (b) Stahl, S. S. *Science* **2005**, *309*, 1824-1826. (c) Wendlandt, A. E.; Suess, A. M.; Stahl, S. S. *Angew. Chem. Int. Ed.* **2011**, *50*, 11062-11087.

(6) For previous reports by Mure and Klinman describing the use of TBHBQ in enzyme model studies, see refs 4e,f.

(7) (a) Corey, E. J.; Achiwa, K., *J. Am. Chem Soc.* **1969**, *91*, 1429-1432. (b) Klein, R. F. X.; Bargas, L. M.; Horak, V.; Navarro, M., *Tetrahedron Lett.* **1988**, *29*, 851-852.

(8) For an example involving C–H bond oxidation, see: (a) Ohshiro, Y.; Itoh, S.; Kurokawa, K.; Kato, J.; Hirao, T.; Agawa, T., *Tetrahedon Lett.***1983**, *24*, 3465-3468. For examples involving C–C bond activation, see: (b) Itoh, S.; Kato, N.; Ohshiro, Y.; Agawa, T., *Tetrahedron Lett.* **1984,** 25, 4753-4756. (c) Mure, M.; Suzuki, A.; Itoh, S.; Ohshiro, Y., *J. Chem. Soc., Chem. Commun.* **1990**, 1608-1611.

(9) Largeron, M.; Chiaroni, A.; Fleury, M.-B., *Chem. Eur. J.* **2008,** *14*, 996-1003.

(10) Largeron, M.; Fleury, M.-B., *Org. Lett.* **2009,** *11*, 883-886.

(11) M. Largeron, M.-B. Fleury, *Angew. Chem. Int. Ed.* **2012**, *51*, 5409-5412.

(12) Belowich, M. E.; Stoddart, J. F., *Chem. Soc. Rev.* **2012,** *41*, 2003-2024.

(13) For reviews, see: (a) Corbett, P. T.; Leclaire, J.; Vial, L.; West, K. R.; Wietor, J.-L.; Sanders, J. K. M.; Otto, S., *Chem. Rev.* **2006,** *106*, 3652-3711. (b) Lehn, J.-M., *Chem.*

Soc. Rev. **2007,** *36*, 151-160. (c) Ludlow, R. F.; Otto, S., *Chem. Soc. Rev.* **2008,** *37*, 101-108.

(14) For selected recent applications of dynamic covalent chemistry, pertaining to the exchange of C=N bonds, see: (a) Dirksen, A.; Dirksen, S.; Hackeng, T. M.; Dawson, P. E. *J. Am. Chem. Soc.* **2006,** *128,* 15602-15603. (b) Dirksen, A.; Hackeng, T. M.; Dawson, P. E. *Angew. Chem., Int. Ed.* **2006,** *45,* 7581-7584. (c) Hartley, C. S.; Moore, J. S., *J. Am. Chem. Soc.* **2007,** *129*, 11682-11683.

(15) For representative fundamental studies of equilibrium-controlled exchange of other covalent bonds, such as esters, alkenes and amides, see: (a) Stanton, M. G.; Allen, C. B.; Kissling, R. M.; Lincoln, A. L.; Gagné, M. R. *J. Am. Chem. Soc.* **1998,** *120,* 5981-5989. (b) Kissling, R. M.; Gagné, M. R., *Org. Lett.* **2000,** *2*, 4209-4212. (c) Nyce, G. W.; Lamboy, J. A.; Connor, E. F.; Waymouth, R. M.; Hedrick, J. L. *Org. Lett.* **2002,** *4,* 3587-3590. (d) Eldred, S. E.; Stone, D. A.; Gellman, S. H.; Stahl, S. S. *J. Am. Chem. Soc.* **2003**, *125*, 3422-3423. (e) Singh, R.; Kissling, R. M.; Letellier, M.-A.; Nolan, S. P. *J. Org. Chem.* **2004,** *69,* 209-212. (f) Cantrill, S. J.; Grubbs, R. H.; Lanari, D.; Leung, K. C.-F.; Nelson, A.; Poulin-Kerstien, K. G.; Smidt, S. P.; Stoddart, J. F.; Tirrell, D. A. *Org. Lett.* **2005,** *7,* 4213-4216. (g) Stephenson, N. S.; Zhu, J.; Gellman, S. H.; Stahl, S. S. *J. Am. Chem. Soc.*, **2009**, *131*, 10003–10008.

(16) Lee, Y.; Jeon, H.-B.; Huang, H.; Sayre, L. M., *J. Org. Chem.* **2001,** *66*, 1925-1937.

(17) Cram, D. J.; Reeves, R. A., *J. Am. Chem. Soc.* **1958**, *80*, 3094-3103.

(18) Heiden, Z. M.; Stephan, D. W., *Chem. Commun.* **2011**, *47*, 5729-5731.

(19) Liu, L.; Zhang, S.; Fu, X.; Yan, C.-H.,*Chem. Commun.* **2011,** *47*, 10148-10150.

(20) Johnsen, C.; Stein, P. C.; Nielsen, K. A.; Bond, A. D.; Jeppesen, J. O., *Eur. J. Org. Chem.* **2010,** *4*, 759-769.

(21) Kin, S.-S.; Thakur, S. S.; Song, J.-Y.; Lee, K.-H. *Bull. Korean Chem. Soc.* **2005**, *26*, 499-501.

(22) Miyamura, H.; Morita, M.; Inasaki, T.; Kobayashi, S., *Bull. Chem. Soc. Jpn.* **2011,** *84*, 588-599.

(23) Jiang, L.; Jin, L.; Tian, H.; Yuan, X.; Yu, X.; Xu, Q., *Chem. Commun.* **2011,** *47*, 10833-10835.

(24) Capape, A.; Crespo, M.; Granell, J.; Font-Bardia, M.; Solans, X., *J. Organomet. Chem.* **2005,** *690*, 4309-4318.

(25) Bitencourt, T. B.; Nascimento, M. d. G., *J. Phys. Org. Chem.* **2010,** *23*, 995-999.

(26) Soroka, M. Ç.; Zygmunt, J., *Synthesis* **1988,** *5*, 370-372.

Chapter 3

Bioinspired Aerobic Oxidation of Secondary Amines and Nitrogen Heterocycles with a Bifunctional Quinone Catalyst

This work has been published:

Wendlandt, A. E.; Stahl, S. S. *J. Am. Chem. Soc.* **2014**, *136*, 506-512.

.

3.1 Introduction

Enzymatic transformations have provided the inspiration for numerous advances in synthetic chemistry and catalysis. In connection with widespread interest in the development of aerobic oxidation reactions, numerous researchers have turned to metalloenzymes as a starting point for development of small-molecule transition-metal catalysts. Organic cofactors are also common in naturally occurring oxidases and oxygenases, but these have been less extensively developed for use in synthetic applications. Copper amine oxidases promote aerobic oxidation of primary amines to aldehydes in nature (Figure 3.1).[1] Copper is present in the enzyme, but substrate oxidation is promoted exclusively by a quinone cofactor in the active site. The mechanism of the reaction was the subject of considerable historical debate and focused on two possible pathways:[2,3] a "transamination" pathway involving the formation and oxidation of an iminoquinone intermediate (Figure 3.1A), and an "addition-elimination" pathway involving substrate oxidation via a hemiaminal intermediate (Figure 3.1B). Extensive mechanistic studies of the enzyme and model systems by Klinman, Sayre and others convincingly demonstrated that the reaction proceeds via the transamination pathway.[4,5]

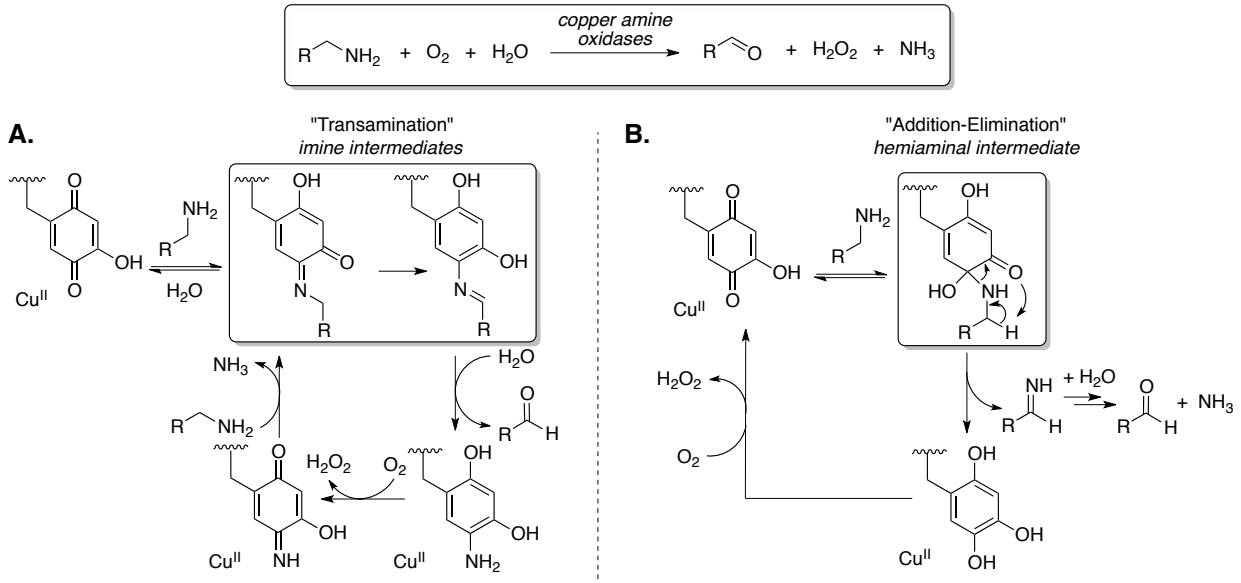

Figure 3.1. Mechanism of aerobic amine oxidation mediated by copper amine oxidase enzymes. (A) "Transamination" mechanism involving covalent imine intermediates. (B) "Addition-elimination" mechanism of amine oxidation, involving a hemiaminal intermediate.

Recently, several groups have begun to explore quinone-based catalysts[6-9] as alternatives to metal-based catalysts for amine dehydrogenation.[10-12] Use of quinones **Q1**[6] and **Q2**[7] (Scheme 3.1) enables efficient and selective production of homo- and heterocoupled imines under mild reaction conditions (Scheme 3.1). These catalysts show exquisite selectivity for primary amines, similar to the native enzymes. Secondary amines are not compatible with the transamination mechanism, and they often serve as inhibitors via formation of irreversible covalent adducts.[13,14]

Scheme 3.1. Biomimetic pre-catalysts **Q1** and **Q2** and their synthetic application to oxidative homo- and cross-coupling of primary amines.

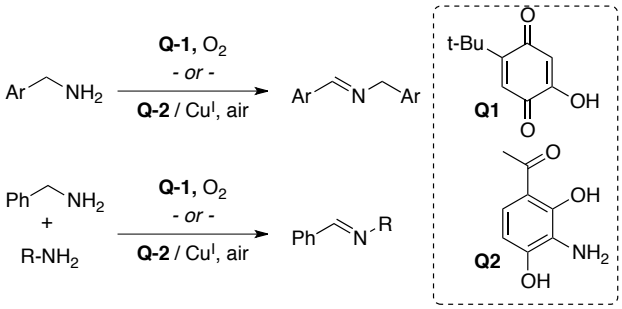

The function of quinone cofactors in nature is not limited to primary amine oxidation. For example, pyrroloquinoline quinone (PQQ)-dependent alcohol dehydrogenases (Figure 3.2) mediate alcohol oxidation via a mechanism that involves a hemiacetal intermediate, resembling the addition-elimination mechanism in Figure 3.1B.[15-17] Identification of new quinone-based catalysts that operate via an addition-elimination mechanism could significantly enhance the synthetic scope of such oxidation reactions. Kobayashi proposed the involvement of hemiaminal intermediates in diverse amine oxidation reactions that use Pt/Ir nanoclusters and 4-*tert*-butylcatechol as cocatalysts.[8] Here, we expand this concept by showing that 1,10-phenanthroline-5,6-dione (phd) (Figure 3.2) is an effective catalyst for secondary amine oxidation. Fundamental studies provide direct evidence for the addition-elimination pathway, including spectroscopic characterization of the hemiaminal intermediate. We further show that coordination of the distal nitrogen atoms to Zn^{2+} enhances phd amine oxidation activity, and that a catalyst system composed of phd/ZnI_2 promotes efficient aerobic oxidation of a variety of secondary amines and nitrogen heterocycles.

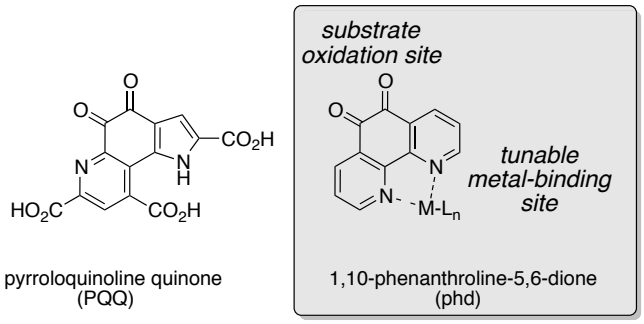

Figure 3.2. Pyrroloquinoline quinone (PQQ), and phd: a modular, bifunctional catalyst for amine oxidation. The *o*-quinone moiety is responsible for substrate oxidation, while remote metal-binding sites can be used to tune the quinone reactivity.

3.2. Results and Discussion

Stoichiometric secondary amine oxidation and characterization of a hemiaminal adduct. In an effort to expand upon our earlier studies of quinone-mediated amine oxidation,[6] we were drawn to the structure of 1,10-phenanthroline-5,6-dione (phd) as a potential catalyst because of its bifunctional character associated with the *o*-quinone and distal chelating nitrogen atoms (Figure 3.2). Independently, the coordination chemistry of phd with a number of different metals has been investigated.[18-20] We speculated that these two features could be combined to achieve unique amine oxidation reactivity.[21] The dehydrogenation of cyclic secondary amines was targeted because these substrates have been ineffective with traditional amine oxidase mimics. For example, Bruice and coworkers have studied isomeric phenanthroline-derived *o*-quinones as models of the cofactor pyrroloquinoline quinone (PQQ), and they observed stoichiometric oxidation of various amines, including the secondary amine morpholine. No catalytic reactivity was observed, however, and the reaction with morpholine led to formation of an irreversible covalent adduct.[14,22] Catalytic dehydrogenation of secondary amines is also an important target because the unsaturated heterocyclic products are prevalent in pharmaceuticals and other biologically active molecules.

Our initial studies probed the stoichiometric reaction of 1,2,3,4-tetrahydroisoquinoline **1** with phd in MeCN. The reaction proceeded quantitatively at room temperature within 18 h to afford 3,4-dihydroisoquinoline **2** and 1,10-phenanthroline-5,6-diol (phd-H_2) as a yellow-green precipitate (eq 1). The effectiveness of this reaction was better than expected in light of Bruice's precedent showing that secondary amines could form irreversible covalent adducts with phd analogs.[14]

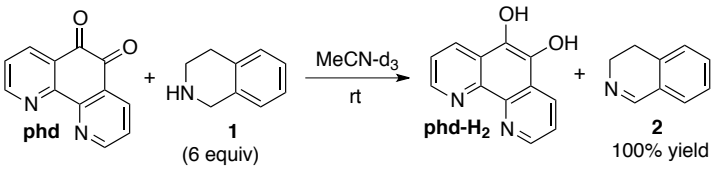

(1)

The reaction of **1** with phd was monitored by ^{1}H NMR spectroscopy to determine whether intermediates could be observed. Upon addition of 6 equiv of **1** in MeCN-d_3 at room temperature, the characteristic phd resonances disappeared with concomitant formation of new broad peaks. Variable temperature studies demonstrated that these broad peaks were associated with an equilibrium exchange process occurring on the NMR time scale. The broad peaks resolved at lower temperature (Figure 3.3 and 3.7) to reveal the presence of a new species, and the chemical exchange process was sufficiently slow at -40 °C to enable full characterization of this intermediate by NMR spectroscopy. It was identified as hemiaminal **A** (Figure 3A) on the basis of ^{1}H-^{13}C and ^{1}H-^{15}N gHSQC and gHMBC as well as 1D NOESY data (see Supporting Information, Figures 3.8-3.12).

NMR titration studies of phd with **1** in MeCN-d_3 (Figure 3.13) were used to establish the equilibrium constant for hemiaminal formation: K = 0.10 mM^{-1} at -40 °C. Exchange spectroscopy (EXSY) experiments were carried out with 6 equiv of **1** and revealed exchange

between **1** and the hemiaminal, and between the hemiaminal and free phd (Figures 3.14 and 3.15).

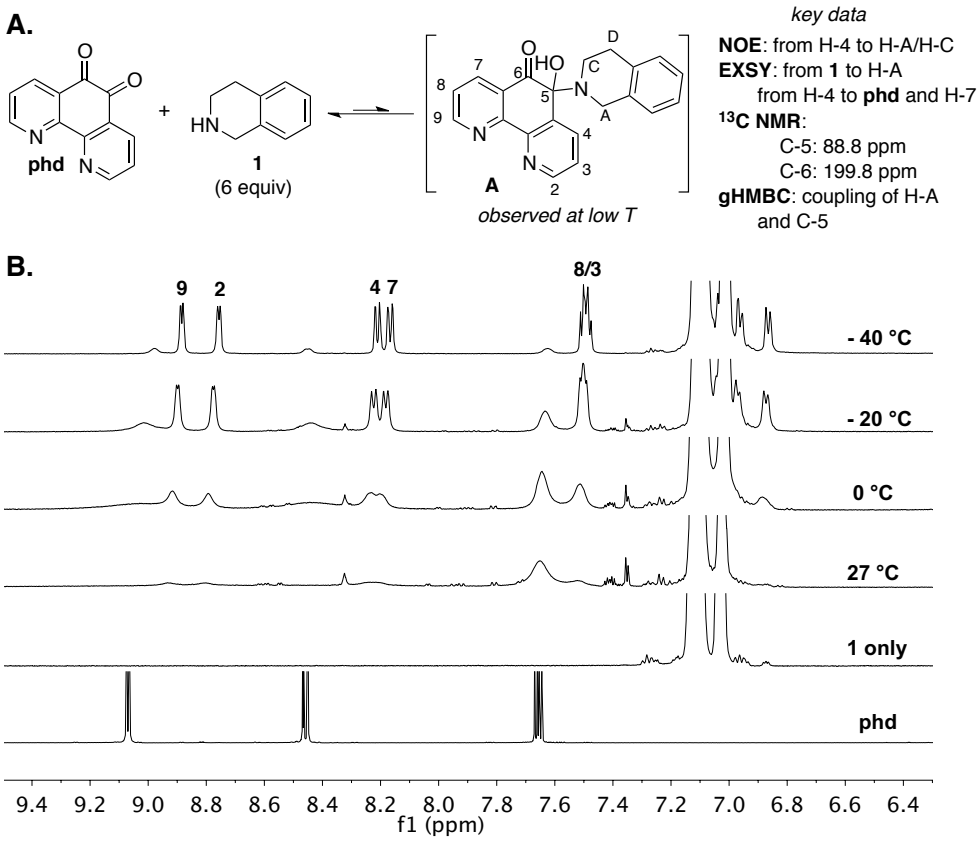

Figure 3.3. Observation of hemiaminal intermediate **A** by variable temperature ^{1}H NMR.

Zn^{2+}-promoted amine oxidation and characterization of Zn-phd complexes. The prospect that metal ions could promote phd-mediated amine oxidation was tested by adding various quantities of $Zn(OTf)_2$ to the reaction mixture. The most significant rate enhancement was observed with 0.5 equiv of $Zn(OTf)_2$ (i.e., phd/Zn^{2+} = 2:1), which led to an 11-fold increase in the initial rate of the oxidation of **1** by phd (Figure 3.4). Formation of large quantities of precipitate, presumably corresponding to a Zn^{2+}/phd-H_2 coordination polymer, slowed the reaction after approx. 40-50% conversion under these conditions.

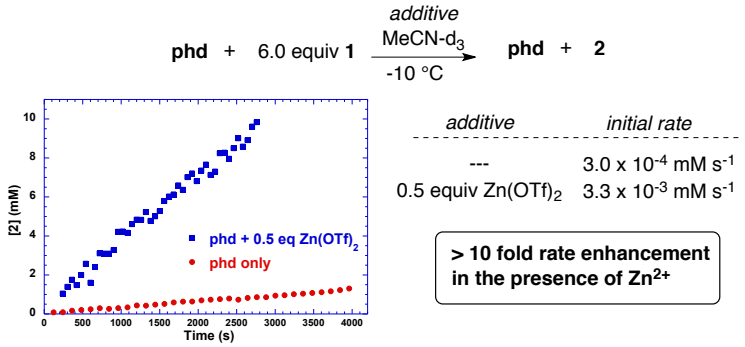

Figure 3.4. Rates for the stoichiometric reaction of **1** with phd at -10 °C in acetonitrile with and without 0.5 equiv $Zn(OTf)_2$. Reaction conditions: [phd] = 19 mM (0.019 mmol), [**1**] = 114 mM (0.114 mmol), [$Zn(OTf)_2$] = 9.5 M (0.095 mmol), MeCN (1 mL), -10 °C.

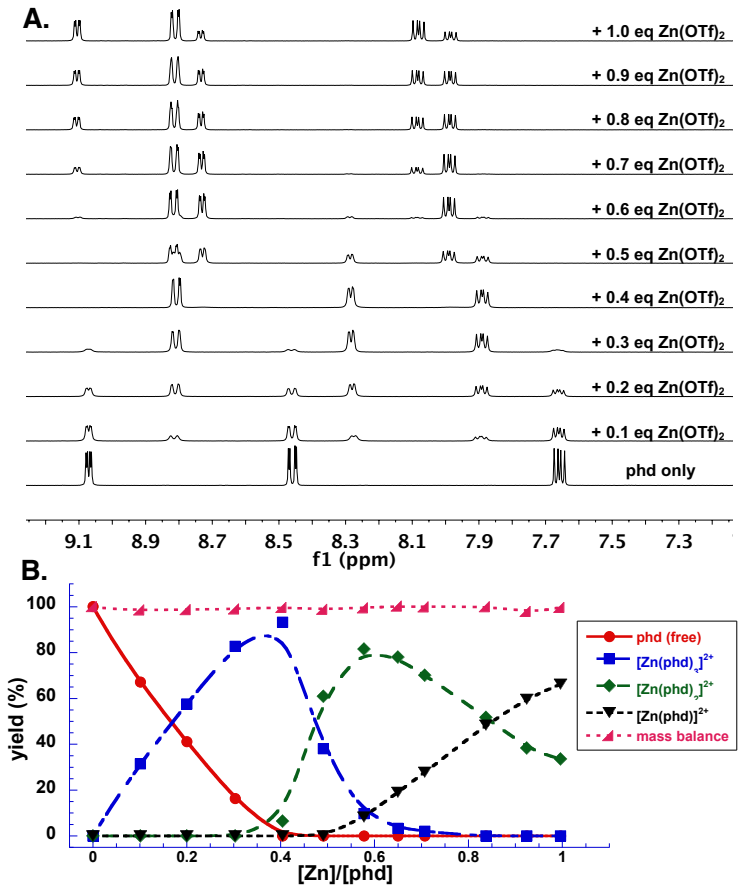

Figure 3.5. ^{1}H NMR titration and speciation plot at different $Zn(OTf)_2$/phd ratios. Lines do not represent fits, but are included to guide the eye.

NMR titration studies of $Zn(OTf)_2$ and phd in MeCN-d_3 revealed sequential formation of three discrete species in solution, corresponding to $[Zn(phd)_3]^{2+}$, $[Zn(phd)_2]^{2+}$ and $[Zn(phd)]^{2+}$ (Figures 3.5 and 3.16). ^{1}H-^{15}N HMBC experiments reveal that the phd ^{15}N resonances shift from 313 ppm to 251 ppm in the presence of $Zn(OTf)_2$ (Figures 3.17 and 3.18), consistent with coordination of the pyridyl nitrogen atoms to Zn. X-ray quality crystals of a $[Zn(phd)_2]^{2+}$ species were obtained from a 2:1 mixture of phd/$Zn(OTf)_2$ in MeCN, confirming phd coordination to Zn (Figure 3.6).

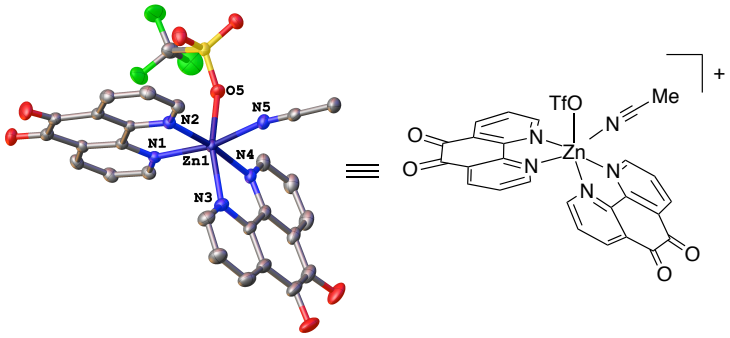

Figure 3.6. X-ray crystal structure of $[Zn(phd)_2(MeCN)(OTf)]^+$ shown with 50% probability ellipsoids. All H atoms and disorder are omitted for clarity (see Supporting Information for details).

Catalytic aerobic oxidation of secondary amines. The oxidation of tetrahydroisoquinoline **1** to the dihydroisoquinoline **2** was then tested with catalytic quantities of phd (5 mol %) and different Zn^{2+} sources (2.5 mol %) under 1 atm of O_2 (Table 3.1). Negligible catalytic turnover was observed in the oxidation of **1** by phd in the absence of Zn^{2+} ions (7% yield), and little improvement was achieved by including $Zn(OTf)_2$, $Zn(OAc)_2$, $ZnCl_2$, or $ZnBr_2$ (Table 1, entries 1–5). Use of ZnI_2, however, resulted in significant catalytic turnover (55% yield; entry 6). The yield further improved upon adding catalytic quantities of a Brønsted acid (75% yield with 15 mol % pyridinium *p*-toluenesulfonic acid, PPTS; entry 7). Control experiments showed that no

amine oxidation occurred in the absence of phd under these conditions (entry 8), and removal of the ZnI_2 leads to only stoichiometric oxidation (7%; entry 9). Replacement of phd with 1,10-phenanthroline also results in no substrate oxidation (entry 10).

Table 3.1. Optimization of the reaction conditions for the catalytic aerobic oxidation of tetrahydroisoquinoline, **1**.[a]

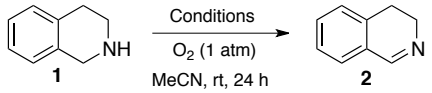

Entry	quinone	additive	additive	% yield **2**
1	5% phd	----	---	7
2	5% phd	2.5% $ZnOTf_2$	---	7
3	5% phd	2.5% $ZnOAc_2$	---	7
4	5% phd	2.5% $ZnCl_2$	---	7
5	5% phd	2.5% $ZnBr_2$	---	10
6	5% phd	2.5% ZnI_2	---	55
7	**5% phd**	**2.5% ZnI_2**	**15% PPTS**	**75**
8	---	2.5% ZnI_2	15% PPTS	NR
9	5% phd	---	15% PPTS	7
10	5% phen	2.5% ZnI_2	15% PPTS	NR

[a] Reaction conditions: 1,2,3,4-tetrahydroisoquinoline (0.130 mmol), MeCN (0.5 mL), O_2 atmosphere, 24 h. PPTS, Pyridinium *p*-toluenesulfonic acid. Yields determined by ^{1}H NMR spectroscopy.

Further studies of the oxidation of **1** to **2**, as well as the oxidation of dibenzylamine **3** to *N*-benzylidene benzylamine **4**, revealed that both Zn^{2+} and iodide are important to the success of the catalytic reactions. Oxidation of **3** under the optimized reaction conditions resulted in an 80% yield of **4** (Table 3.2, entry 1). Upon replacement of ZnI_2 with tetrabutylammonium iodide (Bu_4NI), significant catalytic activity was retained in the oxidation of **1**, but only stoichiometric reactivity was observed in the oxidation of **3** (entry 2). A similar observation was made when ZnI_2 was replaced with molecular iodine (entry 3). Use of catalytic I_2 in the absence of phd led to negligible reactivity, even in the reaction of **1** (entry 4).

Table 3.2. Beneficial effect of Zn^{2+} and iodide on catalytic aerobic amine oxidation.[a]

Entry	quinone	additive	additive	% yield **2**	% yield **4**
1	5% phd	2.5% ZnI_2	15% PPTS	75	80
2	5% phd	5% Bu_4NI	15% PPTS	61	6
3	5% phd	2.5% I_2	15% PPTS	52	8
4	---	2.5% I_2	15% PPTS	2	3

[a] Reaction conditions: amine (0.130 mmol), MeCN (0.5 mL), O_2 atmosphere, 24 h. PPTS, Pyridinium *p*-toluenesulfonic acid. Yields determined by ^{1}H NMR spectroscopy.

The unique beneficial effect of iodide counterions raised the possibility of a catalytic redox role for iodide, and use of a starch-iodine test provides evidence for the formation of I_3^- in the absence of substrate under the standard reaction conditions. On the basis of this result, at least two reasonable mechanisms could be considered for the amine oxidation reactions (Scheme 3.2). Mechanism A involves phd-mediated amine oxidation, similar to the stoichiometric reactivity shown in eq 1 and Figure 4. Catalytic turnover involves an iodide/triiodide cycle[23] that mediates aerobic reoxidation of phd-H_2 (Scheme 3.2A). Mechanism B reflects literature precedents for stoichiometric oxidation of certain amines by molecular iodine,[24] and the catalytic cycle involves I_2/I_3^--promoted amine oxidation coupled to a phd-based redox cycle that mediates aerobic reoxidation of iodide (Scheme 3.2B). The latter pathway resembles metal-catalyzed oxidation reactions in which quinones have been used to facilitate aerobic oxidation of the reduced catalyst.[25]

Scheme 3.2. Two proposed reaction mechanisms.

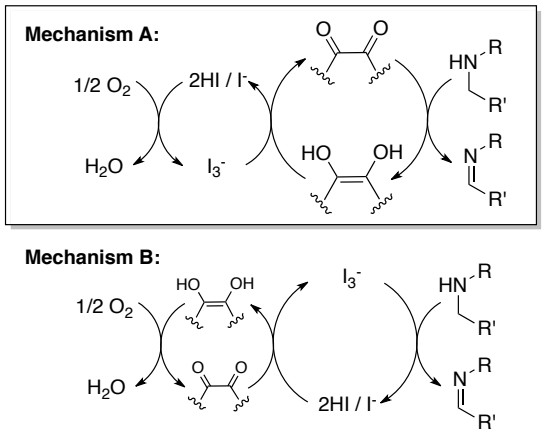

Kinetic isotope effect experiments were carried out in order to distinguish between these possibilities (Scheme 3). The reaction of **1**-d_1 was subjected to three different reaction conditions, including those employing (a) stoichiometric phd as the oxidant under anaerobic conditions, (b) stoichiometric iodine as the oxidant under anaerobic conditions, and (c) the optimized catalytic conditions with 5 mol % phd/2.5 mol % ZnI_2 under aerobic conditions. Comparison of the KIEs from these experiments showed that the KIE obtained under catalytic conditions matched that obtained with stoichiometric phd (KIE = 6.4 in both cases), and differed from the KIE observed with I_2 as the oxidant (KIE = 3.8). These results provide strong support for the quinone-mediated amine oxidation pathway associated with Mechanism A in Scheme 2A.

Scheme 3.3. Intramolecular competition kinetic isotope effect experiments.

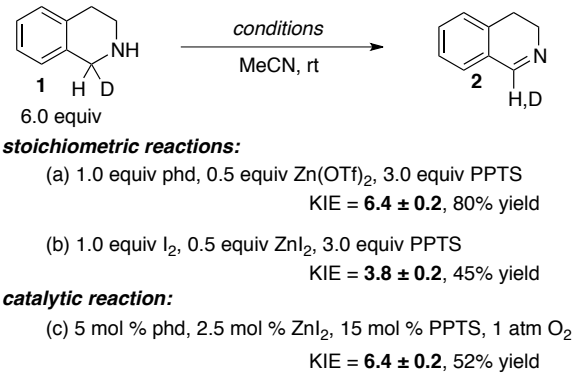

Substrate scope and synthetic applications. The optimized catalytic conditions were tested with a number of different substrates (Table 3.3), ranging from simple dibenzyl amines (A) to various nitrogen heterocycles, such as tetrahydroisoquinolines (B), tetrahydro-β-carbolines (C), and tetrahydroquinazolines (D), as well as indolines (E). Substrate classes (B)–(D) are particular appealing because the saturated heterocycles may be accessed readily via simple condensation and Pictet-Spengler reactions (Table 3.3B–3.3D).

Substituted tetrahydroisoquinolines were smoothly converted to 3,4-dihydroisoquinolines under these conditions (Table 3.3B). Electron-donating groups improved reaction yields and diminished reaction times. 6,7-Dimethoxytetrahydroisoquinoline was oxidized to dihydrobackebergine **6** in 91% isolated yield and proceeds more rapidly than the parent substrate 1. Aryl and alkyl substitution at the 1-position is well-tolerated: 1-phenyl- and 1-cyclohexyl-substituted 6,7-dimethoxy-3,4-dihydroisoquinolines were isolated in excellent yields (98% and 90% yields of **7** and **8**, respectively). The 3,4-dihydroisoquinoline products of these reactions have been widely used as precursors to chiral tetrahydroisoquinolines, which are widely represented in natural products and pharmaceuticals. For example, 1-(4-chlorophenyl)-3,4-dihydro-6,7-dimethoxyisoquinoline **9**, which is obtained in 94% yield under our aerobic

oxidation conditions, is an intermediate to the phase III antiepileptic AMPA receptor agonist **10**.[26]

Substituted tetrahydro-β-carbolines are readily converted to 3,4-dihydro-β-carbolines using the same optimized conditions (Table 3.3C). Aryl substitution in the 1-position is again tolerated, with yields slightly improved for substrates containing electron-rich substituents (**13**, R = OMe, 88% yield), relative to those containing electron-deficient substituents (**11**, R = Cl, 70% yield). *o*-Methyl substitution is also well-tolerated (**14**, 91% yield), and the natural product isoeudistomin U (**15**) was obtained in 63% isolated yield (85% NMR yield).

Quinazolines were formed in good yields from tetrahydroquinazolines (Table 3.3D). Unlike other substrate classes, wherein electron-donating substituents improved yields, quinazoline products containing electron-withdrawing substitution at the 2-position were better substrates. Ring-chain tautomerism in 2-substituted tetrahydroquinazolines could occur, and the improved yields of electron-deficient quinazolines may reflect the stabilization of the ring tautomer in the respective tetrahydroquinazoline substrates.

With slight modification to the reaction conditions (5 mol % phd, 1.0 mol % ZnI_2, and 1.0 mol % PPTS) indoline could be converted to indole **25** (Table 3.3E) in 81% isolated yield. 3-Methyl, and 2-methyl indolines were also oxidized to the corresponding indoles in good yields (80% and 73% isolated yields, **26** and **27** respectively). Even the tertiary amine substrate, 1-methyl indoline, afforded the indole product **28** in 48% yield (Table 3.3E); however, the electron-deficient *N*-tosylindoline **29** was not oxidized under these conditions.

Table 3.3. Substrate scope and synthetic applications.[a]

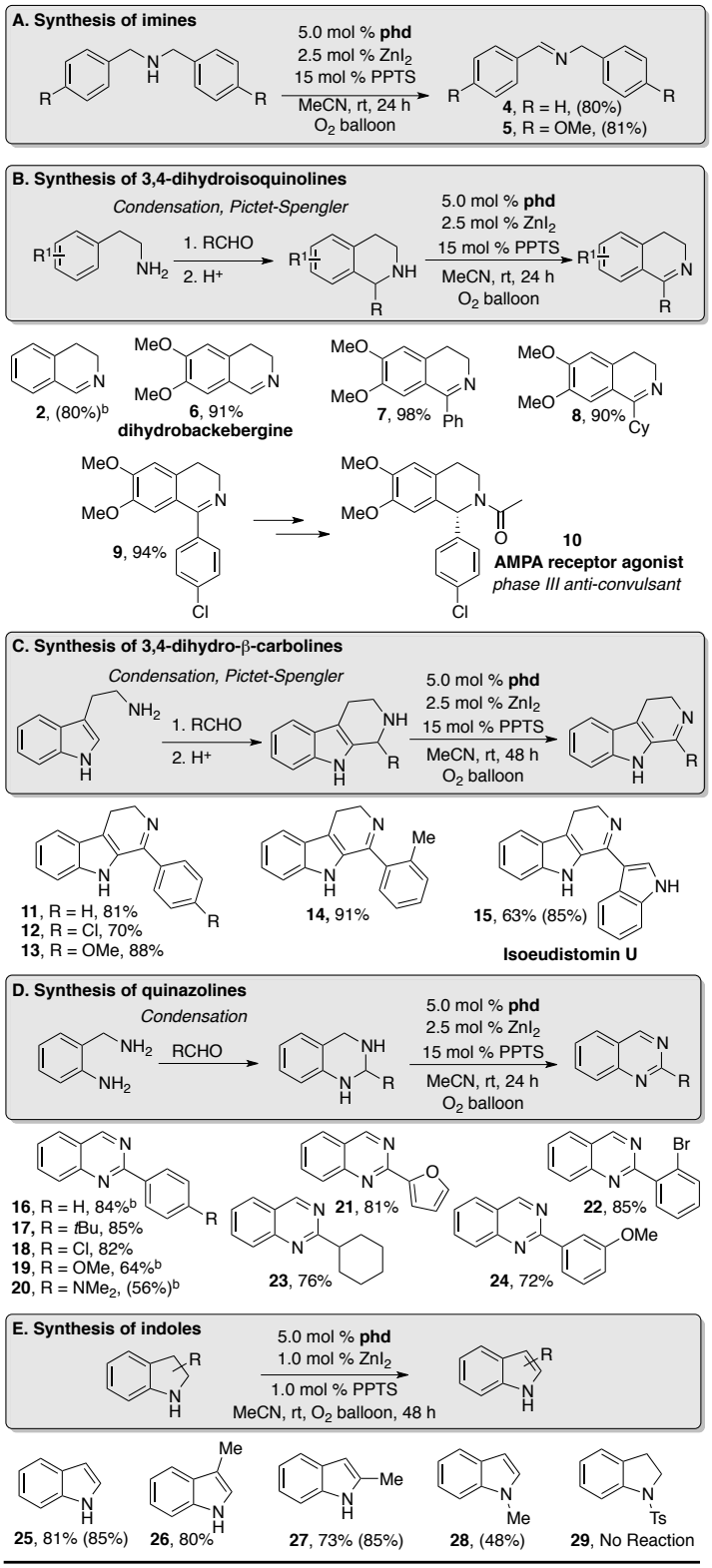

[a] Reaction conditions: substrate amine (1.0 mmol), phd (0.05 mmol), ZnI_2 (0.025 mmol), PPTS (0.15 mmol), MeCN (4.0 mL), O_2 balloon, 24-48 h. [b] 48 h reaction time. Yields are reported as isolated yields, numbers in parenthesis indicate NMR yields.

3.3. Conclusion

In conclusion, we have identified a new strategy for aerobic oxidation of secondary amines, employing 1,10-phenanthroline-5,6-diones as a bifunctional *o*-quinone catalyst. The success of these reactions can be traced to the non-biomimetic reaction mechanism, which involves an addition-elimination pathway, rather than the transamination pathway employed by copper amine oxidase enzymes and many quinone model systems. Direct spectroscopic evidence was obtained for the hemiaminal intermediate. The bifunctional character of the phd catalyst was exploited in the use of Zn^{2+} to promote amine oxidation, and iodide was fortuitously discovered to promote aerobic catalytic turnover. Control experiments and mechanistic studies reveal that iodide plays a critical redox role in mediating aerobic reoxidation of the reduced quinone catalyst. Collectively, these results provide a foundation for broader exploration of quinones and related redox-active organic catalysts in selective aerobic oxidation reactions.

3.4. Acknowledgement

We would like to thank Mr. Paul White for helpful discussions and assistance with NMR studies, and Brian S. Dolinar and Dr. Ilia A. Guzei for X-ray crystallographic determination. We are grateful for financial support from the NIH (R01-GM100143). Analytical instrumentation was partially funded by the National Science Foundation (CHE-1048642, CHE-9208463, CHE-0342998, CHE-9974839, CHE-9304546) and National Institutes of Health (NIH 1 S10 RR13866-01)

3.5. Experimental Details and Supporting Information

3.5.1 General Considerations.

All commercially available compounds were purchased from Sigma-Aldrich, and used as received unless otherwise indicated. Solvents were dried over alumina columns prior to use. ^{1}H and ^{13}C NMR spectra for compound characterization were recorded on Bruker AC-300 MHz, Avance-400 MHz, Avance-500 MHz or Varian Mercury-300 MHz spectrometers. Chemical shift values are given in parts per million relative to residual solvent peaks (^{1}H and ^{13}C) or liquid NH_3 (^{15}N). High-resolution, exact mass measurements were obtained by the mass spectrometry facility at the University of Wisconsin. Melting points were taken on a Mel-Temp II melting point apparatus. Gas chromatographic analysis of reactions was conducted with a Shimadzu GC-2010Plus gas chromatograph with either a DB-Wax or a RTX-5 column. Flash chromatography was performed using SilicaFlash® P60 (Silicycle, particle size 40-63 μm, 230-400 mesh).

3.5.2. Procedure for Stoichiometric Reaction of phd with 1,2,3,4-tetrahydroisoquinoline.

To a solution of phd (4.0 mg, 0.019 mmol) in MeCN-d_3 (1.0 mL) containing internal standard (1,3,5-trimethoxybenzene) was added 6.0 equiv of 1,2,3,4-tetrahydro-isoquinoline (14.5 uL, 0.114 mmol). Reaction progress was monitored by ^{1}H NMR until completion, at which point solids had formed along the walls of the NMR tube. (The liquids could be decanted, and the solids reconstituted in DMSO-d_6 + 1 drop TFA to give a spectrum which matched authentic 1,10-phenanthroline-5,6-diol, prepared according to the literature procedure[27]).

3.5.3. Low Temperature NMR Characterization of Hemiaminal Intermediate A: General considerations for NMR studies

Low temperature characterization data was obtained using Bruker Avance 500 MHz or Varian INOVA 600 MHz spectrometers. Low temperature correlation spectroscopy was acquired using the following pulse parameters: ^{1}H-^{13}C HSQC spectral window (f2) of 230 ppm centered at 105 ppm, j1xh = 140.0 Hz, ni = 256, and ns = 2; ^{1}H-^{13}C HMBC spectral window (f2) of 230 ppm centered at 105 ppm, jnxh = 8.0 Hz, j1xh = 140.0 Hz, ni = 256, ns = 4; ^{1}H-^{15}N HMBC spectral window (f2) of 400 ppm centered at 150 ppm, jnxh = 7.0 Hz, j1xh = 95.0 Hz, ni = 256, and ns = 128. Chemical shift values are given in parts per million relative to residual solvent peaks (^{1}H and ^{13}C) or liquid NH_3 (^{15}N). Unless otherwise indicated, temperature calibrations were determined using a 4% MeOH in CD_3OD external standard.

3.5.4. General Procedure for NMR sample preparation

A solution of phd (4.0 mg, 0.019 mmol) in 1.0 mL MeCN-d_3 was loaded into an NMR tube. 1,2,3,4-Tetrahydroisoquinoline (14.5 uL, 0.114 mmol, 6.0 equiv) was added, and the sample was frozen in a dry ice/acetone bath to prevent further reaction. The sample was quickly thawed prior to loading into a spectrometer already cooled to -40 °C. When relevant, percent yield was determined from quantitative ^{1}H NMR spectra (relaxation delay: 25 s) based on 1,3,5-trimethoxybenzene internal standard.

3.5.5. General Procedure for NMR time courses.

A solution of (a) phd (4.0 mg, 0.019 mmol), or (b) phd (4.0 mg, 0.019 mmol) and 0.5 equiv $Zn(OTf)_2$ (3.45 mg, 0.0095 mmol) in 1.0 mL MeCN-d_3 was loaded into an NMR tube. The sample was locked, tuned and shimmed in an NMR spectrometer already at -10 °C. The sample was quickly ejected, 1,2,3,4-tetrahydroisoquinoline (14.5 μL, 0.114 mmol, 6.0 equiv) was added, and the sample was re-injected into the spectrometer. Quantitative (1 scan) ^{1}H spectra were acquired every 60 or 120 seconds.

3.5.6. Procedures for aerobic reaction screening

In a disposable culture tube, 1,10-phenanthroline-5,6-dione (5 mol %, 0.065 mmol), ZnI_2 (2.5 mol %, 0.00325 mmol), and PPTS (15 mol %, 0.0195 mmol) were dissolved in 0.5 mL MeCN. 1,2,3,4-Tetrahydroisoquinoline or dibenzylamine (0.130 mmol) was added, and the reaction tube was placed into an aluminum block mounted on a Large Capacity Mixer (Glas-Col) that enabled several reactions to be performed simultaneously under a constant pressure of (approx.) 1 atm O_2 with orbital agitation. The headspace above the tubes was filled and purged with oxygen gas multiple times, and then left under constant pressure of O_2 for 24 h. Upon completion, the tube was removed and internal standard was added. The reaction solvents were removed, and the residue suspended in $CDCl_3$ and filtered through a short plug of Celite for NMR analysis.

3.5.7. Kinetic Isotope Effect Studies

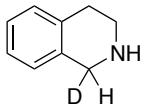

1-d$_1$

Mono-deuterated 1,2,3,4-tetrahydroisoquinoline, **1**-d_1, was prepared with >99:1 deuterium incorporation according to the literature procedure.[28]

Stoichiometric Reactions: Quinone-mediated oxidation

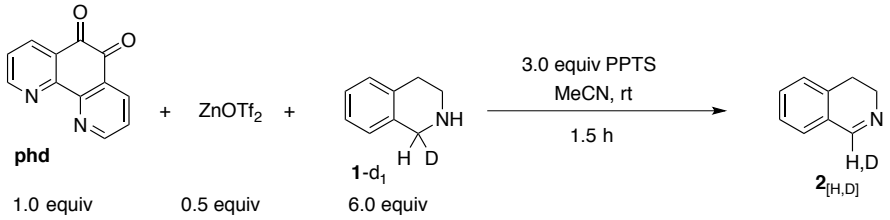

after 1.5 h, 80% yield: KIE = **6.4 ± 0.14**

To a solution containing 1.0 equiv phd (10.0 mg, 0.047 mmol), 0.5 equiv $Zn(OTf)_2$ (8.6 mg, 0.023 mmol) and 3.0 equiv PPTS (35.6 mg, 0.141 mmol) in 2.5 mL MeCN was added 6.0 equiv **1**-d_1 (36 μL, 0.284 mmol). After 1.5 h, a stock solution of 1,3,5-trimethoxybenzene was added and the reaction was concentrated, resuspended in $CDCl_3$, and filtered through a celite plug into an NMR tube. Quantitiative NMR analysis showed the reaction yield to be 80% based on **phd**. The intrinsic KIE was determined to be 6.4 +/- 0.14 (mean +/- s.e.m.) based on three independent experiments.

Stoichiometric Reactions: Iodine/Triiodide-mediated oxidation.

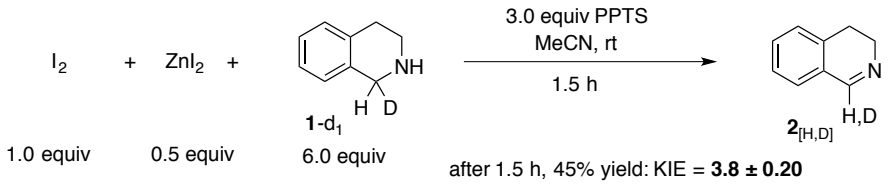

To a solution containing 1.0 equiv I_2 (12.1 mg, 0.047 mmol), 0.5 equiv ZnI_2 (7.6 mg, 0.023 mmol) and 3.0 equiv PPTS (35.6 mg, 0.141 mmol) in 2.5 mL MeCN was added 6.0 equiv **1**-d_1 (36 μL, 0.284 mmol). After 1.5 h a stock solution of 1,3,5-trimethoxybenzene was added to the reaction mixture and the reaction was diluted with EtOAc and washed with a saturated solution of sodium thiosulfate. The organic phase was dried, concentrated and redissolved in $CDCl_3$ for NMR. Quantitiative NMR analysis showed the reaction yield to be 45% based on **phd.** The intrinsic KIE was determined to be 3.8 +/- 0.20 (mean +/- s.e.m.) based on five independent experiments.

Catalytic Reactions: Optimized aerobic conditions.

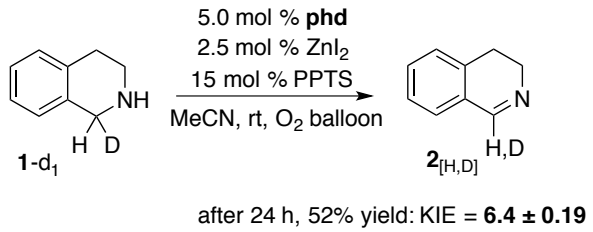

To a solution containing 5 mol % phd (4.14 mg, 0.0195 mmol), 2.5 mol % ZnI_2 (3.14 mg, 0.00975 mmol), and 15 mol % PPTS (14.9 mg, 0.585 mmol) in 1.6 mL MeCN containing 1,3,5-trimethoxybenzene and under an O_2 atmosphere (balloon) was added **1**-d_1 (50 μL, 0.39 mmol). After 24 h the reaction was concentrated, redissolved in $CDCl_3$, and filtered through a Celite

plug. Quantitiative NMR analysis showed the reaction yield to be 52% based on **1** (>10 catalyst turnovers). The intrinsic KIE was determined to be 6.4 +/- 0.19 (mean +/- s.e.m.) based on three independent experiments. A sample run to earlier conversion, stopped after 7 h, was measured to have KIE = 6.5.

3.5.8. Procedures for catalytic secondary amine oxidation

Typical procedure for the oxidation of secondary amines is as follows. A 25 mL flask was charged with 1,10-phenanthroline-5,6-dione (10.5 mg, 0.05 mmol, 5 mol %) and amine substrate (1.0 mmol) and 3.0 mL anhydrous MeCN was added. The flask was flushed with O_2 and equipped with an O_2 balloon. A well-dissolved solution of ZnI_2 (7.98 mg, 0.025 mmol, 2.5 mol %) and pyridinium *p*-toluenesulfonic acid, PPTS (37.7 mg, 0.15 mmol, 15 mol %), in 1.0 mL anhydrous MeCN was then added. (Depending on the substrate, once ZnI_2 was added the mixture was observed to change color and/or form a heterogeneous component over the course of the reaction). The reaction was stirred vigorously at room temperature for 24 h or 48 h, or until TLC indicated completion.

Workup A: Following reaction completion, the mixture was concentrated by rotary evaporation, suspended in a minimum of chloroform, and directly chromatographed over SiO_2 using EtOAc/Hexanes or EtOAc.

Workup B: Following reaction completion, the mixture was diluted in 50 mL EtOAc and washed with 25 mL of 1M NaOH. The aqueous phase was extracted with additional EtOAc (2 x 25 mL). The combined organic phases were washed with 25 mL brine, dried over Na_2SO_4,

filtered, and concentrated. The reaction crude was then chromatographed over SiO_2 using EtOAc/Hexanes or EtOAc.

Figure 3.7. Variable Temperature stackplot of phd with 6.0 equiv **1** from 27 °C to -40 °C, resolving species **A** from the dynamic exchange of phd with **1**.

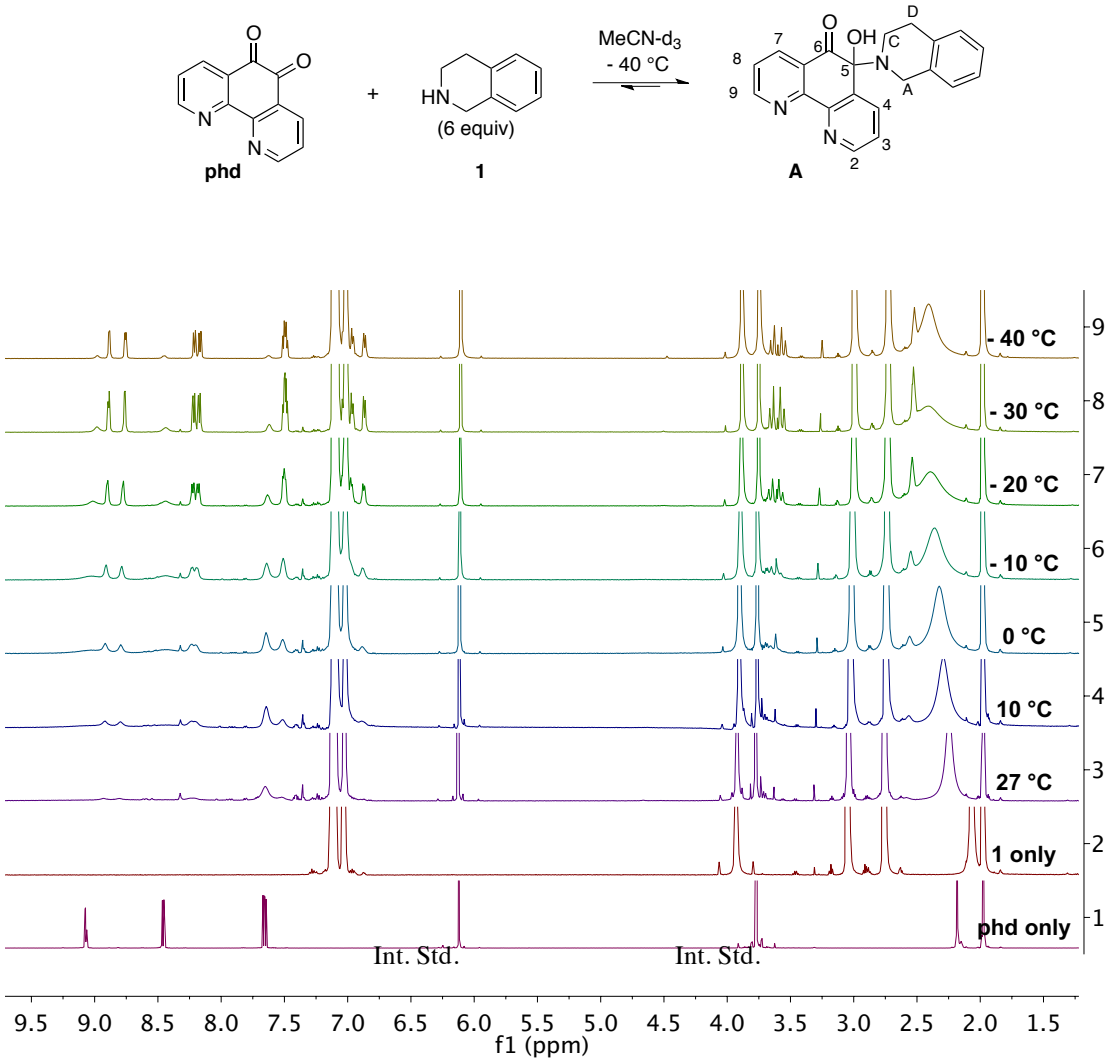

Figure 3.8. Characterization of Hemiaminal species, A ^{1}H NMR at -40 °C.

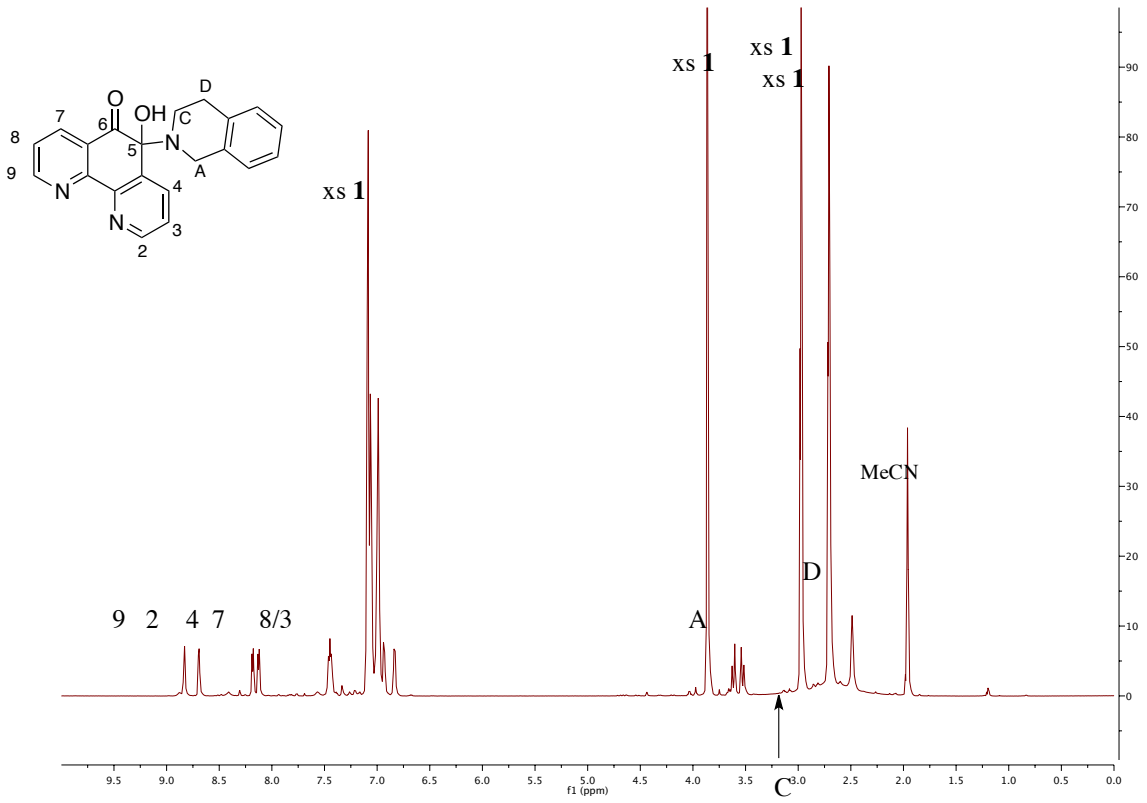

Figure 3.9. Characterization of Hemiaminal species, A ^{1}H – ^{13}C HSQC at -40 °C.

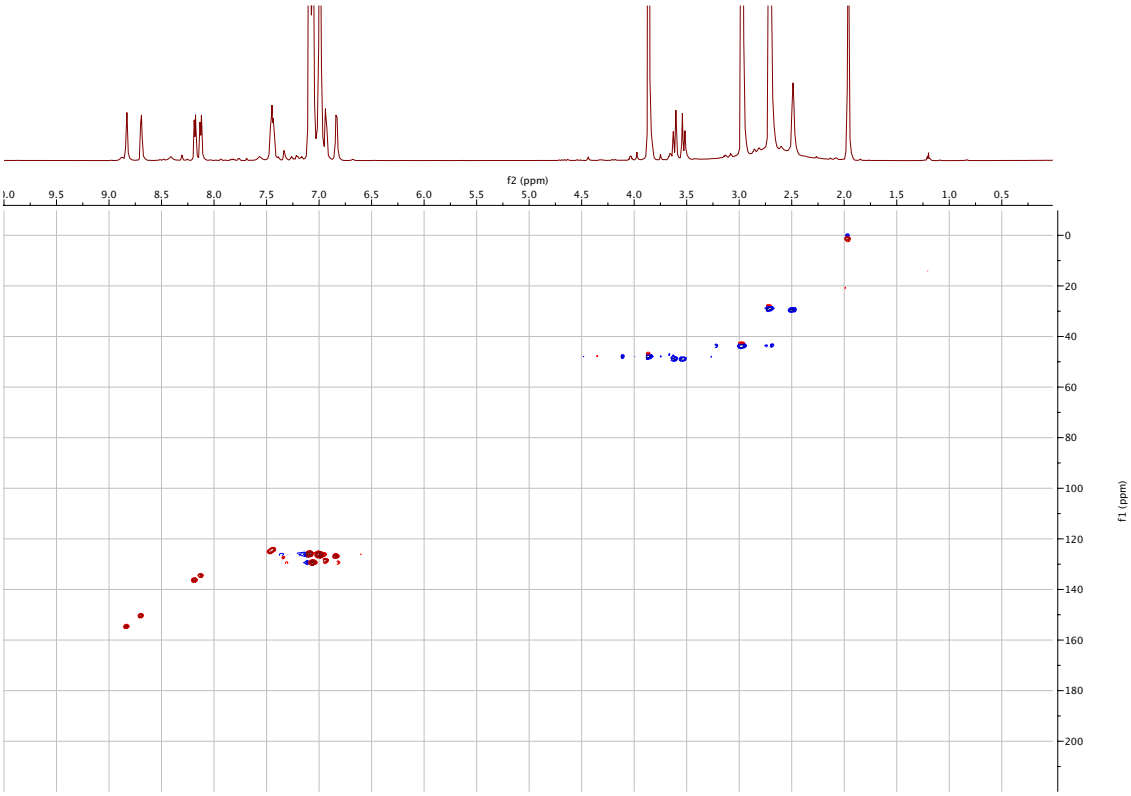

Figure 3.10. Characterization of Hemiaminal species, A ^{1}H-^{13}C HMBC at -40 °C.

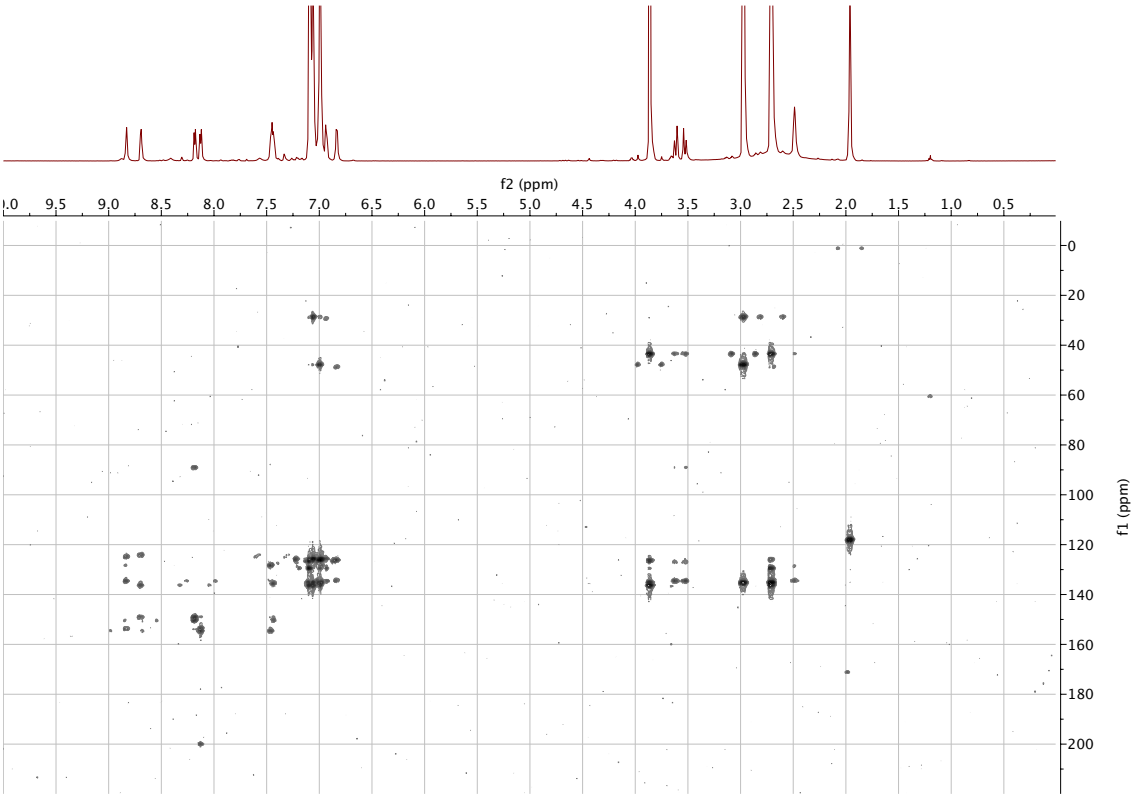

Figure 3.11. Characterization of Hemiaminal species, A ^{1}H-^{15}N HMBC at -40 °C.

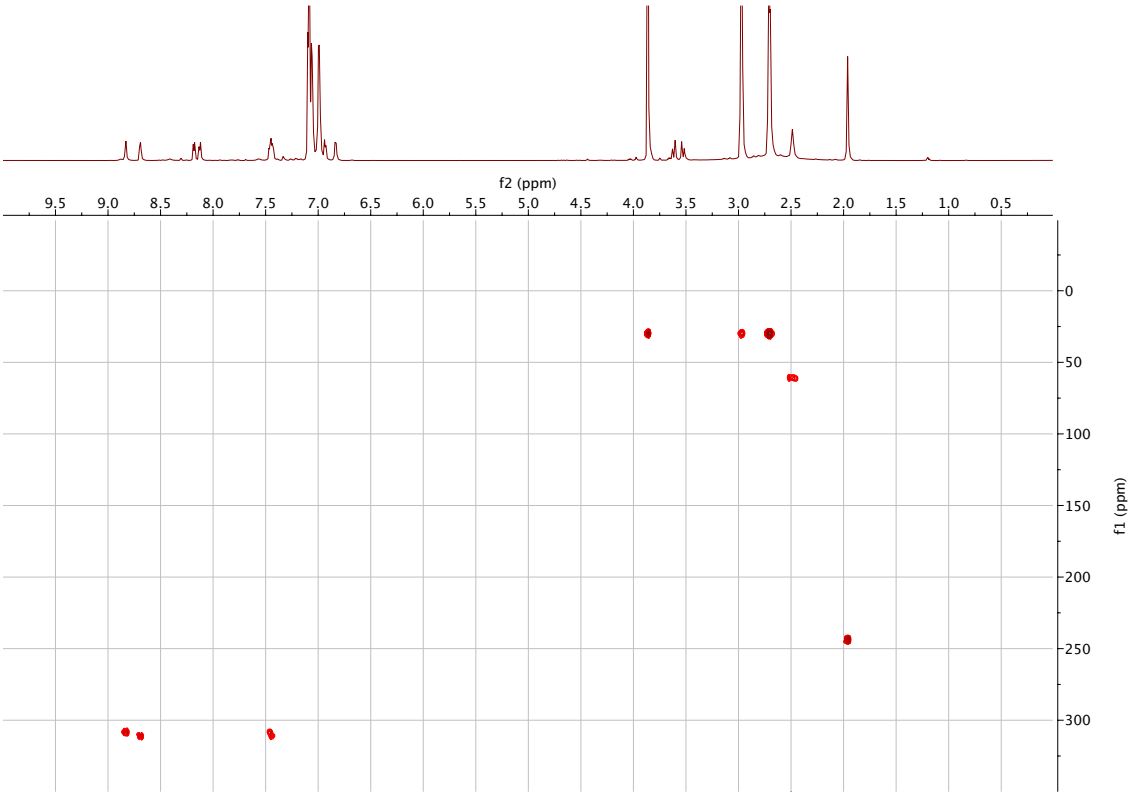

Figure 3.12. Characterization of Hemiaminal species, A 1D-NOESY at -40 °C.

Selective irradiation at 8.12 ppm, mix time 0.3 s. NOE is observed from 4 to 3, A and C. (NOTE: Positive NOE is also observed to free **1** due to the exchange of positively magnetized A/C in species **A** with free **1** – see exchange dynamics).

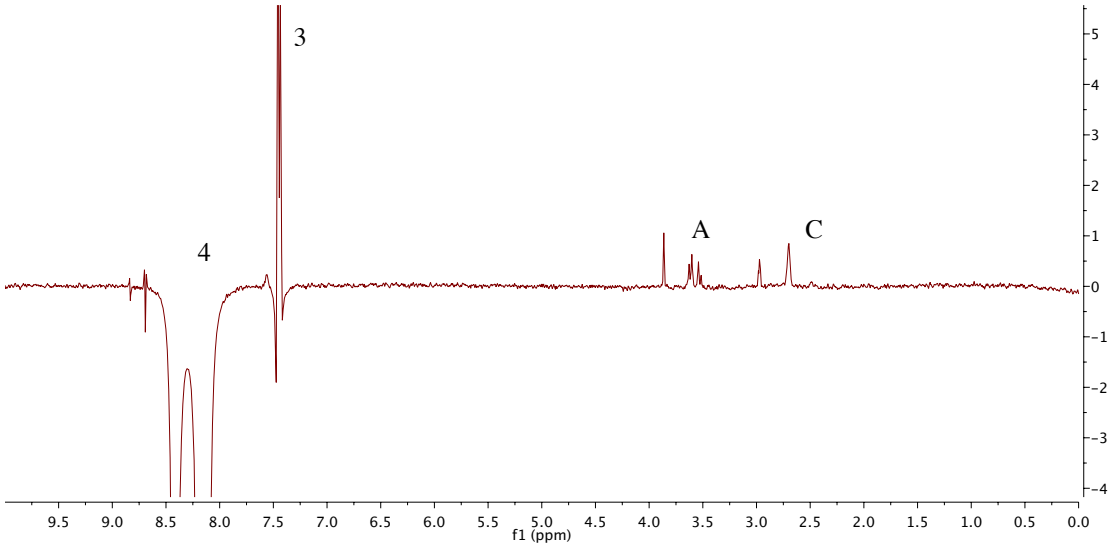

Figure 3.13. NMR titration of phd with 1, demonstrating equilibrium formation of Hemiaminal species, A ^{1}H-NMR stackplot at -40 °C.

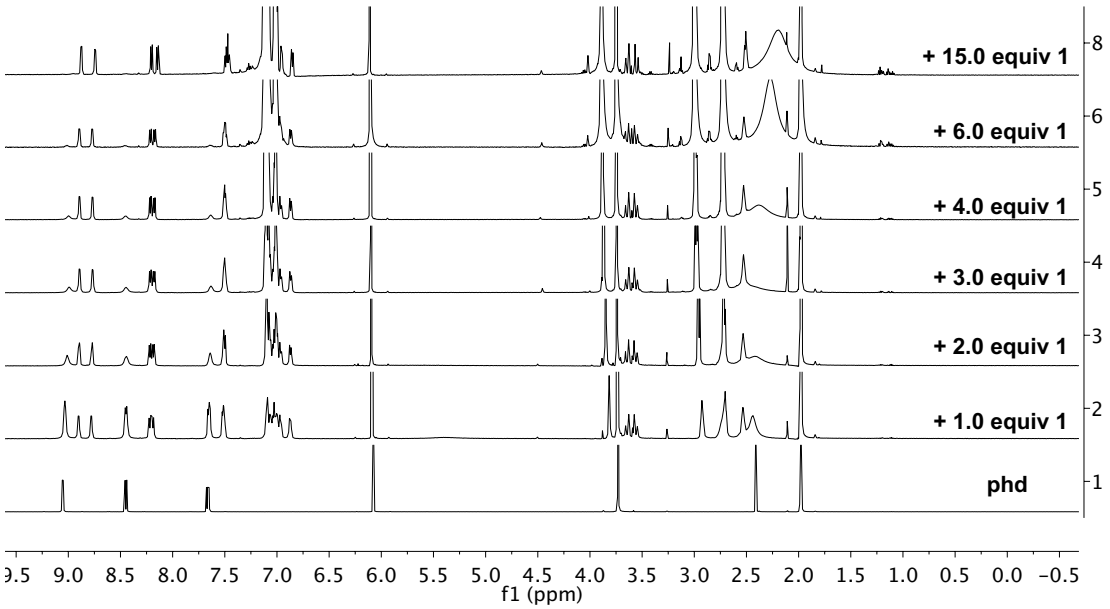

Figure 3.14. **Low Temperature Exchange Dynamics** EXSY-1D at -40 °C.

Selective irradiation at 3.88 ppm with arrayed mix time. Magnetization transfer from free **1** (*) to species **A** (A) indicates exchange.

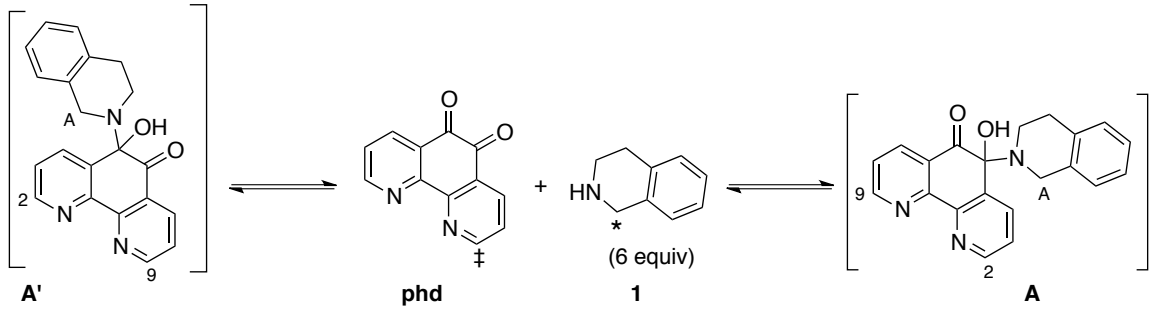

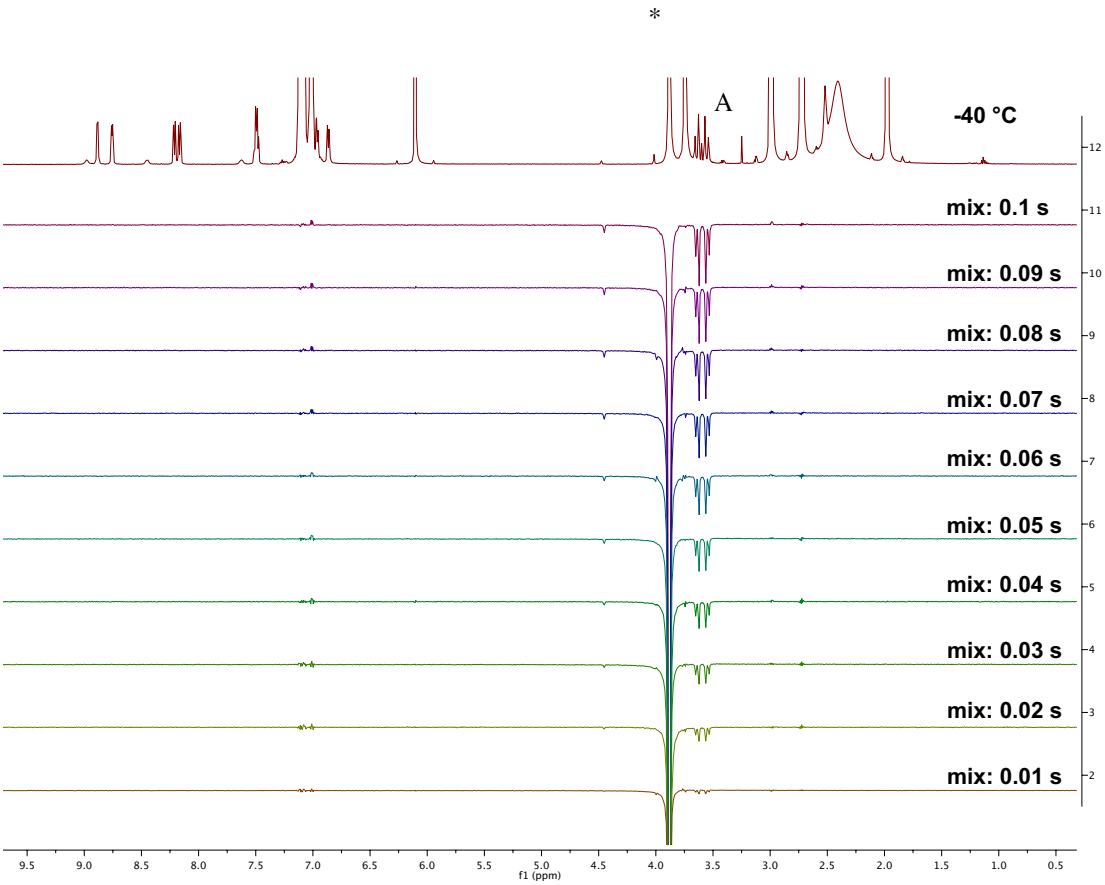

Figure 3.15. Low Temperature Exchange Dynamics EXSY-1D at -40 °C.

Selective irradiation at 8.12 ppm with arrayed mix time. Magnetization transfer from species **A** (2) to free phd (‡) to species **A'** (9) indicates exchange.

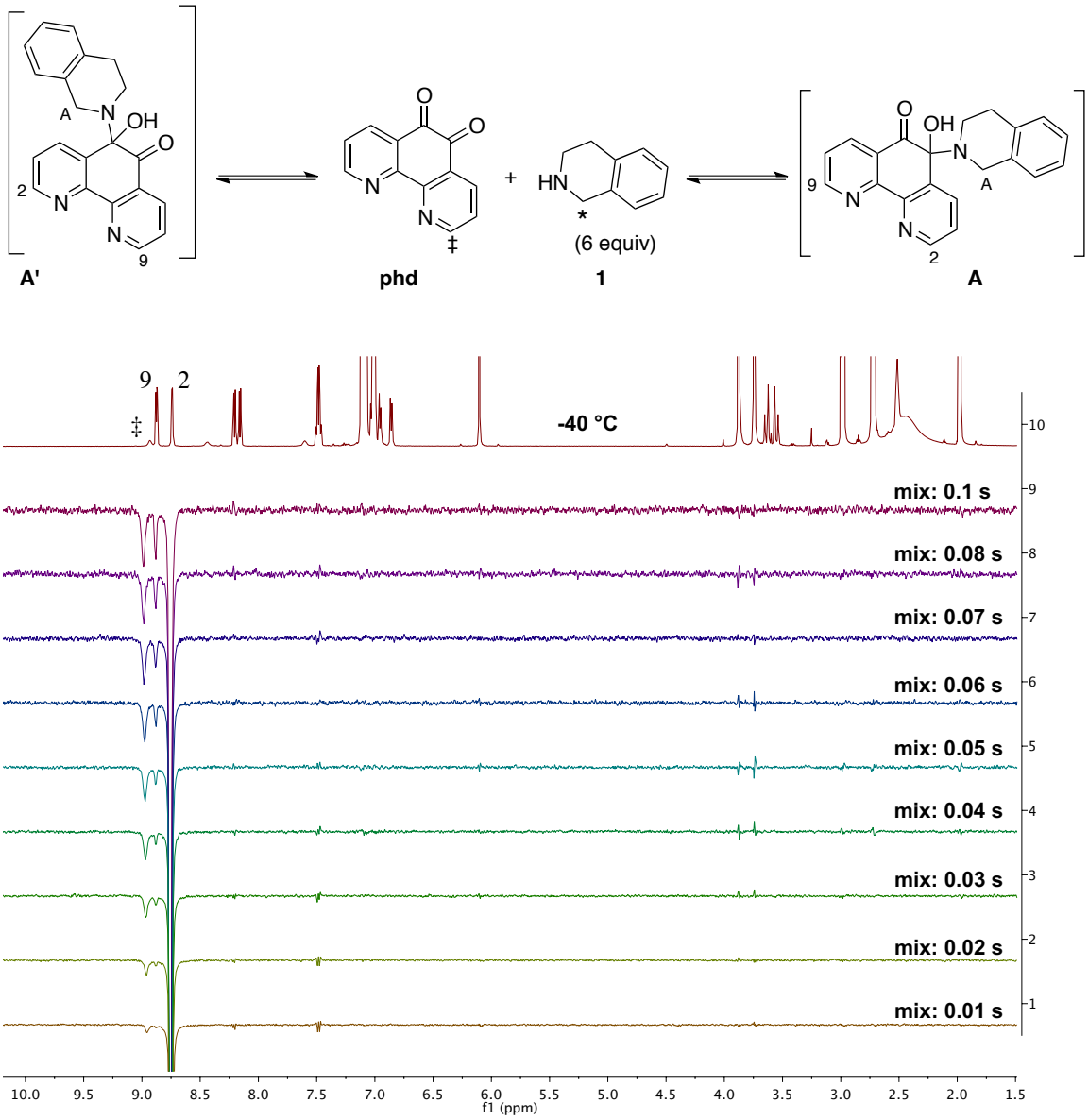

Figure 3.16. $Zn(OTf)_2$/phd NMR Titration stackplot and speciation plot.

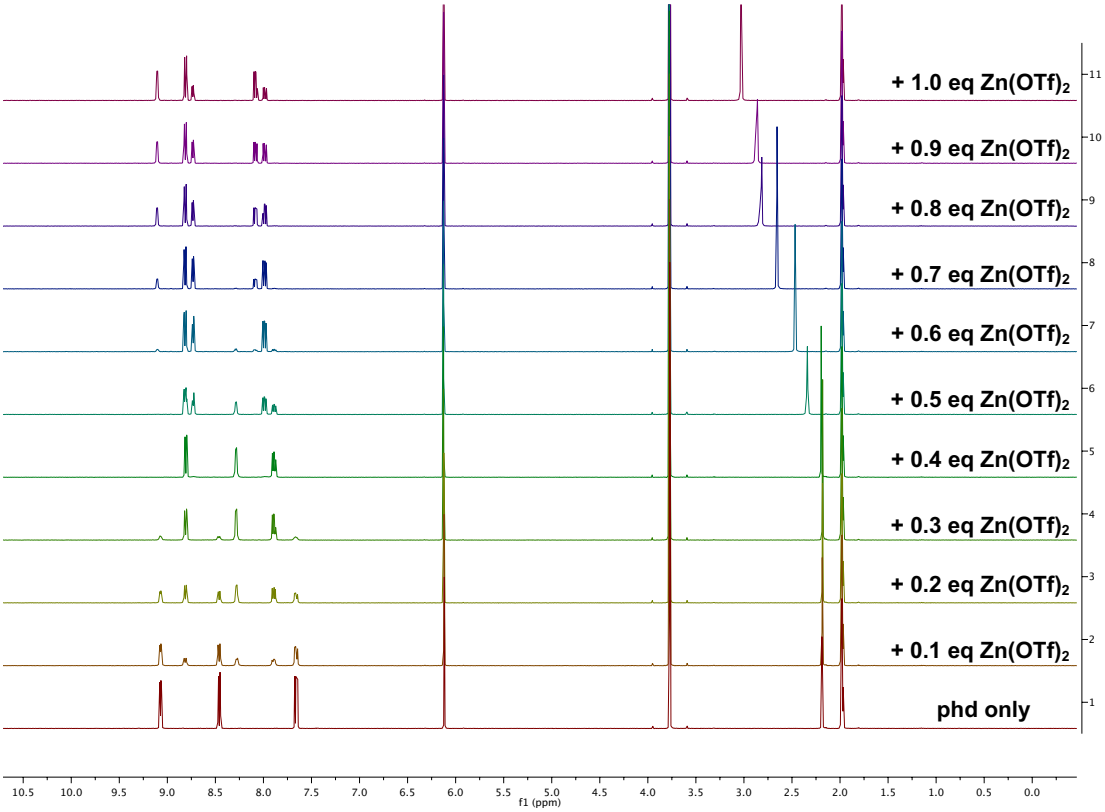

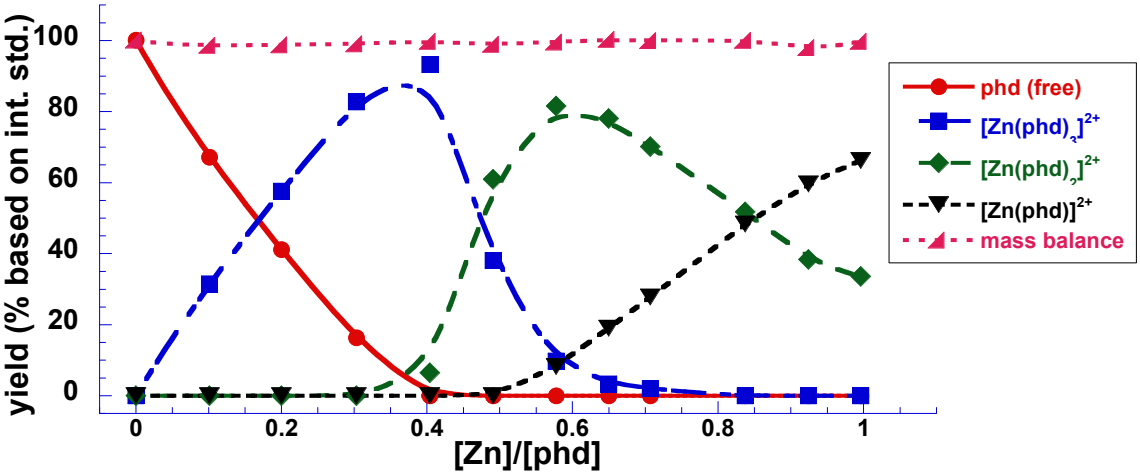

Figure 3.17. ^{1}H-^{15}N HMBC: $Zn(phd)_3OTf_2$ Indirect measurement of ^{15}N chemical shift of free phd is 251 ppm (vs NH_3)

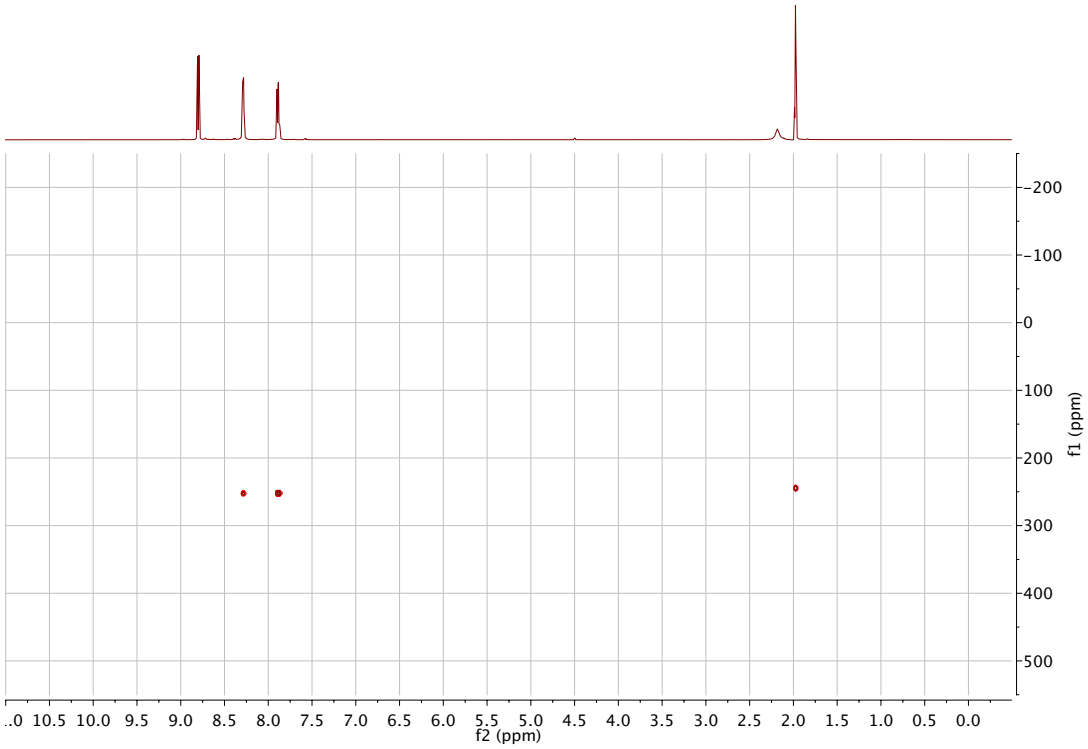

Figure 3.18. ^{1}H-^{15}N HMBC: phd only. Indirect measurement of ^{15}N chemical shift of free phd is 313 ppm (vs NH_3)

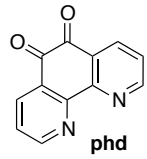

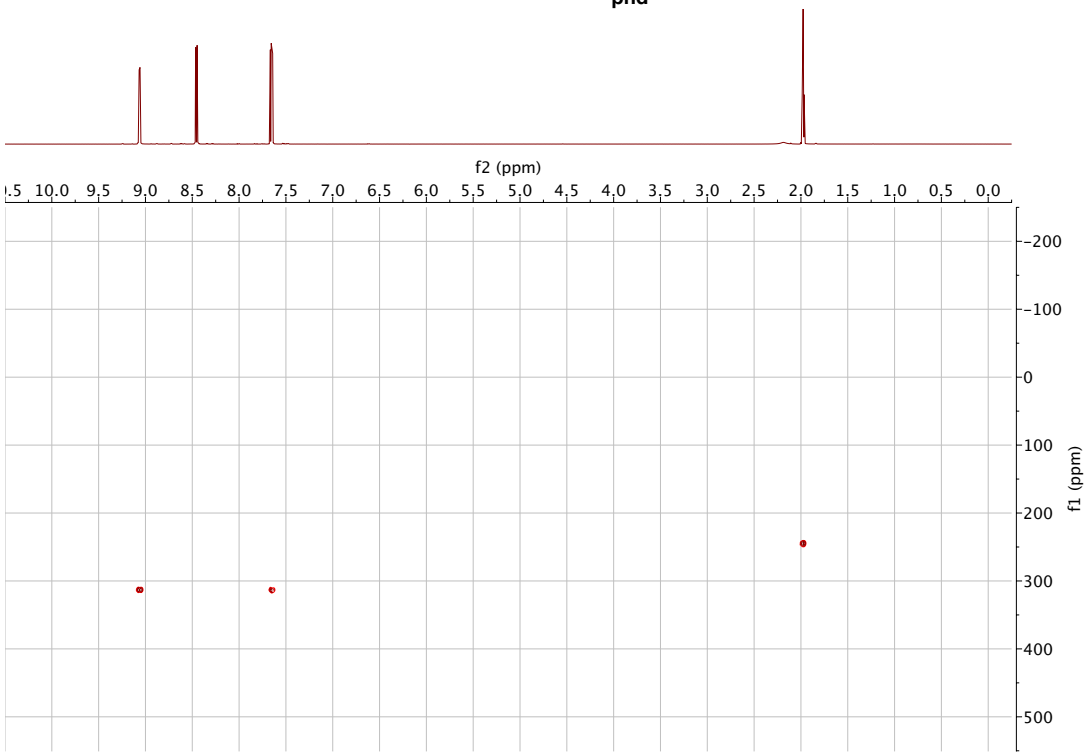

3.5.9. Synthesis of 1,10-phenanthroline-5,6-dione, *phd*

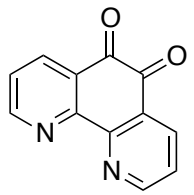

1,10-phenanthroline-5,6-dione, phd

The quinone catalyst, phd, was prepared from commercial 1,10-phenanthroline (Sigma Aldrich) according to the method of Eisenberg.[29] 1,10-phenanthroline (4.0 g, 22.0 mmol) and KBr (4.1 g, 34.4 mmol) were combined in a flask, and an ice-cooled mixture of H_2SO_4 (40 mL) and HNO_3 (20 mL) was slowly added to the solids. The mixture was heated to reflux for 3 h, and then dumped onto 500 mL ice. The yellow aqueous solution was carefully neutralized with NaOH to pH = 6 - 7, extracted into $CHCl_3$, dried over $MgSO_4$, and concentrated to give nearly quantitative 1,10-phenanthroline-5,6-dione. The yellow solids were recrystallized from ethanol to give pale yellow, flat needles (1.65 g, 35%): mp (EtOH): 263-264 °C; ^{1}H NMR (400 MHz, DMSO) δ 9.01 (dd, 2H, J = 4.8, 1.6 Hz), 8.40 (dd, 2H, J = 7.6, 1.6 Hz), 7.69 (dd, 2H, J = 7.6, 4.8 Hz); ^{13}C NMR (101 MHz, DMSO) δ 178.25, 154.83, 152.79, 136.16, 129.60, 125.72; EMM (ESI) Calc for $C_{12}H_6N_2O_2$ (M+H): 211.0503, found 211.0500. 1,10-phenanthroline-5,6-dione is also commercially available (Sigma Aldrich).

3.5.10 Synthesis and Characterization of Substrates

Acyclic Secondary Amines

Dibenzylamine was obtained from commercial sources (Sigma Aldrich) and was used as obtained, without further purification. Other acyclic secondary amines were synthesized by reductive amination, according to the literature method.[30]

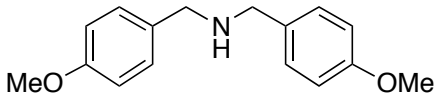

N,N-bis-(4-methoxybenzyl)amine

Synthesized according to the representative procedure to give a colorless oil whose spectroscopic data matched those previously reported:[31] ^{1}H NMR (400 MHz, $CDCl_3$) d 7.29 (d, *J* = 8.6 Hz, 1H), 6.91 (d, *J* = 8.6 Hz, 1H), 3.84 (s, 6H), 3.77 (s, 4H), 1.55 (s, 1H); ^{13}C NMR (101 MHz, $CDCl_3$) d 158.61, 132.58, 129.34, 113.78, 55.30, 52.51.

Tetrahydroisoquinolines

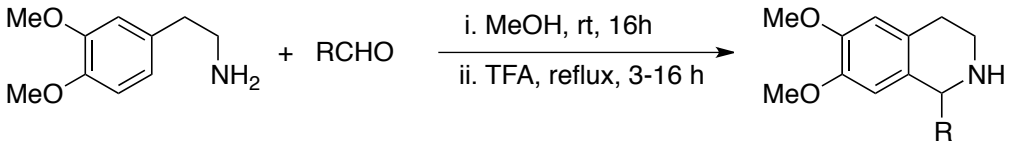

1,2,3,4-tetrahydroisoquinoline was obtained from commercial sources (Sigma Aldrich) and was used without further purification. 6,7-dimethoxy-1,2,3,4-tetrahydroisoquinoline was prepared by basification of an aqueous solution of 6,7-dimethoxy-1,2,3,4-tetrahydroisoquinoline hydrochloride (available from Sigma Aldrich) and extraction of the neutralized compound into organic solvent. 1-substituted tetrahydroisoquinolines were prepared according to the following representative procedure.

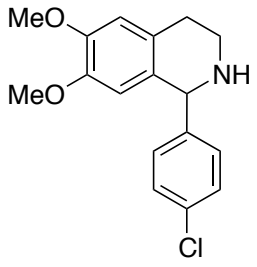

1-(4-chlorophenyl)-1,2,3,4-tetrahydro-6,7-dimethoxyisoquinoline

Representative Procedure for Imine Formation: 4-Chlorobenzaldehyde (2.5 g, 17.8 mmol) was dissolved in 100 mL MeOH, and 3,4-dimethoxyphenethylamine (3.0 mL, 17.8 mmol) was added. The reaction was stirred at room temperature for 16 h, forming a white precipitate over this time. The white solids were collected by vacuum filtration, rinsed with 5 mL MeOH, and dried to afford the desired imine as a fine white solid (4.29 g, 79% yield). The filtrate was concentrated, and the remaining solids were suspended in a minimum of methanol, and similarly collected to give an additional 0.548 g, or 89.6% combined yield of the corresponding imine: ^{1}H NMR (500 MHz, $CDCl_3$) δ 8.09 (s, 1H), 7.65 (d, J = 8.4 Hz, 2H), 7.39 (d, J = 8.4 Hz, 2H), 6.6-6.8 (m, 3H), 3.8-3.9 (m, 8H), 2.97 (t, J = 7.2 Hz, 2H); ^{13}C NMR (126 MHz, $CDCl_3$) δ 160.12, 148.62, 147.36, 136.53, 134.66, 132.40, 129.19, 128.88, 120.86, 112.41, 111.12, 63.33, 55.89, 55.73, 36.93. [In some instances, when imine products did not precipitate from solution, the solvents were evaporated and the residue triturated with - or recrystallized from - hexanes, diethyl ether, EtOH, or another suitable solvent].

Representative Procedure for Pictet-Spengler: The thus obtained imine (1.67 g, 5.5 mmol) was dissolved in TFA (10 mL) and heated to reflux for 3 h, or until TLC indicated completion. The reaction was cooled, diluted with water and the solution basified by the addition of 1M

NaOH. The aqueous solution was extracted (3 x 75 mL EtOAc or CH_2Cl_2), dried over $MgSO_4$, and concentrated to give 1.67 g of the title compound as a white solid whose spectroscopic data match those previously reported:[32] ^{1}H NMR (500 MHz, $CDCl_3$) δ 7.30 (d, *J* = 8.1 Hz, 2H), 7.22 (d, *J* = 8.2 Hz, 2H), 6.65 (s, 1H), 6.22 (s, 1H), 5.05 (s, 1H), 3.89 (s, 3H), 3.67 (s, 3H), 3.20 (dt, *J* = 11.2, 5.2 Hz, 1H), 3.06 (ddd, *J* = 12.5, 8.5, 4.9 Hz, 1H), 2.94 (dd, *J* = 12.3, 5.9 Hz, 1H), 2.6-2.85 (m, 1H), 2.26 (s, 1H); ^{13}C NMR (126 MHz, $CDCl_3$) δ 147.76, 147.13, 143.25, 133.14, 130.31, 129.16, 128.55, 127.59, 111.45, 110.70, 60.74, 55.88, 55.85, 41.79, 29.14.

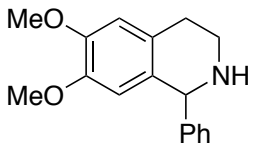

1-phenyl-1,2,3,4-tetrahydro-6,7-dimethoxyisoquinoline

Spectroscopic data match those previously reported.[33] ^{1}H NMR (400 MHz, $CDCl_3$) d 7.1-7.5 (m, 5H), 6.63 (s, 1H), 6.25 (s, 1H), 5.05 (s, 1H), 3.87 (s, 3H), 3.63 (s, 3H), 3.22 (dt, *J* = 12.1, 5.2 Hz, 1H), 3.05 (ddd, *J* = 12.3, 8.2, 4.6 Hz, 1H), 2.93 (ddd, *J* = 14.0, 8.2, 5.3 Hz, 1H), 2.75 (dt, *J* = 16.0, 4.9 Hz, 1H), 1.87 (br s, NH); ^{13}C NMR (101 MHz, $CDCl_3$) d 147.61, 147.05, 144.90, 129.87, 128.91, 128.41, 127.68, 127.37, 111.42, 110.96, 61.49, 55.87, 55.86, 41.90, 29.35.

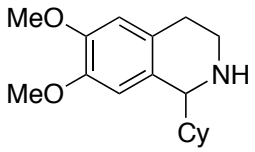

1-cyclohexyl-1,2,3,4-tetrahydro-6,7-dimethoxyisoquinoline

Spectroscopic data match those previously reported.[33] ^{1}H NMR (400 MHz, $CDCl_3$) d 6.64 (s, 1H), 6.56 (s, 1H), 3.87 (s, 3H), 3.83 (s, 3H), 3.26 (ddd, *J* = 12.1, 5.2, 3.6 Hz, 1H), 2.90 (ddd, *J* = 12.1, 9.8, 4.2 Hz, 1H), 2.76 (ddd, *J* = 15.4, 9.8, 5.3 Hz, 1H), 2.58 (dt, *J* = 15.8, 4.0 Hz, 1H), 1.5-2.0 (m,

6H), 1.0-1.5 (m, 6H); ^{13}C NMR (101 MHz, $CDCl_3$) d 147.09, 147.06, 130.27, 128.40, 111.71, 109.29, 60.40, 56.10, 55.81, 43.27, 42.50, 30.93, 29.83, 27.09, 26.72, 26.61, 26.38.

1,2,3,4-Tetrahydro-β-carbolines

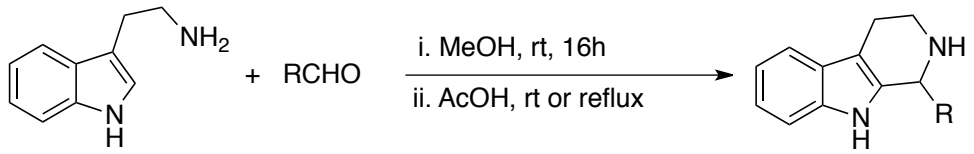

Tetrahydro-b-carbolines were prepared from tryptamine using the general procedure outlined for the preparation of tetrahydroisoquinolines with the modifications described below.

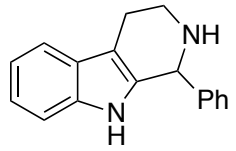

1-phenyl-1,2,3,4-tetrahydro-β-carboline

Representative Procedure for Pictet-Spengler: Following imine formation as indicated above, *N*-benzylidene tryptamine (2.0 g, 8.0 mmol) was dissolved in 20 mL AcOH, and brought to reflux for 30 min. The reaction was cooled, diluted with water, neutralized with 1M NaOH, and extracted into EtOAc (3 x 75 mL). The organic phases were combined, washed with brine, and then dried with Na_2SO_4 to give 1.96 g (7.89 mmol, 98% yield) of the title compound. Spectroscopic data match those previously reported.[33] ^{1}H NMR (400 MHz, $CDCl_3$) δ 7.5-7.6 (m, 2H), 7.28-7.4 (m, 5H), 7.2-7.25 (m, 1H), 7.07-7.17 (m, *J* = 7.1, 5.5 Hz, 2H), 5.17 (t, *J* = 1.8 Hz,

1H), 3.38 (ddd, J = 12.5, 5.3, 3.7 Hz, 1H), 3.15 (ddd, J = 12.9, 8.9, 4.7 Hz, 1H), 2.7-3.0 (m, 2H), 1.85 (br s, NH); ^{13}C NMR (101 MHz, $CDCl_3$) δ 141.85, 135.86, 134.55, 128.85, 128.51, 128.21, 127.43, 121.74, 119.42, 118.26, 110.84, 110.27, 58.20, 42.98, 22.59; EMM (ESI) Calc for $C_{17}H_{15}ClN_2$ (M+H): 247.1230, found 247.1224.

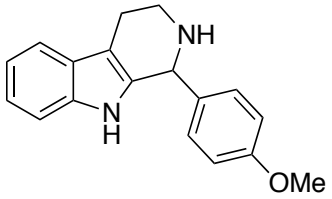

1-(4-methoxyphenyl)-1,2,3,4-tetrahydro- β -carboline

Spectroscopic data match those previously reported.[33] ^{1}H NMR (400 MHz, $CDCl_3$) δ 7.98 (s, 1H), 7.5-7.6 (m, 1H), 7.0-7.25 (m, 5H), 6.86 (d, J = 8.3 Hz, 2H), 5.06 (s, 1H), 3.80 (s, 3H), 3.33 (dt, J = 12.5, 4.5 Hz, 1H), 3.10 (ddd, J = 12.9, 8.8, 4.8 Hz, 1H), 2.7-3.0 (m, 2H), 1.78 (s, 1H); ^{13}C NMR (101 MHz, $CDCl_3$) δ 159.49, 135.91, 134.90, 134.03, 129.71, 127.44, 121.64, 119.32, 118.21, 114.13, 110.90, 110.08, 57.45, 55.38, 42.83, 22.59; EMM (ESI) Calc for $C_{18}H_{18}N_2O$ (M+H): 279.1492, found 279.1482.

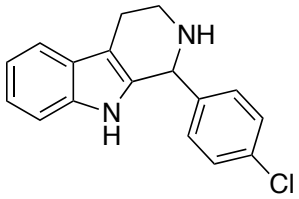

1-(4'-chlorophenyl)-1,2,3,4-tetrahydro- β -carboline

Prepared according to the representative procedure with the following modifications: the reaction was stirred at room temperature for 1.5 h. Spectroscopic data match those previously reported.[34] ^{1}H NMR (400 MHz, $CDCl_3$) δ 7.74 (s, NH), 7.59 (d, J = 8.4 Hz, 1H), 7.3-7.4 (m, 2H), 7.0-7.3 (m,

5H, overlaps with $CDCl_3$ residual peak), 5.14 (t, *J* = 1.8 Hz, 1H), 3.36 (dt, *J* = 12.6, 4.6 Hz, 1H), 3.16 (ddd, *J* = 12.8, 8.6, 4.8 Hz, 1H), 2.75-3.0 (m, 2H), 1.91 (br s, NH); ^{13}C NMR (101 MHz, $CDCl_3$) δ 140.40, 135.93, 134.01, 133.87, 129.92, 128.98, 127.33, 121.94, 119.54, 118.35, 110.91, 110.45, 57.39, 42.68, 22.50; EMM (ESI) Calc for $C_{17}H_{15}ClN_2$ (M+H): 283.0997, found 283.0995.

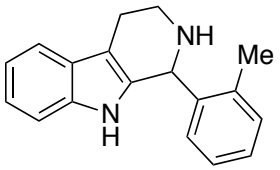

1-(2-methylphenyl)-1,2,3,4-tetrahydro-β-carboline

This compound has been previously reported.[35] ^1H NMR (400 MHz, $CDCl_3$) δ 8.11 (br s, NH), 7.62 (dd, *J* = 5.7, 3.1 Hz, 1H), 7.3-7.4 (m, 3H), 7.15- 7.3 (m, 3H, overlaps with $CDCl_3$ residual peak), 7.06 (d, *J* = 7.6 Hz, 1H), 5.39 (t, *J* = 1.8 Hz, 1H), 3.33 (dt, *J* = 12.7, 4.7 Hz, 1H), 3.13 (ddd, *J* = 12.9, 8.4, 4.9 Hz, 1H), 2.8-3.0 (m, 2H), 2.48 (s, 3H), 1.64 (br s, NH); ^{13}C NMR (101 MHz, $CDCl_3$) δ 139.59, 137.13, 135.94, 134.79, 131.07, 128.89, 128.04, 127.44, 126.25, 121.62, 119.34, 118.15, 110.93, 110.42, 54.71, 42.73, 22.68, 19.12; EMM (ESI) Calc for $C_{18}H_{18}N_2$ (M+H): 263.1543, found 263.1533.

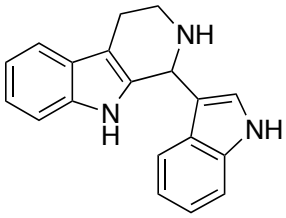

1-(indol-3-yl)-1,2,3,4-tetrahydro-β-carboline

Synthesized according to the literature method.[36] A suspension of tryptamine (2.0 g, mmol) and indole-3-carboxaldehyde (1.99 g, mmol) in 5 mL toluene was heated to reflux for 1 h. After this time, the solvents were removed in vacuo, and the viscous residue dissolved in 20 mL $CHCl_3$. Trifluoroacetic acid (10 mL) was added, and the reaction was stirred for 24 h. The reaction was then neutralized by the addition of Na_2CO_3 (aq) and extracted into $CHCl_3$ (3 x 100 ml). The combined organic phases were dried over $NaSO_4$, concentrated, and chromatographed to afford a pale yellow solid, mp: decomposed at 170 °C; ^{1}H NMR (500 MHz, DMSO-d_6) d 10.99 (s, 1H), 10.39 (s, 1H), 7.44 (d, *J* = 7.5 Hz, 1H), 7.37 (dd, *J* = 7.8, 2.6 Hz, 2H), 7.20 (d, *J* = 7.7 Hz, 1H), 7.16 (d, *J* = 2.4 Hz, 1H), 7.05 (t, *J* = 7.5 Hz, 1H), 6.97 (p, *J* = 7.1 Hz, 2H), 6.88 (t, *J* = 7.5 Hz, 1H), 5.44 (s, 1H), 3.20 (dd, *J* = 11.0, 6.0 Hz, 1H), 3.00 (ddd, *J* = 12.4, 7.6, 4.7 Hz, 1H), 2.80 (q, *J* = 7.4, 6.3 Hz, 1H), 2.6-2.7 (m, 1H); ^{13}C NMR (126 MHz, DMSO-d_6) d 137.02, 136.67, 136.20, 127.44, 126.84, 124.87, 121.42, 120.66, 119.93, 118.78, 118.48, 117.89, 116.30, 111.85, 111.49, 107.92, 50.16, 42.41, 22.82; Calc for $C_{19}H_{17}N_3$ (M+H): 288.1496, found 288.1495.

Tetrahydroquinazolines

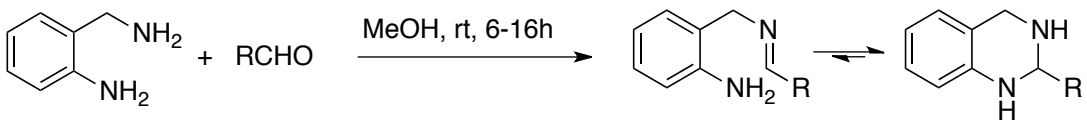

Tetrahydroquinazolines were prepared by condensation of 2-aminobenzylamine with the corresponding aldehyde in MeOH, according to the representative procedure for imine formation, above. Tetrahydroquinazolines exhibit ring-chain tautomerism, resulting in NMR spectra that reflect an equilibrium mixture of species. NMR peak data is given only for the major, ring tautomer unless otherwise indicated.

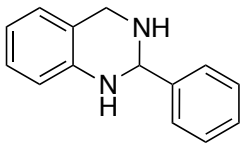

2-phenyl-1,2,3,4-tetrahydroquinazoline

Spectroscopic data match those previously reported.[37] Ratio of Ring to Chain ($CDCl_3$): 15:1; ^{1}H NMR (400 MHz, $CDCl_3$) d 7.56 (m, *J* = 8.8 Hz, 2H), 7.3-7.5 (m, 3H), 7.10 (t, *J* = 7.7 Hz, 1H), 6.99 (d, *J* = 7.4 Hz, 1H), 6.77 (t, *J* = 7.4 Hz, 1H), 6.63 (d, *J* = 7.9 Hz, 1H), 5.29 (s, 1H), 4.32 (d, *J* = 16.6 Hz, 1H), 4.04 (d, *J* = 16.7 Hz, 1H), 3.48 (s, 3H); ^{13}C NMR (126 MHz, $CDCl_3$) d 143.70, 141.49, 128.78, 128.60, 127.33, 126.63, 126.26, 121.20, 118.22, 115.06, 69.60, 46.45.

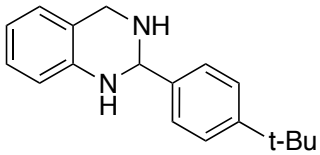

2-(4-tert-butylphenyl)-1,2,3,4-tetrahydroquinazoline

Ratio of Ring to Chain: 13:1 ($CDCl_3$); mp: 119-122 °C; ^{1}H NMR (400 MHz, $CDCl_3$) d 7.4-7.5 (m, 5H), 7.10 (t, *J* = 7.3 Hz, 1H), 6.99 (d, *J* = 7.4 Hz, 1H), 6.77 (t, *J* = 7.4 Hz, 1H), 6.62 (d, *J* = 8.0 Hz, 1H), 5.26 (s, 1H), 4.31 (d, *J* = 16.6 Hz, 1H, overlaps with broad peak at 4.24), 4.24 (br s, 1H), 4.04 (d, *J* = 16.6 Hz, 1H), 2.05 (br s, 1H), 1.38 (s, 9H); ^{13}C NMR (126 MHz, $CDCl_3$) d 151.59, 143.86, 138.66, 127.27, 126.27, 126.24, 125.68, 121.31, 118.10, 115.03, 69.44, 46.65, 34.65, 31.38. EMM (ESI) Calc for $C_{18}H_{22}N_2$ (M+H): 267.1856, found 267.1844.

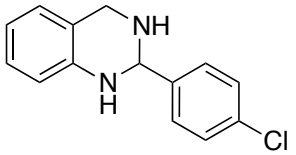

2-(4-chlorophenyl)-1,2,3,4-tetrahydroquinazoline

Spectroscopic data match those previously reported.[37] Ratio of Ring to Chain ($CDCl_3$): 13:1; ^{1}H NMR (400 MHz, $CDCl_3$) d 7.50 (d, *J* = 8.3 Hz, 2H), 7.40 (d, *J* = 8.3 Hz, 2H), 7.10 (t, *J* = 8.0 Hz, 1H), 6.98 (d, *J* = 7.4 Hz, 1H), 6.77 (td, *J* = 7.5, 1.2 Hz, 1H), 6.63 (d, *J* = 7.9 Hz, 1H), 5.26 (s, 1H), 4.26 (d, *J* = 16.7 Hz, 1H), 3.99 (d, *J* = 16.7 Hz, 1H); ^{13}C NMR (126 MHz, $CDCl_3$) d 143.37, 140.15, 134.20, 128.88, 128.12, 127.38, 126.26, 121.28, 118.42, 115.17, 68.86, 46.15.

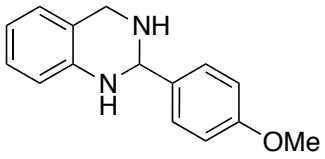

2-(4-methoxyphenyl)-1,2,3,4-tetrahydroquinazoline

Spectroscopic data match those previously reported.[37] Ratio of Ring to Chain ($CDCl_3$): 6:1; ^{1}H NMR (400 MHz, $CDCl_3$) d 7.47 (d, *J* = 8.5 Hz, 2H), 7.09 (t, *J* = 7.6 Hz, 1H), 6.9-7.0 (m, 3H), 6.76 (t, *J* = 7.4 Hz, 1H), 6.61 (d, *J* = 8.0 Hz, 1H), 5.22 (s, 1H), 4.30 (d, *J* = 16.6 Hz, 1H), 4.22 (br s, 1H), 4.02 (d, *J* = 16.6 Hz, 1H), 3.86 (s, 3H), 1.97 (br s, 1H); ^{13}C NMR (126 MHz, $CDCl_3$) d 159.71, 143.86, 133.93, 127.78, 127.26, 126.23, 121.26, 118.10, 115.02, 114.05, 69.21, 55.36, 46.60.

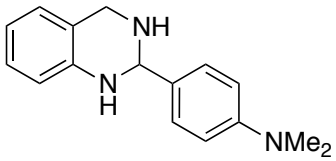

2-(4-N,N-dimethylaminophenyl)-1,2,3,4-tetrahydroquinazoline

Spectroscopic data match those previously reported.[37] Ratio of Ring to Chain ($CDCl_3$): 2:1; ^{1}H NMR (400 MHz, $CDCl_3$) d 8.26 (s, 1H chain tautomer), 7.65 (d, *J* = 8.8 Hz, 2H chain tautomer), 7.41 (d, *J* = 8.6 Hz, 2H ring tautomer), 7.05-7.15 (m, 1H ring tautomer + 1H chain tautomer), 6.98 (d, *J* = 7.4 Hz, 2H chain tautomer), 6.8-6.65 (m, 4H ring tautomer + 3H chain tautomer), 6.60 (d, *J* = 7.9 Hz, 1H, ring tautomer), 5.20 (s, 1H ring tautomer), 4.74 (s, 2H chain tautomer), 4.32 (d, *J* = 16.6 Hz, 1H ring tautomer), 4.19 (s, 1H ring tautomer), 4.04 (d, *J* = 16.5 Hz, 1H ring tautomer), 3.05 (s, 6H chain tautomer), 3.00 (s, 6H ring tautomer). ^{13}C NMR (126 MHz, $CDCl_3$) d 161.17, 152.13, 150.79, 145.93, 144.10, 129.66, 129.50, 129.15, 128.21, 127.34, 127.19, 126.21, 125.11, 124.24, 121.24, 118.16, 117.87, 115.84, 114.91, 112.55, 111.61, 111.55, 69.40, 63.68, 46.81, 40.65, 40.24 (includes both ring and chain tautomers).

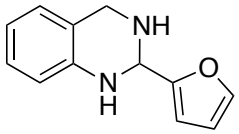

2-(furan-2-yl)-1,2,3,4-tetrahydroquinazoline

Spectroscopic data match those previously reported.[38] Ratio of Ring to Chain ($CDCl_3$): 18:1; ^{1}H NMR (400 MHz, $CDCl_3$) d 7.45 (t, *J* = 1.2 Hz, 1H), 7.09 (td, *J* = 7.7, 1.5 Hz, 1H), 6.95 (dd, *J* = 7.6, 1.5 Hz, 1H), 6.77 (td, *J* = 7.4, 1.2 Hz, 1H), 6.61 (dd, *J* = 8.0, 1.2 Hz, 1H), 6.35-6.5 (m, 2H), 5.34 (s, 1H), 4.40 (s, 1H), 4.18 (d, *J* = 16.7 Hz, 1H), 3.96 (d, *J* = 16.7 Hz, 1H), 2.07 (s, 1H); ^{13}C NMR (101 MHz, $CDCl_3$) d 154.12, 142.89, 142.35, 127.35, 126.23, 121.46, 118.48, 115.35, 110.33, 106.70, 63.78, 45.49.

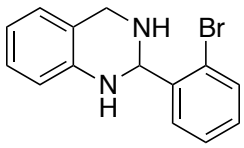

2-(2'-bromophenyl)-1,2,3,4-tetrahydroquinazoline

Isolated as a viscous pale yellow oil. Ratio of Ring to Chain ($CDCl_3$): 48:1; ^{1}H NMR (500 MHz, $CDCl_3$) d 7.64 (d, *J* = 8.3 Hz, 1H), 7.38 (t, *J* = 7.6 Hz, 1H), 7.24 (td, *J* = 7.7, 1.7 Hz, 1H), 7.11 (t, *J* = 7.2 Hz, 1H), 6.99 (d, *J* = 7.5 Hz, 1H), 6.79 (t, *J* = 7.4 Hz, 1H), 6.62 (d, *J* = 8.0 Hz, 1H), 5.60 (s, 1H), 4.28 (d, *J* = 16.5 Hz, 1H), 3.99 (d, *J* = 16.6 Hz, 1H), 3.0-3.8 (br s, 2H); ^{13}C NMR (126 MHz, $CDCl_3$) d 143.79, 140.15, 133.30, 133.29, 129.95, 127.90, 127.88, 127.39, 126.37, 123.30, 121.32, 118.42, 115.26, 68.56, 46.24; EMM (ESI) Calc for $C_{14}H_{13}BrN_2$ (M+H): 289.0335, found 289.0339.

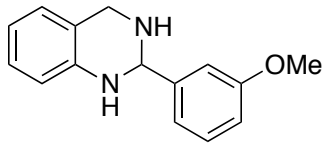

2-(3-methoxyphenyl)-1,2,3,4-tetrahydroquinazoline

Viscous yellow oil. Ratio of Ring to Chain ($CDCl_3$): 4:1; ^{1}H NMR (400 MHz, $CDCl_3$) d 7.3-7.4 (m, 1H), 7.05-7.2 (m, 3H), 6.99 (dt, *J* = 7.5, 1.2 Hz, 1H), 6.94 (ddd, *J* = 8.3, 2.6, 1.0 Hz, 1H), 6.77 (td, *J* = 7.4, 1.2 Hz, 1H), 6.63 (dd, *J* = 8.1, 1.2 Hz, 1H), 5.24 (s, 1H), 4.30 (d, *J* = 16.6 Hz, 1H), 4.03 (d, *J* = 16.6 Hz, 1H), 3.86 (s, 3H); ^{13}C NMR (101 MHz, $CDCl_3$) d 159.99, 143.68, 143.18, 129.84, 127.33, 126.27, 121.24, 118.92, 118.23, 115.11, 114.29, 111.96, 69.58, 55.34, 46.51. Calc for $C_{15}H_{16}N_2O$ (M+H): 241.1336, found 241.1334.

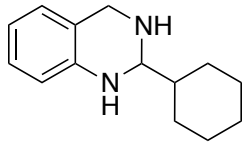

2-cyclohexyl-1,2,3,4-tetrahydroquinazoline

Chain tautomer not observed ($CDCl_3$); mp: 65-67 °C; ^{1}H NMR (400 MHz, $CDCl_3$) d 7.04 (t, *J* = 7.3 Hz, 1H), 6.92 (d, *J* = 7.4 Hz, 1H), 6.70 (t, *J* = 7.4 Hz, 1H), 6.55 (d, *J* = 8.0 Hz, 1H), 4.15 (d, *J* = 16.6 Hz, 1H), 3.99 (d, *J* = 15.7 Hz, 1H, overlaps with peak at 3.98), 3.98 (s, 1H), 1.9-2.0 (m, 1H), 1.7-1.9 (m, 4H), 1.4-1.6 (m, 1H), 1.0-1.4 (m, 5H); ^{13}C NMR (126 MHz, $CDCl_3$) d 144.04, 127.15, 126.09, 121.74, 117.74, 114.96, 71.04, 46.74, 42.87, 28.27, 27.99, 26.52, 26.21, 26.18. EMM (ESI) Calc for $C_{14}H_{20}N_2$ (M+H): 217.1700, found 217.1699.

Indolines

Indoline was obtained from commercial sources (Sigma Aldrich), and was used as received without further purification. Methylindolines were prepared by reduction of the corresponding indole using excess $NaCNBH_3$ in acetic acid, according to literature methods.[39]

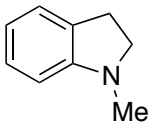

1-methylindoline

Spectroscopic data match those previously reported.[40] ^{1}H NMR (400 MHz, $CDCl_3$) δ 7.1-7.2 (m, 2H), 6.75 (t, *J* = 7.6 Hz, 1H), 6.53 (d, *J* = 8.0 Hz, 1H), 3.32 (t, *J* = 8.1 Hz, 2H), 2.97 (t, *J* = 8.1 Hz, 2H), 2.79 (s, 3H); ^{13}C NMR (101 MHz, $CDCl_3$) δ 153.41, 130.37, 127.36, 124.31, 117.88, 107.35, 56.22, 36.37, 28.80.

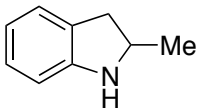

2-methylindoline

Spectroscopic data match those previously reported.[40] ^{1}H NMR (400 MHz, $CDCl_3$) δ 7.08 (d, *J* = 8.8 Hz, 1H), 7.02 (td, *J* = 7.7, 1.4 Hz, 1H), 6.70 (td, *J* = 7.4, 1.0 Hz, 1H), 6.61 (d, *J* = 7.7 Hz, 1H), 4.00 (ddq, *J* = 8.6, 7.8, 6.2 Hz, 1H), 3.78 (br s, NH), 3.15 (dd, *J* = 15.4, 8.5 Hz, 1H), 2.65 (dd, *J* = 15.5, 7.8 Hz, 1H), 1.30 (d, *J* = 6.2 Hz, 3H); ^{13}C NMR (101 MHz, $CDCl_3$) δ 150.98, 128.91, 127.25, 124.74, 118.54, 109.19, 55.25, 37.79, 22.32.

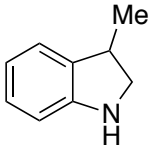

3-methylindoline

Spectroscopic data match those previously reported.[39] ^{1}H NMR (400 MHz, $CDCl_3$) δ 7.10 (d, *J* = 7.2 Hz, 1H), 7.04 (t, *J* = 7.6 Hz, 1H), 6.75 (td, *J* = 7.4, 1.0 Hz, 1H), 6.66 (d, *J* = 7.8 Hz, 1H), 3.71 (t, *J* = 8.6 Hz, 1H, overlaps with NH), 3.5-3.3 (m, 1H), 3.12 (t, *J* = 8.6 Hz, 1H), 1.34 (d, *J* = 6.8 Hz, 3H); ^{13}C NMR (101 MHz, $CDCl_3$) δ 151.25, 134.35, 127.30, 123.38, 118.70, 109.52, 55.47, 36.66, 18.66.

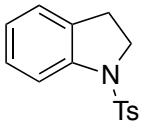

N-toluenesulfonylindoline

Spectroscopic data match those previously reported.[41] ^{1}H NMR (300 MHz, $CDCl_3$) δ 7.7-7.6 (m, 3H), 7.24-7.13 (m, 3H), 7.07 (ddd, *J* = 7.4, 1.5, 0.7 Hz, 1H), 6.96 (td, *J* = 7.4, 1.0 Hz, 1H), 3.91 (t, *J* = 8.4 Hz, 2H), 2.87 (t, *J* = 8.8 Hz, 2H), 2.36 (s, 3H); ^{13}C NMR (75 MHz, $CDCl_3$) δ 144.23, 142.22, 134.27, 131.96, 129.85, 127.91, 127.53, 125.30, 123.91, 115.23, 50.15, 28.10, 21.74.

3.5.11 Characterization of Products

Acyclic imines

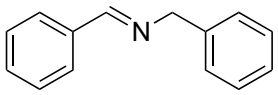

N-benzylidenebenzylamine, **4**

Spectroscopic data match those previously reported.[6] ^{1}H NMR (300 MHz, $CDCl_3$) δ 8.37 (s, 1H), 7.78 (m, 2H), 7.21-7.41 (m, 8H), 4.81 (s, 2H); ^{13}C NMR (75 MHz, $CDCl_3$) δ 162.21, 139.56, 136.42, 131.00, 128.83, 128.73, 128.52, 128.22, 127.22, 65.29.

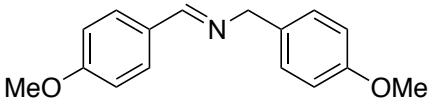

N-(4-methoxybenzylidene)-4-methoxybenzylamine, **5**

Spectroscopic data match those previously reported.[6] ^{1}H NMR (300 MHz, $CDCl_3$) δ 8.30 (s, 1H), 7.73 (d, J = 8.4 Hz, 2H), 7.25 (d, J = 8.4 Hz, 2H), 6.8-6.9 (m, 4H), 4.73 (s, 2H) 3.83 (s, 3H), 3.79 (s, 3H); ^{13}C NMR (75 MHz, $CDCl_3$) δ 161.90, 161.12, 158.87, 131.92 130.02, 129.39, 114.19, 114.12, 64.62, 55.56, 55.51.

3,4-Dihydroisoquinolines

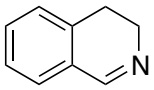

3,4-dihydroisoquinoline, **2**

Spectroscopic data matches those reported in the literature.[42] ^{1}H NMR (400 MHz, $CDCl_3$) δ 8.28 (br s, 1H), 7.2-7.3 (m, 3H, overlaps with $CDCl_3$ residual peak), 7.08 (d, J = 8.8 Hz, 1H), 3.70 (td, J = 8.0, 1.6 Hz, 2H), 2.68 (t, J = 8.0 Hz, 2H); ^{13}C NMR (101MHz, $CDCl_3$) δ 160.83, 136.37, 131.30, 128.45, 127.49, 127.44, 127.17, 47.34, 25.06.

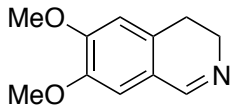

3,4-dihydro-6,7-dimethoxyisoquinoline, **6**

Using workup method B. From 194.6 mg substrate, 176.1 mg (91% yield) of the title compound was collected as a viscous oil. Spectroscopic data matches those reported in the literature.[43] ^{1}H NMR (400 MHz, $CDCl_3$) δ 8.21 (br s, 1H), 6.79 (s, 1H), 6.65 (s, 1H), 3.90 (s, 3H), 3.88 (s, 3H), 3.71 (t, J = 7.6 Hz, 2H), 2.66 (t, J = 7.6 Hz, 2H); ^{13}C NMR (101 MHz, $CDCl_3$) δ 159.69, 151.23, 147.85, 129.90, 121.54, 110.40, 110.38, 56.15, 56.07, 47.35, 24.78; EMM (ESI) Calc for $C_{11}H_{13}NO_2$ (M+H): 192.1020, found 192.1019.

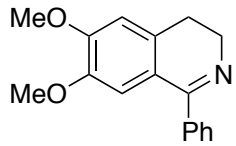

1-phenyl-3,4-dihydro-6,7-dimethoxyisoquinoline, **7**

Using workup method B. From 269.0 mg of starting material, 260.7 mg (97.5%) of the title compound was obtained as a white solid, mp: 119-121 °C. Spectroscopic data matches those reported in the literature.[44] ^{1}H NMR (400 MHz, $CDCl_3$) δ 7.60 (m, 2H), 7.43 (m, 3H), 6.79 (d, J = 5.6 Hz, 2H), 3.95 (s, 3H), 3.81 (t, J = 7.2 Hz, 2H), 3.72 (s, 3H), 2.73 (t, J = 7.2 Hz, 2H); ^{13}C NMR (101 MHz, $CDCl_3$) δ 166.72, 150.90, 147.10, 139.24, 132.63, 129.32, 128.80, 128.20, 121.63, 111.56, 110.28, 56.18, 56.07, 47.76, 26.05; EMM (ESI) Calc for $C_{17}H_{17}NO_2$ (M+H): 268.1333, found 268.1327.

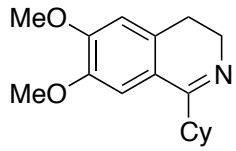

1-cyclohexyl-3,4-dihydro-6,7-dimethoxyisoquinoline, **8**

Using workup method B. From 274.8 mg starting material, 244.3 mg (89.5% yield) was obtained as a colorless oil that eventually solidifies to an off-white solid; mp: 78-80 °C. Spectroscopic data matches those reported in the literature[45] ^{1}H NMR (400 MHz, $CDCl_3$) δ 6.99 (s, 1H), 6.65 (s, 1H), 3.87 (s, 6H), 3.58 (t, *J* = 7.2 Hz, 2H), 2.77 (t, *J* = 10 Hz, 1H), 2.53 (t, *J* = 7.2 Hz, 2H), 1.6-1.9 (m, 5H), 1.2-1.5 (m, 5H); ^{13}C NMR (101 MHz, $CDCl_3$) δ 170.15, 150.55, 147.43, 132.09, 121.69, 110.48, 108.68, 56.38, 55.94, 46.96, 42.27, 31.35, 26.62, 26.32, 26.04; EMM (ESI) Calc for $C_{17}H_{23}NO_2$ (M+H): 274.1802, found 274.1795.

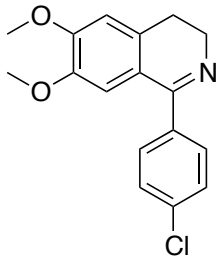

1-(4-chlorophenyl)-3,4-dihydro-6,7-dimethoxyisoquinoline, **9**

Using workup method B. From 304.8 mg starting material, 284.9 mg (94.0% yield) was obtained as a white crystalline solid, mp: 125-127 °C. Spectroscopic data matches those reported in the literature[46] ^{1}H NMR (500 MHz, $CDCl_3$) δ 7.55 (d, *J* = 8.0 Hz, 2H), 7.40 (d, *J* = 8.5 Hz, 2H), 6.77 (s, 1H), 6.73 (s, 1H), 3.94 (s, 3H), 3.79 (t, *J* = 8.0 Hz, 2H), 3.73 (s, 3H), 2.72 (t, *J* = 8.0 Hz, 2H); ^{13}C NMR (126 MHz, $CDCl_3$) δ 165.77, 151.09, 147.18, 137.58, 135.39, 132.67, 130.20, 128.45, 121.20, 111.18, 110.35, 56.18, 56.09, 47.69, 25.96; EMM (ESI) Calc for $C_{17}H_{16}ClNO_2$ (M+H): 302.0943, found 302.0934.

3,4-Dihydro-β-carbolines

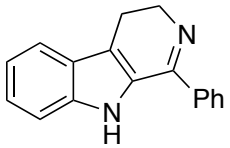

1-phenyl-3,4-dihydro-β-carboline, **11**

Using workup method A or B. From 249.1 mg of starting material, 200.0 mg collected (80.9% yield) as a pale yellow solid, mp: 211-214 °C. Spectroscopic data matches those reported in the literature.[47] ^{1}H NMR (400 MHz, $CDCl_3$) δ 8.23 (s, NH), 7.77 (m, 2H), 7.69 (d, *J* = 8.0 Hz, 1H), 7.5-7.6 (m, 3H), 7.39 (d, *J* = 8.0 Hz, 1H), 7.32 (t, *J* = 7.2 Hz, 1H), 7.21 (t, *J* = 7.6 Hz, 1H), 4.08 (t, *J* = 8.4 Hz, 2H), 3.01 (t, *J* = 8.4 Hz, 2H); ^{13}C NMR (101 MHz, $CDCl_3$) δ 159.33, 137.67, 136.47, 130.00, 128.90, 127.85, 127.81, 125.63, 124.63, 120.46, 120.06, 117.89, 112.01, 48.98, 19.29; EMM (ESI) Calc for $C_{17}H_{14}N_2$ (M+H): 247.1230, found 247.1224.

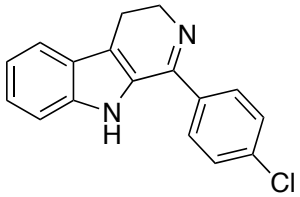

1-(4'-chlorophenyl)-3,4-dihydro-β-carboline, **12**

Using workup method A. From 283.9 mg of starting material, 197.3 mg were collected (70% yield) as a light yellow solid, mp: 220-222 °C. Spectroscopic data matches those reported in the literature.[34] ^{1}H NMR (400 MHz, $CDCl_3$) δ 8.08 (br s, NH), 7.65-7.7 (m, 3H), 7.46 (d, *J* = 8.4 Hz, 2H), 7.37 (d, *J* = 8.4 Hz, 1H), 7.30 (t, *J* = 7.2 Hz, 1H), 7.19 (t, *J* = 7.2 Hz, 1H), 4.04 (t, *J* = 8.4 Hz, 2H), 2.97 (t, *J* = 8.4 Hz, 2H); ^{13}C NMR (101 MHz, $CDCl_3$) δ 158.31, 136.55, 136.14, 136.04, 129.23, 129.14, 127.45, 125.61, 124.88, 120.64, 120.12, 118.32, 112.03, 48.99, 19.24; EMM (ESI) Calc for $C_{17}H_{13}ClN_2$ (M+H): 281.0841, found 281.0835.

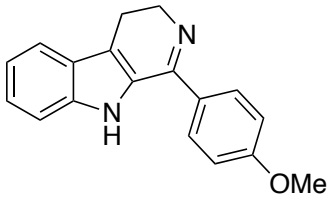

1-(4-methoxyphenyl)-3,4-dihydro-β-carboline, **13**

Using workup method A or B. From 277.6 mg of starting material; 241.4 mg collected (87.6% yield) as a pale white solid, mp: 196-197 °C. Spectroscopic data matches those reported in the literature.[47] ^{1}H NMR (400 MHz, $CDCl_3$) δ 8.18 (br s, NH), 7.70 (d, *J* = 8.8 Hz, 2H) 7.65 (d, *J* = 8.0 Hz, 1H), 7.36 (d, *J* = 8.0 Hz, 1H), 7.28 (t, *J* = 7.2 Hz, 1H overlaps with $CDCl_3$ residual peak), 7.18 (t, *J* = 7.2 Hz, 1H) 7.00 (d, *J* = 8.8 Hz, 2H), 4.00 (t, *J* = 8.4 Hz, 2H), 3.86 (s, 3H), 2.95 (t, *J* = 8.4 Hz, 2H); ^{13}C NMR (101 MHz, $CDCl_3$) δ 161.10, 158.70, 136.40, 130.24, 129.33, 127.97, 125.68, 124.52, 120.42, 120.01, 117.89, 114.22, 111.98, 55.46, 48.81, 19.30; EMM (ESI) Calc for $C_{18}H_{16}N_2O$ (M+H): 277.1336, found 277.1326.

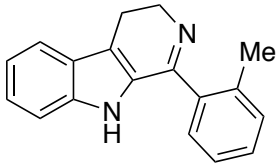

1-(2-methylphenyl)-3,4-dihydro-β-carboline, **14**

Using workup method B. From 263.7 mg of starting material, 240.7 mg (91% yield) were collected as an off-white solid, decomposed above 180 °C. This compound has been previously reported, but full spectroscopic data have not been reported.[35] ^{1}H NMR (500 MHz, $CDCl_3$) δ 7.87 (s, NH), 7.66 (d, *J* = 8.0 Hz, 1H), 7.38 (m, 2H), 7.25-7.35 (m, 4H, overlaps with $CDCl_3$ residual peak), 7.18 (m, 1H), 4.12 (t, *J* = 8.5 Hz, 2H), 3.04 (t, *J* = 8.5 Hz, 2H), 2.28 (s, 3H); ^{13}C NMR (125 MHz, $CDCl_3$) δ 160.45, 136.96, 136.56, 136.23, 130.89, 129.21, 128.63, 128.28,

126.10, 125.67, 120.46, 120.12, 116.80, 111.99 48.90, 19.50, 19.33; EMM (ESI) Calc for $C_{18}H_{16}N_2$ (M+H): 261.1308, found 261.1303.

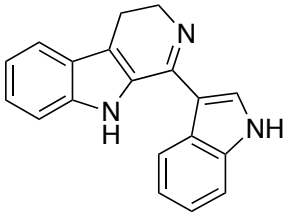

Isoeudistomin U, **15**

Using workup method B. Bright yellow solid, slow decomposition >200 °C; Spectroscopic data match those previously reported.[36,48] ^{1}H NMR (400 MHz, MeOD-d_4 + 1 drop TFA-d_1) δ 8.30 (s, 1H), 7.93 (d, *J* = 7.2 Hz, 1H), 7.74 (d, *J* = 8.0 Hz, 1H), 7.61 (d, *J* = 7.6 Hz, 1H), 7.52 (d, J = 8.4 Hz, 1H), 7.3-7.45 (m, 3H), 7.19 (t, *J* = 7.6 Hz, 1H), 4.00 (t, *J* = 8.0 Hz, 2H), 3.29 (m, 2H, overlaps with MeOD-d_4 residual peak); ^{13}C NMR (101 MHz, MeOD-d_4 + 1 drop TFA-d_1) δ 157.04, 137.78, 141.44, 136.53, 128.00, 125.22, 124.98, 124.92, 124.41, 124.92, 124.41, 124.35, 122.89, 121.44, 120.97, 119.57, 112.98, 112.84, 106.00, 41.25, 19.26; EMM (ESI) Calc for $C_{19}H_{15}N_3$ (M+H): 286.1339, found 286.1350.

Quinazolines

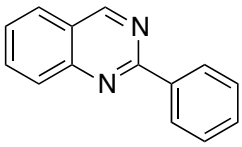

2-phenylquinazoline, **16**

Spectroscopic data matches those reported in the literature.[50] Using workup method A. From 210.2 mg of starting material, 174.0 mg (84.4% yield) were isolated as a bright yellow flaky solid, mp: 96-100 °C. ^{1}H NMR (400 MHz, $CDCl_3$) δ 9.45 (s, 1H), 8.61 (dd, *J* = 8.0, 1.2 Hz, 2H),

8.08 (d, J = 8.4 Hz, 1H), 7.8-7.9 (m, 2H), 7.48-7.62 (m, 4H); ^{13}C NMR (101 MHz, $CDCl_3$) δ 161.13, 160.55, 150.83, 138.09, 134.16, 130.66, 128.70, 128.62, 127.32, 127.18, 123.66; EMM (ESI) Calc for $C_{14}H_{10}N_2$ (M+H): 207.0917, found 207.0921.

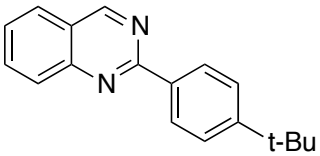

2-(4-tert-butylphenyl)-quinazoline, **17**

Using workup method B. From 270 mg of starting material, 226.8 mg (85.3% yield) were collected as a white crystalline solid, mp: 90-91 °C. ^{1}H NMR (400 MHz, $CDCl_3$) δ 9.45 (s, 1H), 8.53 (d, J = 8.4 Hz, 1H), 8.08 (d, J = 8.8 Hz, 1H), 7.8-7.9 (m, 2H), 7.5-7.6 (m, 3H), 1.39 (s, 9H); ^{13}C NMR (101 MHz, $CDCl_3$) δ 161.20, 160.48, 153.99, 150.88, 135.37, 134.04, 128.67, 128.40, 127.16, 127.06, 125.68, 123.56, 34.93, 31.33; EMM (ESI) Calc for $C_{18}H_{18}N_2$ (M+H): 263.1543, found 263.1548.

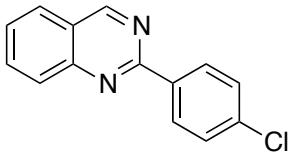

2-(4-chlorophenyl)-quinazoline, **18**

Spectroscopic data matches those reported in the literature.[50] From 248.1 mg of starting materials, 199.6 mg (81.8% yield) were collected as a fine white crystalline solid; mp: 136-137 °C; ^{1}H NMR (400 MHz, $CDCl_3$) δ 9.48 (s, 1H), 8.62 (d, J = 8.4 Hz, 2H), 8.10 (d, J = 8.0 Hz, 1H), 7.94-7.98 (m, 2H), 7.66 (t, J = 7.2 Hz, 1H), 7.35 (d, J = 8.4 Hz, 2H); ^{13}C NMR (101 MHz, $CDCl_3$) δ 160.59, 160.11, 150.75, 136.89, 136.58, 134.32, 129.94, 128.88, 128.66, 127.52, 127.21, 123.68; EMM (ESI) Calc for $C_{14}H_9ClN_2$ (M+H): 241.0528, found 241.0524.

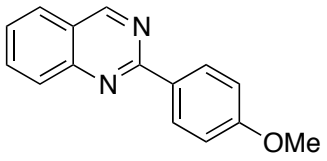

2-(4-methoxyphenyl)-quinazoline, **19**

Spectroscopic data matches those reported in the literature.[50] From 240 mg of starting material, 151.4 mg (64% yield) as a pale yellow crystalline solid; mp: 92-94 °C; ^{1}H NMR (400 MHz, $CDCl_3$) δ 9.45 (s, 1H), 8.61 (d, *J* = 9.2 Hz, 2H), 8.07 (d, *J* = 8.4 Hz, 1H), 7.89-7.93 (m, 2H), 7.60 (t, J = 7.2 Hz, 1H), 7.35 (d, *J* = 8.8 Hz, 2H), 3.93 (s, 3H); ^{13}C NMR (101 MHz, $CDCl_3$) δ 161.88, 160.92, 160.44, 150.89, 134.07, 130.78, 130.25, 128.47, 127.18, 126.83, 123.36, 114.02, 55.44; EMM (ESI) Calc for $C_{15}H_{12}N_2O$ (M+H): 237.1023, found 237.1025.

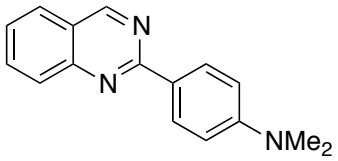

2-(4-(N,N-dimethylamino)-phenyl)-quinazoline, **20**

This compound has been previously reported.[49] Bright yellow needles, mp: 136-138.5 °C; ^{1}H NMR (400 MHz, $CDCl_3$) δ 9.36 (s, 1H), 8.51 (d, *J* = 9.2 Hz, 2H), 8.00 (d, *J* = 8.4 Hz, 1H), 7.8-7.9 (m, 2H), 7.49 (t, *J* = 8.0 Hz, 1H), 6.82 (d, *J* = 9.2 Hz, 2H), 3.06 (s, 6H); ^{13}C NMR (101 MHz, $CDCl_3$) δ 161.53, 160.27, 152.20, 151.07, 133.86, 129.93, 128.23, 127.17, 126.14, 125.74, 123.11, 111.79, 40.31; EMM (ESI) Calc for $C_{16}H_{15}N_3$ (M+H): 250.1339, found 250.1334.

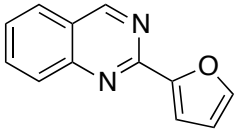

2-(Furan-2-yl)quinazoline, **21**

Using workup method A. From 200.7 mg of starting materials, 159.0 mg (81% yield) of the title compound was collected as pale orange needles, mp: 128-130 °C. Spectroscopic data match those previously reported.[50] ^{1}H NMR (400 MHz, $CDCl_3$) δ 9.37 (s, 1H), 8.09 (d, *J* = 9.2 Hz, 1H), 7.8-7.9 (m, 2H), 7.68 (dd, *J* = 3.6, 2.4 Hz, 1H), 7.59 (td, *J* = 6.9, 0.8 Hz, 1H), 7.45 (dd, *J* = 3.6, 0.8 Hz, 1H), 6.61 (dd, *J* = 3.6, 2.0 Hz, 1H); ^{13}C NMR (101 MHz, $CDCl_3$) δ 160.79, 154.16, 152.56, 150.48, 145.40, 134.56, 128.45, 127.32, 123.42, 114.14, 112.37; EMM (ESI) Calc for $C_{12}H_8N_2O$ (M+H): 197.0710, found 197.0707.

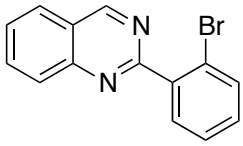

2-(2-bromophenyl)-quinazoline, **22**

From 303 mg of starting material, 254.1 mg (85% yield) of the title compound was obtained as a pale yellow viscous oil; ^{1}H NMR (400 MHz, $CDCl_3$) δ 9.51 (s, 1H), 8.11 (dd, *J* = 8.4, 0.8 Hz, 1H), 7.9-8.0 (m, 2H), 7.77 (dd, *J* = 7.6, 1.6 Hz, 1H), 7.71 (dd, *J* = 8.4, 1.2 Hz, 1H), 7.66 (dt, *J* = 8.0, 1.2 Hz, 1H), 7.44 (dt, *J* = 7.6, 1.2 Hz, 1H), 7.28 (dt, *J* = 7.6, 1.6 Hz, 1H); ^{13}C NMR (101 MHz, $CDCl_3$) δ 162.85, 160.30, 150.31, 140.22, 134.47, 133.75, 131.74, 130.47, 128.66, 128.13, 127.53, 127.21, 123.33, 121.97; EMM (ESI) Calc for $C_{14}H_9BrN_2$ (M+H): 285.0022, found 285.0013.

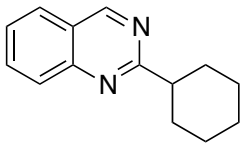

2-cyclohexylquinazoline, **23**

From 216.3 mg starting material, 161.9 mg (76.3% yield) of the title compound was recovered as a glassy colorless solid, mp: 34-37 °C; ^{1}H NMR (400 MHz, $CDCl_3$) δ 9.27 (s, 1H), 7.90 (d, *J* =

8.8 Hz, 1H), 7.7-7.8 (m, 2H), 7.49 (t, J = 6.8 Hz, 1H), 2.97 (tt, J = 11.6, 3.6 Hz, 1H), 2.00 (m, 2H), 1.6-1.8 (m, 5H), 1.2-1.4 (m, 3H); ^{13}C NMR (101 MHz, $CDCl_3$) δ 170.97, 160.42, 150.44, 133.87, 128.08, 127.07, 126.84, 123.31, 47.99, 31.99, 26.36, 26.07; EMM (ESI) Calc for $C_{14}H_{16}N_2$ (M+H): 213.1387, found 213.1387.

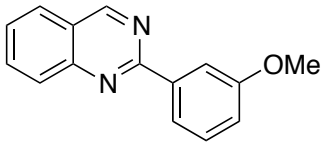

2-(3-methoxyphenyl)-quinazoline, **24**

Spectroscopic data matches those reported in the literature.[51] From 239.3 mg starting material, 169.8 mg (72% yield) of the title compound was obtained as a white crystalline solid, mp: 78-80 °C; ^{1}H NMR (400 MHz, $CDCl_3$) δ 9.45 (s, 1H), 8.14 (dt, J = 8.0, 1.2 Hz, 1H), 8.10 (m, 1H), 8.00 (d, J = 8.4 Hz, 1H), 7.8-7.85 (m, 2H), 7.51 (td, J = 7.6, 1.2 Hz, 1H) 7.36 (t, J = 8.0 Hz, 1H), 6.97 (ddd, J = 8.4, 2.8, 0.8 Hz, 1H), 3.86 (s, 3H); ^{13}C NMR (101 MHz, $CDCl_3$) δ 160.88, 160.48, 160.07, 150.07, 139.56, 134.14, 129.69, 128.72, 127.35, 127.16, 123.70, 121.20, 117.30, 113.06, 55.50; EMM (ESI) Calc for $C_{15}H_{12}N_2O$ (M+H): 237.1023, found 237.1032.

Indoles

The reaction procedure for the oxidation of indoles was identical to that described above, except that 1.0 mol % ZnI_2 and 1.0 mol % PPTS were used. Workup method A was employed in all instances.

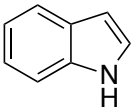

Indole, **25**

From 112 μl of indoline, using workup method A, obtained 95.1 mg (81.2% yield) of indole. Spectroscopic data were identical to commercially available material. ^{1}H NMR (400 MHz, $CDCl_3$) δ 8.01 (br s, NH), 7.64 (d, *J* = 7.6 Hz, 1H), 7.35 (d, *J* = 8.4 Hz, 1H), 7.1-7.25 (m, 3H), 6.54 (t, *J* = 2.0 Hz, 1H); ^{13}C NMR (101 MHz, $CDCl_3$) δ 135.84, 127.91, 124.26, 122.06, 120.82, 119.90, 111.14, 102.65; EMM (EI) Calc for C_8H_7N (M+H): 117.0573, found 117.1579.

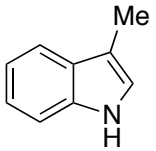

3-methylindole, **26**

From 135.4 mg of 3-methylindoline, using workup method A, obtained 106.6 mg (79.9% yield) of 3-methylindole as a white solid; mp 95-97 °C to red oil; ^{1}H NMR (400 MHz, $CDCl_3$) δ 7.73 (m, 2H), 7.41 (d, *J* = 7.6 Hz, 1H), 7.34 (t, *J* = 6.8 Hz, 1H), 7.28 (t, *J* = 7.2 Hz, 1H), 7.01 (s, 1H), 2.48 (s, 3H); ^{13}C NMR (101 MHz, $CDCl_3$) δ 136.36, 128.39, 121.99, 121.79, 119.25, 118.98, 111.74, 111.13, 9.82; EMM (EI) Calc for C_9H_9N (M+H): 131.0730, found 131.0726. Spectroscopic data were identical to commercially available material.

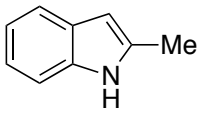

2-methylindole, **27**

From 137.6 mg of the corresponding 2-methylindoline, using workup method A, obtained 124.9 mg as a mixture of product and starting material. This mixture was dissolved in hot hexanes, precipitating out 99.0 mg (73% yield) of title compound as white crystals; mp 58-59°C; ^{1}H NMR (500 MHz, $CDCl_3$) δ 7.65 (br s, NH), 7.52 (d, *J* = 7.5 Hz, 1H), 7.29 (d, *J* = 8.0 Hz, 1H), 7.05-7.15 (m, 2H), 6.23 (br s, 1H), 2.45 (s, 3H); ^{13}C NMR (125 MHz, $CDCl_3$) δ 136.07, 135.06,

129.10, 120.96, 119.66, 110.22, 100.43, 13.77; EMM (EI) Calc for C_9H_9N (M+H): 131.0730, found 131.0726. Spectroscopic data were identical to commercially available material.

3.6 References

(1) For selected reviews, see: (a) Klinman, J. P. *J. Biol. Chem.* **1996**, *271*, 27189. (b) Mure, M. *Acc. Chem. Res.* **2004**, *37*, 131.

(2) Mure, M.; Mills, S. A.; Klinman, J. P. *Biochem.* **2002**, *41*, 9269.

(3) (a) Ohshiro, Y.; Itoh, S. *Bioorg. Chem.* **1991**, *19*, 169; (b) Rodriguez, E. J.; Bruice, T. C. *J. Am. Chem. Soc.* **1989**, *111*, 7947.

(4) (a) Mure, M.; Klinman, J. P. *J. Am. Chem. Soc.* **1995**, *117*, 8698. (b) Mure, M.; Klinman, J. P. *J. Am. Chem. Soc.* **1995**, *117*, 8707.

(5) (a) Lee, Y.; Sayre, L. M. *J. Am. Chem. Soc.* **1995**, *117*, 11823. (b) Lee, Y.; Sayre, L. M. *J. Am. Chem. Soc.* **1995**, *117*, 3096.

(6) Wendlandt, A. E.; Stahl, S. S. *Org. Lett.* **2012**, *14*, 2850.

(7) Largeron, M.; Fleury, M.-B. *Angew. Chem. Int. Ed.* **2012**, *51*, 5409.

(8) (a) Yuan, H.; Yoo, W.-J.; Miyamura, H.; Kobayashi, S. *J. Am. Chem. Soc.* **2012**, *134*, 13970. (b) Yuan, H.; Yoo, W.-J.; Miyamura, H.; Kobayashi, S. *Adv. Synth. Catal.* **2012**, *354*, 2899.

(9) Largeron, M.; Fleury, M.-B. *Science* **2013**, *339*, 43.

(10) For selected reviews highlighting different approaches to amine oxidation, esp employing molecular oxygen as the terminal oxidation, see: (a) Li, C.-J. *Acc. Chem. Res.*, **2009**, *42*, 335. (b) Murahashi, S.-I. *Angew. Chem. Int. Ed.* **1995**, *34*, 2443. (c) Largeron, M. *Eur. J. Org. Chem.* **2013**, 5225. (d) Schümperli, M. T.; Hammond, C.; Hermans, I. *ACS Catalysis* **2012**, *2*, 1108.

(11) For alternative approaches to aerobic, organocatalytic C-N bond dehydrogenation, see: Chen, S.; Hossain, M. S.; Foss, F. W. *ACS Sustainable Chem. Eng.* **2013**, *1*, 1045. (b) Fang, X.; Liu, Y.-C.; Li, C. *J. Org. Chem.* **2007**, *72*, 8608. (c) Liu, L.; Wang, Z.; Fu, X.; Yan, C.-H. *Org. Lett.* **2012**, 14, 5692. (d) Srogl, J.; Voltrova, S. *Org. Lett.* **2009**, *11*, 843.

(12) For selected examples of aerobic, transition-metal catalyzed amine oxidation, see: (a) Sonobe, T.; Oisaki, K.; Kanai, M. *Chem. Sci.* **2012**, *3*, 3249. (b) Samec, J. S. M.; Éll, A. H.; Bäckvall, J.-E. *Chem – Eur. J.* **2005**, *11*, 2327. (c) Yamaguchi, K.; Mizuno, N. *Angew. Chem. Int. Ed.* **2003**, *42*, 1480. (d) Lang, X.; Ji, H.; Chen, C.; Ma, W.; Zhao, J. *Angew. Chem. Int. Ed.* **2011**, *50*, 3934. (e) Wang, J.-R.; Fu, Y.; Zhang, B.-B.; Cui, X.; Liu, L.; Guo, Q.-X. *Tetrahedron Lett.* **2006**, *47*, 8293. (f) Hu, Z.; Kerton, F. M. *Org. Biomol. Chem.* **2012**, *10*, 1618. (g) Zhang, E.; Tian, H.; Xu, S.; Yu, X.; Xu, Q. *Org. Lett.* **2013**, *15*, 2704. (h) Patil, R. D.; Adimurthy, S. *Adv. Synth. Catal.* **2011**, *353*, 1695.

(13) (a) Lee, Y.; Ling, K.-Q.; Lu, X.; Silverman, R. B.; Shepard, E. M.; Dooley, D. M.; Sayre, L. M. *J. Am. Chem. Soc.* **2002**, *124*, 12135. (b) Lee, Y.; Huang, H.; Sayre, L. M. *J. Am. Chem. Soc.* **1996**, *118*, 7241. (c) Zhang, Y.; Ran, C.; Zhou, G.; Sayre, L. M. *Bioorg. Med. Chem.* **2007**, *15*, 1868.

(14) Eckert, T. S.; Bruice, T. C. *J. Am. Chem. Soc.* **1983**, *105*, 4431.

(15) For leading reference, see: Anthony, C.; Ghosh, M.; Blake, C. C. *Biochem. J.* **1994**, *304*, 665.

(16) (a) Itoh, S.; Kawakami, H.; Fukuzumi, S. *J. Am. Chem. Soc.* **1997**, *119*, 439. (b) Itoh, S.; Kawakami, H.; Fukuzumi, S. *Biochem.* **1998**, *37*, 6562.

(17) Itoh, S.; Mure, M.; Ogino, M.; Ohshiro, Y. *J. Org. Chem.* **1991**, *56*, 6857.

(18) For leading reference, see: Goss, C. A.; Abruna, H. D. *Inorg. Chem.* **1985**, *24*, 4263.

(19) Yuasa, J.; Suenobu, T.; Fukuzumi, S. *ChemPhysChem* **2006**, *7*, 942.

(20) Lei, Y.; Anson, F. C. *J. Am. Chem. Soc.* **1995**, *117*, 9849. (b) Lei, Y.; Shi, C.; Anson, F. C. *Inorg. Chem.* **1996**, *35*, 3044.

(21) For an example of Lewis acid-promoted stoichiometric amine oxidation by TTQ model quinones, see: Itoh, S.; Taniguchi, M.; Takada, N.; Nagatomo, S.; Kitagawa, T.; Fukuzumi, S. *J. Am. Chem. Soc.* **2000**, *122*, 12087.

(22) Eckert, T. S.; Bruice, T. C.; Gainor, J. A.; Weinreb, S. M. *Proc. Nat. Acad. Sci.* **1982**, *79*, 2533.

(23) (a) Dhineshkumar, J.; Lamani, M.; Alagiri, K.; Prabhu, K. R. *Org. Lett.* **2013**, *15*, 1092. (b) H. Huang, X. Ji, W. Wu, H. Jiang, *Adv. Synth. Catal.* **2013**, *355*, 170.

(24) For examples of iodine-mediated oxidation of amines, see: (a) Goosen, A.; McCleland, C. W.; Sipamla, A. M. *J. Chem. Res. (S)*, **1995**, 18. (b) Iida, S.; Togo, H. *Tetrahedron* **2007**, *63*, 8274. (c) Leonard, N. J.; Leubner, G. W. *J. Am. Chem. Soc.* **1949**, *71*, 3408. (d) Domínguez, E.; Lete, E. *J. Heterocyclic Chem.* **1984**, 21, 525. (e) Sotomayor, N.; Domínguez, E.; Lete, E. *Tetrahedron* **1995**, *51*, 12721.

(25) Piera, J.; Bäckvall, J.-E. *Angew. Chem. Int. Ed.* **2008**, 47, 3506.

(26) Wu, Z.; Perez, M.; Scalone, M.; Ayad, T.; Ratovelomanana-Vidal, V. *Angew. Chem. Int. Ed.* **2013**, *52*, 4925.

(27) Wu, J.-Z.; Li, H.; Zhang, J.-G.; Xu, J.-H. *Inorg. Chem. Commun.* **2002**, *5*, 71.

(28) Chen, L.; Zhang, L.; Lv, J.; Cheng, J.-P.; Luo, S. *Chem – Eur. J.* **2012**, *18*, 8891.

(29) Paw, W.; Eisenberg, R., *Inorg. Chem.* **1997,** *36*, 2287.

(30) Abdel-Magid, A. F.; Carson, K. G.; Harris, B. D.; Maryanoff, C. A.; Shah, R. D. *J. Org. Chem.* **1996**, *61*, 3849.

(31) Lorentz-Petersen, L. L. R.; Jensen, P.; Madsen, R. *Synthesis* **2009**, 4110.

(32) Gao, M.; Kong, D.; Clearfield, A.; Zheng, Q.-H. *Bioorg. Med. Chem. Lett.* **2006**, *16*, 2229.

(33) Barbero, M.; Bazzi, S.; Cadamuro, S.; Dughera, S. *Tetrahedron Lett.* **2010**, *51*, 6356.

(34) Shen, Y.-C.; Chen, C.-Y.; Hsieh, P.-W.; Duh, C.-Y.; Lin, Y.-M.; Ko, C.-L. *Chem. Pharm. Bull.* **2005**, *53*, 32.

(35) Wawzonek, S.; Nelson, G. E. *J. Org. Chem.* **1962**, *27*, 1377.

(36) Massiot, G.; Nazabadioko, S.; Bliard, C. *J. Nat. Prod.* **1995**, *58*, 1636.

(37) Sinkkonen, J.; Zelenin, K. N.; Potapov, A.-K. A.; Lagoda, I. V.; Alekseyev, V. V.; Pihlaja, K. *Tetrahedron* **2003**, *59*, 1939.

(38) Vanden Eynde, J. J.; Godin, J. r. m.; Mayence, A.; Maquestiau, A.; Anders, E. *Synthesis* **1993**, 867.

(39) Gotor-Fernandez, V.; Fernandez-Torres, P.; Gotor, V. *Tetrahedron: Asymmetry* **2006**, *17*, 2558.

(40) Gribble, G. W.; Hoffman, J. H. *Synthesis* **1977**, *1977*, 859.

(41) Raszka, B.; McKee, J.; Zanger, M. *Synth. Commun.* **2010**, *40*, 1837.

(42) Sasamoto, N.; Dubs, C.; Hamashima, Y.; Sodeoka, M. *J. Am. Chem. Soc.* **2006**, *128*, 14010.

(43) Miyazaki, M.; Ando, N.; Sugai, K.; Seito, Y.; Fukuoka, H.; Kanemitsu, T.; Nagata, K.; Odanaka, Y.; Nakamura, K. T.; Itoh, T. *J. Org. Chem.* **2010**, *76*, 534.

(44) Movassaghi, M.; Hill, M. D. *Org. Lett.* **2008**, *10*, 3485.

(45) Georgiev, V. S.; Carlson, R. P.; Van Inwegen, R. G.; Khandwala, A. *J. Med. Chem.* **1979**, *22*, 348.

(46) Awuah, E.; Capretta, A. *J. Org. Chem.* **2010**, *75*, 5627.

(47) Dong, J.; Shi, X.-X.; Xing, J.; Yan, J.-J. *Synth. Commun.* **2011**, *42*, 2806.

(48) Badre, A.; Boulanger, A.; Abou-Mansour, E.; Banaigs, B.; Combaut, G.; Francisco, C. *J. Nat. Prod.* **1994**, *57*, 528.

(49) Herbich, J.; Kapturkiewicz, A.; Nowacki, J.; Golinski, J.; Dbrowski, Z. *Phys. Chem. Chem. Phys.* **2001**, *3*, 2438.

(50) Han, B.; Yang, X.-L.; Wang, C.; Bai, Y.-W.; Pan, T.-C.; Chen, X.; Yu, W. *J. Org. Chem.* **2012**, *77*, 1136.

(51) Truong, V. L.; Morrow, M. *Tetrahedron Lett.* **2010**, *51*, 758.

Chapter 4

A Modular Ortho-Quinone Catalyst System for Dehydrogenation of Tetrahydroquinolines Under Ambient Conditions

This work has been published:

Wendlandt, A. E.; Stahl, S. S. *J. Am. Chem. Soc.* **2014**, *136*, 11910–11913.

4.1. Introduction

Copper amine oxidases contain a tyrosine-derived *ortho*-quinone in their active site that mediates aerobic oxidation of primary amines to aldehydes (e.g., topaquinone, Scheme 4.1A).[1] Biomimetic *o*-quinones such as **Q1** and **Q2** (Scheme 4.1A) have been shown to be effective synthetic catalysts for aerobic dehydrogenation of primary amines, typically affording homocoupled imines.[2] Both topaquinone and the biomimetic quinone catalysts mediate amine oxidation via a "transamination" pathway, initiated by formation of an imine adduct of the substrate with the quinone. This mechanism accounts for the highly selective oxidation of primary over secondary and tertiary amines. We recently reported that 1,10-phenanthroline-5,6-dione (phd, Scheme 4.1A) promotes amine oxidation by a non-biomimetic "addition-elimination" pathway involving a hemiaminal intermediate (Scheme 4.1B).[3] This novel mechanism enabled the substrate scope to be expanded to include secondary amines. Aerobic dehydrogenation of a number of different nitrogen heterocycles was achieved by using phd in combination with ZnI_2 and pyridinium *p*-toluene sulfonate (PPTS) as a cocatalyst (Scheme 4.1C).

This phd/ZnI_2 catalyst system demonstrated the feasibility of aerobic secondary amine dehydrogenation, but reactions often required up to 48 h to reach completion and certain product classes were not accessible. For example, quinolines are an important class of heterocycles, but even the parent tetrahydroquinoline underwent dehydrogenation to quinoline in only 18% yield (Scheme 4.1C). Here, we describe an octahedral $[Ru(phd)_3]^{2+}$ catalyst that shows considerably higher activity for amine oxidation, including successful aerobic dehydrogenation of diverse tetrahydroquinolines at room temperature with ambient air as the source of O_2.[4] This work highlights the modular nature of the phd *o*-quinone catalyst that makes it readily amenable to

optimization and adaptation to different applications. Replacement of iodide with Co(salophen) (salophen = *N*,*N*'-bis(salicylidene)-1,2-phenylenediamine) as a redox co-catalyst contributes significantly to the efficiency of the reactions.

Scheme 4.1. *Ortho*-Quinone Catalyzed Dehydrogenation of Saturated C–N Bonds.

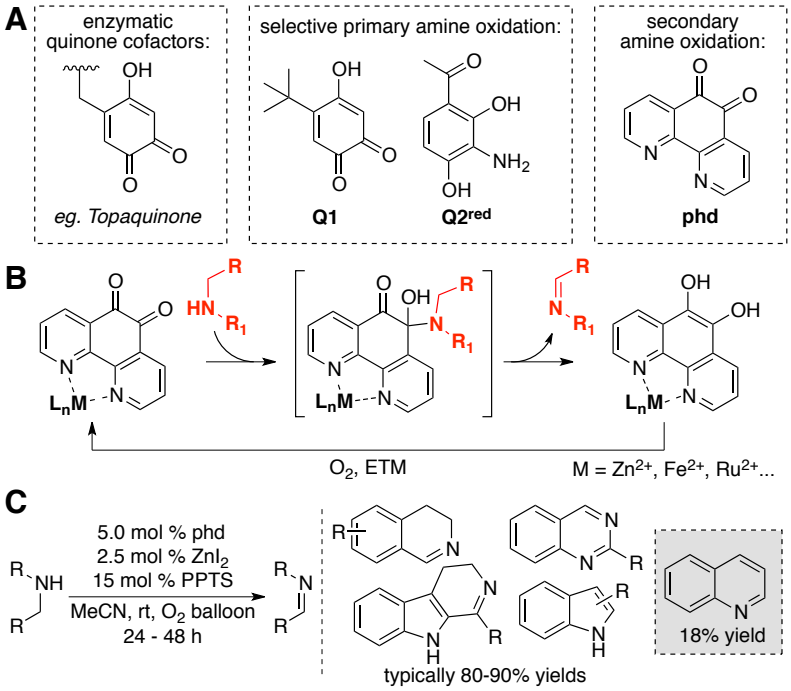

4.2. Results and Discussion

In our initial studies, we compared the previously optimized phd/ZnI_2 catalyst system with simple octahedral $[Fe(phd)_3]^{2+}$ and $[Ru(phd)_3]^{2+}$ complexes in the oxidation of tetrahydroquinoline to quinoline (Figure 4.1). The time course traces (Figure 4.1) show the low activity and conversion of the previously reported employing phd/ZnI_2 catalyst (red trace); the catalyst loses activity approx. 6-7 h into the reaction after reaching ≤20 % conversion to the quinoline product. The Fe and Ru complexes (2.5 mol %) were also tested (green and blue traces, respectively). The use of Bu_4NI (1 mol %) as a cocatalyst reflected previous observations

showing that the I/I_3^- redox couple promotes aerobic oxidation of the reduced, hydroquinone form of the phd catalyst.[5] $[Fe(phd)_3]^{2+}$ showed a similar initial rate to the ZnI_2 catalyst, but it exhibited somewhat improved stability. In contrast, $[Ru(phd)_3]^{2+}$ exhibited a significant increase in activity and a 93% yield of quinoline was obtained after 24 h. On the basis of this result, we characterized $[Ru(phd)_3](ClO_4)_2$ via X-ray crystallography (Figure 4.2).[6,7]

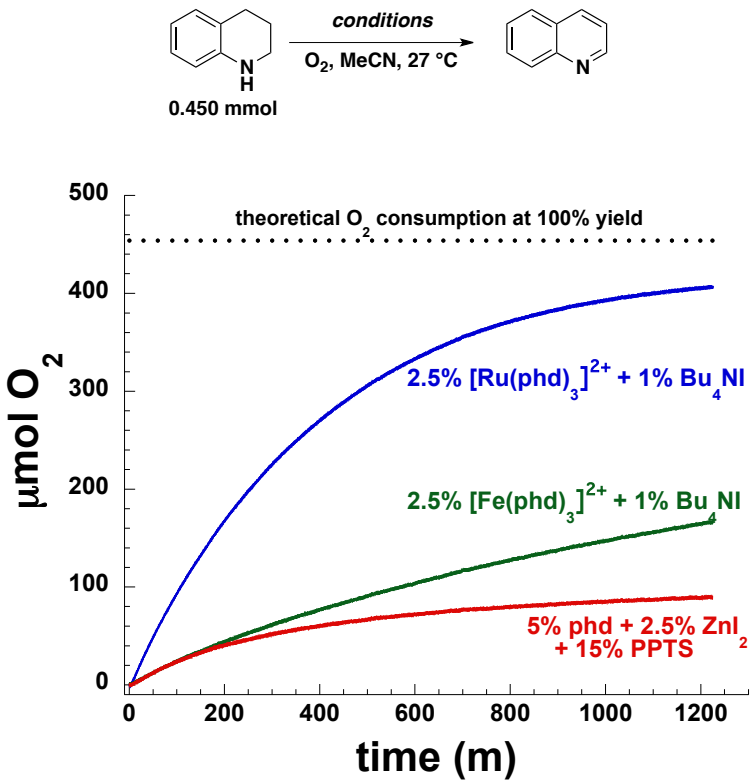

Figure 4.1. Rate comparison of Zn-, Fe-, and Ru-based catalyst systems in the oxidation of tetrahydroquinoline to quinoline.

This $[Ru(phd)_3]^{2+}/Bu_4NI$ catalyst was tested with a series of challenging *N*-heterocyclic substrates that had required 48 h to reach completion with the phd/ZnI_2 catalyst (Scheme 4.2). Improved yields and significantly decreased reaction times were observed in each case, with the most dramatic improvement observed in the dehydrogenation of tetrahydroquinoline.

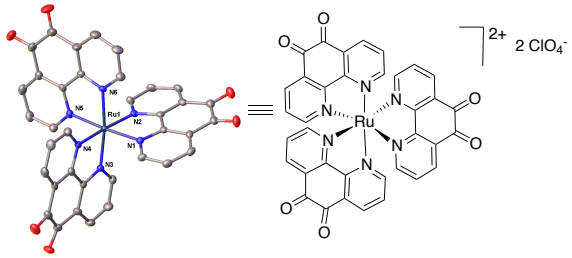

Figure 4.2. X-ray crystal structure of $[Ru(phd)_3](ClO_4)_2$ shown with 50% probablility elipsoids. All H atoms and acetonitrile solvent molecules are omitted for clarity (see Supporting Information, SI).

Iodide was previously shown to mediate aerobic oxidation of the reduced hydroquinone form of the catalyst, and a catalyst sequence for the present dehydrogenation reactions is depicted in Scheme 3, where Co-Cat$^{red/ox}$ = $3I^-/I_3^-$. We speculated that alternative co-catalysts could lead to even better catalytic reactivity. Bäckvall and others have highlighted the role of co-catalysts for aerobic oxidation of benzoquinone in multicomponent catalytic reactions,[8] and molecular catecholase mimics have been identified for aerobic oxidation of hydroquinones.[9] Drawing on these precedents, we tested a number of possible co-catalysts as replacements for Bu_4NI, including Cu(pc), Fe(pc), Co(salophen), and Co(salpr) (pc = phthalocyanine; salpr = bis(salicylideneiminato-3-propyl)methylamine).[10] Co(salophen) proved to be particularly effective, enabling full conversion within 3 h (Figure 4.3).

Scheme 4.2. Aerobic *N*-Heterocycle Dehydrogenation with phd/ZnI_2 and $[Ru(phd)_3](PF_6)_2/Bu_4NI$ Catalyst Systems.

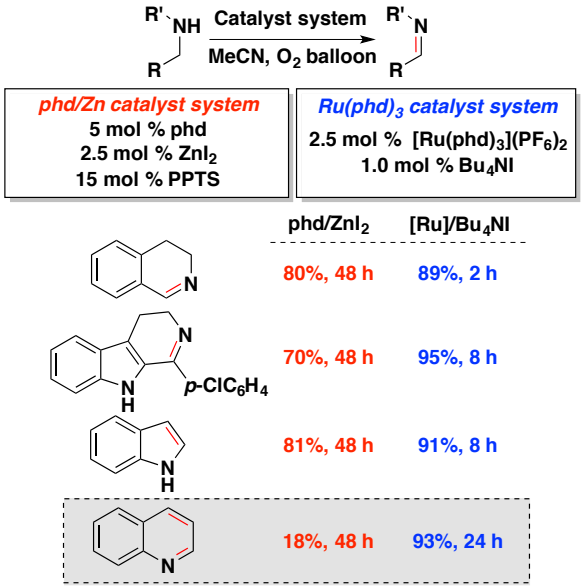

Scheme 4.3. Proposed Catalytic Sequence for $[Ru(phd)_2]^{2+}$-Mediated Dehydrogenation of Tetrahydrodroquinolines.

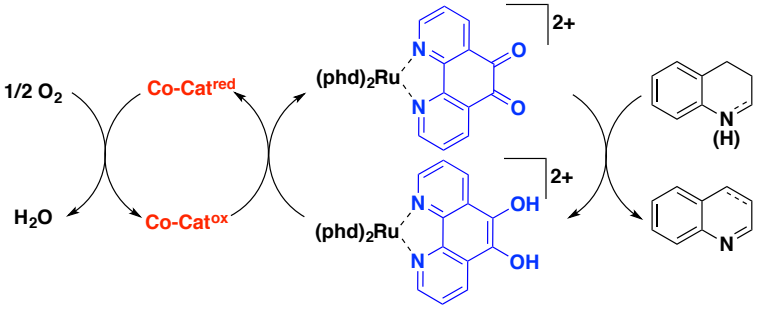

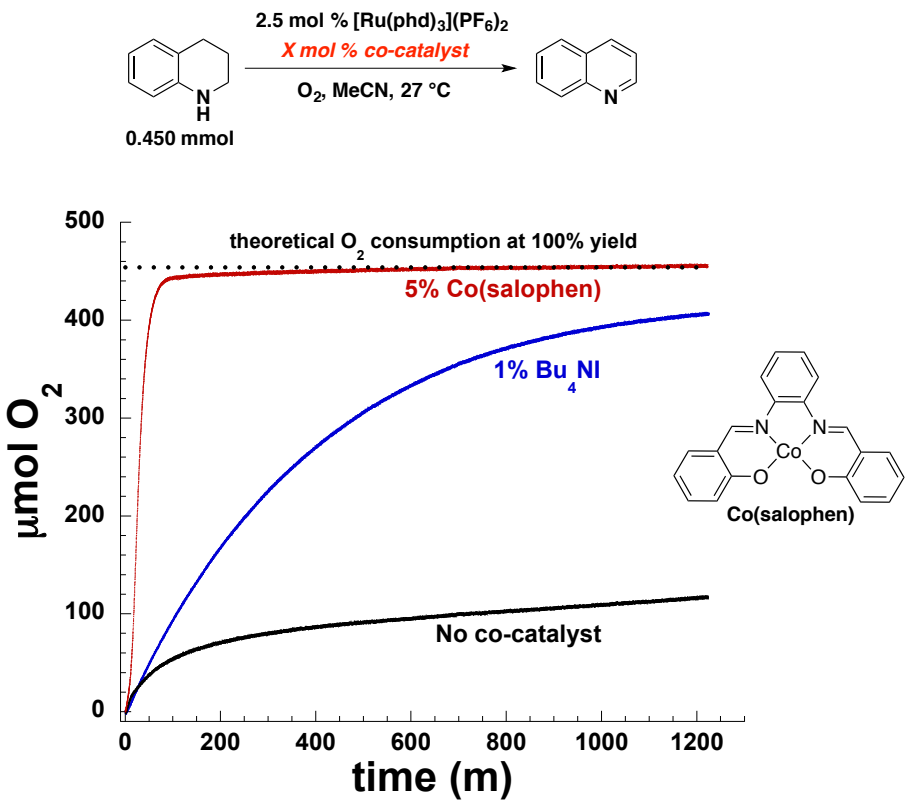

Figure 4.3. Rate comparison of different co-catalysts on the $Ru(phd)_3$-catalyzed aerobic oxidation of tetrahydroquinoline.

Subsequent studies showed that Co(salophen) enabled the reactions to proceed efficiently under ambient conditions (at room temperature with ambient air as the oxidant). The $[Ru(phd)_3]^{2+}$ catalyst structurally resembles Ru-polypyridyl complexes commonly used as photoactive catalysts, but control experiments show that the reactions exhibit identical behavior in the presence and absence of light.[11] In addition, no reaction was observed in the absence of $[Ru(phd)_3]^{2+}$, suggesting that Co(salophen) is not a competent dehydrogenation catalyst under these conditions.

This catalyst system was then demonstrated in the dehydrogenation of a number of other tetrahydroquinolines (Table 4.1). 6-Methylquinoline **3** was obtained cleanly after 6 h (91%

yield), but the more-electron rich 6-methoxyquinoline **4** was isolated in only 74% yield and considerable side-product formation was observed. Excellent yields of this product could be obtained when the reaction was carried out using 1.0 mol % Bu_4NI as the co-catalyst, suggesting that Co(salophen) co-catalyst contributes to side product formation in this reaction. The electron-deficient 6-chloroquinoline **5** was obtained in excellent yield (95%) with the original $[Ru(phd)_3]^{2+}$/Co(salophen) catalyst system.

Substitution at the 2, 3, and 4 position was well-tolerated; 4-methylquinoline **6** (97%), and 3-methylquinoline **7** (92%), were obtained after short reaction times (5–6 h). The sterically-hindered 2-methyl-quinoline **8** (83%) was obtained after slightly longer reaction time if MeOH was used as the solvent instead of MeCN. Other effective 2-substituted tetrahydroquinoline substrates included 2-butyl, 2-phenyl, and 2-styrenyl derivatives, affording quinolines **10**, **11**, and **12** in 82%, 87% and 60% yields, respectively. The medicinally-relevant quinolines, 4-(*p*-fluorophenyl)-7-methylquinoline **16**, an intermediate en route to nM leukotriene biosynthesis inhibitor[12] **17**, was obtained in 65% yield, and the advanced intermediate **18** toward BRD4 inhibitor[13] **19** was obtained in 96% yield.

When probing the reactivity of polycyclic substrate **20** (Scheme 4.4), both dehydrogenation and benzylic oxygenation occurred to afford product **21** in 68% isolated yield. This reaction provides concise access to the indeno[2,1,c]quinoline substructure present in numerous biologically active compounds,[14] including antiprotozoal agent **22**[15] and phase II topoisomerase inhibitor, TAS-103.[16]

Table 4.1. Substrate scope[a]

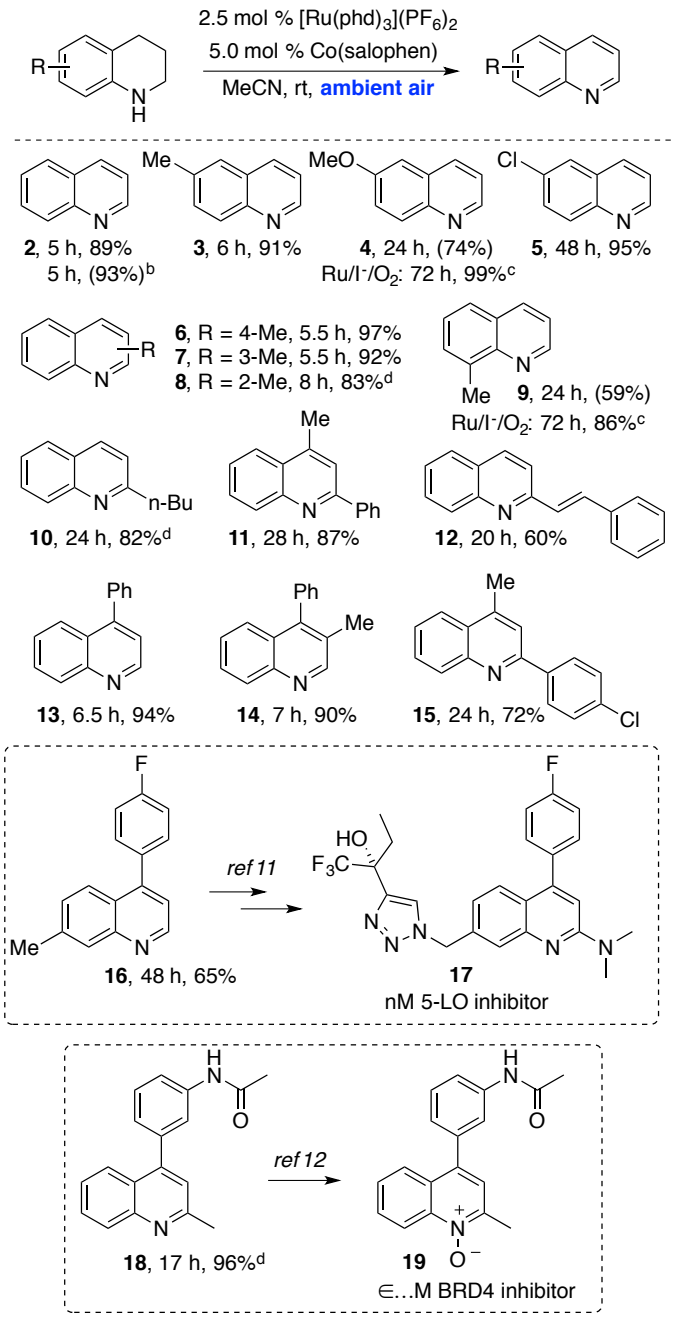

[a] Conditions: tetrahydroquinoline (1.0 mmol), $[Ru(phd)_3](PF_6)_2$ (25.5 mg, 0.025 mmol), Co(salophen) (18.7 mg, 0.05 mmol) in MeCN (4.0 mL), air, r.t. Isolated yields (yields in parentheses determined by ^{1}H NMR). [b] Performed in the dark. [c] Conditions: std conditions, but Bu_4NI (3.7 mg, 0.01 mmol) used instead of Co(salophen) and 1 atm O_2 instead of air. [d] MeOH solvent.

Scheme 4.4. Synthesis of indeno[2,1,c]quinoline **21**.[a]

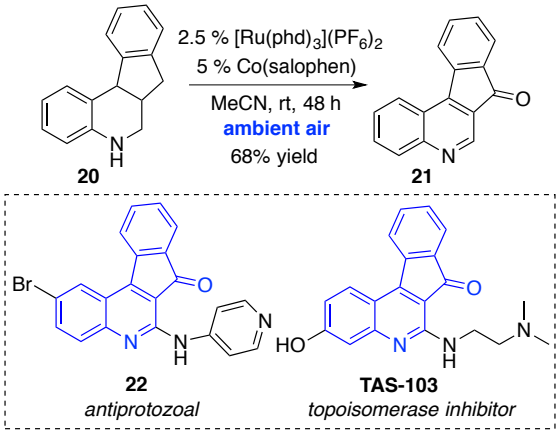

[a] Reactions conditions: tetrahydroquinoline **20** (221.3 mg, 1.0 mmol), $Ru(phd)_3(PF_6)_2$ (25.5 mg, 0.025 mmol), Co(salophen) (18.7 mg, 0.05 mmol) in MeCN (4.0 mL), stirring under air balloon at room temperature.

In conclusion, these results demonstrate the utility of $[Ru(phd)_3]^{2+}$ as a novel *o*-quinone catalyst for dehydrogenation of *N*-heterocycles. The results show that the substitutionally inert Ru^{2+} ion is more effective than Zn^{2+} in activating phd toward secondary amine dehydrogenation. Replacement of iodide with Co(salophen) as a redox cocatalyst to promote aerobic oxidation of the hydroquinone catalyst leads to substantial improvement in catalyst activity and enables the reactions to proceed under ambient conditions. The modular nature of the catalyst system described here has important implications for future studies targeting other aerobic quinone-mediated oxidation reactions.

4.3. Acknowledgements

We thank Kelsey Miles for X-ray crystallographic determination. We are grateful for financial support from the NIH (R01-GM100143). Analytical instrumentation was partially funded by the

National Science Foundation (CHE-1048642, CHE-9208463, CHE-0342998, CHE-9974839, CHE-9304546) and National Institutes of Health (NIH 1 S10 RR13866-01).

4.4. Experimental Details and Supplementary Information

4.4.1. General Considerations.

All commercially available compounds were purchased from Sigma-Aldrich, and used as received unless otherwise indicated. Solvents were dried over alumina columns prior to use. ^{1}H and ^{13}C NMR spectra for compound characterization were recorded on Bruker AC-300 MHz, Avance-400 MHz, Avance-500 MHz or Varian Mercury-300 MHz spectrometers. Chemical shift values are given in parts per million relative to residual solvent peaks (^{1}H and ^{13}C). High-resolution, exact mass measurements were obtained by the mass spectrometry facility at the University of Wisconsin. C, H, N elemental analyses were carried out by Robertson Microlit Laboratories. Melting points were taken on a Mel-Temp II melting point apparatus. Flash chromatography was performed using SilicaFlash® P60 (Silicycle, particle size 40-63 μm, 230-400 mesh).

4.4.2. Procedure for Multiwell Gas Uptake Kinetics Measurements (Figures 4.1 and 4.3)

Each set of data was collected using a 6-well gas uptake apparatus which holds individually calibrated 50 mL round bottom flasks, each connected to a pressure transducer designed to measure the gas pressure within each sealed reaction vessel. Five vessels contained various reaction mixtures, and the sixth well used as a solvent control for variations in pressure. The

apparatus was evacuated and filled with O2 to 600 torr three times. The pressure was established at 600 torr with the flasks heated to 27 °C. Solution A (see below) was added via syringe through a septum, and the pressure and temperature allowed to equilibrate. When the pressure (approximately 700 torr) and temperature (27 °C) stabilized, solution B (see below) was added via syringe through a septum. Data were acquired using custom software written within LabVIEW (National Instruments).

Specific conditions for Figure 1

- "5% phd + 2.5% ZnI_2 + 15% PPTS"

Solution A: phd (4.74 mg, 0.0225 mmol, 0.05 equiv) in 1.0 mL MeCN. Solution B: PPTS (16.98 mg, 0.0676 mmol, 0.15 equiv), ZnI_2 (3.59 mg, 0.0112 mmol, 0.025 equiv) and tetrahydroquinoline (60.1 mg, 0.451 mmol, 1.0 equiv) in 1.0 mL MeCN.

- "2.5% $Fe(phd)_3$ + 1% Bu_4NI"

Solution A: Bu_4NI (1.66 mg, 0.0045 mmol, 0.01 equiv) and tetrahydroquinoline (60.1 mg, 0.451 mmol, 1.0 equiv) in 1.0 mL MeCN. Solution B: $Fe(phd)_3$ $2PF_6$ (11.0 mg, 0.0113 mmol, 0.025 equiv) in 1.0 mL MeCN.

- "2.5% $Ru(phd)_3$ + 1% Bu_4NI"

Solution A: Bu_4NI (1.66 mg, 0.0045 mmol, 0.01 equiv) and tetrahydroquinoline (60.1 mg, 0.451 mmol, 1.0 equiv) in 1.0 mL MeCN. Solution B: $Ru(phd)_3$ $2PF_6$ (11.5 mg, 0.0113 mmol, 0.025 equiv) in 1.0 mL MeCN.

Specific conditions for Figure 3

- "no co-catalyst"

Solution A: tetrahydroquinoline (60.1 mg, 0.451 mmol, 1.0 equiv) in 1.0 mL MeCN. Solution B: $Ru(phd)_3$ $2PF_6$ (11.5 mg, 0.0113 mmol, 0.025 equiv) in 1.0 mL MeCN.

- "1% Bu_4NI"

As "2.5% $Ru(phd)_3$ + 1% Bu_4NI" in Figure 1.

- "5% Co(salophen)"

Co(salophen) (8.41 mg, 0.0225 mmol, 0.05 equiv) was added as a solid to the flask prior to evacuating/backfilling with O_2. Solution A: tetrahydroquinoline (60.1 mg, 0.451 mmol, 1.0 equiv) in 1.0 mL MeCN. Solution B: $Ru(phd)_3$ $2PF_6$ (11.5 mg, 0.0113 mmol, 0.025 equiv) in 1.0 mL MeCN.

4.4.3. Procedures for aerobic reaction screening

In a disposable culture tube, a solution of $[Ru(phd)_3]2PF_6$ (2.5 mol %, 0.065 mmol) in 0.25 mL was added to Bu_4NI (0.5 to 2.5 mol %), Co(salophen) (5.0 mol %), or other co-catalyst (5.0 mol %) in 0.25 mL MeCN. 1,2,3,4-Tetrahydroquinoline (15 μL, 0.130 mmol) was added, and the reaction tube was placed into an aluminum block mounted on a Large Capacity Mixer (Glas-Col) that enabled several reactions to be performed simultaneously under a constant pressure of

(approx.) 1 atm O_2 with orbital agitation. The headspace above the tubes was filled and purged with oxygen gas multiple times, and then left under constant pressure of O_2 for 24 h. Upon completion, the tube was removed and 1,3,5-trimethoxybenzene was added as an internal standard. The reaction solvents were removed under vacuum, and the residue was suspended in $CDCl_3$ and filtered through a short plug of Celite for NMR analysis. The yield was determined by ^{1}H NMR spectroscopy (relaxation delay >25 s) versus the internal standard.

4.4.4. Additional Tables and Figures

Table 4.2. Additional Co-catalyst Screening Data (see above for conditions)

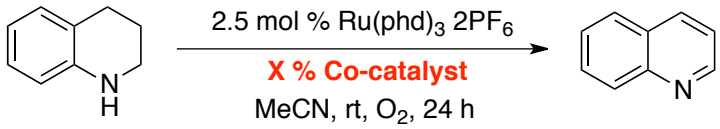

entry	co-catalyst	NMR Yields
1	----	16 %
2	0.5 % TBAI	82 %
3	**1.0 % TBAI**	**93 %**
4	1.5 % TBAI	74 %
5	2.0 % TBAI	61 %
6	2.5 % TBAI	48 %
7	5.0 % Cu(pc)	7 %
8	5.0 % Fe(pc)	79 %
9	5.0 % Co(salpr)	33 %
10	**5.0 % Co(salophen)**	**89 %**

Figure 4.4. Multiwell gas uptake plot for 1% to 5% Co(salophen)

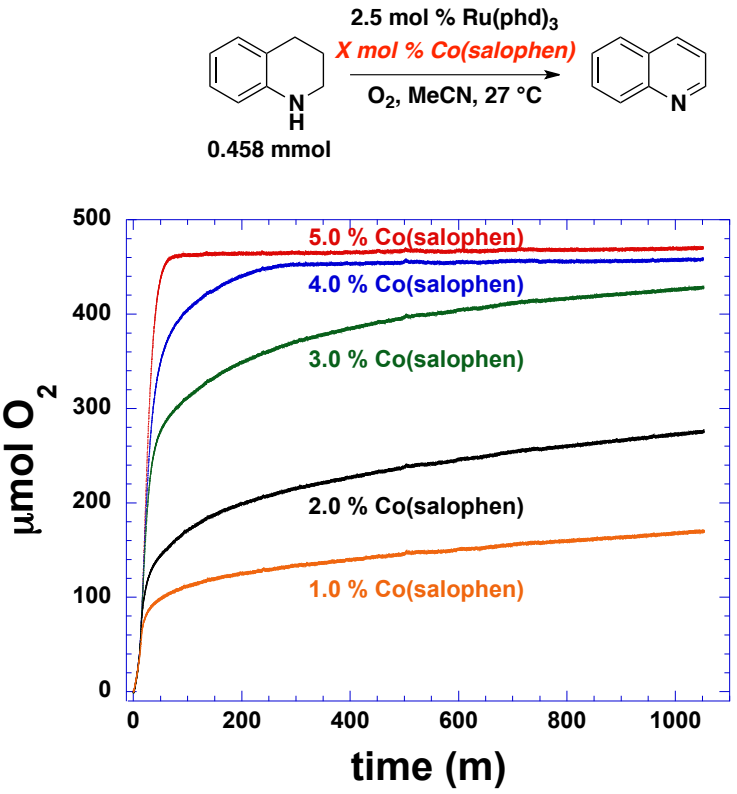

4.4.5. Synthesis and Characterization of Catalysts

1,10-Phenanthroline-5,6-dione, phd, was prepared according to the method previously reported,[3] and is also commercially available. Co(salophen) was prepared according to the method of Backvall,[17] and is also commercially available.

$[Fe(phd)_3](PF_6)_2 H_2O$

$[Fe(phd)_3]2PF_6$ was prepared based on the method reported previously.[7a] To a solution of phd (695 mg, 3.3 mmol, 3.2 equiv) in 1:1 EtOH/H_2O was added $(NH_4)_2Fe(SO_4)_2{\cdot}6H_2O$ (405 mg, 1.03 mmol, 1.0 equiv). The reaction was stirred for 60 minutes at room temperature, and then precipitated with a saturated aqueous solution of NH_4PF_6. The solids were collected and washed

sequentially with H_2O, EtOH, and Et_2O. The complex was then dissolved in a minimum of MeCN, filtered through celite, and reprecipitated by slow addition of Et_2O to give 772 mg (76% yield) of the title complex as a black crystalline solid. ^{1}H NMR (500 MHz, CD_3CN) δ 8.66 (dd, *J* = 7.9, 1.3 Hz, 6H), 7.81 (dd, *J* = 5.6, 1.4 Hz, 6H), 7.73 (dd, *J* = 7.9, 5.6 Hz, 6H). ^{13}C NMR (126 MHz, CD_3CN) δ 175.55, 160.32, 158.70, 138.30, 131.37, 129.50; Anal. Calc for $C_{36}H_{20}F_{12}FeN_6O_7P_2$: C, 43.48; H, 2.03; N, 8.45. Found: C, 42.89; H, 2.30; N, 8.71.

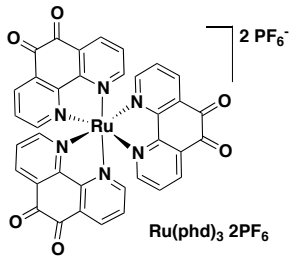

[Ru(phd)$_3$]2PF$_6$

$Ru(dmso)_4Cl_2$ was prepared from $RuCl_3$ according to a previously reported procedure.[18] $Ru(dmso)_4Cl_2$ (598 mg, 1.23 mmol) and phd (870 mg, 4.13 mmol, 3.3 equiv) were loaded into a round bottom flask and 25 mL of 1:1 EtOH/H_2O was added. The sample was quickly frozen and degassed three times by the method of freeze-pump-thaw. The sample was the equipped with a condenser and refluxed under nitrogen overnight. After cooling to room temperature, the sample was precipitated by the addition of a saturated aqueous solution of NH_4PF_6. Solid was collected, washed with water, EtOH, then Et_2O and dried under vacuum. The sample was then redissolved in a minimum of MeCN and filtered through a pad of celite. The pad was washed with MeCN, and Et_2O was slowly added to the collected filtrate to give 693 mg (55% yield) of [Ru(phd)$_3$]2PF$_6$ as a brown solid: ^{1}H NMR (500 MHz, CD_3CN) δ 8.62 (dd, *J* = 8.1, 1.4 Hz, 6H),

8.13 (d, J = 5.1 Hz, 6H), 7.72 (dd, J = 8.0, 5.6 Hz, 6H); ^{13}C NMR (126 MHz, CD_3CN) δ 175.54, 157.65, 156.78, 137.50, 131.46, 129.56; Anal. Calc for $C_{36}H_{18}F_{12}N_6O_6P_2Ru$: C, 42.33; H, 1.78; N, 8.23. Found: C, 42.12; H, 2.03; N, 8.13.

4.4.6. Synthesis and Characterization of Substrates

1,2,3,4-Tetrahydroquinoline, 6-methyltetrahydroquinoline, 6-methoxytetrahydroquinoline, 6-chlorotetrahydroquinoline were obtained from commercial sources and used as received. 2-methyltetrahydroquinoline, 3-methyltetrahydroquinoline, 4-methyltetrahydroquinoline, and 8-methyltetrahydroquinoline were obtained by high-pressure hydrogenation of the corresponding quinoline (commercial) according to literature procedure.[19] 4-phenyltetrahydroquinoline and 3-methyl-4-phenyltetrahydroquinoline were obtained according to literature procedure.[20] 2-butyltetrahydroquinoline, 2-styrenyltetrahydroquinoline were obtained from the method of Miyata.[21] 4-methyl-2-phenyltetrahydroquinoline and 4-methyl-2-(*p*-chlorophenyl)-tetrahydroquinoline were obtained according to a literature method.[22]

The synthesis of 4-(*p*-fluorophenyl)-7-methyltetrahydroquinoline, 4-(*m*-acetamido-phenyl)-2-methyltetrahydroquinoline, and compound **20** were synthesized according to the following common method. Desired benzylic azide was obtained from the appropriate benzylic bromide based on literature procedure.[23] The hetero-Diels-Alder reaction was carried out according to the procedure of Pearson.[24]

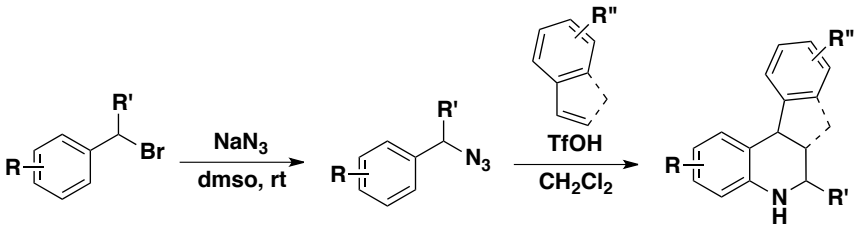

To 400 mL of DMSO was added NaN_3 (1.45g, 22 mmol, 1.1 equiv), and the suspension was allowed to stir for 1 h or until completely dissolved. The appropriate benzylic bromide was then added (20 mmol, 1.0 equiv), and the mixture was stirred at room temperature overnight. After completion, 400 mL H_2O was added and the solution was allowed to cool to room temperature. The mixture was then extracted with 3 x 200 mL Et_2O, and the organic phase was washed with 2 x 100 mL H_2O followed by 1 x 100 mL brine. The organic phase was then dried over $MgSO_4$, and concentrated to give the corresponding azides (yields >90%), which were used without further purification.

A solution of the appropriate benzylic azide was added to CH_2Cl_2 and cooled to 0 °C. TfOH (1.1 equiv) was added, and the solution allowed to stir for 10 min at room temperature. Indene or the appropriate styrene (2.0 equiv) was then added (either at room temperature, or at 0 °C) and the reaction stirred at the indicated temperature until completion (see below). The reaction was quenched by addition of saturated aqueous Na_2CO_3, and extracted into EtOAc (3 x 100 mL). The organic phase was washed with brine, dried over $MgSO_4$, concentrated, and purified by column chromatography.

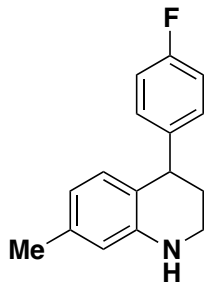

From 3-methylbenzyl azide. 4-fluorostyrene was added at room temperature, and stirred for 1 h at room temperature. ^{1}H NMR (500 MHz, $CDCl_3$) δ 7.15 – 7.06 (m, 2H), 7.03 – 6.92 (m, 2H), 6.61 (d, *J* = 7.6 Hz, 1H), 6.46 – 6.35 (m, 2H), 4.10 (t, *J* = 6.1 Hz, 1H), 3.87 (s, 1H), 3.29 (ddd, *J* = 11.0, 7.2, 3.6 Hz, 1H), 3.21 (ddd, *J* = 11.5, 8.1, 3.4 Hz, 1H), 2.24 (s, 3H), 2.18 (dddd, *J* = 13.3, 8.1, 5.4, 3.5 Hz, 1H), 1.99 (dtd, *J* = 13.0, 7.1, 3.4 Hz, 1H); ^{13}C NMR (126 MHz, $CDCl_3$) δ 161.33 (d, *J* = 243.9 Hz), 144.74, 142.46 (d, *J* = 3.2 Hz), 137.18, 130.20, 129.96 (d, *J* = 7.8 Hz), 120.43, 118.16, 115.08, 114.84 (d, *J* = 17.3 Hz), 41.81, 39.17, 31.46, 21.18; MS: Calc for $C_{16}H_{16}FN$: 242.1340; Meas: 242.1333.

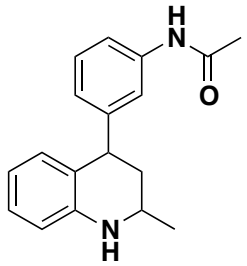

From (1-azidoethyl)benzene. 3-acetamidostyrene was added at room temperature and stirred at reflux overnight. Mp = 175-180 °C; ^{1}H NMR (400 MHz, $CDCl_3$) δ 7.60 – 7.49 (m, 1H), 7.29 (m, overlaps with $CHCl_3$, 1H), 7.22 (t, *J* = 1.8 Hz, 1H), 7.14 (br s, 1H), 7.06 – 6.94 (m, 2H), 6.69 – 6.47 (m, 3H), 4.15 (dd, *J* = 12.4, 5.5 Hz, 1H), 3.81 (br s, 1H), 3.60 (dtt, *J* = 12.5, 6.3, 3.1 Hz, 1H), 2.32 – 2.08 (m, 4H), 1.82 (td, *J* = 12.6, 11.1 Hz, 1H), 1.24 (d, *J* = 6.2 Hz, 3H); ^{13}C NMR

(101 MHz, $CDCl_3$) δ 168.13, 146.97, 145.32, 138.04, 129.75, 129.19, 127.17, 124.75, 124.49, 119.81, 118.06, 117.32, 114.09, 47.62, 44.44, 41.18, 24.67, 22.56; MS: Calc for $C_{18}H_{20}N_2O$: 281.1649; Meas: 281.1649.

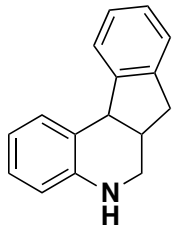

From benzyl azide. Indene was added at 0 °C, and the reaction stirred for 1 h at this temperature. Mp = 89-90 °C. ^{1}H NMR (500 MHz, $CDCl_3$) δ 7.36 (m, 2H), 7.29 – 7.21 (m, 1H), 7.18 – 7.11 (m, 2H), 7.04 (td, *J* = 7.9, 1.5 Hz, 1H), 6.79 (td, *J* = 7.4, 1.2 Hz, 1H), 6.57 (dd, *J* = 7.9, 1.2 Hz, 1H), 4.32 (d, *J* = 6.0 Hz, 1H), 3.84 (br s, 1H), 3.30 – 3.13 (m, 2H), 2.93 – 2.78 (m, 2H), 2.72 (dd, *J* = 15.7, 1.8 Hz, 1H); ^{13}C NMR (126 MHz, $CDCl_3$) δ 146.58, 144.81, 141.39, 130.78, 127.07, 126.52, 126.33, 125.25, 124.53, 122.22, 117.60, 114.87, 45.64, 43.14, 37.14, 36.11; MS: Calc for $C_{16}H_{15}N$: 222.1278; Meas: 222.1277.

4.4.7. Synthesis and Characterization of Products

General procedure for oxidation of tetrahydroquinolines to quinolines.

A 25 mL round bottom flask equipped with a stir bar was loaded with tetrahydroquinoline (1.0 mmol), $[Ru(phd)_3]2PF_6$ (0.025 mmol, 25.5 mg), and Co(salophen) (0.05 mmol, 18.7 mg). MeCN (4.0 mL) or MeOH (if indicated) was added and the reaction was stirred open to ambient air until TLC indicated completion. (Typically, for reaction times longer than 8 h, the reaction was

equipped with an air balloon to minimize solvent evaporation). The crude reaction mixture was then diluted with EtOAc and filtered through a pad of celite. The celite pad was subsequently washed with EtOAc (5 x 50 mL) and the combined filtrate was concentrated *in vacuo*. Purification using SiO_2 chromatography afforded the desired quinoline product.

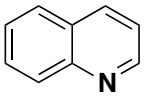

Characterization data matched those of authentic material.[25] ^{1}H NMR (500 MHz, $CDCl_3$) δ 8.89 (dd, *J* = 4.2, 1.7 Hz, 1H), 8.09 (dd, *J* = 8.3, 1.5 Hz, 2H), 7.76 (dd, *J* = 8.1, 1.4 Hz, 1H), 7.68 (ddd, *J* = 8.4, 6.9, 1.4 Hz, 1H), 7.50 (ddd, *J* = 8.0, 6.8, 1.1 Hz, 1H), 7.34 (dd, *J* = 8.2, 4.2 Hz, 1H); ^{13}C NMR (126 MHz, $CDCl_3$) δ 150.42, 148.28, 136.02, 129.46, 129.44, 128.26, 127.79, 126.52, 121.06.

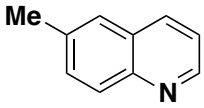

Characterization data matched those of authentic material.[25] ^{1}H NMR (500 MHz, $CDCl_3$) δ 8.82 (dd, *J* = 4.3, 1.7 Hz, 1H), 8.00 (t, *J* = 9.7 Hz, 2H), 7.57 – 7.45 (m, 2H), 7.30 (dd, *J* = 8.2, 4.2 Hz, 1H), 2.49 (s, 3H); ^{13}C NMR (126 MHz, $CDCl_3$) δ 149.53, 146.90, 136.34, 135.32, 131.71, 129.11, 128.29, 126.58, 121.04, 21.57; MS: Calc for $C_{10}H_9N$: 144.0808; Meas: 144.0809.

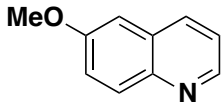

Characterization data matched those of authentic material.[25] ^{1}H NMR (400 MHz, $CDCl_3$) δ 8.76 (dd, *J* = 4.2, 1.7 Hz, 1H), 8.03 (dd, *J* = 8.4, 1.3 Hz, 1H), 7.99 (d, *J* = 9.2 Hz, 1H), 7.43 – 7.27 (m,

2H), 7.06 (d, J = 2.8 Hz, 1H), 3.92 (s, 3H); ^{13}C NMR (101 MHz, $CDCl_3$) δ 157.71, 147.96, 144.45, 134.76, 130.88, 129.29, 122.27, 121.36, 105.10, 55.53; MS: Calc for $C_{10}H_9NO$: 160.0757; Meas: 160.0759.

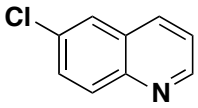

Characterization data matched those of authentic material.[25] Mp = 35-37 °C; ^{1}H NMR (500 MHz, $CDCl_3$) δ 8.91 (dd, J = 4.2, 1.7 Hz, 1H), 8.14 – 7.99 (m, 2H), 7.80 (d, J = 2.3 Hz, 1H), 7.65 (dd, J = 9.0, 2.3 Hz, 1H), 7.42 (dd, J = 8.3, 4.2 Hz, 1H); ^{13}C NMR (126 MHz, $CDCl_3$) δ 149.59, 145.62, 134.10, 131.26, 130.10, 129.39, 127.80, 125.39, 120.89; MS: Calc for C_9H_6ClN: 164.0262; Meas: 164.0260.

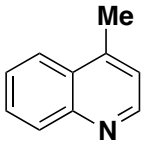

Characterization data matched those of authentic material.[25] ^{1}H NMR (400 MHz, $CDCl_3$) δ 8.78 (d, J = 4.4 Hz, 1H), 8.11 (d, J = 8.5 Hz, 1H), 8.00 (dd, J = 8.3, 0.9 Hz, 1H), 7.71 (ddd, J = 8.4, 6.8, 1.4 Hz, 1H), 7.57 (ddd, J = 8.2, 7.0, 1.2 Hz, 1H), 7.23 (dd, J = 4.4, 1.2 Hz, 1H), 2.71 (s, 3H); ^{13}C NMR (101 MHz, $CDCl_3$) δ 150.20, 147.99, 144.31, 130.03, 129.12, 128.29, 126.29, 123.82, 121.87, 18.69; MS: Calc for $C_{10}H_9N$: 144.0808; Meas: 144.0812.

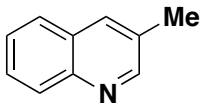

Characterization data matched those of authentic material.[25] ^{1}H NMR (500 MHz, $CDCl_3$) δ 8.77 (d, *J* = 2.2 Hz, 1H), 8.06 (dd, *J* = 8.3, 1.1 Hz, 1H), 7.90 (d, *J* = 1.1 Hz, 1H), 7.73 (dd, *J* = 8.1, 0.7 Hz, 1H), 7.64 (ddd, *J* = 8.4, 6.8, 1.5 Hz, 1H), 7.50 (ddd, *J* = 8.1, 6.8, 1.2 Hz, 1H), 2.51 (s, 3H); ^{13}C NMR (126 MHz, $CDCl_3$) δ 152.44, 146.57, 134.66, 130.47, 129.19, 128.43, 128.13, 127.13, 126.55, 18.77 MS: Calc for $C_{10}H_9N$: 144.0808; Meas: 144.0807.

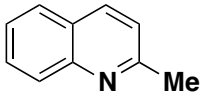

Characterization data matched those of authentic material.[25] ^{1}H NMR (500 MHz, $CDCl_3$) δ 8.02 (d, *J* = 8.7 Hz, 2H), 7.77 (dd, *J* = 8.0, 1.3 Hz, 1H), 7.68 (ddd, *J* = 8.5, 6.9, 1.5 Hz, 1H), 7.48 (ddd, *J* = 8.1, 6.9, 1.2 Hz, 1H), 7.28 (d, *J* = 8.4 Hz, 1H), 2.75 (s, 3H);^{13}C NMR (126 MHz, $CDCl_3$) δ 159.01, 147.89, 136.17, 129.43, 128.65, 127.49, 126.49, 125.67, 122.01, 25.43; MS: Calc for $C_{10}H_9N$: 144.0808; Meas: 144.0810.

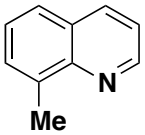

Characterization data matched those of authentic material.[25] ^{1}H NMR (400 MHz, $CDCl_3$) δ 8.95 (dd, *J* = 4.3, 1.8 Hz, 1H), 8.13 (dd, *J* = 8.2, 1.7 Hz, 1H), 7.67 (d, *J* = 8.4 Hz, 1H), 7.57 (dt, *J* = 7.0, 1.3 Hz, 1H), 7.47 – 7.34 (m, 2H), 2.83 (s, 3H); ^{13}C NMR (101 MHz, $CDCl_3$) δ 149.27, 147.40, 137.12, 136.30, 129.61, 128.28, 126.30, 125.87, 120.84, 18.15; MS: Calc for $C_{10}H_9N$: 144.0808; Meas: 144.0809.

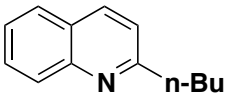

Characterization data matched those previously reported.[26] ^{1}H NMR (400 MHz, $CDCl_3$) δ 8.11 – 8.00 (m, 2H), 7.77 (dd, *J* = 8.2, 1.2 Hz, 1H), 7.67 (ddd, *J* = 8.5, 6.9, 1.5 Hz, 1H), 7.47 (ddd, *J* = 8.1, 6.9, 1.2 Hz, 1H), 7.29 (d, *J* = 8.5 Hz, 1H), 3.10 – 2.89 (m, 2H), 1.89 – 1.71 (m, 2H), 1.54 – 1.34 (m, 2H), 0.96 (t, *J* = 7.4 Hz, 3H); ^{13}C NMR (101 MHz, $CDCl_3$) δ 163.12, 147.93, 136.15, 129.30, 128.85, 127.48, 126.71, 125.62, 121.38, 39.15, 32.22, 22.71, 14.02; MS: Calc for $C_{13}H_{15}N$: 186.1278; Meas: 186.1276.

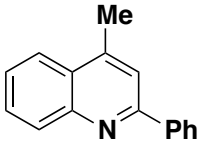

Characterization data matched those of authentic material.[26] ^{1}H NMR (400 MHz, $CDCl_3$) δ 8.17 (ddd, *J* = 9.8, 8.3, 1.4 Hz, 3H), 8.05 – 7.97 (m, 1H), 7.73 (d, *J* = 1.4 Hz, 2H), 7.61 – 7.49 (m, 3H), 7.47 (m, 1H), 2.78 (s, 3H); ^{13}C NMR (101 MHz, $CDCl_3$) δ 157.09, 148.16, 144.79, 139.85, 130.33, 129.32, 129.19, 128.78, 127.54, 127.27, 126.02, 123.61, 119.77, 19.03; MS: Calc for $C_{16}H_{13}N$: 220.1121; Meas: 220.1124.

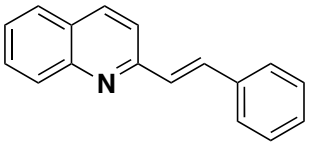

Characterization data matched those previously reported.[27] ^{1}H NMR (500 MHz, $CDCl_3$) δ 8.05 (d, *J* = 8.5 Hz, 1H), 8.01 (dd, *J* = 8.5, 1.1 Hz, 1H), 7.75 – 7.68 (m, 1H), 7.67 – 7.53 (m, 5H), 7.42 (ddd, *J* = 8.1, 6.8, 1.2 Hz, 1H), 7.38 – 7.30 (m, 3H), 7.28 – 7.22 (m, 1H); ^{13}C NMR (126 MHz,

$CDCl_3$) δ 156.01, 148.29, 136.53, 136.35, 134.43, 129.75, 129.23, 129.05, 128.81, 128.64, 127.51, 127.36, 127.28, 126.18, 119.28; MS: Calc for $C_{17}H_{13}N$: 232.1121; Meas: 232.1117.

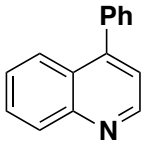

Characterization data matched those previously reported.[28] ^{1}H NMR (500 MHz, $CDCl_3$) δ 8.95 (d, *J* = 4.4 Hz, 1H), 8.18 (dd, *J* = 8.5, 1.2 Hz, 1H), 7.93 (dd, *J* = 8.6, 1.4 Hz, 1H), 7.73 (ddd, *J* = 8.4, 6.8, 1.4 Hz, 1H), 7.59 – 7.44 (m, 6H), 7.34 (d, *J* = 4.3 Hz, 1H); ^{13}C NMR (126 MHz, $CDCl_3$) δ 150.01, 148.71, 148.48, 138.01, 129.88, 129.56, 129.32, 128.59, 128.43, 126.77, 126.63, 125.89, 121.35; MS: Calc for $C_{15}H_{11}N$: 206.0965; Meas: 206.0969.

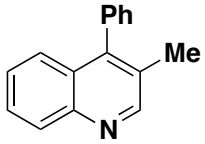

Characterization data matched those previously reported.[29] Mp = 83-85 °C. ^{1}H NMR (400 MHz, $CDCl_3$) δ 8.78 (s, 1H), 8.04 (d, *J* = 8.4 Hz, 1H), 7.56 (td, *J* = 6.8, 1.8 Hz, 0H), 7.52 – 7.27 (m, 5H), 7.20 (d, *J* = 6.9 Hz, 2H), 2.19 (s, 3H); ^{13}C NMR (101 MHz, $CDCl_3$) δ 152.66, 146.91, 146.25, 136.90, 129.37, 129.25, 128.60, 128.18, 128.03, 127.89, 127.56, 126.42, 125.88,17.60; MS: Calc for $C_{16}H_{13}N$: 220.1121; Meas: 220.1120.

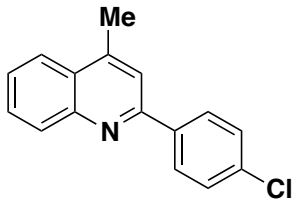

Mp = 65-67 °C.^{1}H NMR (500 MHz, $CDCl_3$) δ 8.15 (d, *J* = 8.5 Hz, 1H), 8.12 (d, *J* = 8.6 Hz, 2H), 8.01 (dd, *J* = 8.3, 1.3 Hz, 1H), 7.73 (ddd, *J* = 8.4, 6.8, 1.4 Hz, 1H), 7.69 (q, *J* = 1.1 Hz, 1H), 7.56 (ddd, *J* = 8.2, 6.8, 1.3 Hz, 1H), 7.49 (d, *J* = 8.8 Hz, 2H), 2.78 (d, *J* = 1.0 Hz, 3H); ^{13}C NMR (126 MHz, $CDCl_3$) δ 155.73, 148.08, 145.08, 138.21, 135.39, 130.27, 129.51, 128.96, 128.79, 127.30, 126.25, 123.65, 119.34, 19.08; MS: Calc for $C_{16}H_{12}ClN$: 254.0732; Meas: 254.0727.

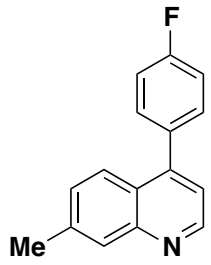

Compound has been previously reported.[12a] Mp = 115-118 °C; ^{1}H NMR (500 MHz, $CDCl_3$) δ 8.82 (d, *J* = 4.4 Hz, 1H), 7.88 (s, 1H), 7.69 (d, *J* = 8.5 Hz, 1H), 7.51 – 7.35 (m, 2H), 7.27 (dd, *J* = 8.6, 1.7 Hz, 1H), 7.22 – 7.05 (m, 3H), 2.50 (s, 3H); ^{13}C NMR (126 MHz, $CDCl_3$) δ 162.88 (d, *J* = 248.1 Hz), 149.94, 148.95, 147.13, 139.74, 134.12 (d, *J* = 3.3 Hz), 131.20 (d, *J* = 8.0 Hz), 129.03, 128.92, 125.25, 124.73, 120.64, 115.63 (d, *J* = 21.6 Hz), 21.73; MS: Calc'd for $C_{16}H_{12}FN$: 238.1027; Meas: 238.1032.

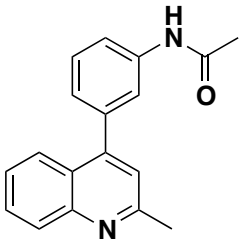

Characterization data matched those previously reported.[13] Mp = 188-190 °C; ^{1}H NMR (500 MHz, $CDCl_3$) δ 8.07 (d, *J* = 8.4 Hz, 1H), 7.84 (d, *J* = 8.5 Hz, 1H), 7.73 – 7.56 (m, 4H), 7.48 – 7.38 (m, 2H), 7.25 – 7.18 (m, 2H), 2.76 (s, 3H), 2.20 (s, 3H); ^{13}C NMR (126 MHz, $CDCl_3$) δ 168.50, 158.49, 148.29, 148.04, 138.91, 138.22, 129.42, 129.19, 128.89, 125.86, 125.58, 125.38, 124.95, 122.19, 120.77, 119.70, 25.30, 24.65; MS: Calc for $C_{18}H_{16}N_2O$: 277.1336; Meas: 277.1334.

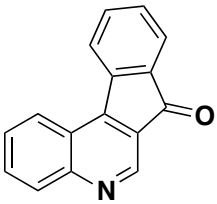

Compound has been previously reported.[30] mp = 223-224 °C; ^{1}H NMR (500 MHz, $CDCl_3$) δ 9.17 (s, 1H), 8.50 (dd, *J* = 8.4, 1.0 Hz, 1H), 8.19 (dt, *J* = 8.5, 0.8 Hz, 1H), 8.14 (d, *J* = 7.5 Hz, 1H), 7.86 (ddd, *J* = 8.2, 6.7, 1.3 Hz, 1H), 7.79 (dt, *J* = 7.4, 0.9 Hz, 1H), 7.71 (ddd, *J* = 8.1, 6.8, 1.3 Hz, 1H), 7.64 (td, *J* = 7.6, 1.2 Hz, 1H), 7.51 (td, *J* = 7.4, 0.9 Hz, 1H); ^{13}C NMR (126 MHz, $CDCl_3$) δ 193.08, 152.66, 151.20, 144.90, 142.57, 134.74, 134.04, 132.18, 131.17, 131.15, 128.26, 125.05, 124.93, 124.87, 124.58, 123.69; MS: Calc for $C_{16}H_9NO$: 232.0757; Meas: 232.0759.

4.5. References and Notes

(1) For selected reviews, see: (a) Klinman, J. P. *J. Biol. Chem.* **1996**, *271*, 27189. (b) Mure, M. *Acc. Chem. Res.* **2004**, *37*, 131.

(2) (a) Wendlandt, A. E.; Stahl, S. S. *Org. Lett.* **2012**, *14*, 2850. (b) Largeron, M.; Fleury, M.-B. *Angew. Chem. Int. Ed.* **2012**, *51*, 5409. (c) Largeron, M.; Fleury, M.-B. *Science* **2013**, *339*, 43.

(3) Wendlandt, A. E.; Stahl, S. S. *J. Am. Chem. Soc.* **2014**, *136*, 506.

(4) For leading references to other catalytic methods for dehydrogenation of tetrahydroquinolines, see: (a) Yamaguchi, K.; Mizuno, N. *Angew. Chem. Int. Ed.* **2003**, *42*, 1480. (b) Yamaguchi, R.; Ikeda, C.; Takahashi, Y.; Fujita, K.-i. *J. Am. Chem. Soc.* **2009**, *131*, 8410. (c) Wu, J.; Talwar, D.; Johnston, S.; Yan, M.; Xiao, J. *Angew. Chem. Int. Ed.* **2013**, *52*, 6983. (d) Chakraborty, S.; Brennessel, W. W.; Jones, W. D. *J. Am. Chem. Soc.* **2014**, *136*, 8564.

(5) Through reaction screening it was determined that 1.0 mol % Bu_4NI was optimal in the case of both the Fe and Ru catalysts. See supporting information for additional details.

(6) For examples of homo- and heteroleptic Ru-phd complexes, see: (a) Nguyen, F.; Anson, F. C. *Electrochim. Acta* **1998**, *44*, 239. (b) Poteet, S. A.; Majewski, M. B.; Breitbach, Z. S.; Griffith, C. A.; Singh, S.; Armstrong, D. W.; Wolf, M. O.; MacDonnell, F. M. *J. Am. Chem. Soc.* **2013**, *135*, 2419. (c) Poteet, S. A.; MacDonnell, F. M. *Dalton Trans.* **2013**, *42*, 13305. (d) Parakh, P.; Gokulakrishnan, S.; Prakash, H. *Sep. Purif. Technol.* **2013**, *109*, 9.

(7) Ru-phd complexes have been applied previously as catalysts for NADH oxidation: (a) Goss, C. A.; Abruña, H. D. *Inorg. Chem.* **1985**, *24*, 4263. (b) Hilt, G.; Steckhan, E. *J. Chem. Soc., Chem. Commun.* **1993**, 1706. (c) Rivera, N.; Colón, Y.; Guadalupe, A. R. *Bioelectroch. Bioener.* **1994**, *34*, 169. (d) Wu, Q.; Maskus, M.; Pariente, F.; Tobalina, F.; Fernández, V. M.; Lorenzo, E.; Abruña, H. D. *Anal. Chem.* **1996**, *68*, 3688. (e) Hilt, G.; Lewall, B.; Montero, G.; Utley, J. H. P.; Steckhan, E. *Liebigs Ann.* **1997**, *1997*, 2289. (f) Hilt, G.; Jarbawi, T.; Heineman, W. R.; Steckhan, E. *Chem. – Eur. J.* **1997**, *3*, 79. (g) Yokoyama, K.; Ueda, Y.; Nakamura, N.; Ohno, H. *Chem. Lett.* **2005**, *34*, 1282. (h) Pinczewska, A.; Sosna, M.; Bloodworth, S.; Kilburn, J. D.; Bartlett, P. N. *J. Am. Chem. Soc.* **2012**, *134*, 18022.

(8) For a recent review of this area, see: Piera, J.; Bäckvall, J.-E. *Angew. Chem. Int. Ed.* **2008**, *47*, 3506.

(9) For leading references: (a) Sakamoto, H.; Funabiki, T.; Yoshida, S.; Tarama, K. *Bull. Chem. Soc. Jpn.* **1979**, *52,* 2760. (b) Tsuruya, S.; Yanai, S.-i.; Masai, M. *Inorg. Chem.* **1986**, *25*, 141. (c) Sakata, K.; Kikutake, T.; Shigaki, Y.; Hashimoto, M.; Ogawa, H. I.; Kato, Y. *Inorg Chim. Acta* **1988**, *144*, 1. (d) Simándi, L. I.; Simándi, T. M.; May, Z.; Besenyei, G. *Coord. Chem. Rev.* **2003**, *245*, 85.

(10) See Supporting Information for details.

(11) Photoexcitation of Ru-phd complexes is typically thought to terminate in non-radiative decay pathways arising from the semiquinone structure. See refs 6b,c.

(12) (a) Delorme, D.; Dubé, D.; Ducharme, Y.; Grimm, E. L.; Friesen, R.; Lepine, C. (Merck Frosst, Canada). US Pat. 5,552,437, Sept 3, 1996. (b) Grimm, E. L.; Ducharme, Y.; Frenette, R.; Friesen, R.; Gagnon, M.; Juteau, H.; Laliberte, S.; MacKay, B.; Gareau, Y. (Merck, USA) US Pat. App. 2008/0188521 A1, Aug 7, 2008.

(13) Vidler, L. R.; Filippakopoulos, P.; Fedorov, O.; Picaud, S.; Martin, S.; Tomsett, M.; Woodward, H.; Brown, N.; Knapp, S.; Hoelder, S. *J. Med. Chem.* **2013**, *56*, 8073.

(14) See, for example: (a) Upadhayaya, R. S.; Shinde, P. D.; Sayyed, A. Y.; Kadam, S. A.; Bawane, A. N.; Poddar, A.; Plashkevych, O.; Földesi, A.; Chattopadhyaya, J. *Org. Biomol. Chem.* **2010**, *8*, 5661. (b) Upadhayaya, R. S.; Lahore, S. V.; Sayyed, A. Y.; Dixit, S. S.; Shinde, P. D.; Chattopadhyaya, J. *Org. Biomol. Chem.* **2010**, *8*, 2180. (c) Upadhayaya, R. S.; Shinde, P. D.; Kadam, S. A.; Bawane, A. N.; Sayyed, A. Y.; Kardile, R. A.; Gitay, P. N.; Lahore, S. V.; Dixit, S. S.; Földesi, A.; Chattopadhyaya, J. *Eur. J. Med. Chem.* **2011**, *46*, 1306.

(15) Upadhayaya, R. S.; Dixit, S. S.; Földesi, A.; Chattopadhyaya, J. *Bioorg. Med. Chem. Lett.* **2013**, *23*, 2750.

(16) (a) Utsugi T.; Aoyagi K.; Asao T.; Okazaki S.; Aoyagi Y.; Sano M.; Wierzba K.; Yamada Y. *Jpn. J. Cancer Res.* **1997**, *88*, 992. (b) Okazaki, S.; Asao, T.; Wakida, M.; Ishida, K.; Washinosu, M.; Utsugi, T.; Yamada, Y. (Taiho Pharmaceutical Co., Japan) Eur. Pat. 0 713 870 B1, July 18, 2001. (c) Fujimoto, S. *Biol. Pharm. Bull.* **2007**, *30*, 1923.

(17) Backvall, J.-E.; Hopkins, R. B.; Grennberg, H.; Mader, M.; Awasthi, A. K. *J. Am. Chem. Soc.* **1990**, *112*, 5160.

(18) Evans, I. P.; Spencer, A.; Wilkinson, G. *J. Chem. Soc., Dalton Trans.* **1973**, 204.

(19) Shaw, J. E.; Stapp, P. R. *J. Het. Chem.* **1987**, *24*, 1477.

(20) Prasada Rao Lingam, V. S.; Thomas, A.; Mukkanti, K.; Gopalan, B. *Synth. Commun.* **2011**, *41*, 1809.

(21) Ueda, M.; Kawai, S.; Hayashi, M.; Naito, T.; Miyata, O. *J. Org. Chem.* **2010**, *75*, 914.

(22) Kouznetsov, V.; Urbina, J.; Palma, A.; López, S.; Devia, C.; Enriz, R.; Zacchino, S. *Molecules* **2000**, *5*, 428.

(23) Alvarez, S. G.; Alvarez, M. T. *Synthesis*, **1997**, 413.

(24) Pearson, W. H.; Fang, W.-K. *Isr. J. Chem.* **1997**, *37*, 39.

(25) Spectroscopic data matched those obtained from authentic material and by comparison to those contained in online spectroscopic databases (either Sigma-Aldich online or Spectral Database for Organic Compounds, SDBS).

(26) Li, H.; Wang, C.; Huang, H.; Xu, X.; Li, Y. *Tetrahedron. Lett.* **2011**, *52*, 1108.

(27) Wang, T.; Zhuo, L.-G.; Li, Z.; Chen, F.; Ding, Z.; He, Y.; Fan, Q.-H.; Xiang, J.; Yu, Z.-X.; Chan, A. S. C. *J. Am. Chem. Soc.* **2011**, *133*, 9878.

(28) Banwell, M. G.; Lupton, D. W.; Ma, X.; Renner, J.; Sydnes, M. O. *Org. Lett.* **2004**, *6*, 2741.

(29) Zhao, P.; Yan, X.; Yin, H.; Xi, C. *Org. Lett.* **2014**, *16*, 1120.

(30) Fuson, R. C.; Miller, J. J. *J. Am. Chem. Soc.* **1957**, *79*, 3477.

Chapter 5

Copper-Catalyzed Aerobic Oxidative C–H Functionalizations: Recent Trends and Mechanistic Insights

This work has been published:

Wendlandt, A. E.; Suess, A. M.; Stahl, S. S. *Angew. Chem. Int. Ed.* **2011**, *50*, 11062-11087.

5.1 Abstract

The selective oxidation of C–H bonds and the use of O_2 as a stoichiometric oxidant represent two prominent challenges in organic chemistry. Copper(II) is a versatile oxidant, capable of promoting a wide range of oxidative coupling reactions initiated by single-electron transfer (SET) from electron-rich organic molecules. Many of these reactions can be rendered catalytic in Cu by employing molecular oxygen as a stoichiometric oxidant to regenerate the active copper(II) catalyst. Meanwhile, numerous other recently reported Cu-catalyzed C–H oxidation reactions feature substrates that are electron-deficient or appear unlikely to undergo single-electron transfer to copper(II). In some of these cases, evidence has been obtained for the involvement of organocopper(III) intermediates in the reaction mechanism. Organometallic C–H oxidation reactions of this type represent important new opportunities for the field of Cu-catalyzed aerobic oxidations.

5.2 Introduction and Historical Context.

The selective oxidation of organic molecules is a topic of critical importance to laboratory and industrial chemical synthesis,[1] and oxidative functionalization of C–H bonds is one of the most challenging classes of oxidation reactions.[2] Molecular oxygen is the ideal oxidant because of its abundance, low cost and lack of toxic by-products, but aerobic oxidation methods often face significant limitations with respect to selectivity and scope. Radical-chain autoxidation reactions are used in the production of important commodity organic molecules, such as terephthalic acid and *tert*-butyl hydroperoxide, but such methods are intrinsically limited to substrates that undergo selective radical chemistry. Consequently, they find limited use in the

synthesis of complex organic molecules, such as pharmaceuticals, or in laboratory-scale oxidations.

Within the field of homogeneous catalysis, palladium-catalyzed reactions are perhaps the most versatile methods for selective aerobic oxidation of organic molecules,[3] and they include methods ranging from alcohol oxidation to oxidative C–C, C–N and C–O bond formation. Advances in this field have occurred in parallel with a rapid growth in Pd-catalyzed methods for C–H oxidation;[4] however, many of the latter methods are not compatible with the use of O_2 as the stoichiometric oxidant. Instead, other oxidants such as $PhI(OAc)_2$, benzoquinone, Cu^{II} or Ag^{I} are required to achieve catalytic turnover. Mechanistic studies suggest that these oxidants are often required to promote reductive elimination of the product from the Pd center via the formation of high-valent intermediates.[5] New Pd catalyst systems may be capable of overcoming this limitation,[6] but another, complementary solution may involve the use of other transition-metal catalysts. In particular, recent advances in homogeneous copper catalysis highlight opportunities to achieve selective aerobic oxidative functionalization of C–H bonds.

Copper is found in the active site of many metalloenzymes that catalyze aerobic oxidation reactions. These enzymes include "oxygenases", which mediate oxygen-atom transfer to organic substrates, and "oxidases", which couple the reduction of O_2 to H_2O (or H_2O_2) to the oxidation of diverse substrates. The latter reactions range from outer-sphere oxidations (e.g., of lignin and Fe^{2+}) to the dehydrogenation of alcohols and amines. Extensive studies in the fields of mechanistic enzymology and bioinorganic chemistry have provided valuable insights into fundamental mechanisms of O_2 activation and substrate oxidation mediated by these enzymes.[7]

Independent of the biological reactions, the facile aerobic oxidation of Cu^{I} ions to Cu^{II} is widely recognized,[8] and a number of important synthetic Cu-catalyzed aerobic oxidation

reactions exist, including industrial applications.[9] These include Glaser-Hay coupling of terminal alkynes (Scheme 5.1A);[10] oxidative polymerization of 2,6-dimethylphenol to produce polyphenylene oxide, a commodity-scale, high-temperature thermoplastic (Scheme 5.1B);[11] synthesis of 2,5,6-trimethyl-*p*-quinone, an intermediate in the commercial synthesis of vitamin E (Scheme 5.1C);[12] oxidative carbonylation of methanol to dimethycarbonate (Scheme 5.1D);[13] and numerous methods for aerobic alcohol oxidation (Scheme 5.1E).[14,15] Each of these examples formally corresponds to an "oxidase" reaction in which the formation of a new carbon-carbon or carbon-heteroatom bonds is coupled to the reduction of O_2. Despite this common feature, the mechanisms by which copper mediates the different substrate oxidation reactions exhibit considerable diversity.

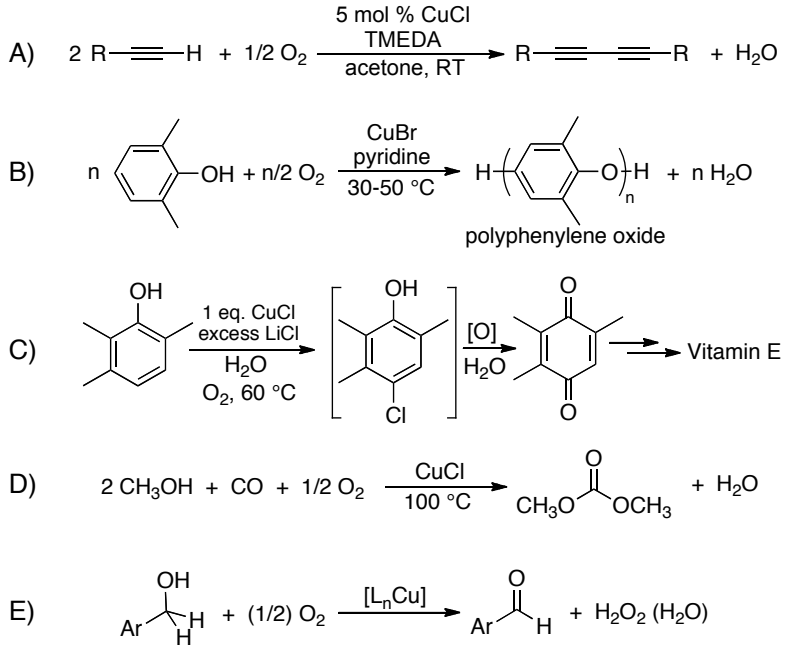

Scheme 5.1. Synthetic copper "oxidase" reactions.

Copper(II) is an effective one-electron oxidant, and it has been used in a number of oxidative-coupling reactions initiated by single-electron transfer from electron-rich organic molecules.[16] The oxidative dimerization of phenols and naphthols is a reaction that can be

traced to the work of Pummerer in 1914,[17] in which the oxidative coupling of 2-naphthols was accomplished with silver oxide or potassium ferricyanide as a one-electron oxidant. Subsequently, analogous reactions were demonstrated with a wide range of other oxidants.[18] In 1959, Hay and coworkers reported that the oxidative polymerization of 2,6-disubstituted phenols could be accomplished by bubbling O_2 through a solution of a phenol derivative, 5 mol % copper(I) chloride and pyridine at room temperature.[11b,19] When substituents are small, as with 2,6-dimethylphenol, carbon-oxygen coupling occurs, allowing preparation of linear, high-molecular-weight polyphenylene oxide (Scheme 5.2, top pathway).[11] The presence of large substituents leads to carbon-carbon coupling products (Scheme 5.2, bottom pathway). Substrates that lack *ortho* substituents form complex mixtures of *ortho* and *para* carbon-carbon and carbon-oxygen coupling products, in addition to the formation of quinone-like products.[29,20] *Ortho*-hydroxylation is often observed in phenol oxidations mediated by Cu/O_2/amine systems [21,22] suggesting that oxygenase-type reactivity can compete with the oxidase (oxidative-coupling) reactions. Overall, these observations are rationalized by mechanisms that involve the formation phenoxyl radical intermediates, where the copper(I) species formed upon one-electron oxidation of the phenols can be reoxidized to copper(II) by molecular oxygen.

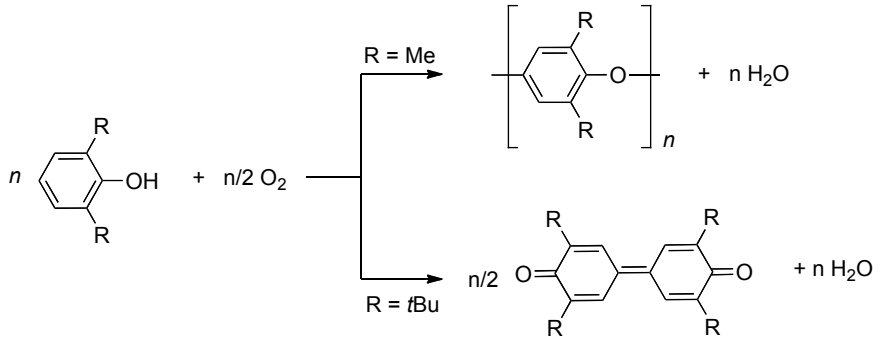

Scheme 5.2. Aerobic, oxidative polymerization or dimerization of 2,6-disubstituted phenols.

Single-electron-transfer (SET) mechanisms similar to those noted above explain many copper-mediated oxidation reactions, but other reactions are not readily rationalized by such

mechanisms. The aerobic, oxidative dimerization of terminal alkynes (Scheme 5.1A) was first reported in 1869 by Glaser, who demonstrated that diphenyldiacetylene could be obtained by treating copper(I) phenylacetylide with air.[23] A thorough survey of Glaser coupling reactions, including their historical development, applications and mechanistic studies, are the subject of an excellent recent review.[10] Several points are worth repeating here. In 1937, Zalkind and Aizikovich found that copper(I) acetylides could be generated *in situ*,[24] and, in 1962, Hay reported that these reactions could carried out with catalytic Cu, if the reaction was performed in the presence of the *N,N,N',N'*-tetramethylethylene diamine (TMEDA) under an atmosphere of O_2.[25]

Despite the nearly 150-year history of this reaction, the mechanism remains poorly understood. Until the 1960s, mechanistic proposals typically featured the formation and coupling of alkynyl radicals. *In situ* deprotonation of the teminal alkyne could afford acetylides susceptible to one-electron oxidation by Cu^{II} to afford the alkynyl radicals. Subsequent kinetic studies, investigation of alkyne electronic effects, and consideration of the low activation barriers for these reactions[26] caused these proposals to be abandoned in favor of organometallic pathways. π-Complexation of the alkyne to Cu^{I} or Cu^{II}, for example, should facilitate deprotonation of the alkyne and formation of Cu-acetylide intermediates. The copper oxidation states involved in different steps of the mechanism remain unclear, and both Cu^{I} and Cu^{II} species have been proposed.[27] One widely accepted mechanism involves formation of dimeric copper(II)-acetylides that undergo coupling of the alkynyl fragments to afford the diyne product (Scheme 5.3).[28]

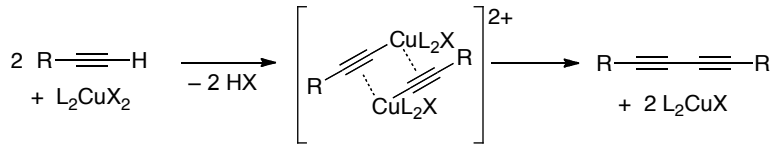

Scheme 5.3. Proposed mechanism for the Glaser Reaction.

The aerobic oxidative coupling of phenols and alkynes proceed with similar Cu catalysts under similar conditions; however, the above discussion suggests that the mechanisms for these reactions are quite different. This conclusion aligns with the observation that a variety of oxidants that promote SET reactions promote the oxidative coupling of phenols,[29] whereas other transition metals that mediate the oxidative coupling of alkynes, such as Pd^{II} and Ni^{II}, typically employ organometallic pathways.[10] This divergence between single electron transfer and organometallic mechanisms provides a framework for the consideration of recent advances in copper-catalyzed aerobic C–H oxidation, and it underlies the organization of this review. Section 5.3 surveys copper-based SET reactions that have been achieved with aerobic catalytic turnover. The content focuses on the different synthetic transformations, but it includes recent insights into the mechanisms of these reactions. Section 5.4 surveys reactions that qualitatively resemble organometallic C–H oxidation reactions catalyzed by Pd and other transition metals. The mechanisms for most of these reactions have not been fully elucidated, but the substrates tend not to be electron-rich molecules commonly associated with SET reactions, and in many cases they are highly electron-deficient. These features suggest that organometallic mechanisms may be involved. The relevance of organocopper intermediates is even more plausible in light of recent insights into the formation and reactivity of organocopper(II) and -copper(III) complexes. The organometallic chemistry of Cu^{II} and Cu^{III} and its prospective role in catalytic oxidation reactions are considered in Section 5.5, together with possible mechanistic similarities between oxidative and non-oxidative Cu-catalyzed coupling reactions. The research summarized in this review includes material published through early May 2011, and emphasizes results from the

past five years. Collectively, the recent advances in this area highlight a wealth of new opportunities to achieve selective aerobic oxidative functionalization of C–H bonds.

5.3. C–H Oxidation Initiated by Single-Electron Transfer

A number of electron-rich substrates, in particular, tertiary amines, enolates, phenols, and electron-rich arenes and heterocycles, are susceptible to one-electron oxidation. Many oxidants, including Cu^{II}, are capable of promoting oxidative coupling reactions with these substrates, initiated by single-electron transfer. Copper(II) is especially attractive as an oxidant in these reactions because, under appropriate conditions and with suitable substrates, the reactions can be carried out with catalytic Cu using ambient air or O_2 as the stoichiometric oxidant. Recent work has demonstrated this principle in the oxidative coupling reactions of electron-rich arenes, α-functionalization of tertiary amines and cyclic ethers, and reactions of stabilized enolates.

5.3.1. Homocouplings of Electron-Rich Arenes

Chiral 1,1'-bi-2-naphthol (BINOL) derivatives are a useful class of chiral ligands and auxiliaries, which may be accessed through oxidative homo- or cross-coupling of naphthols. This well-developed strategy capitalizes on the facile one-electron oxidation of phenols and naphthols, which can be accomplished using a number of different oxidants under relatively mild conditions.[29] Recent research efforts on oxidative binaphthol coupling have focused on replacing stoichiometric oxidants with catalytic methods using first-row transition metals, such as V,[30] Fe,[31] Mn,[32] and Cu[33-39], in particular, for the formation of enantioenriched products via asymmetric catalysis [30c-i, 31a,c-d,34-37,39].

Copper-based procedures for the oxidative dimerization of naphthols and phenols have been studied extensively, and many of these methods are capable of using O_2 as the terminal oxidant (Scheme 5.4).[34-39] These reactions have been the subject of several previous reviews,[40] but the recent results presented here provide a valuable segue to some of the other results discussed herein. Conditions for the aerobic, copper-catalyzed oxidative dimerization of naphthols are quite mild, commonly involving 1-10 mol % Cu catalyst loading, 2-10 mol % chiral amine ligand, and an O_2 or air atmosphere at ambient temperatures (Scheme 5.4). Though high yields and excellent *ee*'s have been obtained, the best results almost universally feature naphthol substrates containing a methyl ester substituent at the C3 position (e.g., **1**, Scheme 5.4). Some of the highest yields and enantioselectivities to date have been achieved by Kozlowski and coworkers with a computationally designed 1,5-diaza-*cis*-decalin ligand.[36] Recently, this catalyst system has been applied in the aerobic copper-catalyzed enantioselective coupling of functionalized 2-naphthols to prepare binaphthyl polymers[41] and homochiral biaryl natural products, such as Nigerone (**3**) and Elsinochrome A (**4**).[40f,42]

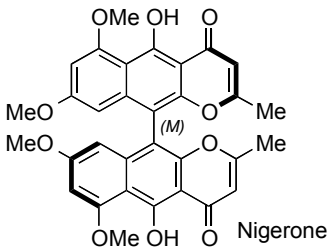

Nigerone
3

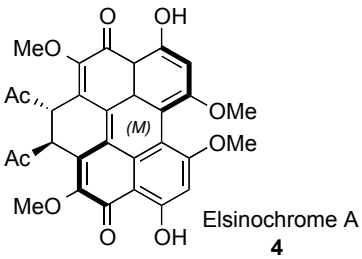

Elsinochrome A
4

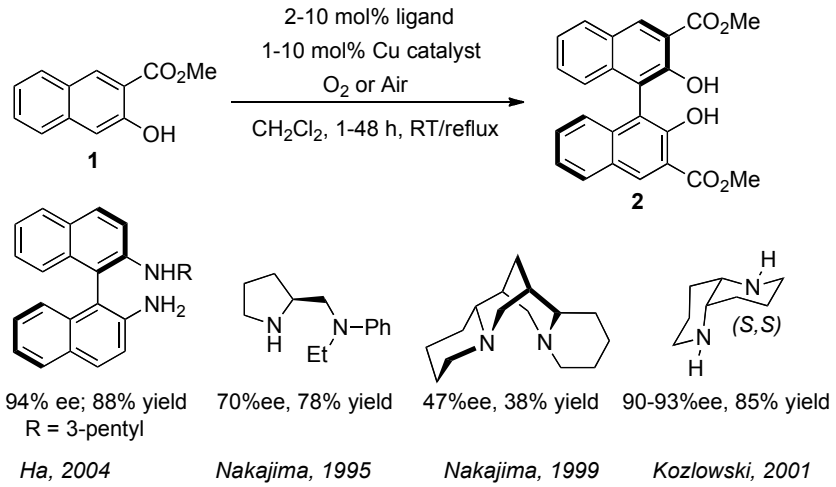

Scheme 5.4. Aerobic, copper-catalyzed, oxidative dimerization of naphthol derivatives using chiral amine ligands.

The prevailing mechanistic proposal for these reactions features formation of a Cu^{II}-naphthoxide (**6**) species that undergoes intramolecular electron transfer from the coordinated naphthoxide to Cu^{II} to form a Cu^{I}-naphthoxyl radical (**7**).[43] The chiral diamine ligand provides the basis for the enantioselective C–C coupling from this species. Details of the C–C coupling step are not well understood, but possibilities include attack of a second naphthol substrate on the naphthoxyl radical or bimolecular coupling of two Cu^{I}-naphthoxyl radicals. Evidence for binuclear Cu intermediates and their potential involvement in the C–C coupling step have been obtained from gas-phase studies of the reaction, catalyzed by Cu(TMEDA)(OH)Cl.[43b,c] A simplified catalytic cycle featuring the diaza-*cis*-decalin ligand is shown in Scheme 5.5.

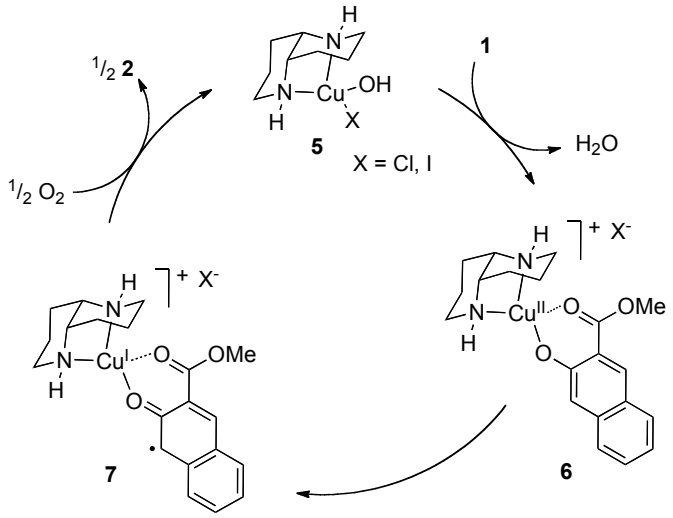

Scheme 5.5. Proposed mechanism for catalytic naphthol dimerization.

Copper(I) and copper(II) 1,5-diaza-*cis*-decalin complexes [$(N_2)Cu$] are effective pre-catalysts for aerobic oxidative coupling of naphthol substrates, but recent mechanistic studies by Kozlowski and Stahl reveal that these complexes are not the reactive form of the catalyst under steady-state conditions.[44] Rather, the active catalyst forms in a pre-steady-state self-processing step that involves oxygenation of the naphthol substrate, **1,** to form an oxygenated "cofactor", $NapH^{OX}$. The identity of this cofactor was not firmly established; however, orthoquinone derivatives of **1** were obtained under single-turnover conditions. Formation of $NapH^{OX}$ is correlated with a kinetic "burst" of O_2 consumption, after which the $(N_2)Cu/NapH^{OX}$ catalyst effects highly selective, steady-state oxidase reactivity (i.e., aerobic oxidative biaryl coupling) (Scheme 5.6). These observations implicate a striking similarity between this synthetic catalyst system and certain biological copper oxidases, such as copper amine oxidases (CAOs),[45] which also undergo preliminary oxidative self-processing to generate an oxygenated cofactor (e.g., topaquinone[46]) that is required for subsequent oxidase-type oxidation catalysis.

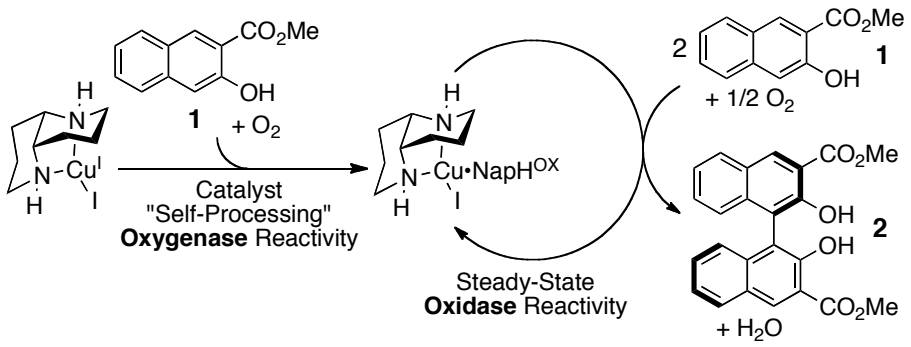

Scheme 5.6. Oxygenase vs. oxidase reactivity identified from mechanistic studies of Cu-catalyzed oxidative coupling of naphthol substrate, **1**.

5.3.2. Oxidative Bromination and Chlorination of Electron-Rich Arenes.

The facile single-electron oxidation of phenols and other electron-rich arenes and heteroarenes has led to the development of copper-catalyzed halogenation protocols for these substrates. Gusevskaya and coworkers reported a highly selective method for oxidative halogenation of phenols under aerobic copper-catalyzed conditions.[47] Para-chlorinated phenols could be obtained with high selectivity[48] using 12.5 mol % $CuCl_2$ and 2 equiv LiCl in AcOH under 1 atmosphere of O_2 (Scheme 5.7A). Para-brominated phenols were obtained with excellent selectivity and good yields under similar reaction conditions (12.5 mol % $Cu(OAc)_2$, 2 equiv LiBr, AcOH under 1 atm O_2) (Scheme 5.7B).[49]

In both reactions, more-electron-rich phenols undergo oxidative halogenation with faster rates, and electron-deficient substrates, such as *p*-nitrophenol, and non-phenolic arenes are unreactive. On the basis of these observations, the authors propose that high selectivity for monochlorination arises from the electron-withdrawing effect of a chlorine substituent, which deactivates the substrate toward further reaction. The phenolic O–H group is proposed to be crucial to substrate activation. A detailed mechanism of these reactions is not known, but the proposed pathway features formation of a Cu^{II}–phenolate, followed by intramolecular electron

transfer to afford a phenoxyl radical. Halogen-atom transfer to the *para* position of the phenoxyl radical by $CuCl_2$ or $CuBr_2$ and tautomerization of the dienone generates the *para*-halogenated phenol (Scheme 5.8).

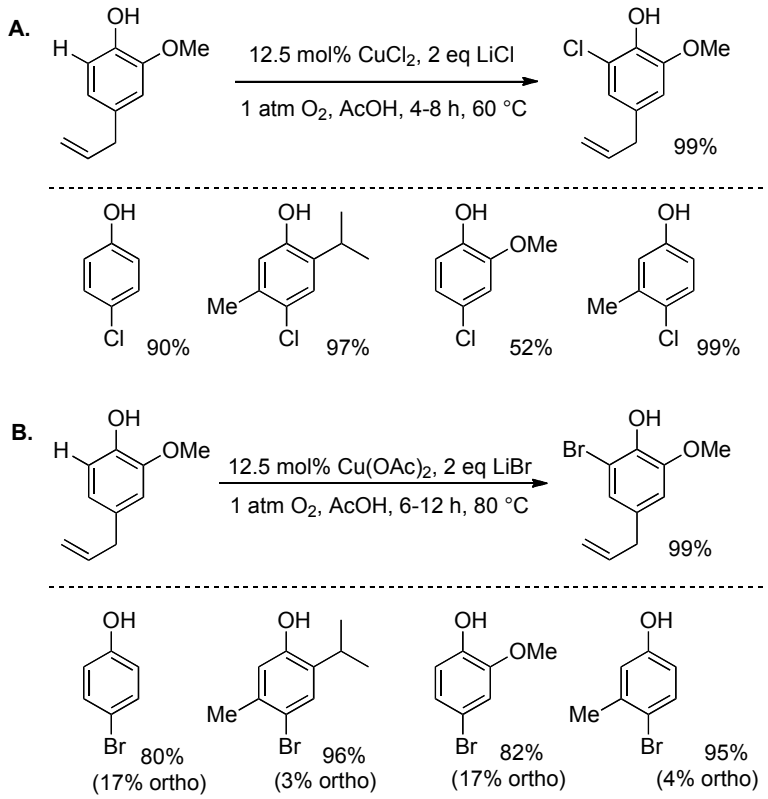

Scheme 5.7. Aerobic oxidative chlorination (A) and bromination (B) of phenols.

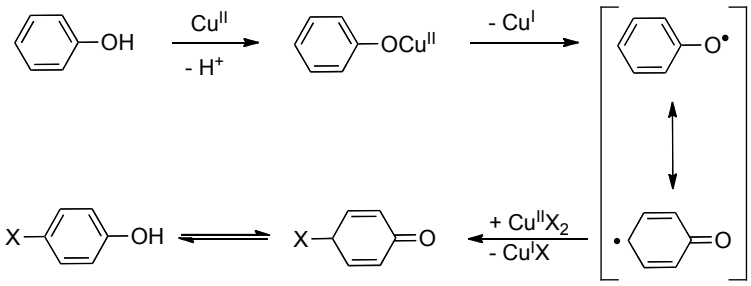

Scheme 5.8. Proposed mechanism for the oxidative halogenation of phenols.

In subsequent studies, Gusevskaya demonstrated that anilines and indoles are also effective substrates for oxidative bromination.[50] Using conditions similar to those developed for the halogenation of phenols, they achieved bromination of unprotected anilines with high regioselectivity. Unlike phenol halogenation, however, monobrominated aniline products could undergo further bromination. Though aniline itself was an excellent substrate under these conditions, *N*-methyl aniline showed almost no reactivity. The chlorination of anilines proved to be much less effective than bromination; formation of *N*-acetylated byproducts competes with chlorination of the heterocycle.

Stahl and coworkers reported a complementary copper-catalyzed method for the regioselective chlorination and bromination of electron-rich arenes that lack O–H or N–H groups.[51] Under conditions similar to those reported by Gusevskaya (25 mol % CuBr, 1 equiv LiBr, in AcOH under an O_2 atmosphere), regioselective monobromination of a range of electron-rich arenes and heteroarenes was achieved (Scheme 5.9A).[52] Arene chlorination was also achieved, but more forcing conditions were typically required (Scheme 5.9B). Appropriate selection of the reaction conditions enabled selective mono- or di-halogenation of the arenes. Li and coworkers have reported a method for aerobic oxidative bromination of arenes, using 1 mol % $Cu(NO_3)_2$, and 1.1 equiv HBr at 100 °C in water under air.[53] Excellent conversions and selectivities were achieved for a range of simple arenes, including toluene, anisole and cresole. The results by Stahl and Li reveal that substrate depronation to form a Cu^{II}-bound adduct, as in formation of a Cu^{II}-phenoxide or -anilide (cf. Scheme 5.8), is not a prerequisite to achieve oxidative halogenation of arenes.

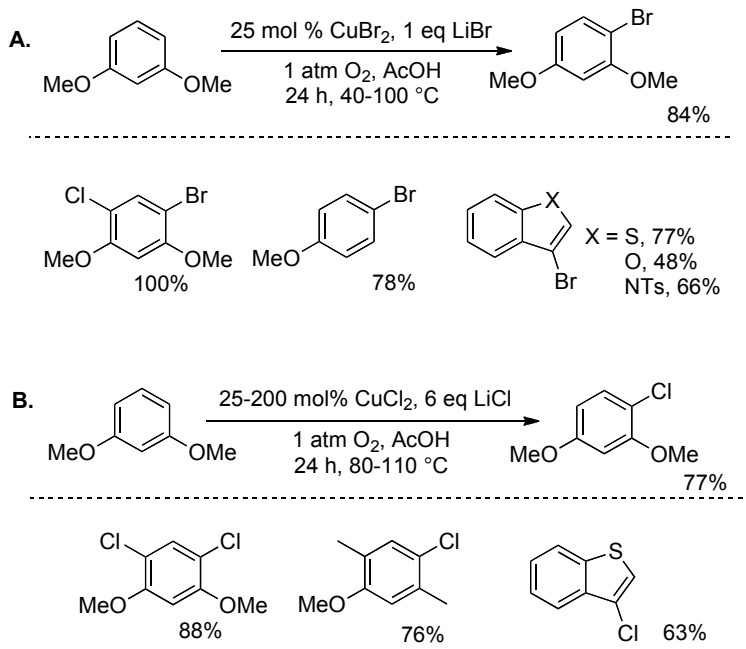

Scheme 5.9. Representative copper-catalyzed oxidative bromination (A) and chlorination (B) reactions of electron-rich arenes.

Preliminary mechanistic studies by Stahl and coworkers into these reactions suggest that bromination and chlorination occur through different pathways (Scheme 5.10). The bromination reactions turn red-brown, and the disproportionation of $CuBr_2$ into CuBr and Br_2 has been described under similar conditions.[54] Accordingly, the arene bromination reactions could proceed via electrophilic bromination by in-situ-generated Br_2. Molecular oxygen will reoxidize CuBr to $CuBr_2$ in the presence of LiBr (Scheme 5.10A). In support of this proposal, exposure of cyclooctene to the arene bromination conditions resulted in the formation of *trans*-1,2-dibromocyclooctane in 75% yield (Scheme 5.10B). The disproportionation of $CuCl_2$ into CuCl and Cl_2 is much less favorable, and chlorination of cyclooctene was not observed under the arene chlorination conditions (Scheme 5.10B). In light of these observations, an SET mechanism was suggested for the arene chlorination reactions (Scheme 5.10C).[16] An arene radical-cation

formed in this step could undergo chorination of the ring via reaction with $CuCl_2$ and loss of a proton.

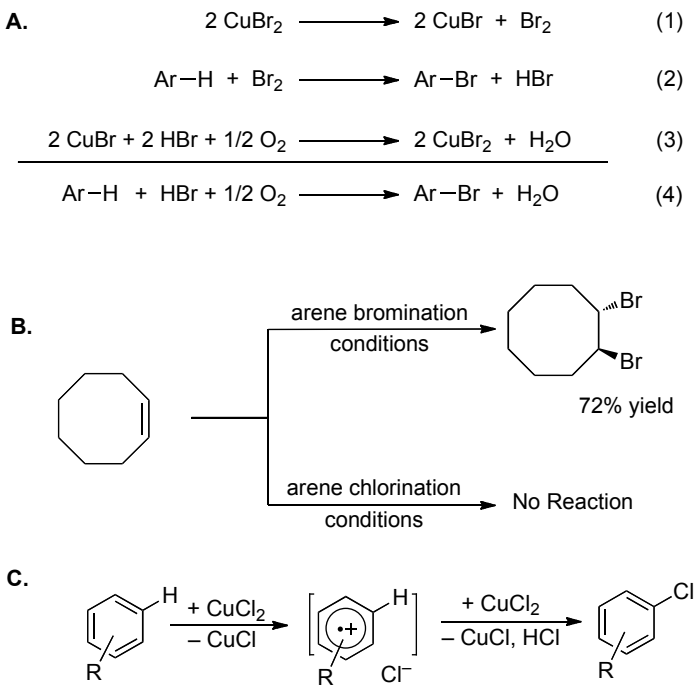

Scheme 5.10. Proposed mechanism for electrophilic bromination of electron-rich arenes (A), divergent outcomes for the reaction of cyclooctene under the arene bromination and chlorination reaction conditions (B), and proposed SET mechanism for oxidative chlorination of electron-rich arenes (C).

5.3.3. Other Oxidative C–H Functionalization Reactions of Electron-Rich Arenes.

Electron-rich arenes and heteroarenes have been shown to undergo other C–H functionalization reactions. Itami and coworkers reported the arylation of electron-rich arenes with boronic acids using 1 equiv $Cu(TFA)_2$, under aerobic conditions at 80 °C.[55] The reaction was selective for formation of cross-coupled products; no homocoupled products arising from the trimethoxybenzene or boronic acid reagents were observed. Reactions with nitrogen heterocycles led to products arising from multiple C–H arylations (Scheme 5.11).

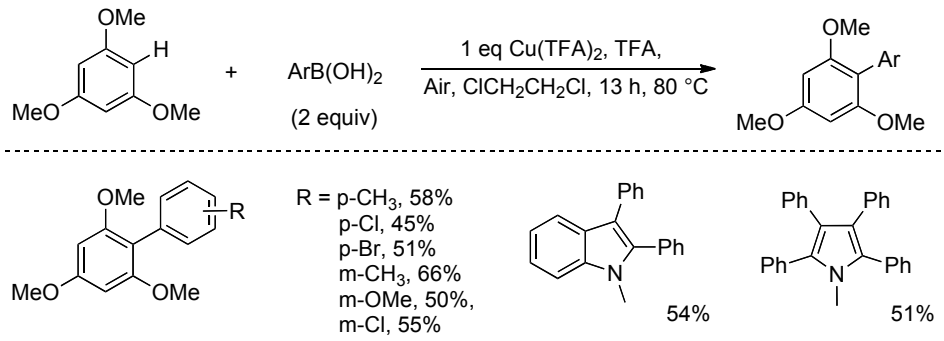

Scheme 5.11. Arylation of trimethoxybenzene and nitrogen heterocycles with aryl boronic acids.

Trimethoxybenzene was also reported to undergo oxidative C–S coupling with disulfides in the presence of 20 mol % CuI, in DMF under air (Scheme 5.12).[56] Substituted phenyl, allyl, and benzyl disulfides were used to thiolate 1,3,5-trimethoxybenzene in variable yields. Aryl thioethers were obtained with 1,2,4-trimethoxybenzene and 1,3-dimethoxybenzene, but the yields were relatively low, and other electron rich arenes were not effective. Examples of mono- and diselenylation of trimethoxybenzene in 70 and 30% yields, respectively, with diphenylselenide were also reported. The synthetic scope of these reactions was rather limited, but they represent an intriguing example of C–S coupling under aerobic conditions.

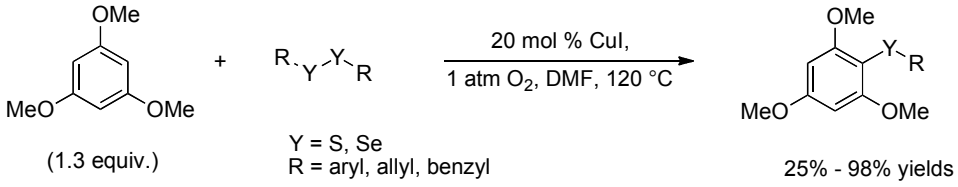

Scheme 5.12. Oxidative functionalization of trimethoxybenzene with disulfides and diselenides.

5.3.4. α-Functionalization of Tertiary Amines.

Tertiary amines are electron rich and susceptible to one-electron oxidation, and this reactivity has been used to enable the oxidative functionalization of C–H bonds adjacent to 3° amines with Ru,[57] Fe[58] and Cu[59] catalysts, typically with oxidants such as *tert*-butylhydroperoxide (TBHP)

or 2,3-dichloro-5,6-dicyano-1,4-benzoquinone (DDQ). Li and coworkers pioneered the development of many different methods within this class of "cross dehydrogenative coupling" reactions, and have written several recent reviews in this area.[60] Recently, a number of these reactions have been shown to be amenable to aerobic catalytic turnover, and these will be the subject of the following discussion. The mechanistic principles that establish when O_2 can be used as an oxidant, rather than TBHP, DDQ or other oxidant, have not yet been established.

These methods are believed to be initiated by SET from a tertiary amine to form an amine radical-cation (Scheme 5.13). Subsequent loss of a hydrogen atom (or H^+ and an electron) from the alpha position, which is often a benzylic position, generates an iminium ion that is susceptible to attack by a wide range of soft nucleophiles. Klussmann and coworkers have recently obtained X-Ray crystal structures of tetrahydroisoquinolinium cuprates having dichlorocuprate and $(Cu_2Br_4)^{2-}$ counterions, **8** and **9**, resulting from oxidation of the tetrahydroisoquinoline by $CuCl_2$ and CuBr, respectively, and O_2 (Scheme 5.13B).[61] Both iminium species react smoothly with added nucleophiles to give expected cross-coupling products. A similar ionic crystal structure was obtained from similar studies where DDQ is used as the oxidant, instead of Cu/O_2.[62]

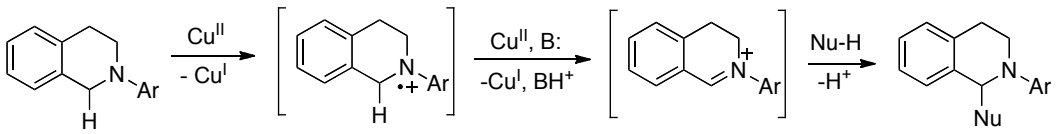

Scheme 5.13. Proposed mechanism for cross-dehydrogenative coupling.

8 **9**

In one of the earliest reported Cu-catalyzed methods compatible with O_2 as the oxidant, Li and coworkers described the coupling of stabilized carbon nucleophiles with *N*-phenyl-1,2,3,4-tetrahydroisoquinoline.[63] The reaction utilizes 5 mol% CuBr at 60 °C in H_2O under ambient air (Scheme 5.14). Various nitroalkanes served as competent substrates, though over-alkylation, in the case of *N*,*N*-dimethyl anilines, was a problem. Dialkyl malonate derivatives were effective nucleophiles in reactions with *N*-phenyltetrahydroisoquinoline as well as cyclic benzyl ethers.[64]

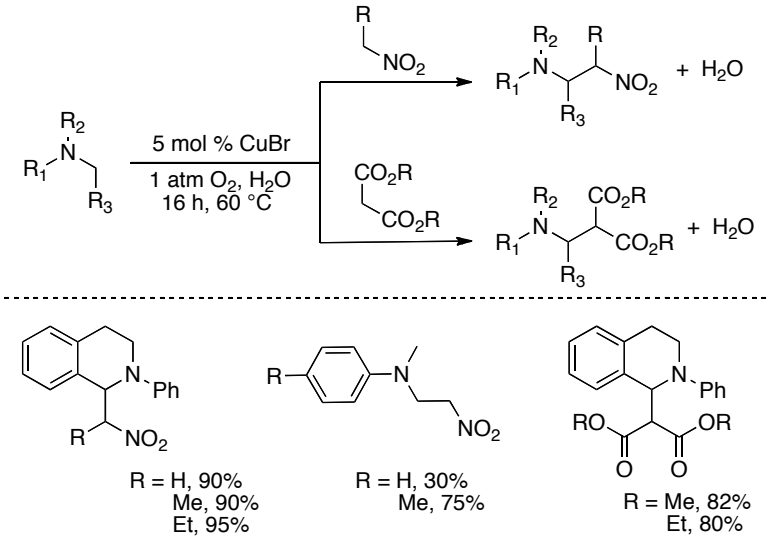

Scheme 5.14. Aerobic Cu-catalyzed oxidative cross-dehydrogenative coupling (CDC) reaction.

Li and coworkers reported the aerobic phosphonation of 2-aryl tetrahydroisoquinolines to afford ⟨-aminophosphonates.[65] Using diethyl phosphonate and *N*-phenyltetrahydroisoquinoline, a variety of copper salts (CuBr, $CuBr_2$, CuOTf, CuCl, CuI) catalyzed C–P bond formation under an O_2 atmosphere in excellent yields (Scheme 5.15). Dimethyl-, diisopropyl-, and dibenzyl-phosphonates were also effective coupling partners. In addition to *N*-phenyltetrahydroisoquinoline, *N*-*p*-methoxy and *N*-*o*-methoxy derivatives could be used.

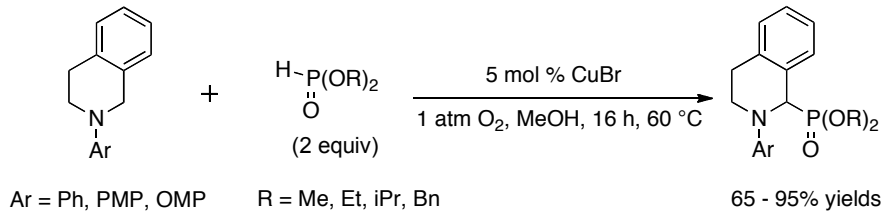

Scheme 5.15. Oxidative synthesis of ⟨-aminophosphates from tertiary benzylamines.

Guo, Tan, and coworkers reported the reaction of tetrahydroisoquinolines with simple methyl ketones using 5 mol % CuI and 4Å molecular sieves at 80 °C under O_2 (Scheme 5.16).[66] Aliphatic ketones and aryl methyl ketones are competent substrates; however, unsymmetrical ketones, such as 2-butanone, can lead to a mixture of regioisomeric products.

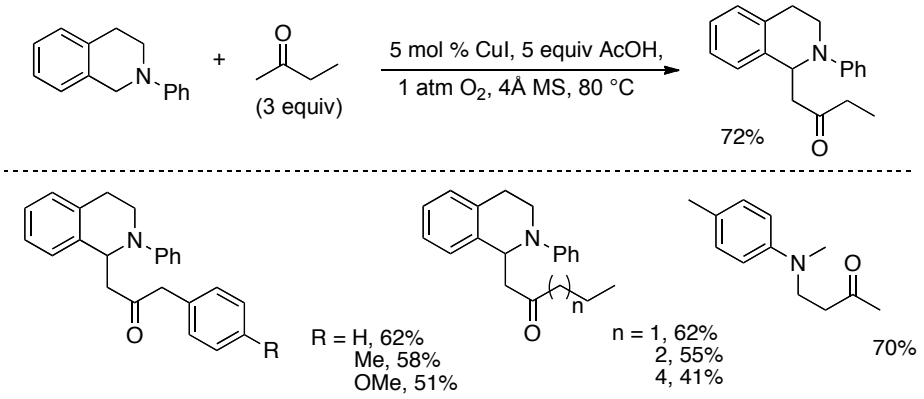

Scheme 5.16. Oxidative functionalization of tetrahydroisoquinolines with methyl ketones.

Finally, Zhang and coworkers reported the copper-catalyzed oxidative coupling of *N*,*N*-dimethylanilines with heteroarenes using 5 mol% CuBr in MeCN at 50 °C under air (Scheme 5.17).[67] A range of methoxy- and nitrile-substituted indolizines underwent cross-coupling under these conditions. Indoles, too, were acceptable substrates, though mixtures of products of mono- and bis-heteroarylation products of *N*,*N*-dimethylaniline were obtained. Only a small number of simple *N*,*N*-dimethylanilines were explored, and the presence of substituents on the aniline were found to have a significant impact on reaction yield.

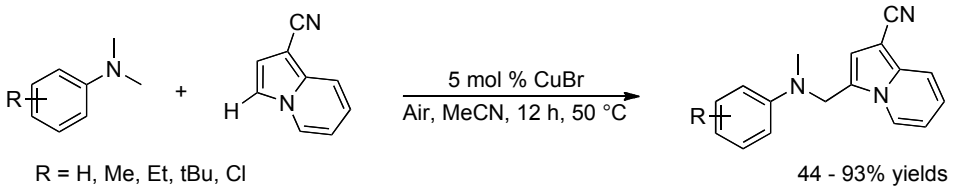

Scheme 5.17. CDC reaction between *N*,*N*-dimethylaniline and substituted indolizines.

5.3.5. Reactions of Amide-Enolates.

A number of important examples of stoichiometric oxidative coupling reactions of enolates with stoichiometric Cu^{II} salts have been reported;[68,69] however, these reactions are not typically amenable to aerobic catalytic turnover. Two groups have recently described copper-mediated C–H oxidation routes for the synthesis of oxindoles from anilides.[70] Taylor and coworkers reported the Cu-catalyzed cyclization of anilides to form 3,3-disubstituted oxindoles using 5 mol% $Cu(OAc)_2{\cdot}H_2O$ in refluxing mesitylene under air (Scheme 5.18).[70a] Yields were best when R^1 was an electron-withdrawing group.

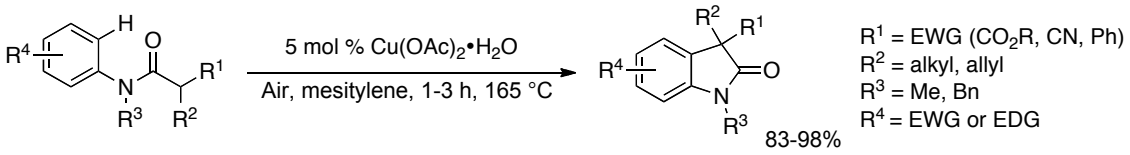

Scheme 5.18. Cyclization of anilides to give oxindoles.

The proposed mechanism begins with single-electron oxidation of the amide-enolate moiety by Cu^{II}, followed by cyclization, oxidation, and aromatization (Scheme 5.19). Consistent with this mechanism, an earlier stoichiometric study by Kündig and coworkers revealed the presence of a secondary isotope effect of 1.25**,** which the authors suggest indicates that C–H bond cleavage is not involved in the rate-determining step (Scheme 5.20).[70b]

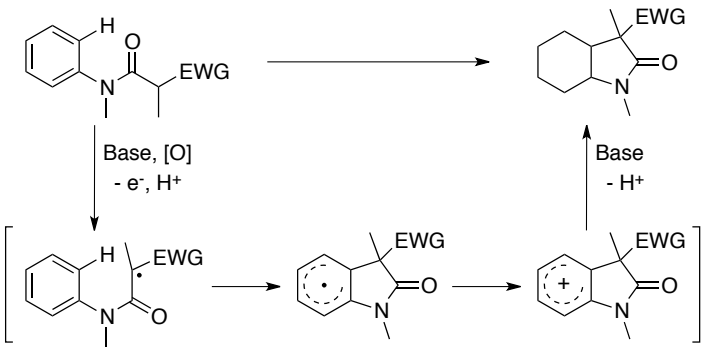

Scheme 5.19. Proposed mechanism involving a radical amide-enolate.

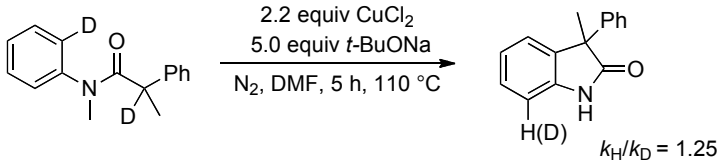

Scheme 5.20. Intramolecular competition experiment reveals a secondary isotope effect.

A subsequent stoichiometric study was carried out by Taylor and coworkers in which the anilide substrate contained a cyclopropyl radical probe (Scheme 5.21).[70c] Oxindole products were not detected in this case. Instead, the dienyl anilide was produced, resulting from the radical fragmentation of the cyclopropyl substituent and further supporting the likelihood of a radical amide-enolate intermediate.

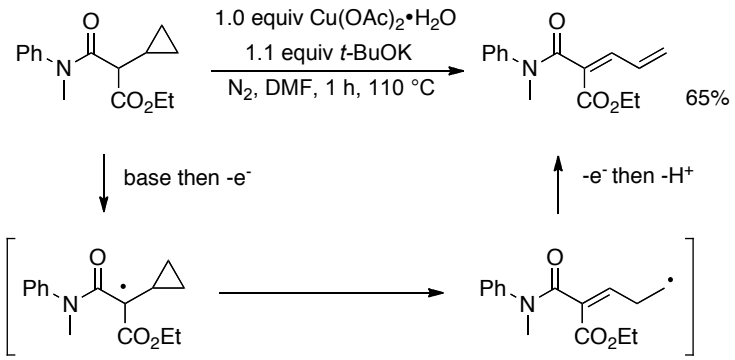

Scheme 5.21. Radical probe experiment suggests SET-initiated mechanism.

5.3.6. Summary of Cu-Catalyzed C–H Oxidation Reactions Initiated by SET.

Each of the reactions highlighted in Section 5.3 is consistent with a mechanistic pathway wherein a Cu^{II} catalyst mediates the one-electron oxidation of an electron-rich substrate – naphthol, phenol, methoxyarene, tertiary amine, or enolate – followed by reaction with of the oxidized intermediate with a suitable nucleophile, before or after loss of another electron. In many of these transformations, copper is one of several viable oxidants capable of promoting the reaction. However, copper is appealing as a reagent because of its low cost and toxicity and, perhaps more importantly, because the Cu^{I} byproduct of these SET steps is capable of undergoing efficient oxidation to Cu^{II} in the presence of O_2. Much work remains to understand the mechanism of these reactions, particularly with respect to understanding the factors that will enable stoichiometric Cu^{II} or undesirable stoichiometric oxidants such as DDQ, to be replaced with catalytic Cu in combination with O_2.

5.4. C–H Oxidations that Resemble Organometallic Reactions.

Over the past five years, a number of copper-catalyzed aerobic oxidation reactions have emerged that resemble organometallic C–H oxidation reactions mediated by 2nd and 3rd row transition metals. In most cases, mechanisms have not been established; however, the reactions employ substrates that are electronically neutral or electron-deficient and, therefore, differ from classical substrates for SET-initiated reactions. Several early studies provided a foundation for the ensuing developments in this area: Yu reported chelate-directed oxidative C–H functionalization reactions of 2-phenylpyridine; [71] the groups of Buchwald and Nagasawa developed oxidative annulation reactions of *N*-aryl amidines and amides for the synthesis of 2-substituted benzimidazoles and benzoxazoles, respectively; [72,73] Stahl described the oxidative amidation of terminal alkynes;[74] and Daugulis reported "aromatic Glaser-Hay" reactions for the

homocoupling of electron-deficient arenes and heteroarenes.[75] These reports provide the basis for the four general reaction classes surveyed below: (1) chelate-directed C–H oxidation reactions, (2) oxidative annulation reactions, (3) heterofunctionalization reactions of alkynes and electron-deficient (hetero)arenes, and (4) homo- and cross-coupling reactions of electron-deficient arenes.

5.4.1. Chelate-Directed C–H Oxidation Reactions.

In 2006, Yu and co-workers reported a Cu^{II}-catalyzed chelate-directed oxidative functionalization of 2-phenylpyridine derivatives.[71] Their report largely focused on *ortho*-chlorination reactions and demonstrated that a variety of 2-arylpyridines could be chlorinated in the presence of 20 mol % $CuCl_2$ in $Cl_2CHCHCl_2$, under 1 atm O_2 at 130 °C (Scheme 5.22A). The solvent serves as an *in situ* source of the chloride nucleophile. High yields of monochlorinated products could be obtained when the pyridyl-directing group was *ortho*-substituted, and monosubstitution could be additionally improved by reducing the reaction temperature and time.

Bromination of the arene ring was achieved by using $Br_2CHCHBr_2$ as a solvent instead of tetrachloroethane and by switching the copper source to $Cu(OAc)_2$. Use of 1 equiv of $Cu(OAc)_2$ and a range of different nucleophiles enabled diverse functional groups to be introduced into the aryl ring (Scheme 5.22B). The hydroxylation reaction was run under anaerobic conditions with $H_2{}^{18}O$, and a lack of label incorporation into the product prompted the authors to propose that the reaction proceeds via $Cu(OAc)_2$-mediated acetoxylation of the arene. Subsequent *in situ* hydrolysis of the acetate to affords the phenol. The reaction could be carried out with catalytic $Cu(OAc)_2$ (10 mol %) by performing the reaction in a mixture of acetic acid and acetic anhydride, resulting in formation of the aryl acetate product.

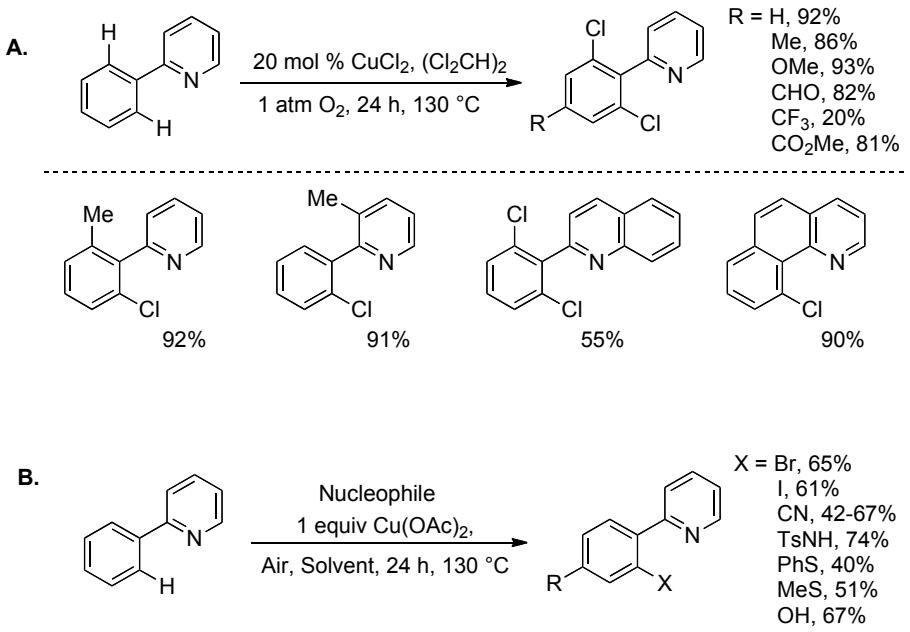

Scheme 5.22. Cu-catalyzed chlorination of 2-phenylpyridine derivatives (A) and Cu^{II}-promoted functionalization of 2-phenylpyridine with various nucleophiles (B).

Cheng and coworkers subsequently expanded upon these results in the acyloxylation of 2-arylpyridines with a range of alkyl and aryl anhydrides.[76] The reactions conditions featured 10 mol % $Cu(OAc)_2$ in toluene under O_2 at 145 °C (Scheme 5.23), and a range of mono- and di-acetoxylated 2-arylpyridines were accessed in this manner. In a subsequent study, the acyloxylation of 2-phenylpyridine was accomplished using acyl chlorides, which can undergo in-situ formation of anhydrides.[77] The procedure is similar to that for anhydrides, but employs 2 equiv of acyl chloride, 20 mol % $Cu(OAc)_2$, and 2 equiv KO*t*Bu in toluene under O_2 at 145 °C for 48 h. The latter protocol enables access to an expanded scope of aryl acyloxylated products due to the broad availability of acyl chloride reagents.

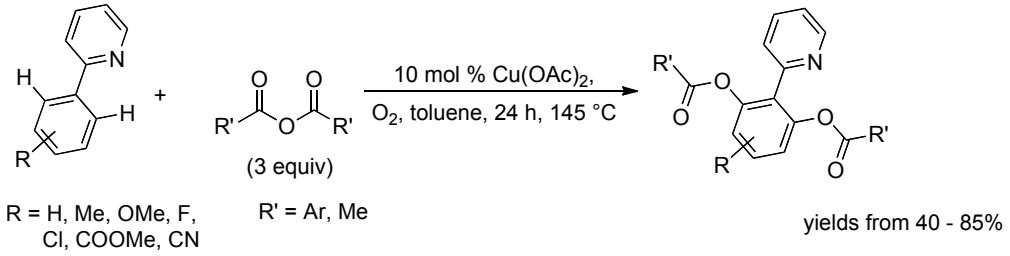

Scheme 5.23. Pyridyl-directed acyloxylation of 2-phenylpyridine.

Concurrent with the original study of Yu, Chatani and coworkers reported chelate-directed amination of 2-phenylpyridine derivatives with aniline, using stoichiometric $Cu(OAc)_2$,[78,79] and Ohno and coworkers later described the use of tetrahydropyrimidine rather than pyridine as a directing group to achieve *ortho* hydroxylation and amidation (with $BocNH_2$ and $TsNH_2$) using stoichiometric $Cu(OAc)_2$.[80] Nicholas and coworkers recently reported conditions for the catalytic amidation of 2-phenylpyridine, using 20 mol % $Cu(OAc)_2$ under 1 atm O_2 in DMSO/Anisole (1:39) at 160 °C for 48 h. (Scheme 5.24).[81] Modest catalytic turnover numbers were observed (from 1.2 to 3.3 turnovers; yields from 26-65%) in the amidation/amination of 2-phenylpyridine with several sulfonamides, carboxamides, and *p*-nitroaniline.

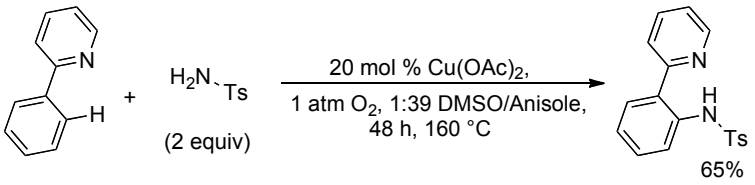

Scheme 5.24. Catalytic amidation of 2-phenylpyridine.

Related reactions employing oxidants other than O_2 have been reported, including the amidation of 2-phenylpyridine and indole derivatives with di-*tert*-butylperoxide, and methylthiolation of 2-phenylpyridines with dimethylsulfoxide as the source of methylthiolate and $K_2S_2O_8$ as the oxidant.[82] Yao and coworkers reported a chelate-directed oxidative C–H

halogenation of pyrazole-3,5-dicarboxylic acid with stoichiometric $CuCl_2$, KOH, and halide salts.[83] After 3 days at 160 °C, halogenated pyrazoles were isolated as Cu^{II} coordination complexes (Scheme 5.25).[84]

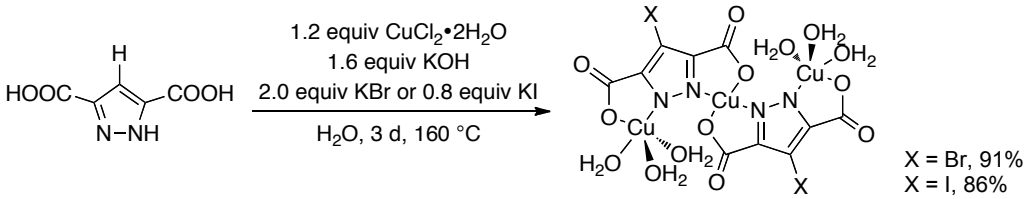

Scheme 5.25. Copper-mediated halogenation of pyrazole -3,5-dicarboxylic acid.

These reactions qualitatively resemble Pd-catalyzed chelate-directed C–H functionalization reactions,[4c] but preliminary mechanistic insights suggest the reactions proceed by a different mechanism. Yu and coworkers noted that Cu-catalyzed chlorination reactions in Scheme 5.21A exhibit a first-order dependence on substrate and $CuCl_2$ and that electron-withdrawing groups lower the rate of the reaction. No deuterium kinetic isotope effect was observed in an intramolecular competition experiment with substrate **10**. The lack of isotopic sensitivity in the C–H cleavage step contrasts observations from Pd-catalyzed reactions. On the basis of these results, Yu and coworkers propose that the reactions are initiated by a SET step (Scheme 5.26), similar to those described in Section 5.3 of this review (cf. Scheme 5.10C). Intramolecular chloride transfer to a radical-cation intermediate is proposed to occur, followed by another SET step and loss of a proton, to afford the chloroarene product. The Cu^{II} catalyst can be regenerated by oxidation of Cu^{I} by O_2. A mechanism initiated by electrophilic activation of the arene was not considered in this work, but also could explain the available results.

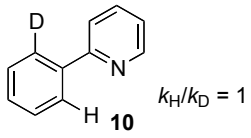

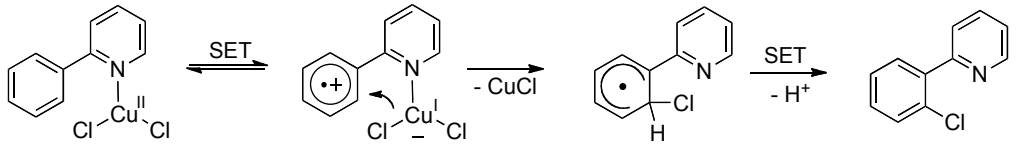

Scheme 5.26. Proposed mechanism for pyridyl-directed monochlorination of 2-phenylpyridine.

5.4.2. Oxidative Annulation Reactions.

Buchwald and coworkers described the aerobic oxidative cyclization of amidines to give benzimidazoles using 15 mol % $Cu(OAc)_2$ and 5 equiv AcOH at 100 °C in DMSO under an oxygen atmosphere (Scheme 5.27).[72] Cyclization was tolerant of both electron-donating and electron-withdrawing substituents, including halogen substituents. Best yields were obtained with substrates that afforded 5- and 6- substituted benzimidazoles; low conversions were obtained for reactions leading to 4-substituted and 4,6-disubstituted products. For reasons that are not clear, amidines with aryl groups lacking *ortho*-substitution showed little conversion to the desired benzimidazole. *N*-methyl-2-phenylbenzimidazoles could be prepared by slight modification of the reaction conditions, and 2-*t*-butyl-benzimidazoles were also accessible (Scheme 5.28).

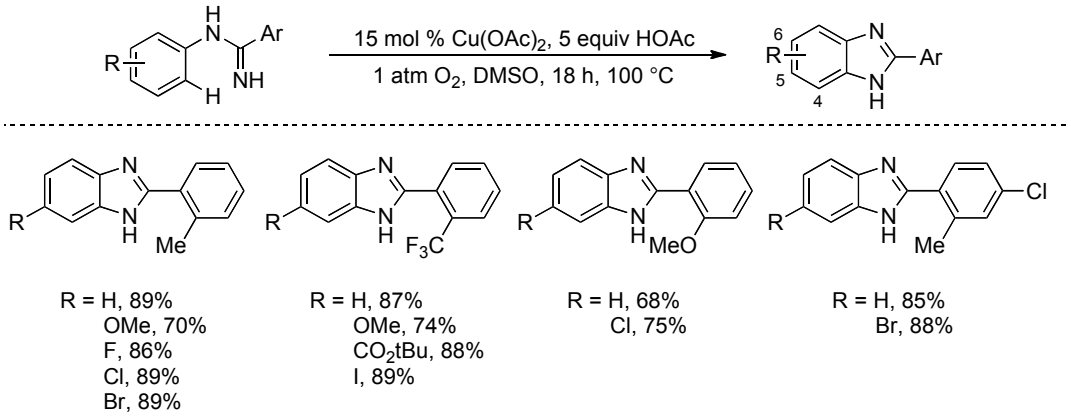

Scheme 5.27. Synthesis of 2-arylated benzimidazoles.

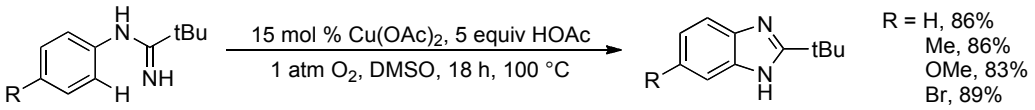

Scheme 5.28. Synthesis of 2-*tert*-butylbenzimidazoles.

The Nagasawa group reported a similar protocol for the preparation of benzoxazoles.[73] Various benzanilides underwent cyclization to the desired benzoxazole products in high yields using 20 mol % $Cu(OTf)_2$ at 140 °C in *o*-xylene under oxygen atmosphere (Scheme 5.29).

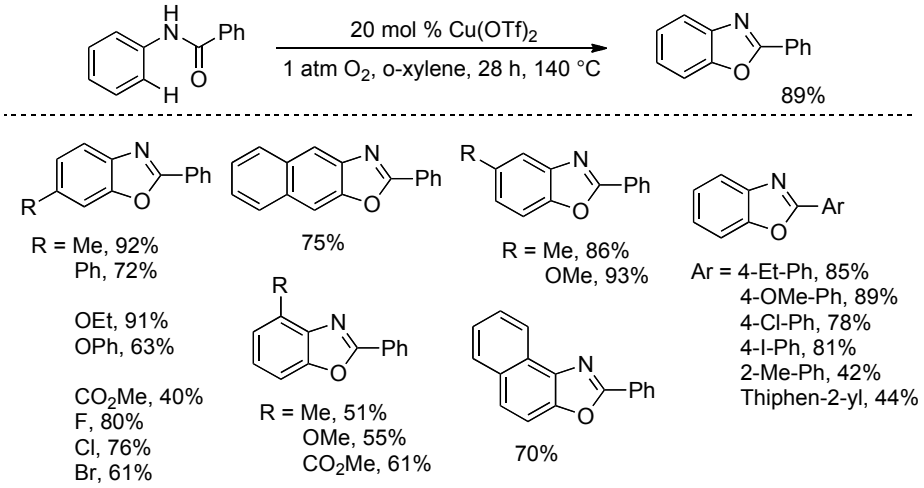

Scheme 5.29. Synthesis of 2-arylated benzoxazoles from anilides.

The highest yields were reported for *meta*- or *para*- substituted benzanilides, while *ortho*-substituted substrates gave lower yields. Electron-withdrawing substituents resulted in lower conversion, with recovered starting material reported in some cases. Regioselectivity of *meta*-substituted benzanilides exclusively favors the least sterically hindered position, resulting in 2,5-disubstituted benzoxazoles. However, when the *meta*-substituent is a pyrrolidinone, benzoyl, acetyl or other directing group, the reaction exclusively forms the more sterically hindered 2,7-disubstituted benzoxazoles (Scheme 5.30).[85]

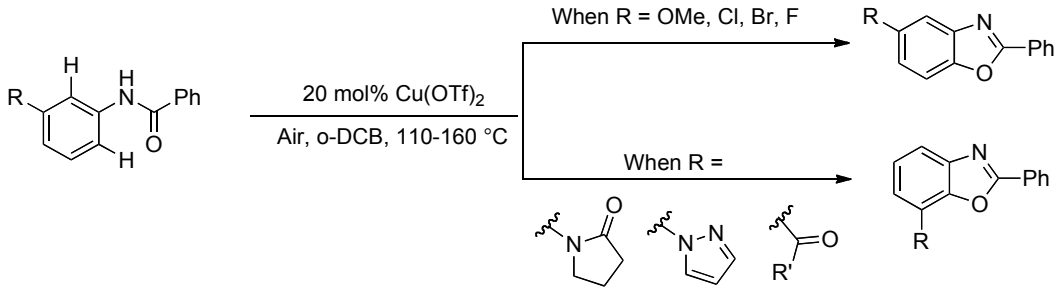

Scheme 5.30. Directing-group effect on benzoxazole cyclization regiochemistry.

The mechanism for benzoxazole and benzimidazole formation is still uncertain. Buchwald postulated three possible mechanisms for oxidative annulation, each originating with coordination of the pendant amidine to the Cu center (Scheme 5.31). Pathway A involves attack of the arene π-system on the Cu-coordinated amidinate ligand, followed by rearomatization to produce benzimidazole. In pathway B, addition of the arene π-system to the Cu center affords an organocopper intermediate, which can then undergo aromatization and reductive elimination to produce desired product. Pathway C involves generation of a Cu-nitrene species that inserts into the arene C–H bond. The Cu is proposed to be in the +2 or +3 oxidation state, although no information is provided into specific redox steps. Both Buchwald and Nagasawa note that the reactions proceed more rapidly with electron-rich substrates. Nagasawa also reported the lack of a deuterium isotope effect in an intramolecular competition study with a mono-*ortho*-deuterated substrate. On the basis of these observations, Nagasawa suggests that Buchwald's electrophilic metalation pathway (Pathway B, Scheme 5.31) is the most reasonable mechanism for the reaction. An SET mechanism (cf. Scheme 5.26) is also consistent with the reported data; however, this mechanism was not considered in these reports.

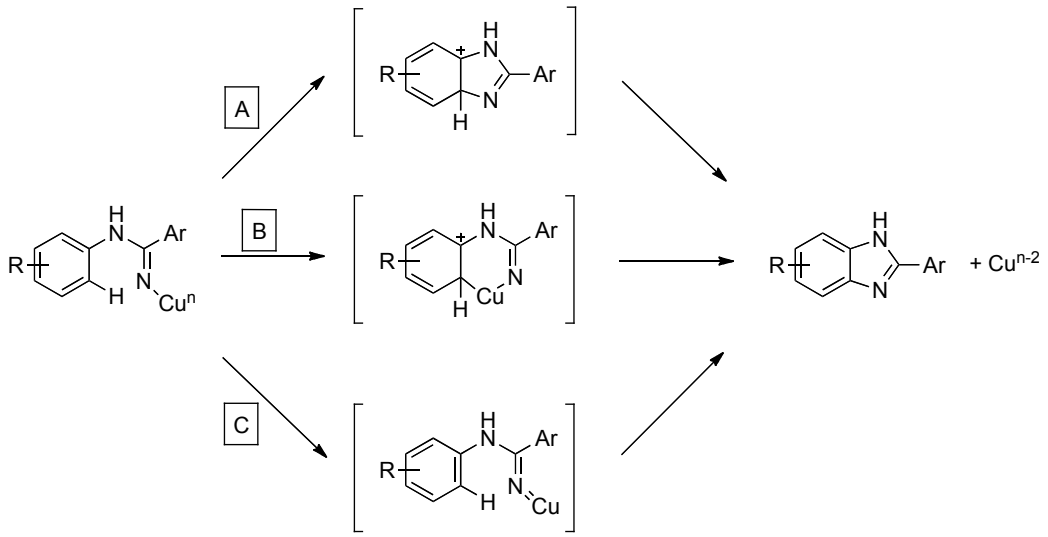

Scheme 5.31. Proposed mechanisms considered for benzoxazole/benzimidazole formation.

Punniyamurthy and coworkers have recently reported an alternative strategy for the preparation of benzoxazoles by rearrangement of bisaryloxime ethers using 20 mol % $Cu(OTf)_2$ under O_2 in toluene at only 80 °C (Scheme 5.32).[86] Though the substrate scope is abbreviated relative to the method reported by Nagasawa, the reaction conditions are much more mild. Punniyamurthy suggests a mechanism beginning with N-O bond scission followed by rearrangement to a copper-containing metallacycle and reductive elimination, possibly via a Cu^{III} intermediate.

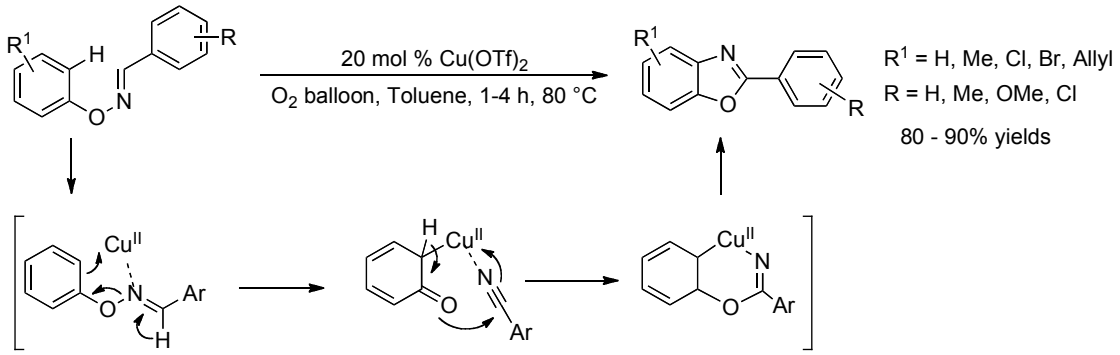

Scheme 5.32. Rearrangement of aryl oximes to give 2-aryl benzoxazoles.

Nagasawa and Ueda reported a copper-catalyzed tandem addition/oxidative cyclization reaction leading to the formation of 1,2,4-triazoles. Aryl nitriles were coupled to substituted 2-aminopyridines with 5 mol % CuBr, 5 mol% 1,10-phenanthroline, and 10 mol % ZnI_2 in dichlorobenzene at 130 °C under O_2 atmosphere (Scheme 5.33).[87]

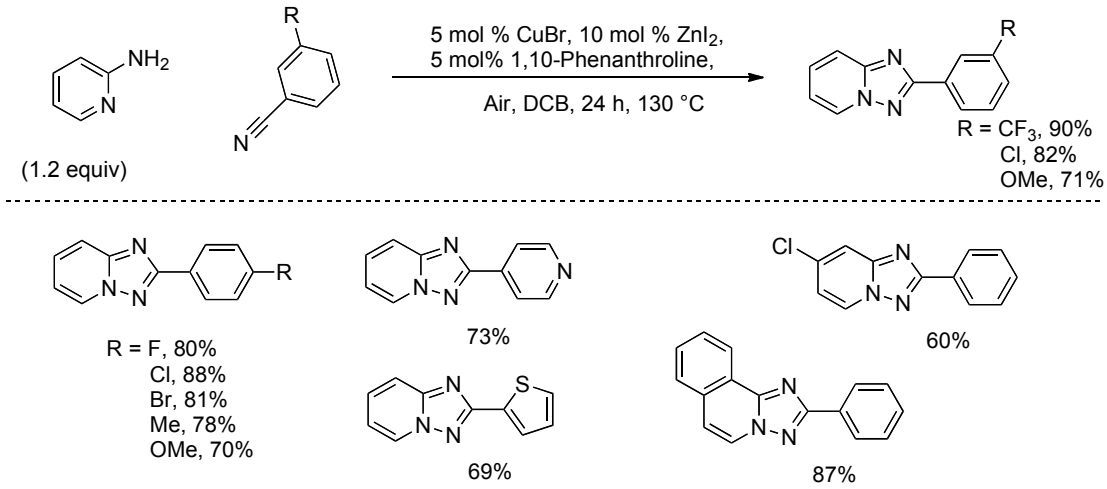

Scheme 5.33. Tandem addition-oxidative coupling of aminopyridines with aryl nitriles.

Mechanistically, the reaction is suggested to proceed via addition of the 2-amino group to the nitrile to form an *N*-2-pyridylamidine, followed by copper-catalyzed oxidative N–N coupling. The oxidative cyclization of a pre-formed amidine proceeds smoothly in the absence of zinc, implying that ZnI_2 assists only in amidine formation. Also, cyclization can also be achieved using stoichiometric $Cu(OAc)_2$ under an argon atmosphere, suggesting that molecular oxygen is only involved in the reoxidation of Cu^I to complete the catalytic cycle. The authors do not speculate on the mechanism of N–N bond formation.

A modified procedure, employing 5 mol % CuBr, 3 equiv Cs_2CO_3 in DMSO with an air atmosphere at 120 °C, provided the addition and oxidative cyclization of aryl nitriles with amidines to give 1*H*-1,2,4-triazoles. In all instances, electron-deficient benzonitriles gave best yields (Scheme 5.34). Bao and colleagues have developed a similar strategy for the preparation

of benzimidazoles and quinazolines. Their cascade strategy begins with C–N bond formation between carbodiimides and various amines, followed by $Cu(OAc)_2/O_2$-catalyzed oxidative annulation to give desired product.[88]

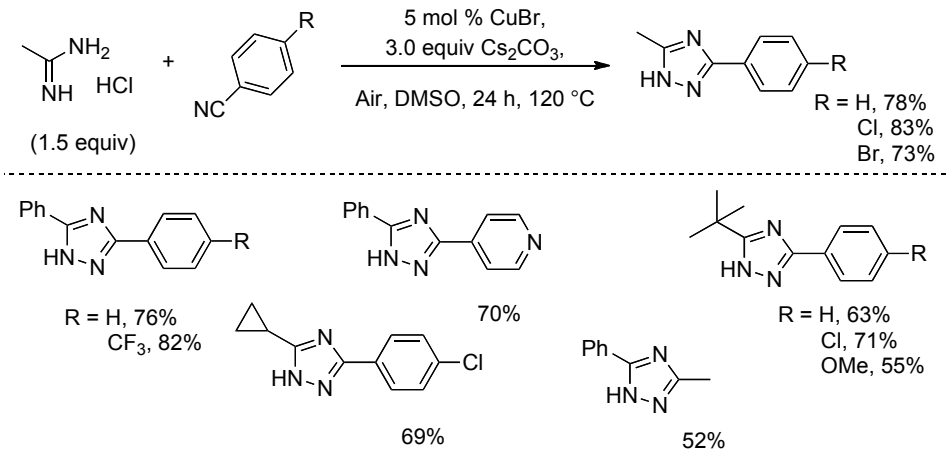

Scheme 5.34. Oxidative coupling and cyclization of aryl nitriles with amidines.

Another tandem strategy, developed by Chiba and coworkers, involves the one-pot, two-step synthesis of phenanthridine derivatives from biaryl-2-carbonitriles.[89] Initial Grignard addition to biaryl nitrile substrates (followed by addition of MeOH) was shown to produce N–H imine intermediates, which, upon treatment with 10 mol % $Cu(OAc)_2$ in DMF under O_2, undergo intramolecular C–H amination to give annulated products in high yields (Scheme 5.35).

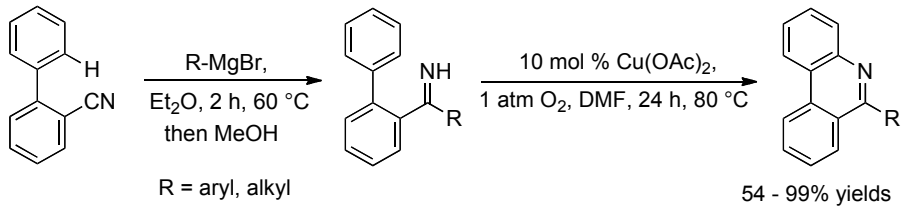

Scheme 5.35. One pot synthesis of phenanthridines from biaryl-2-nitriles.

Zhu and coworkers demonstrate the oxidative annulation of *N*-aryl-2-aminopyridines using 20 mol % $Cu(OAc)_2$, with 10 mol % $Fe(NO_3)_3{\bullet}9H_2O$, and 5 equiv PivOH in DMF under O_2 at

130 °C (Scheme 5.36).[90] Without Fe^{III}, the product yield is diminished from 88% to 58%, even when Cu loading is increased to 2 equiv.[91]

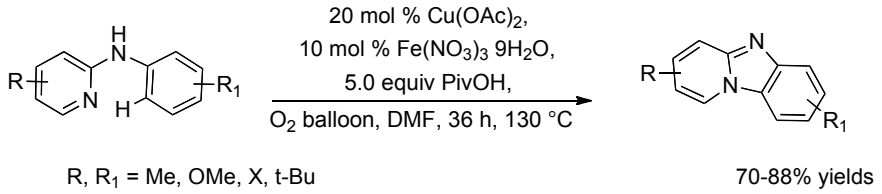

Scheme 5.36. Oxidative annulation of *N*-aryl-2-aminopyridines.

Zhu and coworkers have subsequently extended this method from arene C–H bonds to vinyl C–H bonds; however, instead of obtaining the expected oxidative amination products, aminooxygenation products were observed (Scheme 5.37).[92] Using 20 mol % copper(II) hexafluoroacetylacetonate (hfacac) in DMF under O_2 at 105 °C, a range of imidazo[1,2-a]pyridine-3-carbaldehydes were formed from simple acyclic precursors (Scheme 5.37). Addition of iron nitrate, which proved essential in the previous study, had no beneficial effect on yield in this case. With slight modification of the reaction conditions, 1,2-disubstituted imidazole-4-carbaldehydes could be similarly obtained (Scheme 5.36).

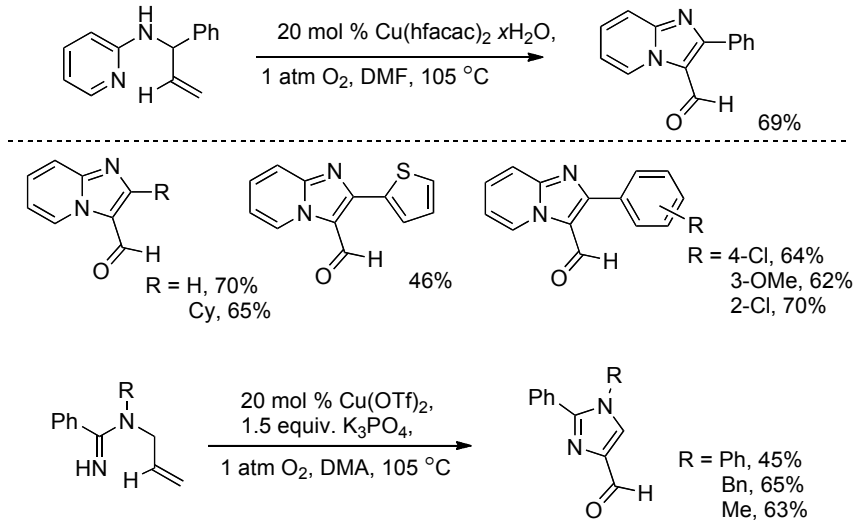

Scheme 5.37. Aminooxygenation for preparation of imidazo[1,2-a]pyridine carbaldehydes, and imidazole carbaldehydes.

Finally, Li and coworkers reported an aerobic, copper-catalyzed oxidative C–H acylation procedure for the preparation of indoline-2,3-diones.[93] *N*-methyl-2-oxo-*N*-phenylacetamide could be cyclized in 90% yield using 20 mol % $CuCl_2$ and 1 atm O_2 in THF at 100 °C (Scheme 5.38). A range of *N*- and aryl-substituted substrates could be cyclized, with electron rich substrates affording higher yields than electron deficient substrates.

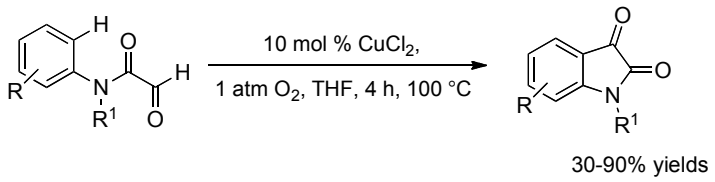

Scheme 5.38. Aerobic, copper-catalyzed synthesis of indoline-2,3-diones.

5.4.3. Hetero-Functionalization of Terminal Alkynes and Electron-Deficient Heteroarenes.

In 2008, Stahl and coworkers reported the oxidative coupling of terminal alkynes with a wide range of nitrogen nucleophiles using 20 mol % $CuCl_2$, 2 equiv of Na_2CO_3 and 2 equiv of pyridine in toluene under an O_2 atmosphere (Scheme 5.39).[74] The use of excess amine nucleophile (5 equiv) minimized the quantity of Glaser alkyne homocoupling byproduct. Screening results showed that $Cu(OAc)_2$ is also an effective catalyst, and a respectable yield of the ynamide (69%) can be obtained with a 1:1 stoichiometry of alkyne and amine under catalytic conditions. Cyclic carbamate, amide, and urea nucleophiles, as well as substituted indoles and *N*-alkyl benzenesulfonamides, were all good coupling partners. Effective substrates all had a pK_a between 15-23 (DMSO), although not all amines within this pK_a range were effective. For example, acyclic nucleophiles other than sulfonamides exhibited poor reactivity. Terminal alkynes substituted with aryl, alkyl, and silyl groups were effective, with electron-rich alkynes being the most effective.

Alkynyl chloride byproducts were isolated from the reaction mixture, suggesting that C–N bond formation may originate through an alkynyl chloride intermediate, but, when alkynyl chlorides were subjected to the reaction conditions, little conversion to the ynamides was observed. The authors invoked a simplified mechanism involving the sequential activation of alkyne C–H and nucleophile N–H groups at a Cu^{II} center, followed by C–N bond formation to give ynamide product. Details of the C–N coupling process and aerobic reoxidation of the catalyst were not addressed.

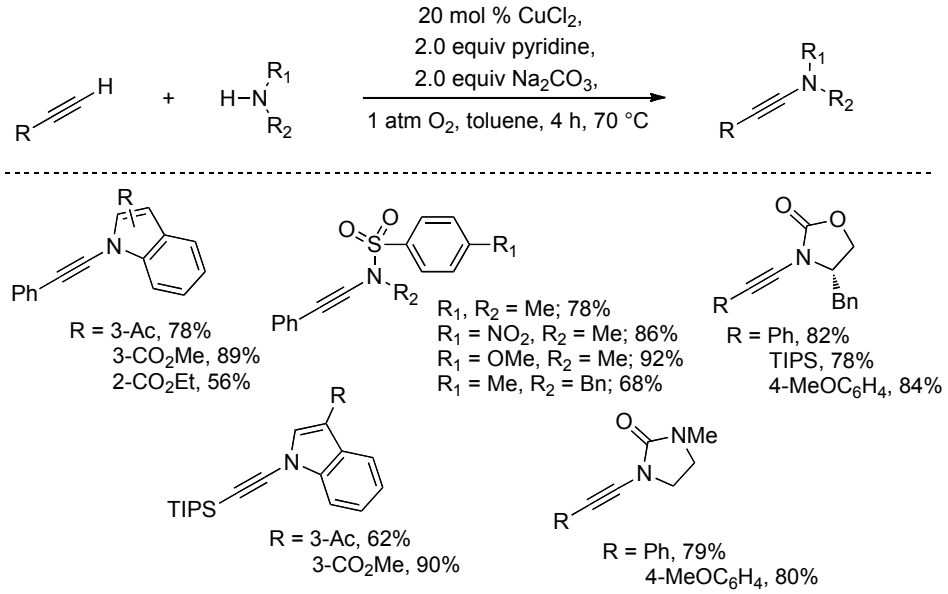

Scheme 5.39. Aerobic copper-catalyzed synthesis of ynamides from terminal alkynes.

This reactivity expands upon an early report by Peterson in 1968, who described the oxidative coupling of phenylacetylene with simple secondary amines.[94] Dimethylamine, diethylamine, and piperidine were reported to react with phenylacetylene in the presence of 20 mol % $Cu(OAc)_2$-H_2O in benzene under a steady stream of oxygen (Scheme 5.40). Isolation of the products is complicated by the reactivity of these products toward hydrolysis, which forms the corresponding *N*,*N*-dialkylamides. When primary amines, such as ethylamine, were used as

the nitrogen nucleophile, *N*-ethyl-2-phenylacetamide was obtained instead of the ynamide. In some cases the amide product may be desired;[95] however, the ability to stop at the intermediate ynamide expands the synthetic versatility of the reactions.

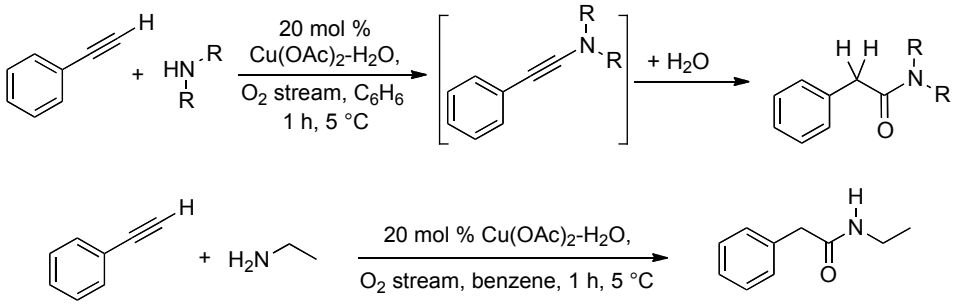

Scheme 5.40. Ynamidation of phenylacetylene with simple secondary and primary amines.

Jiao et al. reported an aerobic copper-catalyzed ynamination reaction with concomitant dioxygenation of the alkyne using 10 mol % $CuBr_2$, 10 mol % TEMPO, and 4 equiv pyridine in toluene and water under an O_2 atmosphere (Scheme 5.41).[96] This tandem amination-diketonization was effective with both electron rich and electron deficient alkynes with a variety of anilines. Electron-deficient anilines performed more efficiently, and halo-substituted anilines were partially compatible with the reaction conditions, affording products in low yields. The reaction is performed with 10 equiv H_2O, but ^{18}O-labeling studies revealed that both oxygen atoms in the diketone come from O_2, and not H_2O. Under the reaction conditions, oxidative coupling of the anilines was also observed, forming *trans*-1,2-diphenyldiazene; this reactivity was the subject of a later independent report.[97]

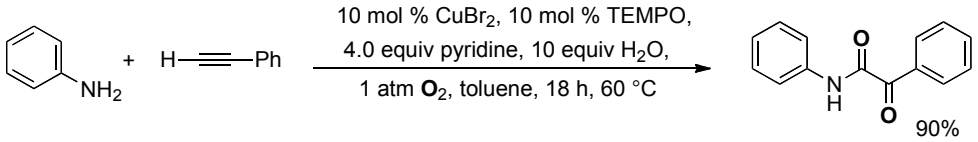

Scheme 5.41. Tandem ynamidation-diketonization reaction.

Other alkyne heterofunctionalization reactions have also been developed. Han and coworkers reported the oxidative phosphonation of terminal alkynes under aerobic conditions.[98] Using 10 mol % CuI or $Cu(OAc)_2$, 2 equiv Et_3N or Et_2NH, in DMSO under dry air, *H*-phosphonates could be coupled to terminal alkynes to yield alkynylphosphonates in excellent yields (Scheme 5.42). A wide range of terminal alkynes could be used, including aliphatic, aryl, and highly functionalized alkynes, giving high yields of desired alkynylphosphonate diethyl, diisopropyl, dibutyl, and dibenzyl esters. Interestingly, only very small quantities (10%) of Glaser dimerization products are formed under these reaction conditions. When oxygen was excluded from the reaction mixture, hydrophosphorylation occured to give alkenylphosphorus compounds.[99] The authors report that a copper acetylide precipitates at the beginning of the reaction and disappears over the course of the reaction. Subjection of the Cu-acetylide to the reaction conditions was reported to give both alkynylphosphonate and Glaser diyne coupling products. If coordination of *H*-phosphonate to copper acetylide is fast relative to the reaction of copper acetylide with oxygen, the formation of Glaser products can be minimized.

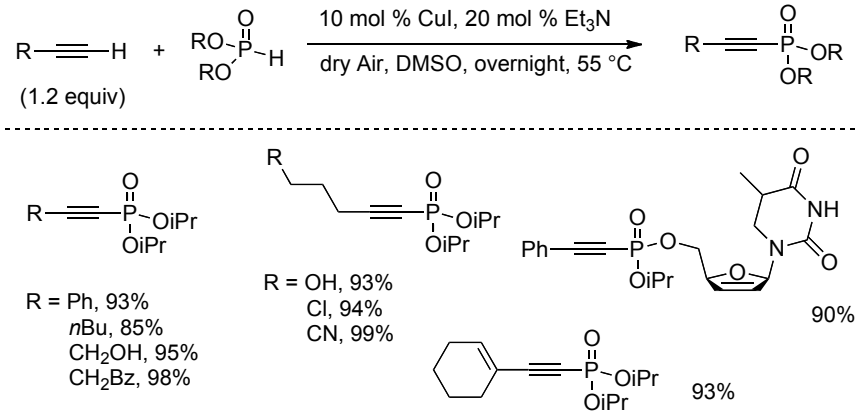

Scheme 5.42. Synthesis of alkynylphosphonates.

Qing et al. reported the oxidative trifluoromethylation of alkynes using 1 equiv CuI, 1 equiv phenanthroline, and 5 equiv Me_3SiCF_3 in DMF under air atmosphere.[100] A range of aryl

alkynes, and a few aliphatic alkynes, were trifluoromethylated using this procedure in good-to-excellent yields (Scheme 5.43). When O_2 was used instead of air, Glaser alkyne dimers were the sole product. The authors speculate that this effect arises from the quenching of a $CuCF_3$ species in the presence of high concentrations of O_2.

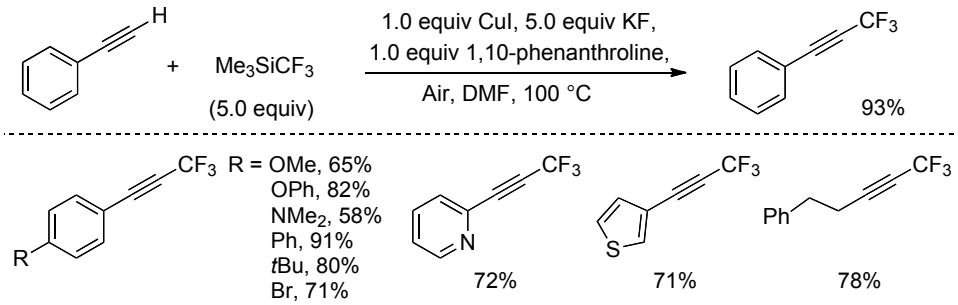

Scheme 5.43. Aerobic copper-mediated trifluoromethylation of alkynes.

Alkynes, heteroaromatics, and electron-deficient arenes share very similar C–H bond acidities. For example, the pK_a values of pentafluorobenzene, benzoxazole, benzothiazole, and phenylacetylene are 21, 24, 27, and 28.8, respectively. Reactions across these classes of molecules show remarkable similarities, and a number of oxidative heterofunctionalization reactions for electron-deficient heteroaromatics and arenes analogous to those described for alkynes have also been developed.[101]

In 2009, Mori and coworkers reported conditions for the oxidative intermolecular coupling of benzothiazole with *N*-methylaniline with 20 mol % $Cu(OAc)_2$, 40 mol % PPh_3, 4 equiv NaOAc, at 140 °C in xylenes under an O_2 atmosphere (Scheme 5.44).[102] The substrate scope encompassed benzoxazoles and benzimidazoles, and aromatic and some aliphatic amines were effective in the amination reactions.

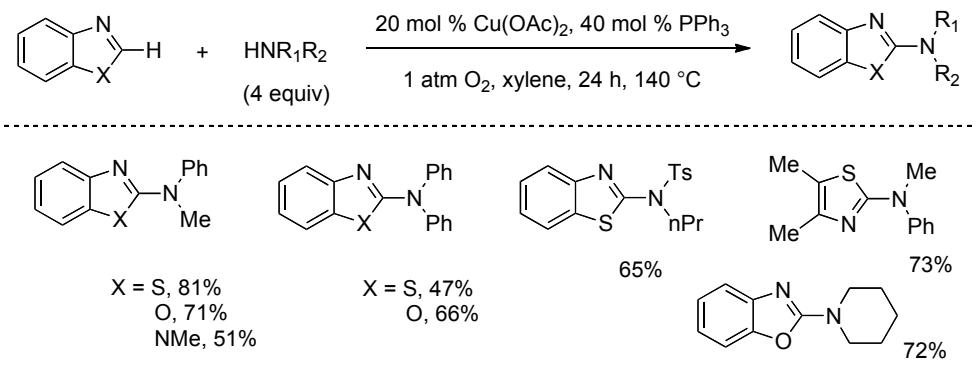

Scheme 5.44. Synthesis of 2-aminobenzimidazoles, oxazoles, and thiazoles.

Shortly after the report by Mori, Schreiber and coworkers reported a similar procedure for the preparation of 2-aminobenzimidazoles, using 20 mol % $Cu(OAc)_2$ and 2 equiv Na_2CO_3, with pyridine as an additive in toluene.[103] Homocoupling of the heteroarene was observed as a byproduct under many conditions, but could be suppressed by the use of 5 equiv of the nitrogen nucleophile. Under these conditions various cyclic amide, urea, and carbamate nucleophiles afforded the desired aminobenzimidazoles (Scheme 5.45). *N*-Methylbenzenesulfonamide was also an effective nucleophile; however, other acyclic secondary amide derivatives were not effective. In contrast, a number of primary amides were successful in the reactions. Other aromatic and heterocyclic C–H bonds were also investigated; benzothiazole, oxazole derivatives, and 1,2,4,5-tetrafluorobenzene derivatives were included in the substrate scope.

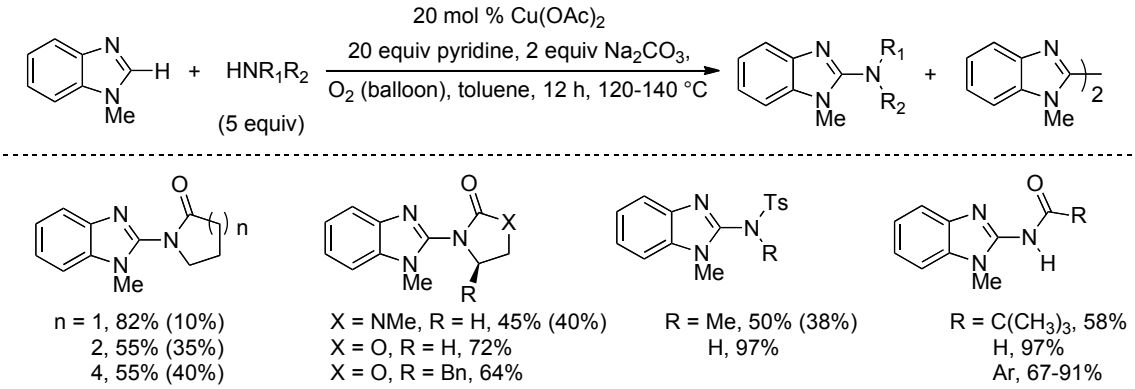

Scheme 5.45. Synthesis of 2-aminobenzimidazoles.

Subsequently, Su and colleagues described the C–H amination of perfluorinated arenes as well as heteroarenes with simple nitroanilines using 20 mol % $Cu(OAc)_2$, 2-3 equiv *t*BuOK, 50 mol % TEMPO, under O_2 in DMF.[104] In reactions with electron-deficient arenes (Scheme 5.46), a number of tetra- and pentafluoroarenes underwent coupling with various electron-deficient anilines. In the absence of a Cu catalyst, nucleophilic aromatic substitution of a fluoro group by the amine nucleophile was observed. The C–H amination of benzoxazoles and benzothiazoles can be carried out using the same conditions, albeit at slightly higher temperature. Though the substrate scope is limited to amination with simple nitroaniline derivatives, this reaction proceeds under milder conditions than the earlier methods developed by Mori and Schreiber.

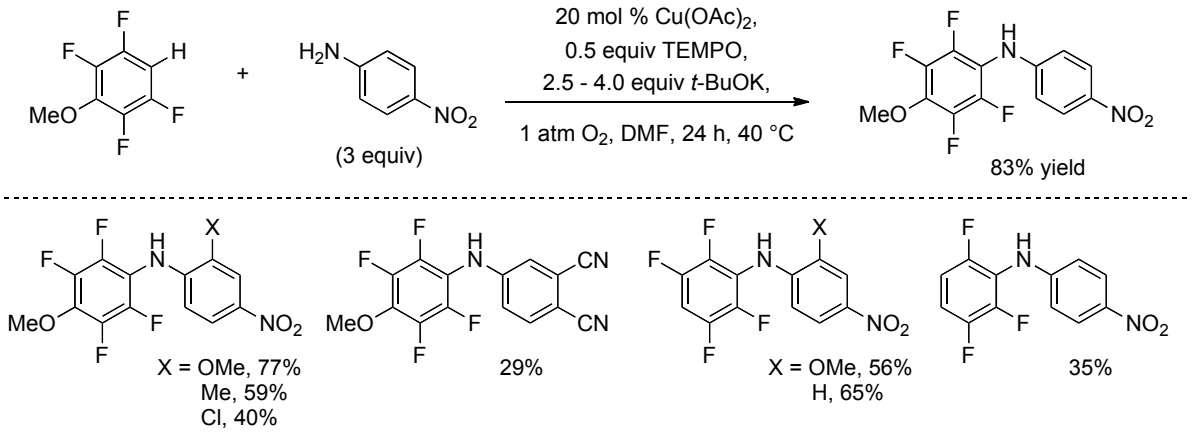

Scheme 5.46. C–H amination of electron-deficient arenes.

Other heterocoupling reactions of electron deficient arenes and alkynes have also been reported. For example, polyfluoroarenes and electron-deficient arenes will undergo aerobic, copper-catalyzed sulfoximation.[105] Fukuzawa and colleagues showed that benzoxazoles could also be thiolated with aryl disulfides using 20 mol% CuI, 20 mol % 2,2'-bipyridine, and 4 equiv Cs_2CO_3 in DMF under an O_2 atmosphere (Scheme 5.47).[106] And, Huang and coworkers have shown that tertiary amines can be used in the amination of benzoxazole in the presence of 20 mol

% $CuBr_2$, and 10 mol % AcOH under O_2 to give *N,N*–dialkyl-2-aminobenzoxazoles (Scheme 5.48).[107] The latter reactions presumably arise from oxidative degradation of the tertiary amine to a secondary amine, followed by oxidative coupling of the benzoxazole with the secondary amine.

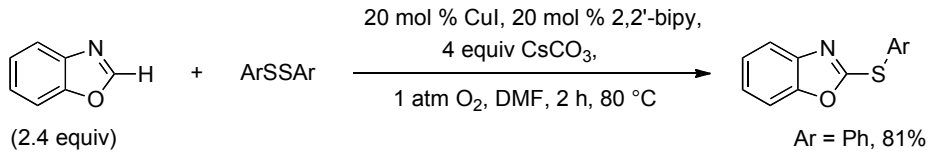

Scheme 5.47. Thiolation of benzoxazole.

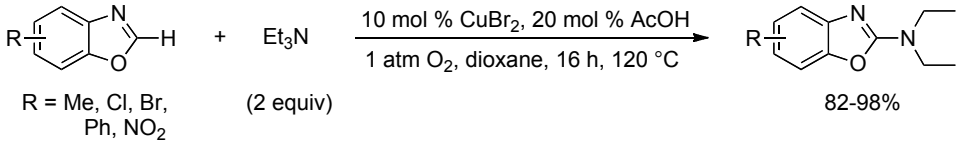

Scheme 5.48. Oxidative amination of benzoxazole using tertiary amines.

5.4.4. Homo- and Cross-Coupling Reactions of Terminal Alkynes and Electron-Deficient Arenes

The similarity in C–H bond acidity between alkynes and electron-deficient arenes appears to provide the basis for a number of oxidative coupling reactions that resemble the Glaser-Hay reaction. Daugulis and coworkers reported an aerobic copper-catalyzed method for the homocoupling of electron-deficient (hetero)aromatics, so-called "aromatic Glaser-Hay" reactions.[75] Using only 1-3 mol% $CuCl_2$ and a Zn/Mg amide base, in THF at room temperature under an O_2 atmosphere, good yields of arene homodimers could be obtained (Scheme 5.49). The reaction exhibited good tolerance of functional groups. Cross-coupling reactions were not examined in this report.[108]

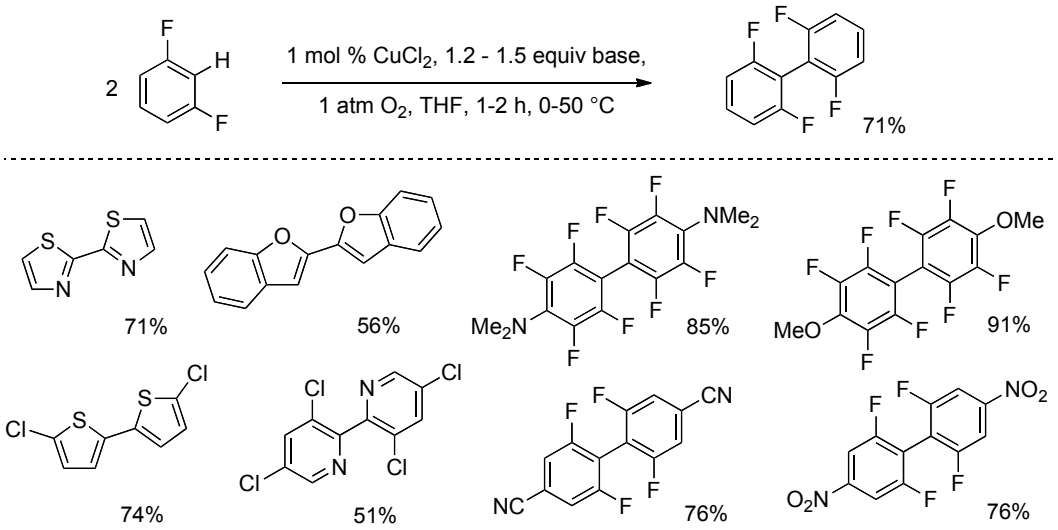

Scheme 5.49. Aerobic oxidative copper-catalyzed homodimerization of functionalized arenes.

Bao recently reported an aerobic $Cu(OAc)_2$-mediated homo- and cross-coupling reaction at the 2-position of a range of azoles.[109] The homocoupling reactions were achieved with 20 mol % $Cu(OAc)_2$ in xylenes at 140 °C under an air or O_2 atmosphere. This method was applied to the oxidative homocoupling of imidazoles, benzimidazoles, thiazoles, oxadiazoles and benzoxazoles (Scheme 5.50). Moderate yields of cross-coupling products could be obtained, but the selectivity was not high. Generally, not more than 50-60% yields were achieved for cross-coupling products.

Su, Hong and coworkers described oxidative cross-coupling reactions of terminal alkynes with electron-deficient arenes and heteroarenes (Scheme 5.51).[110] The reactions employed 3 equiv of *t*-BuOLi, 30 mol % $CuCl_2$, 30 mol % 1,10-phenanthroline, and 15 mol % DDQ in DMSO with O_2 as the oxidant at 40 °C. Excess fluoroarene (5 equiv) was used to enhance the cross-coupling selectivity. When Brønsted bases weaker than tBuO$^-$ were used, such as $NaHCO_3$ and K_3PO_4, Glaser dimerization products dominated. The addition of catalytic DDQ also improved the reaction by suppressing diyne formation. The mechanistic origin of this effect is

not understood, and other quinones did not exhibit a similar effect. Under these conditions, pentafluorobenzene could be coupled to a variety of simple arylalkynes; both electron-rich and electron-deficient alkynes were effective. Other polyfluorinated aromatics could be coupled to terminal alkynes as well. Di- and trifluoroarenes were unreactive, presumably due to the difference in acidity of the aryl C–H bonds and phenylacetylene.

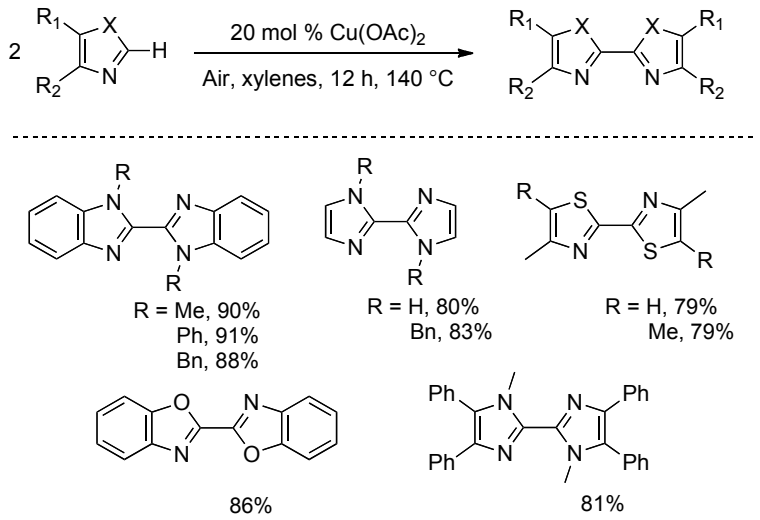

Scheme 5.50. Aerobic oxidative copper-catalyzed dimerization of 2-*H* azoles, oxazoles, and thiazoles.

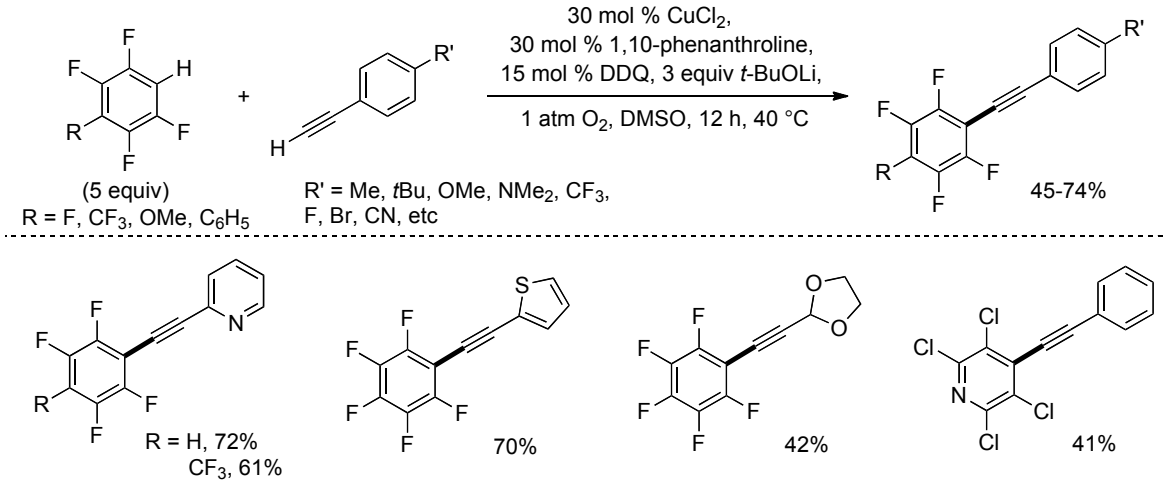

Scheme 5.51. Sonagashira-type aryl-alkynyl coupling reaction.

In a concurrent study, Miura and coworkers reported the aerobic cross-coupling of terminal alkynes with heteroarenes.[111] The 2-position of 1,3,4-oxadiazoles could be functionalized with a range of terminal alkynes using 1 equiv $CuCl_2$ and 2 equiv Na_2CO_3 in *N*, *N*'–dimethylacetamide under 1 atm O_2. When run under air the reaction was sluggish; no reaction occurred under N_2. Oxazoles, too, could be coupled to terminal alkynes in slightly lower yields using a similar procedure, which required increased temperatures and the use of DMSO as a solvent. Electron-rich alkynes were more effective substrates than electron-deficient alkynes, which is attributed to the increased rate of alkyne dimerization with electron-poor alkynes. Aliphatic alkynes and alkynes bearing heterocyclic substituents were also fine coupling partners (Scheme 5.52) in each of these reactions.

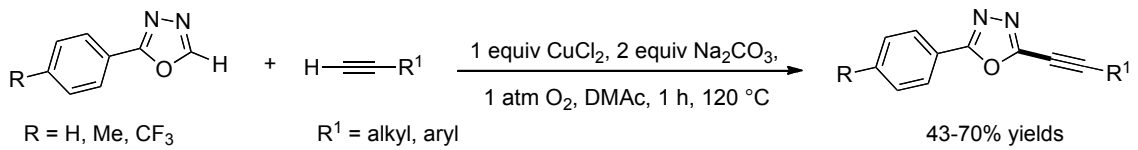

Scheme 5.52. Aerobic copper-mediated oxidative coupling of coupling of alkyness and azoles.

Immediately thereafter, Miura et al. reported methods for the oxidative coupling of polyfluorobenzenes with arylalkynes using 20 mol % $Cu(OTf)_2$, 40 mol % 1,10-phenanthroline, and 1 equivalent LiO*t*Bu in DMSO at room temperature under air (Scheme 5.53).[112] Once again, electron-rich arylalkynes gave higher yields than electron-poor derivatives; use of the latter substrates led to significant formation of diyne byproducts. This study also described a Ni-catalyzed method for aerobic oxidative coupling of alkynes and azoles.

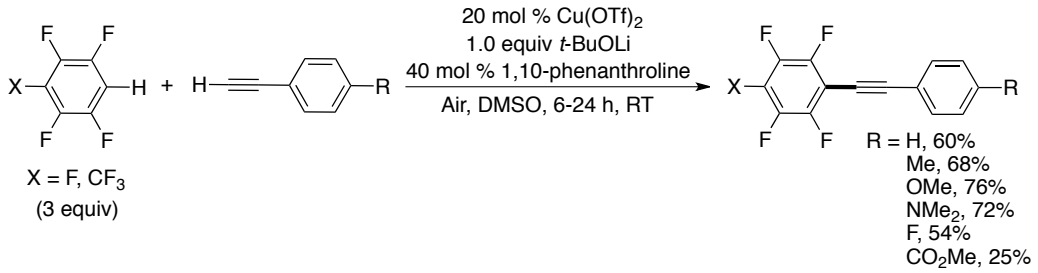

Scheme 5.53. Cu-catalyzed oxidative coupling of polyfluorinated arenes and arylalkynes.

5.4.5. Summary of C–H Oxidations that Resemble Organometallic Reactions.

This section has highlighted a number of oxidative C–H functionalization reactions with substrates that are electronically neutral or electron-deficient, properties not typically associated with SET reactions mediated by Cu^{II}. The similarity between some of these reactions and those mediated by Pd and Rh (e.g., chelate-directed C–H functionalizations and annulation reactions in Sections 5.4.1 and 5.4.2) make it tempting to propose an electrophilic C–H activation pathway by the Cu center, followed by organometallic functionalization of a Cu–C bond. Preliminary mechanistic insights, however, do not necessarily support such a pathway. For example, the lack of deuterium isotope effects from intramolecular competition experiments seem more consistent with electrophilic activation of the arene π-system or SET-initiated C–H functionalization. Further studies will be needed to clarify the mechanisms of these reactions. Sections 5.4.3 and 5.4.4 highlight a wealth of new C–H oxidation reactions involving substrates with acidic C–H bonds. These reactions closely resemble Glaser-Hay couplings; however, they employ substrates and achieve transformations for which the Glaser-Hay analogy was not previously recognized. The mechanisms of these reactions are not well understood, but they seem almost certain to proceed via organometallic intermediates, presumably involving Cu in the +2 or +3 oxidation states. Some insights can be gleaned from recent fundamental studies of the organocopper chemistry.

5.5. Organometallic Copper Chemistry Relevant to C–H Oxidation Reactions.

The organometallic chemistry of Cu^{II} and Cu^{III} is still in a nascent stage of development, but a number of advances in recent years have important implications for the chemical reactions described above. Organocopper(III) intermediates have been widely proposed in non-oxidative Cu-mediated reactions, with prominent examples including conjugate additions and nucleophilic substitution reactions mediated by Cu^{I} organocuprates[113] and Ullmann-type coupling reactions of aryl halides.[114] In contrast, the role of organocopper species in Cu-catalyzed oxidative coupling reactions has received much less consideration.

5.5.1. Survey of High-Valent Organocopper Complexes in Non-Oxidative Reactions.

Experimental characterization of organocopper(III) intermediates in the reactions of cuprates were reported for the first time in 2007 by Bertz and Ogle[115,116] and Gschwind,[117] using low-temperature NMR techniques. Subsequent work has led to spectroscopic characterization of a number of related reactive intermediates (Scheme 5.54).[118]

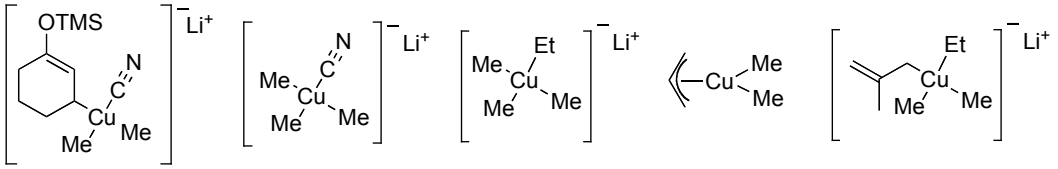

Scheme 5.54. Examples of organocopper(III) species observed using low-temperature NMR spectroscopy.

Ullmann-type cross-coupling reactions of aryl halides are commonly proposed to proceed via a Cu^{I}/Cu^{III} catalytic cycle (Scheme 5.55),[114,119] analogous to the well-established Pd^{0}/Pd^{II} cycle for Pd-catalyzed cross-coupling reactions. The involvement of arylcopper(III) intermediates in these reactions was recently challenged,[120] and subsequently defended,[121] on the basis of DFT computational studies. In addition, the first direct experimental evidence for the involvement of

a Cu^{III} intermediate in an Ullmann-type coupling reactions was reported by Ribas and Stahl in 2010, using a macrocyclic aryl-halide substrate.[122] Aryl-Cu^{III}-halide species were independently synthesized and characterized by X-ray crystallography, and they were shown to undergo reversible reductive elimination/oxidative addition of the aryl halide at the Cu center. Aryl-Cu^{III}-Br species **11** was directly detected by NMR and UV-visible spectroscopy as an intermediate in an Ullmann-type coupling reaction with pyridone as a nitrogen nucleophile.

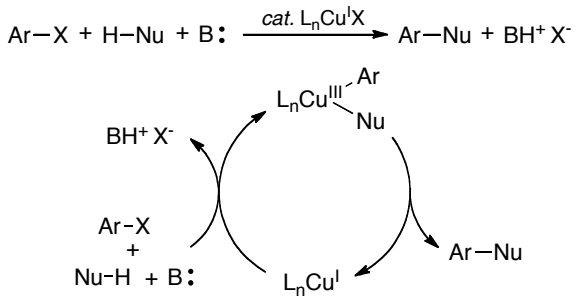

Scheme 5.55. Simplified mechanism commonly proposed for Ullmann-type cross-coupling reactions.

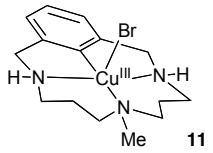

5.5.2. Formation of Organocopper(II) and Copper(III) Complexes via Cu^{II}-Mediated C–H Activation.

Many of the Cu-catalyzed aerobic oxidation reactions described in this review can be carried out under anaerobic conditions by employing Cu^{II} as a stoichiometric reagent. This observation, together with the thermodynamic stability of the +2 oxidation state of copper in the presence of molecular oxygen, suggests that C–H activation steps in the catalytic reactions will be initiated by Cu^{II}. Consequently, the ensuing discussion will emphasize the formation of organocopper

species originating from Cu^{II}. Organometallic C–H activation reactions mediated by Cu^{I} and Cu^{III}, relevant to other (non-aerobic) catalytic reactions, have been discussed elsewhere.[123-127]

A number of organocopper(II) and -copper(III) complexes have been synthesized and crystallographically characterized in recent years,[128-134] and these results provide a useful starting point for the consideration of such intermediates in Cu-catalyzed oxidation reactions. Several of these complexes have been prepared via Cu(II)-mediated activation of a C–H bond within a macrocycle. Starting in 2000, the groups of Latos-Grażyński[130] and Otsuka and Furuta[131] reported a number of organocopper(II) and copper(III) complexes derived from *N*- and *O*-confused porphyrins. The first crystallographically characterized example of an organocopper(II) complex, reported by Furuta and coworkers in 2001,[131b] was obtained by direct metalation of the ligand by $Cu(OAc)_2$ (**13**, Scheme 5.56).[135] Similarly, *N*-confused porphyrins with *meso*-aryl groups (aryl = Ph, C_6F_5) undergo metalation in the presence of $Cu(OAc)_2$ to afford the corresponding macrocyclic organocopper(II) complexes **15**.[130a,131d,e] The pentafluorophenyl derivative of **15** was later shown to undergo oxidation to organocopper(III) derivative **16**, coupled with the loss of the N–H proton, upon treatment with a chemical oxidant (DDQ) (Scheme 5.56).[131e] The reverse reaction was accomplished by the reaction of **16** with a reductant (*p*-toluenesulfonylhydrazide).

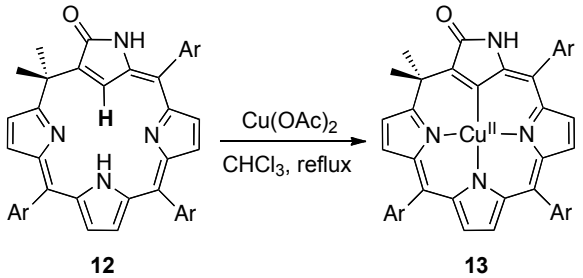

Scheme 5.56. First crystallographically characterized organocopper(II) and its preparation via C–H metalation.

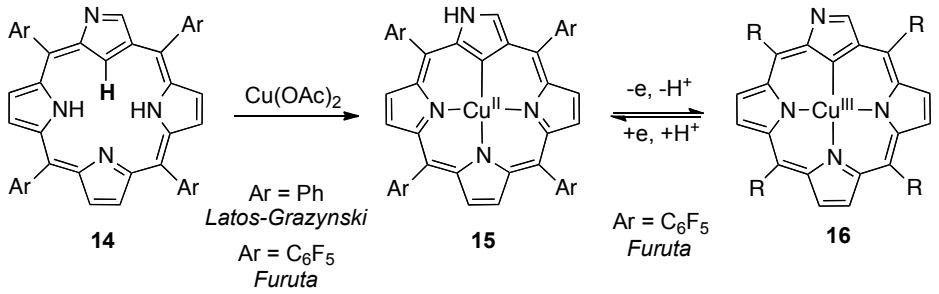

Scheme 5.57. C–H metalation of *N*-confused porphyrins to afford well-defined organocopper(II) species, and the reversible formation of an organocopper(III) derivative (Ar = C_6F_5).

In 2002, Ribas, Llobet, Stack and coworkers reported a different Cu^{II}-mediated C–H activation mechanism.[132a] Reaction of the macrocyclic arene **17** with 1 equiv $Cu^{II}(ClO_4)_2$ in acetonitrile at room temperature resulted in formation of 0.5 equiv of aryl-Cu^{III} species **18** and 0.5 equiv of a ligated Cu^{I} product **19** (Scheme 5.58). Evidence was provided for formation of an arene C–H agostic complex **20** prior to C–H activation, and insights into the C–H···Cu^{II} interaction were recently provided through pulsed-EPR spectroscopic studies and DFT computational methods.[136] The C–H activation step was initially proposed to proceed via a base-assisted electrophilic activation of the arene C–H bond by Cu^{II} (**20** → **21**). A subsequent Cu^{II}-disproportionation reaction between the aryl-Cu^{II} species **21** and another equivalent of the ligated Cu^{II} species **20** would afford the 1:1 product ratio of **18** and **19** (Scheme 5.58). Recently, however, a thorough kinetic and mechanistic study provided evidence that formation of the aryl-Cu^{III} complex **18** proceeds via concerted proton-coupled electron transfer (PCET) directly from **20**. Additional support for this mechanism, which represents a novel route to reactive aryl-Cu^{III} species, was obtained from the reaction of **20** with 2,2,6,6-tetramethylpiperidine-1-oxyl (TEMPO).[136]

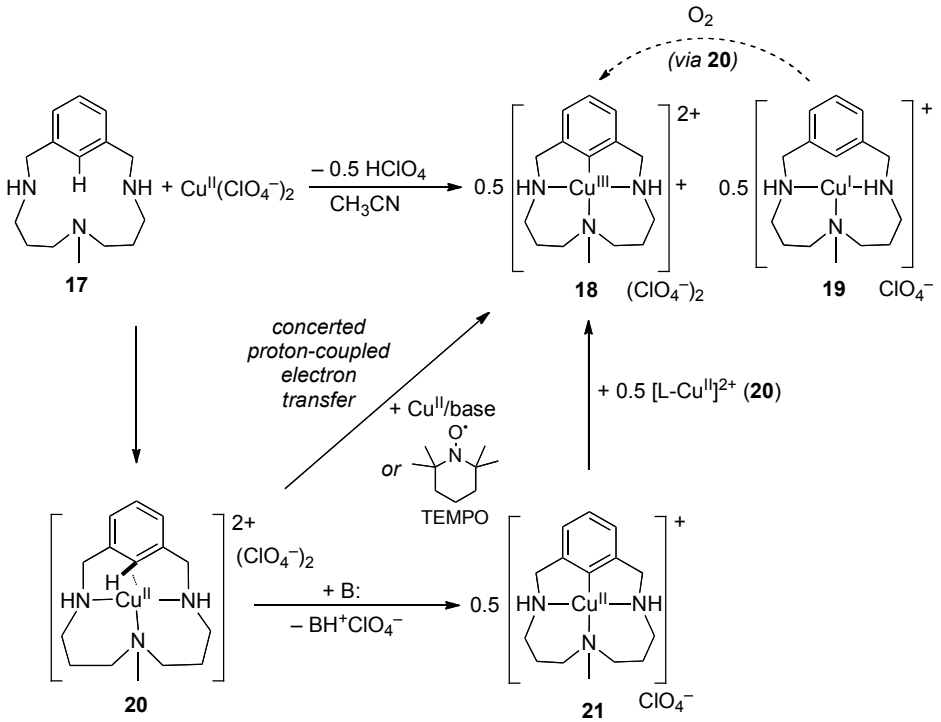

Scheme 5.58. Possible mechanistic pathways for disproportionation of Cu^{II} macrocycle **20** to give aryl-Cu^{III} **19** and Cu^{I}-macrocycle **19**.

The reaction of another macrocyclic arene substrate, reported by Wang and coworkers, reacts with Cu^{II} very similarly to **17**.[134] The azacalix[1]arene[3]pyridine **22** reacts with $Cu^{II}(ClO_4)_2$ to afford the aryl-Cu^{III} complex **23**. An important observation from this study was the improved yields of **23** that could be obtained by performing the reaction under an aerobic atmosphere. Stahl and Ribas made similar observations in the aerobic synthesis of aryl-Cu^{III} complex **18** (see further discussion below). The beneficial effect of O_2 in these reactions can be rationalized by the ability of O_2 to promote the oxidation of Cu^{I} that forms upon disproportionation of Cu^{II} (i.e., Scheme 5.58, **19** → **20** → **18**).

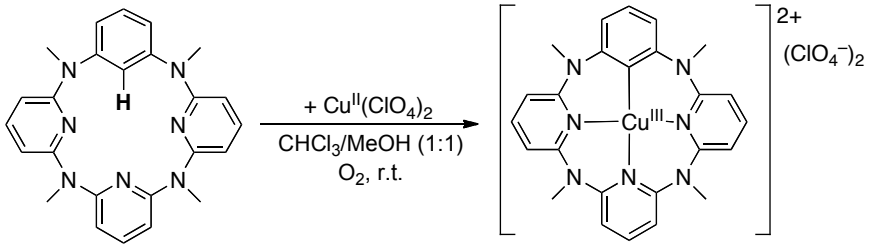

22 **23**

Scheme 5.59. Synthesis of a macrocyclic aryl-Cu^{III} complex under aerobic conditions.

5.5.3. Reactivity of Organocopper(III) Complexes and Cu-Catalyzed C–H Oxidations.

The fundamental insights into Cu^{II}-mediated C–H activation reactions described above have been complemented recently by systematic reactivity studies of organometallic copper(III) complexes.[124,134,137-139] This work includes the first direct evidence for the involvement of an aryl-Cu^{III} intermediate in a Cu-catalyzed C–H oxidation reaction.[140]

In 2008, Huffman and Stahl reported the reaction of a number of different nitrogen nucleophiles with the triazamacrocyclic aryl-Cu^{III} complex **18**, which closely resembles high-valent Cu intermediates proposed in oxidative[141] and non-oxidative[114] Cu-catalyzed coupling reactions. The reactions proceed readily from room temperature to 50 °C, even in the absence of added base and despite the stabilizing effect of the macrocyclic ligand. These observations highlight the innate reactivity of organocopper(III) species relative to isoelectronic Pd^{II} complexes. The reaction exhibited bimolecular reaction kinetics, and no intermediate was observed in the reaction. The reactions were faster with more-acidic nucleophiles, implicating proton loss as a key step prior to C–N bond formation (Scheme 5.60). In a later study carried out jointly by Stahl and Ribas groups,[138] analogous reactions with oxygen nucleophiles were investigated. Carboxylic acids and phenols reacted considerably more rapidly than the nitrogen nucleophiles, and spectroscopic evidence was obtained for the formation of adducts between the

nucleophile and aryl-Cu^{III} that precede C–O bond formation. Wang and coworkers demonstrated similar reactions with the macrocyclic aryl-Cu^{III} complex **23**. A diverse scope of anionic nucleophiles was shown to react very efficiently to afford the C_{aryl}–Nu coupling products (Scheme 5.61).[134]

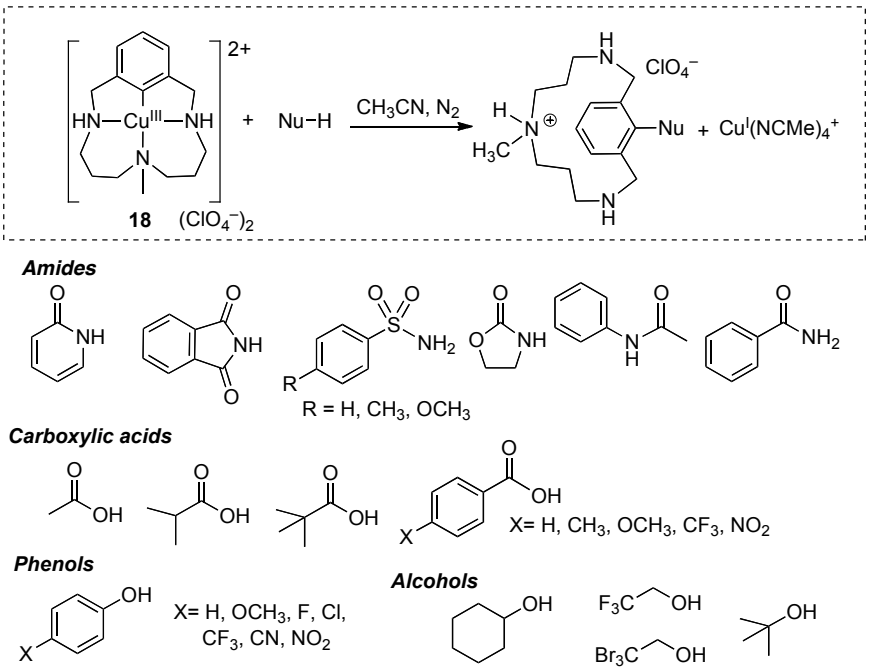

Scheme 5.60. Reductive elimination from macrocyclic aryl-Cu^{III} complexes.

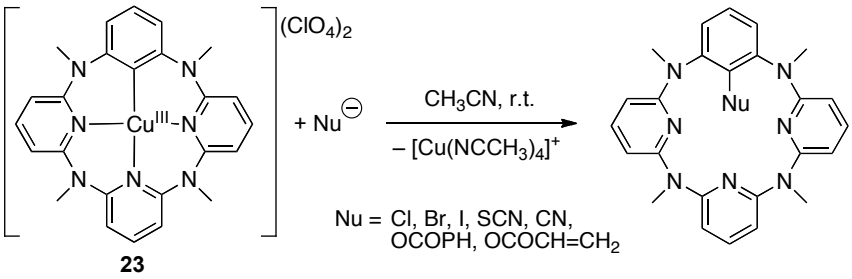

Scheme 5.61. Reductive elimination from macrocyclic aryl-Cu^{III} complexes.

Stahl and Ribas recently demonstrated that the macrocyclic arene **17** can undergo catalytic C–H oxidation under 1 atm O_2 with 10 mol % $Cu(ClO_4)_2$ or $CuBr_2$ (Scheme 5.62).[140] Kinetic and

spectroscopic analysis of the methoxylation reaction, employing simultaneous O_2-uptake methods and UV-visible spectroscopy, provided direct evidence for the formation and disappearance of an aryl-Cu^{III}-Br intermediate in the reaction. These and related observations from the catalytic reactions, together with independent studies of the formation and reaction of the aryl-Cu^{III} intermediate, provide the clearest mechanistic insights to date into a Cu-catalyzed aerobic C–H oxidation reaction. The proposed mechanism (Scheme 5.63) is initiated by complexation of the macrocyclic arene to Cu^{II} (step *i*), followed by C–H activation via Cu^{II} disproportionation to give the aryl-Cu^{III} intermediate (step *ii*) (cf. Scheme 5.58). Subsequent reaction of the aryl-Cu^{III} with methanol results in formation of the methoxylated arene and Cu^{I} (step *iii*) (cf. Scheme 5.60). Rapid reoxidation of Cu^{I} to Cu^{II} by O_2 (step *iv*) completes the catalytic cycle; the same aerobic reoxidation of Cu^{I} occurs in the stoichiometric synthesis of the aryl-Cu^{III} complex (dashed arrows).

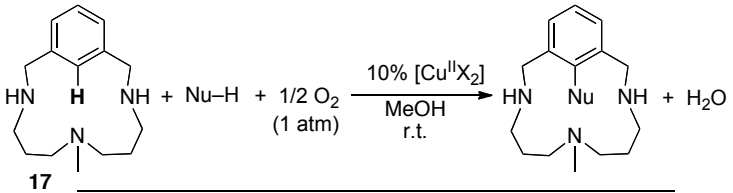

Nu–H	10% $Cu(ClO_4)_2 \cdot 6\ H_2O$	10% $CuBr_2$
MeOH (solvent)	72%	81%
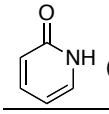 (5 equiv)	77%	84%

Scheme 5.62. Cu-Catalyzed Aerobic Oxidative C–H Functionalization of Arene **17**.

The catalytic cycle in Scheme 5.63 exhibits distinct similarities to the Cu^{I}/Cu^{III} catalytic cycle commonly proposed for Ullmann-type coupling reactions. (cf. Scheme 5.55). Aryl-Cu^{III} species can form via oxidative addition of aryl halides to Cu^{I} in Ullmann-type reactions, whereas the analogous aryl-Cu^{III} intermediate arises here from a Cu^{II}-disproportionation C–H activation

process (cf. Scheme 5.58). Subsequent reductive elimination from the aryl-Cu^{III} intermediate accounts for product formation in both the oxidative and non-oxidative reactions.

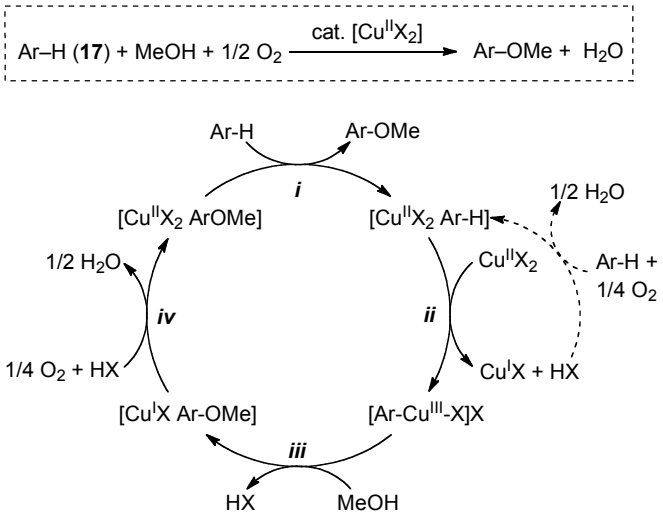

Scheme 5.63. Proposed Catalytic Cycle for Cu-Catalyzed Aerobic Oxidative Methoxylation of Arene **17**.

This organometallic mechanism for C–H oxidation of an arene represents an intriguing alternative to SET mechanisms commonly proposed Cu-catalyzed oxidative coupling reactions. Steps *ii* and *iii* of the mechanism in Scheme 5.63 involve loss of a proton from the Ar–H and MeO–H coupling partners. This feature may explain the observation that many Cu-catalyzed oxidative coupling reactions, such as those in Sections 5.4.3 and 5.4.4, utilize substrates with acidic C–H bonds (alkynes, fluoroarenes, electron-deficient heterocycles). Despite the extensive history of Glaser-Hay reactions of alkynes, alkynyl-Cu^{III} intermediates have never been proposed, to our knowledge; however, the results summarized here suggest that such a pathway might be viable.

5.6. Summary and Outlook

This review highlights the broad array of Cu-catalyzed aerobic C–H oxidation reactions that have been developed in recent years, and it also clarifies key challenges that lie ahead. The emphasis of the content above on synthetic advances largely reflects the relatively poor mechanistic understanding of many of these reactions. For example, many SET-based oxidative coupling reactions are not yet capable of using O_2 as the oxidant. The factors that control the success or failure of different oxidants in these reactions are not well understood. In addition, the vast majority of the reactions discussed here represent "oxidase"-type reactions, but oxygen-atom-transfer ("oxygenase") reactions were also noted (see Schemes 5.6, 5.37 and 5.41). Recent studies of fundamental Cu/O_2 reactivity have largely focused on work relevant to enzymatic and bioinorganic chemistry. Elucidating principles of Cu/O_2 reactivity relevant to important synthetic transformations could provide an important foundation for expanding the scope of useful aerobic oxidation reactions.

This review was generally divided into Cu-catalyzed aerobic oxidation reactions initiated by SET from the substrate to Cu^{II} and those that resemble organometallic C–H oxidation reactions. The line dividing these two reaction classes is not especially clear, however, and the importance of organocopper chemistry in aerobic oxidation reactions remains an open question. The reactions that provide direct evidence for an organometallic mechanism generally feature macrocyclic substrates that impose rather significant constraints on the reaction pathway. As the field expands, it will be important to begin bridging the gap between experimental model studies, of the type described in Section 5.5, and the synthetically useful catalytic oxidation reactions. Despite the uncertainties that exist, the organometallic aerobic oxidation pathways supported by recent studies are quite exciting because they represent a significant departure from classical Cu-

catalyzed oxidative coupling mechanisms, and they offer new modes of reactivity that could enable new types of synthetic transformations. If the rapid pace of advances in this field over the past five years is a representative guide, it seems reasonable to expect that these challenges will be addressed and many new opportunities in Cu-catalyzed aerobic C–H oxidation will be realized.

5.7. Acknowledgments.

We thank the U.S. Department of Energy (DE-FG02-05ER15690) for generous financial support of our work on copper-catalyzed aerobic oxidation reactions. SSS is grateful to Amanda E. King and Lauren M. Huffman for their contributions in starting this project in the group, and Xavi Ribas and Alicia Casitas (University of Girona) for an enjoyable and fruitful collaboration over the past several years.

5.8 References and Notes

---

[1] a) J.-E. Bäckvall, *Modern Oxidation Methods*, 2nd Ed., Wiley-VCH, Weinheim, **2011**; b) F. Cavani, J. H. Teles, *ChemSusChem* **2009**, *2*, 508-534; c) S. Caron, R. W. Dugger, S. G. Ruggeri, J. A. Ragan, D. H. B. Ripin, *Chem. Rev.* **2006**, *106*, 2943-2989.

[2] a) A. R. Dick, M. S. Sanford, *Tetrahedron* **2006**, *62*, 2439-2463; b) J. A. Labinger, J. E. Bercaw, *Nature* **2002**, *417*, 507-514; c) H. M. L. Davies, J. R. Manning, *Nature* **2008**, *451*, 417-424.

[3] a) S. S. Stahl, *Angew. Chem.* **2004**, *116*, 3480-3501; *Angew. Chem. Int. Ed.* **2004**, *43*, 3400-3420; b) T. Punniyamurthy, S. Velusamy, J. Iqbal, *Chem. Rev.* **2005**, *105*, 2329-2364; c) K. M. Gilgorich, M. S. Sigman, *Chem. Commun.* **2009**, 3854-3867; d) S. S. Stahl, *Science* **2005**, *309*, 1824-1826; d) R. A. Sheldon, I. W. C. E. Arends, G.-J. ten Brink, A. Dijksman, *Acc. Chem. Res.* **2002**, *35*, 774-781; e) B. M. Stoltz, *Chem. Lett.* **2004**, *33*, 362-367; f) T. Nishimura, S. Uemura. *Synlett* **2004**, 201-216; g) M. Toyota, M. Ihara, *Synlett* **2002**, 1211-1222.

[4] For some lead reviews on Pd-catalyzed C–H oxidation, see: a) C. S. Yeung, V. M. Dong, *Chem. Rev.* **2011**, *111*, 1215-1292; b) L. Ackermann, *Chem. Rev.* **2011**, *111*, 1315-1345; c) T. W. Lyons, M. S. Sanford, *Chem. Rev.* **2010**, *110*, 1147-1169; d) X. Chen, K. M. Engle, D.-H. Wang, J.-Q. Yu, *Angew. Chem.* **2009**, *121*, 5196-5217; *Angew. Chem. Int. Ed.* **2009**, *48*, 5094-5115; e) V. Ritleng, C. Sirlin, M. Pfeffer, *Chem. Rev.* **2002**, *102*, 1731-1770; f) C. Jia, T. Kitamura, Y. Fujiwara, *Acc. Chem. Res.* **2001**, *34*, 633-639.

[5] For reviews on high-valent Pd chemistry, see: a) K. Muñiz, *Angew. Chem.* **2009**, *121*, 9576-9588; *Angew. Chem. Int. Ed.* **2009**, *48*, 9412-9423; b) L.-M. Xu, B.-J. Li, Z. Yang,

Z.-J. Shi, *Chem. Soc. Rev.* **2010**, *39*, 712-733; c) P. Sehnal, R. J. K. Taylor, I. J. S. Fairlamb, *Chem. Rev.* **2010**, *110*, 824-889.

[6] For recent progress in addressing this problem, see: a) Y.-H. Zhang, J.-Q. Yu, *J. Am. Chem. Soc.* **2009**, *131*, 14654-14655; b) J. Zhang, E. Khaskin, N. P. Anderson, P. Y. Zavalij, A. N. Vedernikov, *Chem. Commun.* **2008**, 3625-3627; c) A. N. Campell, P. B. White, I. A. Guzei, S. S. Stahl *J. Am. Chem. Soc.* **2009**, *132*, 15116-15119; d) G. Brasche, J. Garcia-Fortanet, S. L. Buchwald, *Org. Lett*. **2008**, *10*, 2207-2210.

[7] For representative reviews, see: a) R. A. Himes, K. D. Karlin, *Curr. Opin. Chem. Biol.* **2009,** 13, 119-131; b) L. Que, W. B. Tolman, *Nature* **2008,** *455*, 333-340; c) E. E. Chufán, S. C. Puiu, K. D. Karlin, *Acc. Chem. Res.* **2007,** *40*, 563-572; d) A. C. Rosenzweig, M. H. Sazinsky, *Curr. Op Struct. Bio.* **2006,** *16*, 729-735; e) L. M. Mirica, X. Ottenwaelder, T. D. P. Stack, *Chem. Rev.* **2004,** 104, 1013-1046; f) E. A. Lewis, W. B. Tolman, *Chem. Rev.* **2004**, *104*, 1047-1076; h) E. I. Solomon, P. Chen, M. Metz, S. K. Lee, A. E. Palmer, *Angew. Chem.* **2001***, 113,* 4702-4724; *Angew. Chem., Int. Ed.* **2001**, *40*, 4570-4590; g) V. Mahadevan, R. J. M. K. Gebbink, T. D. P. Stack, *Curr. Opin. Chem. Biol.* **2000,** *4*, 228-234; h) J. P. Klinman, *Chem Rev.* **1996,** *96*, 2541-2562; i) E. I. Solomon, U. M. Sundaram, T. E. Machonkin, *Chem. Rev.* **1996**, *96*, 2563-2606.

[8] A. D. Zuberbühler "Interaction of Cu(I) complexes with Dioxygen" In *Metal Ions in Biological Systems*; H. Sigel, Ed.; M. Dekker: New York, 1976; Vol. 5, pp 325-368.

[9] a) H. Gampp, A. D. Zuberbühler, In *Metal Ions in Biological Systems*; Sigel, H., Sigel, A., Eds.; Dekker: New York, 1981; Vol. 12, p 133. b) P. Gamez, P. G. Aubel, W. L. Driessen, J. Reedijk, *Chem. Soc. Rev.* **2001**, *30*, 376–385; c) J. I. van der Vlugt, F. Meyer, *Top. Organomet. Chem.* **2007**, 22, 191-240.

[10] P. Siemsen, R. C. Livingston, F. Diederich, *Angew. Chem.* **2000**, *112*, 2740-2767; *Angew. Chem. Int. Ed.* **2000**, *39*, 2632-2657.

[11] a) J. Bussink, H. T. van de Grampel, Poly(Phenylene Oxides). In *Ullmann's Encyclopedia of Industrial Chemistry;* W. Gerhartz, Y. S. Yamamoto, F. T. Campbell, R. Pfefferkorn, J. F. Rounsaville Eds, 5th Ed.; VCH: New York, 1985; b) A. S. Hay, H. S. Blanchard, G. F. Endres, J. W. Eustance, *J. Am. Chem. Soc.* **1959,** *81*, 6335-6336; c) General Electric Co., US 3 306 875, 1967 (A. S. Hay).

[12] a) M. Eggersdorfer et al., Vitamins. In *Ullmann's Encyclopedia of Industrial Chemistry*; W. Gerhartz, Y. S. Yamamoto, F. T. Campbell, R. Pfefferkorn, J. F. Rounsaville, Eds, 5th Ed.; VCH: New York, 1985; b) M. Shimizu, Y. Watanabe, H. Orita, T. Hayakawa, K. Takehira, *Bull. Chem. Soc. Jpn.* **1992**, *65*, 1522-1526; c) Hoffmann-La Roche, DE 2 221 624, 1972 (W. Brenner).

[13] a) P. Tundo, M. Selva, *Acc. Chem. Res.* **2002**, *35*, 706-716; b) U. Romano, R. Tesel, M. M. Mauri, P. Rebora, *Ind. En. Chem. Prod. Res. Dev.* **1980**, *19*, 396-403; c) U. Romano, F. Rivetti, N. Di Muzio, U.S. 4,318,862, 1979.

[14] a) I. E. Markó, P. R. Giles, M. Tsukazaki, S. M. Brown, C. J. Urch, *Science* **1996**, *274*, 2044-2046; b) I. E. Markó, A. Gautier, I. Chellé-Regnaut, P. R. Giles, M. Tsukazaki, C. J. Urch, S. M. Brown, *J. Org. Chem.* **1998,** *63*, 7576-7577; c) I. E. Markó, P. R. Giles, M. Tsukazaki, I. Chellé-Regnaut, A. Gautier, S. M. Brown, C. J. Urch, *J. Org. Chem.* **1999**, *64*, 2433-2439.

[15] For selected Cu-TEMPO-based methods, see: a) P. Gamez, I. W. C. E. Arends, J. Reedijk, R. A. Sheldon, *Chem. Commun.* **2003**, 2414-2415; b) A. Dijksman, I. W. C. E.

Arends, R. A. Sheldon, *Org. Biomol. Chem.* **2003,** *1*, 3232-3237; c) M. F. Semmelhack, C. R. Schmid, D. A. Cortes, C. S. Chou, *J. Am. Chem. Soc.* **1984,** *106*, 3374-3376.

[16] M. Schmittel, A. Burghart, *Angew. Chem.* **1997**, *109*, 2658-2699; *Angew. Chem. Int. Ed.* **1997**, *36*, 2550-2589.

[17] a) R. Pummerer, F. Frankfurter, *Chem. Ber.* **1914**, *47*, 1472-1493; see also b) R. Pummerer, F. Frankfurter, *Chem. Ber.* **1919**, *52*, 1416-1420; c) R. Pummerer, E. Prell, A. Rieche, *Chem. Ber.* **1926**, *59*, 2159-2161; R. Pummerer, A. Rieche, *Chem. Ber.* **1926**, *59*, 2161-2175.

[18] A. I. Scott, *Q. Rev. Chem. Soc.* **1965**, *19*, 1-35.

[19] a) A. S. Hay, *J. Polym. Sci.* **1962**, *58*, 581-591; b) G. F. Endres, J. Kwiatek, *J. Polym. Sci.* **1962**, *58*, 593-609; c) G. F. Endres, A. S. Hay, J. W. Eustance, *J. Org. Chem.* **1963**, *28*, 1300-1305; d) H. Finkbeiner, A. S. Hay, H. S. Blanchard, G. F. Endres, *J. Org. Chem.* **1966**, *31*, 549-555.

[20] a) D. R. Armstrong, C. Cameron, D. C. Nonhebel, P. G. Perkins, *J. Chem. Soc. Perk. Trans. 2* **1983**, 581-585; b) D. R. Armstrong, C. Cameron, D. C. Nonhebel, P. G. Perkins, *J. Chem. Soc. Perk. Trans. 2* **1983**, 587-589.

[21] G. Engelsma, E. Havinga, *Tetrahedron* **1958**, *2*, 289-295.

[22] W. Brackman, E. Havinga, *Recl. Trav. Chim. Pays-Bas* **1955**, *74*, 937-955.

[23] C. Glaser, *Chem. Ber.* **1869**, *2*, 422-424.

[24] Y. S. Zalkind, M. A. Aizikovich, *J. Gen. Chem. USSR* **1937**, *7*, 227-233.

[25] A. S. Hay, *J. Org. Chem.* **1962**, *27*, 3320-3321.

[26] a) L. G. Fedenok, V. M. Berdnikov, M. S. Shvartsberg, *J. Org. Chem. USSR* **1974**, *10*, 934-936; b) L. G. Fedenok, V. M. Berdnikov, M. S. Shvartsberg, *J. Org. Chem. USSR* **1973**, *9*, 1806-1809.

[27] For a handful of examples involving Cu^{II} species, see: a) G. Challa, H.C. Meinders, *J. Mol. Cat.* **1977**, *3*, 185-190; b) H. J. Kevelam, K. P. de Jong, H. C. Meinders, G. Challa, *Makromol. Chem.* **1975**, *176*, 1369-1381; c) E. G. Derouane, J. N. Braham, R. Hubin, *Chem. Phys. Lett.* **1974**, *25*, 243-246. For an example involving Cu^{I}, see: A. A. Clifford, W. A. Waters, *J. Chem. Soc.* **1963**, 3056-3062.

[28] F. Bohlmann, H. Schonowsky, E. Inhoffen, G. Grau, *Chem. Ber.* **1964** 97, 794-800.

[29] D. A. Whiting. Oxidative Coupling of Phenols and Phenol Ethers. In *Comprehensive Organic Synthesis*, Ed. B. M. Trost, I. Fleming and G. Pattenden; Pergamon: Oxford, 1991; vol 3; pp 659-703.

[30] For a few examples, see: a) D.-R. Hwang, C.-P. Chen, B.-J. Uang, *Chem. Commun.* **1999**, 1207-1208; b) M. A. Schwartz, R. A. Holton, S. W. Scott, *J. Am. Chem. Soc.* **1969**, *91*, 2800-2800; c) S.-W. Hon, C.-H. Li, J.-H. Kuo, N. B. Barhate, Y.-H. Liu, Y. Wang, C.-T. Chen. *Org. Lett.* **2001**, *3*, 869-872; d) N. B. Barhate, C-.T-. Chen, *Org. Lett.* **2002**, *4*, 2529-2532; e) Q. X. Guo, Z.-J. Wu, Z.-B. Luo, Q.-Z Liu, J.-L. Ye, S.-W. Luo, L.-F. Cun, L.-Z. Gong, *J. Am. Chem. Soc.* **2007**, *129*, 13927-13938; f) C.-Y. Chu, D.-R. Hwang, S.-K. Wang, B.-J. Uang, *Chem. Commun.* **2001**, 980-981; g) M. Tada, T. Taniike, L. M. Kantam, Y. Iwasawa, *Chem. Commun.* **2004**, 2542-2543; h) S. Takizawa, T. Katayama, H. Sasai, *Chem. Commun.* **2008**, 4113-4122.

[31] a) H. Egami, T. Katsuki, *J. Am. Chem. Soc.* **2009**, *131*, 6082-6083; b) F. Toda, K. Tanaka, S. Iwata, *J. Org. Chem.* **1989**, *54*, 3007-3009; c) K. Wang, M. Lu, A. Yu, X.

Zhu, Q. Wang, *J. Org. Chem.* **2009**, *74*, 935-938; d) H. Egami, K. Matsumoto, T. Oguma, T. Kunisu, T. Katsuki, *J. Am. Chem. Soc.* **2010**, *132*, 13633-13635; e) K. Ding, W. Yang, L. Zhang, W. Yangjie, T. Matsuura, *Tetrahedron* **1996**, *52*, 1005-1010.

[32] a) K. Yamamoto, H. Fukushima, Y. Okamoto, K. Hatada, M. Nakazaki, *J. Chem. Soc., Chem. Commun.* **1984**, 1111-1112; b) H. Nishino, N. Itoh, M. Nagashima, K. Kurosawa, *Bull. Chem. Soc. Jpn.* **1992**, *65*, 620-622; c) M. J. S. Dewar, T. Nakaya, *J. Am. Chem. Soc.* **1968**, *90*, 7134-7135.

[33] A few examples of non-aerobic, copper-based oxidative biaryl coupling strategies: a) B. Feringa, H. Wynberg, *Bioorg. Chem.* **1978**, *7*, 397-408; b) J. Brussee, A. C. A. Jansen, *Tetrahedron Lett.* **1983**, *24*, 3261-3262; c) J. Brussee, J. L. G. Groenendijk, J. M. te Koppele, A. C. A. Jansen, *Tetrahedron* **1985**, *41*, 3313-3319; d) K. Yamamoto, H. Fukushima, M. Nakazaki, *J. Chem. Soc., Chem. Commun.* **1984**, 1490-1491; e) M. Smrčina, M. Lorenc, V. Hanuš, P. Sedmera, P. Kočovsky, *J. Org. Chem.* **1992**, *57*, 1917-1920; f) M. Smrčina, J. Poláková, S. Vyskočil, P. Kočovsky, *J. Org. Chem.* **1993**, *58*, 4534-4538; g) M. Hovorka, R. Ščigel, J. Gunterová, M. Tichý, J. Závada, *Tetrahedron* **1992**, *48*, 9503-9516; h) M. Hovorka, J. Günterová, J. Závada, *Tetrahedron Lett.* **1990**, *31*, 413-416.

[34] a) M. Nakajima, K. Kanayama, I. Miyoshi, S.-I. Hashimoto, *Tetrahedron Lett.* **1995**, *36*, 9519-9520; b) M. Nakajima, I. Miyoshi, K. Kanayama, S.-I. Hashimoto, M. Noji, K. Koga, *J. Org. Chem.* **1999**, *64*, 2264-2271; c) M. Noji, M. Nakajima, K. Koga, *Tetrahedron Lett.* **1994**, *35*, 7983-7984.

[35] K. H. Kim, D.-W. Lee, Y.-S. Lee, D.-H. Ko, D.-C. Ha, *Tetrahedron* **2004**, *60*, 9037-9042.

[36] X. Li, J. Yang, M. C. Kozlowski, *Org. Lett.* **2001**, *3*, 1137-1140.

[37] A. Caselli, G. B. Giovenzana, G. Palmisano, M. Sisti, T. Pilati, *Tetrahedron: Asymmetry* **2003**, *14*, 1451-1454.

[38] a) T. Sakamoto, H. Yonehara, C. Pac, *J. Org. Chem.* **1997**, *62*, 3194-3199 b) T. Sakamoto, H. Yonehara, C. Pac, *J. Org. Chem.* **1994**, *59*, 6859-6861.

[39] J. Gao, J. H. Reibenspies, A. E. Martell, *Angew. Chem.* **2003**, *115*, 6190-6194; *Angew. Chem. Int. Ed.* **2003**, *42*, 6008-6012.

[40] a) J. M. Brunel, *Chem. Rev.* **2005**, *105*, 857-898; b) M. Sainsbury, *Tetrahedron* **1980**, *36*, 3327-3359; c) J. A. Ashenhurst, *Chem. Soc. Rev.* **2010**, *39*, 540-548; d) P. Kocovský, Š. Vyskocil, M. Smrčina, *Chem. Rev.* **2003**, *103*, 3213-3246; e) C. Rosini, L. Franzini, A. Raffaelli, P. Salvadori, *Synthesis* **1992**, *1992*, 503-517; f) M. C. Kozlowski, B. J. Morgan, E. C. Linton, *Chem. Soc. Rev.* **2009**, *38*, 3193-3207; g) H. Wang, *Chirality* **2010**, *22*, 827-837.

[41] See, for example: B. J. Morgan, X. Xie, P.-W. Phuan, M. C. Kozlowski, *J. Org. Chem.* **2007**, *72*, 6171-6182.

[42] See, for example: C. A. Mulrooney, X. Li, E. S. DiVirgilio, M. C. Kozlowski, *J. Am. Chem. Soc.* **2003**, *125*, 6856-6857. b) B. J. Morgan, C. A. Mulrooney, E. M. O'Brien, M. C. Kozlowski, *J. Org. Chem.* **2010**, *75*, 30-43. c) E. M. O'Brien, B. J. Morgan, C. A. Mulrooney, P. J. Carroll, M. C. Kozlowski, *J. Org. Chem.* **2010**, *75*, 57-68.

[43] a) X. Li, J. B. Hewgley, C. A. Mulrooney, J. Yang, M. C. Kozlowski, *J. Org. Chem.* **2003**, *68*, 5500-5511; For more detailed mechanistic studies see: b) J. Roithová, D. Schröder, *Chem. - Eur. J.* **2008**, *14*, 2180-2188; c) J. Roithová, P. Milko, *J. Am. Chem. Soc.* **2009**, *132*, 281-288.

[44] B. Hewgley, S. S. Stahl, M. C. Kozlowski, *J. Am. Chem. Soc.* **2008**, *130*, 12232-12233.

[45] a) H. M. Kagan, W. Li, *J. Cell. Biochem.* **2003**, *88*, 660-672; b) N. M. Okeley, W. A. van der Donk, *Chem. Biol.* **2000,** 7, 159-171.

[46] a) S. X. Wang, M. Mure, K. F. Medzihradszky, A. L. Burlingame, D. E. Brown, D. M. Dooley, A. J. Smith, H. M. Kagan, J. P. Klinman, *Science* **1996,** *273*, 1078-1084; b) J. P. Klinman, *J. Biol. Chem.* **1996,** *271*, 27189-27192; c) M. Mure, S. A. Mills, J. P. Klinman, *Biochem.* **2002,** *41*, 9269-9278; d) M. Mure, *Acc. Chem. Res.* **2004,** 37, 131-139.

[47] a) L. Menini, E. V. Gusevskaya, *Chem. Commun.* **2006**, 209-211; b) L. Menini, E. V. Gusevskaya, *Appl. Catal. A – Gen.* **2006**, *309*, 122-128.

[48] The para-isomers were obtained in all of the substrates tested, with the exception of eugenol, which contains a para-allyl substituent. In the case of eugenol, the ortho isomer was obtained. Remarkably, in no instances was overchlorination observed, even at longer reaction times.

[49] L. Menini, L. A. Parreira, E. V. Gusevskaya, *Tetrahedron Lett.* **2007**, *48*, 6401-6404.

[50] L. Menini, J. C. da Cruz Santos, E. V. Gusevskaya, *Adv. Synth. Catal.* **2008**, *350*, 2052-2058.

[51] L. Yang, Z. Lu, S. S. Stahl, *Chem. Commun.* **2009**, 6460-6462.

[52] When 2 eq of LiBr were used, dibrominated arenes were isolated as the sole product.

[53] J. Wang, W. Wang, J.-H. Li, *Green Chem.* **2010**, *12*, 2124-2126.

[54] a) J. C. Barnes, D. N. Hume, *Inorg. Chem.* **1963**, *2*, 444–448; b) C. E. Castro, E. J. Gaughan, D. C. Owsley, *J. Org. Chem.* **1965**, *30*, 587–592.

[55] I. Ban, T. Sudo, T. Taniguchi, K. Itami, *Org. Lett.* **2008**, *10*, 3607-3609.

[56] S. Zhang, P. Qian, M. Zhang, M. Hu, J. Cheng, *J. Org. Chem.* **2010**, *75*, 6732-6735.

[57] See, for example: a) S.-I. Murahashi, N. Komiya, H. Terai, T. Nakae, *J. Am. Chem. Soc.* **2003**, *125*, 15312-15313; b) S.-I. Murahashi, N. Komiya, H. Terai, *Angew. Chem.* **2005**, *117*, 7091-7093; *Angew. Chem. Int. Ed.* **2005**, *44*, 6931-6933; c) S.-I. Murahashi, T. Naota, K. Yonemura, *J. Am. Chem. Soc.* **1988**, *110*, 8256-8258; d) I. Jovel, S. Prateeptongkum, R. Jackstell, N. Vogl, C. Weckbecker, M. Beller, *Chem. Commun.* **2010**, *46*, 1956-1958; e) M. North, *Angew. Chem.* **2004**, *116*, 4218-4220; *Angew. Chem. Int. Ed.* **2004**, *43*, 4126-4128.

[58] See, for example: a) B. Chiavarino, R. Cipollini, M. E. Crestoni, S. Fornarini, F. Lanucara, A. Lapi, *J. Am. Chem. Soc.* **2008**, *130*, 3208-3217; b) E. Shirakawa, N. Uchiyama, T. Hayashi, *J. Org. Chem.* **2010**, *76*, 25-34; c) C. M. R. Volla, P. Vogel, *Org. Lett.* **2009**, *11*, 1701-1704; d) S. Murata, M. Miura, M. Nomura, *J. Org. Chem.* **1989**, *54*, 4700-4702; e) W. Han, A. R. Ofial, *Chem. Commun.* **2009**, 6023-6025; f) P. Liu, C.-Y. Zhou, S. Xiang, C.-M. Che, *Chem. Commun.* **2010**, *46*, 2739-2741; g) N. Chatani, T. Asaumi, S. Yorimitsu, T. Ikeda, F. Kakiuchi, S. Murai, *J. Am. Chem. Soc.* **2001**, *123*, 10935-10941.

[59] See, for example: a) Z. Li, C.-J. Li, *J. Am. Chem. Soc.* **2004**, *126*, 11810-11811; b) Z. Li, C.-J. Li, *J. Am. Chem. Soc.* **2005**, *127*, 6968-6969; c) F. Yang, J. Li, J. Xie, Z.-Z. Huang, *Org. Lett.* **2010**, *12*, 5214-5217; d) Z. Li, C.-J. Li, *J. Am. Chem. Soc.* **2005**, *127*, 3672-3673; e) Z. Li, C.-J. Li, *Org. Lett.* **2004**, *6*, 4997-4999; f) O. Baslé, C.-J. Li, *Org. Lett.* **2008**, *10*, 3661-3663; g) Z. Li, C.-J. Li, *Eur. J. Org. Chem.* **2005**, *2005*, 3173-3176; h) Z. Li, C.-J. Li, *J. Am. Chem. Soc.* **2006**, *128*, 56-57.

[60] a) C.-J. Li, *Acc. Chem. Res.* **2008**, *42*, 335-344; b) C.-J. Li, Z. Li, *Pure Appl. Chem.* **2006**, *78*, 935-945; c) Z. Li, D. S. Bohle, C.-J. Li, *P. Natl. Acad. Sci.* **2006**, *103*, 8928-8933.

[61] E. Boess, D. Sureshkumar, A. Sud, C. Wirtz, C. Farès, M. Klussmann, *J. Am. Chem. Soc.* **2011**, *133*, 8106-8109.

[62] A. S.-K. Tsang, P. Jensen, J. M. Hook, A. S. K. Hashmi, M. H. Todd, *Pure Appl. Chem.* **2011**, *83,* 655-665.

[63] O. Baslé, C.-J. Li, *Green Chemistry* **2007**, *9*, 1047-1050.

[64] W.-J. Yoo, C. A. Correia, Y. Zhang, C.-J. Li, *Synlett* **2009**, *1*, 138-142.

[65] O. Baslé, C.-J. Li, *Chem. Commun.* **2009**, 4124-4126.

[66] Y. Shen, M. Li, S. Wang, T. Zhan, Z. Tan, C.-C. Guo, *Chem. Commun.* **2009**, 953-955.

[67] L. Huang, T. Niu, J. Wu, Y. Zhang, *J. Org. Chem.* **2011**, *76*, 1759-1766.

[68] For a few examples of copper-mediated oxidative enolate homo- and hetero-coupling see: a) M. W. Rathke, A. Lindert, *J. Am. Chem. Soc*. **1971**, *93*, 4605-4606; b) Y. Ito, T. Konoike, T. Saegusa, *J. Am. Chem. Soc.* **1975**, *97*, 2912-2914; c) Y. Ito, T. Konoike, T. Harada, T. Saegusa, *J. Am. Chem. Soc*. **1977**, *99*, 1487-1493; d) P. S. Baran, J. M. Richter, *J. Am. Chem. Soc.* **2004**, *126*, 7450-7451; e) P. S. Baran, J. M. Richter, *J. Am. Chem. Soc.* **2004**, *126*, 7450-7451.

[69] For good reviews of oxidative enolate homo- and cross-coupling, see, and references therein: a) A. G. Csákÿ, J. Plumet, *Chem. Soc. Rev.* **2001**, *30*, 313-320; b) M. P. DeMartino, K. Chen, P. S. Baran, *J. Am. Chem. Soc.* **2008**, *130*, 11546-11560; c) J. M. Richter, B. W. Whitefield, T. J. Maimone, D. W. Lin, M. P. Castroviejo, P. S. Baran, *J. Am. Chem. Soc.* **2007**, *129*, 12857-12869.

[70] a) J. E. M. N. Klein, A. Perry, D. S. Pugh, R. J. K. Taylor, *Org. Lett.* **2010**, *12*, 3446-3449; b) Y.-X. Jia, E. P. Kündig, *Angew. Chem.* **2009**, *121*, 1664-1667; *Angew. Chem. Int. Ed.* **2009**, *48*, 1636-1639; c) A. Perry, R. J. K. Taylor, *Chem. Commun.* **2009**, 3249-

3251; d) D. S. Pugh, J. E. M. N. Klein, A. Perry, R. J. K. Taylor, *Synlett* **2010**, *2010*, 934-938.

[71] X. Chen, X.-S. Hao, C. E. Goodhue, J.-Q. Yu, *J. Am. Chem. Soc.* **2006**, *128*, 6790-6791.

[72] G. Brasche, S. L. Buchwald, *Angew. Chem.* **2008**, *120*, 1958-1960; *Angew. Chem. Int. Ed.* **2008**, *47*, 1932-1934.

[73] S. Ueda, H. Nagasawa, *Angew. Chem.* **2008**, *120*, 6511-6513; *Angew. Chem. Int. Ed.* **2008**, *47*, 6411-6413.

[74] T. Hamada, X. Ye, S. S. Stahl, *J. Am. Chem. Soc.* **2008**, *130*, 833-835.

[75] H.-Q. Do, O. Daugulis, *J. Am. Chem. Soc.* **2009**, *131*, 17052-17053.

[76] W. Wang, F. Luo, S. Zhang, J. Cheng, *J. Org. Chem.* **2010**, *75*, 2415-2418.

[77] W. Wang, C, Pan, F. Chen, J. Cheng, *Chem. Commun.* **2011**, 47, 3978-3980.

[78] T. Uemura, S. Imoto, N. Chatani, *Chem. Lett.* **2006**, *35*, 842-843.

[79] Q. Shuai, G. Deng, Z. Chua, D. S. Bohle, C.-J. Li, *Adv. Synth. Catal.* **2010**, *352*, 632-636.

[80] T. Mizuhara, S. Inuki, S. Oishi, N. Fujii, H. Ohno, *Chem. Commun.* **2009**, 3413-3415.

[81] A. John, K. M. Nicholas, *J. Org. Chem.* **2011**, *76*, 4158-4162.

[82] L. Chu, X. Yue, F.-L. Qing, *Org. Lett.* **2010**, *12*, 1644-1647.

[83] L.-F. Chen, X.-Y. Cao, Z.-J. Li, J.-K. Cheng, Q.-P. Lin, Y.-G. Yao, *Inorg. Chem. Commun.* **2008**, *11*, 961-964.

[84] Yao and coworkers propose a similar mechanism to the work of Yu and coworkers - single electron transfer from the pyrazolecarboxylate ring to carboxylate-coordinated Cu^{II}, after which nucleophilic attack on the cation-radical intermediate by halide followed by H-abstraction yields the halogenated product. In this case no mechanistic studies of the system were carried out.

[85] S. Ueda, H. Nagasawa, *J. Org. Chem.* **2009**, *74*, 4272-4277.

[86] a) M. M. Guru, M. A. Ali, T. Punniyamurthy, *Org. Lett.* **2011**, *13*, 1194-1197; see also: b) M. M. Guru, M. A. Ali, T. Punniyamurthy, *J. Org. Chem.* **2011**, *76*, 5295-5308.

[87] S. Ueda, H. Nagasawa, *J. Am. Chem. Soc.* **2009**, *131*, 15080-15081.

[88] H.-F. He, Z.-J. Wang, W. Bao, *Adv. Synth. Catal.* **2010**, *352*, 2905-2912.

[89] L. Zhang, G. Y. Ang, S. Chiba, *Org. Lett.* **2010**, *12*, 3682-3685.

[90] H. Wang, Y. Wang, C. Peng, J. Zhang, Q. Zhu, *J. Am. Chem. Soc.* **2010**, *132*, 13217-13219.

[91] Under these iron-free conditions, the authors suggest that the reaction mechanism is likely electrophilic aromatic substitution. Mechanistic studies indicate a primary H/D kinetic isotope effect of 2.4 when Fe^{III} is present, suggesting that C–H bond cleavage is rate-limiting under these conditions. The authors theorize that the presence of Fe^{III} is necessary to generate the electrophilic Cu^{III} reactive species, which they suggest supports an electrophilic activation mechanism by copper, rather than an electron transfer mechanism.

[92] H. Wang, Y. Wang, D. Liang, L. Liu, J. Zhang, Q, Zhu, *Angew. Chem. Int. Ed.* **2011**, *50*, 5678-5681.

[93] B.-X. Tang, R.-J. Song, C.-Y. Wu, Y. Liu, M.-B. Zhou, W.-T. Wei, G.-B. Deng, D.-L. Yin, J.-H. Li, *J. Am. Chem. Soc.* **2010**, *132*, 8900-8902.

[94] L. I. Peterson, E. C. Britton, *Tetrahedron Lett.* **1968**, *9*, 5357-5360.

[95] For example, the formation of amides has been accomplished by Cu-catalyzed amidation of terminal alkynes with tosylazide, followed by in-situ hydrolysis of the product: S. H. Cho, E. J. Yoo, I. Bae, S. Chang *J. Am. Chem. Soc.*, **2005**, *127*, 16046–16047.

[96] C. Zhang, N. Jiao, *J. Am. Chem. Soc.* **2010**, *132*, 28-29.

[97] A full report on the copper-catalyzed, aerobic oxidative coupling of anilines to yield diazenes has since been reported: C. Zhang, N. Jiao, *Angew. Chem.* **2010**, *122*, 6310-6313; *Angew. Chem. Int. Ed.* **2010**, *49*, 6174-6177.

[98] Y. Gao, G. Wang, L. Chen, P. Xu, Y. Zhao, Y. Zhou, L.-B. Han, *J. Am. Chem. Soc.* **2009**, *131*, 7956-7957.

[99] M. Niu, H. Fu, Y. Jiang, Y. Zhao, *Chem. Commun.* **2007**, 272-274. See also: b) L.-B. Han, M. Tanaka, *J. Am. Chem. Soc.* **1996**, *118*, 1571-1572; c) L.-B. Han, Y. Ono, S. Shimada, *J. Am. Chem. Soc.* **2008**, *130*, 2752-2753.

[100] L. Chu, F.-L. Qing, *J. Am. Chem. Soc.* **2010**, *132*, 7262-7263.

[101] For two recent highlights describing this reactivity, see: a) A. Armstrong, J. C. Collins, *Angew. Chem.* **2010**, *122*, 2332-2335; *Angew. Chem. Int. Ed.* **2010**, *49*, 2282-2285; b) C. A. de Parrodi, P. J. Walsh, *Angew. Chem.* **2009**, *121*, 4773-4776; *Angew. Chem. Int. Ed.* **2009**, *48*, 4679-4682.

[102] D. Monguchi, T. Fujiwara, H. Furukawa, A. Mori, *Org. Lett.* **2009**, *11*, 1607-1610.

[103] Q. Wang, S. L. Schreiber, *Org. Lett.* **2009**, *11*, 5178-5180.

[104] H. Zhao, M. Wang, W. Su, M. Hong, *Adv. Synth. Catal.* **2010**, *352*, 1301-1306.

[105] M. Miyasaka, K. Hirano, T. Satoh, R. Kowalczyk, C. Bolm, M. Miura, *Org. Lett.* **2010**, *13*, 359-361.

[106] S.-I. Fukuzawa, E. Shimizu, Y. Atsuumi, M. Haga, K. Ogata, *Tetrahedron Lett.* **2009**, *50*, 2374-2376.

[107] S. Guo, B. Qian, Y. Xie, C. Xia, H. Huang, *Org. Lett.* **2010**, *13*, 522-525.

[108] Liu reports the copper-mediated decarboxylative cross-coupling of perfluorinated benzoates with aryl iodides yielding hetero-coupled biaryls: R. Shang, Y. Fu, Y. Wang, Q. Xu, H.-Z. Yu, L. Liu, *Angew. Chem.* **2009**, *121*, 9514-9518; *Angew. Chem. Int. Ed.* **2009**, *48*, 9350-9354.

[109] Y. Li, J. Jin, W. Qian, W. Bao, *Org. Biomol. Chem.* **2010**, *8*, 326-330.

[110] Y. Wei, H. Zhao, J. Kan, W. Su, M. Hong, *J. Am. Chem. Soc.* **2010**, *132*, 2522-2523.

[111] M. Kitahara, K. Hirano, H. Tsurugi, T. Satoh, M. Miura, *Chem.-Eur. J.* **2010**, *16*, 1772-1775.

[112] N. Matsuyama, M. Kitahara, K. Hirano, T. Satoh, M. Miura, *Org. Lett.* **2010**, *12*, 2358-2361.

[113] E. Nakamura, S. Mori, *Angew. Chem*. **2000**, *112*, 3902-3924; *Angew. Chem. Int. Ed.* **2000**, *39*, 3750-3771.

[114] a) S. V. Ley, A. W. Thomas, *Angew. Chem.* **2003**, *115*, 5558-5607; *Angew. Chem. Int Ed.* **2003**, *42*, 5400-5449; b) I. P. Beletskaya, A. V. Cheprakov, *Coord. Chem. Rev.* **2004**, *248*, 2337-2364; c) F. Monnier, M. Taillefer *Angew. Chem.* **2009***, 121,* 7088-7105*; Angew. Chem. Int. Ed.* **2009**, *48*, 6954 – 6971; d) D. S. Surry, S. L. Buchwald *Chem. Sci.* **2010**, *1*, 13-31.

[115] a) S. H. Bertz, S. Cope, M. Murphy, C. A. Ogle, B. J. Taylor, *J. Am. Chem. Soc.* **2007**, *129*, 7208-7209; b) S. H. Bertz, S. Cope, D. Dorton, M. Murphy, C. A. Ogle, *Angew Chem.* **2007**, *37*, 7212-7215; *Angew. Chem. Int. Ed.* **2007**, *46*, 7082-7085.

[116] See also: H. P. Hu, J. P. Snyder, *J. Am. Chem. Soc.* **2007**, *129*, 7210-7211.

[117] T. Gaertner, W. Henze, R. M. Gschwind, *J. Am. Chem. Soc.* **2007**, *129*, 11362-11363.

[118] a) E. R. Bartholomew, S. H. Bertz, S. Cope, D. C. Dorton, M. Murphy, C. A. Ogle, *Chem Commun.* **2008**, 1176-1177; b) E. R. Bartholomew, S. H. Bertz, S. Cope, M. Murphy, C. A. Ogle, *J. Am. Chem. Soc.* **2008**, *130*, 11244-11245; c) E. R. Bartholomew, S. H, Bertz, S. K. Cope, M. D. Murphy, C. A. Ogle, A. A. Thomas, *Chem. Commun.* **2010**, *46*, 1253-1254; d) S. H. Bertz, M. D. Murphy, C. A. Ogle, A. A. Thomas, *Chem Commun.* **2010**, *46*, 1255-1256.

[119] For additional leading references, see: a) T. Cohen, J. Wood, A. G. Dietz Jr., *Tetrahedron Lett.* **1974**, *15*, 3555-3558; b) A. J. Paine, *J. Am. Chem. Soc.* **1987**, *109*, 1496-1502; c) E. R. Strieter, B. Bhayana, S. L. Buchwald, *J. Am. Chem. Soc.* **2008**, *131*, 78-88; d) J. W. Tye, Z. Weng, A. M. Johns, C. D. Incarvito, J. F. Hartwig, *J. Am. Chem. Soc.* **2008**, *130*, 9971-9983.

[120] G. O. Jones, P. Liu, K. N. Houk, S. L. Buchwald, *J. Am. Chem. Soc.* **2010**, *132*, 6205-6213.

[121] H.-Z. Yu, Y.-Y. Jiang, Y. Fu, L. Liu, *J. Am. Chem. Soc.* **2010**, *132*, 18078-18091.

[122] A. Casitas, A. E. King, T. Parella, M. Costas, S. S. Stahl, X. Ribas, *Chem. Sci.* **2010**, 326-330.

[123] M. Zhang, *Appl. Organomet. Chem.* **2010**, *24*, 269-284.

[124] X. Ribas, R. Xifra, T. Parella, A. Poater, M. Solà, A. Llobet, *Angew. Chem.* **2006**, *118*, 3007-3010; *Angew. Chem. Int Ed.* **2006**, *45*, 2941-2944.

[125] a) T. B. Gunnoe *Eur. J. Inorg. Chem.* **2007**, 1185–1203. b) S. Usui, Y. Hashimoto, J. V. Morey, A. E. H. Wheatley, M. Uchiyama, *J. Am. Chem. Soc.*, **2007**, *129*, 15102–15103.

[126] For example, direct arylation of C–H bonds with aryl halides are believed to be initiated by metalation of the C–H bond at Cu^{I}: a) I. Popov, S. Lindeman, O. Daugulis, *J. Am.*

Chem. Soc. **2011**, 133, 9286-9289; b) H.-Q. Do, O. Daugulis, *J. Am. Chem. Soc.* **2008**, *130*, 1128-1129; c) H.-Q. Do, R. M. K. Kahn, O. Daugulis, *J. Am. Chem. Soc.* **2008**, *130*, 15185-15192; d) H.-Q. Do, O. Daugulis, J. Am. Chem. Soc. **2007**, *129*, 12404-12405.

[127] In the presence of hypervalent iodine reagents, C–H activation by Cu^{III} has been proposed. See, for example: a) R. J. Phipps, N. P. Grimster, M. J. Gaunt, *J. Am. Chem. Soc.* **2008**, *130*, 8172-8174; b) R. J. Phipps, M. J. Gaunt, *Science*, **2009**, *323*, 1593-1597; c) S. H. Cho, J. Yoon, S. Chang, *J. Am. Chem. Soc.* **2011**, *133*, 5996-6005; d) B. Chen, X.-L. Hou, Y.-X. Li, Y.-D. Wu, *J. Am. Chem. Soc.* **2011**, *133*, 7668-7671.

[128] M. A. Willert-Porada, D. J. Burton, N. C. Baenziger, *J. Chem. Soc. Chem. Commun.* **1989**, 1633-1634.

[129] D. Naumann, T. Roy, K.-F. Tebbe, W. Crump, *Angew. Chem.* **1993**, *105*, 1555-1556; *Angew. Chem. Int. Ed. Engl.* **1993**, *32*, 1482-1483.

[130] a) P. J. Chmielewski, L. Latos-Grażyński, I. Schmidt, *Inorg. Chem.* **2000**, *39*, 5475-5482; b) M. Pawlicki, I. Kańska, L. Latos-Grażyński, *Inorg. Chem.* **2007**, *46*, 6575-6584; c) N. Grzegorzek, M. Pawlicki, L. Szterenberg, L. Latos-Grażyński, *J. Am. Chem. Soc.* **2009**, *131*, 7224-7225.

[131] a) H. Furuta, H. Maeda, A. Osuka, *J. Am. Chem. Soc.* **2000**, *122*, 803-807; b) H. Furuta, T. Ishizuka, A. Osuka, Y. Uwatoko, Y. Ishikawa, *Angew. Chem.* **2001**, *113*, 2385-2387; *Angew. Chem. Int. Ed.* **2001**, *40*, 2323-2325; c) H. Furuta, H. Maeda, A. Osuka, *Org. Lett.* **2002**, *4*, 181-184; d) H. Maeda, A. Osuka, Y. Ishikawa, I. Aritome, Y. Hisaeda, H. Furuta, *Org. Lett.* **2003**, *5*, 1293-1296; e) H. Maeda, Y. Ishikawa, T. Matsuda, A. Osuka, H. Furuta, *J. Am. Chem. Soc.* **2003**, *125*, 11822-11823; f) H. Maeda, A. Osuka, H. Furuta, *J. Am. Chem. Soc.* **2003**, *125*, 15690-15691.

[132] a) X. Ribas, D. A. Jackson, B. Donnadieu, J. Mahía, T. Parella, R. Xifra, B. Hedman, K. O. Hodgson, A. Llobet, T. D. P. Stack, *Angew. Chem.* **2002**, *114*, 3117-3120; *Angew. Chem. Int. Ed.* **2002**, *41*, 2991-2994; b) R. Xifra, X. Ribas, A. Llobet, A. Poater, M. Duran, M. Solà, T. D. P Stack, J. Benet-Buchholz, B. Donnadieu, J. Mahía, T. Parella, *Chem.–Eur. J.* **2005**, *11*, 5146-5156.

[133] a) I. Kinoshita, L. J. Wright, S. Kubo, K. Kimura, A. Sakata, T. Yano, R. Miyamoto, T. Nishioka, K. Isobe, *Dalton Trans.* **2003**, 1993-2003; b) R. Santo, R. Miyamoto, R. Tanaka, T. Nishioka, K. Sato, K. Toyota, M. Obata, S. Yano, I. Kinoshita, A. Ichimura, T. Takui, *Angew. Chem.* **2006**, *118*, 7773-7776; *Angew. Chem. Int. Ed.* **2006**, *45*, 7611-7614.

[134] B. Yao, D.-X. Wang, Z.-T. Huang, M.-X. Wang, *Chem. Commun.* **2009**, 2899-2901.

[135] Similar reactivity had been reported a year earlier by Latos-Grażyński and coworkers, although the resulting organocopper(II) complex was not crystallographically characterized. See ref. 130a.

[136] X. Ribas, C. Calle, A. Poater, A. Casitas, L. Gómez, R. Xifra, T. Parella, J. Benet-Buchholz, A. Schweiger, G. Mitrikas, M. Solà, A. Llobet, T. D. P. Stack, *J. Am. Chem. Soc.* **2010**, *132*, 12299-12306.

[137] L. M. Huffman, S. S. Stahl, *J. Am. Chem. Soc.* **2008**, *130*, 9196-9197.

[138] L. M. Huffman, A. Casitas, M. Font, M. Canta, M. Costas, X. Ribas, S. S. Stahl, *Chem., Eur. J.* **2011**, *17*, 10643-10650.

[139] a) L. M. Huffman, S. S. Stahl, *Dalton Trans.* **2011**, *40*, 8959-8963; b) A. Casitas, N. Ioannidis, G. Mitrikas, M. Costas, X. Ribas, *Dalton Trans*. **2011**, 40, 8796-8799.

[140] A. E. King, L. M. Huffman, A. Casitas, M. Costas, X. Ribas, S. S. Stahl, *J. Am. Chem. Soc.* **2010**, *132*, 12068-12073.

[141] In addition to the C–H oxidation reactions proposed here, aryl-Cu^{III} intermediates have been implicated in Cu^{II}-catalyzed oxidative coupling reactions of boronic acids and heteroatom nucleophiles ("Chan-Lam reactions"). For a recent review and mechanistic study of these reactions, see: a) J. X. Qiao, P. Y. S. Lam, *Synthesis* **2011**, *2011*, 829-856; b) A. E. King, T. C. Brunold, S. S. Stahl, *J. Am. Chem. Soc.* **2009**, *131*, 5044-5045.

Chapter 6

Copper(II)-Mediated Oxidative Cyclization of Enamides to Oxazoles

This work has been published:

Wendlandt, A. E.; Stahl, S. S. *Org. Biomol. Chem.* **2012**, *10*, 3866-3870.

6.1. Introduction

Copper(II)-mediated C–H oxidation reactions have been the focus of extensive attention in recent years.[1,2] Many applications of these reactions are oxidative cyclizations involving heterofunctionalization of arene C–H bonds.[3] Two early examples, reported by the groups of Buchwald[3a] and Nagasawa,[3b,c] feature copper-catalyzed oxidative cyclization of substituted benzamidines and benzanilides to benzimidazoles (Eqn 6.1) and benzoxazoles (Eqn 6.2), respectively. In connection with our broader interest in the oxidative functionalization of alkenes,[4] we wondered whether analogous C–H oxidation reactions could be achieved with enamides (Eqn 6.3). Here, we present a method for the synthesis of 2,5-disubstituted oxazoles via sequential anti-Markovnikov hydroamidation of terminal alkynes, followed by Cu-mediated cyclization of the resulting enamides.

Buchwald et al.

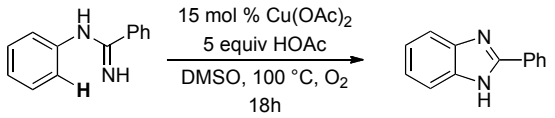

(6.1)

Nagasawa et al.

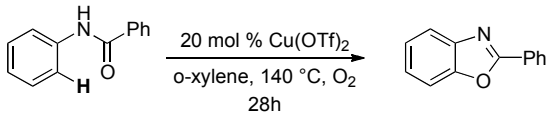

(6.2)

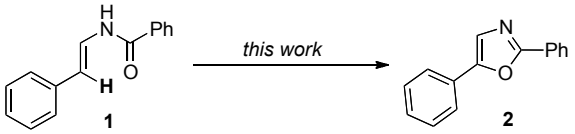

(6.3)

Oxazoles are an important class of heterocycles that are ubiquitous in biologically active molecules, including pharmaceuticals and natural products.[5] Annulation methods are among numerous approaches used in the preparation of substituted oxazoles. Recent examples include multicomponent coupling reactions,[6] intramolecular additions to alkynes,[7] and oxidative and

non-oxidative condensation and substitution reactions.[8] Several methods are particularly relevant to the work described here. Yoshimura and coworkers[8a] developed a heterocyclization method involving base-mediated *O*-vinylation via *O*-addition/HBr-elimination of *β*-bromoenamides. A similar method was later implemented by Pattenden et al.[8b] Glorius and coworkers have reported a method for copper-catalyzed coupling of primary amides with 1,2-dihalogenated olefins, which affords mixtures of 2,4- and 2,5-disubstituted oxazoles.[8c] Buchwald et al. have developed a two-step, one-pot method for copper-catalyzed cross-coupling of vinyl halides with primary amides, followed by intramolecular *O*-vinylation via iodine-mediated *O*-addition to the alkene and elimination of HI.[8d]

Each of the methods just noted requires access to vinyl halide precursors. We envisioned a complementary route to oxazoles originating from readily available terminal alkynes and primary amides (Scheme 6.1). This strategy draws upon recent work of Gooβen and coworkers, who have shown that enamides may be accessed efficiently via Ru-catalyzed anti-Markovnikov hydroamidation of alkynes.[9]

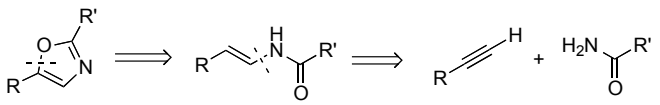

Scheme 6.1. Retrosynthetic strategy for the synthesis of oxazoles.

6.1. Results and Discussion

Our efforts to develop Cu-mediated methods for oxidative cyclization of enamides were initiated with *N*-[(*E*)-2-phenylethenyl]benzamide **1** as the substrate. Use of the catalytic conditions reported previously for oxidative cyclization of aromatic substrates (Eqns 1 and 2) were not successful with **1**. These conditions led to complete consumption of **1**, but only trace quantities of the desired 2,5-diphenyloxazole product **2** (see Supplementary Information, Table

6.3). Subsequent efforts to identify alternative conditions compatible with the use of catalytic quantities of Cu were similarly unsuccessful (see Supp. Info.). Measurable yields of the desired product **2** were obtained, however, by using stoichiometric $CuCl_2$ in toluene (Table 6.1, entry 1). Further screening of reaction conditions revealed that higher product yields could be obtained with dioxane as the solvent. Addition of various amine bases significantly improved the reaction outcome (Table 6.1, entries 2-6), and imidazole was the optimal base in the initial experiments (31% yield, entry 6). The amine bases appear to serve as ligands for Cu^{II}, evidenced by significant color changes and improved Cu solubility upon their addition to the reaction mixture. Use of chelating ligands, such as 2,2'-bipyridine and 1,10-phenanthroline, led to lower yields of **2** relative to reactions with imidazole (Table 6.3). Whereas a Cu:base stoichiometry of 4:1 was optimal for some bases (e.g., DMAP; see ESI) the best results with imidazole were obtained with a 1:1 Cu:base stoichiometry (59%, entry 7). Screening of alternate Cu sources [e.g., $Cu(OAc)_2$, $Cu(OTf)_2$] failed to improve the yield (entries 8 and 9). Subsequent screening showed that replacement of imidazole with N-methylimidazole, NMI (Cu:NMI = 1:1) led to the highest observed yield of **2** (67%, entry 10).

Efforts to lower the Cu loading and achieve catalytic turnover were not successful, despite the use of aerobic (ambient air) conditions in these reactions (entries 11 and 12). Nevertheless, the use of an air atmosphere is beneficial to the reaction. The product yield diminished to 54% when the reaction was performed under anaerobic (N_2) conditions, and the use of pure O_2 (1 atm) also led to a lower yield (50%). The latter result correlates with an increase in the formation of unidentified side-products in the reaction.

Table 6.1 Optimization of copper-mediated annulation of enamides.[a]

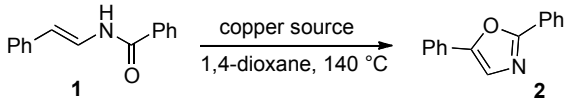

Entry	Copper Source	Additive	Yield[b]
1	2.0 equiv $CuCl_2$	------	8%[c]
2	2.0 equiv $CuCl_2$	0.5 equiv pyridine	23%
3	2.0 equiv $CuCl_2$	0.5 equiv Et_3N	26%
4	2.0 equiv $CuCl_2$	0.5 equiv DMAP[d]	22%
5	2.0 equiv $CuCl_2$	0.5 equiv DBU[e]	24%
6	2.0 equiv $CuCl_2$	0.5 equiv imidazole	31%
7	2.0 equiv $CuCl_2$	2.0 equiv Imidazole	59%
8	2.0 equiv $Cu(OAc)_2$	2.0 equiv Imidazole	6.8%
9	2.0 equiv $Cu(OTf)_2$	2.0 equiv Imidazole	10%
10	**2.0 equiv $CuCl_2$**	**2.0 equiv NMI[f]**	**67% (74%)[g]**
11	1.0 equiv $CuCl_2$	1.0 equiv NMI	56%
12	0.5 equiv $CuCl_2$	0.5 equiv NMI	40%

[a] Reaction conditions: reactions were run on 0.05 mmol scale, at 0.1 M in a sealed vessel at 140 °C under air. [b] GC yield. [c] In toluene. [d] 4-Dimethyl-aminopyridine. [e] 1,8-Diazabicyclo[5.4.0]undec-7-ene. [f] N-methylimidazole. [g] NMR yield, 0.2 mmol scale.

The optimized conditions were employed with a number of different substrates to explore the reaction scope (Table 6.2). The Ru-catalyzed hydroamidation protocol of Gooβen et al. enabled efficient access to diverse secondary enamide substrates.[9a,10] The enamides obtained from this method are obtained initially with (*Z*)-alkene stereochemistry, but *(E)*-enamides may be obtained by Et_3N-promoted isomerization of the crude hydroamidation product at elevated temperatures. The geometry of the starting enamide did not influence the outcome of the oxidative cyclization reactions; both *(Z)*- and *(E)*-**1** afforded the oxazole **2** in the same yield (78% and 74%, respectively; Table 6.1, entry 10 and Eqn 6.4). A control experiment showed that (*Z*)-**1** isomerizes to *(E)*-**1** in the absence of $CuCl_2$ under the cyclization conditions.

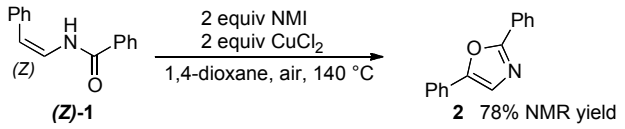

(6.4)

Substrates were varied at both the amide- or alkyne-derived portion of the molecule. In general, good yields were obtained with substrates bearing aromatic substituents, particularly electron-rich groups (Table 6.2, entries 1–6 and 8–10). A modest reduction in yield was observed for substrates bearing electron-deficient aromatic substituents (entries 5 and 8). Poor yields were obtained with substrates derived from alkyl-substituted amides. For example, the pivalamide derivative (entry 7) led to only 29% yield of the oxazole, and no desired product was obtained with the corresponding *i*Pr derivative (not shown). In contrast, a *β*-*n*Bu-enamide derived from 1-hexyne underwent cyclization in moderate yield (58%, entry 12).

The *β*-cyclohexyl enamide **3** underwent cyclization to the desired oxazole **4** in 38% yield (Eqn 6.5); however, a significant amount of the vinylic chlorination product **5** was observed as a side product (41% yield). Vinylic chlorination is not a significant side-reaction with the other substrates in Table 6.2. Chlorination of the *β* C–H bond of **3** resembles $CuCl_2$-mediated chlorination of electron-rich arene C–H bonds, which are believed to be initiated by single-electron transfer from the arene to Cu^{II}.[1b,11] By analogy, we speculate that the present reactions involve initial Cu^{II}-mediated one-electron oxidation of enamide. Addition of the amide oxygen to the radical-cation intermediate, followed by loss of two protons and another electron, affords the oxazole product (Scheme 6.2). This mechanism seems more plausible than an organometallic pathway involving directed C–H activation.[12] Single-electron-transfer mechanisms have also been proposed in another Cu^{II}-mediated arene annulation reaction.[3e]

Table 6.2 Substrate scope of copper-mediated annulation of enamides.[a]

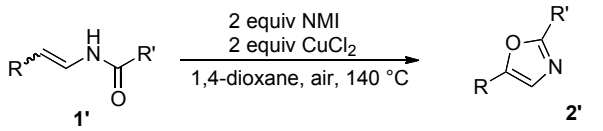

Entry	Product		Yield[b]
1	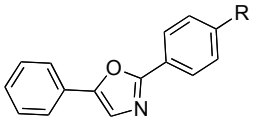	R = H	67%[c]
2		R = OMe	74%[c]
3	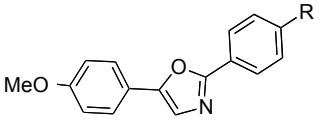	R = H	72%
4		R = OMe	69%
5		R = NO_2	49%
6	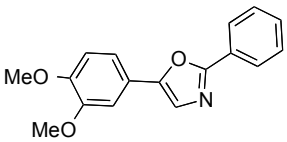		67%
7	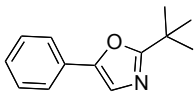		29%
8	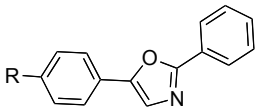	R = Cl	57% (52%)[d]
9		R = Me	69%
10		R = *t*Bu	73%
11	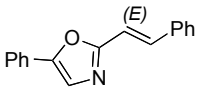		38%
12	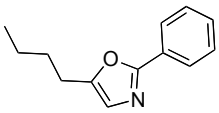		58%

[a] Reaction conditions: 0.4 mmol enamide, 0.8 mmol $CuCl_2$, and 0.8 mmol NMI in 0.1 M 1,4-dioxane in a sealed tube under air for 20 h at 140 °C. [b] Isolated yield. [c] Average of two runs. [d] 0.9 mmol enamide, 1.8 mmol $CuCl_2$, and 1.8 mmol NMI in a sealed tube under air for 20 h at 140 °C.

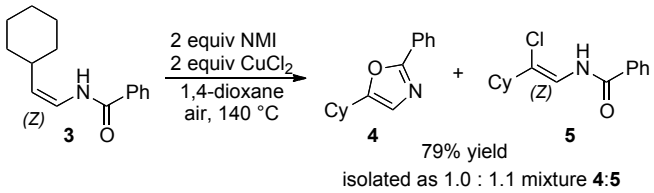

(6.5)

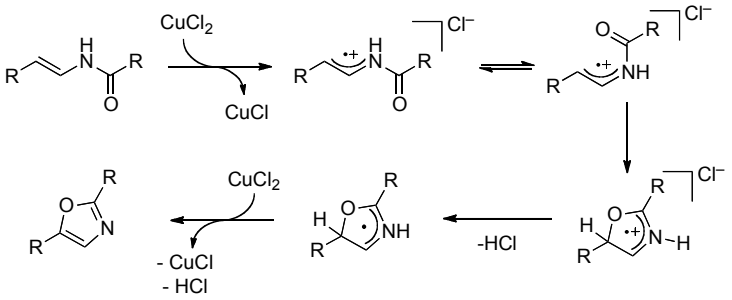

Scheme 6.2 Proposed mechanism for oxazole synthesis.

In summary, we have developed an efficient route for the preparation of 2,5-disubstituted oxazoles from simple alkyne and amide precursors. These methods, based on oxidative cyclization of enamides, complement the growing collection of Cu^{II}-based methods for heterofunctionalization of C–H bonds.

6.3 Acknowledgements

We thank the U.S. Department of Energy (DE-FG02-05ER15690) for financial support of this work. Analytical instrumentation was partially funded by the NSF (CHE-9208463, CHE-0342998, CHE-9629688, CHE-9974839).

6.4 Experimental Details and Supplementary Information

6.4.1 General Considerations

All commercially available compounds were purchased from Sigma-Aldrich, and used as received unless otherwise indicated. Solvents were dried over alumina columns prior to use; anhydrous 1,4-dioxane was used as received. ^{1}H and ^{13}C NMR spectra were recorded on Bruker AC-300 MHz or Varian Mercury-300 MHz spectrometers. Chemical shift values are given in parts per million relative to residual solvent peaks or TMS internal standard. Exact mass

measurements were obtained by the mass spectrometry facility at the University of Wisconsin. Melting points were taken on a Mel-Temp II melting point apparatus. Gas Chromatography was done on a Shimadzu GC-17A using Shimadzu RTX-5MS (15m) column and referenced to an internal standard (trimethoxybenzene). Flash chromatography was performed using SilicaFlash® P60 (Silicycle, particle size 40-63 μm, 230-400 mesh) from Sigma Aldrich.

6.4.2 Procedure for Reaction Screening

Reaction screening was carried out as follows. Under ambient air, a 1.5 dr vial containing a flea stirbar was loaded with 10 mg (0.045 mmol) of *N*-[(*E*)-2-phenylethenyl]benzamide, **1**, followed by the addition of 12.1 mg (0.09 mmol) of anhydrous $CuCl_2$. Anhydrous 1,4-dioxane was added (0.5 mL), followed by 7.2 uL of *N*-methylimidazole. The vial was sealed firmly with a Teflon cap, and a dark blue coloration was observed. (If N_2 or O_2 atmosphere was desired the vial was equipped at this point with a septum, and flushed for 5-7minutes with dry O_2 or N_2 before being sealed with a Teflon cap. The vial(s) were then clamped in an oil bath already stabilized at 140 °C, and heated with gentle stirring for 20 h (although timecourse studies indicate that reaction is 90% complete after around 6 hrs). Within 5 minutes of heating, the reaction had turned from dark blue to green. By the end of the reaction vials contained a clear to pale yellow solution with a black residue at the bottom. Vials were removed from heat and allowed to cool. Samples were diluted with 3 mL EtOAc, and 1 mL of internal standard stock solution (1,3,5-trimethoxybenzene in EtOAc) was added. Approximately 0.5 to 1.0 mL of saturated Na_2S solution was then added and the vial was shaken vigorously to precipitate out CuS salts. An aliquot of the organic phase was then filtered through celite and analyzed by Gas Chromatography. Yields were determined by comparision with internal standard, with retention factor corrections previously ascertained though calibration curves.

6.4.3. Additional Screening Data

Table 6.3. Additional Screening Data for Enamide Cyclization to Oxazoles.

Table S1. Additional Screening Data[a]

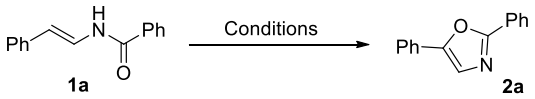

Entry	Cu Source	Solvent	Additive	Temp	% yield[b]
1.	15% $Cu(OAc)_2$	DMSO	5eq AcOH	100C	<1 %
2.	20% $Cu(OTf)_2$	o-xylene	-----	140C	<1 %
3.	20% $Cu(OTf)_2$	toluene	-----	140C	<1 %
4.	20% $Cu(OAc)_2$	toluene	-----	140C	1.7%
5.	20% $Cu(OAc)_2$	toluene	2.0 eq pyridine	140C	<1 %
6.	20% $Cu(OAc)_2$	toluene	2.0 eq NaOAc	140C	<1 %
7.	20% $Cu(OAc)_2$	toluene	5.0 eq AcOH	140C	<1 %
8.	200% $Cu(OAc)_2$	toluene	-----	140C	5.8 %
9.	200% $CuCl_2$	toluene	-----	140C	7.9 %
10.	200% $CuCl_2$	toluene	3.0 eq $NaHCO_3$	140C	7.9%
11.	200% $CuCl_2$	toluene	3.0 eq Na_2CO_3	140C	4.1%
12.	200% $CuCl_2$	toluene	3.0 eq K_2CO_3	140C	5.1%
13.	200% $CuCl_2$	toluene	3.0 eq Cs_2CO_3	140C	2.5%
14.	200% $CuCl_2$	toluene	3.0 eq NaOAc	140C	9.4%
15.	200% $CuCl_2$	toluene	0.8 eq pyridine	140C	14.4%
16.	200% $CuCl_2$	toluene	0.8 eq imidazole	140C	19.2%
17.	200% $CuCl_2$	toluene	0.8 eq DBU[c]	140C	17.8%
18.	200% $CuCl_2$	toluene	0.8 eq DABCO[d]	140C	2.3%
19.	200% $CuCl_2$	toluene	0.8 eq pyrrolidine	140C	18.6%
20.	200% $CuCl_2$	toluene	0.8 eq bipy	140C	3.5%
21.	200% $CuCl_2$	toluene	0.8 eq phen	140C	1.9%
22.	200% $CuCl_2$	toluene	0.4 eq bipy	140C	3.9%
23.	200% $CuCl_2$	toluene	0.4 eq phen	140C	5.0%
24.	200% $CuCl_2$	toluene	0.3 eq DMAP	140C	16.3%
25.	200% $CuCl_2$	toluene	0.5 eq DMAP	140C	19.1%
26.	200% $CuCl_2$	toluene	0.8 eq DMAP	140C	15.4%
27.	200% $CuCl_2$	toluene	1.0 eq DMAP	140C	13.9%
28.	200% $CuCl_2$	toluene	2.0 eq DMAP	140C	6.4%
29.	200% $CuCl_2$	1,4-dioxane	0.5 eq DMAP	140C	23.7%
30.	200% $CuCl_2$	1,4-dioxane	0.5 eq imidazole	140C	31%
31.	200% $CuCl_2$	1,4-dioxane	2 eq imidazole	140C	57.4%
32.	100% $CuCl_2$	1,4-dioxane	2 eq imidazole	140C	1.7%
33.	100% $CuCl_2$	1,4-dioxane	1 eq imidazole	140C	53.8%
34.	50% $CuCl_2$	1,4-dioxane	2 eq imidazole	140C	2.3%
35.	50% $CuCl_2$	1,4-dioxane	0.5 eq imidazole	140C	39.4%

[a] Reaction Conditions: reactions were run on 0.05mmol scale, at 0.1M in a sealed vessel at 140 C under air unless otherwise specified. [b] GC Yield. [c] 1,8-Diazabicyclo[5.4.0]undec-7-ene. [d] DABCO.

6.4.4. Substrate Synthesis

All enamides substrates were prepared using the procedure developed by Gooβen et al.[9a] Characterization data for substrates not reported therein are included below. Though not noted in their initial report, we found that trace carboxylic acid impurities in the amide substrates poisoned the catalyst; an additional base wash (10 % Na_2CO_3) was utilized on commercial amides containing these impurities. $Ru(mta)_2cod$ is commercially available, but was prepared from $RuCl_3$ according to the procedure of Genet et al.[13] An alternative, metal-free preparation of *N*-[(*E*)-2-phenylethenyl]benzamide, **1**, was adapted from Katritzky and coworkers.[14]

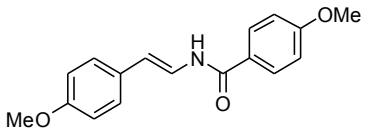

4-methoxy-N-[(E)-2-(4-methoxyphenyl)ethenyl]benzamide

Isolated as a cream-colored solid, mp = 200-203 °C. ^{1}H NMR (300 MHz, DMSO-d_6): δ 10.37 (d, NH, 9.9 Hz), 7.95 (d, 2H, J = 8.7 Hz), 7.49 (dd, 1H, J = 14.4, 9.6 Hz), 7.30 (d, 2H, J= 8.7 Hz), 7.05 (d, 2H, J = 8.7 Hz), 6.88 (d, 2H, J = 8.8 Hz), 6.37 (d, 1H, J =14.7Hz), 3.83 (s, 3H), 3.74 (s, 3H); ^{13}C NMR (75 MHz, DMSO-d_6): δ 163.93, 162.73, 158.58, 130.18, 129.87, 127.01, 126.25, 123.22, 114.91, 114.37, 112.81, 56.11, 55.75; EMM (ESI) *m/z* calcd for $C_{17}H_{17}NO_3$ $[M+H]^+$: 284.1282, meas: 284.1288.

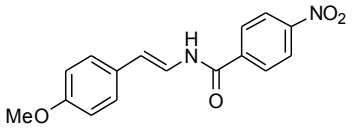

N-[(E)-2-(4-methoxyphenyl)ethenyl]-4-nitrobenzamide

Isolated as a yellow solid, decomposition to red oil at 217 °C. ^{1}H NMR (300 MHz, DMSO-d_6): δ 10.83 (d, NH, 9.3 Hz), 8.37 (dt, 2H**,** J=6.9, 2.1 Hz), 8.20 (dt, 2H, J = 9.0, 2.1 Hz), 7.50 (dd, 1H, 14.4, 9.3 Hz), 7.36 (d, 2H, J = 6.6 Hz), 6.90 (d, 2H, J = 6.9 Hz), 6.47 (d, 1H, J = 14.7 Hz); ^{13}C NMR (75 MHz, DMSO-d_6): δ 162.81, 158.89, 149.93, 139.74, 129.74, 129.35, 127.34, 124.31, 122.60, 114.94, 114.77, 55.77; EMM (ESI) *m/z* calcd for $C_{16}H_{14}N_2O_4$ $[M]^+$: 298.0949, meas: 298.0953.

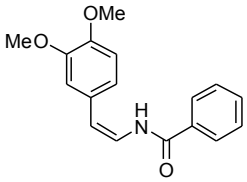

N-[(Z)-2-(3,4-dimethoxyphenyl)ethenyl]benzamide

Isolated as a white solid, mp 132-133 °C. ^{1}H NMR (300 MHz, DMSO- d_6): δ 9.94 (d, NH, J = 9.3 Hz), 7.95 (m, 2H), 7.58 (t, 1H, J = 7.2 Hz), 7.50 (t, 2H, J = 7.5 Hz), 7.09 (d, 1H, J = 1.5 Hz), 7.03 (dd, 1H, J = 8.4, 1.5 Hz), 6.97 (d, 1H, J = 8.4 Hz), 6.85 (t, 1H, J = 9.6 Hz), 5.81 (d, 1H, J = 9.9 Hz), 3.79 (s, 3H), 3.77 (s, 3H); ^{13}C NMR (75 MHz, DMSO-d_6): δ 165.81, 149.24, 148.38, 134.19, 132.44, 129.21, 129.04, 128.43, 122.05, 121.72, 113.72, 112.76, 112.62, 56.22, 55.99; EMM (ESI): *m/z* calcd for $C_{17}H_{17}NO_3$ $[M]^+$: 283.1203, meas 283.1212.

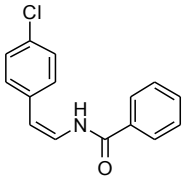

N-[(Z)-2-(4-chlorophenyl)ethenyl]benzamide

Isolated as a white solid, Mp = 131-133°C; ^{1}H NMR (300 MHz, DMSO-d_6): δ 10.05 (d, NH, J = 9.3 Hz), 7.91 (d, 2H, J = 6.9 Hz), 7.38-7.59 (m, 6H), 6.94 (t, 1H, J = 9.6 Hz), 5.75 (d, 1H, J = 9.6

Hz); ^{13}C NMR (75 MHz, DMSO-d^6): δ 166.15, 135.42, 134.06, 132.55, 131.48, 130.85, 129.12, 129.02, 128.61, 124.29, 112.06; EMM (ESI) m/z calcd for $C_{15}H_{12}ClNO$ [M+Na]: 280.0500, meas: 280.0504.

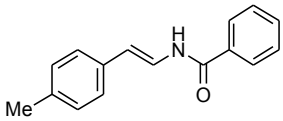

N-[(E)-2-(4-methylphenyl)ethenyl]benzamide

Isolated as a white solid, Mp = 178-179 °C. ^{1}H NMR (300 MHz, DMSO-d_6): δ 10.55 (d, NH, J = 9.9 Hz), 7.94 (d, 2H, J = 6.9 Hz), 7.47-7.61 (m, 4H), 7.27 (d, 2H, J = 8.1 Hz), 7.10 (d, 2H, J = 7.8 Hz), 6.42 (d, 1H, J = 15 Hz), 2.25 (s, 3H); ^{13}C NMR (75 MHz, DMSO-d_6): δ 164.63, 136.14, 134.38, 134.09, 132.51, 130.00, 129.14, 128.26, 125.86, 123.99, 113.64, 21.40. EMM (ESI) m/z calcd for $C_{16}H_{15}NO$ $[M+Na]^+$:260.1046, meas: 260.1053.

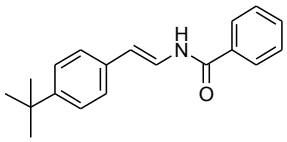

N-[(E)-2-(4-tert-butylphenyl)ethenyl]benzamide

Isolated as a white solid, Mp = 196-199°C. ^{1}H NMR (300 MHz, DMSO-d_6): δ 10.56 (d, NH, J = 9.9 Hz), 7.95 (d, 2H, J = 6.6 Hz), 7.47-7.63 (m, 4H), 7.30 (virtual s, 4H), 6.42 (d, 1H, J = 14.4 Hz), 1.25, (s, 9H); ^{13}C NMR (75 MHz, DMSO-d_6): δ 164.64, 149.43, 134.38, 134.08, 132.52, 129.15, 128.26, 126.16, 125.67, 124.12, 113.49, 34.87, 31.77. EMM (ESI) m/z calcd for $C_{19}H_{21}NO$ $[M+H]^+$:280.1696, meas: 280.1697.

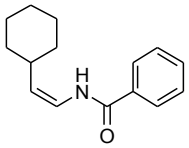

N-[(*Z*)-2-cyclohexylethenyl]benzamide

Isolated as an oil which solidified over time, mp: 90-93 °C.^{1}H NMR (300MHz, $CDCl_3$): δ 7.79 (d, 2H, J = 6.9 Hz), 7.67 (br d, 1H, J = 9.3 Hz), 7.41-7.59 (m, 3H), 6.79 (t, 1H, J = 10.2 Hz), 4.75 (t, 1H, J = 9.3 Hz), 2.20 (m, 1H), 1.69 (m, 5H), 1.14-1.34 (m, 5H); ^{13}C NMR (75 MHz, $CDCl_3$): δ 164.58, 134.31, 132.08, 128.96, 127.25, 119.63, 118.52, 35.80, 33.26, 26.10, 26.01. EMM(ESI) *m/z* calcd for $C_{15}H_{19}NO$ $[M+Na]^+$: 252.1359, Meas (M+Na): 252.1353.

6.4.5. Kinetic Isotope Effect Determination

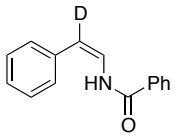

N - [2'-Deutero-(*Z*)-2-phenylethenyl]benzamide*,* **1**-d_1

Deuterated enamide substrate **1**-d_1 was prepared from benzamide-d_2 according to the method of Goossen,[9c] with slight modifications to the standard protocol. A Schlenk flask, which had been washed three times with a D_2O solution acidified with a few drops of aqueous DCl, then flame dried under vacuum, was introduced into a glovebox. The solid reaction components, benzamide-d_2 (0.485 g, 4.0 mmol), 1,4-bis(dicyclohexylphosphino)butane (0.108 g, 0.32 mmol), $Ru(mta)_2cod$ (0.064 g, 0.20 mmol), and ytterbium triflate (0.099 g, 0.16 mmol) were then added under inert atmosphere, followed by the addition of dry, degassed DMF (12 mL). After the reaction was removed from the glovebox, phenylacetylene (0.878 mL, 8.0 mmol) and degassed

D_2O (0.432 mL, 24 mmol) was added in place of H_2O. The reaction was subsequently carried out according to the literature procedures. After repeated purification, the title compound was obtained (224 mg, 25%) with 93% deuterium incorporation based on ^{1}H NMR. ^{1}H NMR (300MHz, $CDCl_3$): δ 8.36 (br s, 1H), 7.74 (d, 2H, J = 6.9 Hz), 7.1-7.5 (m, 9H); ^{13}C NMR (75 MHz, $CDCl_3$): δ 164.58, 135.95, 133.62, 132.38, 129.48, 129.07, 128.08, 127.30, 122.55, 110 .83 (t, J=24.9Hz); EMM (ESI) m/z calcd for $C_{15}H_{12}DNO$ [M+H]: 225.1133, meas: 225.1138.

A kinetic isotope effect was determined by independent rate measurements of (Z)-**1** and (Z)-**1**-d_1. A comparison of the initial linear region of the reaction timecourse (t=0 to t=10 min) results in a measured k_H/k_D of 0.96.

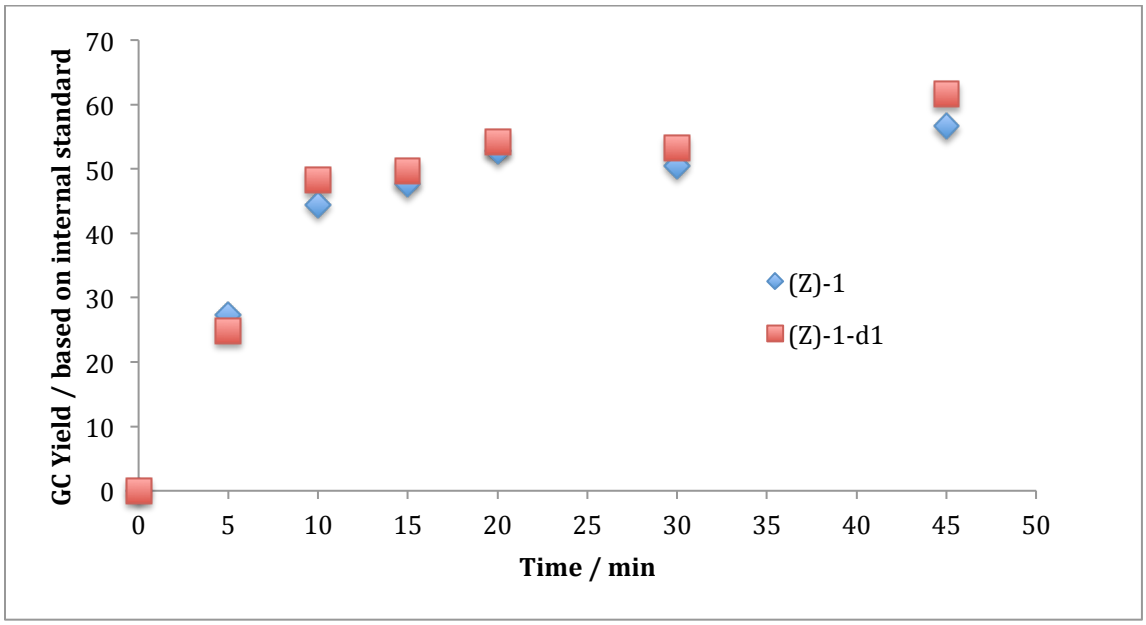

Figure 6.1. Reaction Timecourse of (*Z*)-**1** and (*Z*)-**1**-d_1.

6.5 References and Notes

1. For leading references in this area, see: (a) X. Li, J. B. Hewgley, C. A. Mulrooney, J. Yang, M. C. Kozlowski, *J. Org. Chem.,* 2003, **68**, 5500; (b) L. Menini, E. V. Gusevskaya, *Chem. Commun.,* 2006, 209; (c) Chen, X.-S. Hao, C. E. Goodhue, J.-Q. Yu, *J. Am. Chem. Soc.,* 2006, **128**, 6790; (d) T. Hamada, X. Ye, S. S. Stahl, *J. Am. Chem. Soc.,* 2008, **130**, 833; (e) H.-Q. Do, O. Daugulis, *J. Am. Chem. Soc.,* 2009, **131**, 17052; (f) C. Zhang, N. Jiao, *J. Am. Chem. Soc.*, 2010, **132**, 28.
2. For recent reviews, see: (a) A. E. Wendlandt, A. M. Suess, S. S. Stahl, *Angew. Chem. Int. Ed.* 2011, **50**, 11062; (b) T. Punniyamurthy, L. Rout, *Coord. Chem. Rev.* 2008, **252**, 134.
3. For representative examples, see: (a) G. Brasche, S. L. Buchwald, *Angew. Chem. Int. Ed.,* 2008, **47**, 1932; (b) S. Ueda, H. Nagasawa *Angew. Chem. Int. Ed.,* 2008, **47**, 6411; (c) S. Ueda, H. Nagasawa, *J. Org. Chem.,* 2009, **74**, 4272; (d) S. Ueda, H. Nagasawa, *J. Am. Chem. Soc.,* 2009, **131**, 15080; (e) Y.-X. Jia, E. P. Kündig, *Angew. Chem. Int. Ed.,* 2009, **48**, 1636; (f) A. Perry, R. J. K. Taylor, *Chem. Commun.,* 2009, 3249; (g) D. S. Pugh, J. E. M. N. Klein, A. Perry, R. J. K. Taylor, *Synlett,* 2010, 934; (h) J. E. M. N. Klein, A. Perry, D. S. Pugh, R. J. K. Taylor, *Org. Lett.,* 2010, **12**, 3446; (i) H.-F. He, Z.-J. Wang, W. Bao, *Adv. Synth. Catal.,* 2010, **352**, 2905; (j) L. Zhang, G. Y. Ang, S. Chiba, *Org. Lett.,* 2010, **12**, 3682; (k) H. Wang, Y. Wang, C. Peng, J. Zhang, Q. Zhu, *J. Am. Chem. Soc.,* 2010, **132**, 13217; (l) B.-X. Tang, R.-J. Song, C.-Y. Wu, Y. Liu, M.-B. Zhou, W.-T. Wei, G.-B. Deng, D.-L. Yin, J.-H. Li, *J. Am. Chem. Soc.,* 2010, **132**, 8900; (m) M. M. Guru, M. A. Ali, T. Punniyamurthy, *Org. Lett.,* 2011, **13**, 1194; (n) H. Wang, Y. Wang, D. Liang, L. Liu, J. Zhang, Q. Zhu, *Angew. Chem. Int. Ed.* 2011, **50**, 5678; (o) J. Lu, Y. Jin, H. Liu, Y. Jiang, H. Fu, *Org. Lett.,* 2011, **13**, 3694.

4. For reviews, see: (a) V. Kotov, C. C. Scarborough, S. S. Stahl, *Inorg. Chem*. 2007, **46**, 1910; (b) R. I. McDonald, G. Liu, S. S. Stahl, *Chem. Rev.* 2011, **111**, 2981.

5. See, for example: (a) Palmer, D. C.; Taylor, E. C. The *Chemistry of Heterocyclic Compounds*. *Oxazoles: Synthesis, Reactions, and Spectroscopy, Parts A & B*; Wiley: New Jersey, 2004; Vol. 60; (b) Turchi, I. J., *Ind. Eng. Chem. Prod. Res. Dev.* 1981, **20**, 32; (c) Turchi, I. J.; Dewar, M. J. S., *Chem. Rev.* 1975, **75**, 389.

6. (a) W. He, C. Li, L. Zhang, *J. Am. Chem. Soc.*, 2011, **133**, 8482; (b) I. Cano, E. Álvarez, M. C. Nicasio, P. J. Pérez, *J. Am. Chem. Soc.* 2010, **133**, 191; (c) A. S. K. Hashmi, J. P. Weyrauch, W. Frey, J. W. Bats, *Org. Lett.,* 2004, **6**, 4391.

7. (a) A. Arcadi, S. Cacchi, L. Cascia, G. Fabrizi, F. Marinelli, *Org. Lett.*, 2001, **3**, 2501; (b) P. Wipf, Y. Aoyama, T. E. Benedum, *Org. Lett.*, 2004, **6**, 3593; (c) Y.-m. Pan, F.-j. Zheng, H.-x. Lin, Z.-p. Zhan, *J. Org. Chem.,* 2009, **74**, 3148.

8. (a) C-g Shin, Y. Sato, H. Sugivama, K. Nanjo, J. Yoshimura, *Bull. Chem. Soc. Jpn,* 1977, **50**, 1788; (b) S. K. Chattopadhyay, J. Kempson, A. McNeil, G. Pattenden, M. Reader, D. E. Rippon, D. Waite, *J. Chem. Soc. Perkin Trans. 1*, 2000, 2415; (c) K. Schuh, F. Glorius, *Synthesis*, 2007, 2297; (d) R. Martín, A. Cuenca, S. L. Buchwald, *Org. Lett.,* 2007, **9**, 5521; (e) C. Wan, L. Gao, Q. Wang, J. Zhang, Z. Wang, *Org. Lett.*, 2010, **12**, 3902; (f) C. Wan, J. Zhang, S. Wang, J. Fan, Z. Wang, *Org. Lett*., 2010, **12**, 2338; (g) H. Jiang, H. Huang, H. Cao, C. Qi, *Org. Lett.,* 2010, **12**, 5561; (h) D. J. Ritson, C. Spiteri, J. E. Moses, *J. Org. Chem.,* 2011, **76**, 3519.

9. (a) L. J. Gooben, K. S. M. Salih, M. Blanchot, *Angew. Chem. Int. Ed.* 2008, **47**, 8492; (b) L. J. Gooben, M. Blanchot, K. S. M. Salih, K. Gooβen, *Synthesis,* 2009, 2283; (c) M.

Arndt, K. S. M. Salih, A. Fromm, L. J. Goossen, F. Menges, G. Niedner-Schatteburg, *J. Am. Chem. Soc.,* 2011, **133**, 7428.

10. For reviews describing alternate routes to enamides, see: (a) Carbery, D. R., *Org. Biomol. Chem.* 2008, **6**, 3455; (b) J. R. Dehli, J. Legros, C. Bolm, *Chem. Commun.* 2005, 973.

11. (a) L. Menini, E. V. Gusevskaya, *Applied Catalysis A: General* 2006, **309**, 122; (b) Y.-F. Song, G. A. van Albada, J. Tang, I. Mutikainen, U. Turpeinen, C. Massera, O. Roubeau, J. S. Costa, P. Gamez, J. Reedijk, *Inorg. Chem.* 2007, **46**, 4944; (c) L. Yang, S. S. Stahl, *Chem. Commun.*, 2009, 6460.

12. For characterization of an organometallic oxidative C–H amidation reaction mediated by Cu^{II}, see: A. E. King, L. M. Huffman, A. Casitas, M. Costas, X. Ribas, S. S. Stahl, *J. Am. Chem. Soc.* **2010,** 132, 12068.

13. J. P. Genêt, C. Pinel, V. Ratovelomanana-Vidal, S. Mallart, X. Pfister, M. C. C. De Andrade, J. A. Laffitte, *Tetrahedron: Asymmetry* 1994, **5**, 665.

14. A. R. Katritzky, A. V. Ignatchenko, H. Lang, *Synthetic Commun.* 1995, **25,** 1197.

Appendix 1

NMR Spectra for Chapter 2

This work has been published:

Wendlandt, A. E.; Stahl, S. S. *Org. Lett.* **2012**, *14*, 2850-2853.

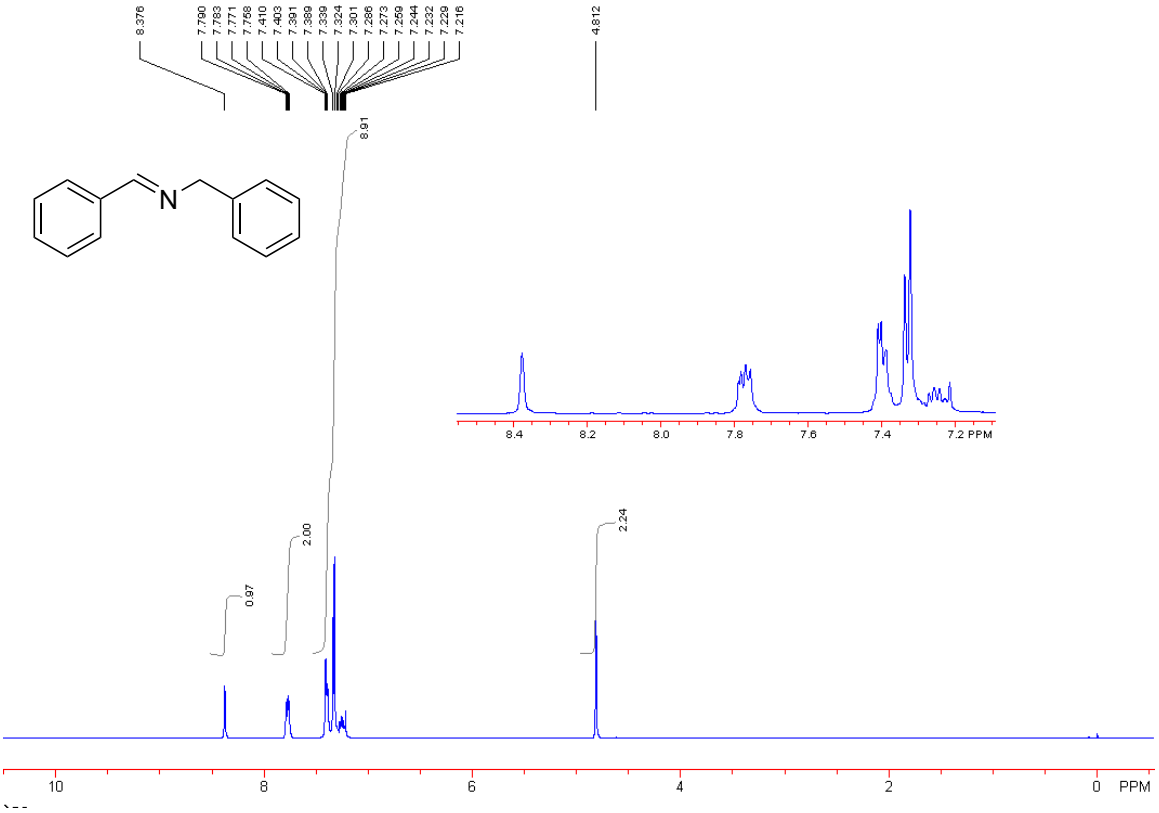
8.376
7.790
7.783
7.771
7.768
7.410
7.403
7.391
7.389
7.339
7.324
7.301
7.286
7.273
7.259
7.244
7.232
7.229
7.216
4.812
8.91
2.00
0.97
2.24
N
8.4
8.2
8.0
7.8
7.6
7.4
7.2 PPM
10
8
6
4
2
0
PPM

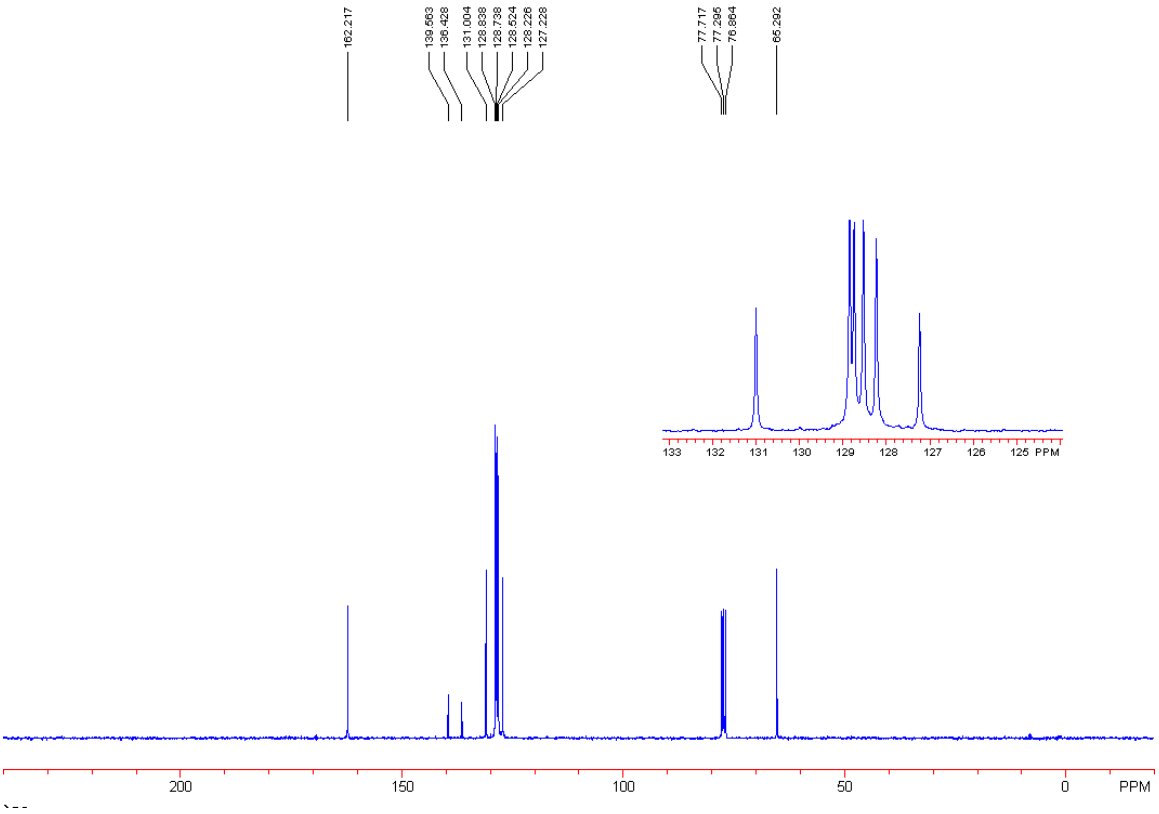
162.217
139.563
136.428
131.004
128.838
128.738
128.524
128.226
127.228
77.717
77.296
76.864
65.292
133
132
131
130
129
128
127
126
125 PPM
200
150
100
50
0
PPM

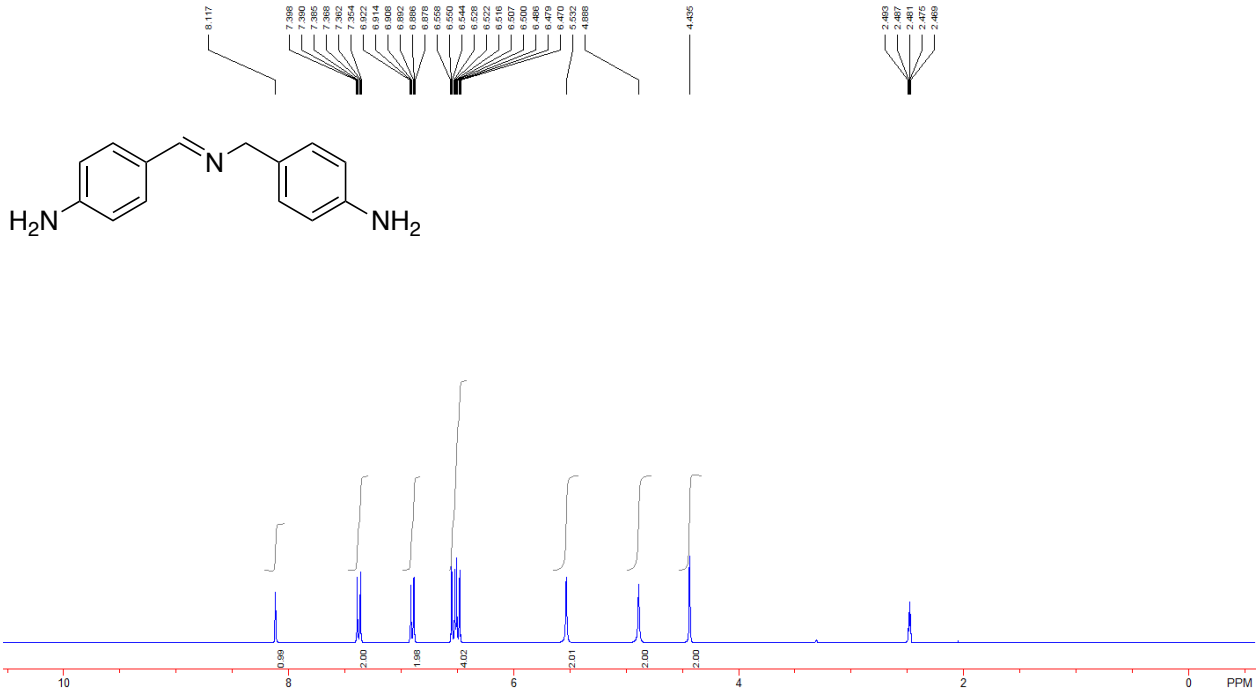
8.117
7.368
7.360
7.356
7.368
7.362
7.354
6.922
6.914
6.908
6.892
6.886
6.878
6.558
6.550
6.544
6.528
6.522
6.516
6.507
6.500
6.486
6.479
6.470
5.532
4.888
4.435
2.493
2.487
2.481
2.475
2.469
N
H2N
NH2
0.99
2.00
1.98
4.02
2.01
2.00
2.00
10
8
6
4
2
0
PPM

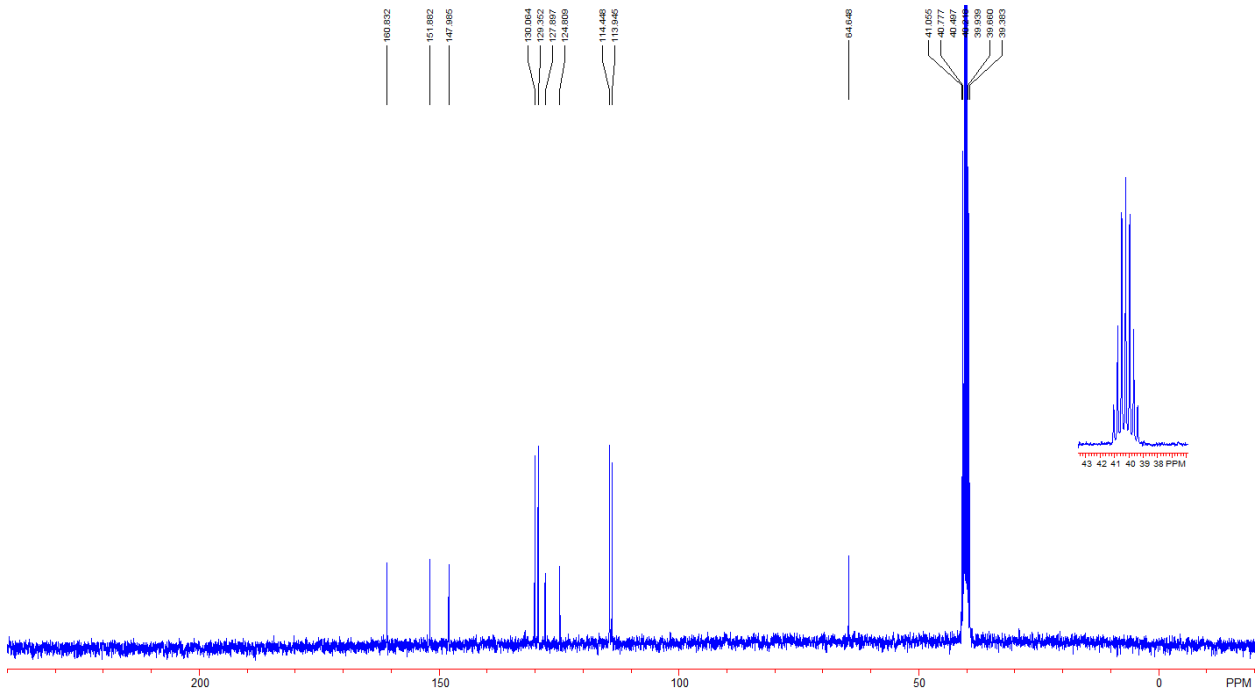
160.832
151.862
147.985
130.064
129.352
127.997
124.809
114.448
113.945
64.648
41.056
40.777
40.497
39.939
39.660
39.363
43 42 41 40 39 38 PPM
200
150
100
50
0
PPM

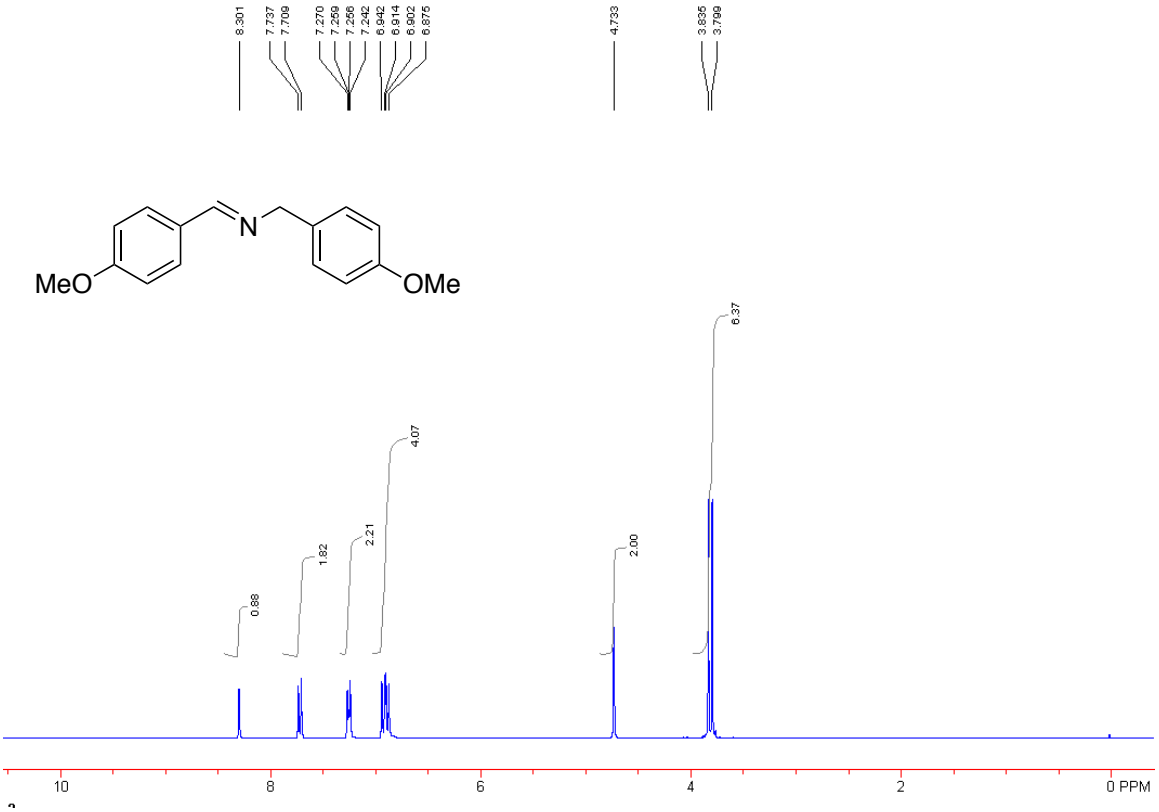
8.301
7.737
7.709
7.270
7.259
7.256
7.242
6.942
6.914
6.902
6.875
4.733
3.835
3.799
MeO
N
OMe
6.37
4.07
2.21
1.82
0.88
2.00
10
8
6
4
2
0 PPM

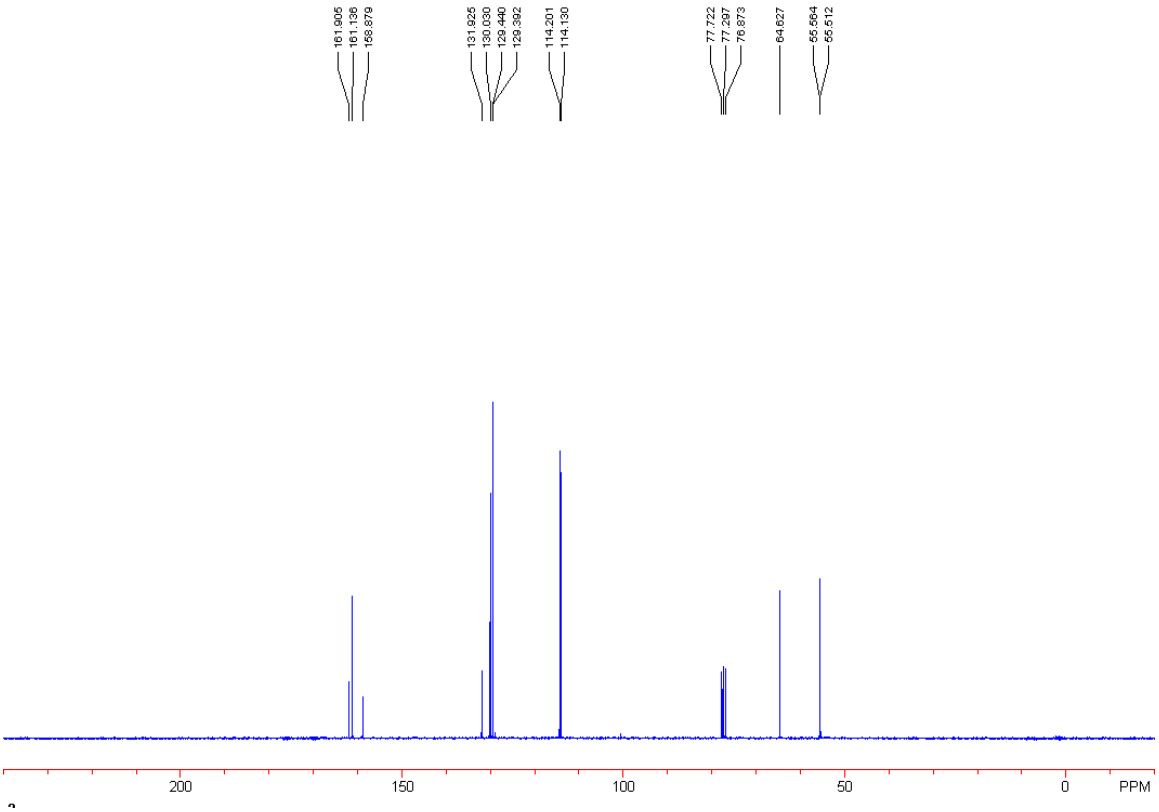
161.905
161.136
158.879
131.925
130.030
129.440
129.392
114.201
114.130
77.722
77.297
76.873
64.627
55.564
55.512
200
150
100
50
0
PPM

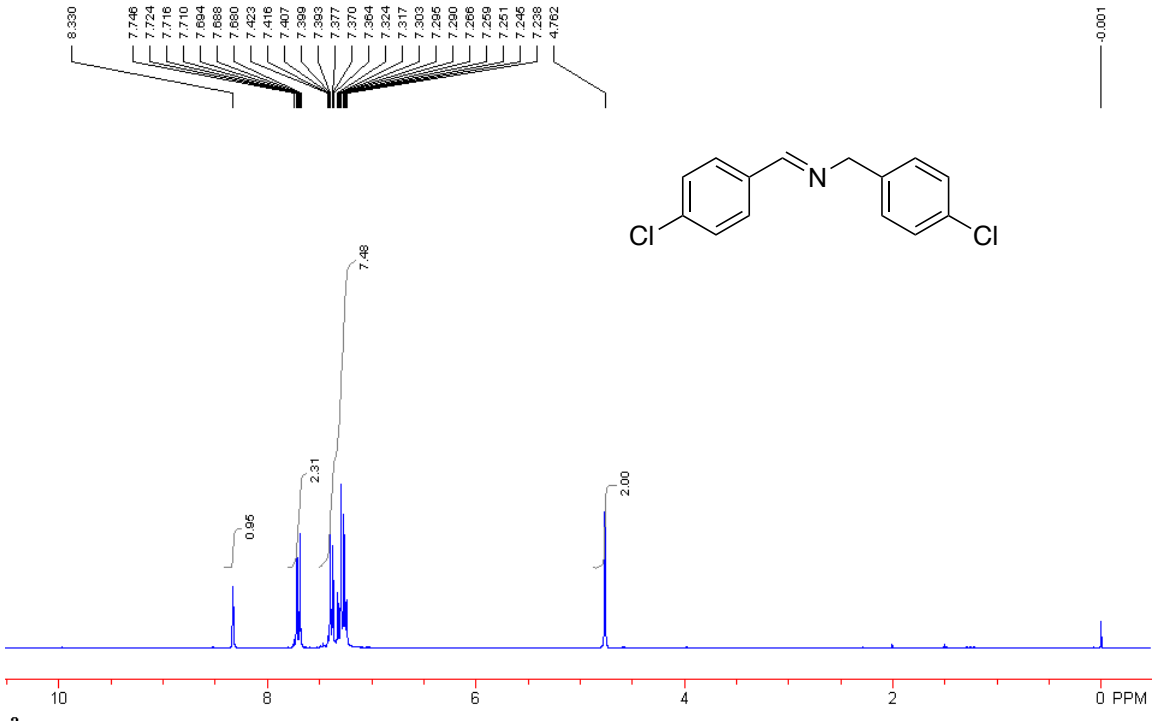
8.330
7.746
7.724
7.716
7.710
7.694
7.688
7.680
7.423
7.416
7.407
7.399
7.393
7.377
7.370
7.364
7.324
7.317
7.303
7.295
7.290
7.266
7.259
7.251
7.245
7.238
4.762
-0.001
N
Cl
Cl
7.48
2.31
0.95
2.00
10
8
6
4
2
0 PPM

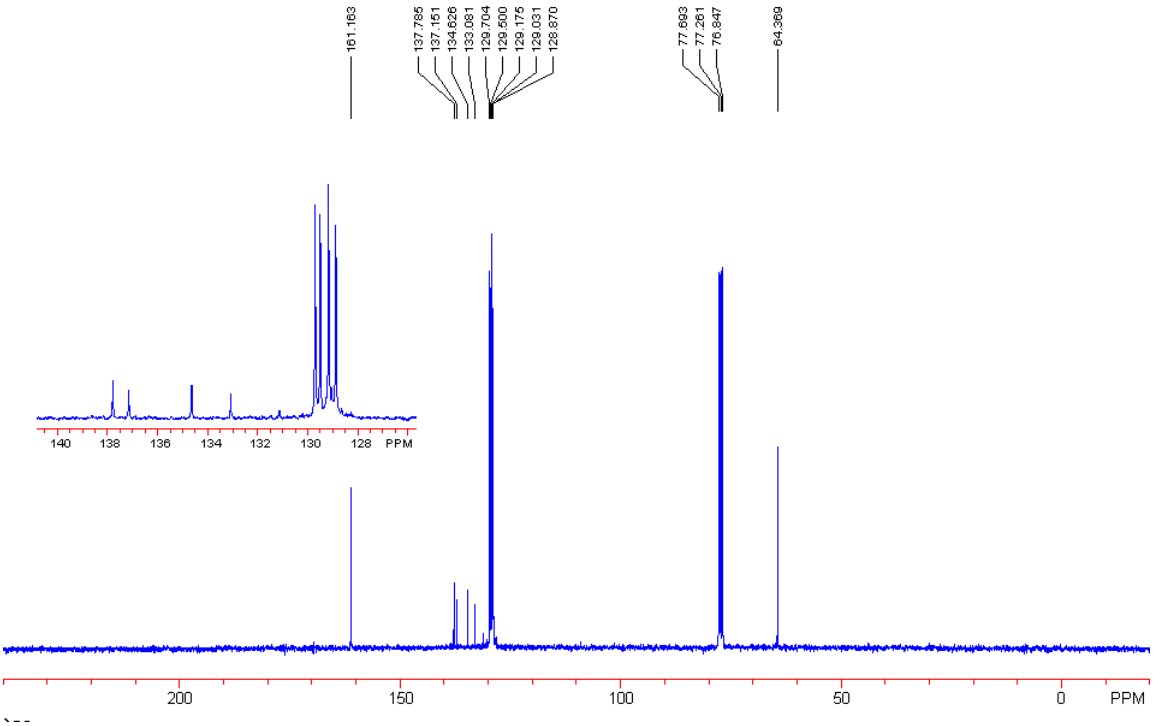
161.163
137.785
137.151
134.626
133.081
129.704
129.500
129.175
129.031
128.870
77.693
77.261
76.847
64.369
140
138
136
134
132
130
128
PPM
200
150
100
50
0
PPM

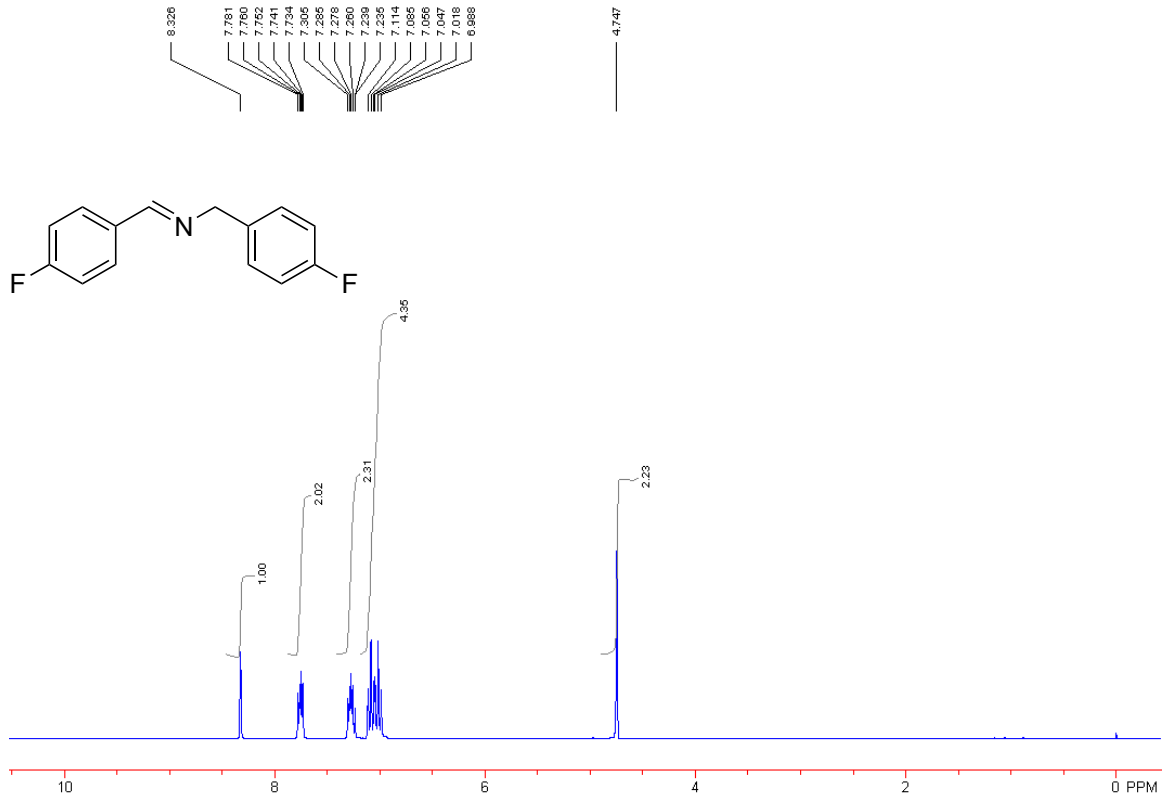
8.326
7.781
7.760
7.752
7.741
7.734
7.305
7.285
7.278
7.260
7.239
7.235
7.114
7.085
7.056
7.047
7.018
6.988
4.747
N
F
F
4.35
2.31
2.02
1.00
2.23
10
8
6
4
2
0 PPM

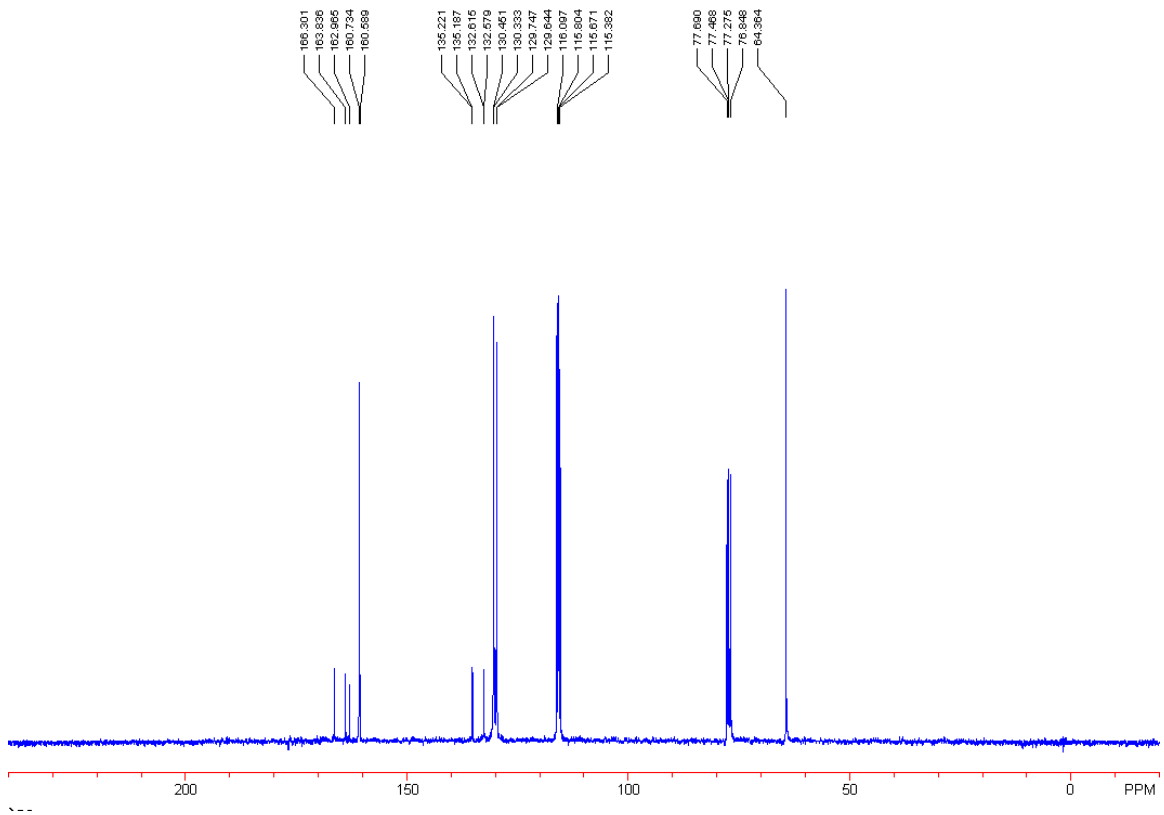
166.301
163.836
162.965
160.734
160.589
135.221
135.187
132.615
132.579
130.451
130.333
129.747
129.644
116.097
115.804
115.671
115.382
77.690
77.408
77.275
76.848
64.364
200
150
100
50
0
PPM

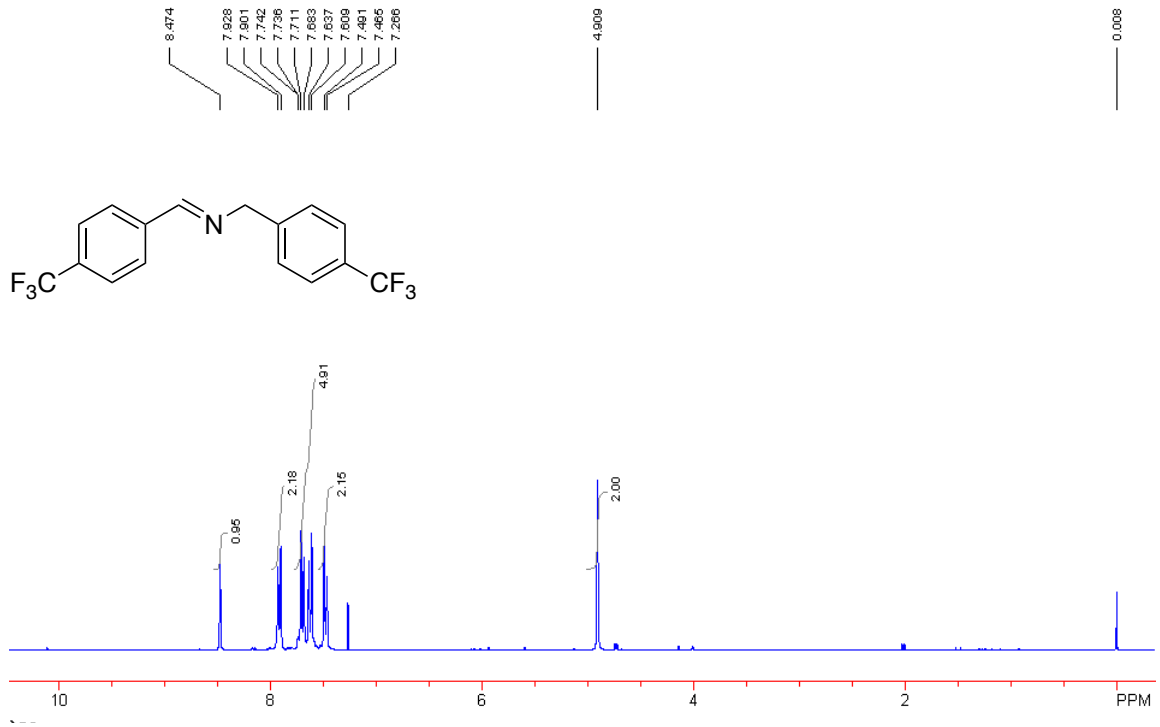
8.474
7.928
7.901
7.742
7.736
7.711
7.683
7.637
7.609
7.491
7.465
7.266
4.909
0.008
N
F3C
CF3
4.91
2.18
2.15
0.95
2.00
10
8
6
4
2
PPM

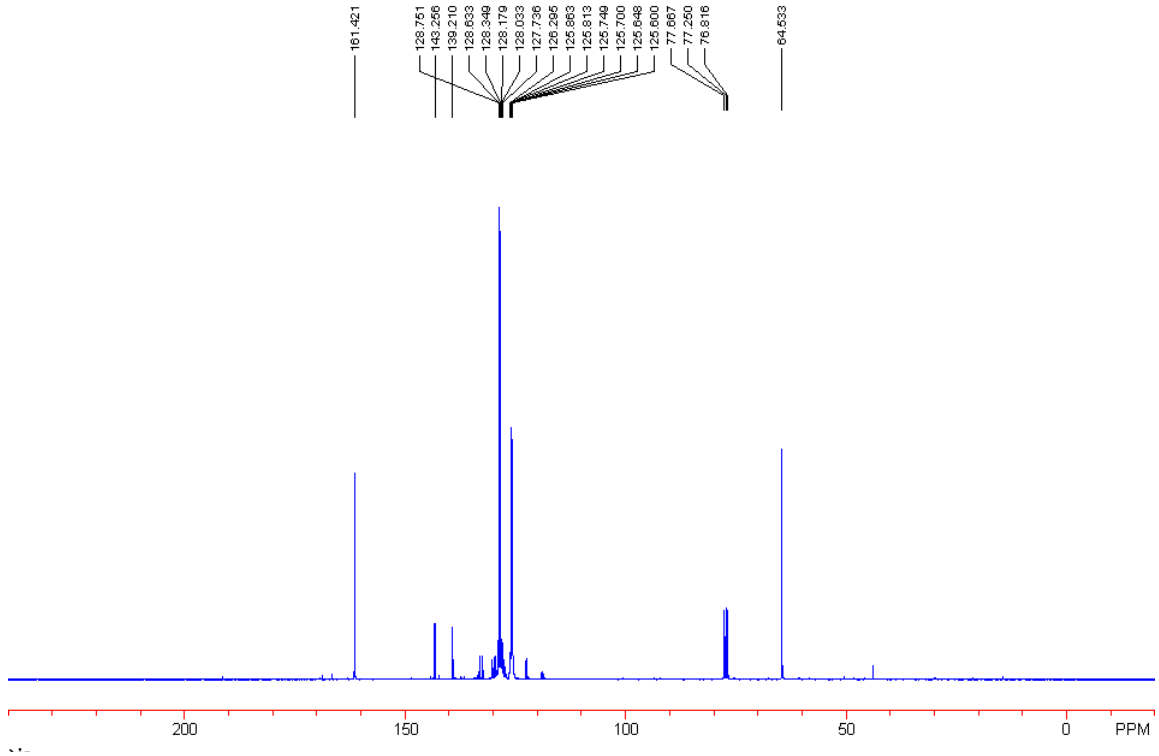
161.421
128.751
143.256
139.210
128.633
128.349
128.179
128.033
127.736
126.295
125.863
125.813
125.749
125.700
125.648
125.600
77.667
77.250
76.816
64.533
200
150
100
50
0
PPM

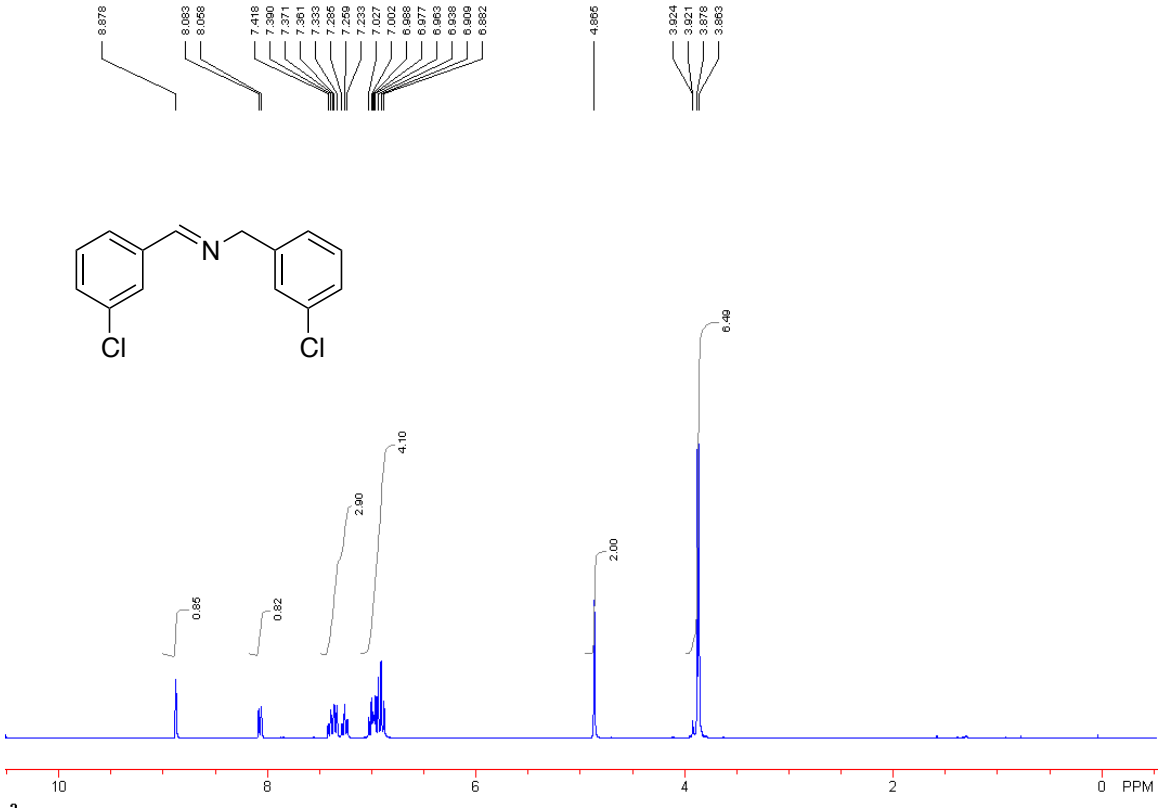
8.878
8.083
8.058
7.418
7.390
7.371
7.361
7.333
7.285
7.259
7.233
7.027
7.002
6.988
6.977
6.963
6.938
6.909
6.882
4.866
3.924
3.921
3.878
3.863
N
Cl
Cl
0.85
0.82
2.90
4.10
2.00
6.49
10
8
6
4
2
0
PPM

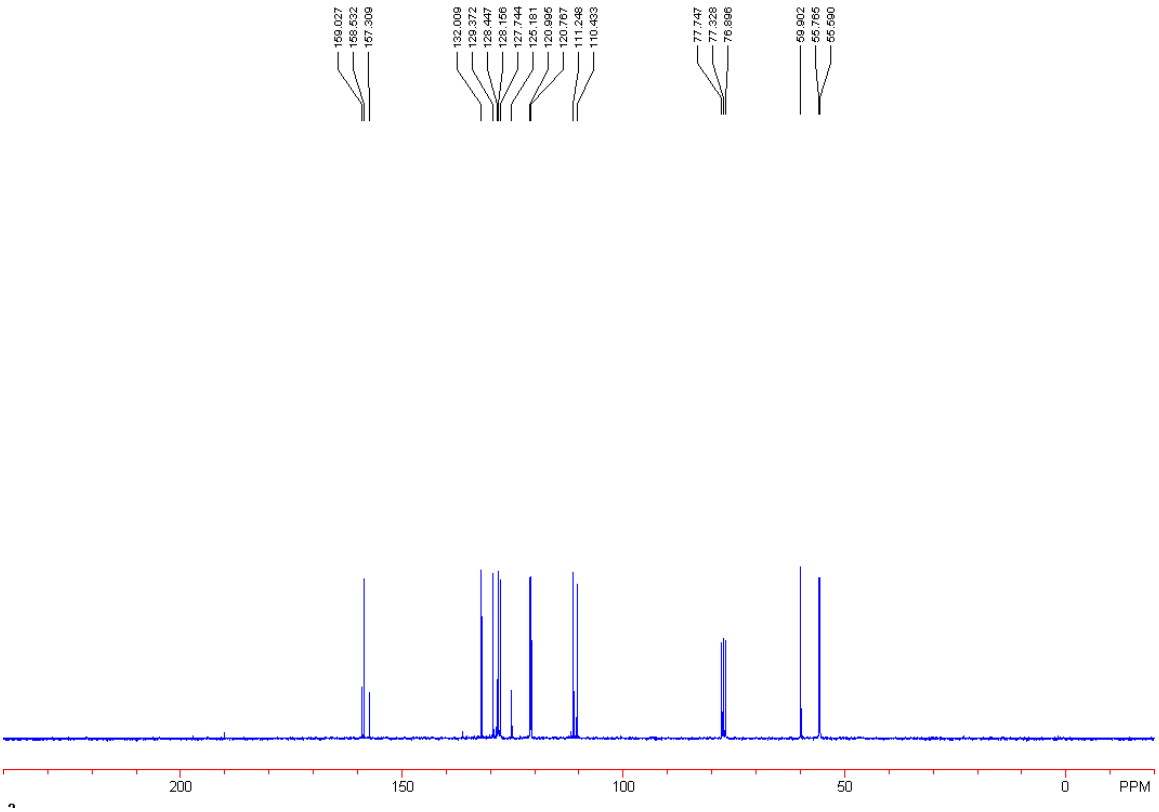
159.027
158.532
157.309
132.009
129.372
128.447
128.156
127.744
125.181
120.995
120.767
111.248
110.433
77.747
77.328
76.896
59.902
55.766
55.590
200
150
100
50
0
PPM

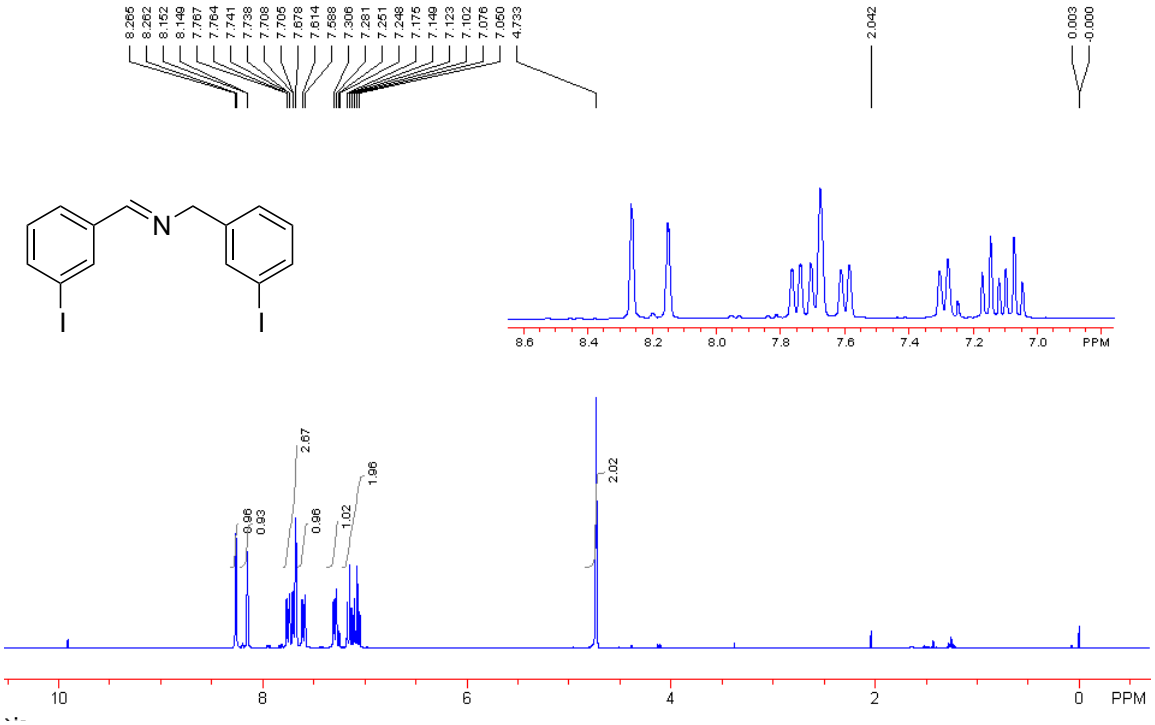
8.265
8.262
8.152
8.149
7.767
7.764
7.741
7.738
7.708
7.705
7.678
7.614
7.588
7.306
7.281
7.251
7.248
7.175
7.149
7.123
7.102
7.076
7.050
4.733
2.042
0.003
-0.000
N
I
I
8.6
8.4
8.2
8.0
7.8
7.6
7.4
7.2
7.0
PPM
2.67
1.96
2.02
0.96
0.93
0.96
1.02
10
8
6
4
2
0
PPM

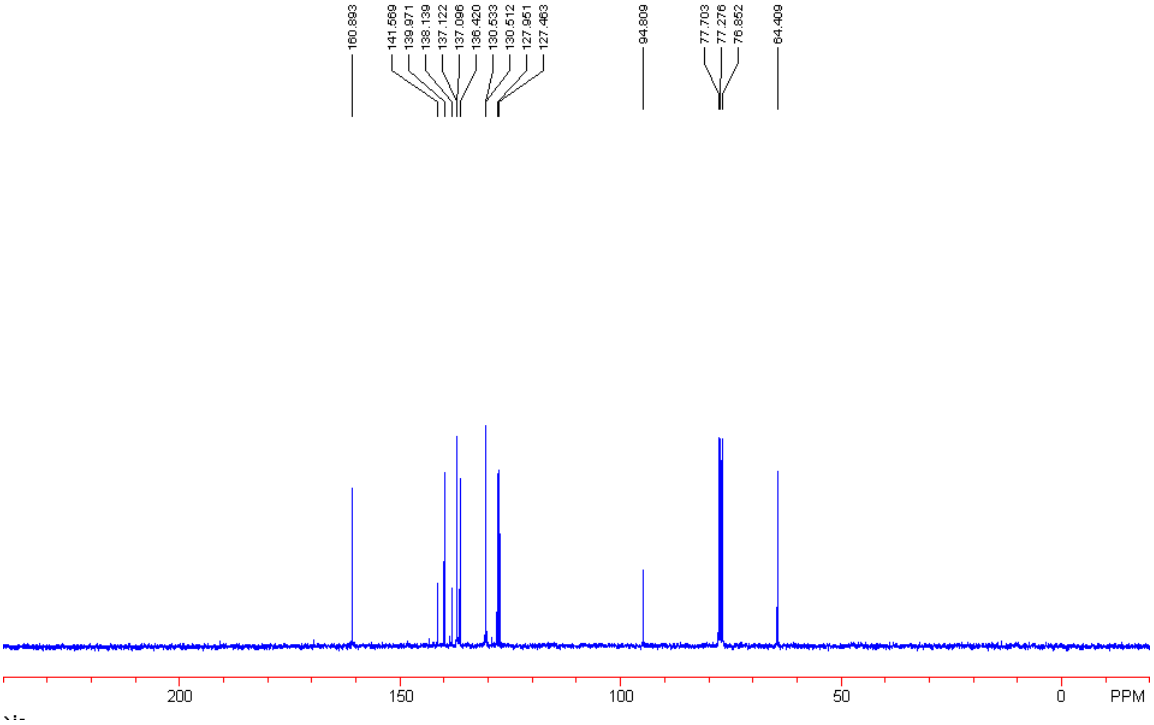
160.893
141.569
139.971
138.139
137.122
137.096
136.420
130.533
130.512
127.951
127.463
94.809
77.703
77.276
76.852
64.409
200
150
100
50
0
PPM

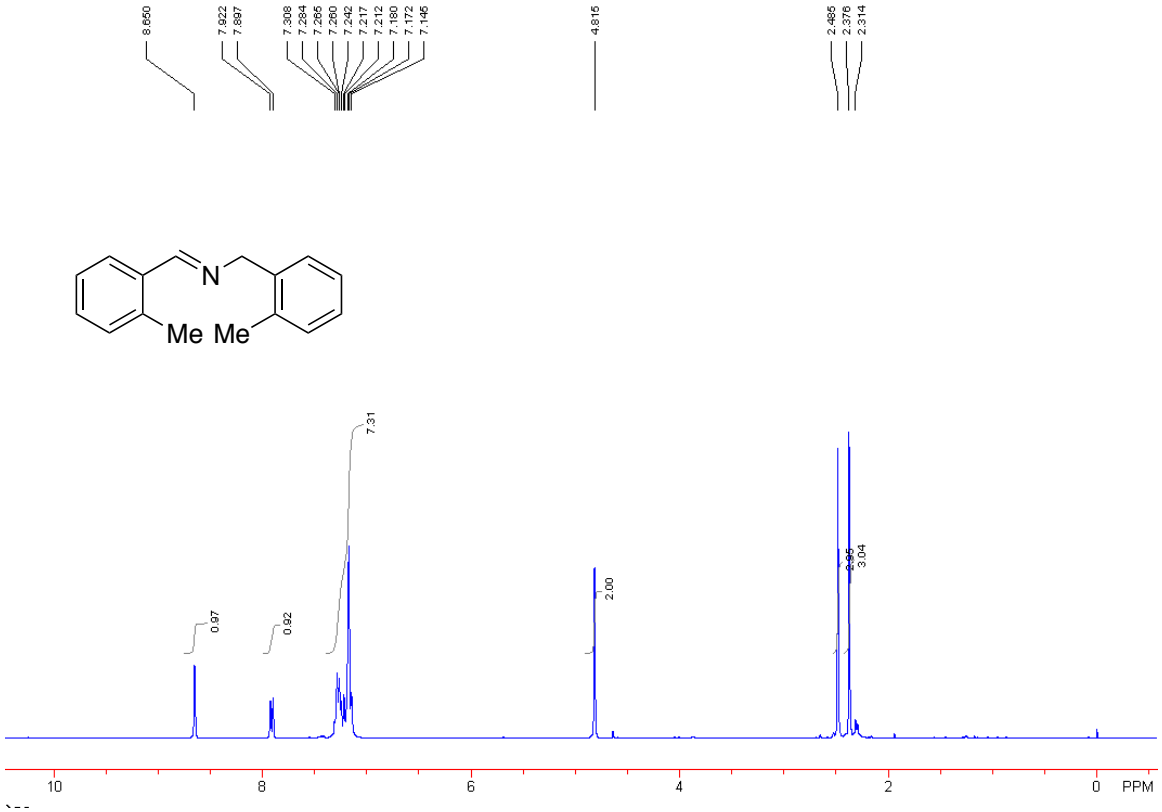
8.650
7.922
7.897
7.308
7.284
7.266
7.260
7.242
7.217
7.212
7.180
7.172
7.145
4.815
2.485
2.376
2.314
N
Me Me
7.31
0.97
0.92
2.00
2.35
3.04
10
8
6
4
2
0
PPM

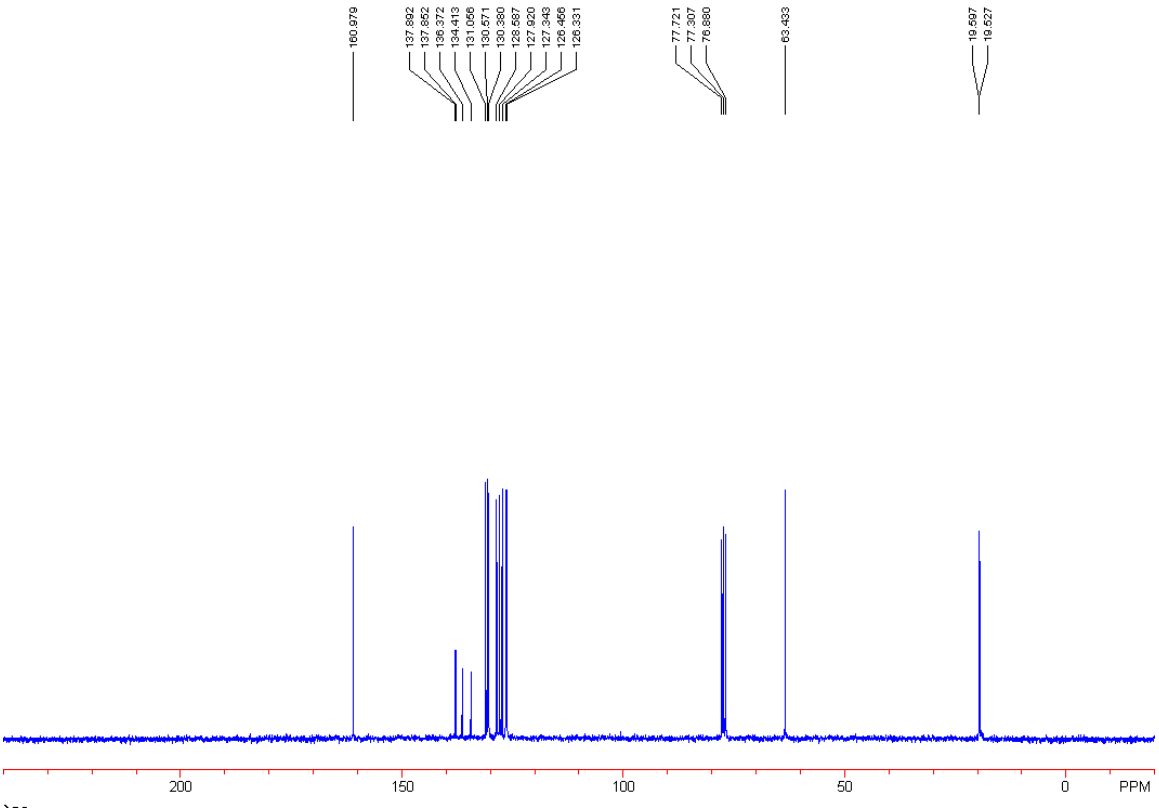
160.979
137.892
137.852
136.372
134.413
131.056
130.571
130.380
128.587
127.920
127.343
126.456
126.331
77.721
77.307
76.890
63.433
19.597
19.527
200
150
100
50
0
PPM

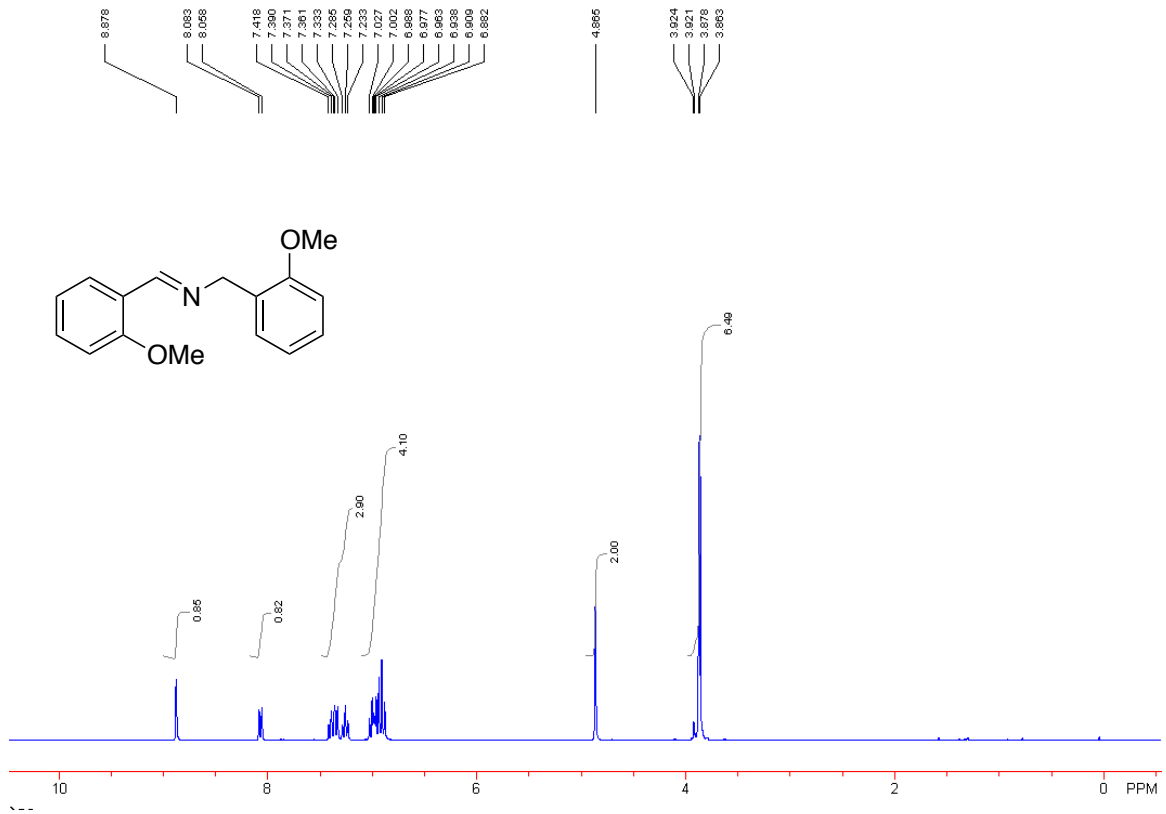
8.878
8.083
8.058
7.418
7.390
7.371
7.361
7.333
7.285
7.259
7.233
7.027
7.002
6.988
6.977
6.963
6.938
6.909
6.882
4.865
3.924
3.921
3.878
3.863
OMe
N
OMe
6.49
4.10
2.90
2.00
0.85
0.82
10
8
6
4
2
0
PPM

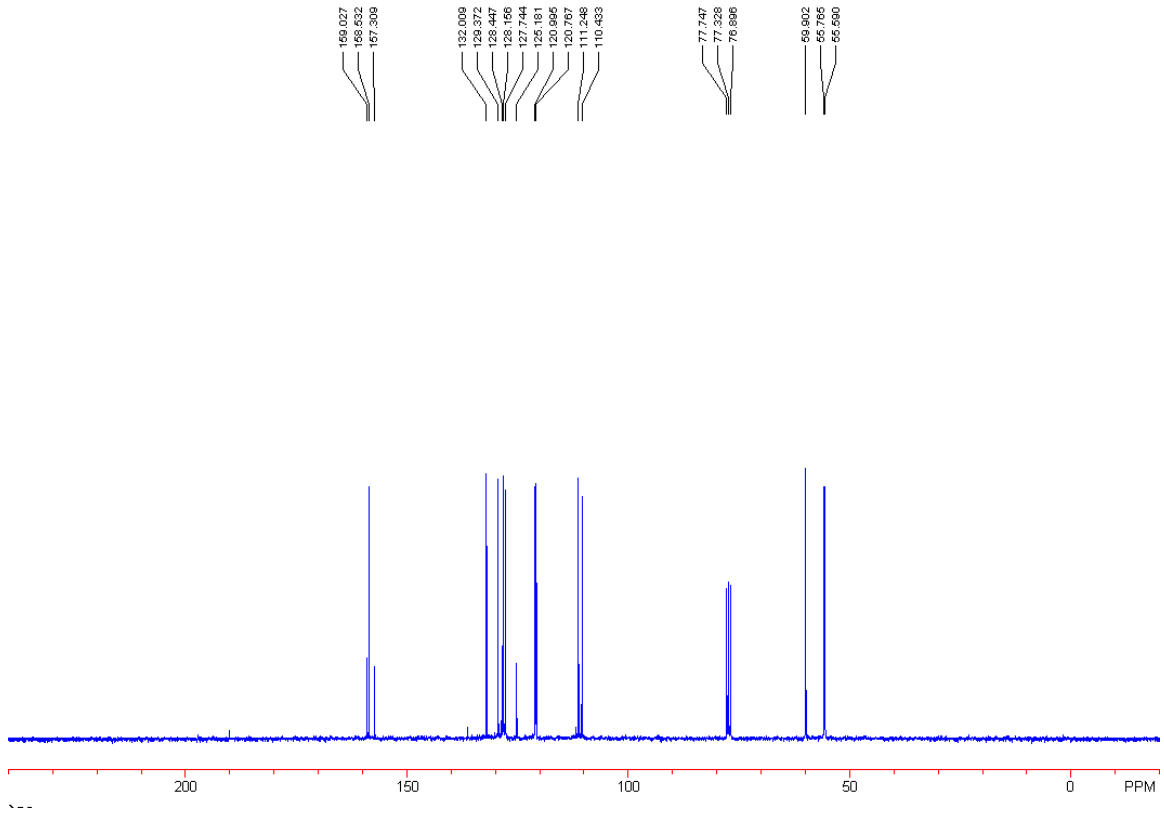
159.027
158.532
157.309
132.009
129.372
128.447
128.156
127.744
125.181
120.995
120.767
111.248
110.433
77.747
77.328
76.896
59.902
55.766
55.590
200
150
100
50
0
PPM

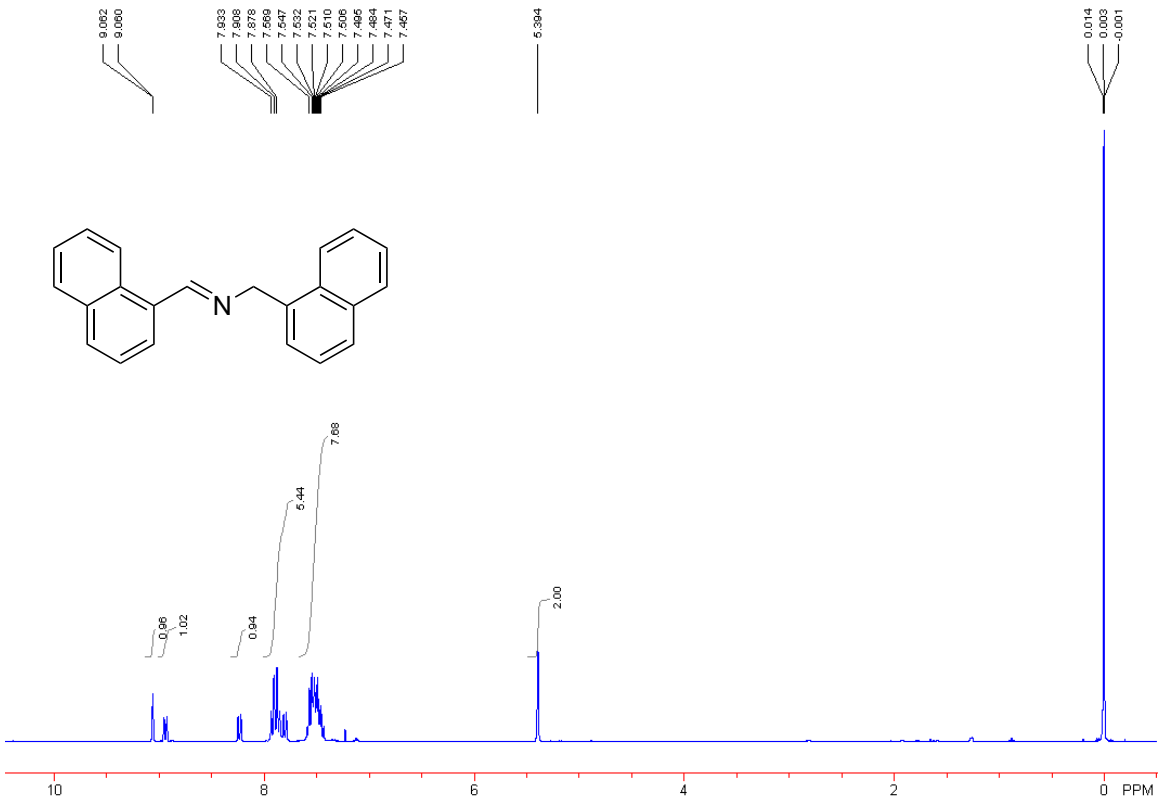
9.062
9.060
7.933
7.908
7.878
7.569
7.547
7.532
7.521
7.510
7.506
7.495
7.484
7.471
7.457
5.394
0.014
0.003
-0.001
N
7.68
5.44
2.00
0.96
1.02
0.94
10
8
6
4
2
0
PPM

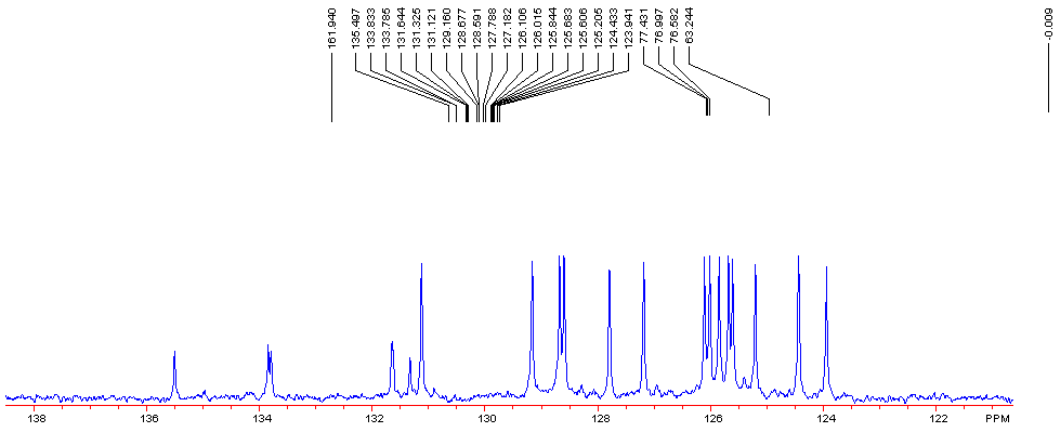
161.940
135.497
133.833
133.785
131.844
131.325
131.121
129.160
128.677
128.591
127.788
127.182
126.106
126.015
125.844
125.683
125.606
125.205
124.433
123.941
77.431
76.997
76.582
63.244
-0.009
138
136
134
132
130
128
126
124
122
PPM

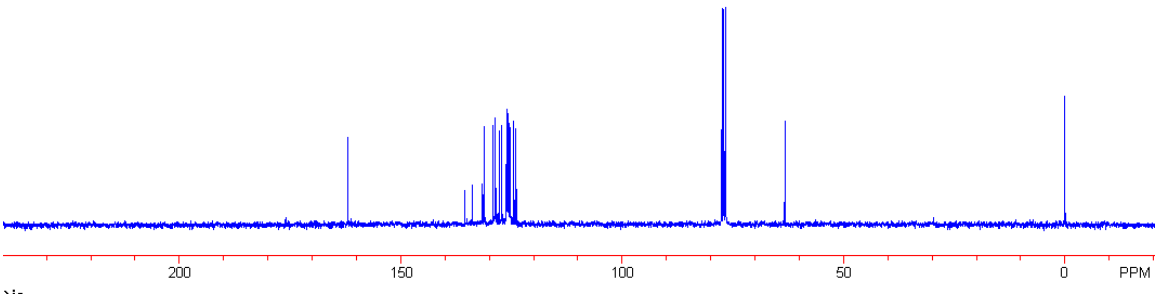
200
150
100
50
0
PPM

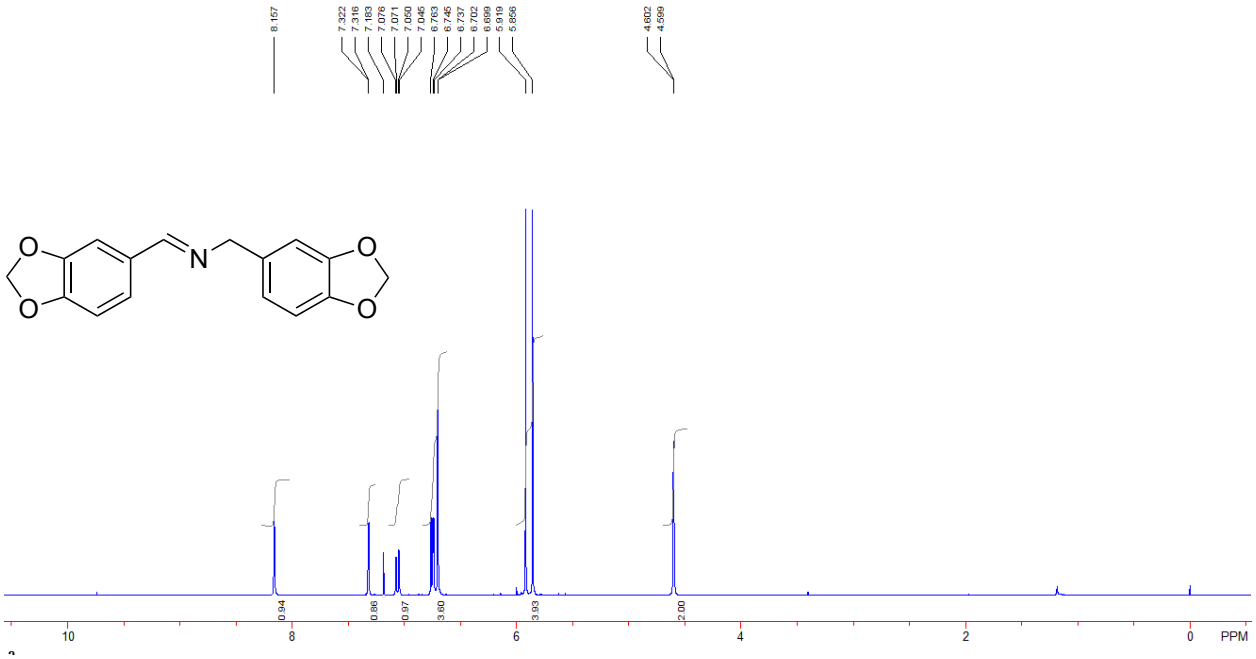
8.157
7.322
7.316
7.093
7.076
7.071
7.050
7.045
6.763
6.745
6.737
6.702
6.699
5.919
5.856
4.602
4.598
O
O
N
O
O
0.94
0.86
0.97
3.60
3.93
2.00
10
8
6
4
2
0
PPM

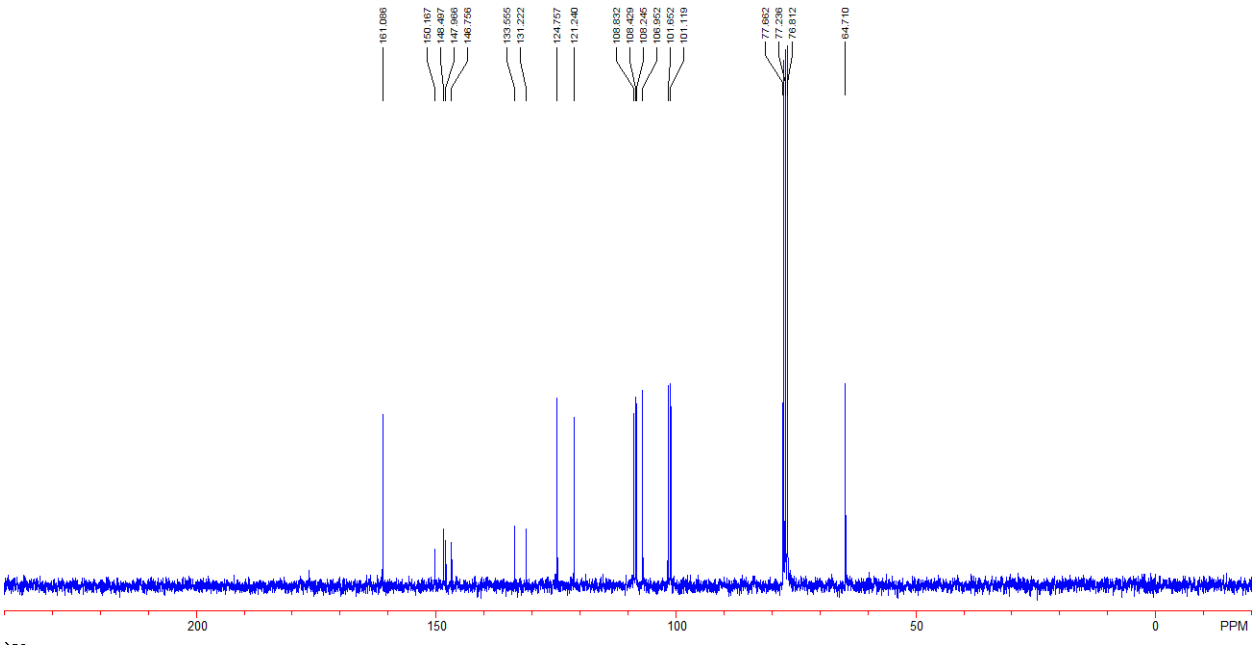
161.086
150.167
148.487
147.966
146.756
133.555
131.222
124.757
121.240
108.832
108.429
108.245
106.952
101.652
101.119
77.662
77.236
76.812
64.710
200
150
100
50
0
PPM

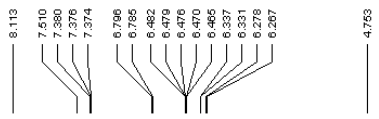
8.113
7.510
7.380
7.376
7.374
6.796
6.785
6.482
6.479
6.476
6.470
6.465
6.337
6.331
6.278
6.267
4.753

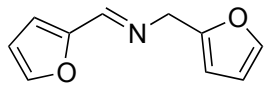
N
O
O

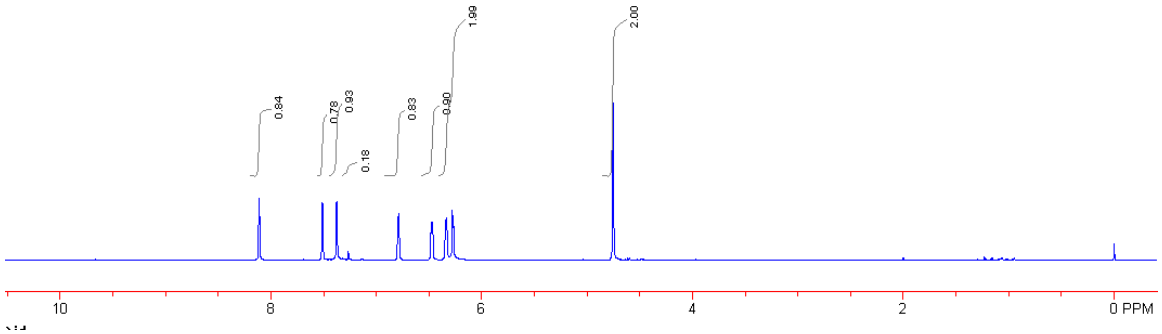
0.84
0.78
0.93
0.18
0.83
0.90
1.99
2.00
10
8
6
4
2
0 PPM

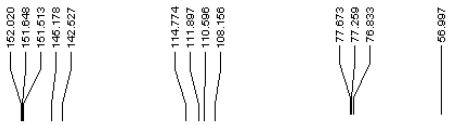
152.020
151.648
151.513
145.178
142.527
114.774
111.897
110.596
108.156
77.673
77.259
76.833
55.997

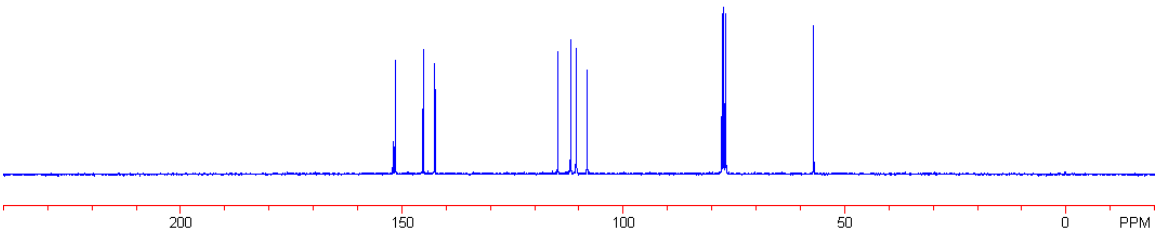
200
150
100
50
0
PPM

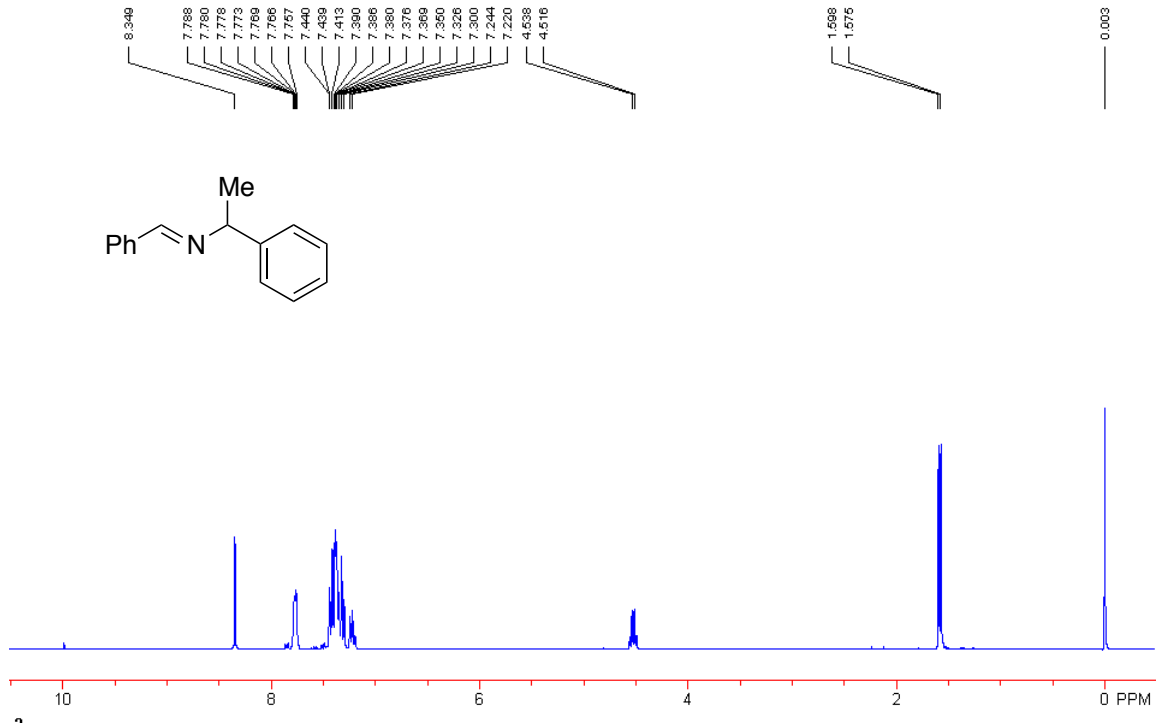
8.349
7.788
7.780
7.778
7.773
7.769
7.766
7.757
7.440
7.439
7.413
7.390
7.386
7.380
7.376
7.369
7.350
7.326
7.300
7.244
7.220
4.538
4.516
1.598
1.575
0.003
Me
Ph
N
10
8
6
4
2
0 PPM

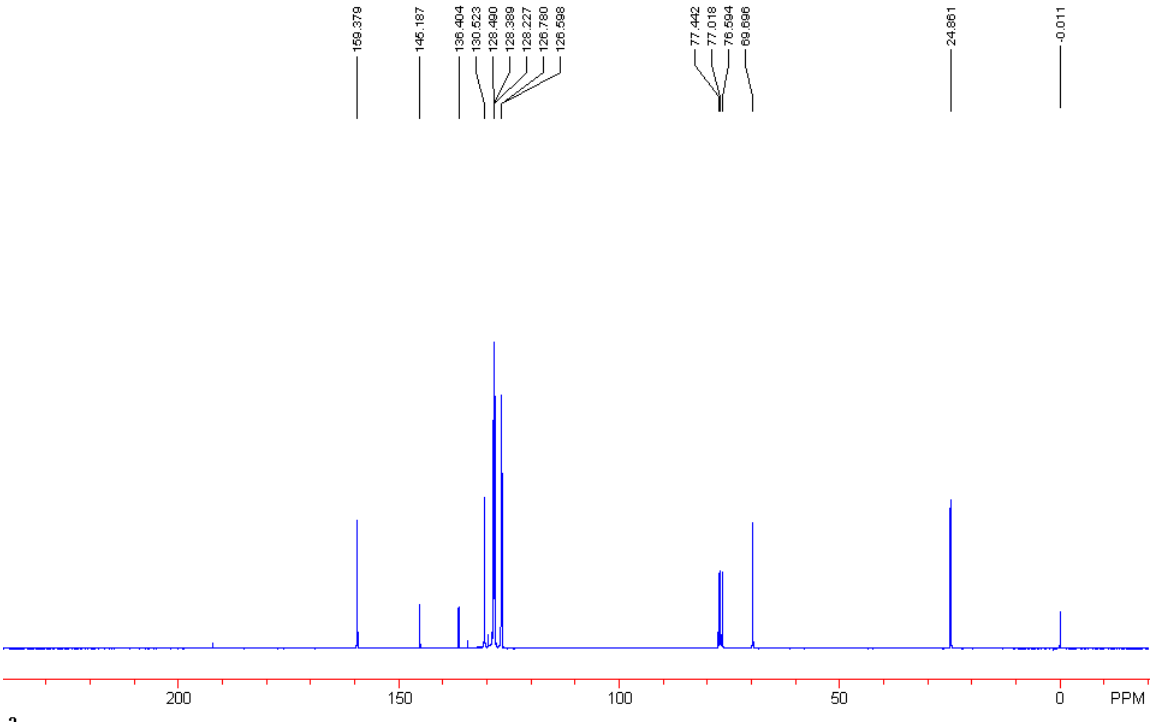
159.379
145.187
136.404
130.523
128.490
128.389
128.227
126.780
126.598
77.442
77.018
76.594
69.696
24.861
-0.011
200
150
100
50
0
PPM

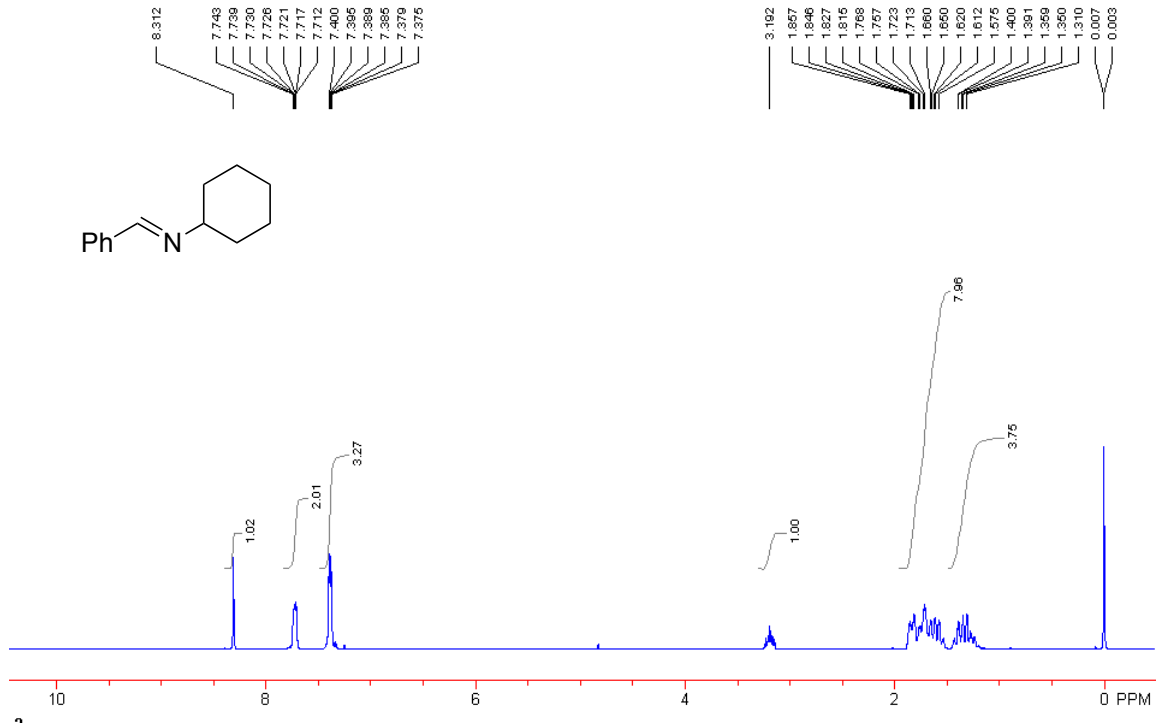
8.312
7.743
7.739
7.730
7.726
7.721
7.717
7.712
7.400
7.395
7.389
7.385
7.379
7.375
3.192
1.857
1.846
1.827
1.815
1.768
1.757
1.723
1.713
1.660
1.650
1.620
1.612
1.575
1.400
1.391
1.359
1.350
1.310
0.007
0.003
Ph
N
7.96
3.75
3.27
2.01
1.02
1.00
10
8
6
4
2
0 PPM

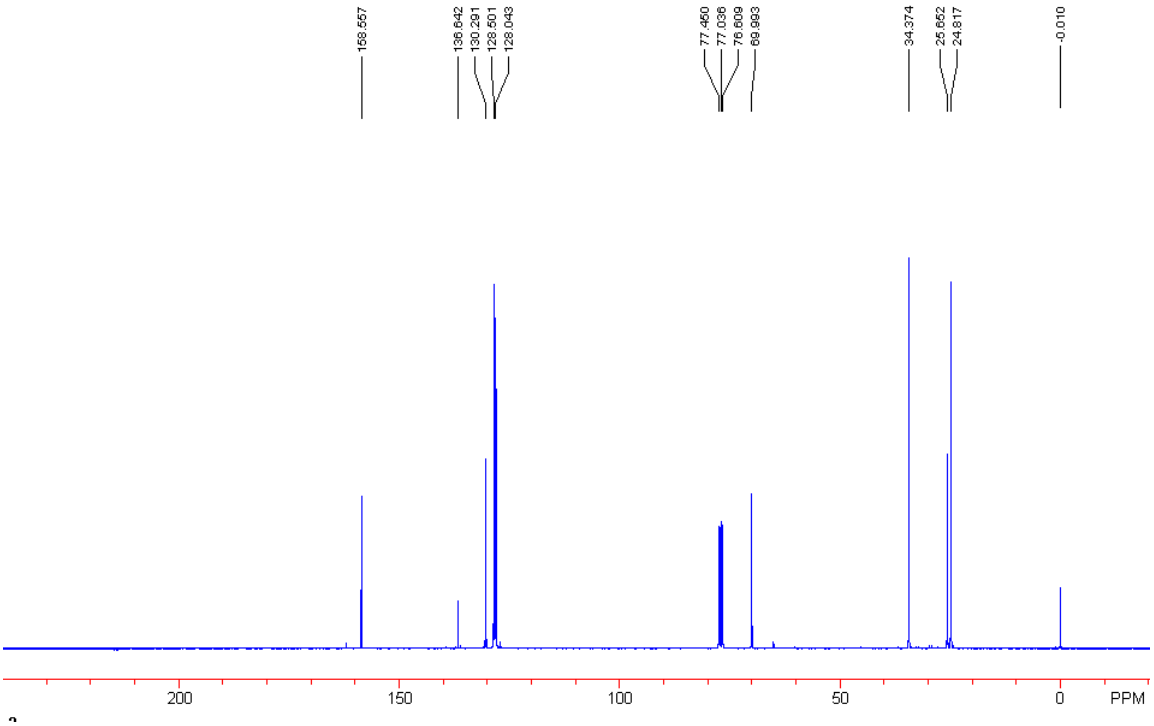
158.557
136.642
130.291
128.501
128.043
77.450
77.036
76.609
69.993
34.374
25.652
24.817
-0.010
200
150
100
50
0
PPM

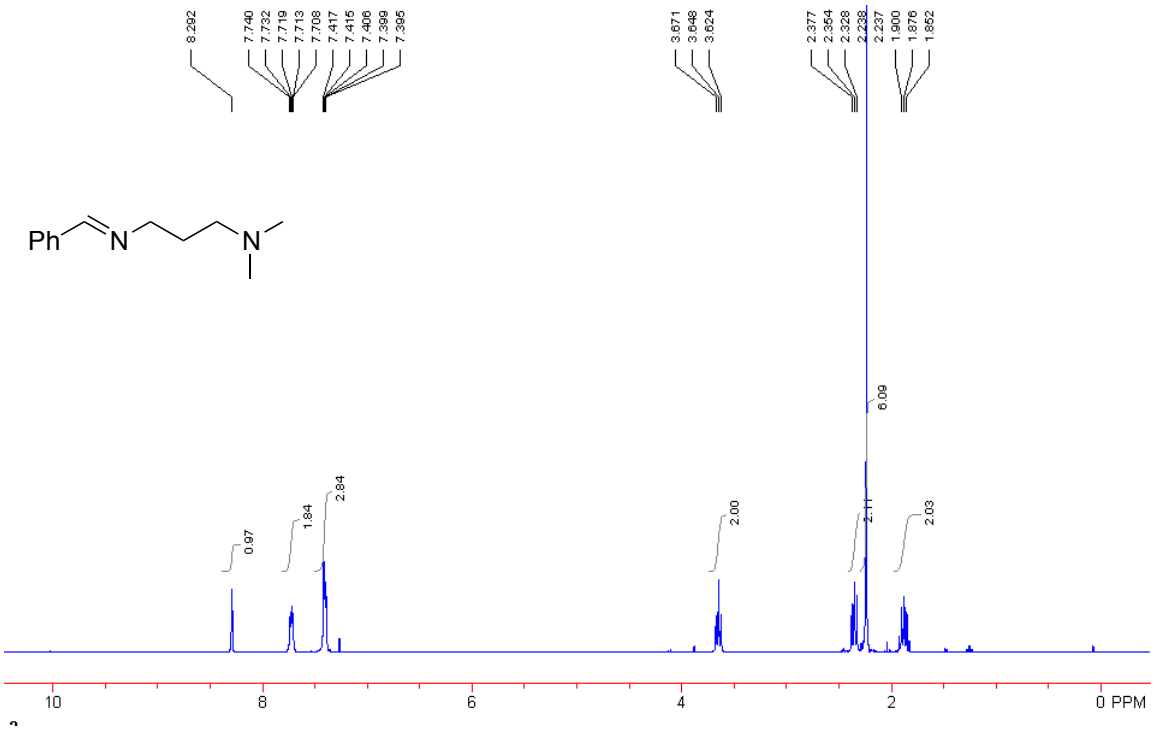
8.292
7.740
7.732
7.719
7.713
7.708
7.417
7.416
7.406
7.399
7.395
3.671
3.648
3.624
2.377
2.354
2.328
2.238
2.237
1.900
1.876
1.852
Ph
N
N
6.09
0.97
1.84
2.84
2.00
2.11
2.03
10
8
6
4
2
0 PPM

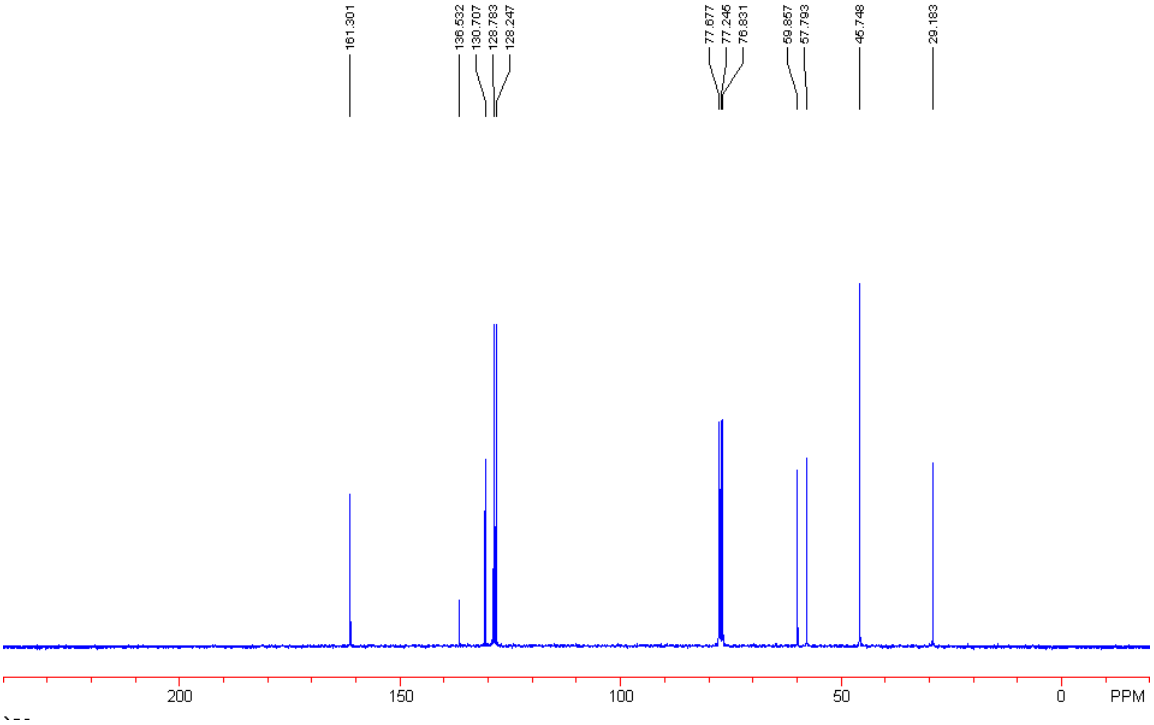
161.301
136.532
130.707
128.783
128.247
77.677
77.246
76.831
59.857
57.793
45.748
29.183
200
150
100
50
0
PPM

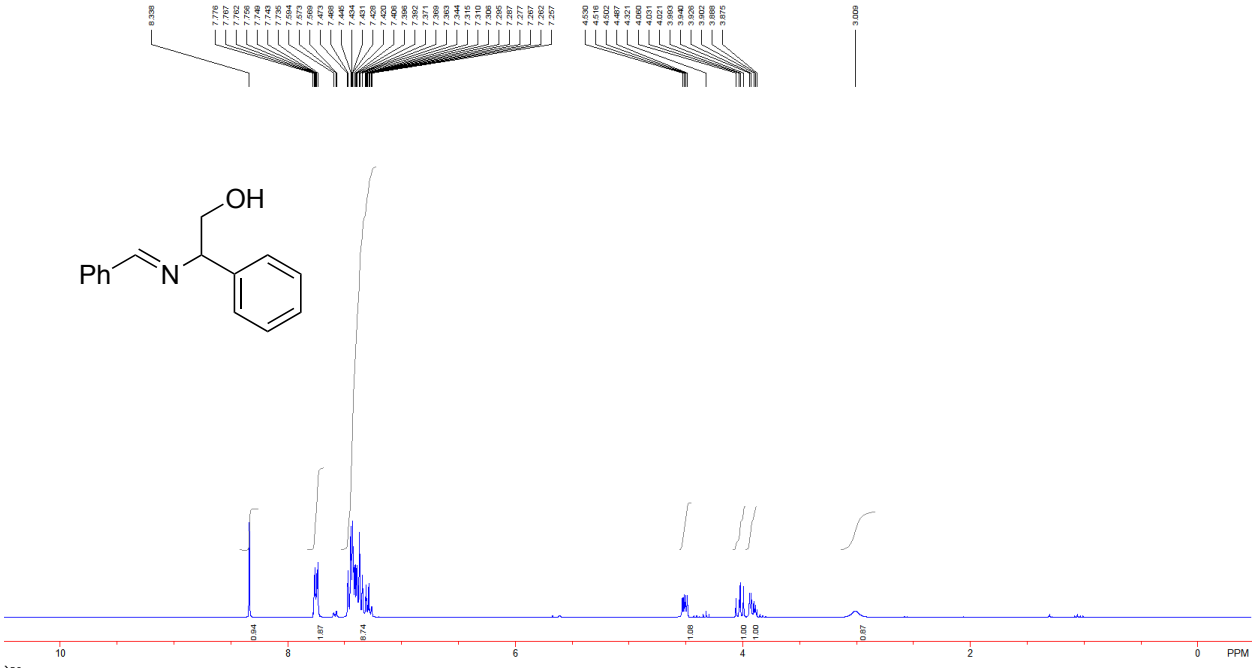
8.338
7.776
7.767
7.762
7.756
7.749
7.743
7.735
7.594
7.573
7.569
7.473
7.468
7.446
7.444
7.431
7.428
7.420
7.416
7.396
7.392
7.391
7.389
7.383
7.344
7.316
7.310
7.306
7.295
7.287
7.277
7.267
7.262
7.257
4.530
4.516
4.507
4.492
4.321
4.060
4.051
4.021
3.993
3.940
3.926
3.902
3.888
3.875
3.009
OH
Ph
N
0.94
1.87
8.74
1.06
1.00
1.00
0.87
10
8
6
4
2
0
PPM

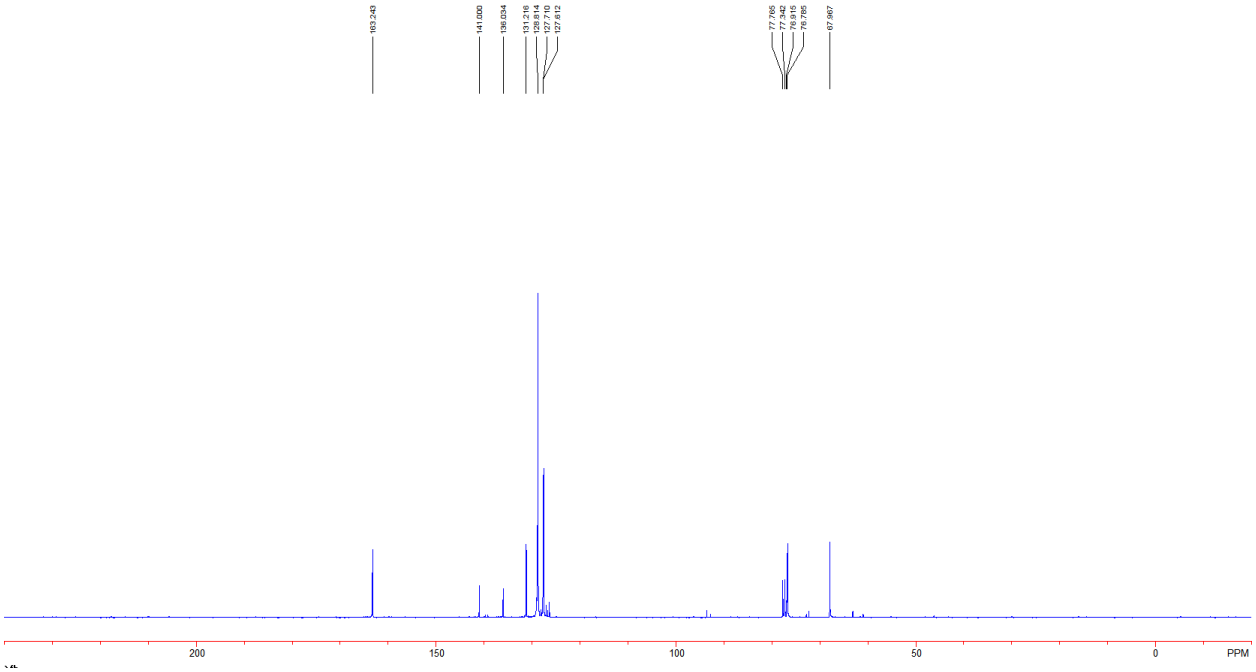
163.243
141.000
136.034
131.218
129.614
128.014
127.710
127.612
77.765
77.342
76.915
76.785
67.987
200
150
100
50
0
PPM

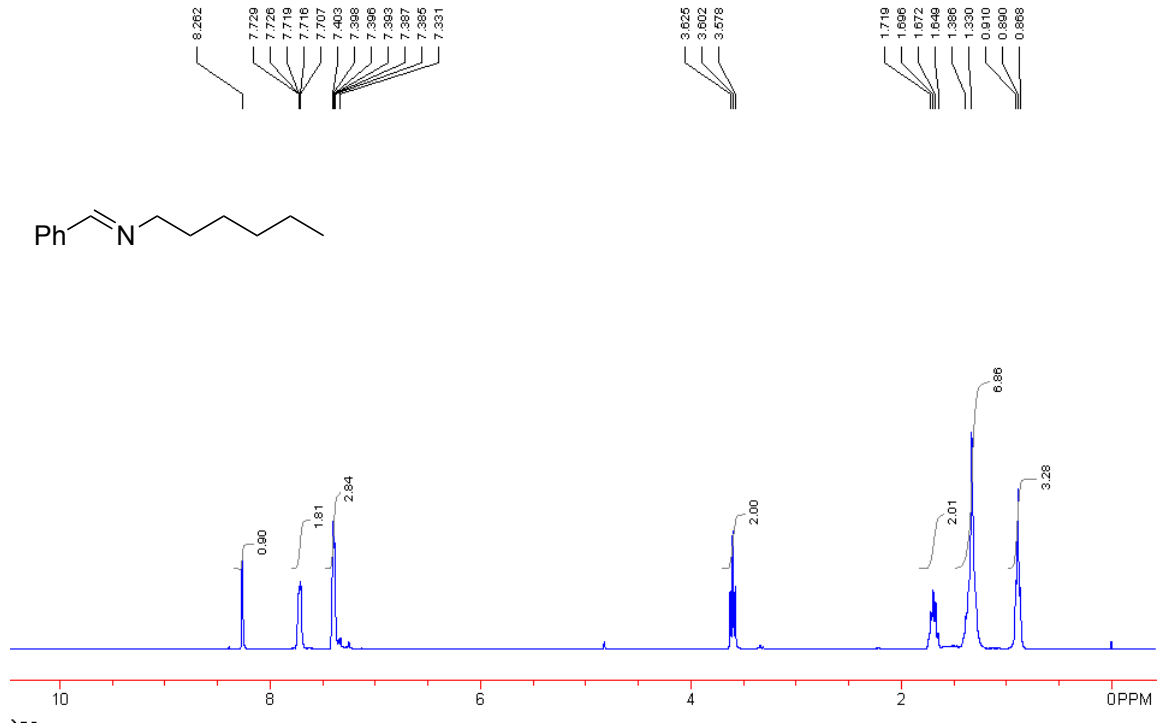
8.262
7.729
7.726
7.719
7.716
7.707
7.403
7.398
7.396
7.393
7.387
7.385
7.331
3.625
3.602
3.578
1.719
1.696
1.672
1.649
1.386
1.330
0.910
0.890
0.868
Ph
N
0.90
1.81
2.84
2.00
2.01
6.86
3.28
10
8
6
4
2
0PPM

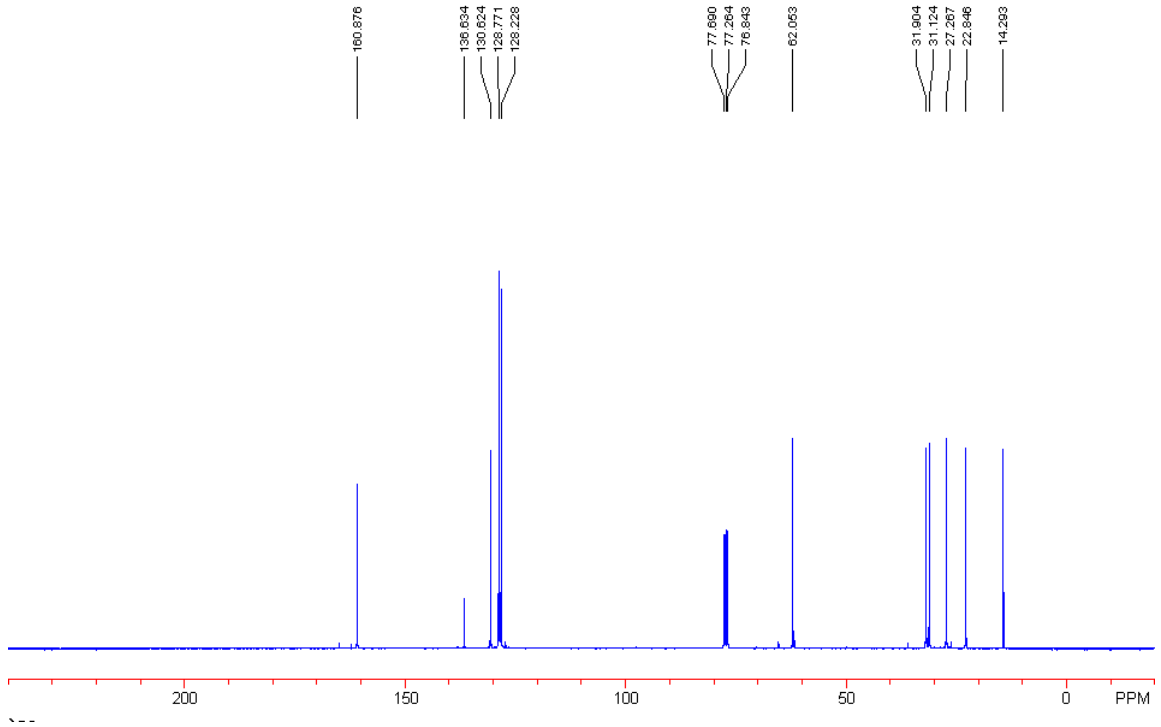
160.876
136.634
130.624
128.771
128.228
77.690
77.264
76.843
62.053
31.904
31.124
27.267
22.846
14.293
200
150
100
50
0
PPM

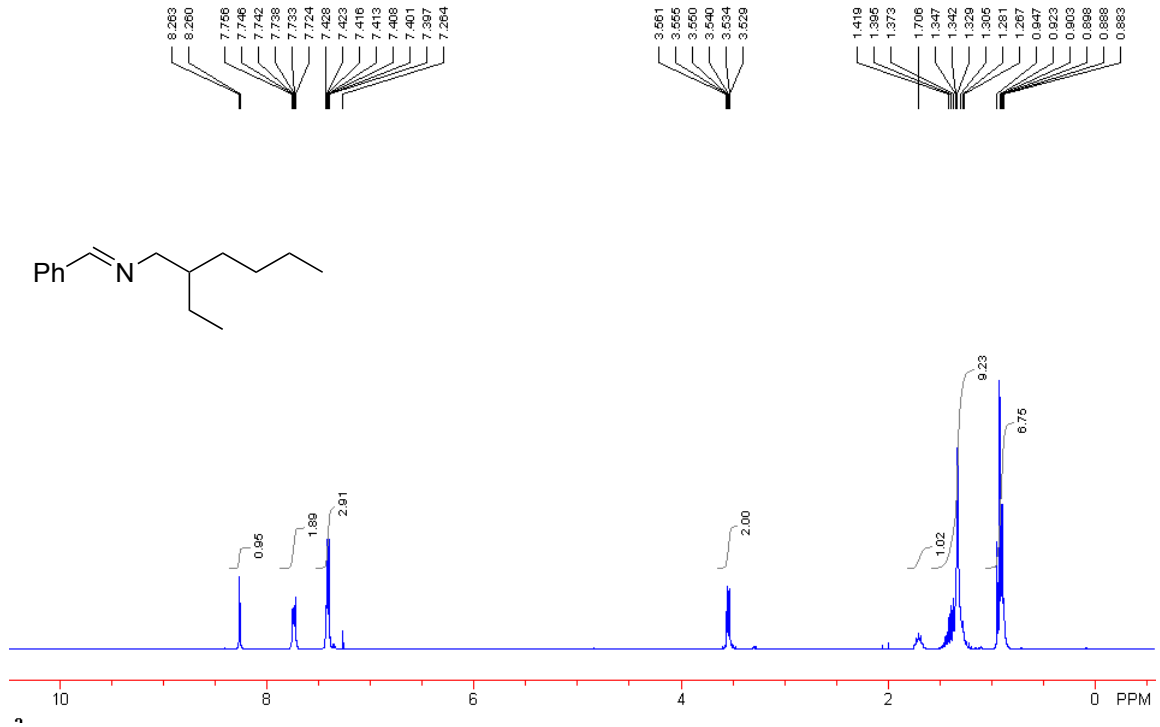
8.263
8.260
7.756
7.746
7.742
7.738
7.733
7.724
7.428
7.423
7.416
7.413
7.408
7.401
7.397
7.264
3.561
3.555
3.550
3.540
3.534
3.529
1.419
1.395
1.373
1.706
1.347
1.342
1.329
1.305
1.281
1.267
0.947
0.923
0.903
0.898
0.888
0.883
Ph
N
0.95
1.89
2.91
2.00
1.02
9.23
6.75
10
8
6
4
2
0
PPM

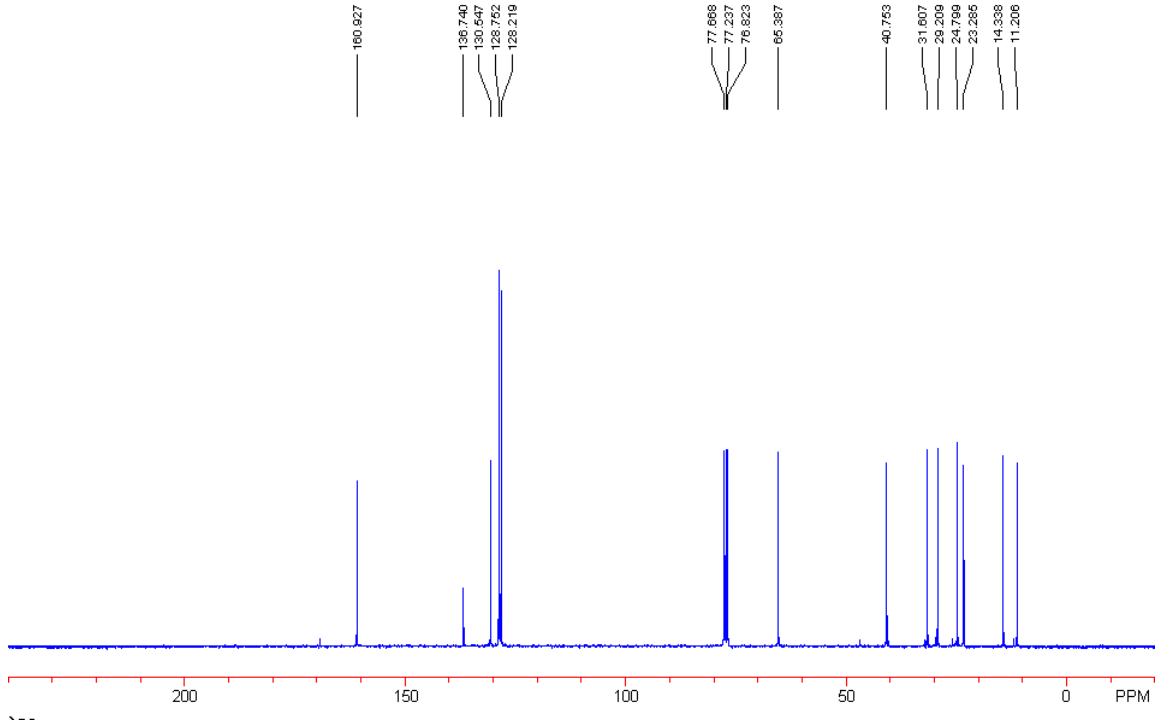
160.927
136.740
130.547
128.752
128.219
77.668
77.237
76.823
65.387
40.753
31.607
29.209
24.799
23.285
14.338
11.206
200
150
100
50
0
PPM

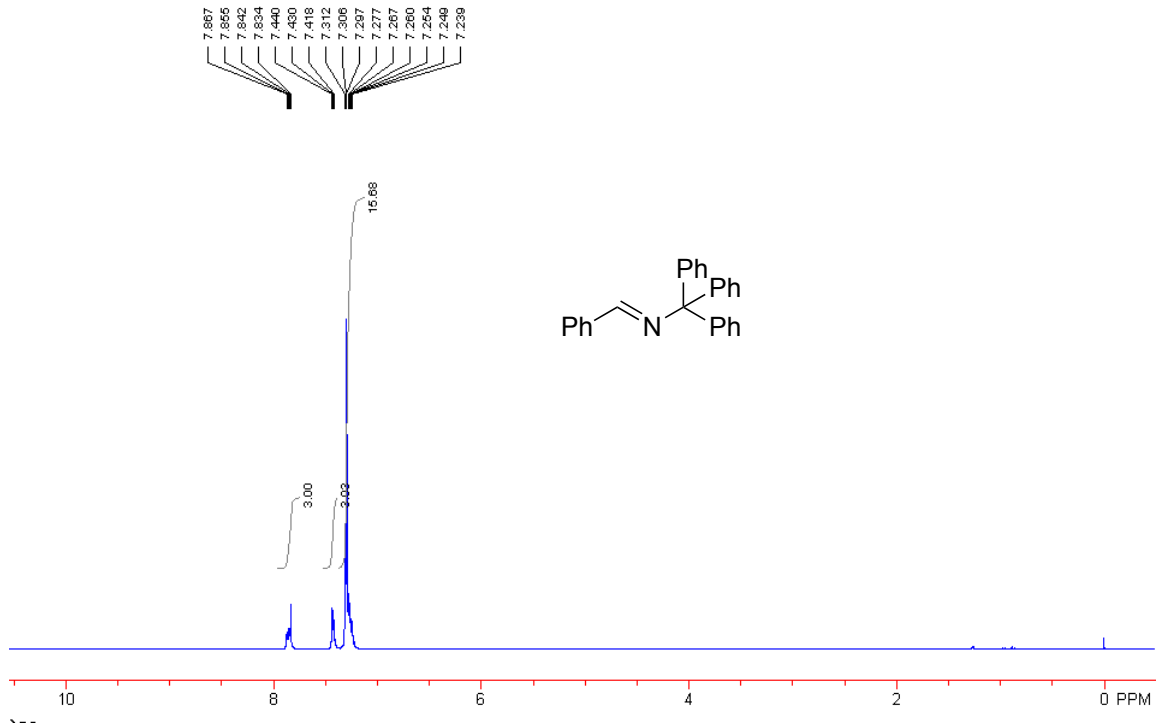
7.867
7.856
7.842
7.834
7.440
7.430
7.418
7.312
7.306
7.297
7.277
7.267
7.260
7.254
7.249
7.239
15.68
3.00
3.03
Ph
Ph
Ph
Ph
N
10
8
6
4
2
0 PPM

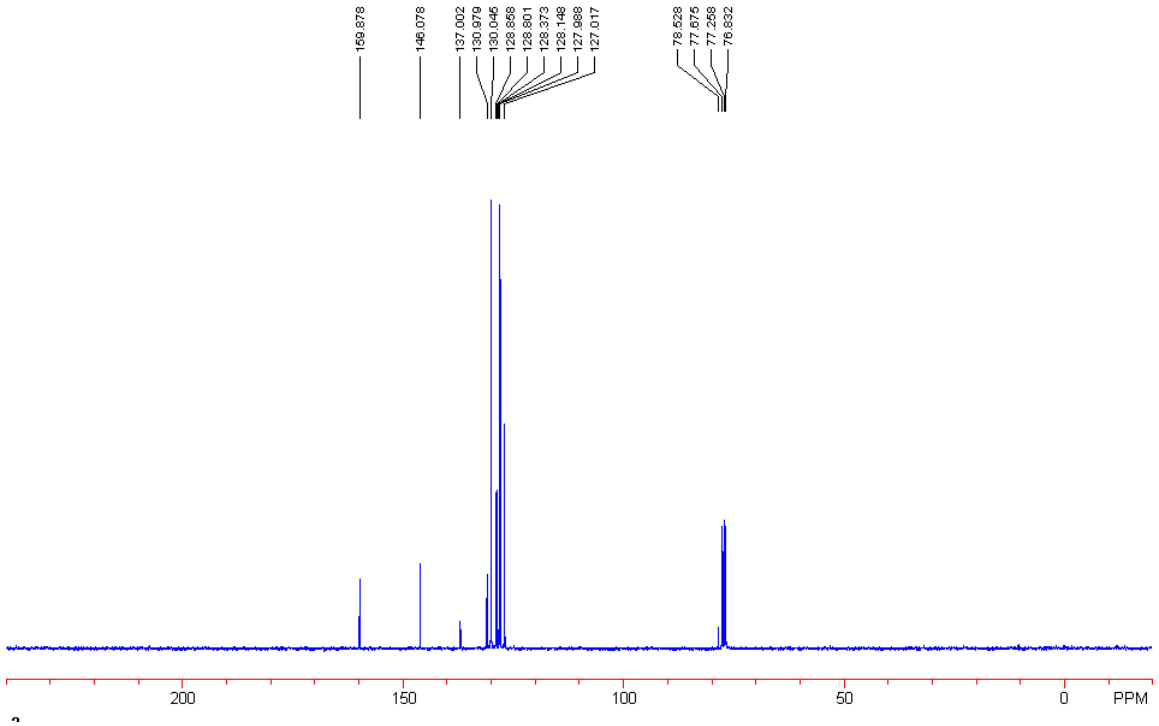
159.878
146.078
137.002
130.979
130.045
128.858
128.801
128.373
128.148
127.988
127.017
78.528
77.675
77.258
76.832
200
150
100
50
0
PPM

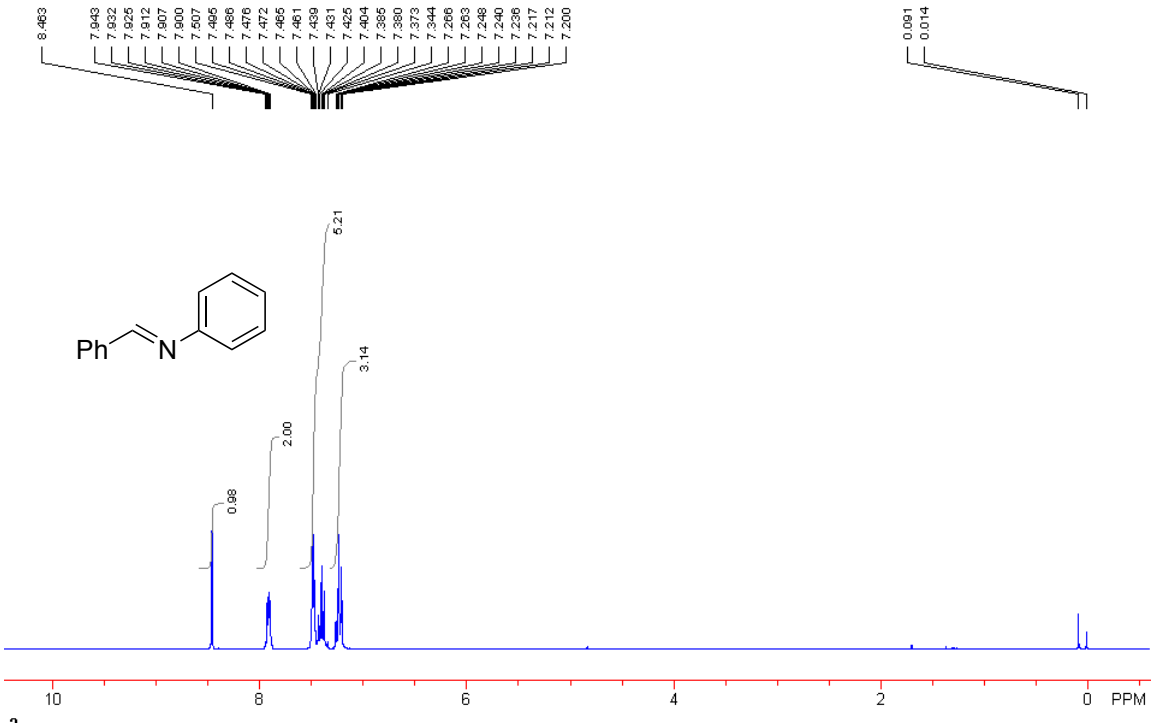
8.463
7.943
7.932
7.925
7.912
7.907
7.900
7.507
7.495
7.486
7.476
7.472
7.465
7.461
7.439
7.431
7.425
7.404
7.385
7.380
7.373
7.344
7.266
7.263
7.248
7.240
7.236
7.217
7.212
7.200
0.091
0.014
Ph
N
6.21
3.14
2.00
0.98
10
8
6
4
2
0
PPM

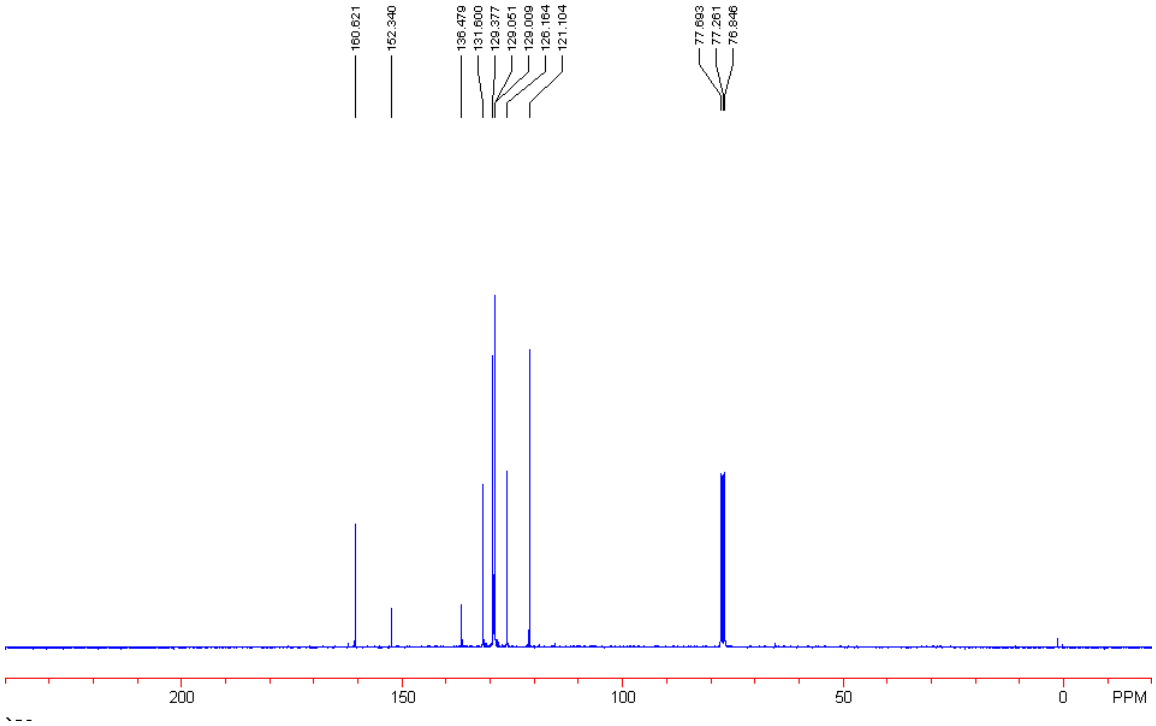
160.621
152.340
136.479
131.600
129.377
129.051
129.009
126.164
121.104
77.693
77.261
76.846
200
150
100
50
0
PPM

O
OH
O

TBHBQ

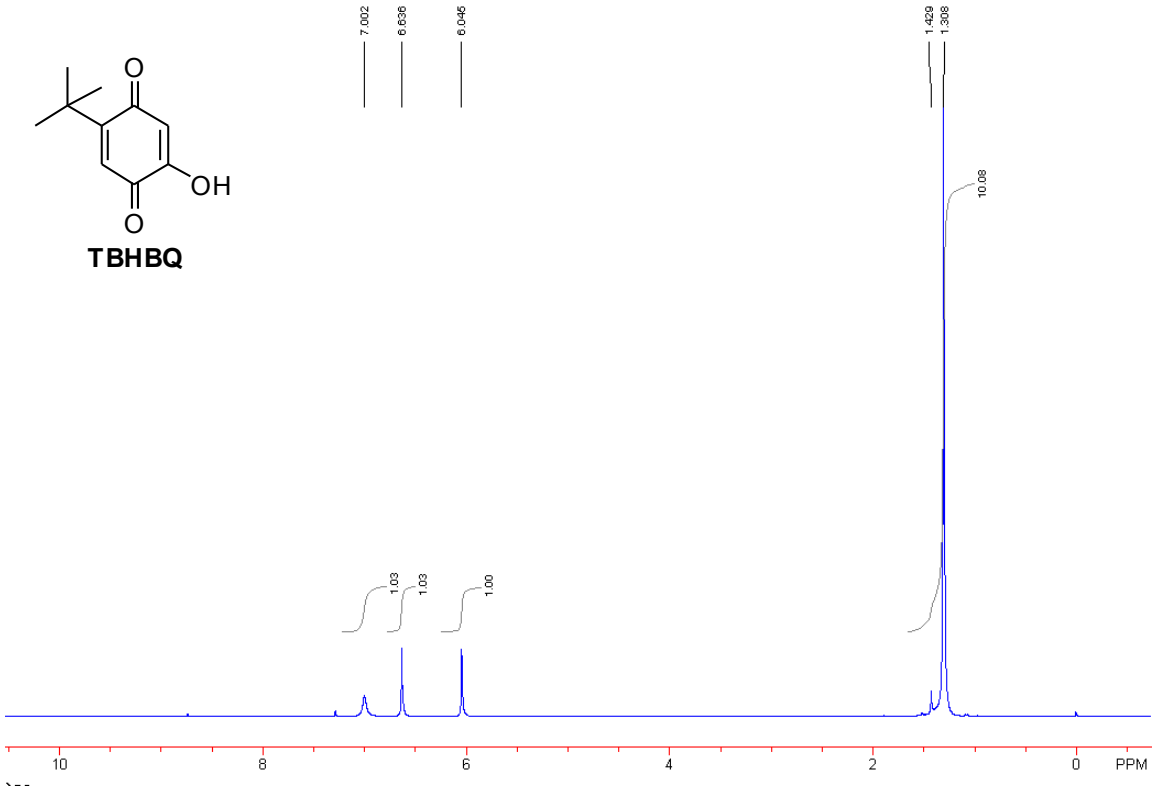
7.002
6.636
6.045
1.429
1.308
10.08
1.03
1.03
1.00
10
8
6
4
2
0
PPM

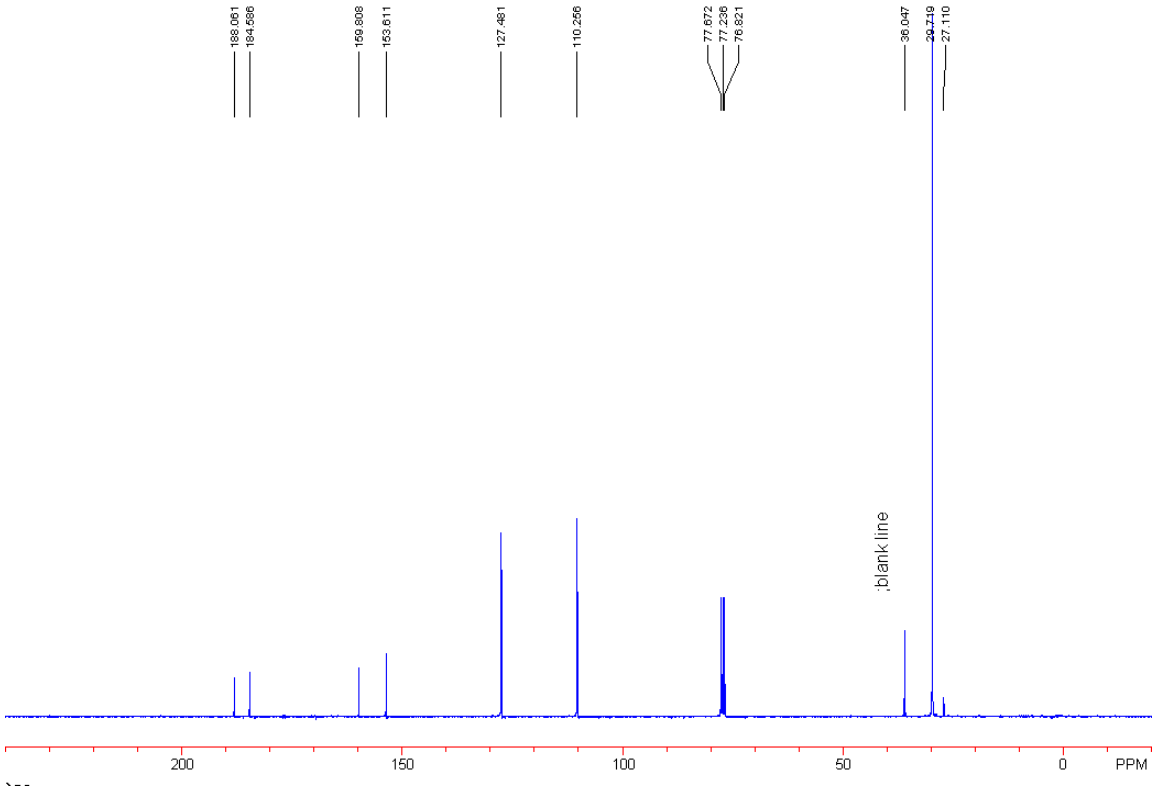
186.061
184.586
159.808
153.611
127.481
110.256
77.672
77.236
76.821
36.047
29.719
27.110
blank line
200
150
100
50
0
PPM

Appendix 2

Supplemental Information for Chapter 3

This work has been published:

Wendlandt, A. E.; Stahl, S. S. *J. Am. Chem. Soc.* **2014**, *136*, 506-512.

.

^{1}H and ^{13}C NMR of 1,10-phenanthroline-5,6-dione, phd

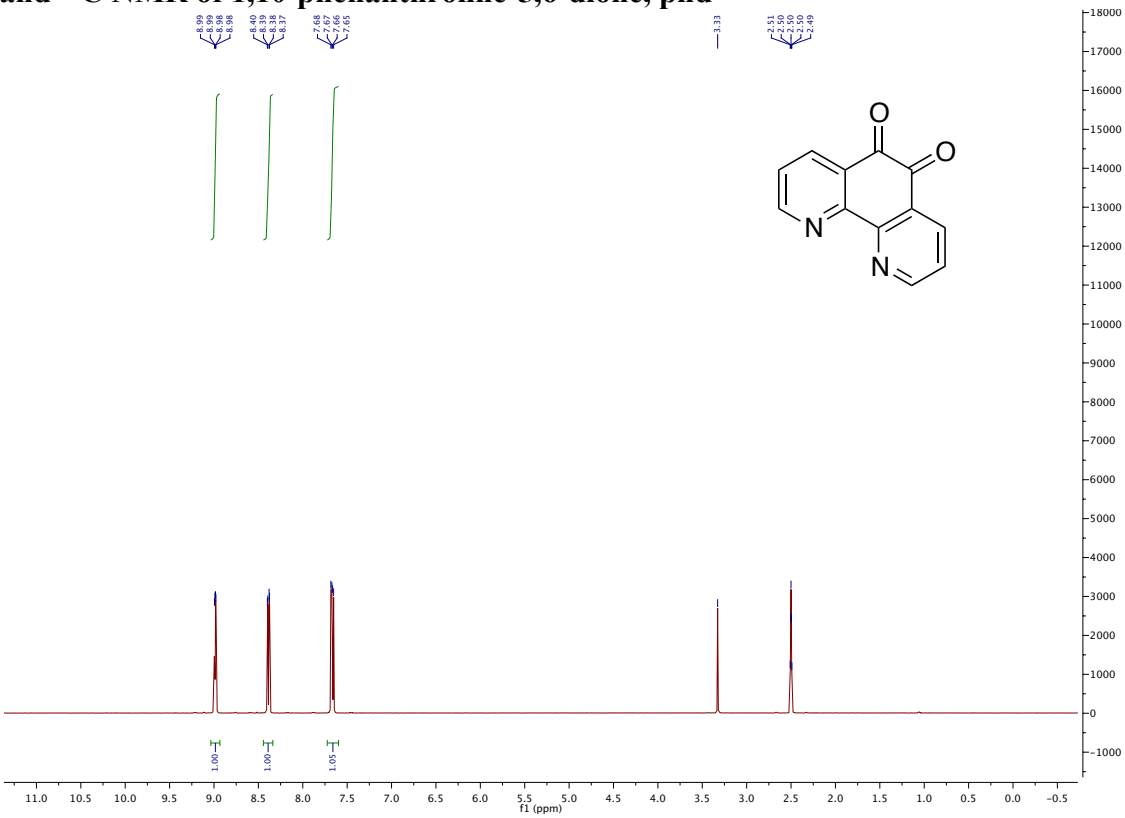

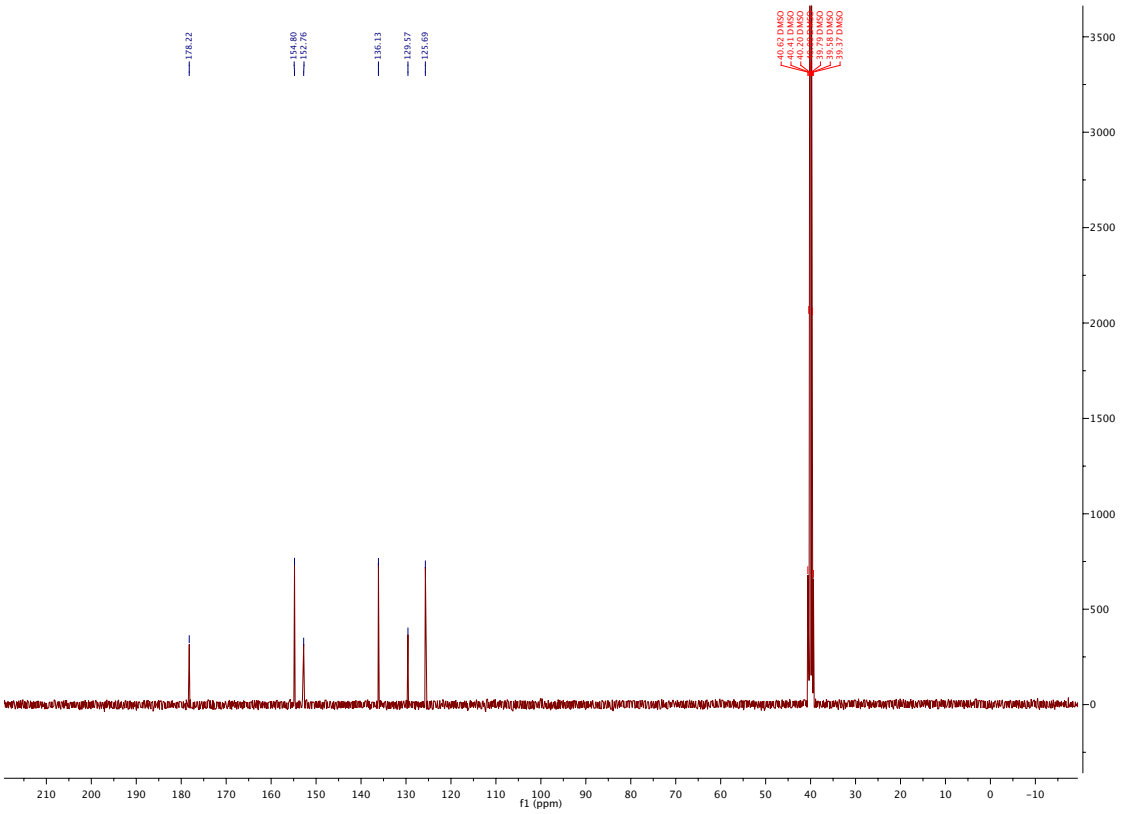

^{1}H and ^{13}C NMR of 1,10-phenanthroline-5,6-diol, phd-H_2

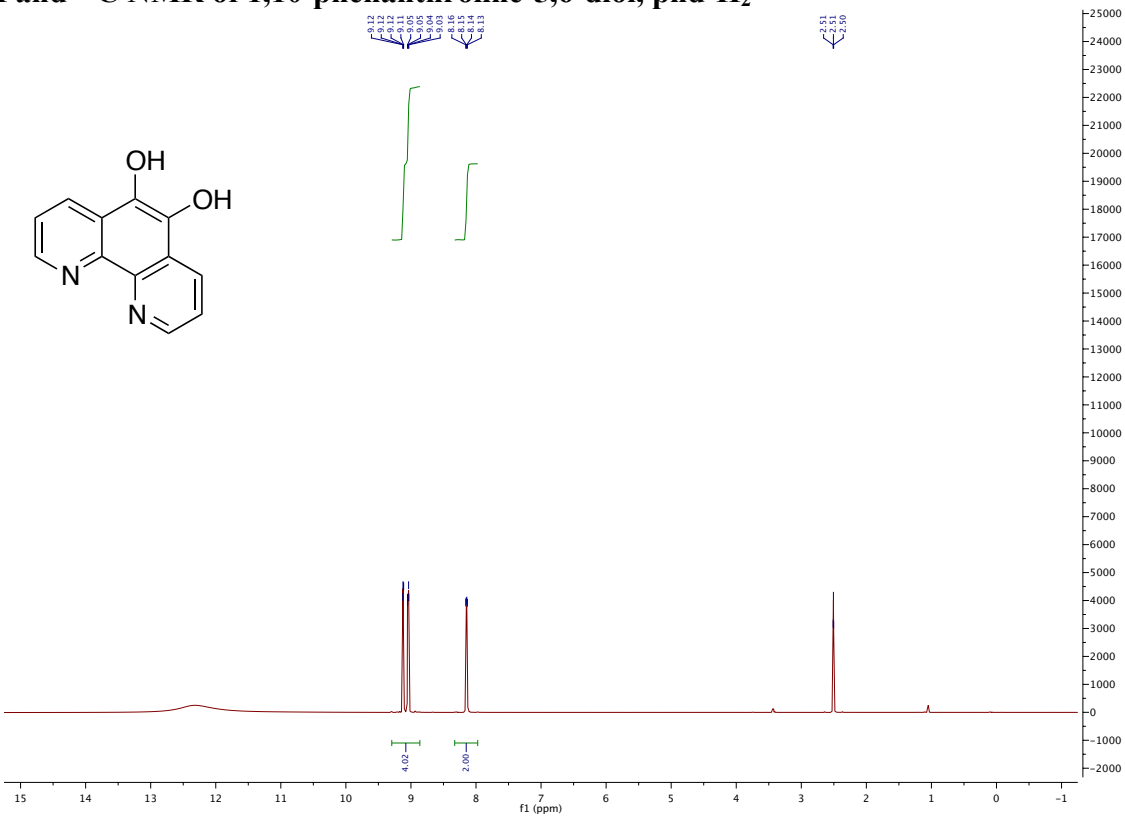

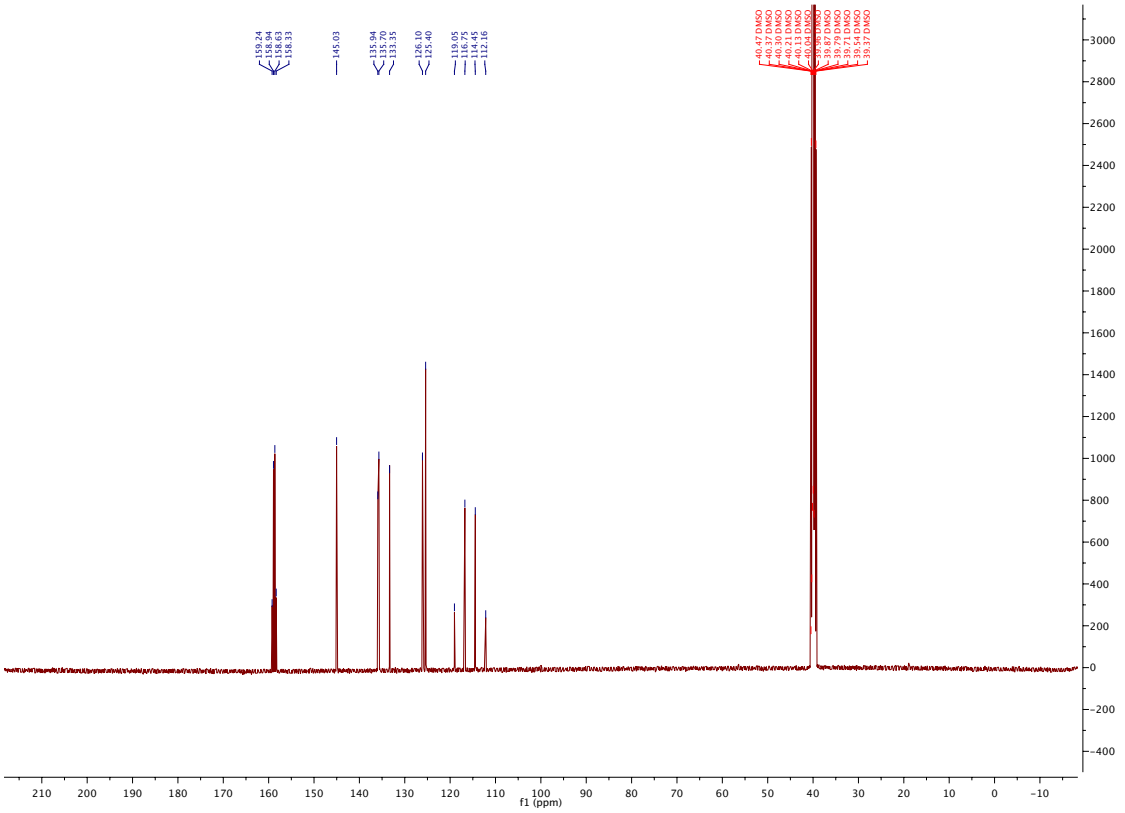

^{1}H and ^{13}C NMR Spectra of Products

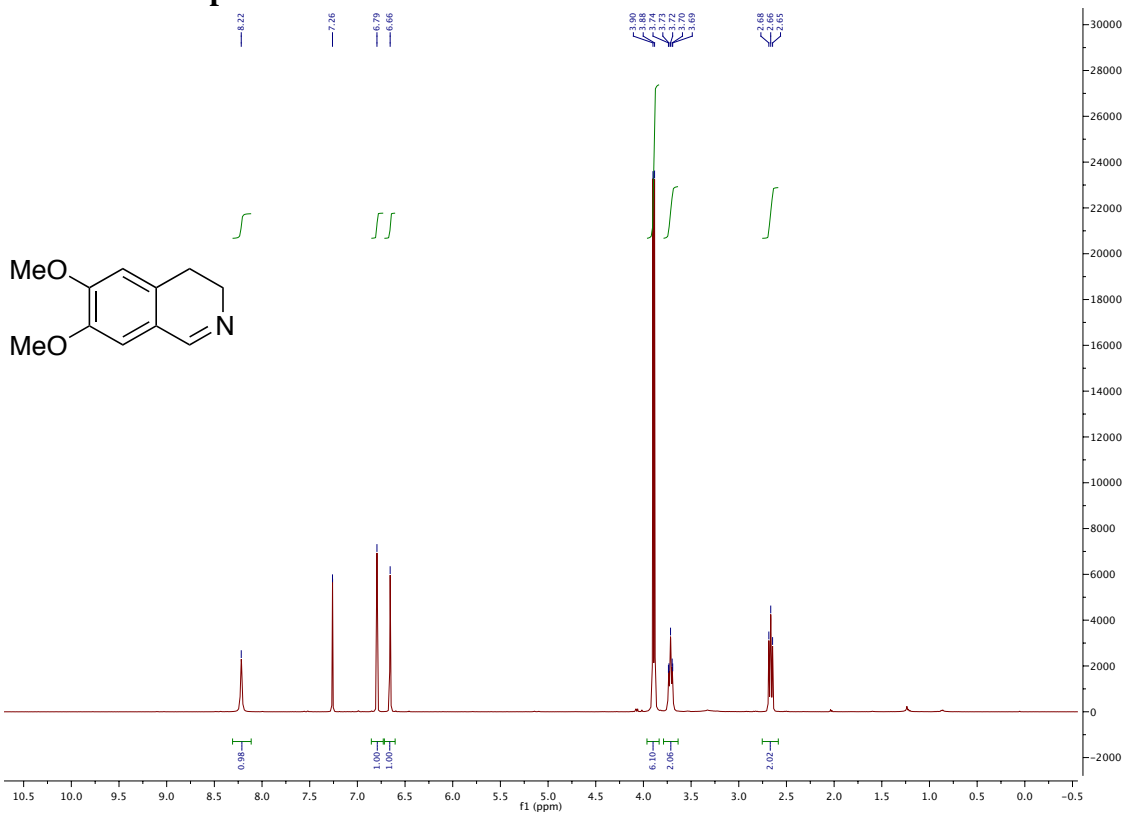

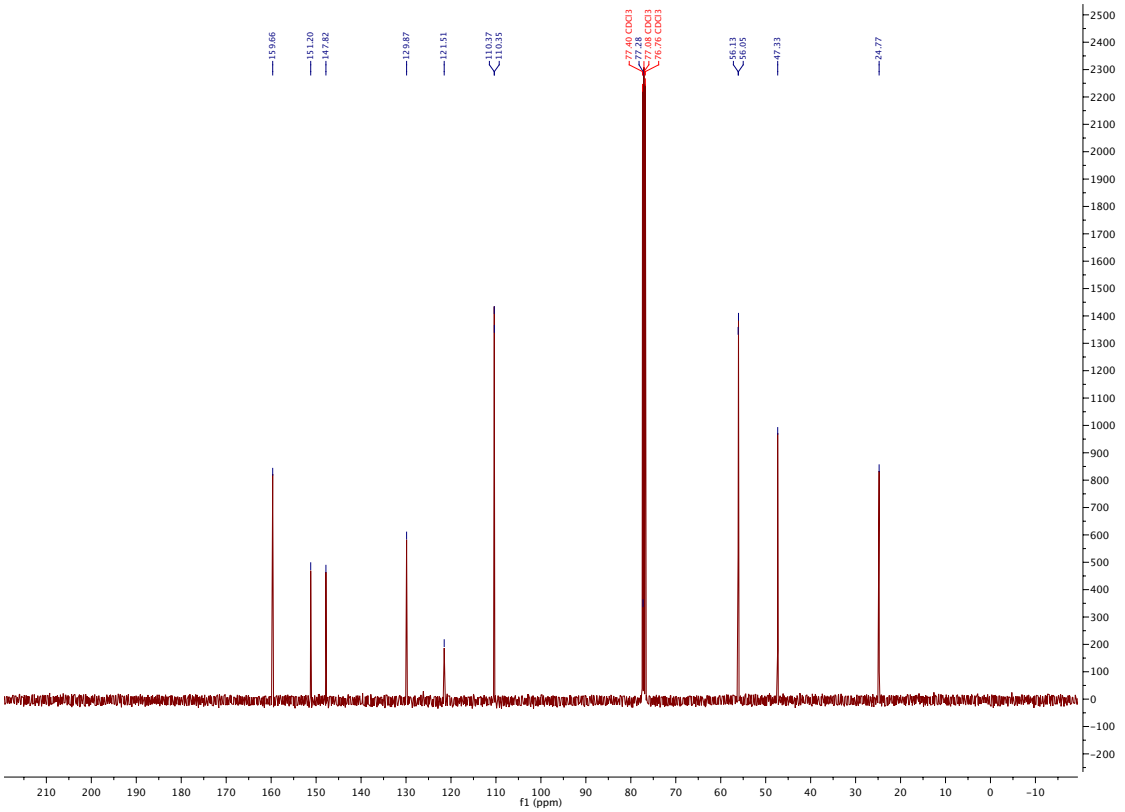

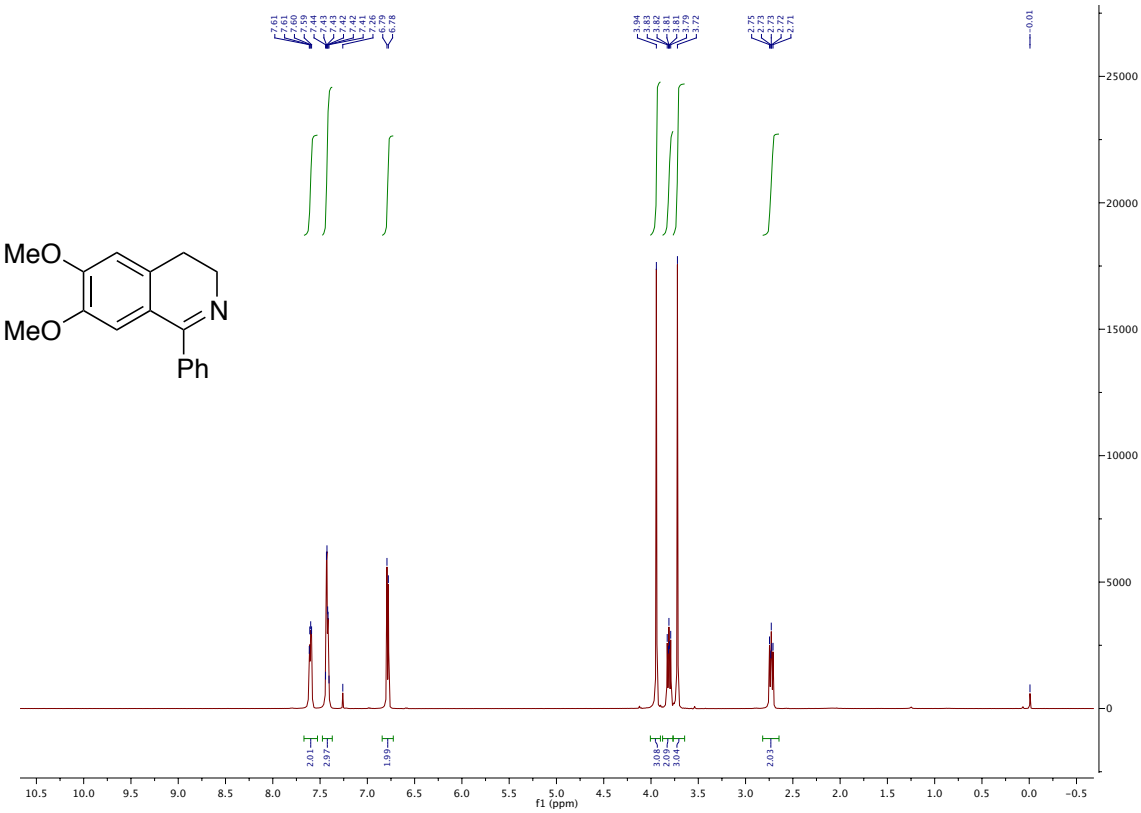
MeO
MeO
N
Ph
f1 (ppm)

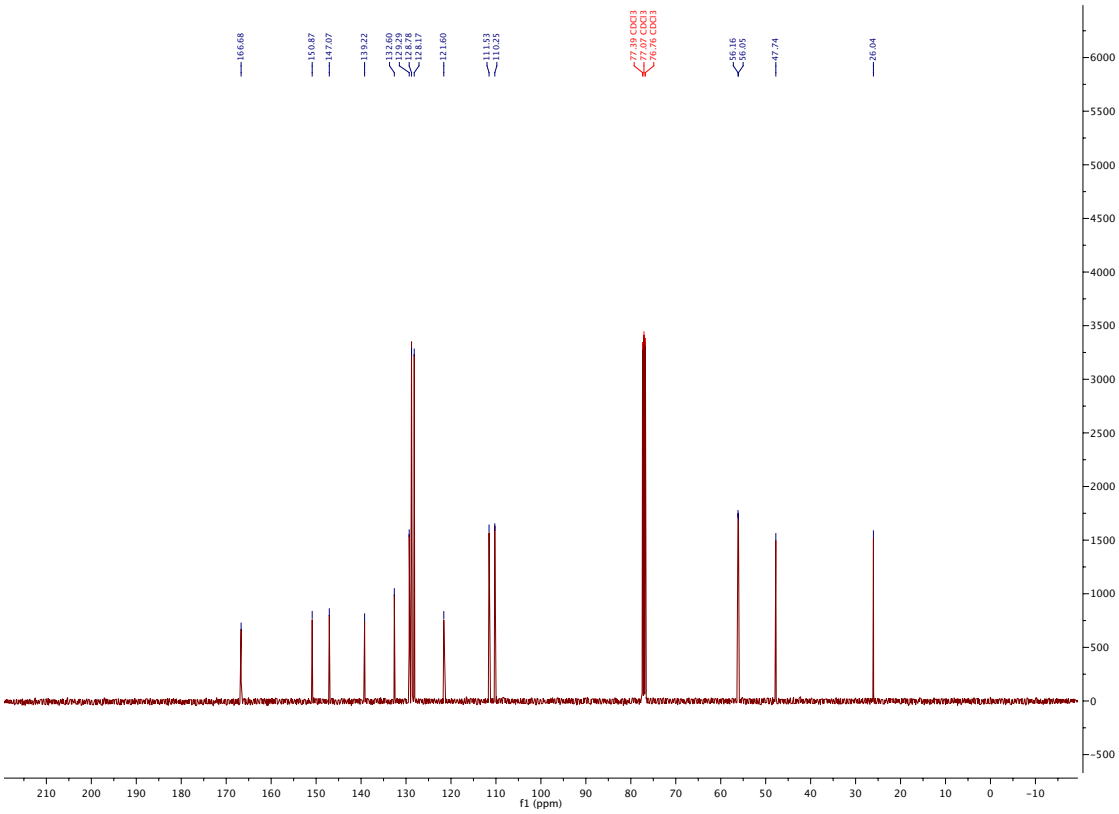
f1 (ppm)

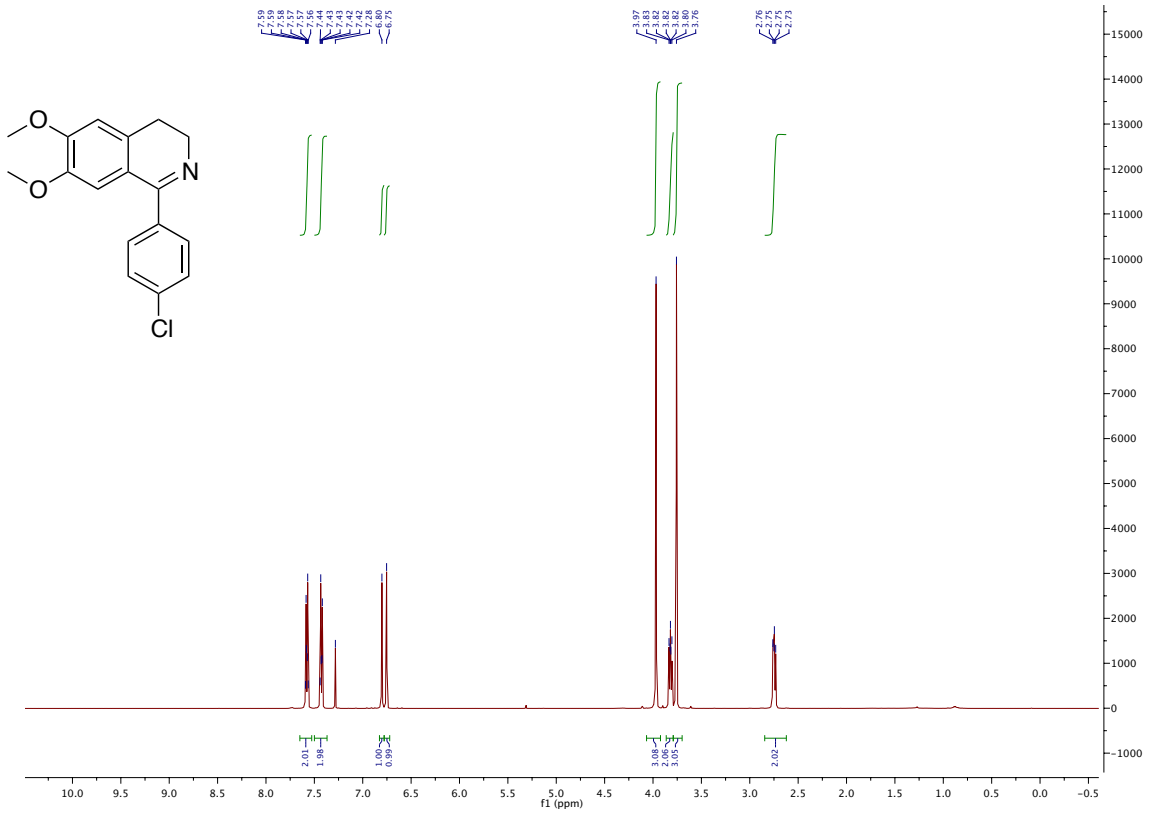
O
O
N
Cl
7.59
7.59
7.58
7.58
7.57
7.57
7.56
7.56
7.44
7.43
7.43
7.42
7.42
7.28
6.80
6.75
3.97
3.83
3.82
3.82
3.82
3.80
3.76
2.76
2.75
2.75
2.73
2.01
1.98
1.00
0.99
3.08
2.06
3.05
2.02
f1 (ppm)

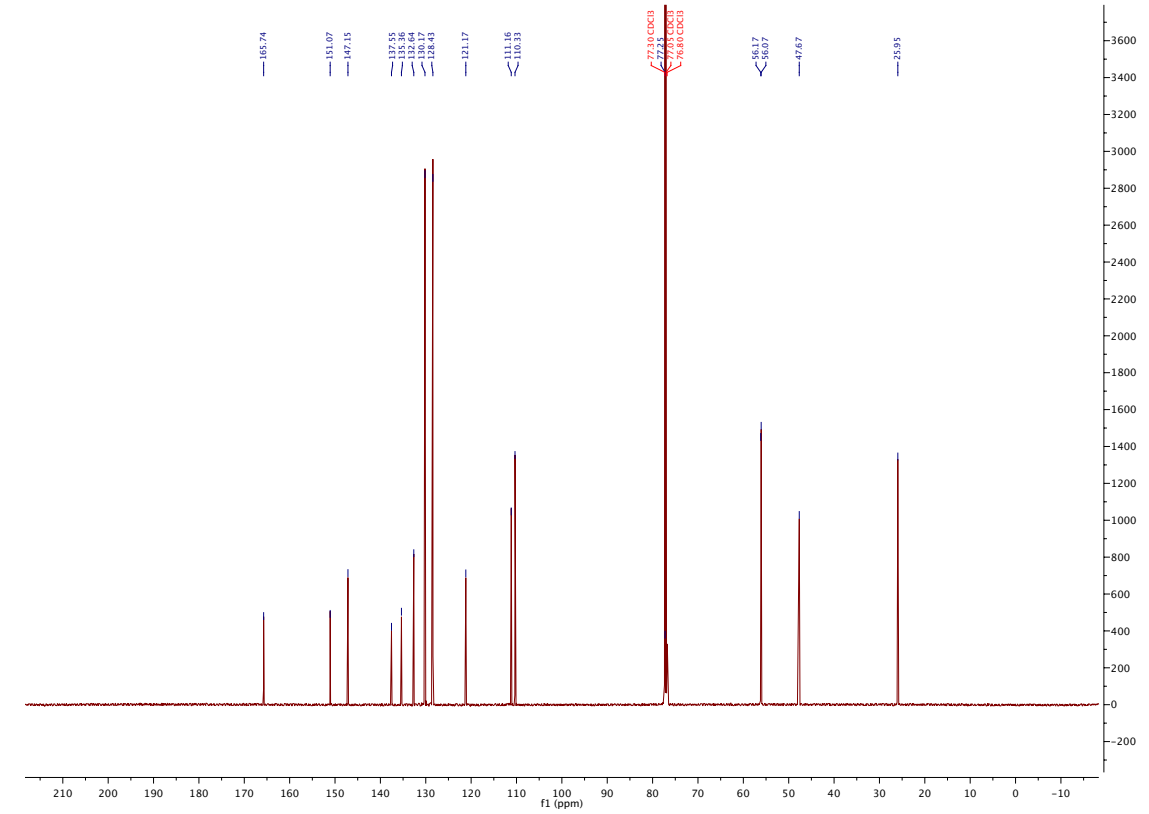
165.74
151.07
147.15
137.55
135.46
132.64
130.17
128.43
121.17
111.16
110.33
77.30 CDCl3
77.25
77.05 CDCl3
76.80 CDCl3
56.17
56.07
47.67
25.95
f1 (ppm)

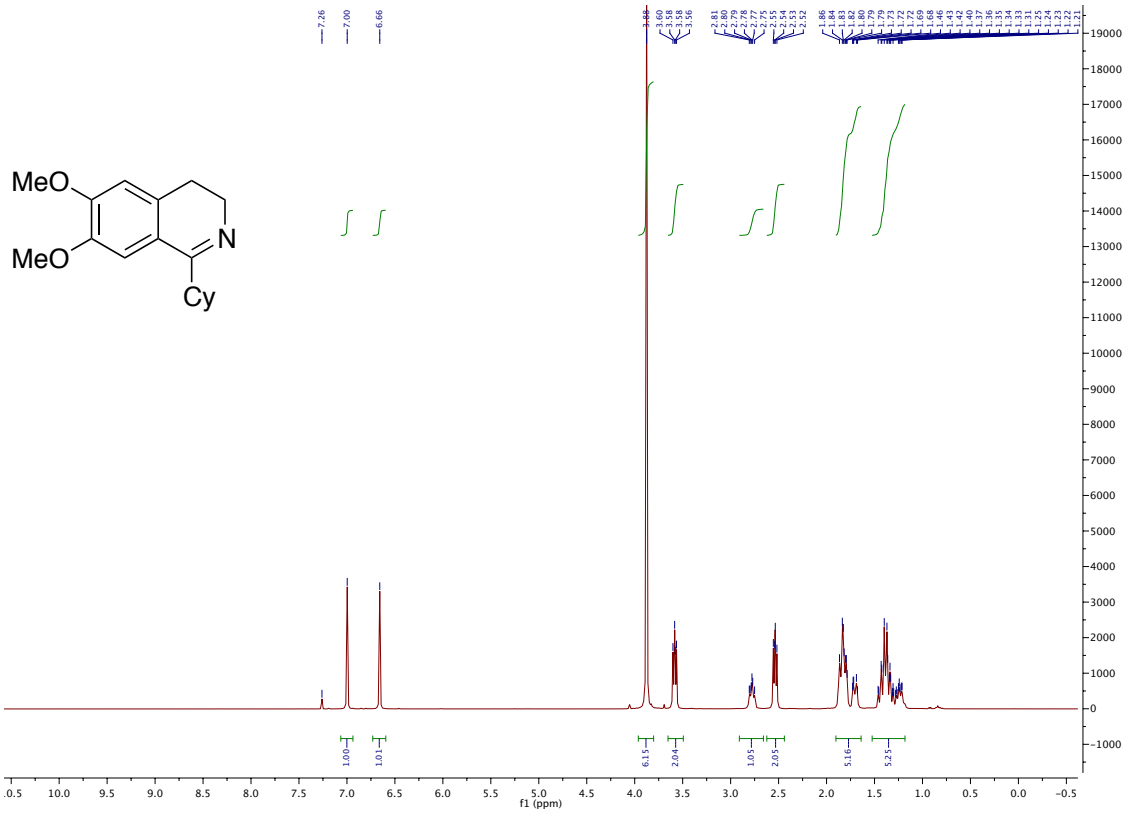
MeO
MeO
N
Cy
7.26
7.00
6.66
3.88
3.60
3.58
3.56
2.81
2.80
2.79
2.78
2.77
2.75
2.55
2.54
2.53
2.52
1.86
1.84
1.83
1.82
1.80
1.79
1.78
1.73
1.72
1.71
1.69
1.68
1.46
1.43
1.42
1.40
1.37
1.36
1.35
1.34
1.33
1.31
1.25
1.24
1.23
1.22
1.21
1.00
1.01
6.15
2.04
1.05
2.05
5.16
5.25
f1 (ppm)

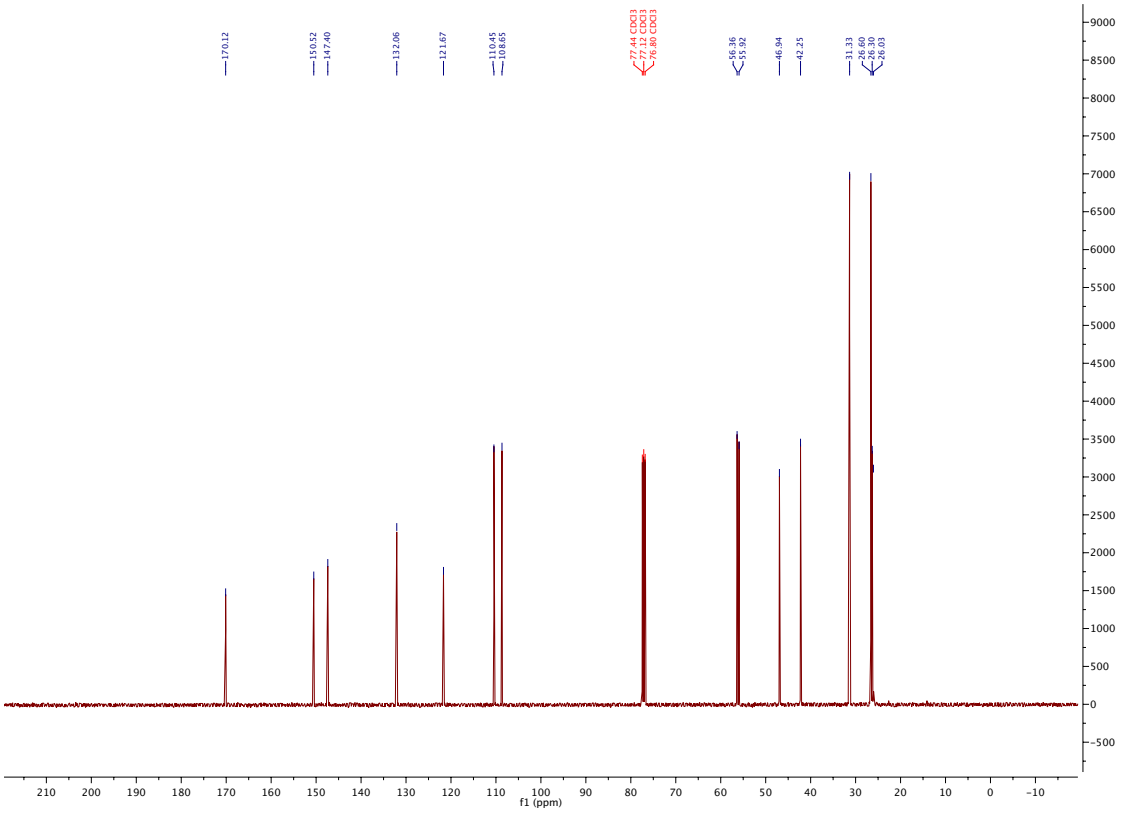
170.12
150.52
147.40
132.06
121.67
110.45
108.65
77.44 CDCl3
77.12 CDCl3
76.80 CDCl3
56.36
55.92
46.94
42.25
31.33
26.60
26.30
26.03
f1 (ppm)

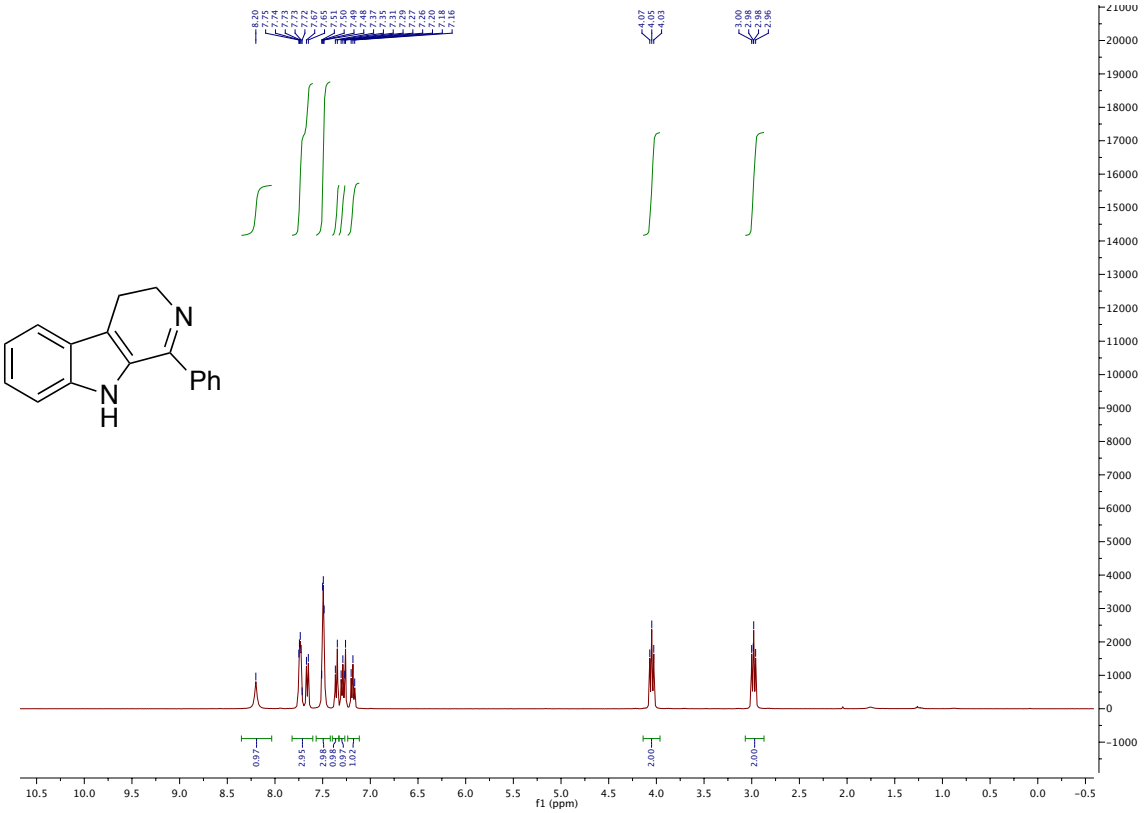
N
Ph
N
H
f1 (ppm)

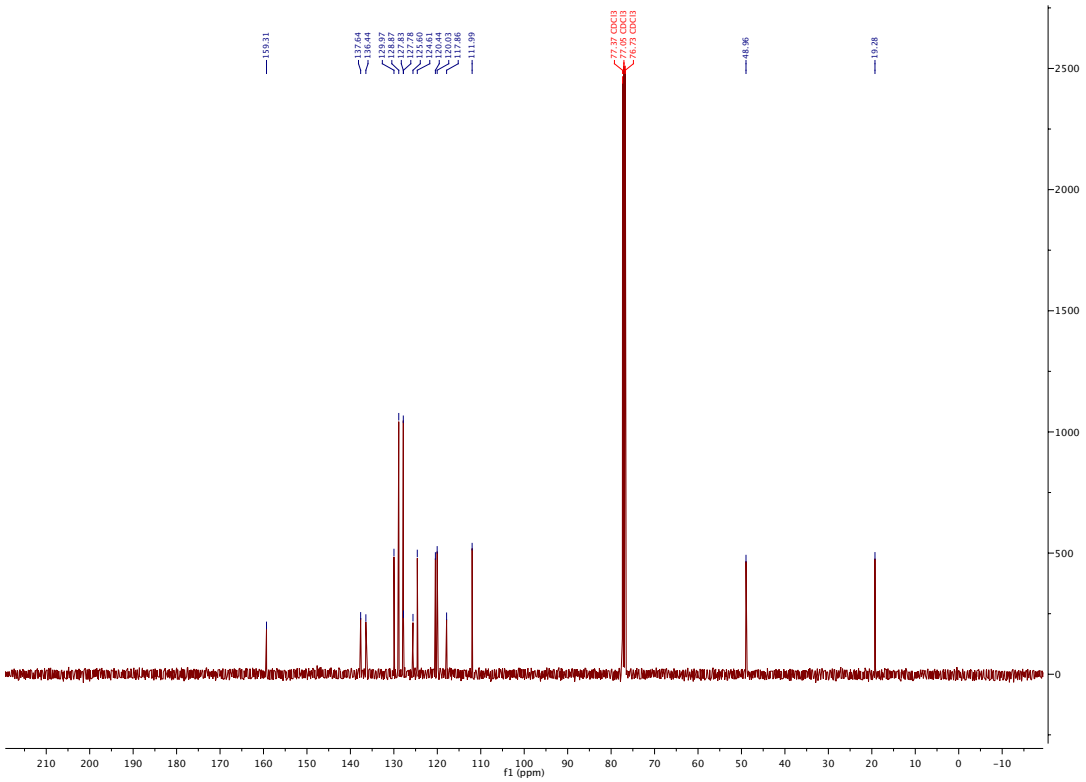
159.31
137.64
136.44
129.97
128.87
128.83
127.78
125.60
124.61
120.03
117.86
111.99
77.37 CDCl3
77.05 CDCl3
76.73 CDCl3
48.96
19.28
f1 (ppm)

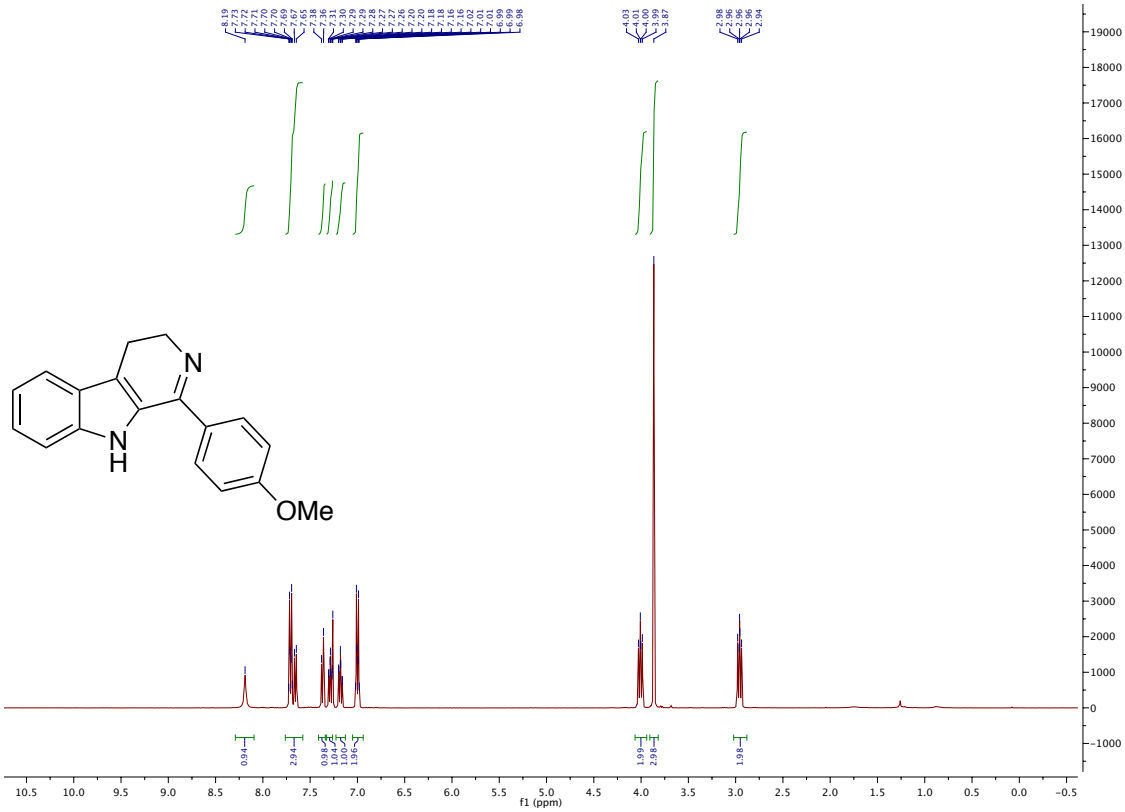
N
N
H
OMe
f1 (ppm)

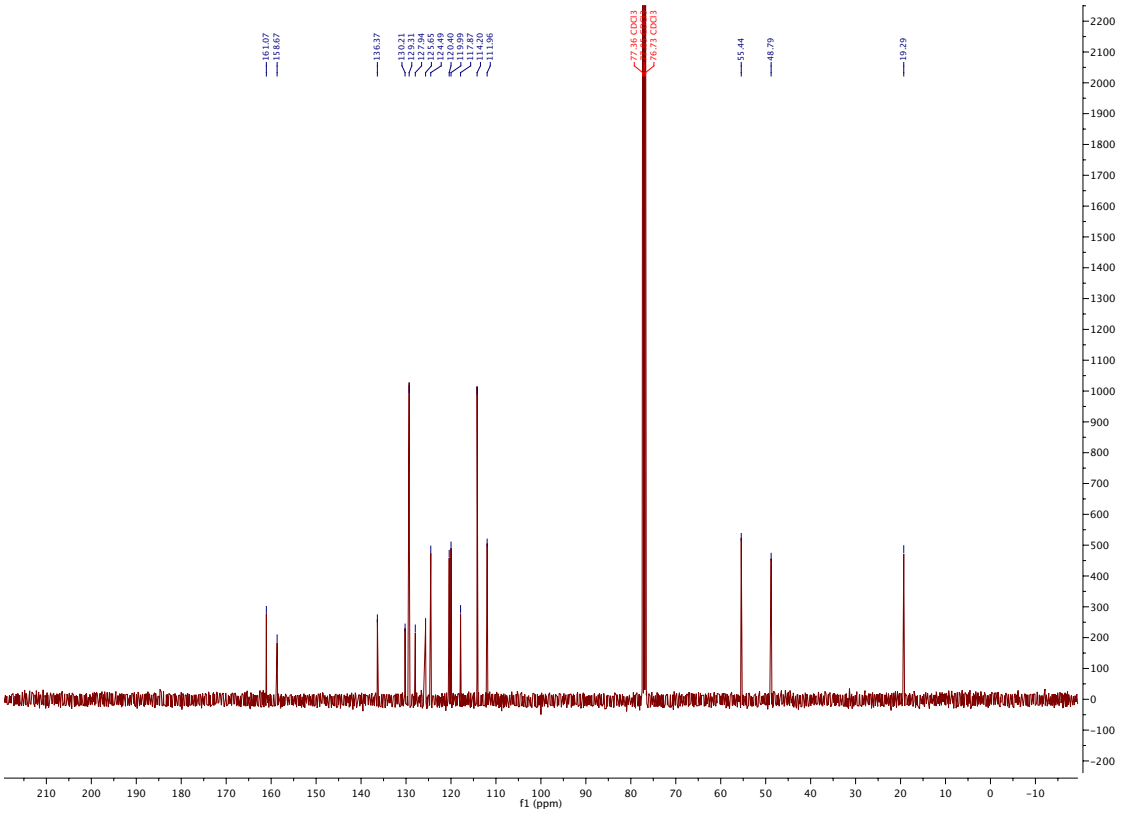
77.36 CDCl3
77.04 CDCl3
76.73 CDCl3
f1 (ppm)

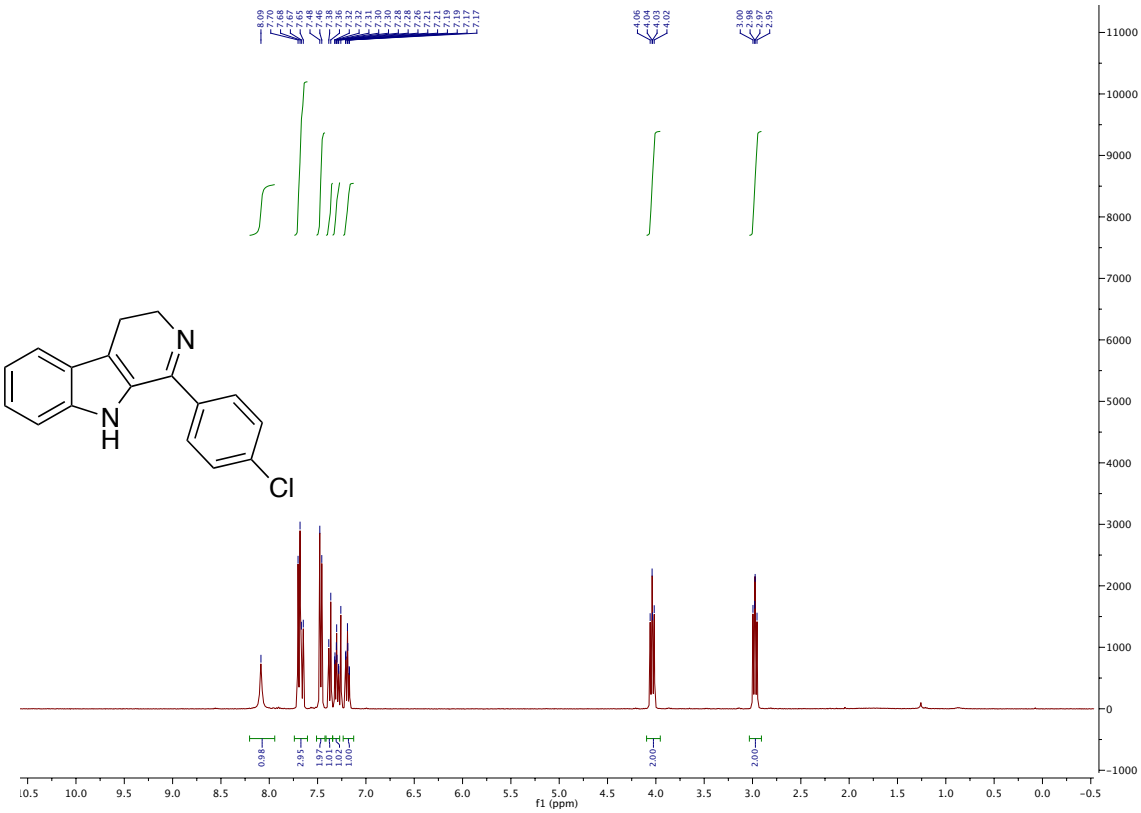
N
N
H
Cl
f1 (ppm)

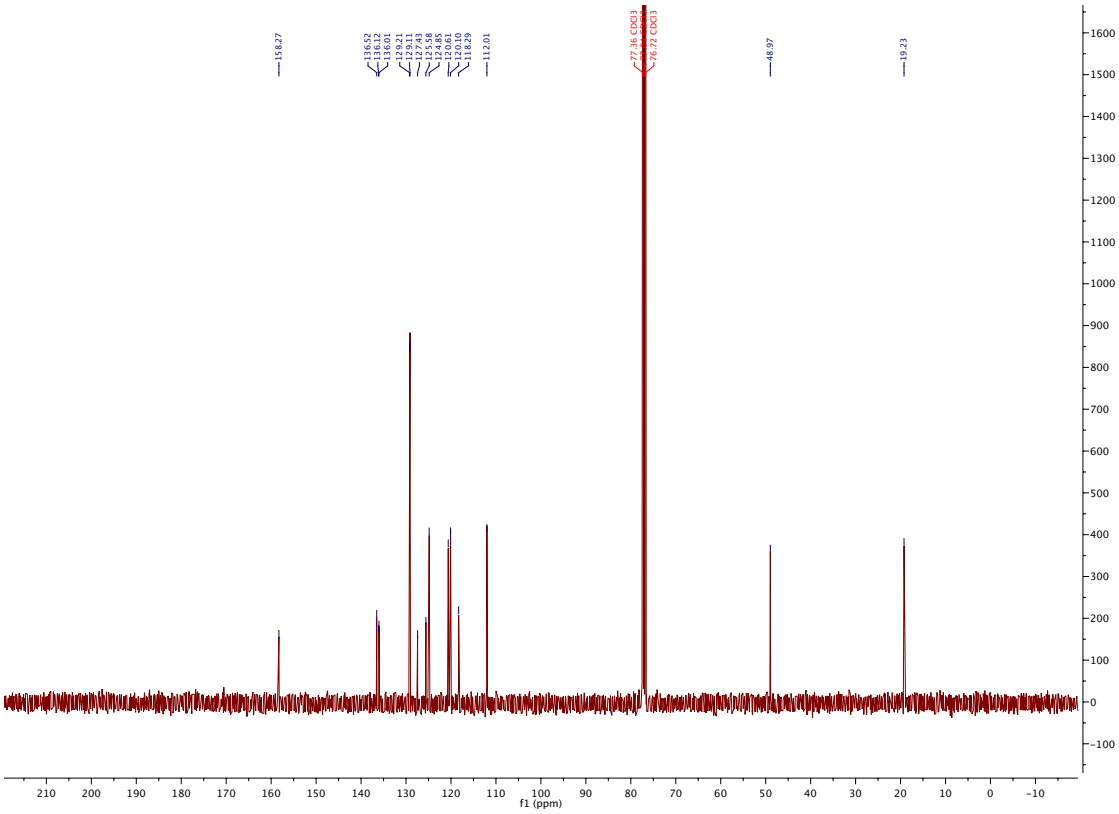
f1 (ppm)

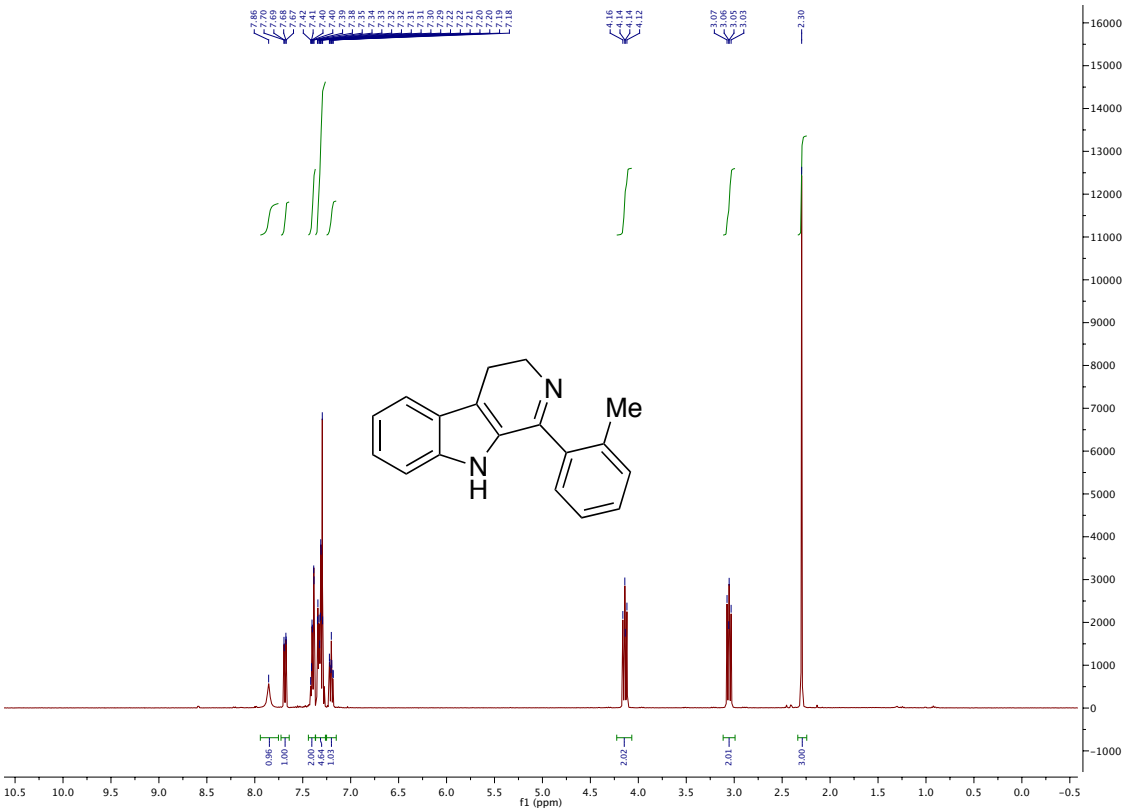
N
Me
N
H
f1 (ppm)

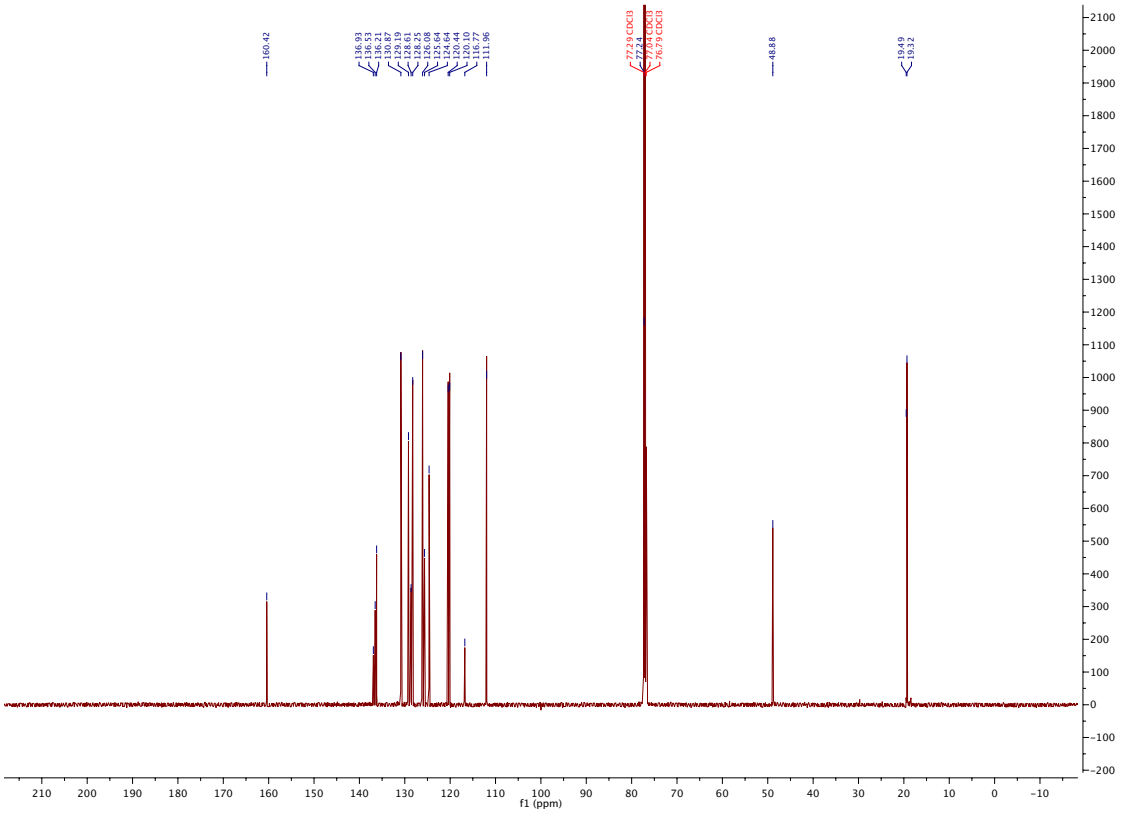
f1 (ppm)

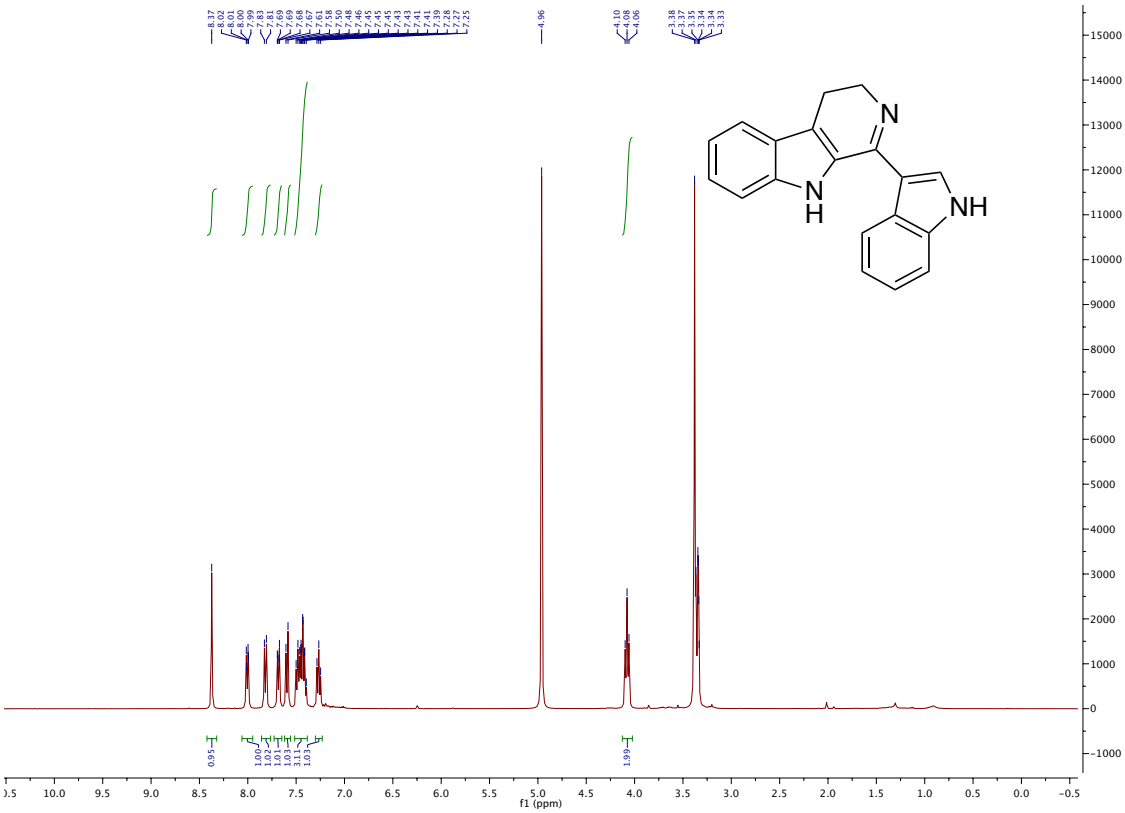
8.37
8.02
8.01
8.00
7.99
7.83
7.81
7.69
7.69
7.68
7.67
7.67
7.61
7.58
7.50
7.49
7.48
7.46
7.45
7.45
7.45
7.43
7.43
7.41
7.41
7.39
7.38
7.27
7.25
4.96
4.10
4.08
4.06
3.38
3.37
3.35
3.34
3.34
3.33
N
N
H
NH
0.95
1.00
1.02
1.01
1.01
1.01
1.17
1.01
1.99
f1 (ppm)

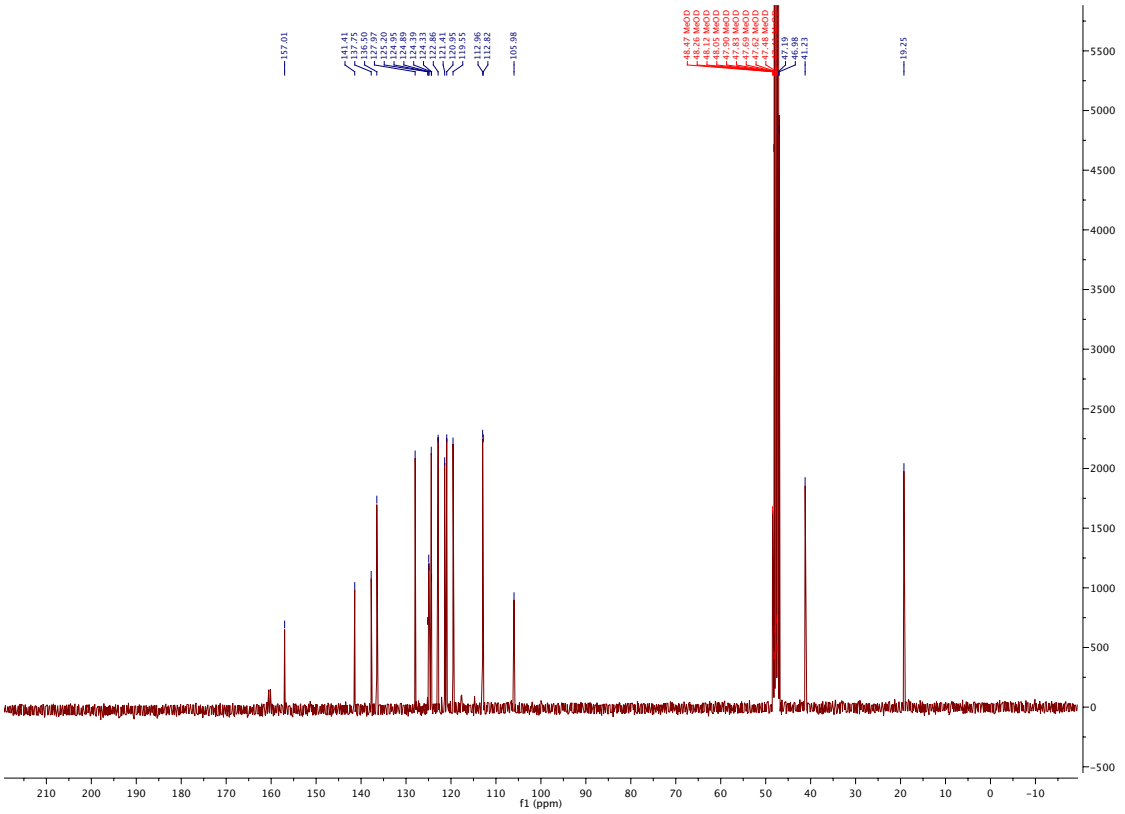
157.01
141.41
137.75
136.50
127.97
125.20
124.89
124.89
124.39
123.33
122.86
121.41
120.95
119.55
112.96
112.82
105.98
48.47 MeOD
48.26 MeOD
48.12 MeOD
48.05 MeOD
47.90 MeOD
47.83 MeOD
47.69 MeOD
47.62 MeOD
47.48 MeOD
47.19
46.98
41.23
19.25
f1 (ppm)

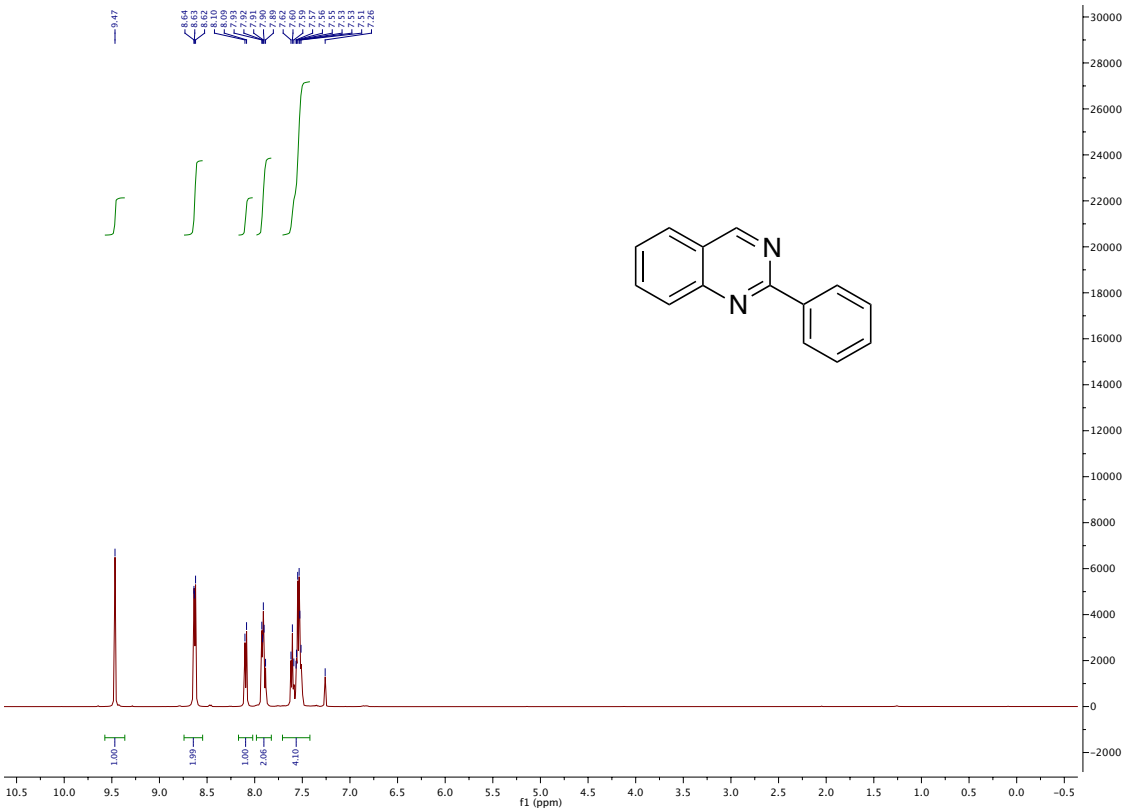
9.47
8.64
8.63
8.62
8.10
8.09
7.93
7.92
7.91
7.90
7.89
7.62
7.60
7.59
7.57
7.56
7.55
7.53
7.53
7.51
7.26
1.00
1.99
1.00
2.06
4.10
N
N
f1 (ppm)

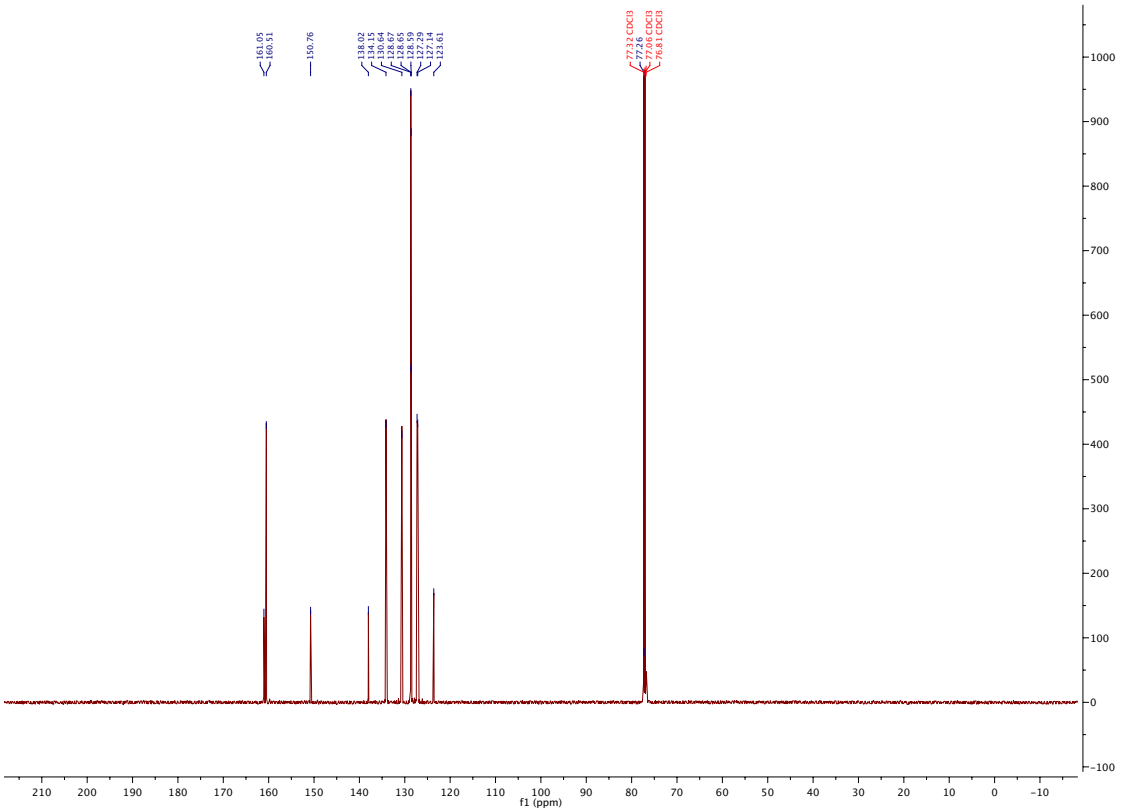
161.05
160.51
150.76
138.02
134.15
130.64
128.67
128.65
126.59
125.29
127.14
123.61
77.32 CDCl3
77.26
77.06 CDCl3
76.81 CDCl3
f1 (ppm)

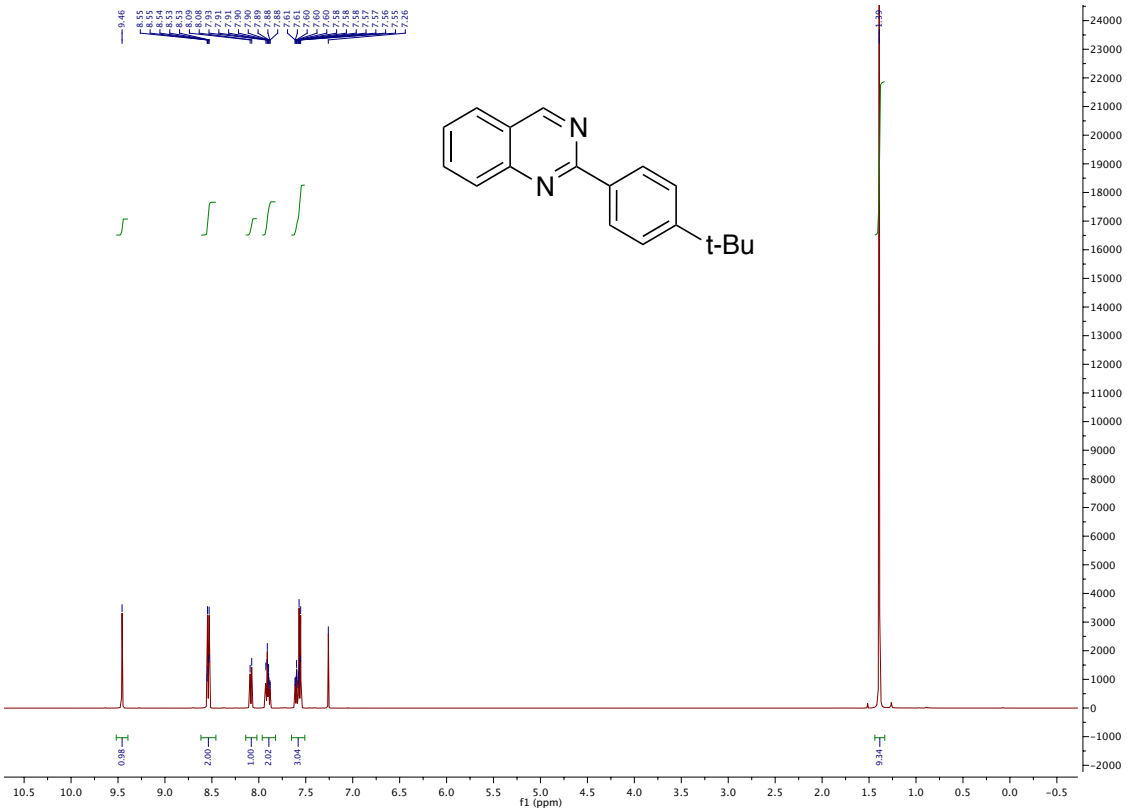
N
N
t-Bu
f1 (ppm)

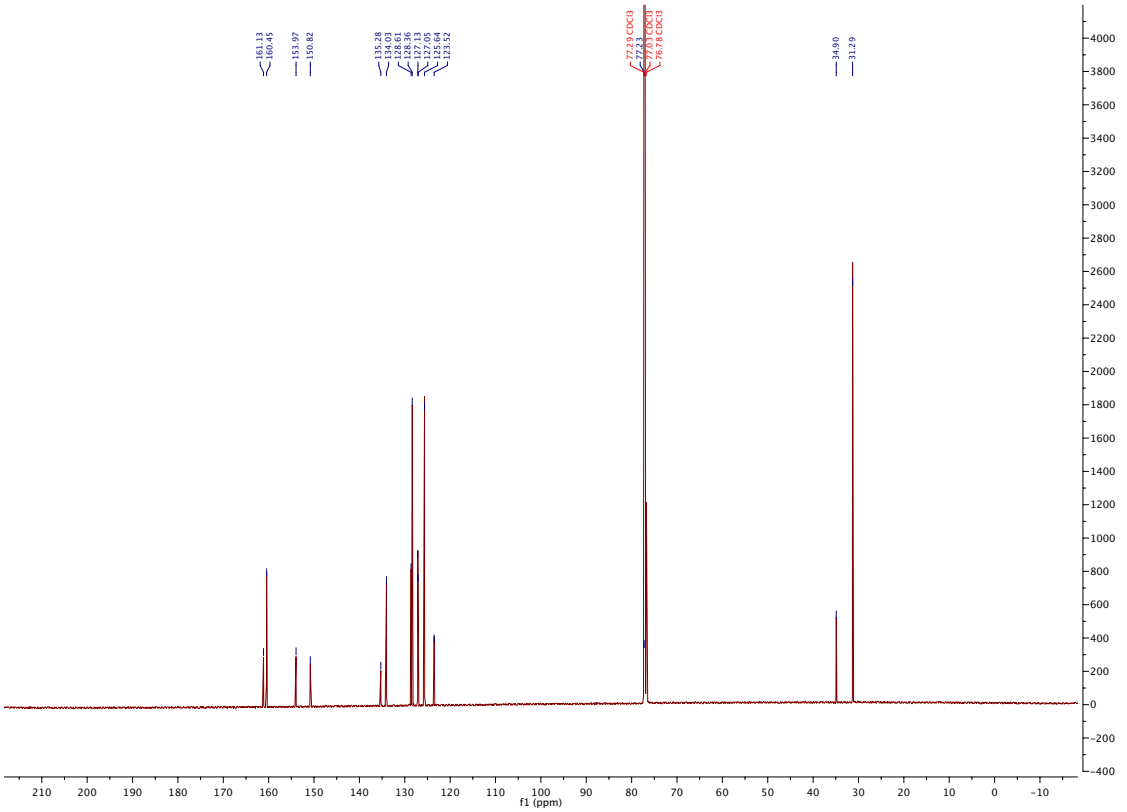
f1 (ppm)

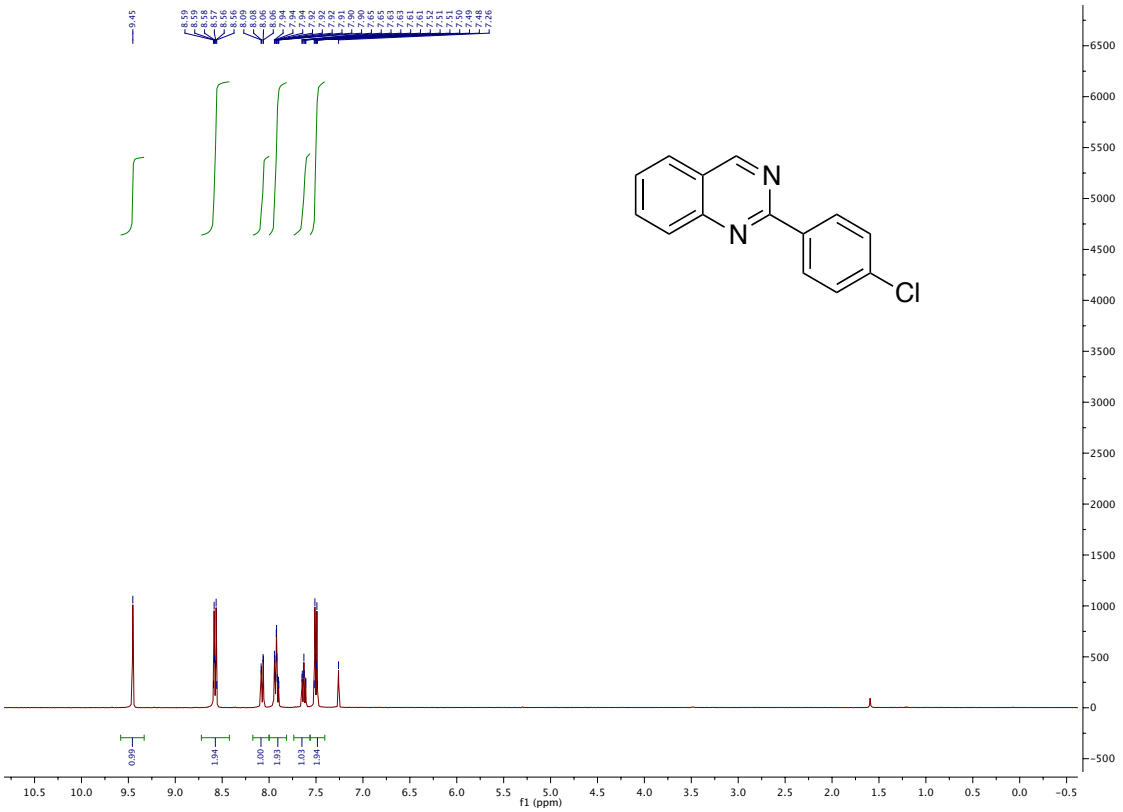
9.45
8.59
8.58
8.57
8.56
8.09
8.08
8.06
7.94
7.92
7.91
7.90
7.65
7.63
7.61
7.52
7.51
7.50
7.49
7.48
7.26
N
N
Cl
0.99
1.94
1.00
1.93
1.03
1.94
f1 (ppm)

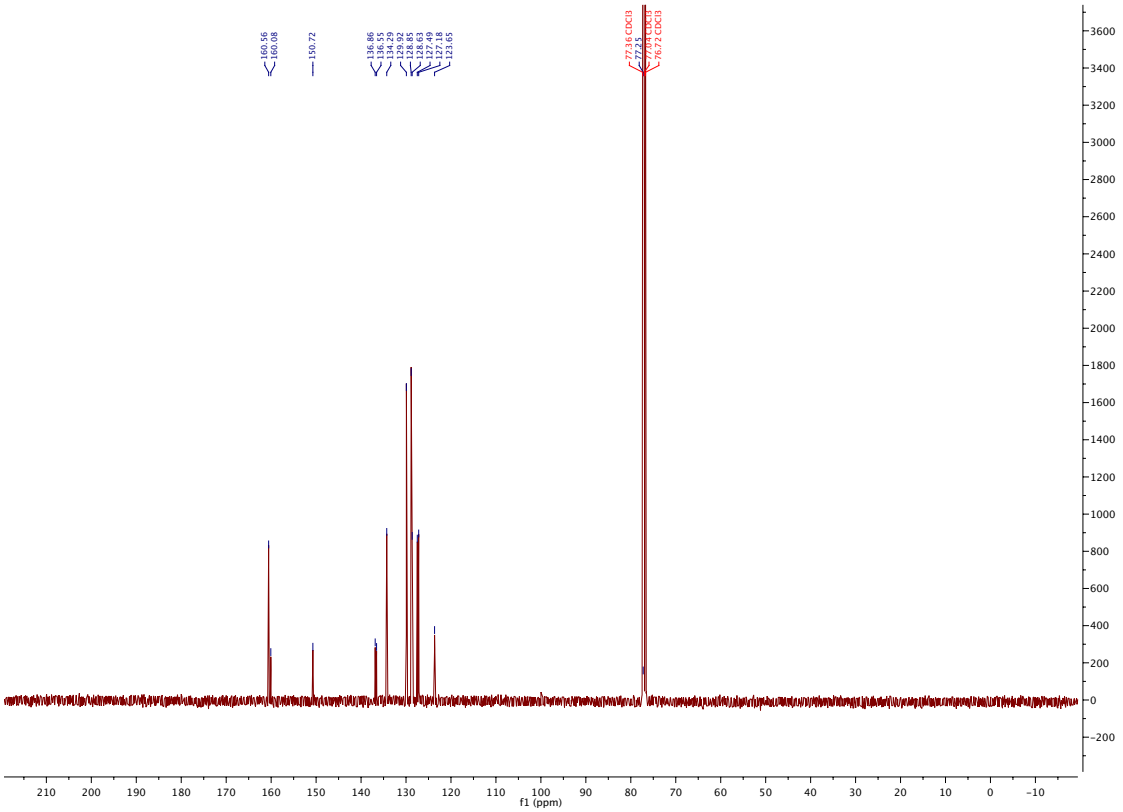
160.56
160.08
150.72
136.86
136.55
134.29
129.92
128.85
128.65
127.49
127.18
123.65
77.36 CDCl3
77.25
77.04 CDCl3
76.72 CDCl3
f1 (ppm)

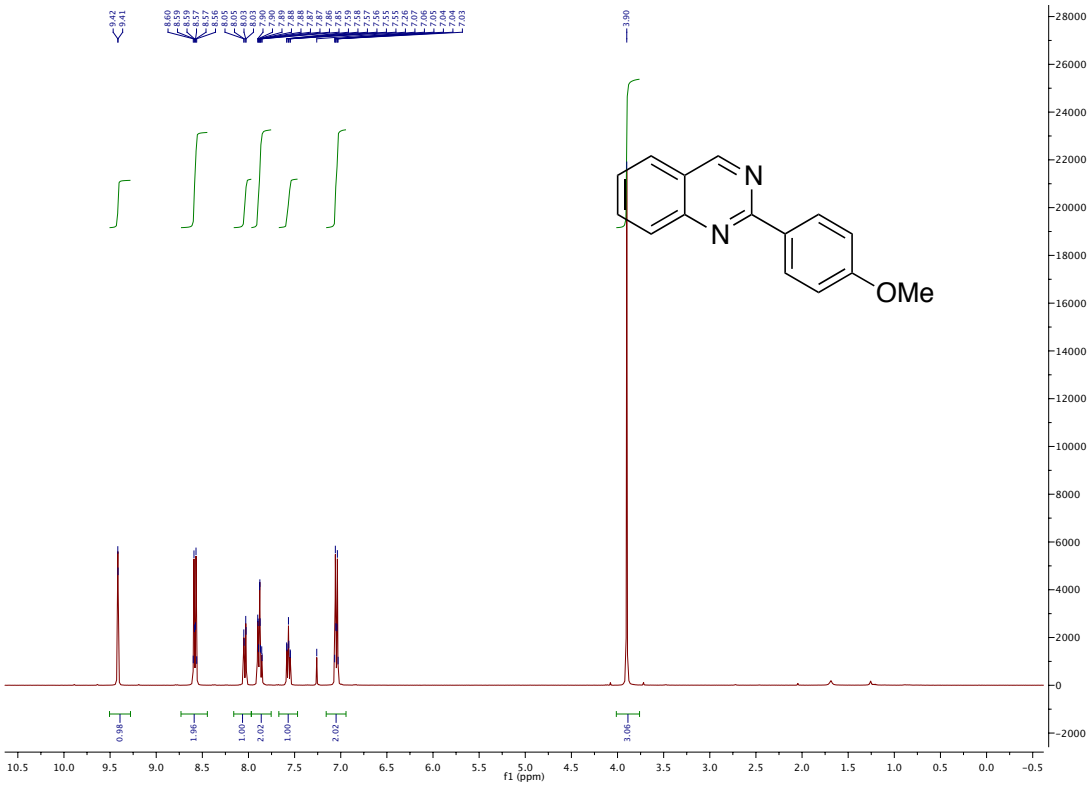
9.42
9.41
8.60
8.59
8.59
8.57
8.57
8.56
8.05
8.05
8.03
8.03
7.90
7.90
7.89
7.89
7.88
7.88
7.87
7.87
7.87
7.87
7.86
7.85
7.85
7.59
7.58
7.57
7.57
7.56
7.55
7.55
7.36
7.07
7.07
7.06
7.05
7.04
7.04
7.03
3.90
N
N
OMe
0.98
1.96
1.00
2.02
1.00
2.02
3.06
f1 (ppm)

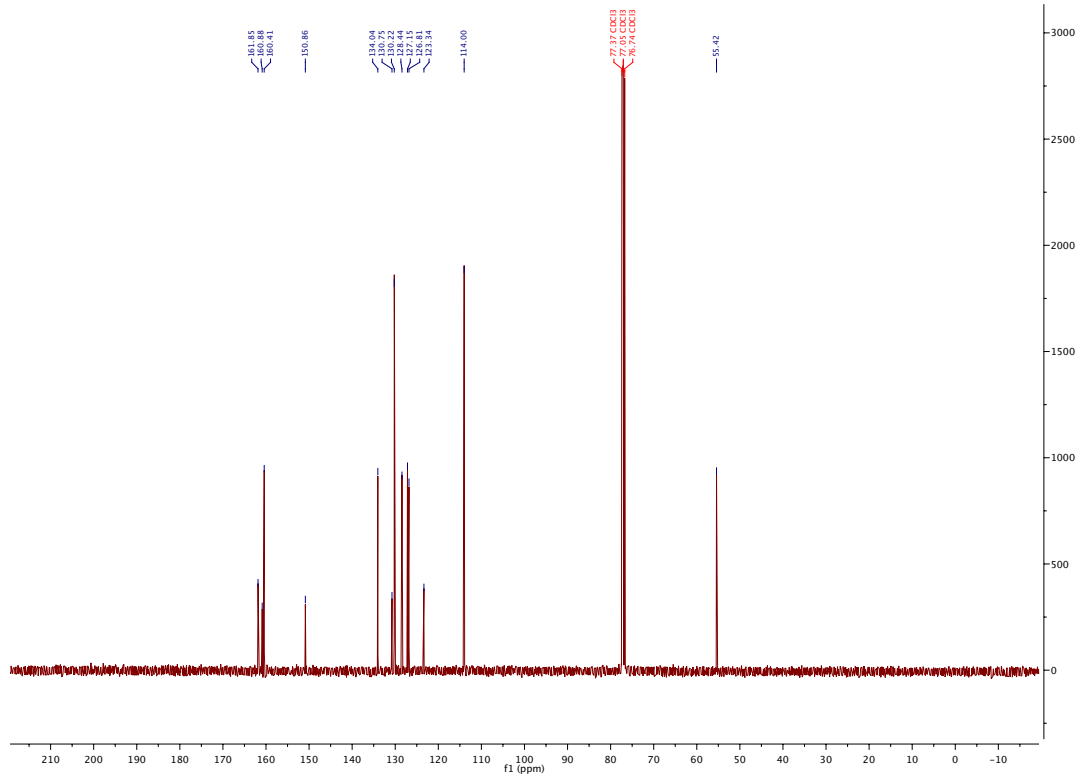
161.85
160.88
160.41
150.86
134.04
130.75
130.22
128.44
127.15
125.81
124.34
114.00
77.37 CDCl3
77.05 CDCl3
76.74 CDCl3
55.42
f1 (ppm)

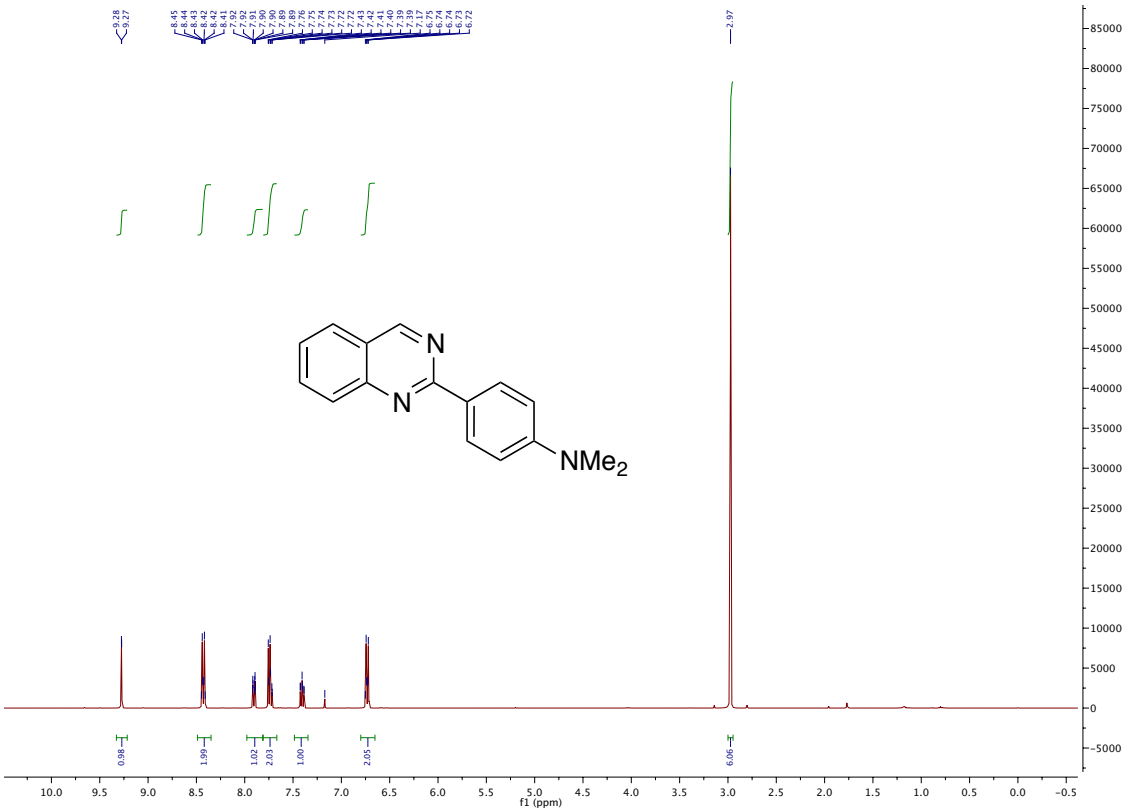
9.28
9.27
8.45
8.44
8.43
8.42
8.42
8.41
8.41
7.92
7.91
7.91
7.90
7.90
7.89
7.89
7.76
7.75
7.74
7.74
7.73
7.72
7.72
7.72
7.43
7.42
7.41
7.41
7.40
7.39
7.39
7.37
7.37
6.75
6.74
6.74
6.74
6.73
6.72
2.97
N
N
NMe2
0.98
1.99
1.02
2.03
1.00
2.05
6.06
f1 (ppm)

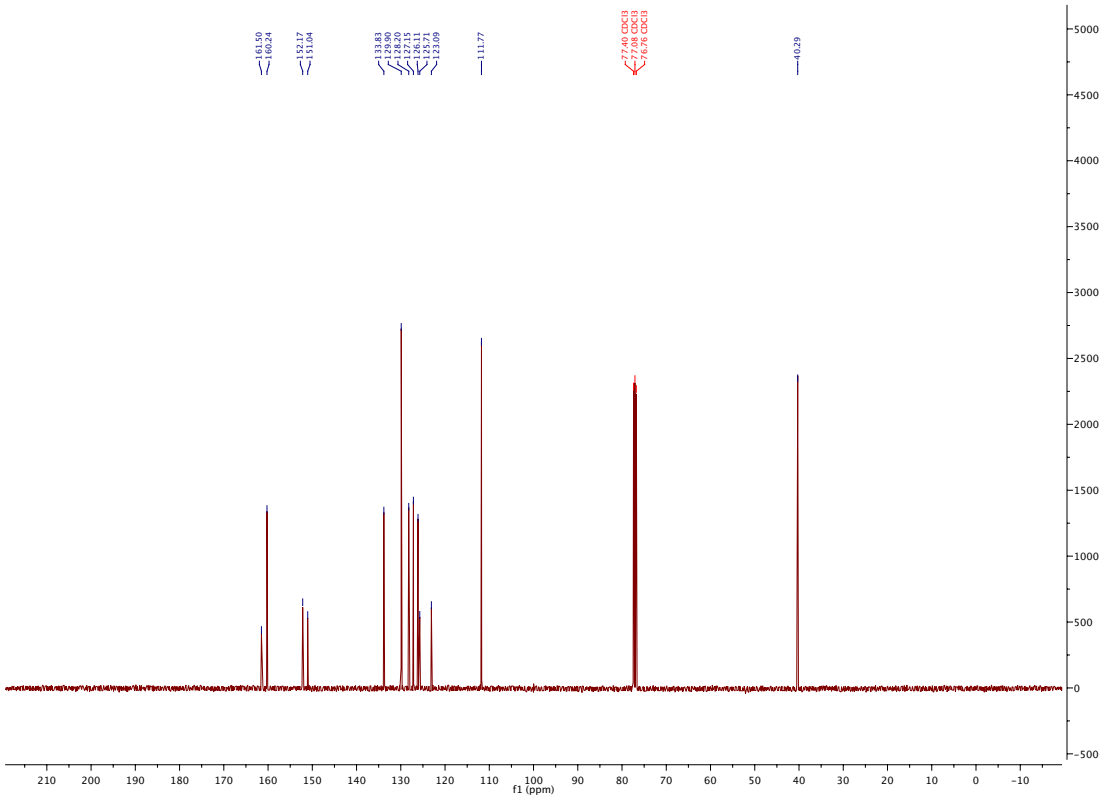
161.50
160.24
152.17
151.04
133.83
129.90
129.20
127.15
126.11
122.77
123.09
111.77
77.40 CDCl3
77.08 CDCl3
76.76 CDCl3
40.29
f1 (ppm)

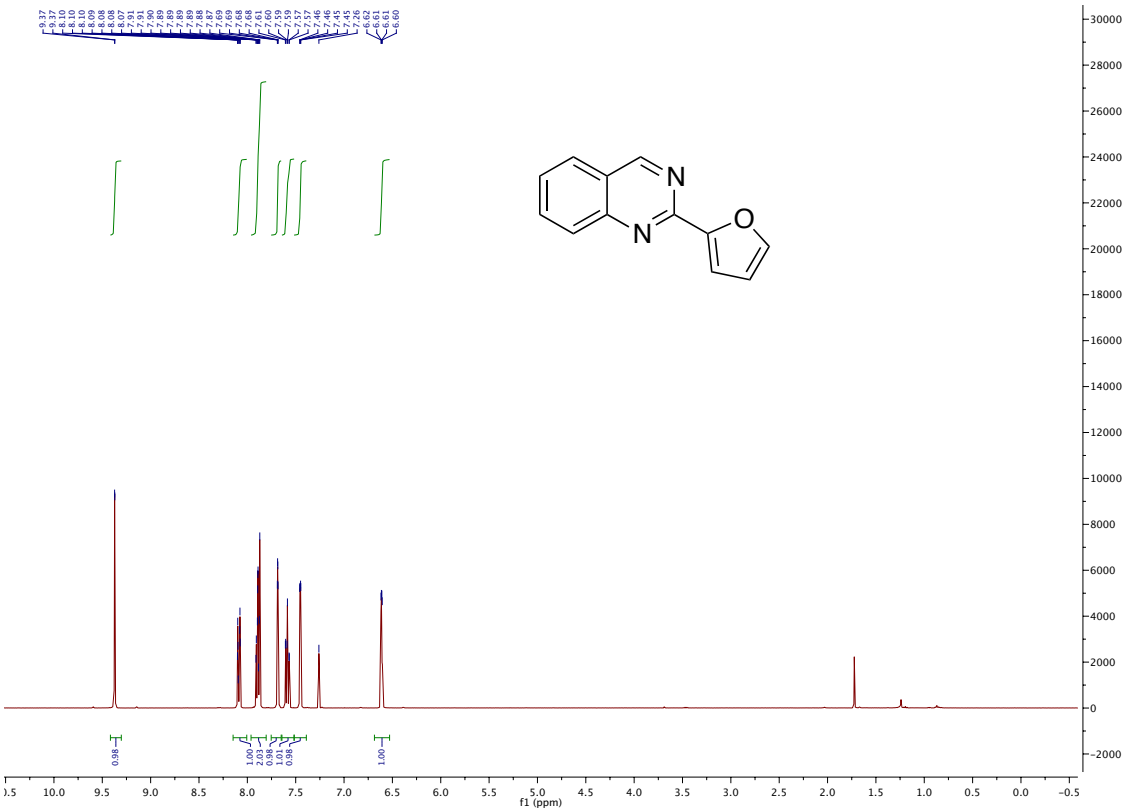
N
N
O
f1 (ppm)

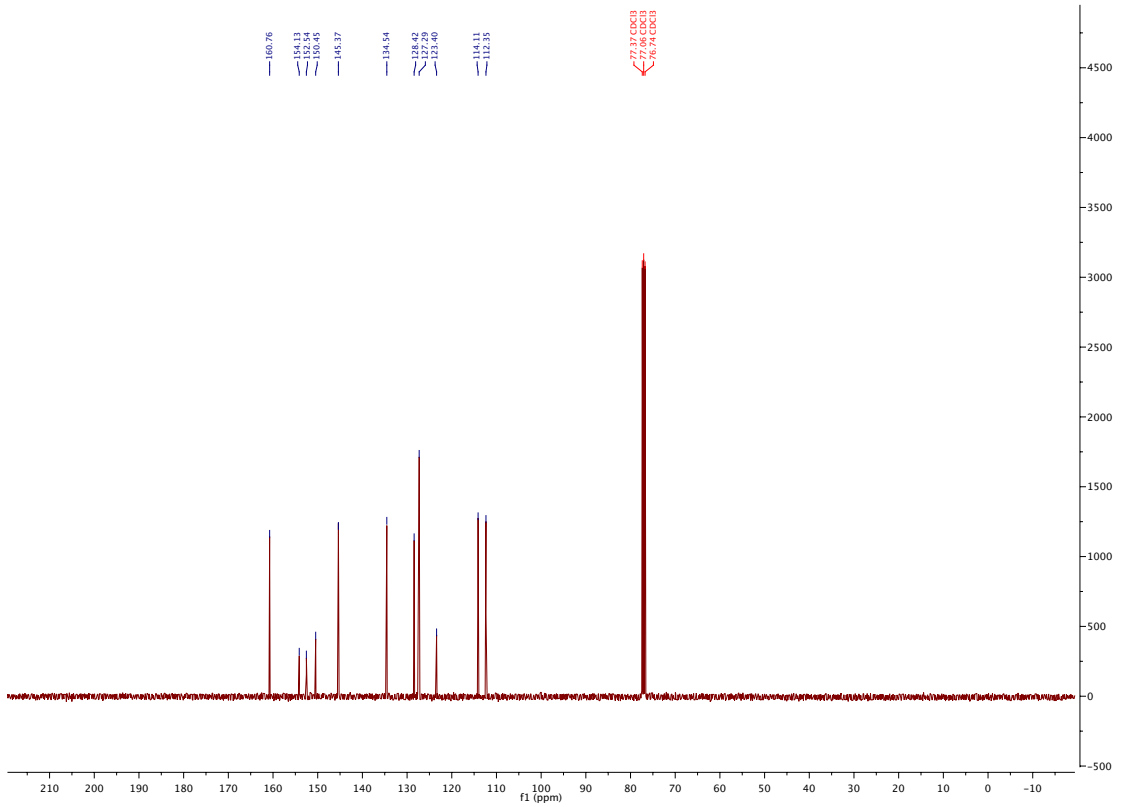
160.76
154.13
152.54
150.45
145.37
134.54
128.42
127.29
123.40
114.11
112.35
77.37 CDCl3
77.06 CDCl3
76.74 CDCl3
f1 (ppm)

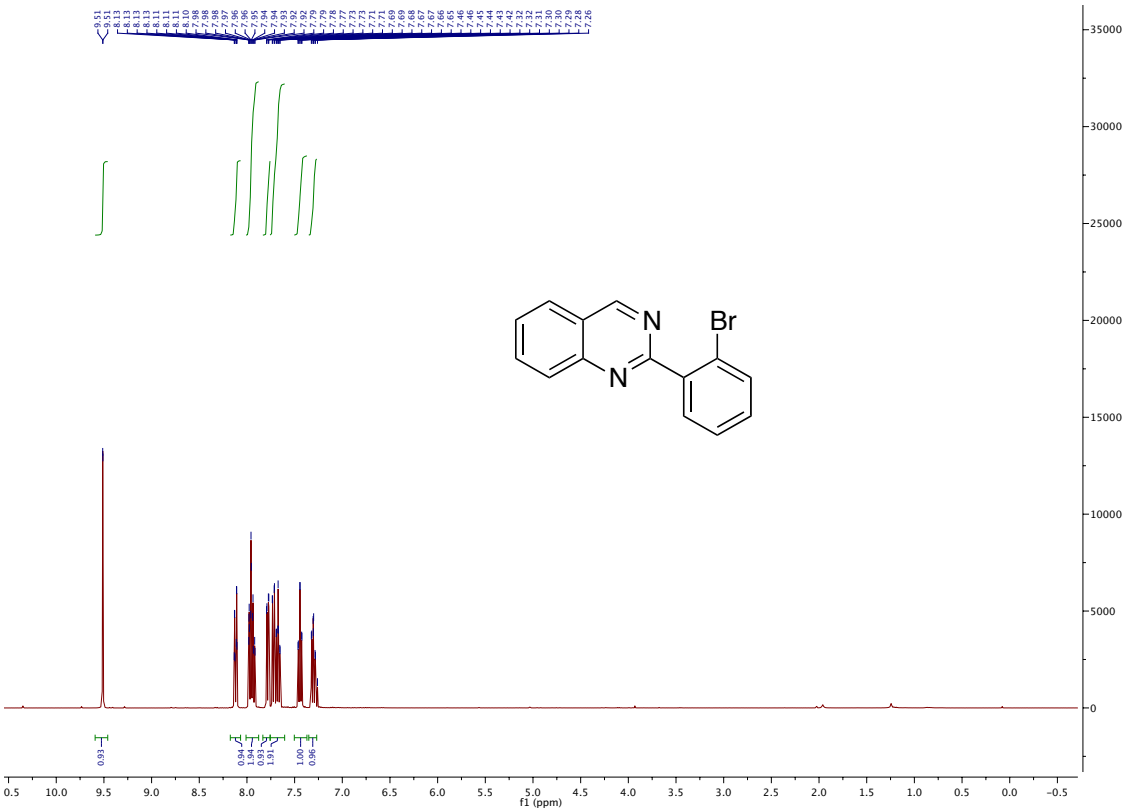
N
Br
N
f1 (ppm)

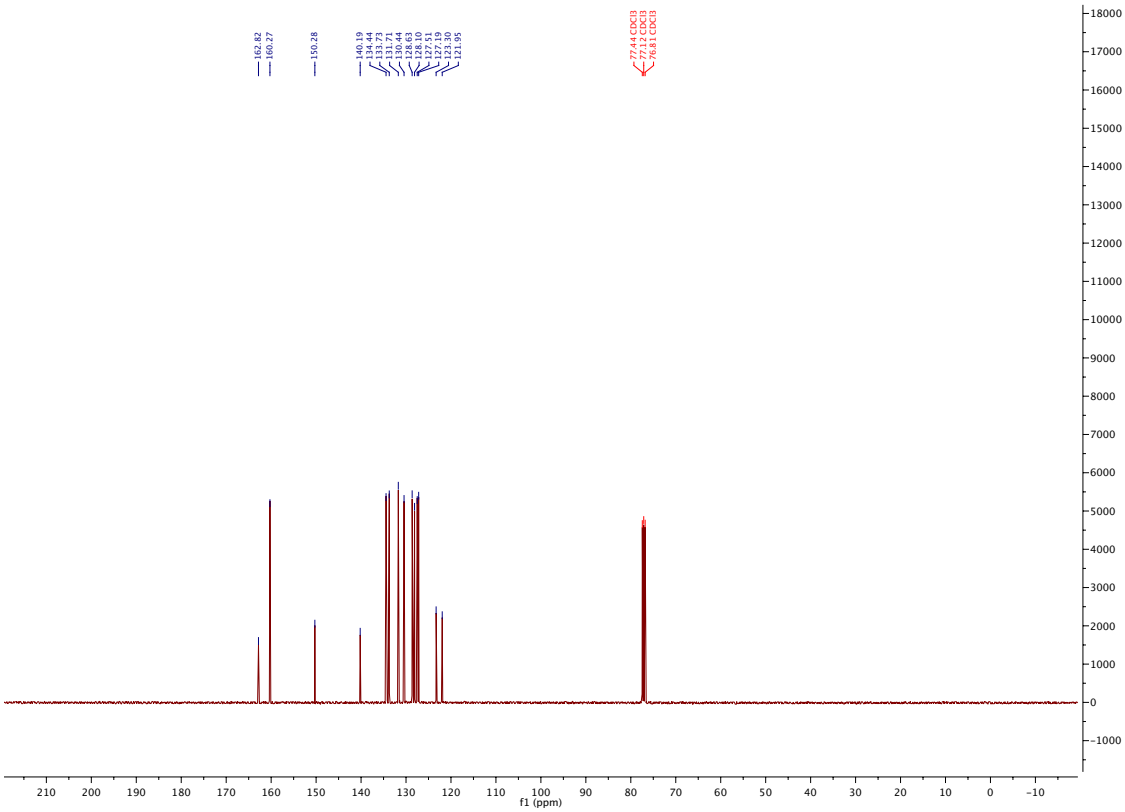
162.82
160.27
150.28
140.19
134.44
133.72
131.71
130.44
129.45
128.10
127.51
127.19
122.30
121.95
77.44 CDCl3
77.12 CDCl3
76.81 CDCl3
f1 (ppm)

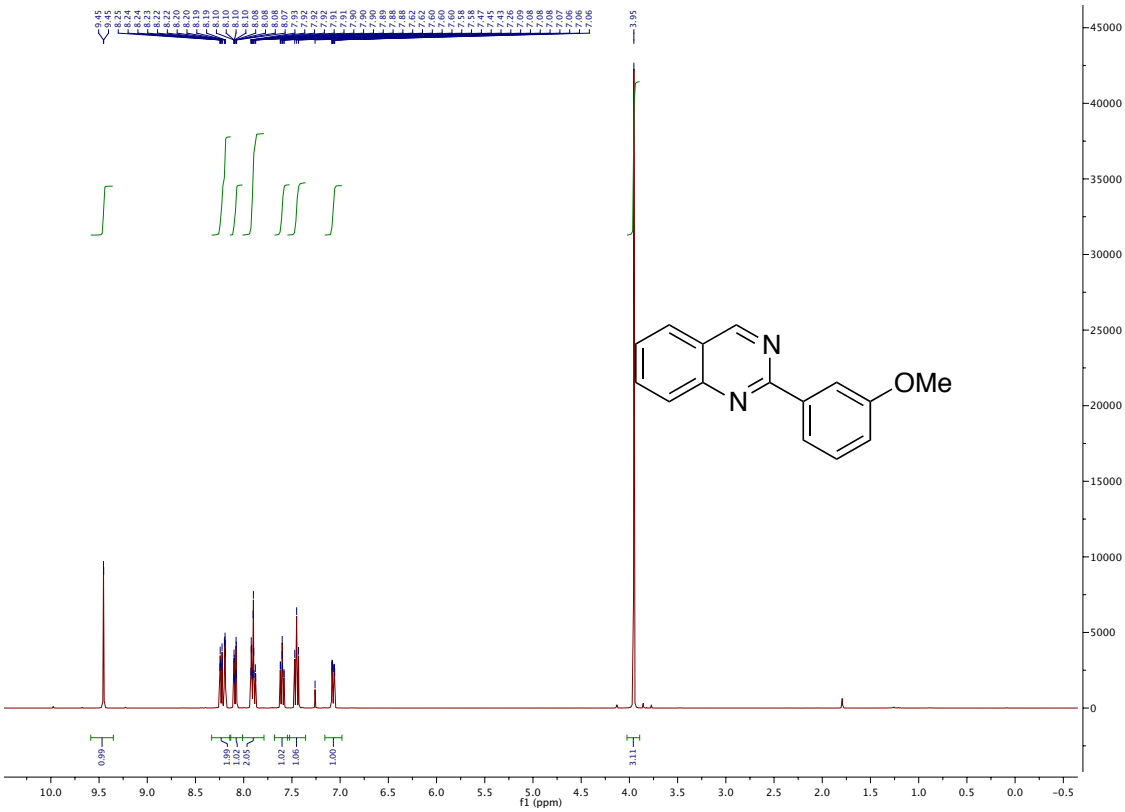
N
N
OMe
f1 (ppm)

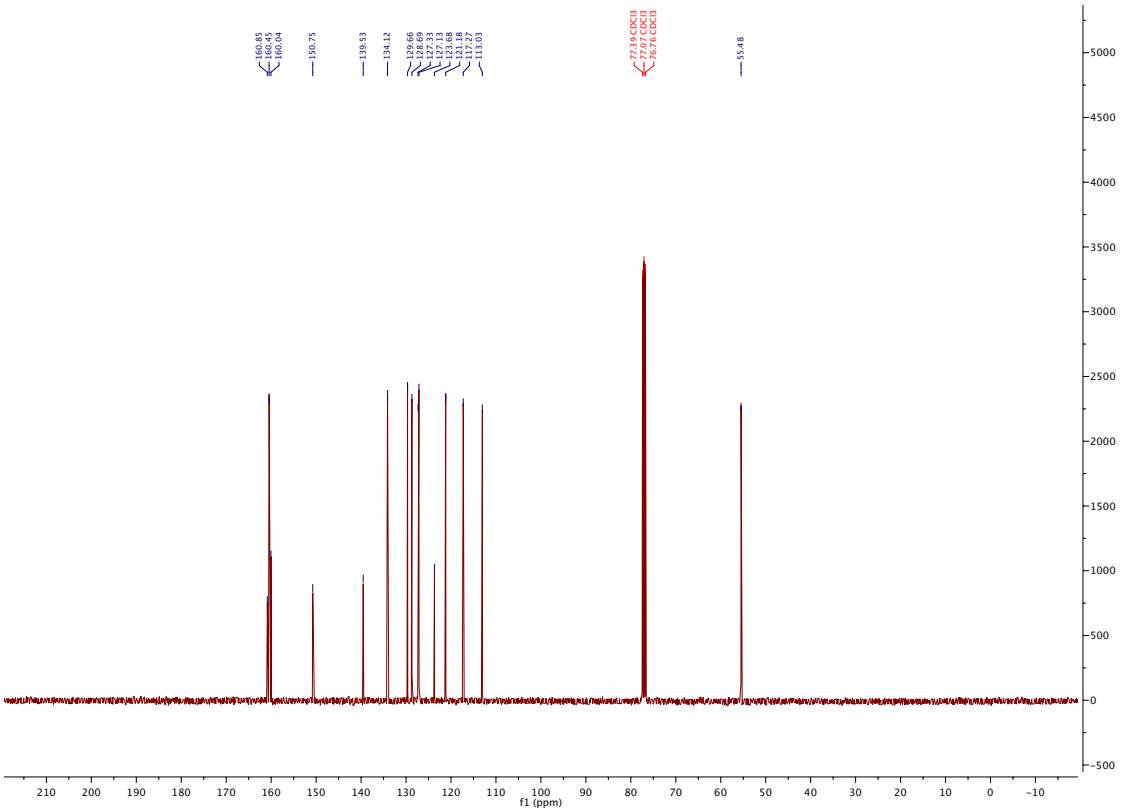
160.85
160.45
160.04
150.75
139.53
134.12
129.66
129.60
127.33
127.13
122.68
121.18
117.27
113.03
77.39 CDCl3
77.07 CDCl3
76.76 CDCl3
55.48
f1 (ppm)

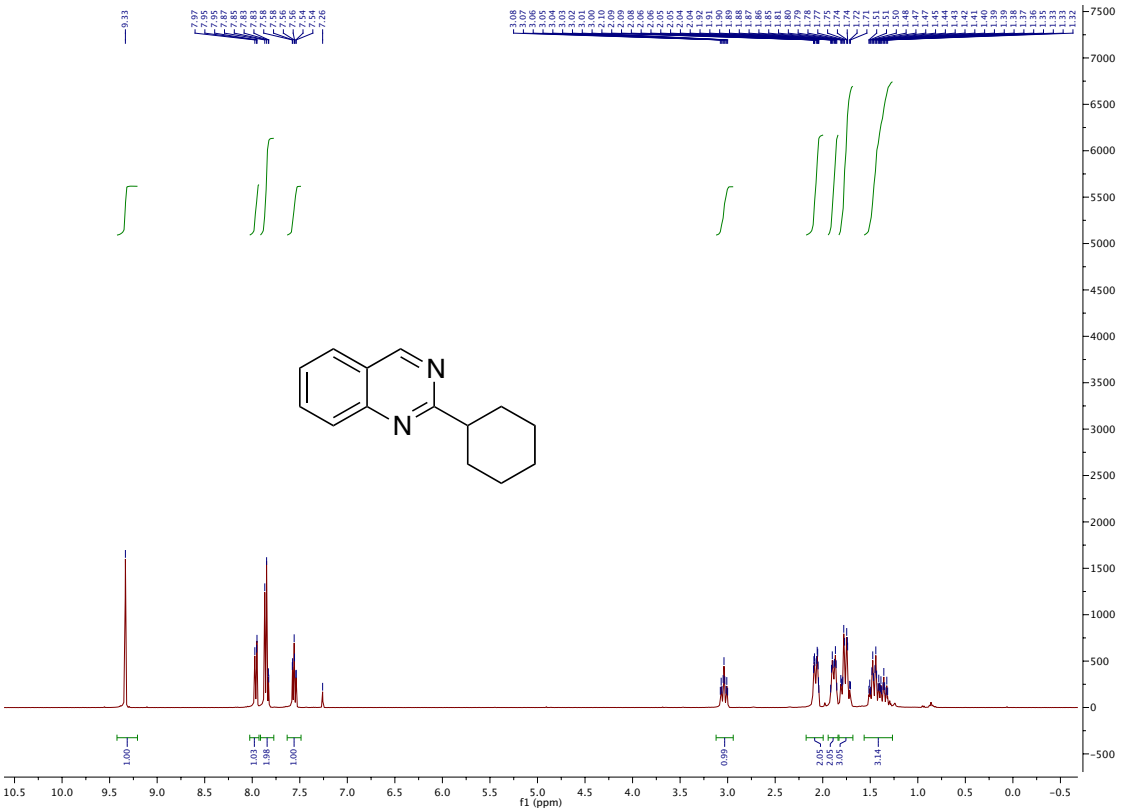
9.33
7.97
7.95
7.95
7.87
7.87
7.85
7.83
7.83
7.58
7.58
7.56
7.56
7.54
7.54
7.26
3.08
3.07
3.06
3.05
3.04
3.03
3.02
3.01
3.00
2.10
2.09
2.08
2.06
2.05
2.04
2.04
2.02
1.91
1.90
1.89
1.88
1.87
1.86
1.85
1.81
1.80
1.79
1.78
1.77
1.75
1.74
1.74
1.72
1.71
1.51
1.51
1.51
1.50
1.48
1.47
1.47
1.45
1.44
1.43
1.42
1.41
1.40
1.39
1.39
1.38
1.37
1.36
1.35
1.33
1.33
1.32
N
N
1.00
1.03
1.98
1.00
0.99
2.05
2.05
3.05
3.14
f1 (ppm)

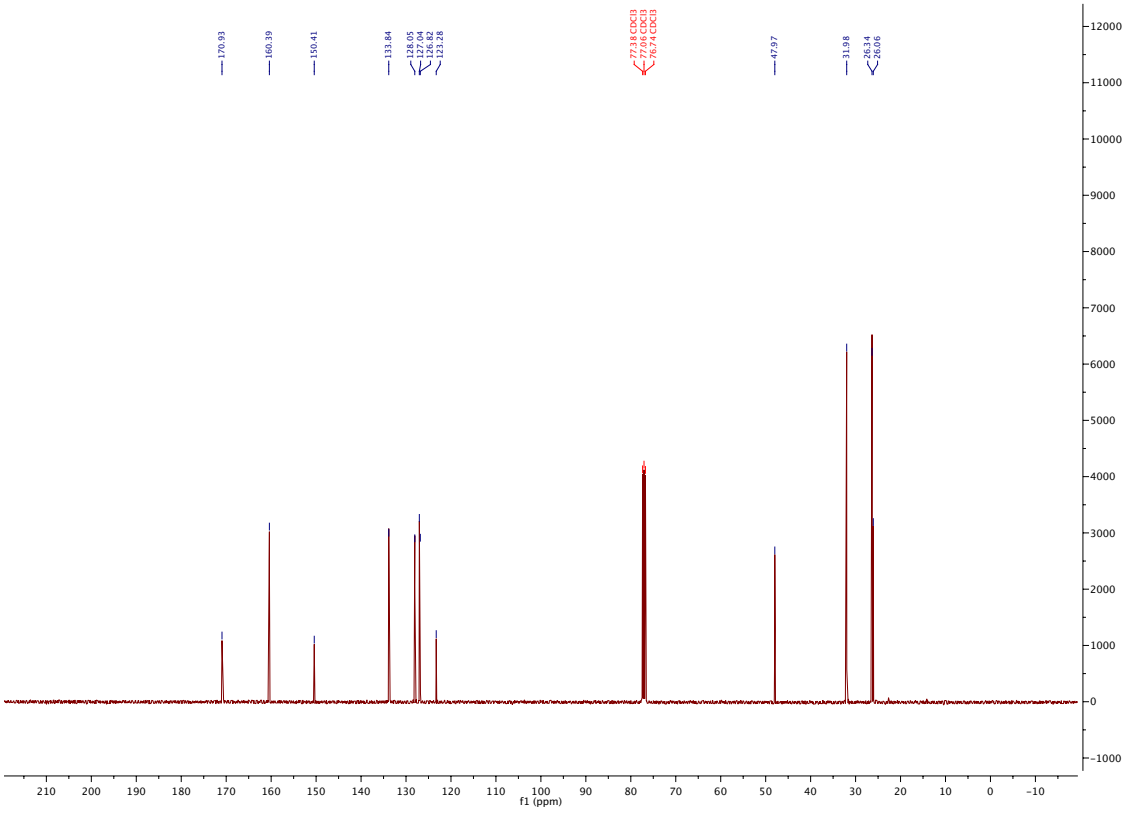
170.93
160.39
150.41
133.84
128.05
127.04
126.82
123.28
77.38 CDCl3
77.06 CDCl3
76.74 CDCl3
47.97
31.98
26.34
26.06
f1 (ppm)

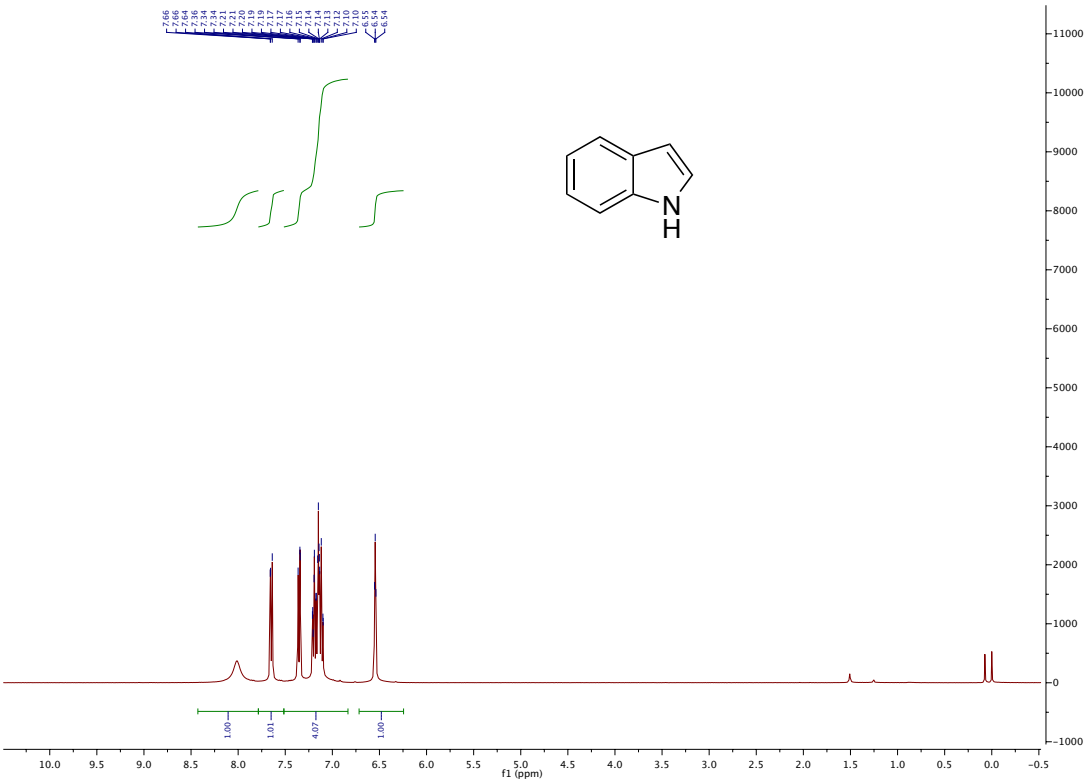
7.66
7.66
7.64
7.36
7.34
7.34
7.21
7.21
7.20
7.19
7.19
7.17
7.17
7.16
7.15
7.14
7.14
7.13
7.12
7.10
7.10
6.55
6.54
6.54
N
H
1.00
1.01
4.07
1.00
f1 (ppm)

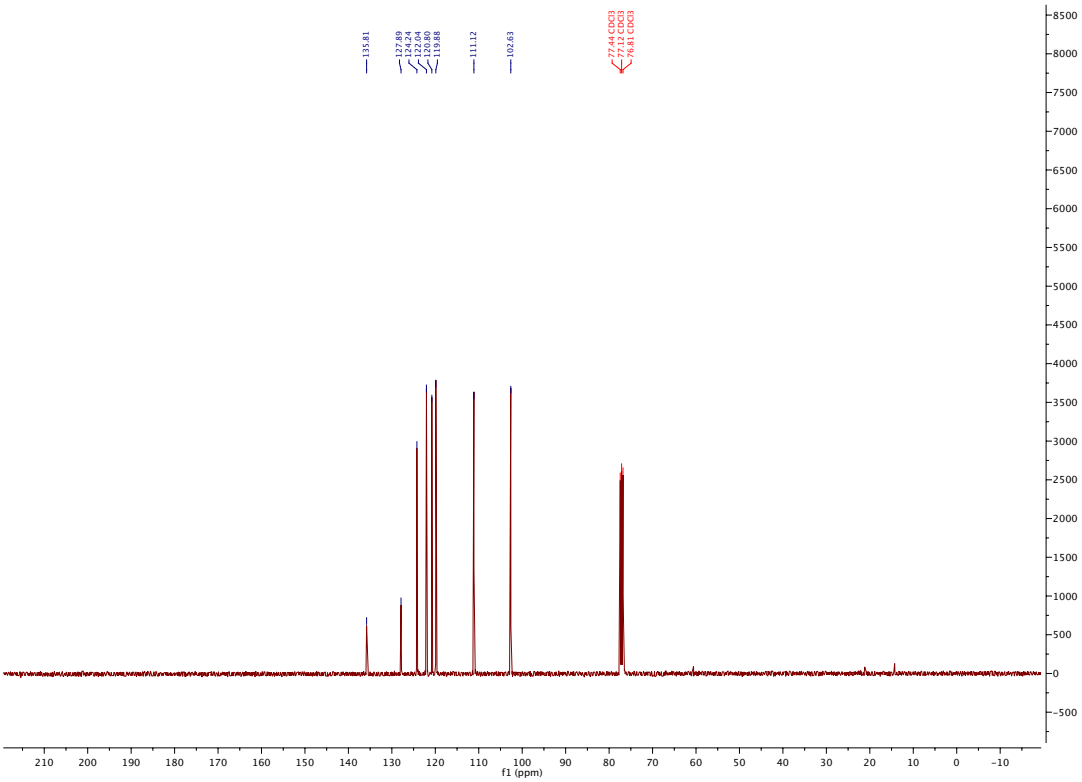
135.81
127.89
124.24
122.04
120.60
119.88
111.12
102.63
77.44 CDCl3
77.12 CDCl3
76.81 CDCl3
f1 (ppm)

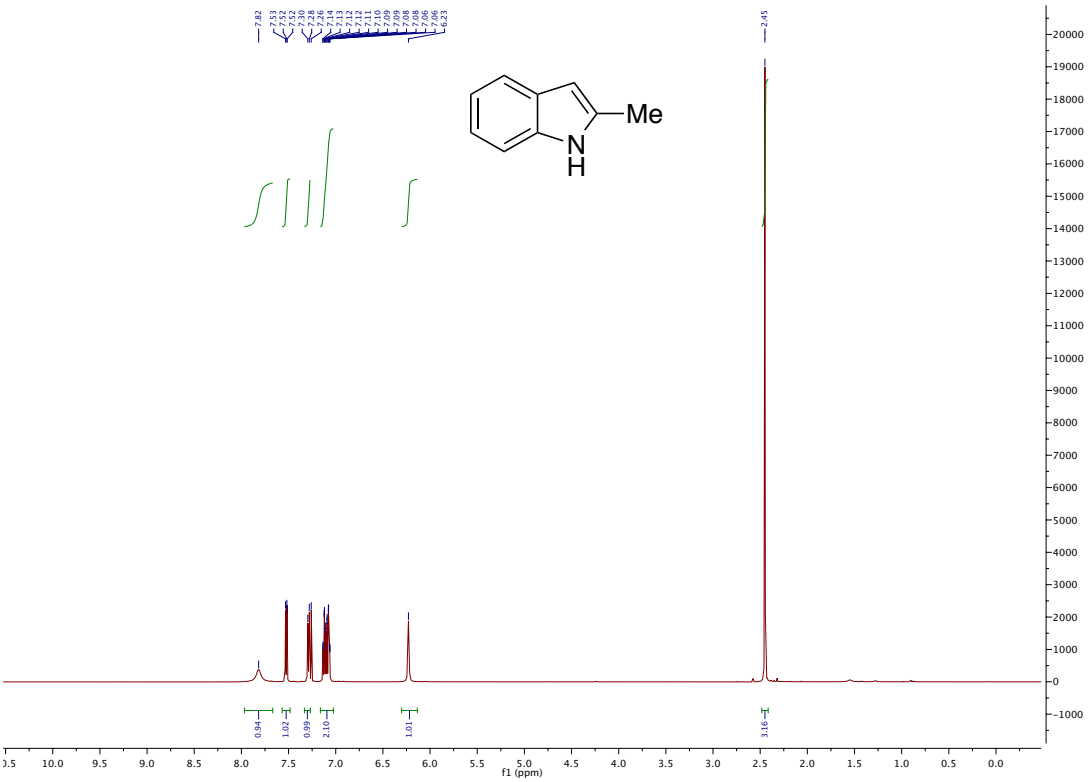
Me
N
H
f1 (ppm)

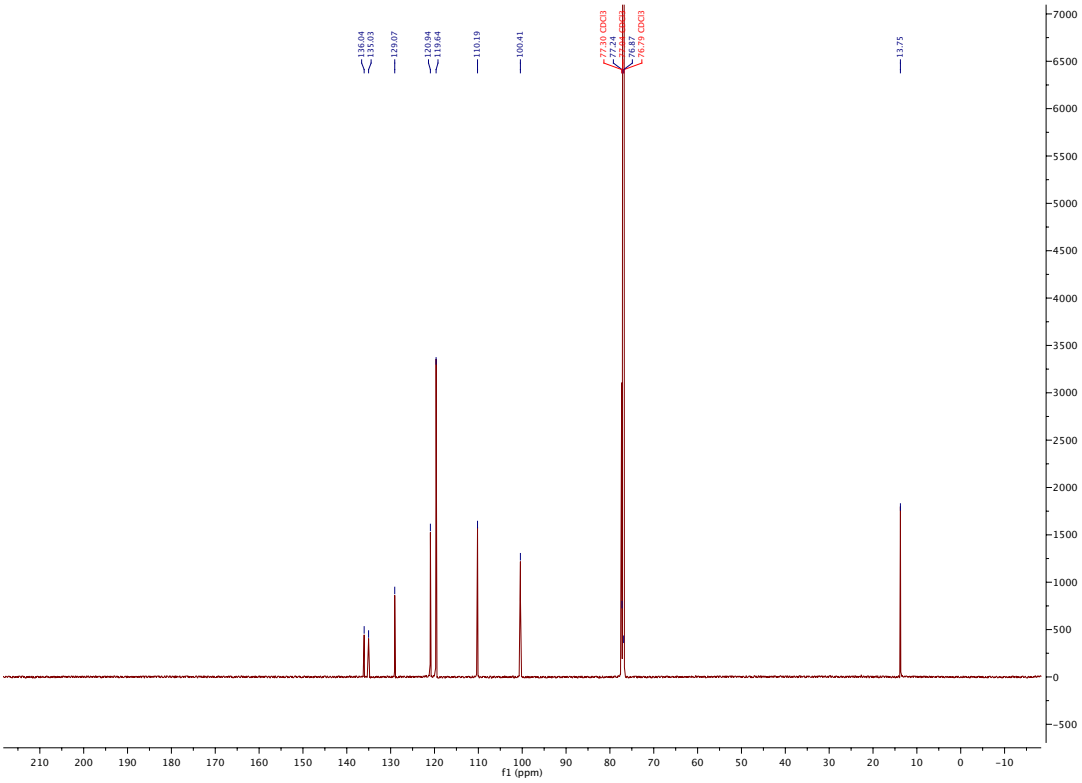
f1 (ppm)

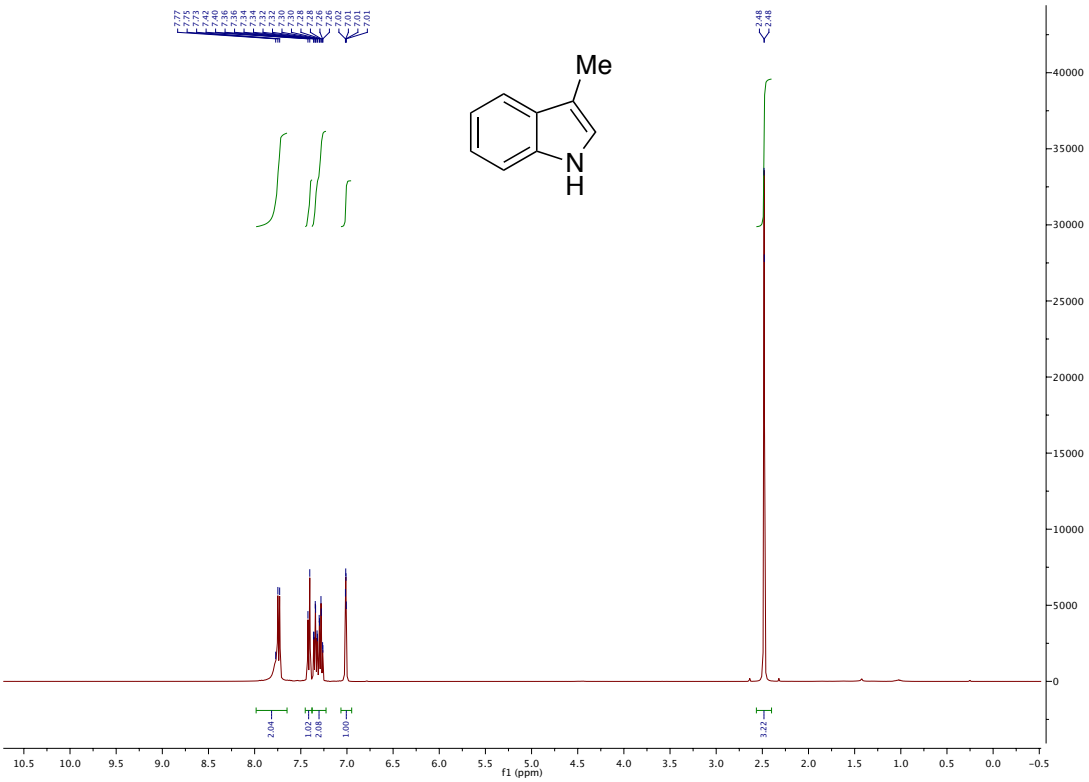
Me
N
H
f1 (ppm)

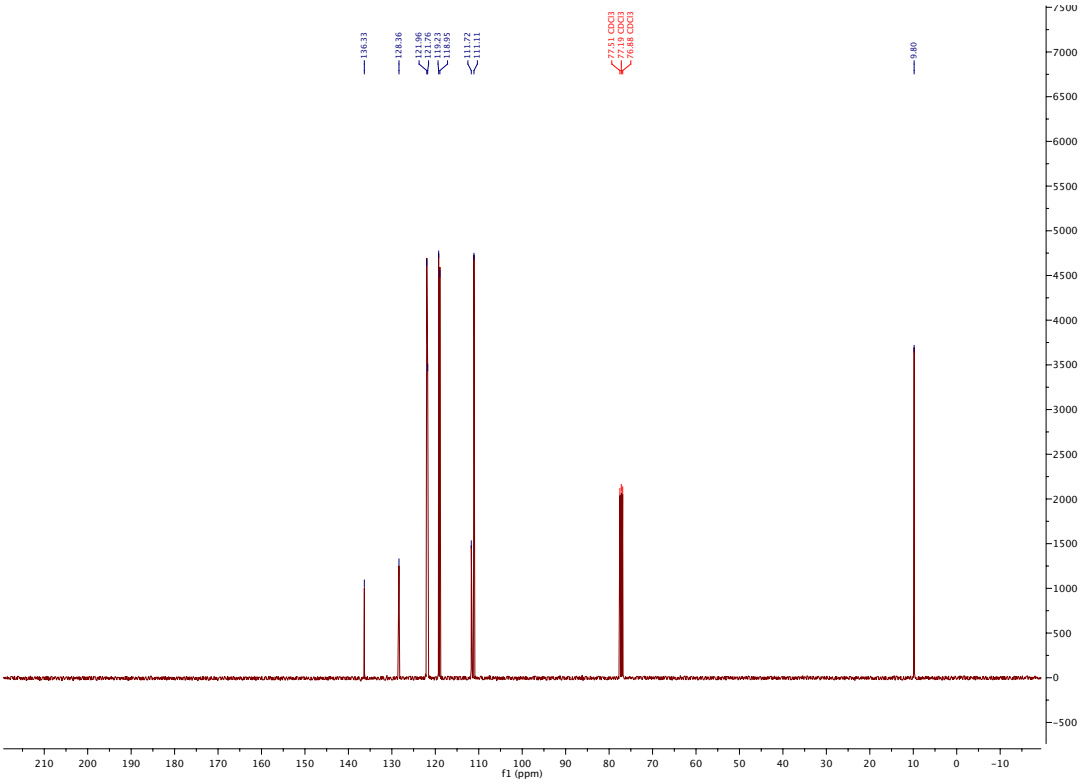
136.33
128.36
121.96
121.46
119.23
118.95
111.72
111.11
77.51 CDCl3
77.19 CDCl3
76.88 CDCl3
9.80
f1 (ppm)

X Ray Crystallographic Data for $Zn(phd)_2^{2+}$ complex, Stahl171

A molecular drawing of the Zn complex of phd shown with 50% probability ellipsoids. All H atoms and disordered parts are omitted for clarity.

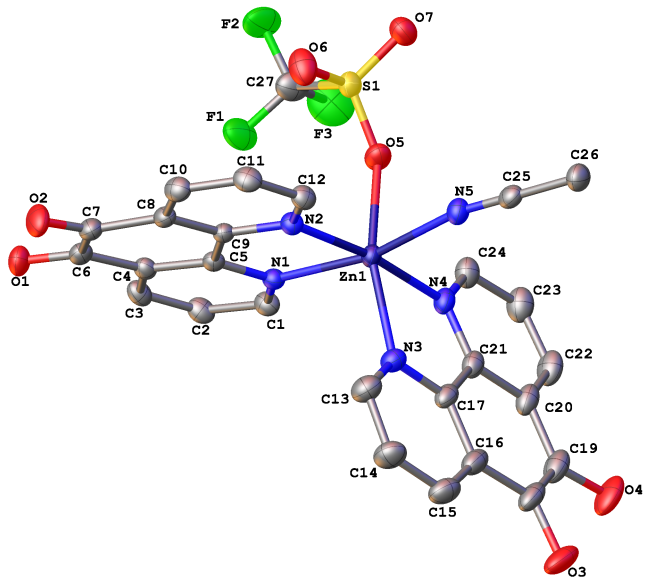

Crystallographic Experimental Section

Data Collection

A red crystal with approximate dimensions 0.733 x 0.133 x 0.119 mm^3 was selected under oil under ambient conditions and attached to the tip of a MiTeGen MicroMount©. The crystal was mounted in a stream of cold nitrogen at 100(1) K and centered in the X-ray beam by using a video camera.

The crystal evaluation and data collection were performed on a Bruker Quazar SMART APEXII diffractometer with Mo K_α (λ = 0.71073 Å) radiation and the diffractometer to crystal distance of 4.96 cm.

The initial cell constants were obtained from three series of ω scans at different starting angles. Each series consisted of 12 frames collected at intervals of 0.5° in a 6° range about ω with the exposure time of 10 seconds per frame. The reflections were successfully indexed by an automated indexing routine built in the APEXII program suite. The final cell constants were calculated from a set of 9785 strong reflections from the actual data collection.

The data were collected by using the full sphere data collection routine to survey the reciprocal space to the extent of a full sphere to a resolution of 0.70 Å. A total of 153282 data were harvested by collecting 6 sets of frames with 0.5° scans in ω and ϕ with exposure times of 20 sec per frame. These highly redundant datasets were corrected for Lorentz and polarization effects. The absorption correction was based on fitting a function to the empirical transmission surface as sampled by multiple equivalent measurements. [1]

Structure Solution and Refinement

The systematic absences in the diffraction data were consistent for the space groups *Pnma* and $Pna2_1$. The *E*-statistics strongly suggested the centrosymmetric space group *Pnma* that yielded chemically reasonable and computationally stable results of refinement [2-4].

A successful solution by the direct methods provided most non-hydrogen atoms from the *E*-map. The remaining non-hydrogen atoms were located in an alternating series of least-squares cycles and difference Fourier maps. All non-hydrogen atoms were refined with anisotropic displacement coefficients. All hydrogen atoms were included in the structure factor calculation at idealized positions and were allowed to ride on the neighboring atoms with relative isotropic displacement coefficients.

The asymmetric unit contains one Zn complex as well as a heavily disordered non-coordinated triflate anion and two partially occupied acetonitrile molecules. Ligand N3 of the Zn complex is disordered over two positions (major component: 82.0(10)%). Triflate ligand S1 is also disordered over two positions (major component: 92.8(2)%). Bond distance and thermal parameter restraints and constraints were applied to the disordered species to enable a computationally stable and chemically reasonable refinement.

A significant amount of time was invested in identifying and refining the disordered non-coordinated triflate anion and acetonitrile molecules. Bond length restraints were applied to model the diffuse species but the resulting isotropic displacement coefficients suggested that the species were mobile. In addition, the refinement was computationally unstable. Option SQUEEZE of program PLATON [5] was used to correct the diffraction data for diffuse scattering effects and to identify the species. PLATON calculated the upper limit of volume that can be occupied by the species to be 1828 $Å^3$, or 27.3% of the unit cell volume. The program

calculated 820 electrons in the unit cell for the diffuse species. This approximately corresponds to one triflate anion (592 electrons/cell) and 1.4 molecules of acetonitrile (246 electrons/cell) in the asymmetric unit. It is very likely that these species are disordered over several positions. Based on these results, the formula for the asymmetric unit is: $[(C_{12}H_6N_2O_2)_2(O_3SCF_3)(C_2H_3N)Zn]^+$; $[O_3SCF_3]^-$; 1.4 (C_2H_3N). Please note that all derived results in the following tables are based on the known contents. No data are given for the diffusely scattering species.

The final least-squares refinement of 551 parameters against 7908 data resulted in residuals R (based on F^2 for $I \geq 2\sigma$) and wR (based on F^2 for all data) of 0.0365 and 0.0939, respectively.

Summary

Crystal data for $C_{30.8}H_{19.2}N_{6.4}O_{10}F_6S_2Zn$ (M =882.41): orthorhombic, space group *Pnma* (no. 62), a = 21.111(7) Å, b = 22.086(6) Å, c = 14.348(6) Å, V = 6690(4) Å^3, Z = 8, T = 100.0 K, μ(Mo Kα) = 0.963 mm^{-1}, *Dcalc* = 1.752 g/mm^3, 153282 reflections measured ($3.384 \leq 2\Theta \leq 55.094$), 7908 unique ($R_{int}$ = 0.0451) which were used in all calculations. The final R_1 was 0.0429 ($I > 2\sigma(I)$) and wR_2 was 0.1159 (all data).

References

[1] Bruker-AXS. (2007-2013) APEX2 (Ver. 2013.2-0), SADABS (2012-1), and SAINT+ (Ver. 8.30C) Software Reference Manuals. Bruker-AXS, Madison, Wisconsin, USA.

[2] Sheldrick, G. M. (2008) SHELXL. *Acta Cryst*. **A64**, 112-122.

[3] Dolomanov, O.V.; Bourhis, L.J.; Gildea, R.J.; Howard, J.A.K.; Puschmann, H. "OLEX2: a complete structure solution, refinement and analysis program". *J. Appl. Cryst*. (2009) **42**, *339-341*.

[4] Guzei, I.A. (2013). Internal laboratory computer programs Gn.

[5] A.L. Spek (1990) Acta Cryst. A46, C34.

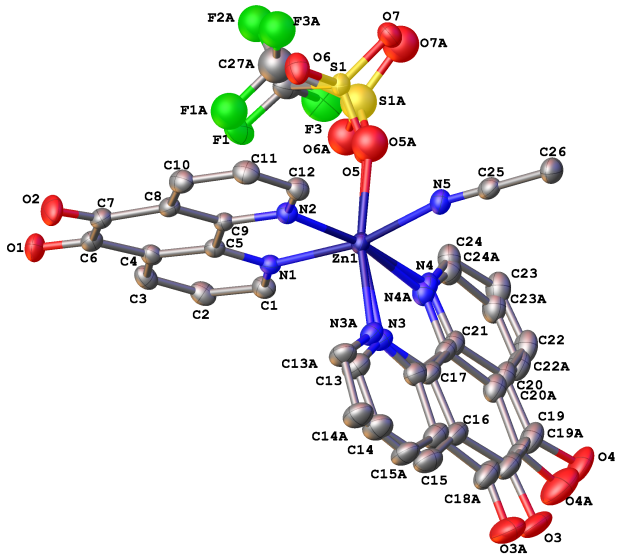

A molecular drawing of the Zn complex of phd showing the disordered component. All atoms are drawn with 50% probability ellipsoids. All H atoms are omitted for clarity.

Table A2.1. Crystal data and structure refinement for Stahl171

Identification code	Stahl171
Empirical formula	$[(C_{12}H_6N_2O_2)_2(O_3SCF_3)(C_2H_3N)Zn]^+$; $[O_3SCF_3]^-$; 1.4 (C_2H_3N)
Formula weight	882.41
Temperature/K	100.0
Crystal system	orthorhombic
Space group	*Pnma*
a/Å	21.111(7)
b/Å	22.086(6)
c/Å	14.348(6)
α/°	90
β/°	90
γ/°	90
Volume/Å^3	6690(4)
Z	8
ρ_{calc} mg/mm^3	1.752
μ/mm^{-1}	0.963
F(000)	3558.0
Crystal size/mm^3	0.733 × 0.133 × 0.119
2Θ range for data collection	3.384 to 55.094°
Index ranges	$-27 \leq h \leq 27$, $-28 \leq k \leq 28$, $-18 \leq l \leq 18$
Reflections collected	153282
Independent reflections	7908[R(int) = 0.0451]
Data/restraints/parameters	7908/616/551
Goodness-of-fit on F^2	1.077
Final R indexes [I>=2σ (I)]	R_1 = 0.0365, wR_2 = 0.0898
Final R indexes [all data]	R_1 = 0.0431, wR_2 = 0.0939
Largest diff. peak/hole / e Å^{-3}	0.44/-0.50

Table A2.2. Fractional Atomic Coordinates (×10⁴) and Equivalent Isotropic Displacement Parameters (Å²×10³) for Stahl171. U_{eq} is defined as 1/3 of of the trace of the orthogonalised U_{IJ} tensor.

Atom	*x*	*y*	*z*	U(eq)
Zn1	1396.9(2)	5124.1(2)	2854.6(2)	19.22(7)
S1	2005.5(3)	4292.8(3)	4677.4(4)	21.07(15)
F1	2759.1(8)	3782.1(8)	3458.2(11)	42.7(4)
F2	2865.4(10)	3452.7(10)	4854.8(15)	57.1(7)
F3	2057.4(11)	3191.5(8)	4056.4(15)	59.2(6)
O6	2471.9(9)	4753.5(9)	4840.5(13)	34.6(4)
O7	1696.0(8)	4055.2(8)	5493.2(12)	29.6(4)
O5	1578.4(8)	4428.4(8)	3914.5(12)	28.0(4)
C27	2447.0(13)	3644.4(12)	4230.9(18)	32.4(6)
O1	4320.4(7)	4906.9(8)	1310.4(12)	31.3(4)
O2	4340.2(8)	5996.6(9)	2211.6(12)	36.5(4)
N1	2127.5(8)	4709.9(8)	2047.8(11)	19.1(3)
N2	2184.9(8)	5700.2(8)	3110.3(12)	19.8(3)
C1	2086.7(10)	4196.8(10)	1559.2(14)	23.3(4)
C2	2605.0(11)	3927.6(10)	1131.1(15)	25.6(4)
C3	3184.3(11)	4208.5(10)	1183.6(15)	24.8(4)
C4	3235.6(10)	4750.9(9)	1675.0(14)	20.7(4)
C5	2695.0(9)	4982.4(9)	2109.2(13)	18.5(4)
C6	3835.7(10)	5090.7(10)	1701.8(15)	23.6(4)
C7	3853.4(10)	5688.4(11)	2224.7(15)	25.1(4)
C8	3278.8(9)	5879(1)	2733.9(14)	20.8(4)
C9	2721.9(9)	5538.7(9)	2669.5(13)	18.2(4)
C10	3274.7(10)	6398.3(10)	3287.0(15)	25.9(4)
C11	2726.3(11)	6560.7(10)	3739.3(15)	26.1(4)
C12	2190.1(10)	6201.5(10)	3632.1(14)	23.6(4)
O3	-1002.7(17)	5743.0(19)	-23(2)	48.5(10)
O4	-1287.7(14)	4626(2)	650(3)	50(1)
N3	953(3)	5678(2)	1794(5)	24.2(8)
N4	627(3)	4571(3)	2421(5)	23.7(9)
C13	1130(2)	6215(2)	1484(4)	32.8(9)
C14	769(2)	6551.1(19)	848(3)	35.8(9)
C15	200(2)	6326(2)	547(3)	34.7(9)
C16	-5.4(19)	5757(2)	864(3)	31.2(8)
C17	395.1(18)	5447(2)	1491(3)	25.1(8)

C18	-593.9(18)	5482(2)	577(3)	35.4(9)
C19	-751.2(18)	4908(2)	891(3)	35.8(9)
C20	-340.9(19)	4578(2)	1514(3)	30.3(9)
C21	228(2)	4850(2)	1818(4)	25.1(8)
C22	-475(2)	3990(2)	1829(4)	35.6(10)
C23	-67(3)	3713(2)	2423(4)	35(1)
C24	484(3)	4018(3)	2704(5)	29.2(9)
O3A	-748(8)	6008(9)	-145(10)	59(4)
O4A	-1155(8)	4859(9)	340(15)	64(4)
N3A	1058(13)	5746(11)	1850(20)	25(2)
N4A	647(16)	4626(13)	2310(30)	26(3)
C13A	1286(10)	6280(9)	1599(18)	29(2)
C14A	988(10)	6665(8)	960(15)	36(3)
C15A	436(10)	6476(8)	587(13)	32(3)
C16A	181(8)	5912(8)	797(13)	32(2)
C17A	529(9)	5549(9)	1442(17)	27(2)
C18A	-412(8)	5678(8)	418(13)	39(3)
C19A	-656(8)	5091(9)	710(15)	34(3)
C20A	-280(9)	4718(9)	1353(17)	30(2)
C21A	290(11)	4963(10)	1710(20)	26(2)
C22A	-457(11)	4140(10)	1597(16)	34(3)
C23A	-85(13)	3794(10)	2166(17)	33(3)
C24A	448(16)	4080(13)	2550(30)	31(3)
N5	819.6(8)	5556.3(8)	3889.3(13)	24.3(4)
C25	429.8(10)	5752.3(10)	4343.7(15)	23.6(4)
C26	-68.3(11)	6002.7(12)	4929.7(16)	30.0(5)
S1A	1774(5)	3986(5)	4427(7)	58(3)
O5A	1580(7)	4572(7)	4082(10)	58(3)
O7A	1556(7)	3835(7)	5353(8)	58(3)
O6A	1753(7)	3499(7)	3755(12)	58(3)
C27A	2636(5)	4090(6)	4605(10)	58(3)
F2A	2912(6)	3587(9)	4929(16)	58(3)
F1A	2932(6)	4236(9)	3811(12)	58(3)
F3A	2759(7)	4532(9)	5217(12)	58(3)

Table A2.3. Anisotropic Displacement Parameters ($Å^2 \times 10^3$) for Stahl171. The Anisotropic displacement factor exponent takes the form: $-2\pi^2[h^2a^{*2}U_{11}+...+2hka \times b \times U_{12}]$

Atom	U_{11}	U_{22}	U_{33}	U_{23}	U_{13}	U_{12}
Zn1	15.36(11)	21.75(12)	20.54(12)	-1.34(9)	-0.05(8)	-0.46(9)
S1	18.0(3)	23.6(3)	21.7(3)	-0.8(2)	2.1(2)	1.9(2)
F1	47.0(9)	52.2(10)	28.8(8)	-2.0(7)	9.5(7)	23.4(8)
F2	56.0(12)	72.6(15)	42.7(10)	13.1(10)	-1.6(9)	40.9(11)
F3	81.1(14)	25.4(9)	71.0(13)	-13.7(9)	2.7(11)	-2.0(9)
O6	29.2(9)	37(1)	37.7(10)	-10.5(8)	4.6(8)	-7.3(8)
O7	29.5(9)	33.4(10)	26.0(9)	3.3(7)	4.9(7)	1.4(7)
O5	24.6(8)	30.1(9)	29.3(9)	8.6(7)	-0.8(7)	4.5(7)
C27	37.8(14)	29.1(13)	30.2(13)	-0.7(10)	-0.9(11)	11.6(11)
O1	19.8(7)	38.9(9)	35.2(9)	0.7(7)	4.6(7)	5.4(7)
O2	21.3(8)	50.6(11)	37.7(9)	-8.1(8)	1.5(7)	-11.4(7)
N1	20.0(8)	20.5(8)	16.8(8)	0.0(6)	-0.8(6)	-0.7(7)
N2	20.8(8)	19.3(8)	19.3(8)	-2.3(7)	0.2(6)	-0.1(7)
C1	25.6(10)	22.9(10)	21.5(10)	-1.0(8)	-0.2(8)	-3.2(8)
C2	33.6(12)	21.1(10)	22.1(10)	-3.5(8)	3.2(9)	-0.1(9)
C3	28.6(11)	23.8(10)	22.1(10)	-0.1(8)	6.2(8)	4.4(9)
C4	21.7(10)	21.6(10)	18.8(9)	2.8(8)	1.3(8)	0.9(8)
C5	19.3(9)	19.2(9)	16.9(9)	2.1(7)	-1.0(7)	0.7(7)
C6	21(1)	27.8(11)	22.2(10)	3.9(8)	-1.9(8)	3.0(8)
C7	20.8(10)	33.3(12)	21(1)	0.7(9)	-3.1(8)	-0.4(9)
C8	19.1(9)	24.4(10)	18.9(9)	1.3(8)	-2.5(7)	-1.4(8)
C9	17.9(9)	20.5(9)	16.2(9)	0.8(7)	-1.2(7)	1.1(7)
C10	26.3(11)	26.1(11)	25.3(10)	-0.5(9)	-3.0(8)	-5.8(9)
C11	32.5(11)	22.4(10)	23.5(10)	-5.4(8)	-2.2(9)	-3.1(9)
C12	26(1)	23.3(10)	21.5(10)	-2.6(8)	2.2(8)	2.6(8)
O3	34.4(16)	74(2)	37.5(14)	-12.6(14)	-18.1(12)	20.8(15)
O4	22.5(13)	65(2)	62(2)	-22.3(17)	-13.0(13)	-0.9(13)
N3	23(2)	26.4(16)	23.4(15)	-1.5(14)	-4.3(14)	1.3(12)
N4	17.0(12)	29.8(18)	24(2)	-4.8(12)	1.2(14)	-1.8(12)
C13	31(2)	33.5(18)	34.1(19)	-1.1(14)	-7.5(15)	0.0(15)
C14	38(3)	32.8(18)	36.8(18)	6.8(15)	-6.9(18)	1.7(17)
C15	35(2)	38(2)	31.4(15)	-1.5(15)	-8.2(15)	10.8(17)
C16	23.8(17)	43(2)	26.6(14)	-8.1(14)	-4.9(13)	8.6(14)
C17	19.0(17)	33.5(19)	22.8(14)	-8.1(13)	-3.0(13)	3.5(13)
C18	22.4(17)	50(2)	33.5(17)	-13.4(17)	-8.9(13)	8.4(17)

C19	22.0(16)	44(2)	42(2)	-18.7(16)	-4.8(14)	1.2(14)
C20	19.7(14)	35(2)	36(2)	-13.1(15)	-0.6(14)	1.2(14)
C21	18.7(15)	30(2)	26.4(18)	-9.1(14)	0.8(13)	1.0(13)
C22	24.7(15)	36(2)	47(3)	-13.8(17)	0.6(17)	-7.2(16)
C23	29.6(15)	31.2(19)	44(3)	-9.3(17)	4.1(19)	-4.4(14)
C24	24.9(16)	28.7(18)	34(3)	-5.6(14)	4.0(15)	-2.1(15)
O3A	45(7)	87(9)	45(6)	14(6)	-20(6)	-5(7)
O4A	46(8)	73(9)	73(9)	-18(7)	-28(7)	4(7)
N3A	21(5)	28(4)	26(4)	-4(4)	-4(4)	2(4)
N4A	24(4)	27(4)	28(5)	-4(4)	1(4)	-1(4)
C13A	30(5)	26(4)	31(4)	8(4)	-6(4)	1(4)
C14A	36(6)	34(5)	37(5)	8(4)	-9(5)	3(5)
C15A	30(5)	33(5)	34(5)	8(4)	-11(5)	1(5)
C16A	25(4)	40(4)	32(4)	-7(4)	-6(4)	7(4)
C17A	26(4)	32(4)	24(4)	-3(4)	1(4)	5(4)
C18A	25(5)	52(5)	40(5)	-11(4)	-8(4)	6(4)
C19A	16(4)	46(5)	41(5)	-10(5)	-14(4)	3(5)
C20A	24(4)	32(4)	35(4)	-11(4)	0(4)	1(4)
C21A	19(4)	33(4)	26(4)	-8(4)	-4(4)	5(4)
C22A	24(4)	38(5)	40(5)	-14(5)	-2(5)	0(5)
C23A	26(4)	34(5)	40(5)	-6(4)	2(5)	-4(4)
C24A	27(4)	33(5)	33(5)	-5(4)	2(4)	3(4)
N5	19.4(8)	26.4(9)	27.2(9)	-2.6(7)	0.7(7)	-0.4(7)
C25	20.1(10)	25.9(11)	24.8(10)	1.1(8)	-4.7(8)	-2.5(8)
C26	23.8(11)	37.5(13)	28.7(11)	-2.7(10)	1.8(9)	6.2(9)

Table A2.4. Bond Lengths for Stahl171.

Atom	**Atom**	**Length/Å**	**Atom**	**Atom**	**Length/Å**
Zn1	O5	2.1956(17)	C13	C14	1.402(5)
Zn1	N1	2.1344(18)	C14	C15	1.368(5)
Zn1	N2	2.1263(18)	C15	C16	1.406(5)
Zn1	N3	2.166(4)	C16	C17	1.412(4)
Zn1	N4	2.126(5)	C16	C18	1.443(5)
Zn1	N3A	2.11(2)	C17	C21	1.445(5)
Zn1	N4A	2.08(2)	C18	C19	1.386(5)
Zn1	N5	2.1449(19)	C19	C20	1.442(5)

Zn1	O5A	2.177(9)	C20	C21	1.412(4)
S1	O6	1.4351(19)	C20	C22	1.403(5)
S1	O7	1.4396(18)	C22	C23	1.359(5)
S1	O5	1.4495(18)	C23	C24	1.403(5)
S1	C27	1.825(3)	O3A	C18A	1.300(13)
F1	C27	1.325(3)	O4A	C19A	1.287(13)
F2	C27	1.327(3)	N3A	C13A	1.326(14)
F3	C27	1.319(3)	N3A	C17A	1.335(14)
O1	C6	1.236(3)	N4A	C21A	1.360(14)
O2	C7	1.233(3)	N4A	C24A	1.323(15)
N1	C1	1.335(3)	C13A	C14A	1.399(14)
N1	C5	1.344(3)	C14A	C15A	1.349(14)
N2	C9	1.346(3)	C15A	C16A	1.389(13)
N2	C12	1.337(3)	C16A	C17A	1.428(13)
C1	C2	1.389(3)	C16A	C18A	1.459(13)
C2	C3	1.373(3)	C17A	C21A	1.444(13)
C3	C4	1.394(3)	C18A	C19A	1.455(13)
C4	C5	1.397(3)	C19A	C20A	1.470(13)
C4	C6	1.473(3)	C20A	C21A	1.416(13)
C5	C9	1.469(3)	C20A	C22A	1.375(14)
C6	C7	1.519(3)	C22A	C23A	1.369(15)
C7	C8	1.477(3)	C23A	C24A	1.406(15)
C8	C9	1.398(3)	N5	C25	1.136(3)
C8	C10	1.395(3)	C25	C26	1.456(3)
C10	C11	1.375(3)	S1A	O5A	1.4450
C11	C12	1.391(3)	S1A	O7A	1.4449
O3	C18	1.349(4)	S1A	O6A	1.4453
O4	C19	1.338(4)	S1A	C27A	1.8515
N3	C13	1.319(5)	C27A	F2A	1.3386
N3	C17	1.356(4)	C27A	F1A	1.3385
N4	C21	1.355(4)	C27A	F3A	1.3381
N4	C24	1.322(5)			

Table A2.5. Bond Angles for Stahl171.

Atom	**Atom**	**Atom**	**Angle/°**	**Atom**	**Atom**	**Atom**	**Angle/°**
N1	Zn1	O5	87.11(7)	C21	N4	Zn1	113.7(3)

N1	Zn1	N3	100.0(2)	C24	N4	Zn1	128.0(3)
N1	Zn1	N5	167.61(7)	C24	N4	C21	118.3(4)
N1	Zn1	O5A	94.1(4)	N3	C13	C14	122.8(3)
N2	Zn1	O5	99.37(7)	C15	C14	C13	119.3(3)
N2	Zn1	N1	77.57(7)	C14	C15	C16	119.6(3)
N2	Zn1	N3	96.96(12)	C15	C16	C17	117.0(3)
N2	Zn1	N4	172.9(2)	C15	C16	C18	123.4(3)
N2	Zn1	N5	93.37(7)	C17	C16	C18	119.5(3)
N2	Zn1	O5A	93.3(5)	N3	C17	C16	122.8(3)
N3	Zn1	O5	163.27(13)	N3	C17	C21	116.9(3)
N4	Zn1	O5	86.22(13)	C16	C17	C21	120.2(3)
N4	Zn1	N1	98.5(3)	O3	C18	C16	123.5(4)
N4	Zn1	N3	77.80(14)	O3	C18	C19	116.5(3)
N4	Zn1	N5	91.4(3)	C19	C18	C16	119.9(3)
N3A	Zn1	N1	98.9(11)	O4	C19	C18	123.0(3)
N3A	Zn1	N2	89.6(5)	O4	C19	C20	115.7(3)
N3A	Zn1	N5	89.4(11)	C18	C19	C20	121.3(3)
N3A	Zn1	O5A	167.1(12)	C21	C20	C19	119.2(3)
N4A	Zn1	N1	96.8(15)	C22	C20	C19	123.1(3)
N4A	Zn1	N2	167.5(10)	C22	C20	C21	117.7(3)
N4A	Zn1	N3A	80.2(7)	N4	C21	C17	118.1(3)
N4A	Zn1	N5	93.7(15)	N4	C21	C20	122.2(3)
N4A	Zn1	O5A	98.3(8)	C20	C21	C17	119.7(3)
N5	Zn1	O5	86.06(7)	C23	C22	C20	119.4(3)
N5	Zn1	N3	89.4(2)	C22	C23	C24	119.3(4)
N5	Zn1	O5A	77.9(4)	N4	C24	C23	123.1(4)
O6	S1	O7	115.93(11)	C13A	N3A	Zn1	130.0(13)
O6	S1	O5	113.79(12)	C13A	N3A	C17A	118.1(15)
O6	S1	C27	105.27(12)	C17A	N3A	Zn1	111.9(11)
O7	S1	O5	114.01(11)	C21A	N4A	Zn1	111.6(13)
O7	S1	C27	103.37(12)	C24A	N4A	Zn1	128.4(15)
O5	S1	C27	102.40(11)	C24A	N4A	C21A	119.4(17)
S1	O5	Zn1	140.91(12)	N3A	C13A	C14A	123.9(15)
F1	C27	S1	111.56(18)	C15A	C14A	C13A	117.4(14)
F1	C27	F2	107.9(2)	C14A	C15A	C16A	121.7(13)
F2	C27	S1	110.70(19)	C15A	C16A	C17A	116.3(12)
F3	C27	S1	110.08(19)	C15A	C16A	C18A	124.7(13)

F3	C27	F1	109.0(2)	C17A	C16A	C18A	119.0(12)
F3	C27	F2	107.5(2)	N3A	C17A	C16A	122.4(13)
C1	N1	Zn1	127.01(14)	N3A	C17A	C21A	117.7(13)
C1	N1	C5	118.16(18)	C16A	C17A	C21A	119.8(13)
C5	N1	Zn1	114.64(13)	O3A	C18A	C16A	120.1(13)
C9	N2	Zn1	114.79(13)	O3A	C18A	C19A	119.0(12)
C12	N2	Zn1	126.78(14)	C19A	C18A	C16A	120.8(11)
C12	N2	C9	118.41(18)	O4A	C19A	C18A	121.8(13)
N1	C1	C2	123.0(2)	O4A	C19A	C20A	118.5(14)
C3	C2	C1	118.9(2)	C18A	C19A	C20A	119.2(11)
C2	C3	C4	119.0(2)	C21A	C20A	C19A	118.3(13)
C3	C4	C5	118.44(19)	C22A	C20A	C19A	122.2(13)
C3	C4	C6	121.18(19)	C22A	C20A	C21A	119.5(13)
C5	C4	C6	120.31(19)	N4A	C21A	C17A	117.8(13)
N1	C5	C4	122.37(18)	N4A	C21A	C20A	119.3(13)
N1	C5	C9	116.42(17)	C20A	C21A	C17A	122.8(13)
C4	C5	C9	121.21(18)	C23A	C22A	C20A	120.9(15)
O1	C6	C4	122.2(2)	C22A	C23A	C24A	116.4(16)
O1	C6	C7	119.3(2)	N4A	C24A	C23A	123.9(18)
C4	C6	C7	118.47(18)	C25	N5	Zn1	168.17(17)
O2	C7	C6	119.5(2)	N5	C25	C26	179.7(3)
O2	C7	C8	122.3(2)	O5A	S1A	O6A	115.5
C8	C7	C6	118.16(18)	O5A	S1A	C27A	102.4
C9	C8	C7	120.29(19)	O7A	S1A	O5A	115.6
C10	C8	C7	121.40(19)	O7A	S1A	O6A	115.5
C10	C8	C9	118.32(19)	O7A	S1A	C27A	102.4
N2	C9	C5	116.48(17)	O6A	S1A	C27A	102.4
N2	C9	C8	122.30(18)	S1A	O5A	Zn1	146.0(10)
C8	C9	C5	121.21(18)	F2A	C27A	S1A	111.9
C11	C10	C8	119.2(2)	F1A	C27A	S1A	111.9
C10	C11	C12	119.0(2)	F1A	C27A	F2A	107.0
N2	C12	C11	122.8(2)	F3A	C27A	S1A	111.9
C13	N3	Zn1	128.5(3)	F3A	C27A	F2A	107.0
C13	N3	C17	118.4(3)	F3A	C27A	F1A	107.0
C17	N3	Zn1	112.8(3)				

Table A2.6. Torsion Angles for Stahl171.

A	B	C	D	Angle/°	A	B	C	D	Angle/°
Zn1	N1	C1	C2	-173.20(16)	C14	C15	C16	C17	0.4(5)
Zn1	N1	C5	C4	175.89(15)	C14	C15	C16	C18	-179.4(4)
Zn1	N1	C5	C9	-3.5(2)	C15	C16	C17	N3	0.5(7)
Zn1	N2	C9	C5	-2.2(2)	C15	C16	C17	C21	-177.5(4)
Zn1	N2	C9	C8	177.70(15)	C15	C16	C18	O3	0.1(6)
Zn1	N2	C12	C11	-178.17(16)	C15	C16	C18	C19	177.3(4)
Zn1	N3	C13	C14	-174.3(5)	C16	C17	C21	N4	-179.9(6)
Zn1	N3	C17	C16	174.2(4)	C16	C17	C21	C20	-0.5(7)
Zn1	N3	C17	C21	-7.7(7)	C16	C18	C19	O4	-179.8(4)
Zn1	N4	C21	C17	5.1(8)	C16	C18	C19	C20	0.8(6)
Zn1	N4	C21	C20	-174.3(5)	C17	N3	C13	C14	-0.8(9)
Zn1	N4	C24	C23	174.8(6)	C17	C16	C18	O3	-179.6(4)
Zn1	N3A	C13A	C14A	-176(3)	C17	C16	C18	C19	-2.4(5)
Zn1	N3A	C17A	C16A	175(2)	C18	C16	C17	N3	-179.8(5)
Zn1	N3A	C17A	C21A	-2(4)	C18	C16	C17	C21	2.2(6)
Zn1	N4A	C21A	C17A	10(4)	C18	C19	C20	C21	0.9(6)
Zn1	N4A	C21A	C20A	-173(3)	C18	C19	C20	C22	-178.4(4)
Zn1	N4A	C24A	C23A	177(3)	C19	C20	C21	N4	178.4(6)
O6	S1	O5	Zn1	1.3(2)	C19	C20	C21	C17	-1.0(7)
O6	S1	C27	F1	-58.8(2)	C19	C20	C22	C23	-179.3(4)
O6	S1	C27	F2	61.3(2)	C20	C22	C23	C24	-0.5(7)
O6	S1	C27	F3	-179.96(19)	C21	N4	C24	C23	-1.2(12)
O7	S1	O5	Zn1	137.29(16)	C21	C20	C22	C23	1.5(7)
O7	S1	C27	F1	179.11(18)	C22	C20	C21	N4	-2.4(8)
O7	S1	C27	F2	-60.8(2)	C22	C20	C21	C17	178.3(5)
O7	S1	C27	F3	58.0(2)	C22	C23	C24	N4	0.3(11)
O5	S1	C27	F1	60.4(2)	C24	N4	C21	C17	-178.4(7)
O5	S1	C27	F2	-179.5(2)	C24	N4	C21	C20	2.2(11)
O5	S1	C27	F3	-60.7(2)	O3A	C18A	C19A	O4A	9(3)
C27	S1	O5	Zn1	-111.78(18)	O3A	C18A	C19A	C20A	-179(2)
O1	C6	C7	O2	3.7(3)	O4A	C19A	C20A	C21A	176(2)
O1	C6	C7	C8	-176.33(19)	O4A	C19A	C20A	C22A	-2(4)
O2	C7	C8	C9	175.0(2)	N3A	C13A	C14A	C15A	0(4)
O2	C7	C8	C10	-5.0(3)	N3A	C17A	C21A	N4A	-6(5)
N1	C1	C2	C3	-2.1(3)	N3A	C17A	C21A	C20A	177(3)

N1	C5	C9	N2	3.8(3)	C13A	N3A	C17A	C16A	-5(5)
N1	C5	C9	C8	-176.05(18)	C13A	N3A	C17A	C21A	179(3)
C1	N1	C5	C4	0.6(3)	C13A	C14A	C15A	C16A	-3(3)
C1	N1	C5	C9	-178.75(17)	C14A	C15A	C16A	C17A	1(3)
C1	C2	C3	C4	0.8(3)	C14A	C15A	C16A	C18A	-180(2)
C2	C3	C4	C5	1.1(3)	C15A	C16A	C17A	N3A	2(4)
C2	C3	C4	C6	-176.0(2)	C15A	C16A	C17A	C21A	179(2)
C3	C4	C5	N1	-1.8(3)	C15A	C16A	C18A	O3A	-1(3)
C3	C4	C5	C9	177.49(18)	C15A	C16A	C18A	C19A	-177(2)
C3	C4	C6	O1	-1.5(3)	C16A	C17A	C21A	N4A	178(3)
C3	C4	C6	C7	178.09(19)	C16A	C17A	C21A	C20A	1(4)
C4	C5	C9	N2	-175.57(18)	C16A	C18A	C19A	O4A	-175(2)
C4	C5	C9	C8	4.6(3)	C16A	C18A	C19A	C20A	-3(3)
C4	C6	C7	O2	-175.9(2)	C17A	N3A	C13A	C14A	3(5)
C4	C6	C7	C8	4.0(3)	C17A	C16A	C18A	O3A	178(2)
C5	N1	C1	C2	1.4(3)	C17A	C16A	C18A	C19A	2(3)
C5	C4	C6	O1	-178.5(2)	C18A	C16A	C17A	N3A	-177(3)
C5	C4	C6	C7	1.1(3)	C18A	C16A	C17A	C21A	0(3)
C6	C4	C5	N1	175.23(18)	C18A	C19A	C20A	C21A	4(3)
C6	C4	C5	C9	-5.4(3)	C18A	C19A	C20A	C22A	-175(2)
C6	C7	C8	C9	-5.0(3)	C19A	C20A	C21A	N4A	-180(3)
C6	C7	C8	C10	175.07(19)	C19A	C20A	C21A	C17A	-3(4)
C7	C8	C9	N2	-179.00(18)	C19A	C20A	C22A	C23A	177(2)
C7	C8	C9	C5	0.8(3)	C20A	C22A	C23A	C24A	6(4)
C7	C8	C10	C11	179.3(2)	C21A	N4A	C24A	C23A	7(7)
C8	C10	C11	C12	0.0(3)	C21A	C20A	C22A	C23A	-1(4)
C9	N2	C12	C11	-0.2(3)	C22A	C20A	C21A	N4A	-1(4)
C9	C8	C10	C11	-0.7(3)	C22A	C20A	C21A	C17A	176(3)
C10	C8	C9	N2	0.9(3)	C22A	C23A	C24A	N4A	-9(5)
C10	C8	C9	C5	-179.20(18)	C24A	N4A	C21A	C17A	-179(4)
C10	C11	C12	N2	0.4(3)	C24A	N4A	C21A	C20A	-1(6)
C12	N2	C9	C5	179.61(18)	O5A	S1A	C27A	F2A	-180.0
C12	N2	C9	C8	-0.5(3)	O5A	S1A	C27A	F1A	-60.0
O3	C18	C19	O4	-2.3(6)	O5A	S1A	C27A	F3A	60.0
O3	C18	C19	C20	178.3(4)	O7A	S1A	O5A	Zn1	-155.6(14)
O4	C19	C20	C21	-178.6(4)	O7A	S1A	C27A	F2A	60.0
O4	C19	C20	C22	2.2(6)	O7A	S1A	C27A	F1A	180.0

N3	C13	C14	C15	1.6(7)	O7A	S1A	C27A	F3A	-60.0
N3	C17	C21	N4	1.9(9)	O6A	S1A	O5A	Zn1	-16.3(14)
N3	C17	C21	C20	-178.7(6)	O6A	S1A	C27A	F2A	-60.0
C13	N3	C17	C16	-0.3(9)	O6A	S1A	C27A	F1A	60.0
C13	N3	C17	C21	177.8(6)	O6A	S1A	C27A	F3A	-180.0
C13	C14	C15	C16	-1.4(6)	C27A	S1A	O5A	Zn1	94.0(14)

Table A2.7. Hydrogen Atom Coordinates (Å×10^4) and Isotropic Displacement Parameters ($Å^2$×10^3) for Stahl171.

Atom	*x*	*y*	*z*	U(eq)
H1	1685	4007	1502	28
H2	2560	3555	807	31
H3	3545	4036	889	30
H10	3646	6637	3350	31
H11	2714	6913	4119	31
H12	1812	6317	3943	28
H13	1518	6380	1700	39
H14	917	6931	628	43
H15	-53	6554	127	42
H22	-848	3788	1628	43
H23	-153	3316	2646	42
H24	766	3819	3117	35
H13A	1674	6410	1867	35
H14A	1168	7044	795	43
H15A	215	6735	171	39
H22A	-844	3980	1366	41
H23A	-180	3381	2291	40
H24A	679	3870	3021	37
H26A	-416	6149	4537	45
H26B	102	6340	5296	45
H26C	-227	5688	5351	45

Appendix 3

Supplementary Information for Chapter 4

This work has been published:

Wendlandt, A. E.; Stahl, S. S. *J. Am. Chem. Soc.* **2014**, *136*, 11910–11913.

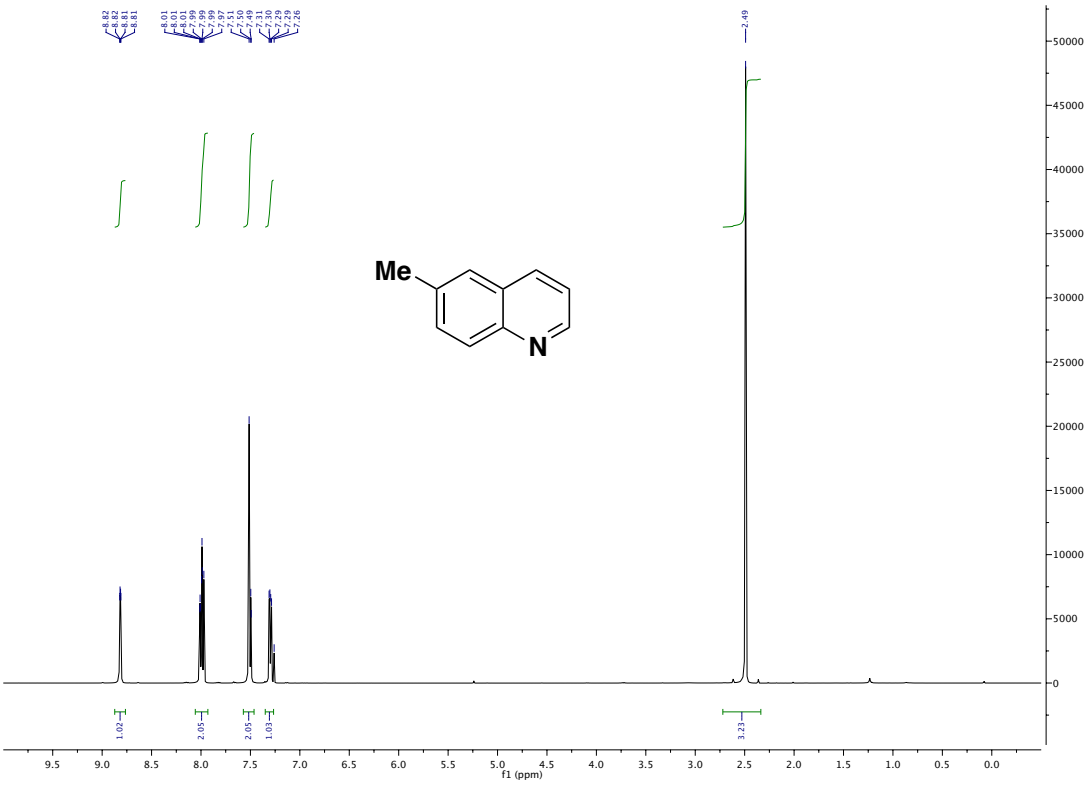
8.82
8.82
8.81
8.81
8.01
8.01
8.00
8.00
7.99
7.99
7.97
7.97
7.51
7.50
7.49
7.31
7.30
7.29
7.28
7.26
2.49
Me
N
1.02
2.05
2.05
1.03
3.23
f1 (ppm)

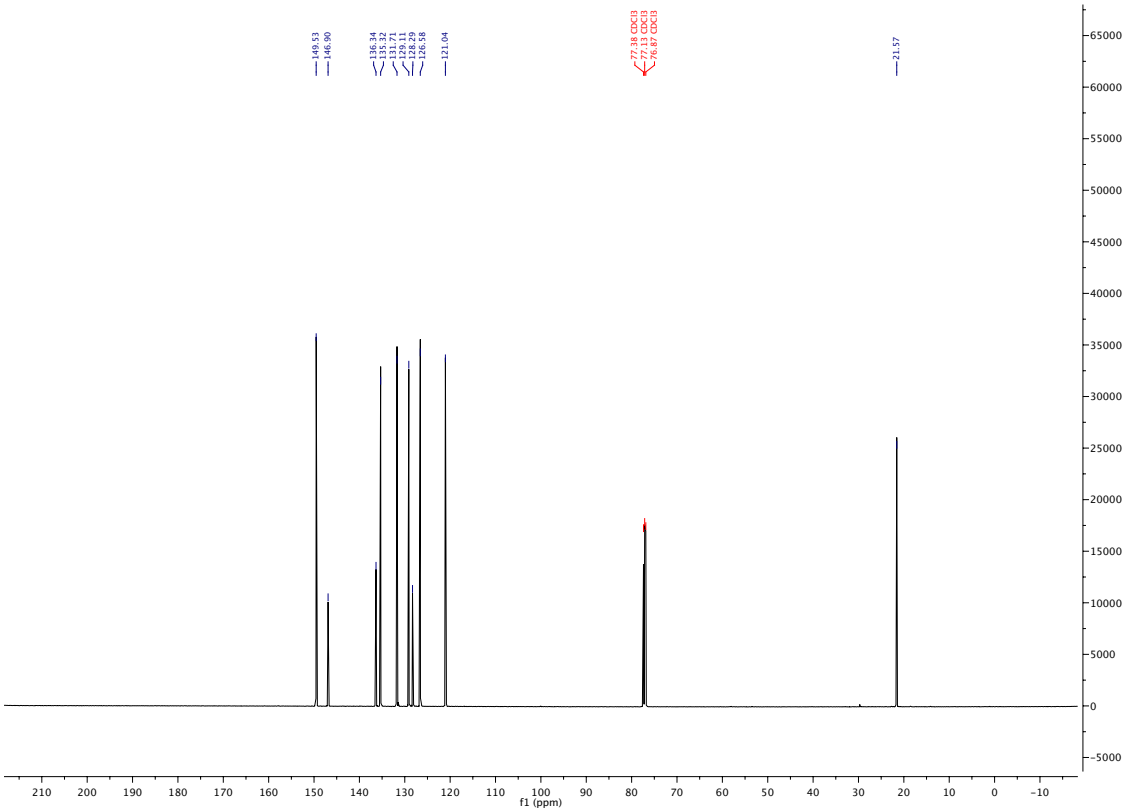
149.53
146.90
136.34
135.32
131.71
129.11
128.29
126.58
121.04
77.38 CDCl3
77.13 CDCl3
76.87 CDCl3
21.57
f1 (ppm)

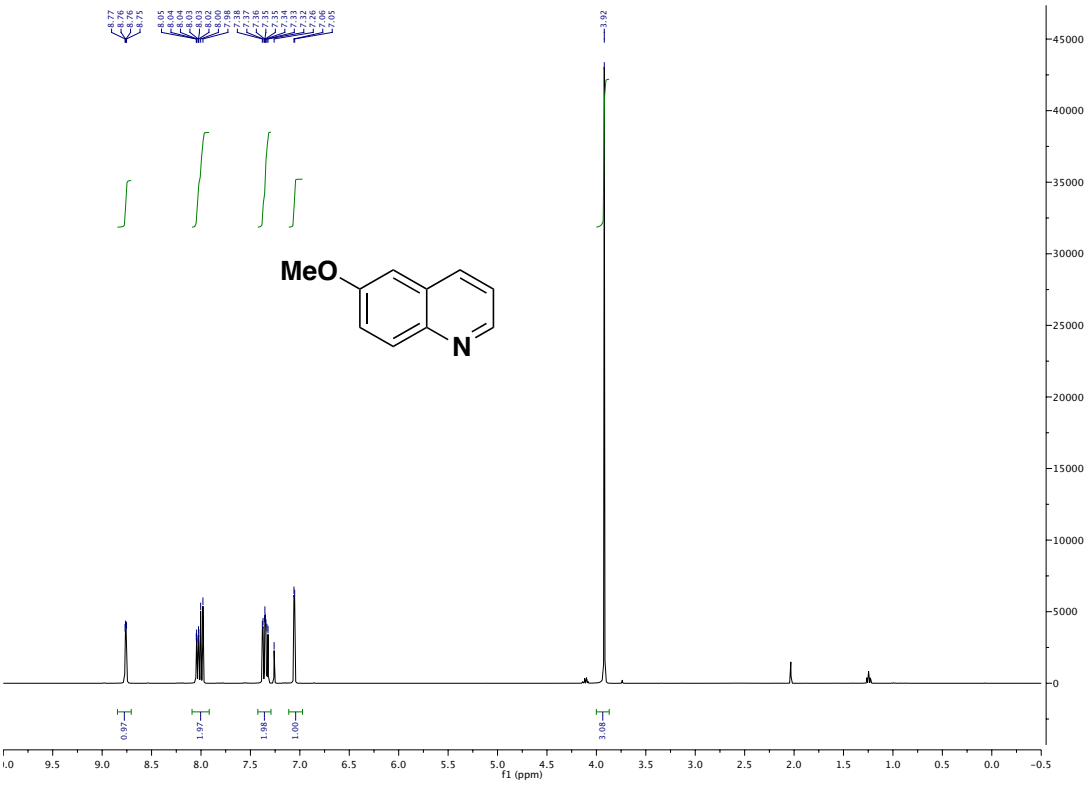
8.77
8.76
8.76
8.75
8.05
8.04
8.04
8.03
8.03
8.02
8.00
7.98
7.38
7.37
7.37
7.36
7.35
7.35
7.34
7.33
7.32
7.26
7.06
7.05
3.92
MeO
N
0.97
1.97
1.98
1.00
3.08
f1 (ppm)

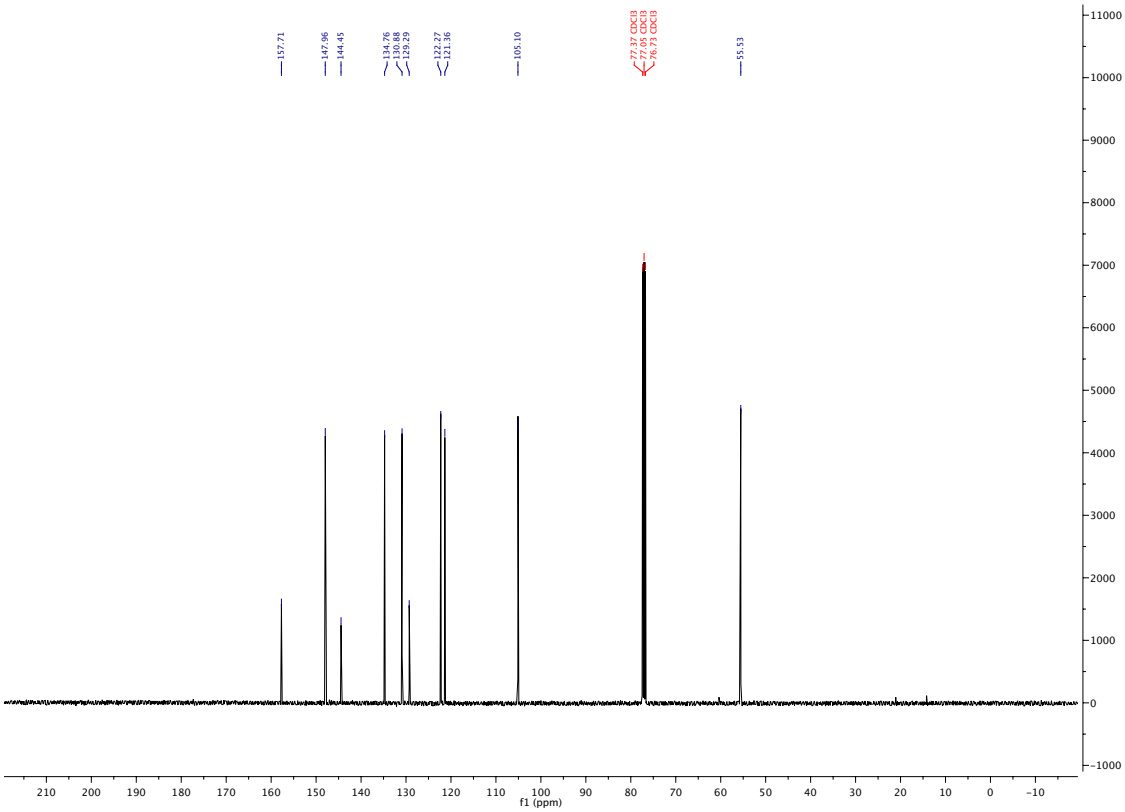
157.71
147.96
144.45
134.76
130.88
129.29
122.27
121.36
105.10
77.37 CDCl3
77.05 CDCl3
76.73 CDCl3
55.53
f1 (ppm)

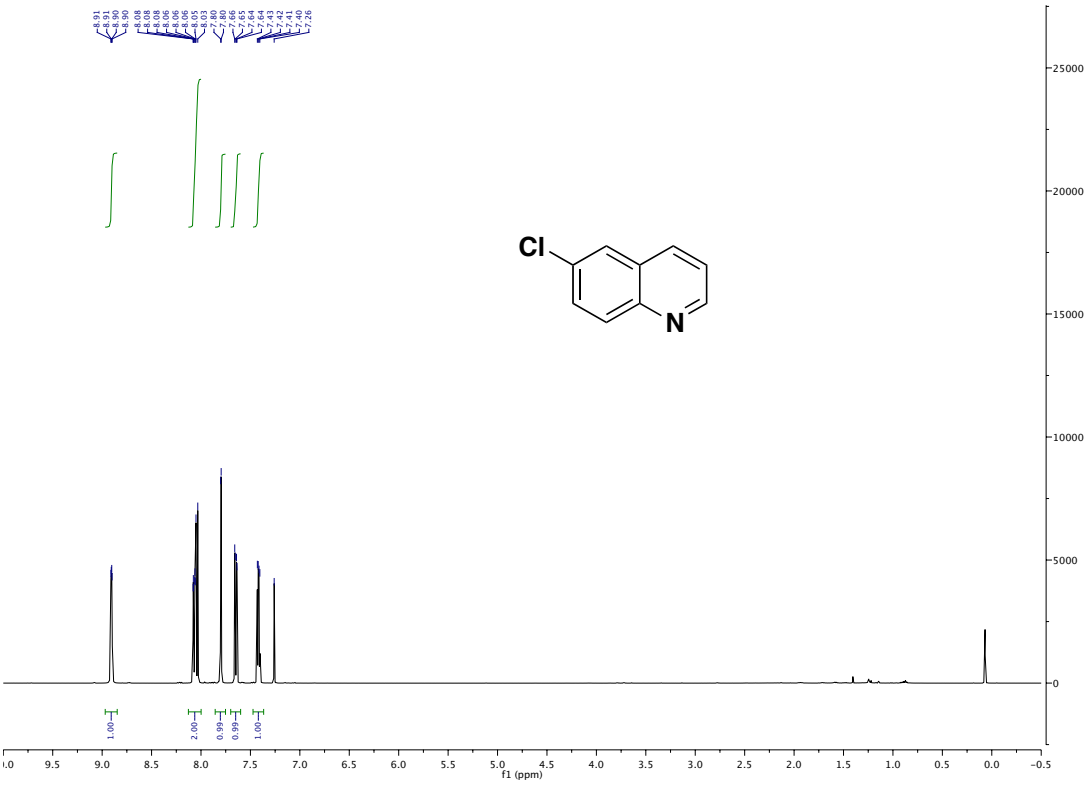
8.91
8.91
8.90
8.90
8.08
8.08
8.08
8.08
8.06
8.06
8.06
8.06
8.05
8.05
7.80
7.80
7.79
7.66
7.65
7.64
7.44
7.43
7.42
7.41
7.40
7.26
Cl
N
1.00
2.00
0.99
0.99
1.00
f1 (ppm)

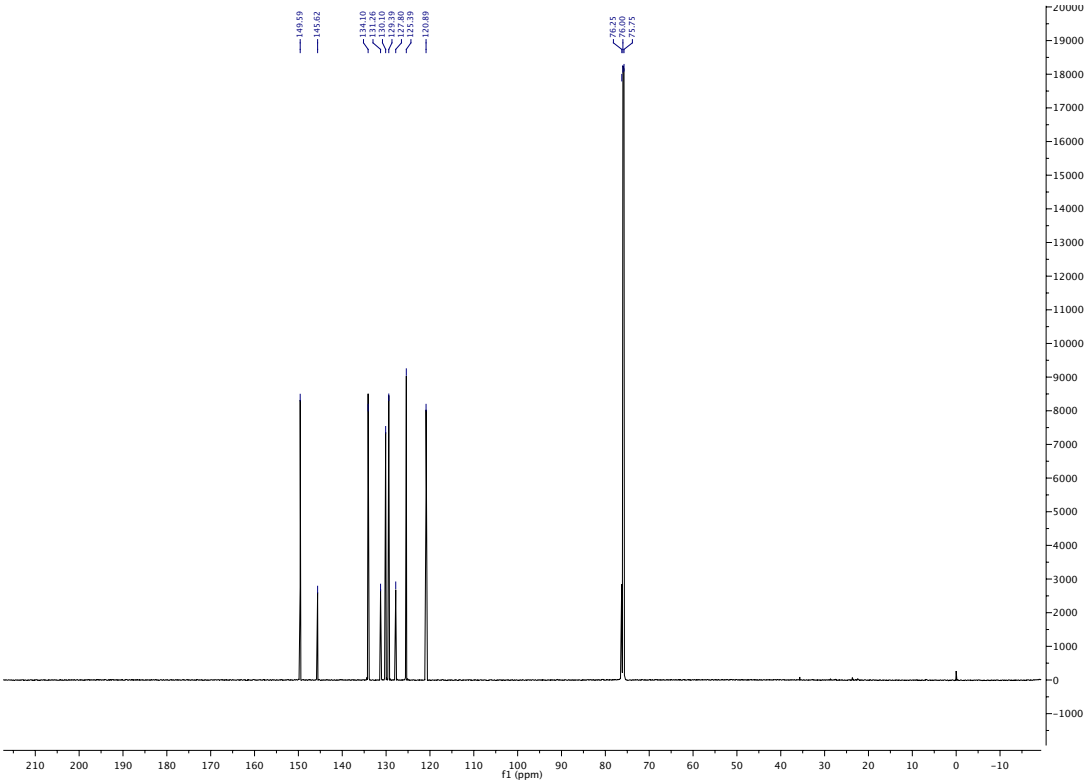
149.59
145.62
134.10
131.46
130.10
129.39
129.00
125.39
120.89
76.35
76.00
75.75
f1 (ppm)

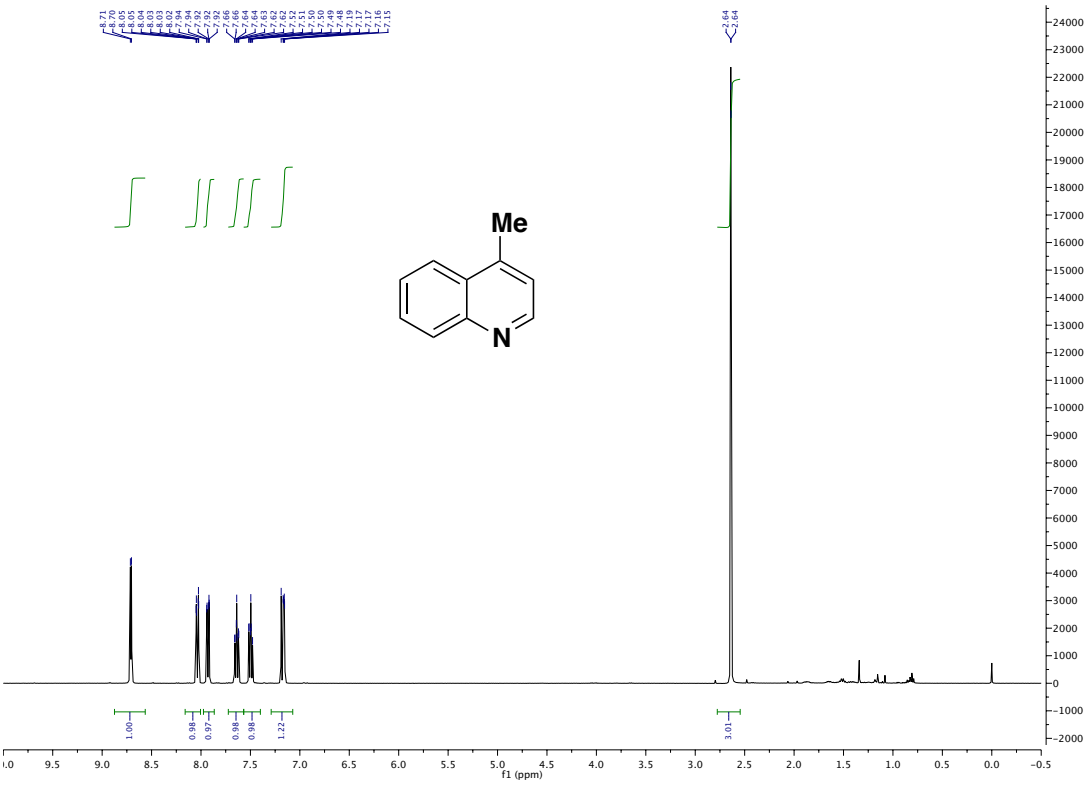
Me
N
f1 (ppm)

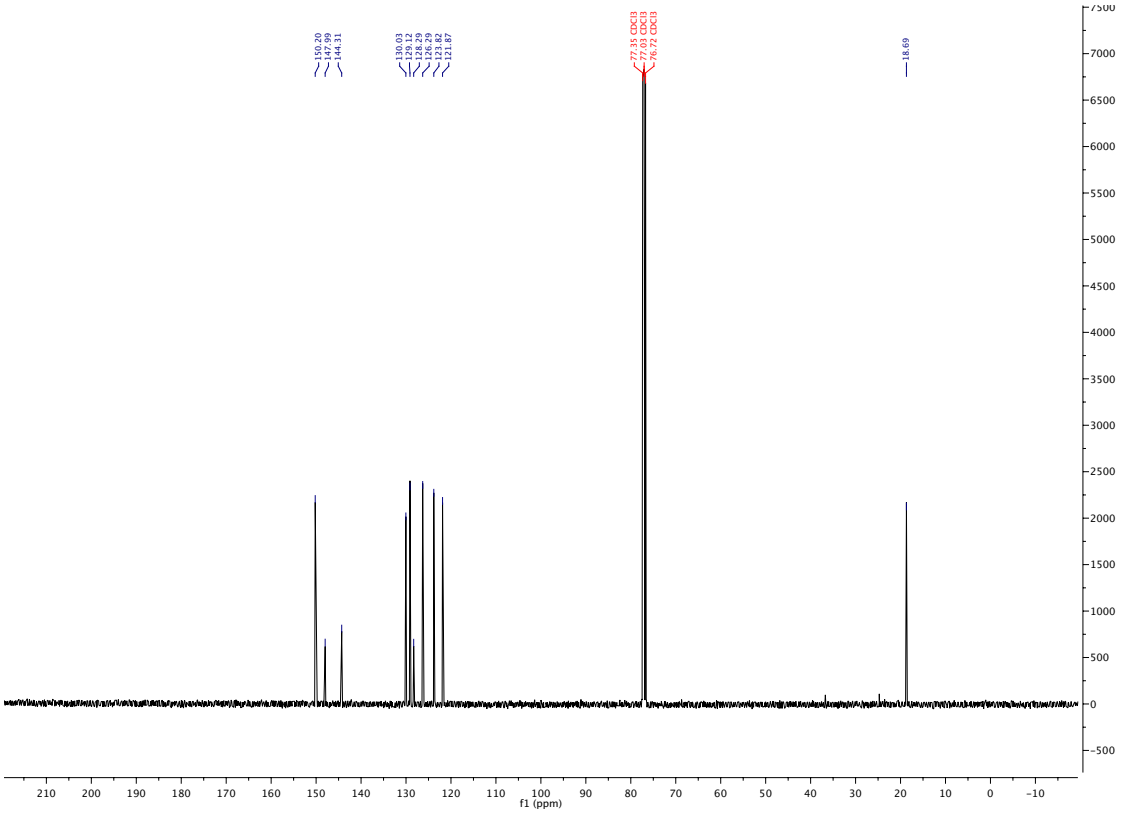
150.20
147.99
144.31
130.03
129.13
128.29
126.29
123.82
121.87
77.35 CDCl3
77.03 CDCl3
76.72 CDCl3
18.69
f1 (ppm)

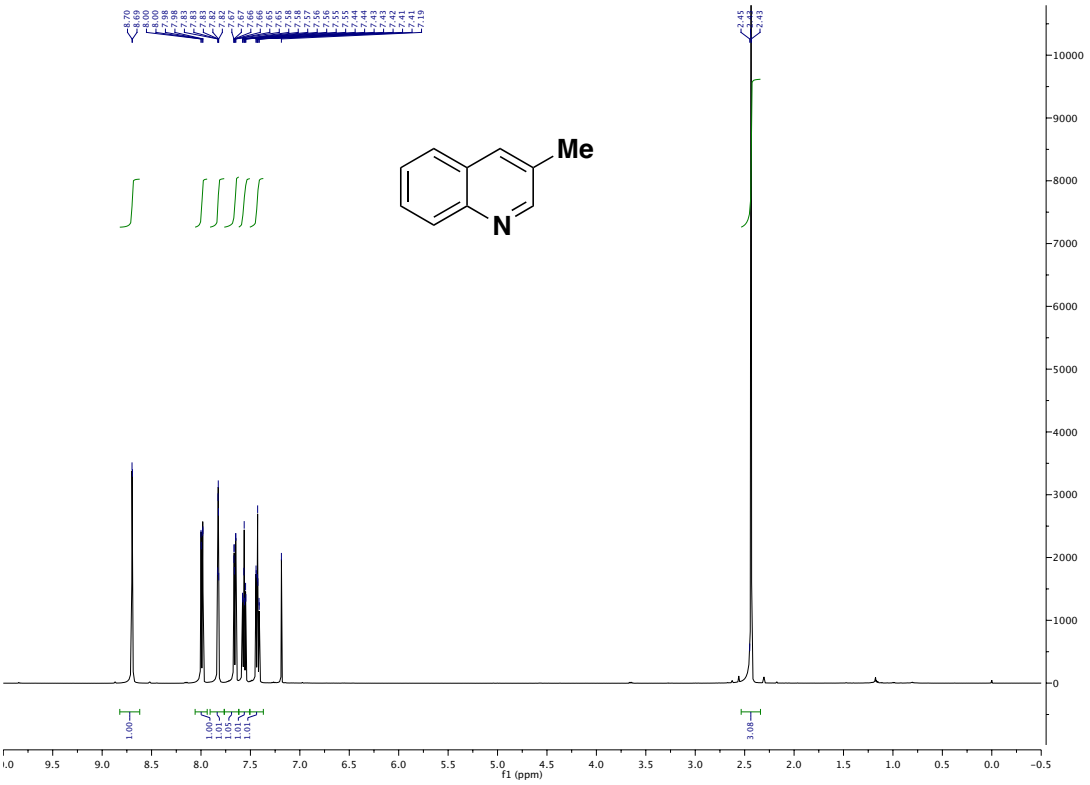
Me
N
f1 (ppm)

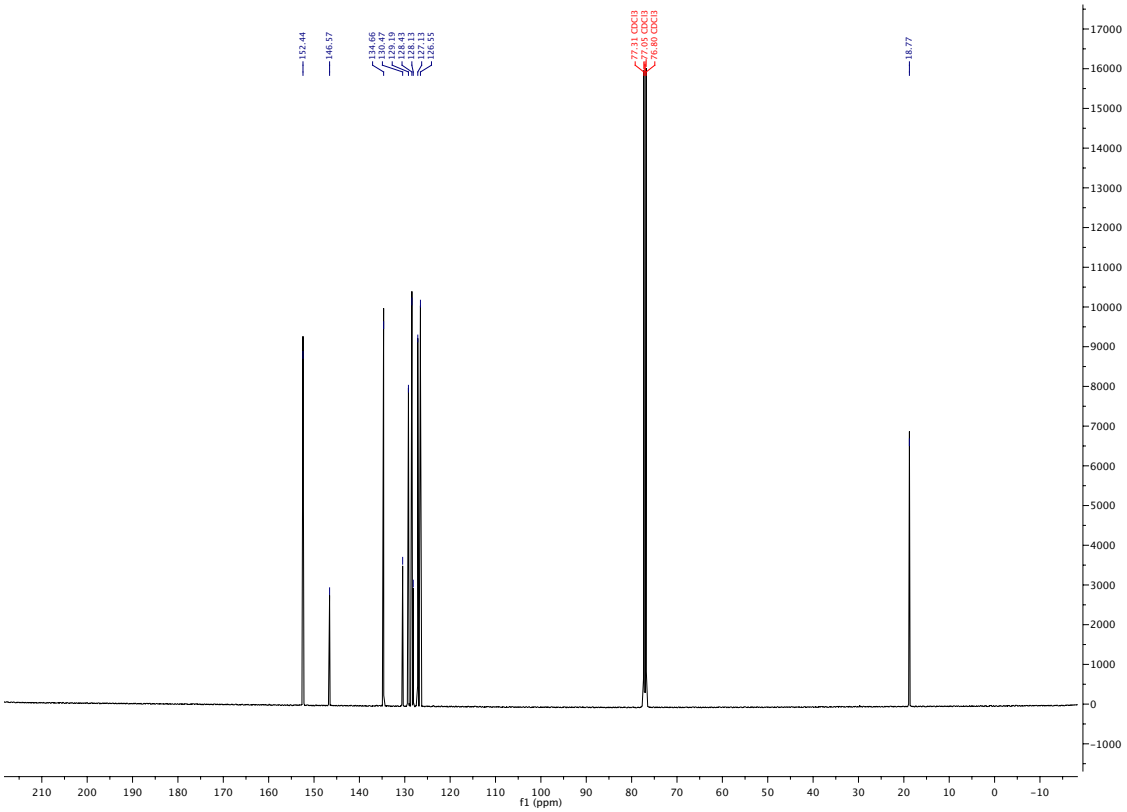
152.44
146.57
134.66
130.47
129.39
128.43
129.13
127.71
126.55
77.31 CDCl3
77.05 CDCl3
76.80 CDCl3
18.77
f1 (ppm)

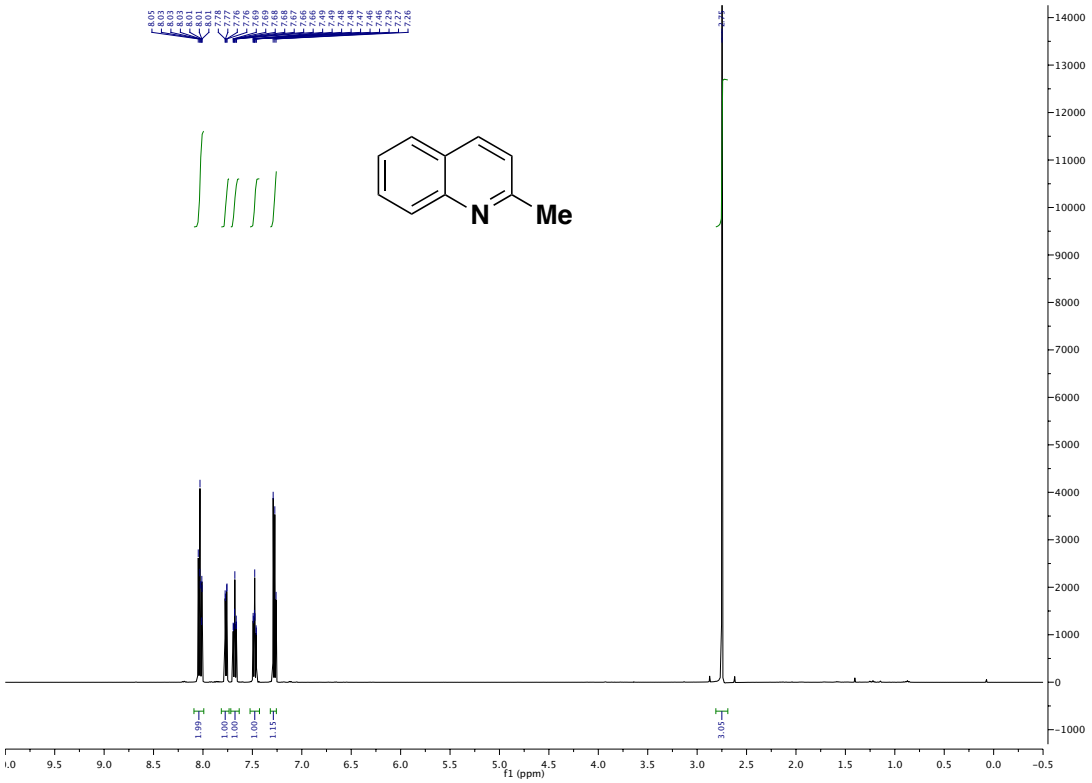
N
Me
f1 (ppm)

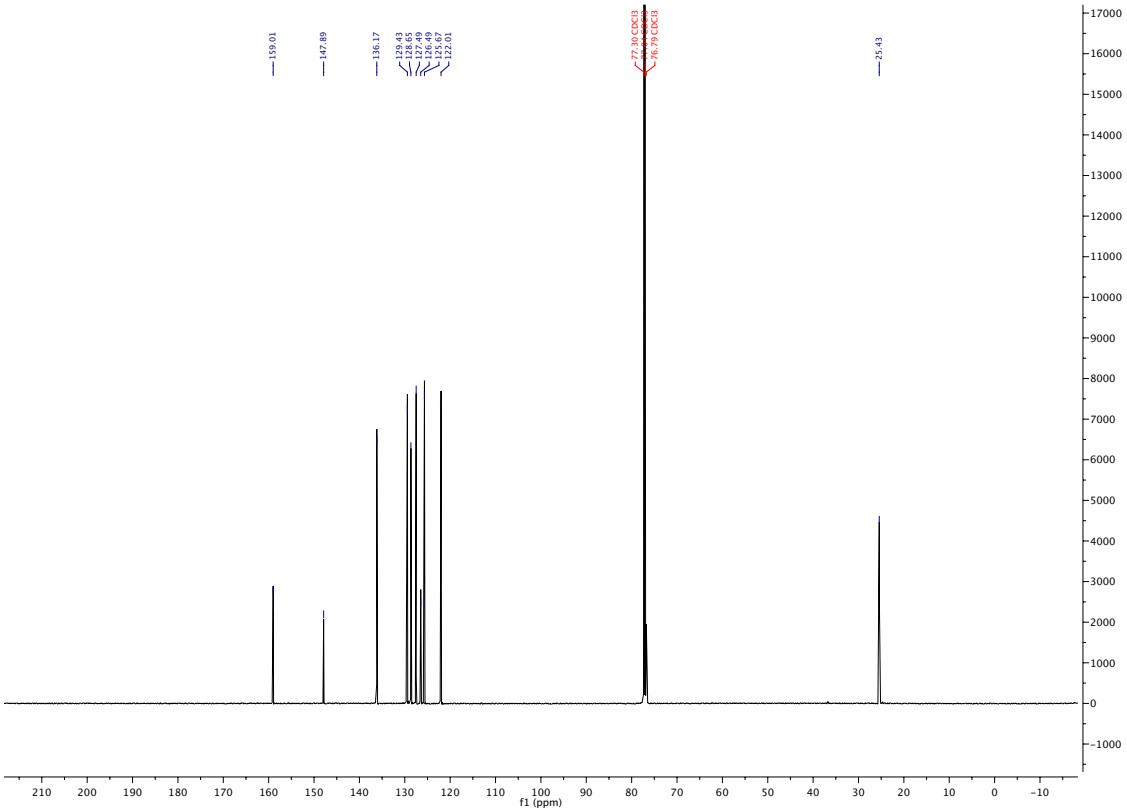
159.01
147.89
136.17
129.43
129.45
127.49
126.49
125.67
122.01
77.30 CDCl3
77.04 CDCl3
76.79 CDCl3
25.43
f1 (ppm)

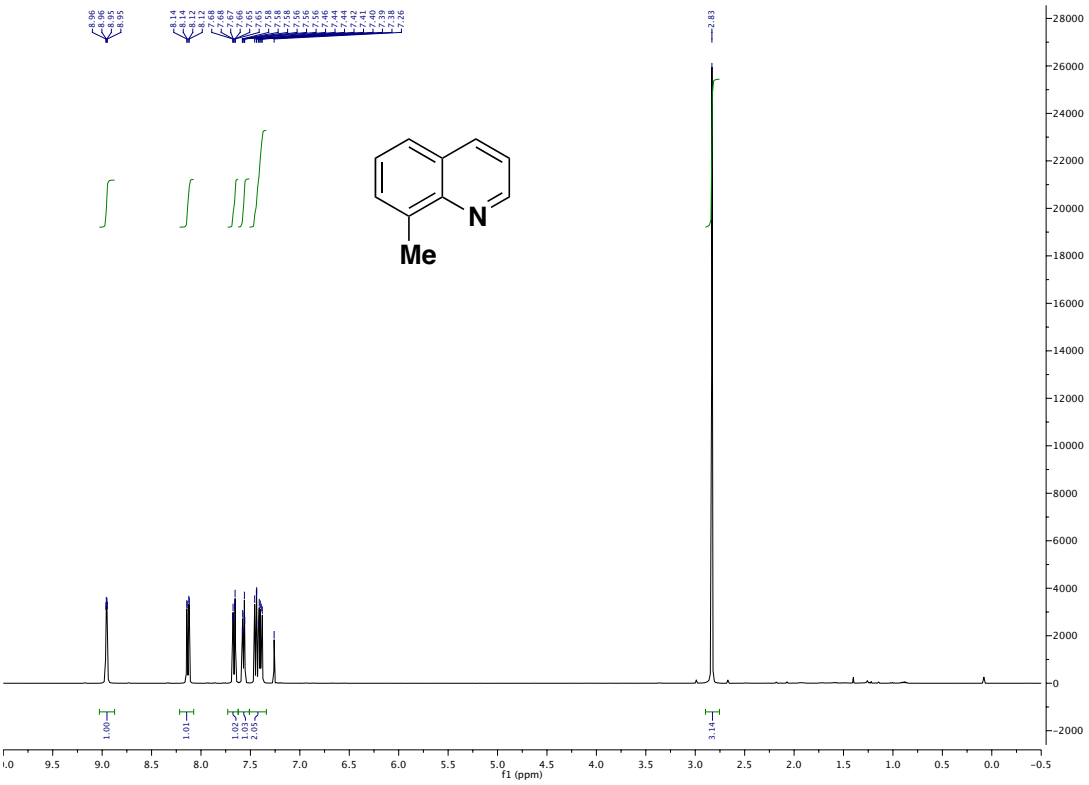
8.96
8.95
8.14
8.12
7.68
7.67
7.66
7.65
7.58
7.56
7.46
7.44
7.42
7.41
7.40
7.39
7.38
7.26
2.83
N
Me
1.00
1.01
1.02
1.03
2.05
3.14
f1 (ppm)

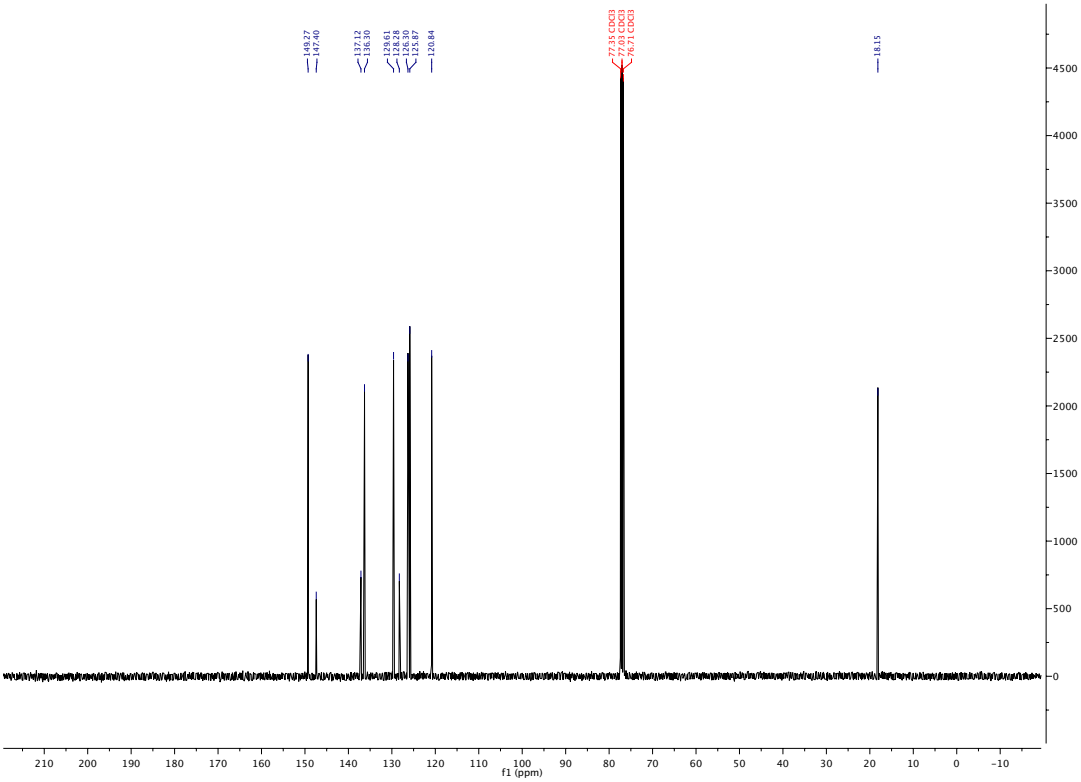
149.27
147.40
137.12
136.30
129.61
128.28
126.30
125.87
120.84
77.35 CDCl3
77.03 CDCl3
76.71 CDCl3
18.15
f1 (ppm)

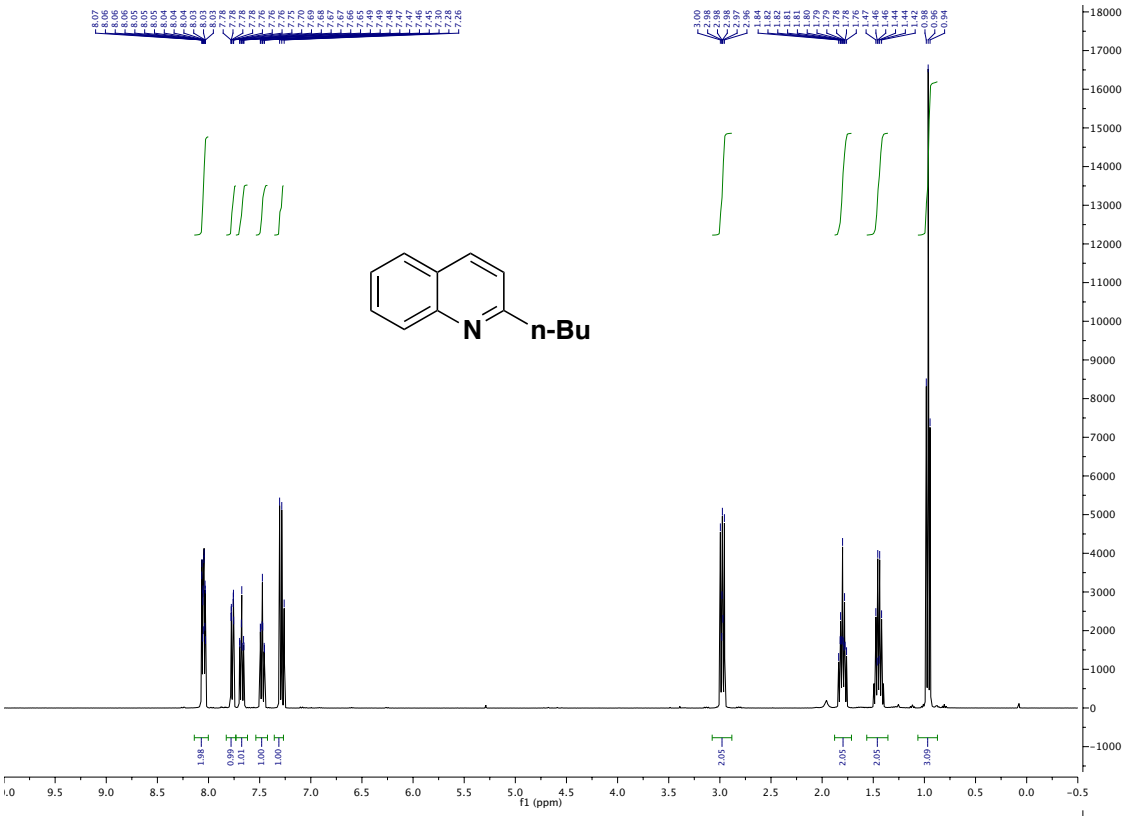
N
n-Bu
f1 (ppm)

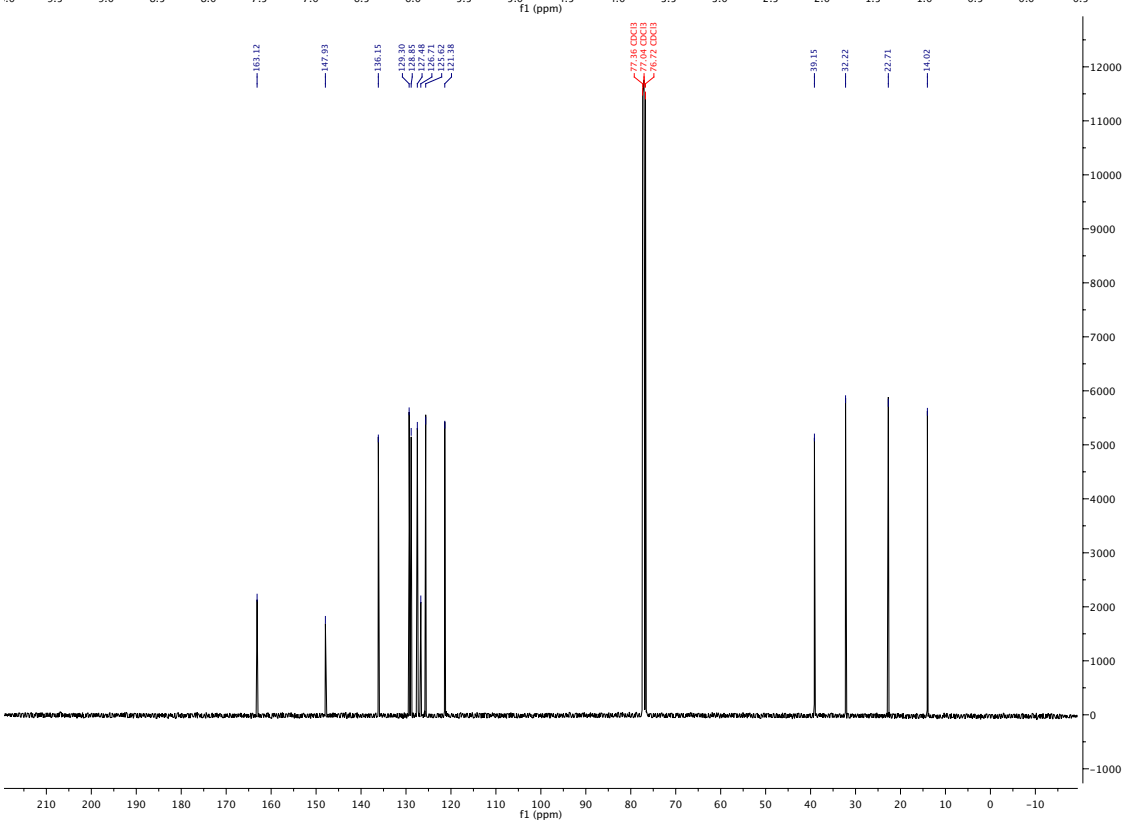
163.12
147.93
136.15
129.30
128.85
127.48
127.46
126.71
125.62
121.38
77.36 CDCl3
77.04 CDCl3
76.72 CDCl3
39.15
32.22
22.71
14.02
f1 (ppm)

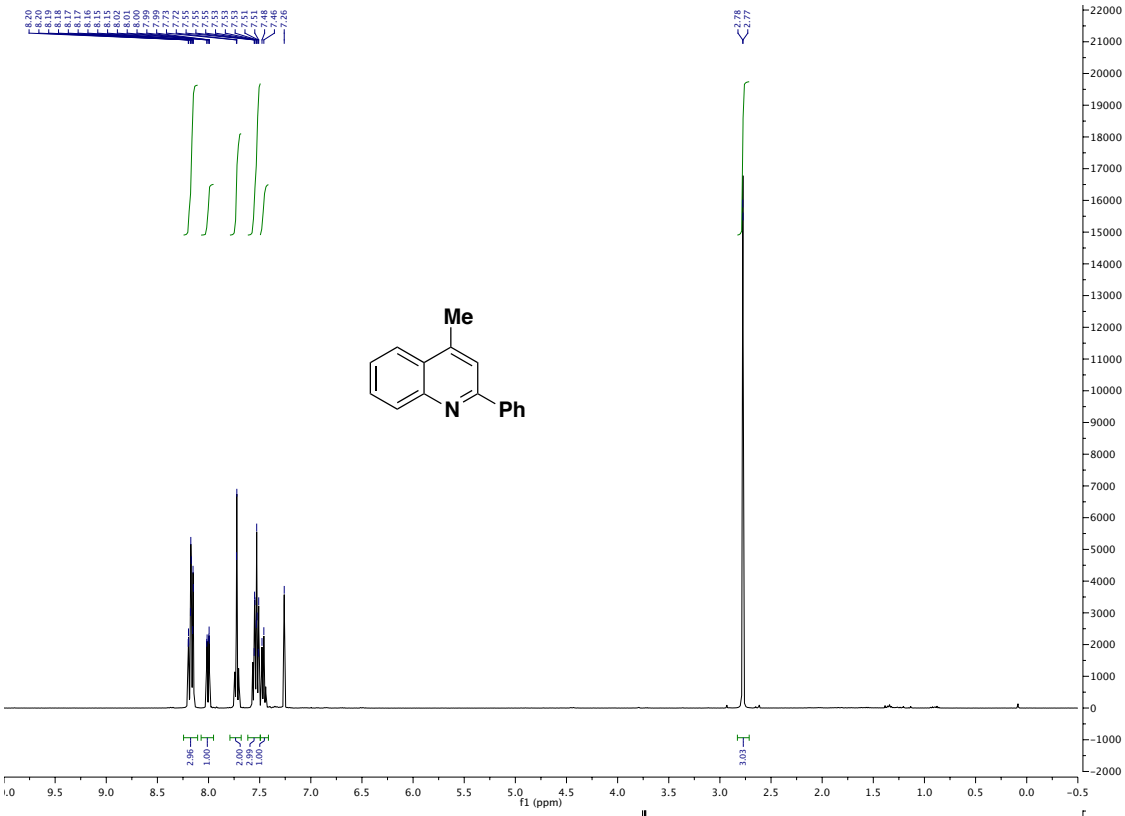
Me
N
Ph
f1 (ppm)

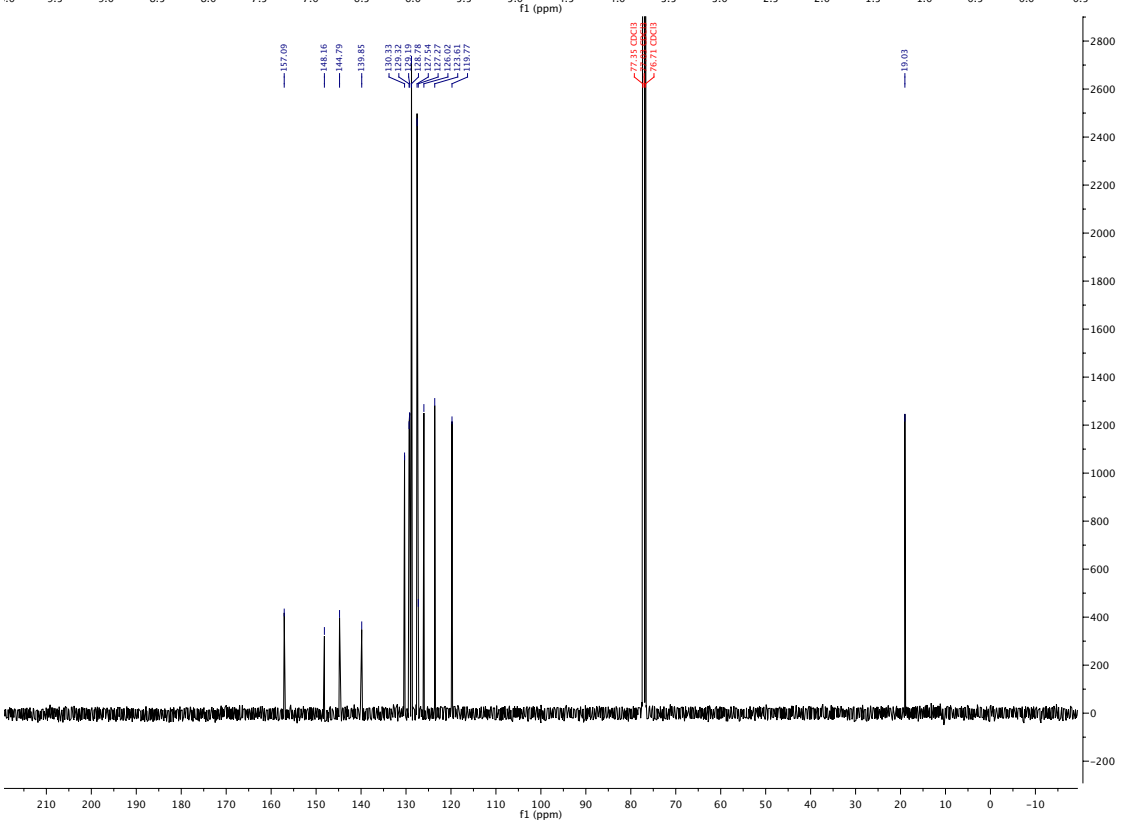
157.09
148.16
144.79
139.85
130.33
129.32
129.19
128.78
127.54
127.27
126.02
123.61
119.77
77.35 CDCl3
77.04 CDCl3
76.71 CDCl3
19.03
f1 (ppm)

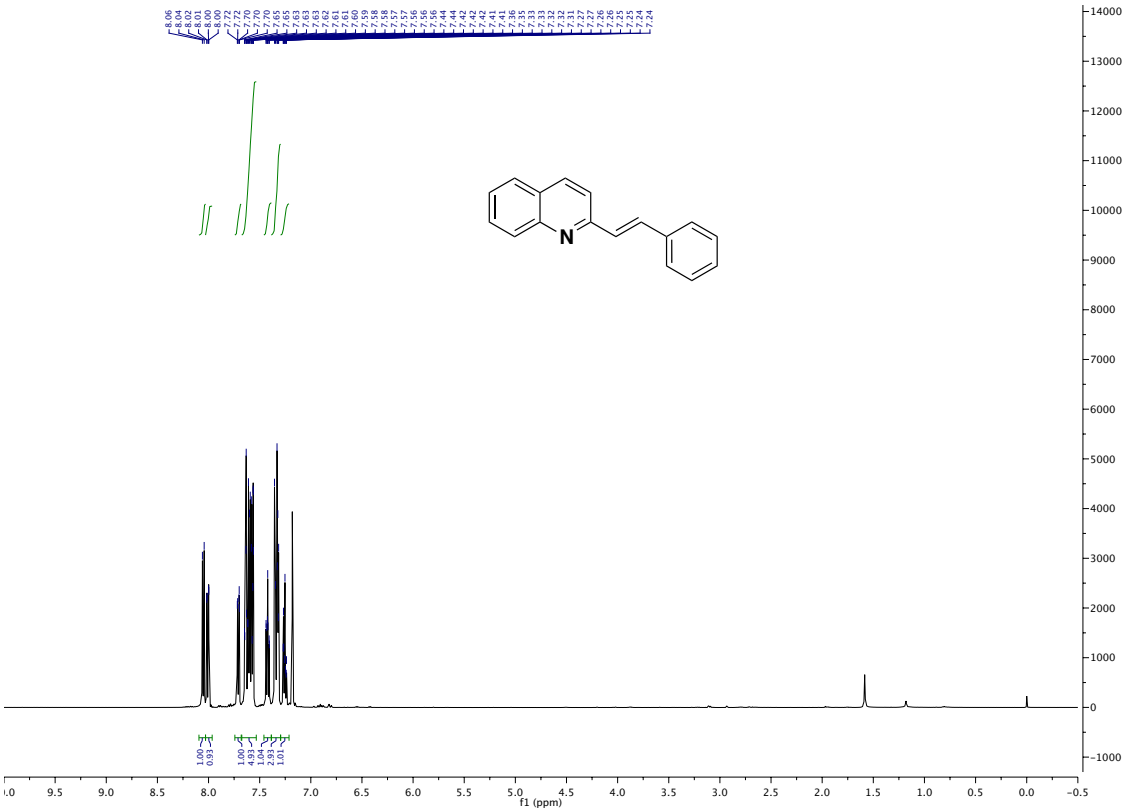
N
f1 (ppm)

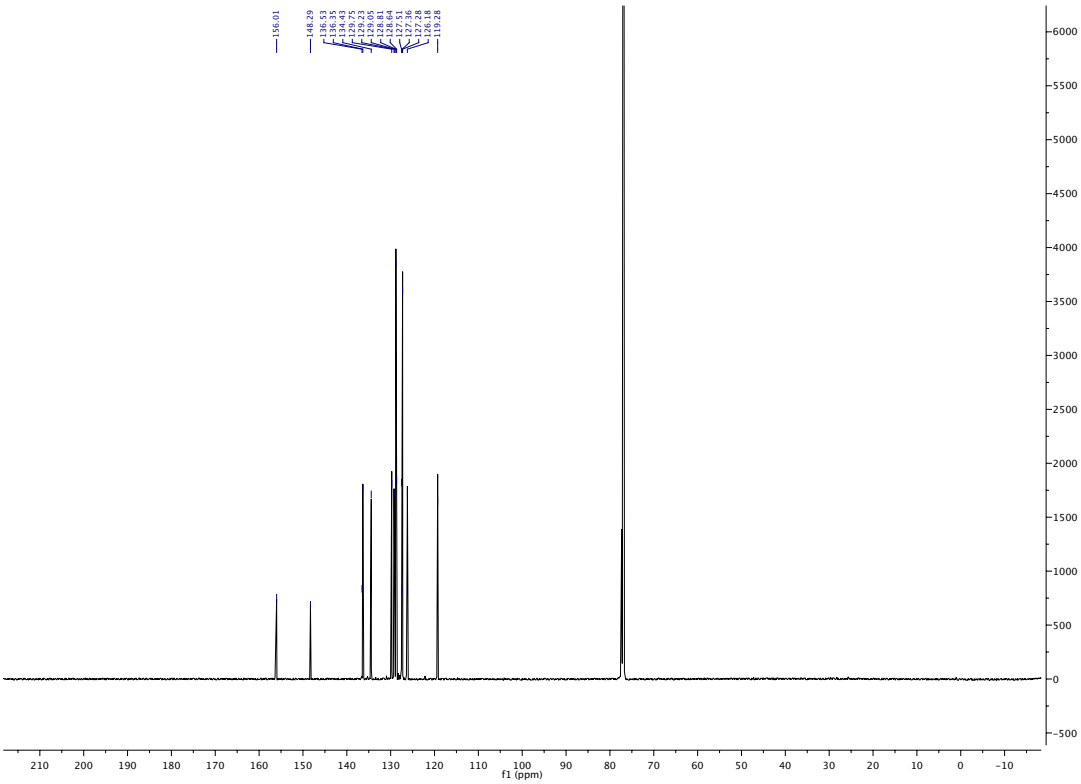
156.01
148.29
136.53
135.55
134.43
129.75
129.23
129.05
128.81
128.64
125.51
127.36
127.28
126.18
119.28
f1 (ppm)

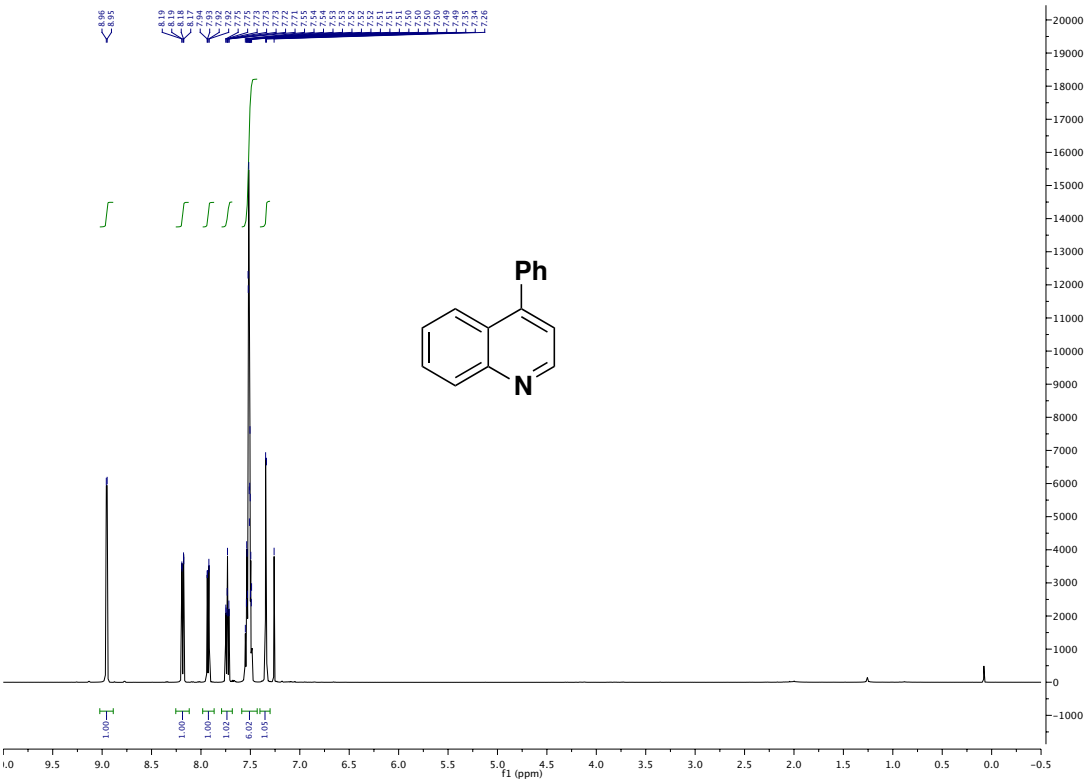
Ph
N
f1 (ppm)

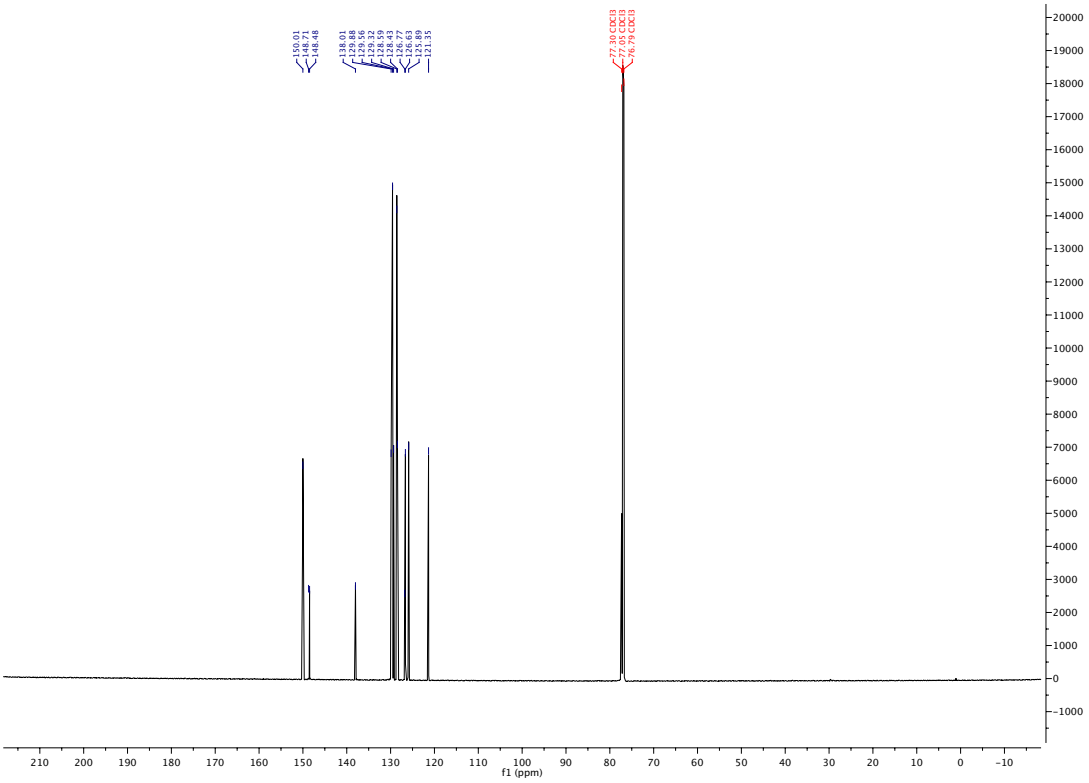
f1 (ppm)

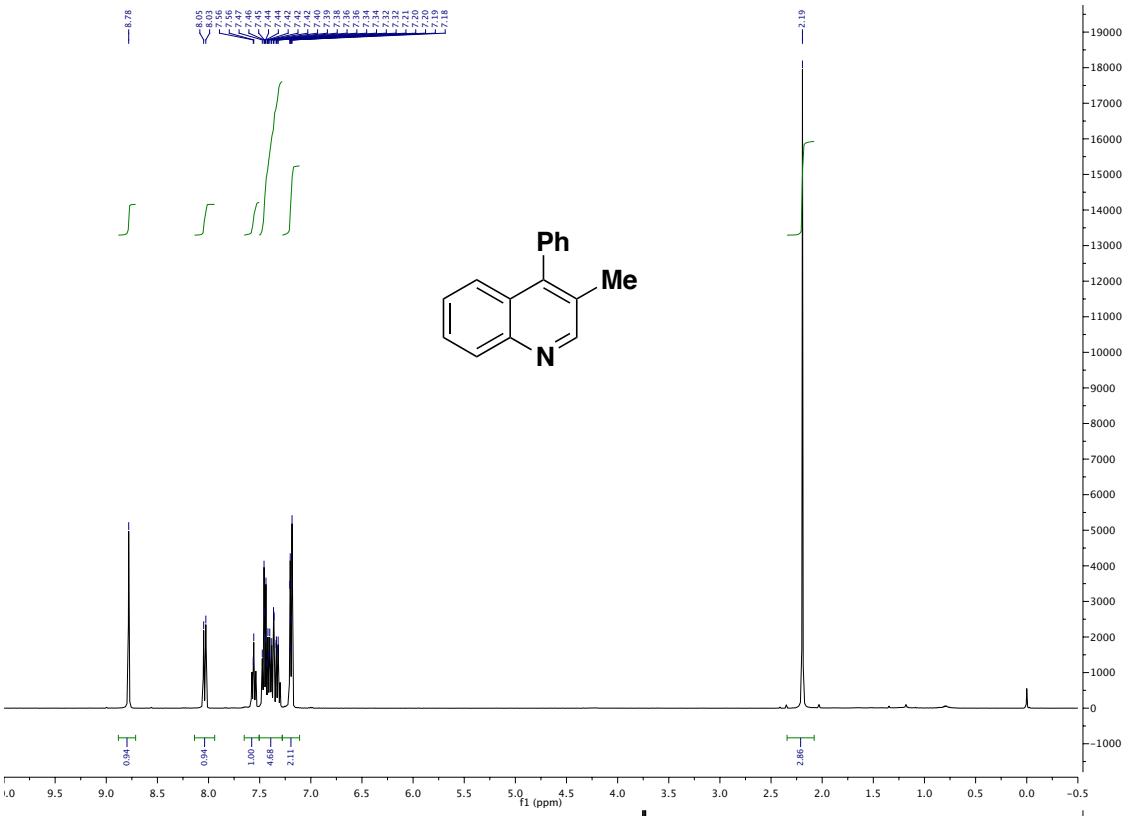
Ph
Me
N
f1 (ppm)

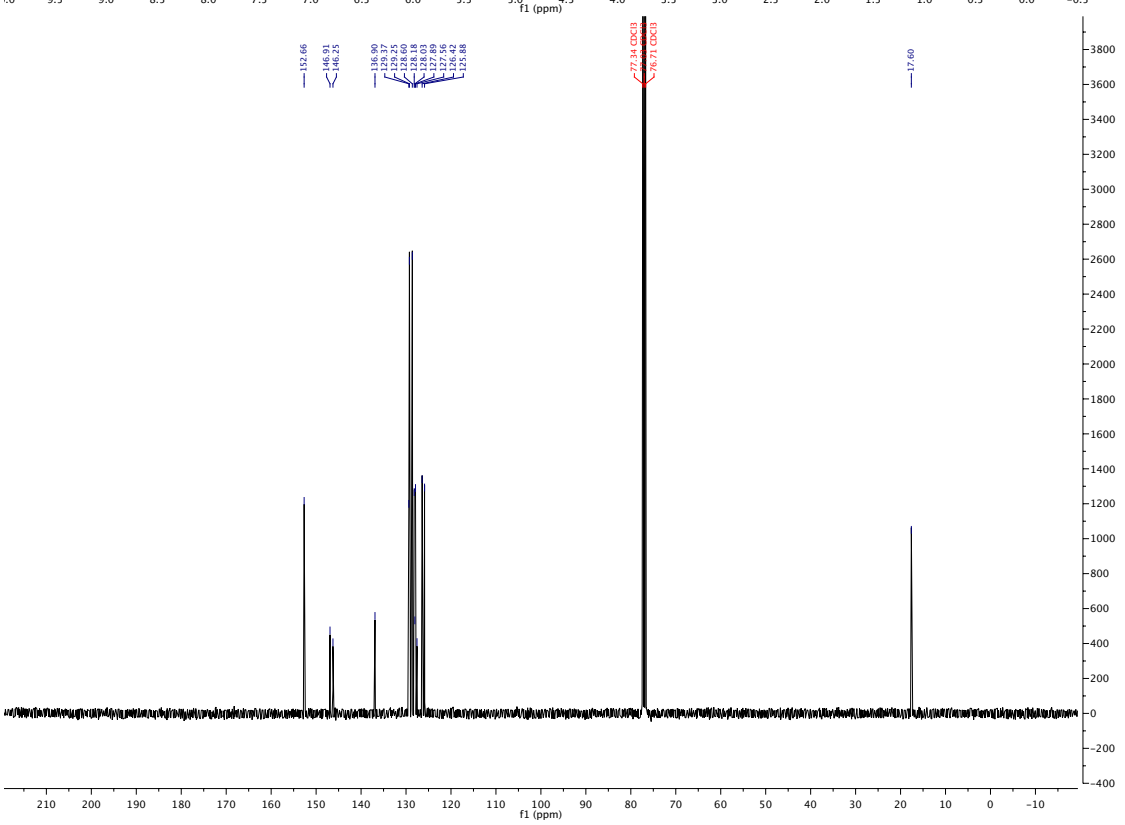
f1 (ppm)

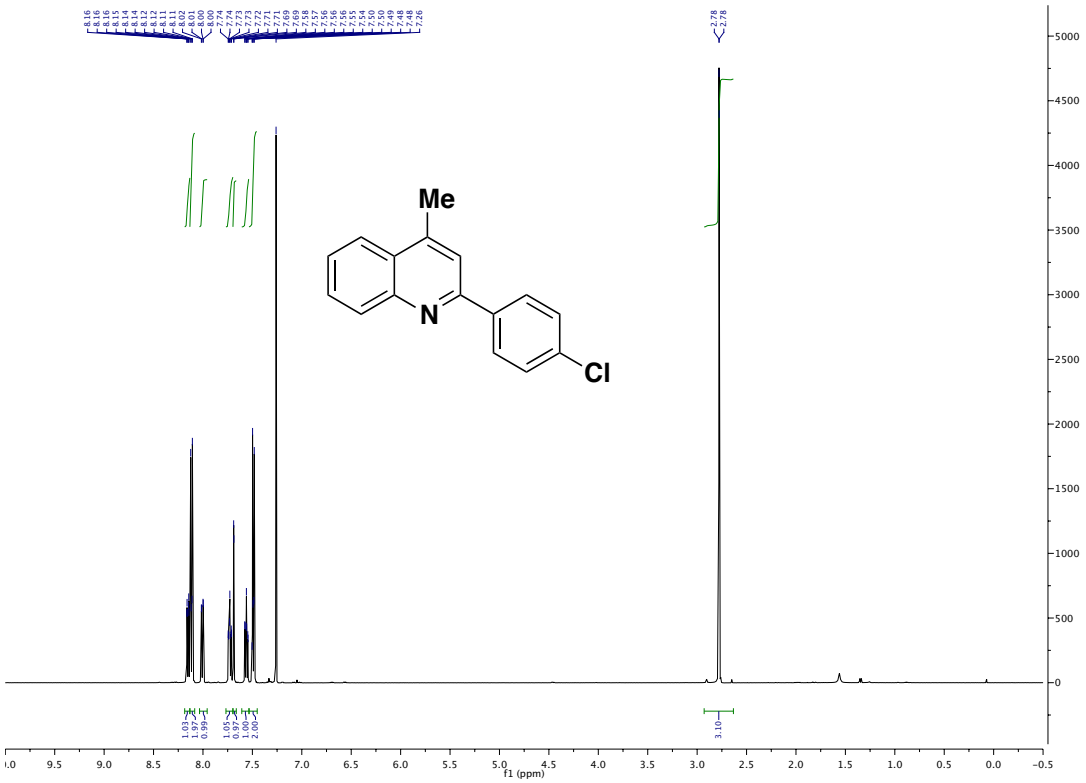
Me
N
Cl
f1 (ppm)

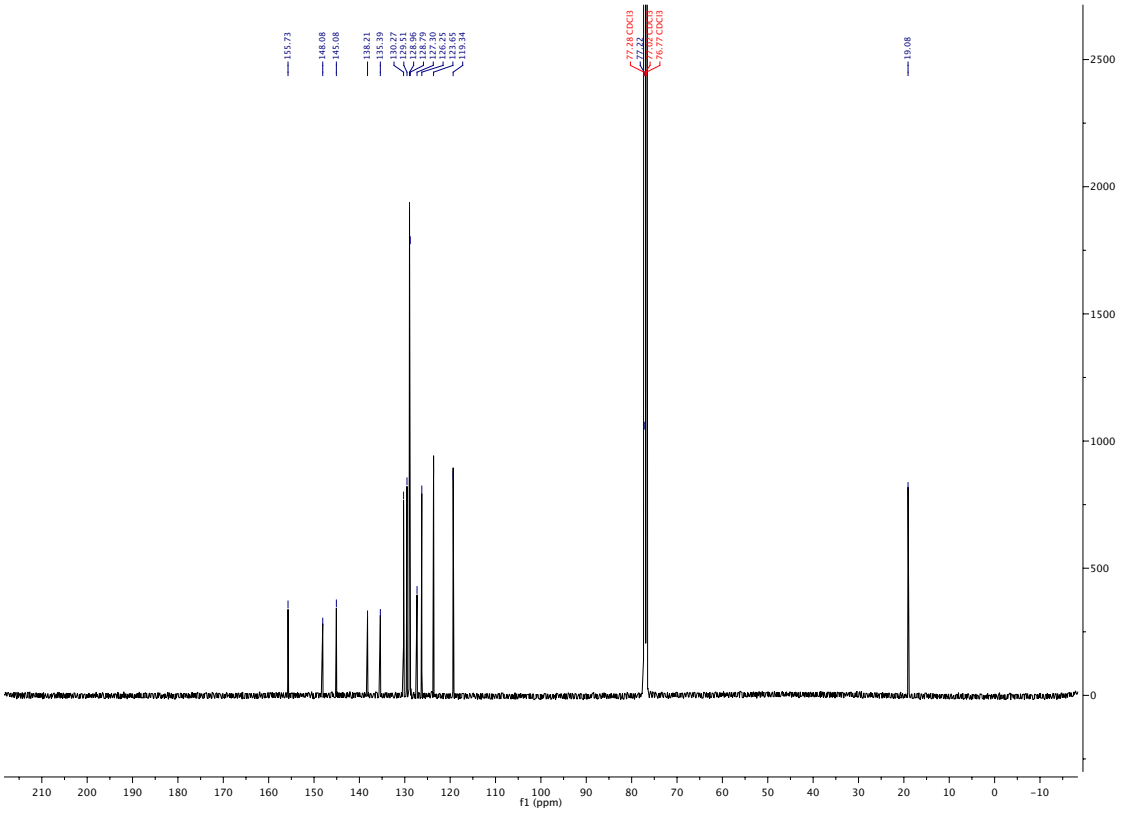
155.73
148.08
145.08
138.21
131.39
130.27
129.51
128.96
127.79
127.30
126.25
123.65
119.34
77.28 CDCl3
77.02 CDCl3
76.77 CDCl3
19.08
f1 (ppm)

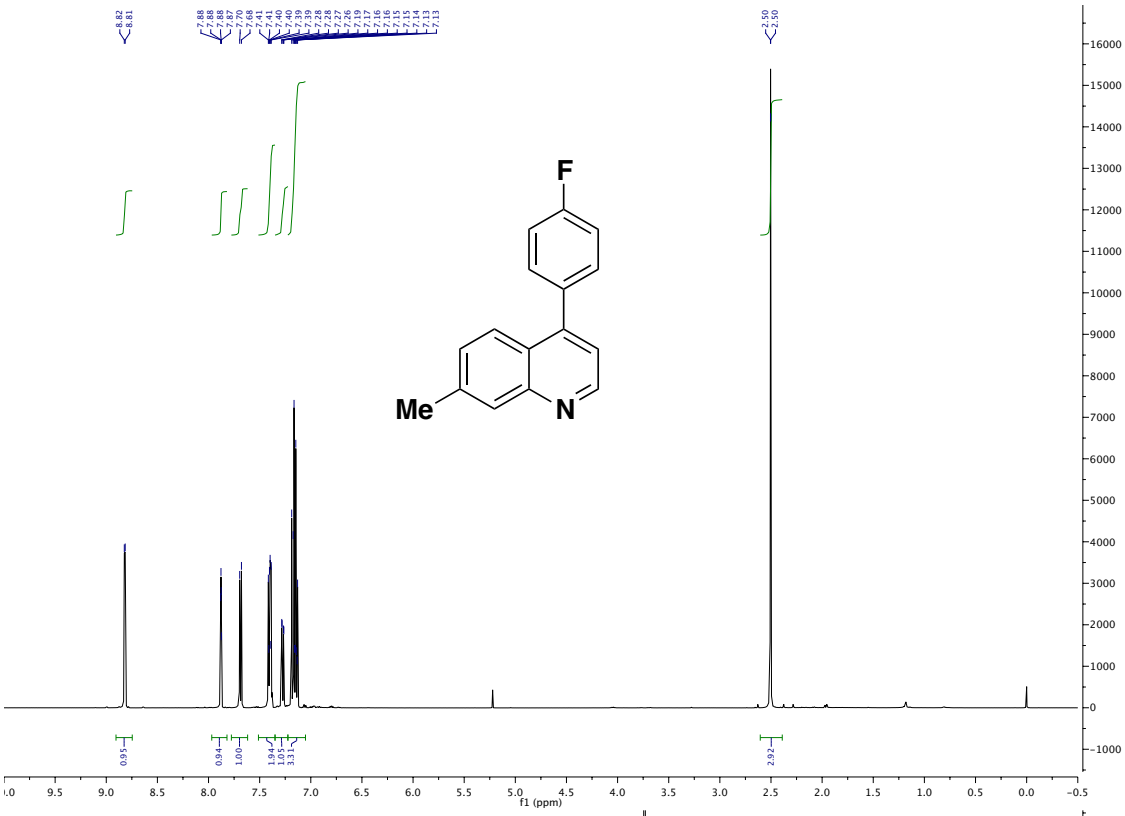
F
Me
N
f1 (ppm)

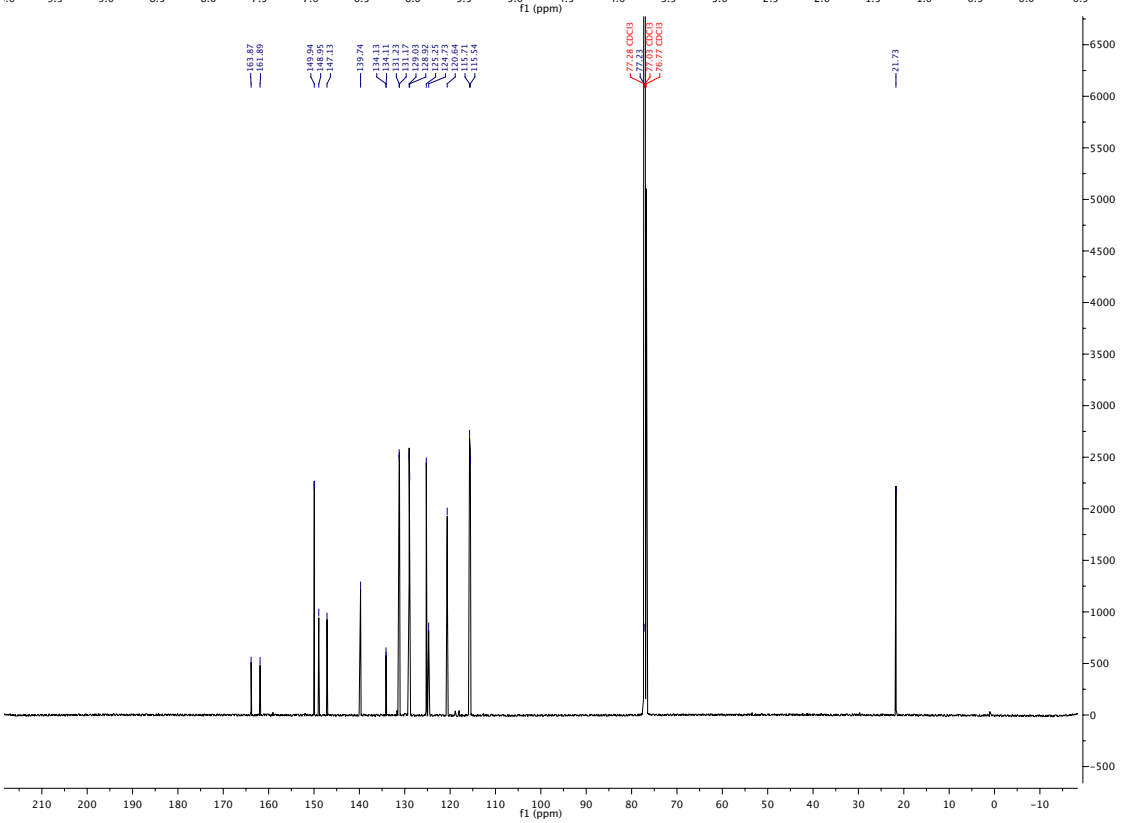
f1 (ppm)

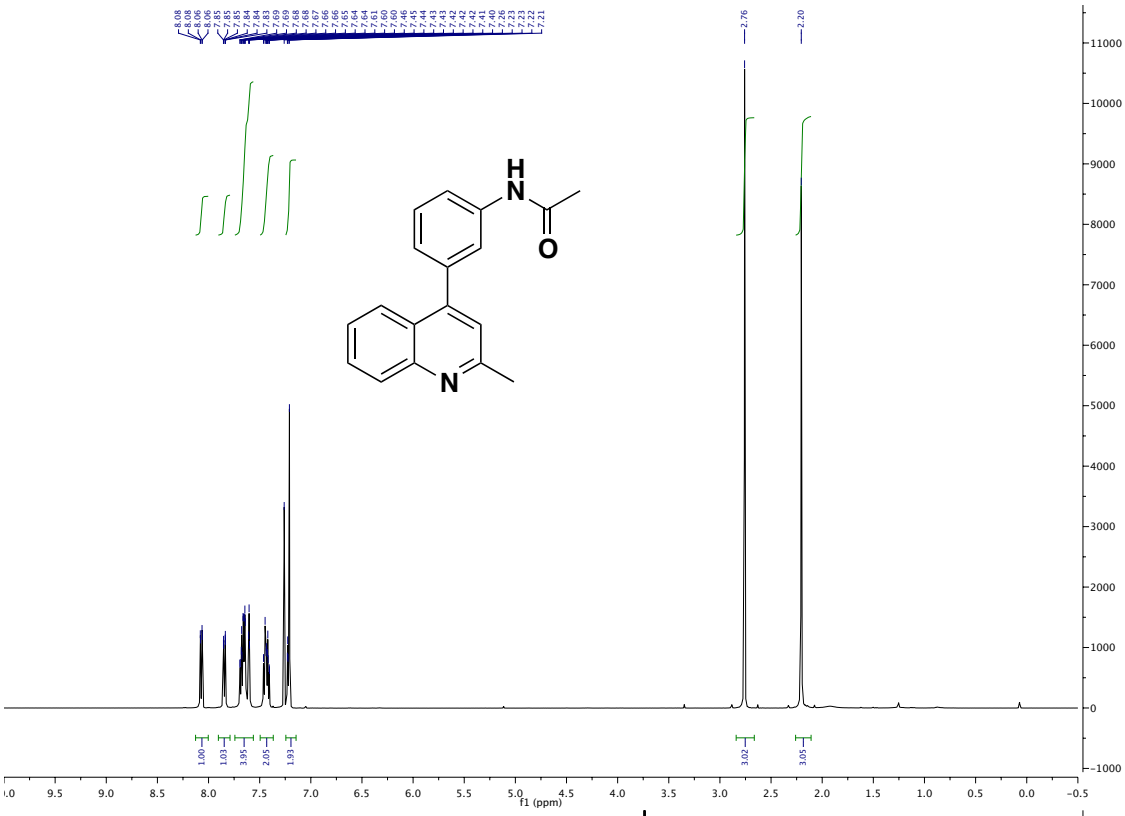
8.08
8.08
8.06
8.06
7.85
7.85
7.85
7.85
7.84
7.84
7.84
7.83
7.69
7.69
7.68
7.68
7.67
7.67
7.66
7.66
7.65
7.65
7.64
7.64
7.61
7.60
7.60
7.60
7.46
7.45
7.44
7.43
7.43
7.42
7.42
7.42
7.41
7.40
7.26
7.23
7.23
7.22
7.21
2.76
2.20
H
N
O
N
1.00
1.03
3.95
2.05
1.93
3.02
3.05
f1 (ppm)

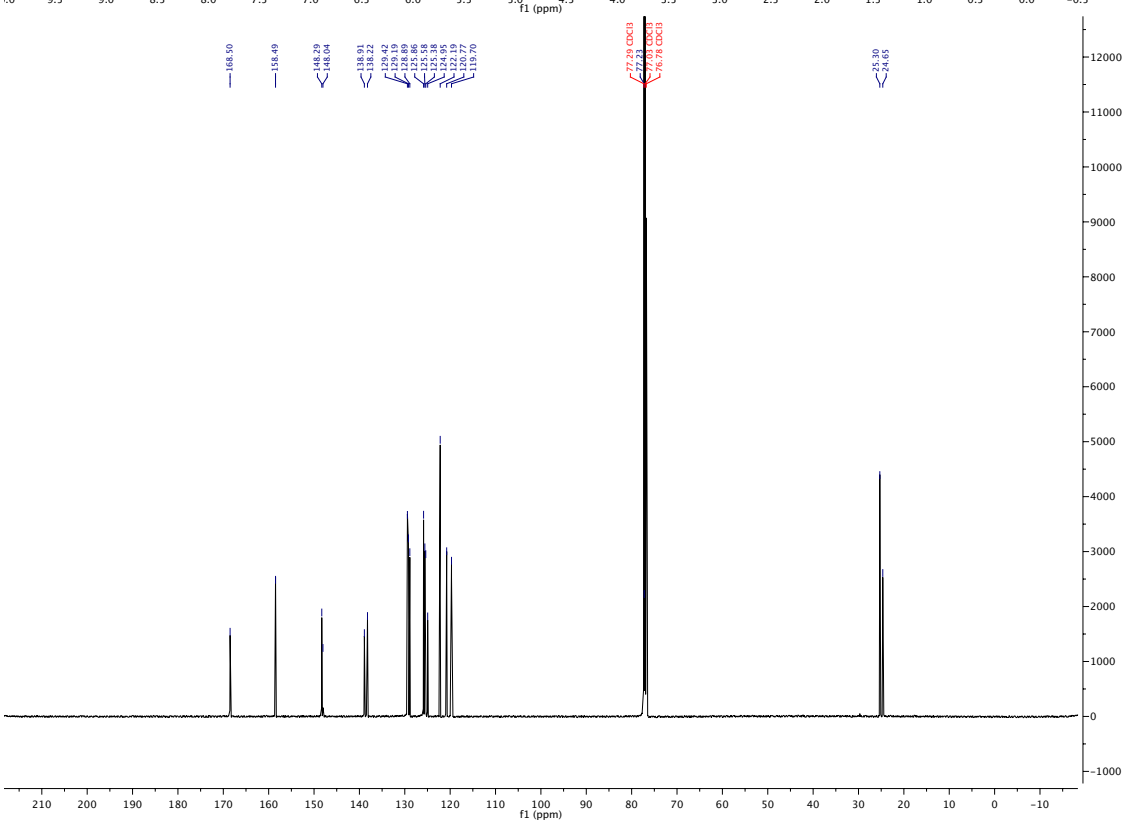
168.50
158.49
148.29
148.04
138.91
138.22
129.42
129.19
128.89
125.86
125.58
125.38
124.95
122.19
120.77
119.70
77.29 CDCl3
77.03 CDCl3
76.78 CDCl3
25.30
24.65
f1 (ppm)

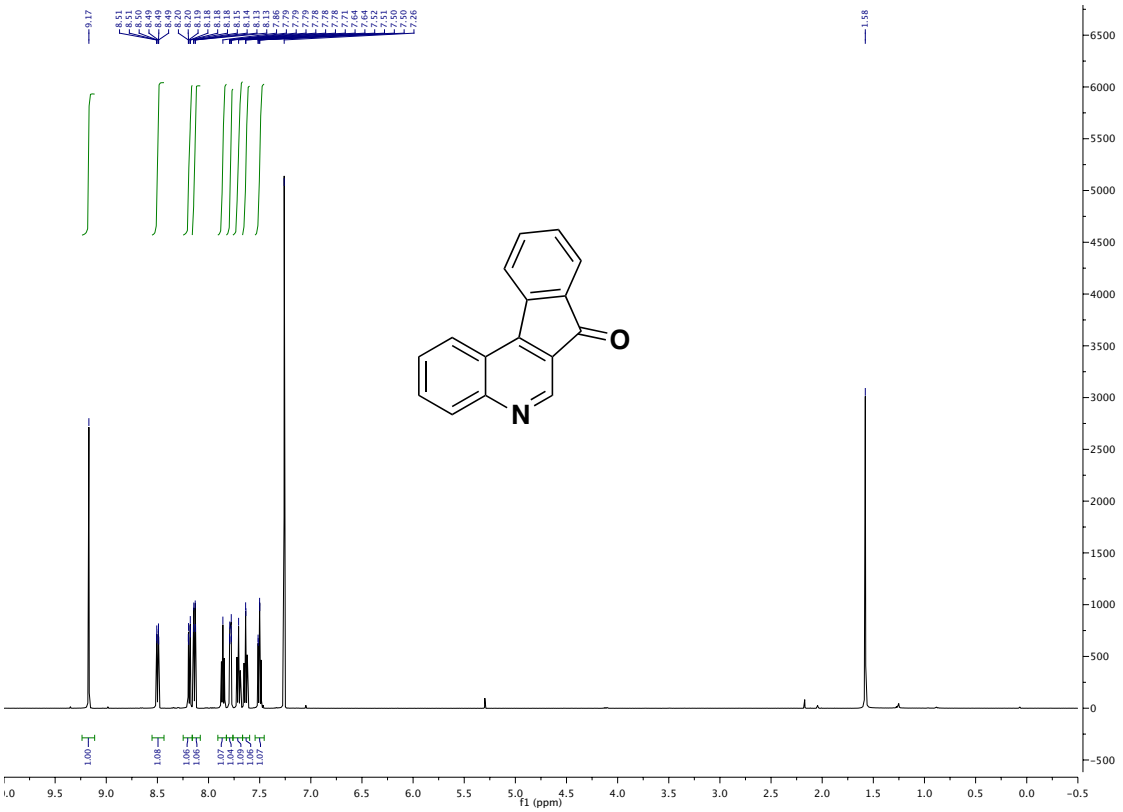
9.17
8.51
8.50
8.49
8.49
8.49
8.20
8.19
8.18
8.18
8.18
8.15
8.15
8.14
8.13
8.11
7.86
7.79
7.79
7.79
7.78
7.78
7.78
7.78
7.71
7.64
7.64
7.52
7.51
7.50
7.50
7.26
1.58
O
N
1.00
1.08
1.06
1.06
1.07
1.04
1.04
1.06
1.07
f1 (ppm)

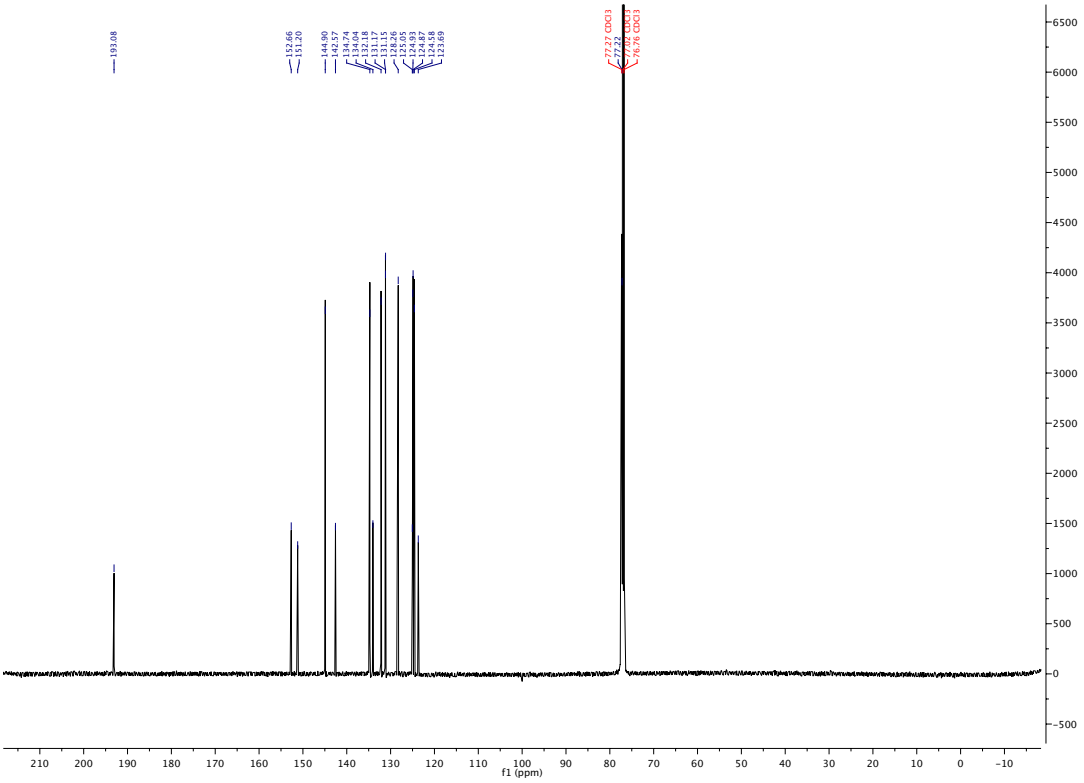
193.08
152.66
151.20
144.90
142.57
134.74
134.04
132.18
131.17
131.15
128.26
125.35
124.95
124.87
124.58
123.98
77.27 CDCl3
77.21
76.96 CDCl3
f1 (ppm)

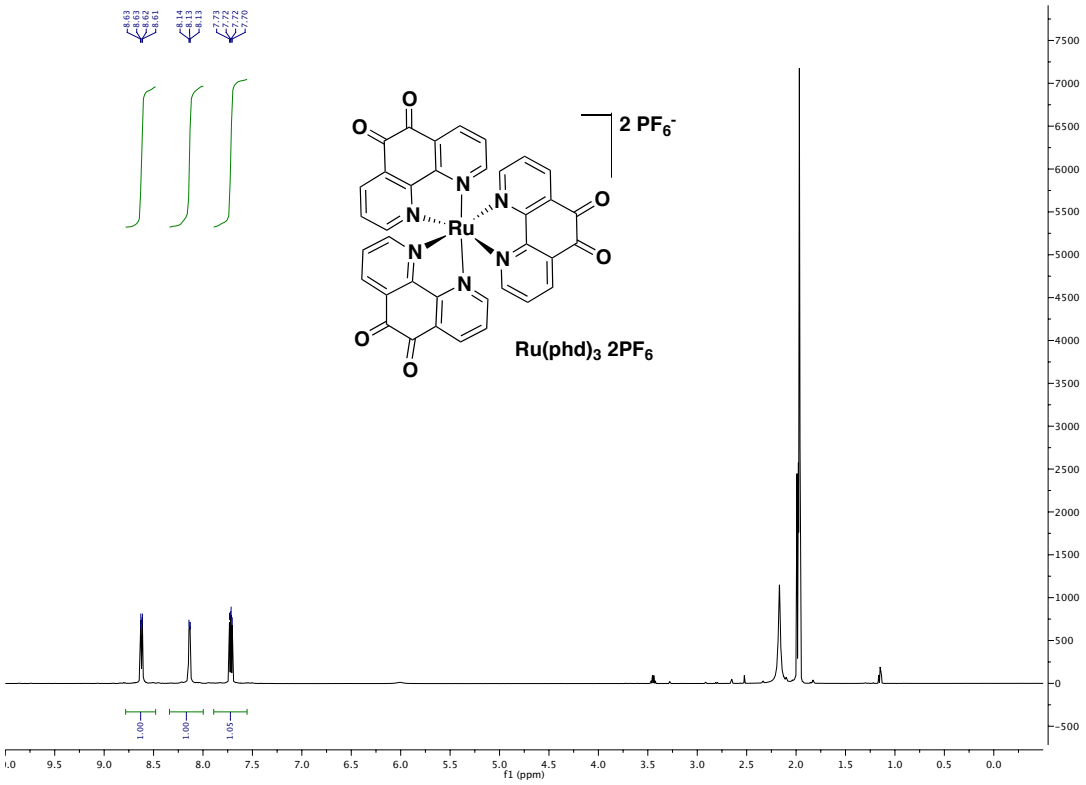
8.63
8.63
8.62
8.61
8.14
8.13
8.13
7.73
7.72
7.72
7.72
7.70
2 PF6-
Ru(phd)3 2PF6
1.00
1.00
1.05
f1 (ppm)

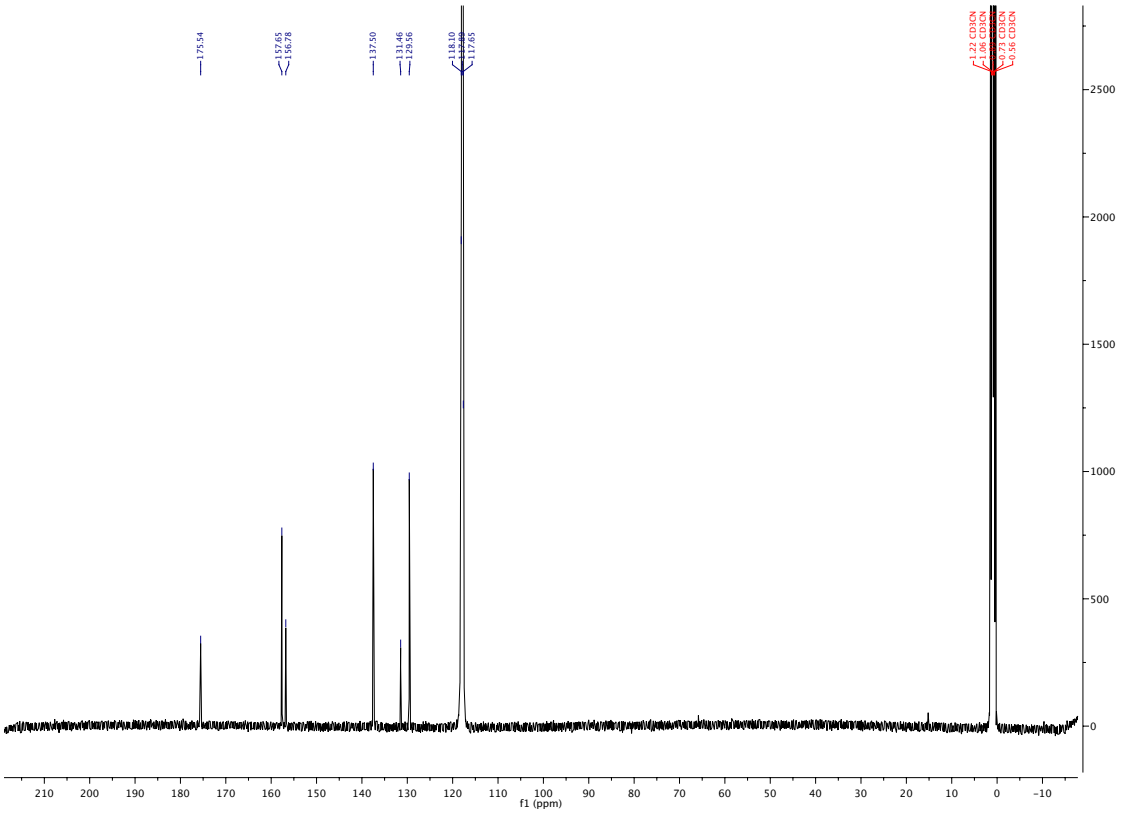
175.54
157.65
156.78
137.50
131.46
129.56
118.10
118.03
117.65
1.22 CD3CN
1.96 CD3CN
1.96 CD3CN
0.23 CD3CN
0.56 CD3CN
f1 (ppm)

V. X Ray Crystallographic Data

Data Collection

A dark red crystal with approximate dimensions 0.27 x 0.12 x 0.07 mm^3 was selected under oil under ambient conditions and attached to the tip of a MiTeGen MicroMount©. The crystal was mounted in a stream of cold nitrogen at 100(1) K and centered in the X-ray beam by using a video camera.

The crystal evaluation and data collection were performed on a Bruker Quazar SMART APEXII diffractometer with Mo K_α (λ = 0.71073 Å) radiation and the diffractometer to crystal distance of 4.96 cm.

The initial cell constants were obtained from three series of ω scans at different starting angles. Each series consisted of 12 frames collected at intervals of 0.5° in a 6° range about ω with the exposure time of 10 second per frame. The reflections were successfully indexed by an automated indexing routine built in the APEXII program suite. The final cell constants were calculated from a set of 9849 strong reflections from the actual data collection.

The data were collected by using the full sphere data collection routine to survey the reciprocal space to the extent of a full sphere to a resolution of 0.70 Å. A total of 77039 data were harvested by collecting 4 sets of frames with 0.5° scans in ω and ϕ with an exposure time 40 sec per frame. These highly redundant datasets were corrected for Lorentz and polarization effects. The absorption correction was based on fitting a function to the empirical transmission surface as sampled by multiple equivalent measurements.[1]

Structure Solution and Refinement

The systematic absences in the diffraction data were uniquely consistent for the space group $P2_12_12_1$ that yielded chemically reasonable and computationally stable results of refinement.[2,3,4]

A successful solution by the direct methods provided most non-hydrogen atoms from the *E*-map. The remaining non-hydrogen atoms were located in an alternating series of least-squares cycles and difference Fourier maps. All non-hydrogen atoms were refined with anisotropic displacement coefficients. All hydrogen atoms were included in the structure factor calculation at idealized positions and were allowed to ride on the neighboring atoms with relative isotropic displacement coefficients.

There were two fully occupied molecules of acetonitrile solvent in the asymmetric unit. There was a disordered and partially occupied acetonitrile solvent molecule which was set to a chemical occupancy of 50%. Bond distance restraints and thermal parameter constraints were applied to the disordered solvent molecule to ensure a chemically reasonable and computationally stable refinement. The carbonyl (C30, O6) of one of the quinone ligands was disordered over two positions with a major component occupancy of 52(7)%. Two perchlorate ions were also in the asymmetric unit. One of them was disordered over two positions with a major component occupancy of 57(2)%. The oxygen atoms of the disordered perchlorate were refined isotropically and bond distance constraints were applied to ensure a chemically reasonable and computationally stable refinement.

The structure was refined as an inversion twin with a minor component contribution of 37(3) %.

The final least-squares refinement of 672 parameters against 12129 data resulted in residuals R (based on F^2 for $I \geq 2\sigma$) and wR (based on F^2 for all data) of 0.0383 and 0.0934, respectively. The final difference Fourier map had one noticeable peak (ca. 1.00 e/Å^3) in the vicinity of the disordered acetonitrile molecule and could not be accounted for with a chemically reasonable and computationally stable model.

Summary

Crystal Data for $C_{41}H_{25.5}Cl_2N_{8.5}O_{14}Ru$ (M =1033.17): orthorhombic, space group $P2_12_12_1$ (no. 19), a = 13.744(5) Å, b = 14.024(6) Å, c = 20.665(8) Å, V = 3983(3) Å^3, Z = 4, T = 100.0 K, μ(MoKα) = 0.613 mm^{-1}, $Dcalc$ = 1.723 g/mm^3, 76925 reflections measured ($3.51 \leq 2\Theta \leq 61.044$), 12129 unique ($R_{int}$ = 0.0586, R_{sigma} = 0.0427) which were used in all calculations. The final R_1 was 0.0383 ($I > 2\sigma(I)$) and wR_2 was 0.0934 (all data).

References

[1] Bruker-AXS. (2007-2013) APEX2 (Ver. 2013.2-0), SADABS (2012-1), and SAINT+ (Ver. 8.30C) Software Reference Manuals. Bruker-AXS, Madison, Wisconsin, USA.

[2] Sheldrick, G. M. (2008) SHELXL. *Acta Cryst*. **A64**, 112-122.

[3] Dolomanov, O.V.; Bourhis, L.J.; Gildea, R.J.; Howard, J.A.K.; Puschmann, H. "OLEX2: a complete structure solution, refinement and analysis program". *J. Appl. Cryst*. (2009) **42**, *339-341*.

[4] Guzei, I.A. (2013). Internal laboratory computer programs Gn.

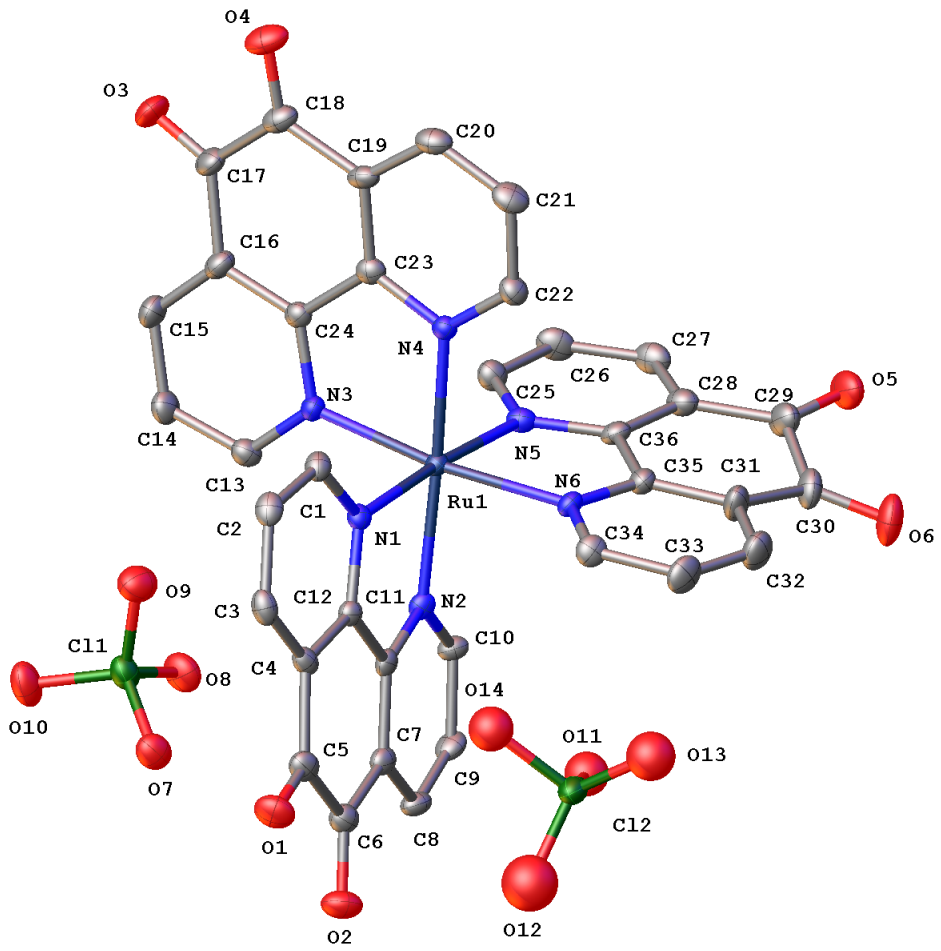

Figure A3.1. A molecular drawing of the Ruthenium complex of Stahl194 shown with 50% probability ellipsoids. All H atoms, acetonitrile solvent molecules, and minor components of the disordered atoms are omitted for clarity.

Table A3.1 Crystal data and structure refinement for stahl194**.**

Identification code	stahl194
Empirical formula	$Ru(C_{12}H_6N_2O_2)_3(ClO_4)_2(CH_3CN)_{2.5}$
Formula weight	1033.17
Temperature/K	100.0
Crystal system	orthorhombic
Space group	$P2_12_12_1$
a/Å	13.744(5)
b/Å	14.024(6)
c/Å	20.665(8)
α/°	90
β/°	90
γ/°	90
Volume/Å^3	3983(3)
Z	4
ρ_{calc}mg/mm^3	1.723
m/mm^{-1}	0.613
F(000)	2084.0
Crystal size/mm^3	0.274 × 0.124 × 0.074
Radiation	MoKα (λ = 0.71073)
2Θ range for data collection	3.51 to 61.044°
Index ranges	$-17 \leq h \leq 19$, $-19 \leq k \leq 19$, $-29 \leq l \leq 26$
Reflections collected	76925
Independent reflections	12129 [R_{int} = 0.0586, R_{sigma} = 0.0427]
Data/restraints/parameters	12129/50/632
Goodness-of-fit on F^2	1.038
Final R indexes [I>=2σ (I)]	R_1 = 0.0383, wR_2 = 0.0880
Final R indexes [all data]	R_1 = 0.0489, wR_2 = 0.0934
Largest diff. peak/hole / e Å^{-3}	1.00/-0.73
Flack parameter	0.37(3)

Table A3.2 Fractional Atomic Coordinates (×10⁴) and Equivalent Isotropic Displacement Parameters (Å²×10³) for stahl194. U_{eq} is defined as 1/3 of of the trace of the orthogonalised U_{IJ} tensor.

Atom	*x*	*y*	*z*	U(eq)
Ru1	7108.6(2)	5103.9(2)	5633.4(2)	11.90(7)
Cl1	8453.5(7)	4844.6(8)	8014.8(5)	22.9(2)
O1	5274(3)	3952(2)	8414.0(17)	28.5(8)
O2	5290(3)	5887(2)	8478.1(17)	28.1(8)
O3	11162(3)	3087(3)	4822.6(17)	31.7(8)
O4	9835(3)	2070(2)	4115.2(17)	29.2(7)
O7	7552(2)	4819(3)	8381.8(15)	27.2(7)
O8	8533(3)	5753(2)	7693.6(17)	31.2(8)
O9	8458(3)	4090(3)	7541.2(19)	33.9(8)
O10	9263(2)	4730(3)	8449.9(17)	34.5(9)
N1	6783(3)	4127(2)	6346.3(17)	13.4(7)
N2	6822(2)	5993(2)	6412.6(18)	14.2(7)
N3	8559(2)	4819(2)	5781.8(15)	14.9(6)
N4	7350(2)	4112(2)	4923.2(17)	13.8(7)
N5	7346(3)	6141(2)	4939.1(17)	15.8(7)
N6	5699(2)	5406(2)	5353.4(17)	14.2(6)
N8	9220(4)	1805(3)	5718(2)	45.2(13)
C1	6893(3)	3177(3)	6315(2)	17.1(8)
C2	6626(3)	2576(3)	6818(2)	18.6(8)
C3	6205(3)	2959(3)	7367(2)	19.4(9)
C4	6101(3)	3943(3)	7413(2)	16.2(8)
C5	5648(3)	4404(3)	7982(2)	19.6(9)
C6	5643(3)	5502(3)	8010(2)	19.4(9)
C7	6071(3)	6034(3)	7462(2)	17.0(8)
C8	6129(3)	7026(3)	7472(2)	18.6(8)
C9	6548(3)	7486(3)	6948(2)	19.9(8)
C10	6880(3)	6949(3)	6430(2)	16.6(8)
C11	6424(3)	5543(3)	6932(2)	14.2(7)
C12	6418(3)	4505(3)	6898(2)	13.9(7)
C13	9152(3)	5189(3)	6235.7(19)	18.5(7)
C14	10127(3)	4947(3)	6288(2)	22.8(8)
C15	10518(3)	4310(3)	5849(2)	23.9(9)
C16	9926(3)	3919(3)	5382(2)	20.7(8)
C17	10308(4)	3237(3)	4892(2)	22.6(9)

C18	9562(3)	2714(3)	4455(2)	22.2(9)
C19	8541(3)	3061(3)	4457(2)	18.0(8)
C20	7848(4)	2689(3)	4039(2)	22.1(8)
C21	6924(3)	3061(3)	4052(2)	23.1(9)
C22	6699(3)	3764(3)	4501(2)	19.1(8)
C23	8271(3)	3772(3)	4895(2)	16.6(8)
C24	8949(3)	4176(3)	5364.0(19)	15.8(7)
C25	8213(3)	6478(3)	4736(2)	19.5(9)
C26	8294(4)	7143(3)	4241(2)	24.5(10)
C27	7458(4)	7467(3)	3937(2)	24.3(9)
C28	6575(3)	7119(3)	4133(2)	21.2(9)
C29	5658(4)	7434(3)	3832(2)	28.4(10)
O5	5634(3)	7960(3)	3364.7(17)	35.3(9)
C30	4723(12)	7207(17)	4176(14)	25(4)
O6	3979(8)	7608(18)	4023(13)	37(4)
C31	4733(3)	6354(4)	4633(2)	26.8(10)
C32	3887(3)	5962(4)	4888(3)	29.8(10)
C33	3958(3)	5297(3)	5375(2)	26.2(9)
C34	4873(3)	5040(3)	5599(2)	19.4(7)
C35	5624(3)	6065(3)	4876(2)	17.1(8)
C36	6538(3)	6460(3)	4637(2)	16.9(8)
N7	5640(4)	8501(4)	5092(2)	40.4(12)
C37	6048(4)	9056(4)	5393(3)	31.5(11)
C38	6550(4)	9780(4)	5776(3)	44.6(14)
C39	9156(4)	1692(4)	6255(3)	32.8(11)
C40	9091(5)	1560(6)	6942(3)	63(2)
Cl2	3298(6)	5109(6)	7075(4)	22.6(11)
O11	3863(6)	5915(5)	6826(5)	42(2)
O12	3088(8)	5195(8)	7765(4)	67(3)
O13	2539(6)	4772(8)	6635(4)	51(2)
O14	4034(7)	4352(6)	7098(4)	43(2)
Cl3	3195(9)	4997(8)	7131(5)	29(2)
O15	3633(11)	5901(9)	7077(8)	67(4)
O16	2396(7)	5189(9)	6731(5)	44(3)
O17	3731(8)	4204(6)	6916(5)	34(3)
O18	2723(10)	4854(10)	7736(5)	58(4)
N9	8502(11)	9224(10)	6654(6)	77(3)

C41	8739(14)	8761(12)	7086(7)	77(3)
C42	8911(14)	8141(11)	7660(7)	77(3)
C30A	4651(16)	6950(30)	4071(13)	32(5)
O6A	3893(14)	7210(40)	3843(14)	53(8)

Table A3.3 Anisotropic Displacement Parameters ($Å^2 \times 10^3$) for stahl194. The Anisotropic displacement factor exponent takes the form: $-2\pi^2[h^2a^{*2}U_{11}+2hka^*b^*U_{12}+\ldots]$.

Atom	U_{11}	U_{22}	U_{33}	U_{23}	U_{13}	U_{12}
Ru1	11.31(12)	11.01(11)	13.36(12)	-0.15(10)	0.09(11)	0.26(10)
Cl1	20.5(5)	29.1(5)	19.1(4)	2.3(4)	-2.7(4)	-2.1(4)
O1	32(2)	32.5(17)	20.6(17)	3.4(14)	7.9(15)	-4.1(14)
O2	29(2)	33.0(18)	22.8(18)	-6.3(14)	7.6(15)	-1.3(14)
O3	21.6(18)	42.2(19)	31.3(19)	-2.9(15)	3.7(15)	14.7(14)
O4	34.5(19)	19.3(14)	33.9(19)	-2.7(13)	12.1(16)	4.0(13)
O7	20.7(14)	35.8(17)	25.0(15)	0.1(14)	0.5(12)	-4.4(14)
O8	37(2)	32.9(18)	23.2(18)	8.6(14)	1.4(16)	-1.3(15)
O9	29(2)	40(2)	33(2)	-8.0(16)	-1.4(17)	0.3(16)
O10	23.9(17)	52(2)	28.1(18)	7.4(16)	-7.7(14)	-3.8(16)
N1	13.6(17)	12.7(14)	14.0(17)	-0.3(12)	-1.8(13)	-0.9(11)
N2	10.6(17)	14.2(15)	17.8(18)	1.6(12)	1.7(13)	-1.7(11)
N3	14.0(14)	16.2(13)	14.6(15)	0.8(12)	0.0(11)	2.5(12)
N4	14.7(18)	14.1(14)	12.7(16)	0.3(11)	0.8(13)	0.9(11)
N5	18.1(19)	14.4(14)	15.1(17)	-0.8(12)	2.7(14)	-1.3(12)
N6	11.4(15)	13.8(14)	17.4(16)	-0.9(12)	0.4(13)	2.0(11)
N8	57(3)	48(3)	31(3)	13(2)	12(2)	17(2)
C1	18(2)	14.2(17)	19(2)	-0.7(14)	-3.8(15)	0.1(13)
C2	20(2)	11.4(16)	24(2)	1.0(14)	-4.6(18)	-2.3(14)
C3	19(2)	19.7(18)	20(2)	6.1(15)	-4.6(17)	-4.4(15)
C4	13(2)	22.3(18)	13(2)	0.8(14)	-1.0(16)	-3.1(14)
C5	14(2)	26(2)	19(2)	0.1(16)	1.0(17)	-2.6(15)
C6	16(2)	23.2(19)	19(2)	-1.0(16)	0.4(18)	-0.9(15)
C7	12(2)	19.8(18)	19(2)	-2.9(15)	-2.4(17)	0.5(14)
C8	16(2)	19.5(18)	20(2)	-6.2(15)	1.7(17)	2.1(15)
C9	20(2)	13.0(17)	27(2)	-4.7(15)	-0.8(18)	2.8(14)
C10	16(2)	14.8(17)	19(2)	-2.6(14)	3.6(15)	-0.2(13)
C11	9.5(18)	15.8(16)	17(2)	0.7(14)	-2.1(16)	0.4(13)

C12	11.5(18)	15.4(16)	14.7(19)	-0.5(13)	-1.1(16)	-0.3(13)
C13	18.7(18)	20.8(17)	16.2(17)	-1.0(15)	0.9(14)	-2.4(15)
C14	17.2(17)	28(2)	22.9(19)	-0.9(18)	-5.0(15)	-0.7(17)
C15	16(2)	29(2)	26(2)	-0.3(17)	-1.8(17)	6.0(16)
C16	18(2)	20.8(19)	23(2)	0.6(16)	3.2(17)	5.6(15)
C17	25(2)	20.9(19)	22(2)	0.8(16)	2.3(18)	10.1(16)
C18	25(2)	17.4(17)	24(2)	0.9(16)	7.3(18)	4.0(15)
C19	24(2)	15.4(16)	15(2)	0.2(14)	6.1(17)	2.9(14)
C20	31(2)	17.0(17)	19(2)	-2.8(14)	5(2)	-0.8(18)
C21	27(3)	20.8(19)	21(2)	-5.0(16)	-0.5(18)	-7.0(16)
C22	19(2)	20.4(18)	18(2)	-1.1(14)	-1.9(16)	-1.4(15)
C23	19(2)	15.6(17)	16(2)	1.5(14)	3.2(16)	-1.1(14)
C24	17.1(19)	16.2(16)	13.9(18)	1.9(13)	1.7(15)	0.8(14)
C25	17(2)	22.2(19)	19(2)	0.6(16)	-0.3(16)	-2.3(15)
C26	25(2)	27(2)	22(3)	1.4(17)	5.6(18)	-7.9(17)
C27	35(3)	17.5(18)	21(2)	3.5(16)	4.4(19)	-0.1(17)
C28	26(2)	19.6(19)	18(2)	0.1(15)	3.3(18)	3.2(16)
C29	33(3)	30(2)	22(2)	8.5(18)	3(2)	11.5(19)
O5	46(2)	35.1(18)	24.4(18)	10.6(15)	0.4(16)	15.1(16)
C30	25(5)	21(7)	30(9)	6(5)	-9(5)	4(4)
O6	25(4)	37(8)	47(8)	17(6)	-11(4)	5(4)
C31	16(2)	39(3)	25(2)	6.1(19)	-1.1(18)	8.1(18)
C32	16(2)	40(3)	34(3)	3(2)	-1.2(19)	5.4(19)
C33	12.9(19)	29(2)	37(2)	-1.2(18)	-1.0(18)	-2.3(16)
C34	17.0(16)	17.6(16)	23.6(18)	-0.2(18)	-0.3(15)	-4.0(13)
C35	16.6(19)	17.5(17)	17.2(19)	-0.8(14)	0.3(16)	3.4(14)
C36	18(2)	15.5(17)	18(2)	-1.4(14)	4.3(16)	3.4(14)
N7	45(3)	43(3)	33(3)	1(2)	12(2)	16(2)
C37	28(3)	36(3)	30(3)	6(2)	9(2)	14(2)
C38	37(3)	49(3)	48(3)	-2(3)	12(2)	5(3)
C39	28(3)	37(3)	34(3)	2(2)	2(2)	6(2)
C40	52(4)	115(6)	22(3)	6(3)	3(3)	40(4)
Cl2	21.2(15)	26(2)	20.8(18)	-5.3(16)	-2.4(13)	6.2(14)
Cl3	36(4)	23(2)	28(3)	2.3(17)	1(2)	9(2)
N9	76(6)	80(7)	74(7)	-33(5)	-5(6)	23(5)
C41	76(6)	80(7)	74(7)	-33(5)	-5(6)	23(5)
C42	76(6)	80(7)	74(7)	-33(5)	-5(6)	23(5)

C30A	30(6)	40(10)	27(7)	4(7)	3(5)	17(7)
O6A	31(6)	79(18)	49(9)	25(10)	-6(5)	21(7)

Table A3.4. Bond Lengths for stahl194.

Atom	Atom	Length/Å	Atom	Atom	Length/Å
Ru1	N1	2.061(3)	C15	C16	1.377(6)
Ru1	N2	2.074(4)	C16	C17	1.489(6)
Ru1	N3	2.057(3)	C16	C24	1.390(6)
Ru1	N4	2.049(3)	C17	C18	1.549(7)
Ru1	N5	2.069(3)	C18	C19	1.486(6)
Ru1	N6	2.065(3)	C19	C20	1.387(6)
Cl1	O7	1.453(3)	C19	C23	1.397(5)
Cl1	O8	1.441(4)	C20	C21	1.373(7)
Cl1	O9	1.441(4)	C21	C22	1.389(6)
Cl1	O10	1.439(3)	C23	C24	1.459(6)
O1	C5	1.209(5)	C25	C26	1.390(6)
O2	C6	1.210(6)	C26	C27	1.386(7)
O3	C17	1.201(6)	C27	C28	1.369(7)
O4	C18	1.205(5)	C28	C29	1.473(7)
N1	C1	1.342(5)	C28	C36	1.394(6)
N1	C12	1.354(5)	C29	O5	1.215(5)
N2	C10	1.344(5)	C29	C30	1.50(2)
N2	C11	1.360(5)	C29	C30A	1.62(3)
N3	C13	1.346(5)	C30	O6	1.209(9)
N3	C24	1.358(5)	C30	C31	1.52(2)
N4	C22	1.341(5)	C31	C32	1.390(7)
N4	C23	1.354(5)	C31	C35	1.385(6)
N5	C25	1.349(5)	C31	C30A	1.44(3)
N5	C36	1.350(6)	C32	C33	1.375(7)
N6	C34	1.346(5)	C33	C34	1.387(6)
N6	C35	1.356(5)	C35	C36	1.458(6)
N8	C39	1.124(7)	N7	C37	1.142(7)
C1	C2	1.388(6)	C37	C38	1.462(8)
C2	C3	1.382(6)	C39	C40	1.435(8)
C3	C4	1.390(6)	Cl2	O11	1.464(10)
C4	C5	1.479(6)	Cl2	O12	1.461(10)

C4	C12	1.395(6)	Cl2	O13	1.462(9)
C5	C6	1.541(6)	Cl2	O14	1.467(9)
C6	C7	1.477(6)	Cl3	O15	1.407(12)
C7	C8	1.393(6)	Cl3	O16	1.401(11)
C7	C11	1.382(6)	Cl3	O17	1.406(11)
C8	C9	1.385(6)	Cl3	O18	1.423(12)
C9	C10	1.386(6)	N9	C41	1.150(12)
C11	C12	1.456(5)	C41	C42	1.490(13)
C13	C14	1.387(6)	C30A	O6A	1.200(10)
C14	C15	1.383(6)			

Table A3.5 Bond Angles for stahl194.

Atom	**Atom**	**Atom**	**Angle/°**	**Atom**	**Atom**	**Atom**	**Angle/°**
N1	Ru1	N2	78.66(13)	C15	C16	C24	119.1(4)
N1	Ru1	N5	175.76(14)	C24	C16	C17	119.3(4)
N1	Ru1	N6	97.64(14)	O3	C17	C16	122.6(5)
N3	Ru1	N1	88.54(13)	O3	C17	C18	119.6(4)
N3	Ru1	N2	100.67(13)	C16	C17	C18	117.8(4)
N3	Ru1	N5	95.02(13)	O4	C18	C17	119.3(4)
N3	Ru1	N6	172.25(13)	O4	C18	C19	122.7(4)
N4	Ru1	N1	95.49(13)	C19	C18	C17	118.0(4)
N4	Ru1	N2	174.12(13)	C20	C19	C18	121.6(4)
N4	Ru1	N3	79.51(13)	C20	C19	C23	119.3(4)
N4	Ru1	N5	87.43(12)	C23	C19	C18	119.1(4)
N4	Ru1	N6	95.18(13)	C21	C20	C19	118.7(4)
N5	Ru1	N2	98.39(13)	C20	C21	C22	119.3(4)
N6	Ru1	N2	85.20(14)	N4	C22	C21	123.0(4)
N6	Ru1	N5	79.01(14)	N4	C23	C19	121.8(4)
O8	Cl1	O7	109.1(2)	N4	C23	C24	115.6(4)
O8	Cl1	O9	109.6(2)	C19	C23	C24	122.6(4)
O9	Cl1	O7	109.9(2)	N3	C24	C16	122.4(4)
O10	Cl1	O7	109.3(2)	N3	C24	C23	115.4(4)
O10	Cl1	O8	109.2(2)	C16	C24	C23	122.2(4)
O10	Cl1	O9	109.8(2)	N5	C25	C26	122.4(4)
C1	N1	Ru1	126.9(3)	C27	C26	C25	119.1(4)
C1	N1	C12	118.1(4)	C28	C27	C26	119.0(4)

C12	N1	Ru1	114.9(2)	C27	C28	C29	121.8(4)
C10	N2	Ru1	127.5(3)	C27	C28	C36	119.3(4)
C10	N2	C11	117.7(4)	C36	C28	C29	118.9(4)
C11	N2	Ru1	114.2(3)	C28	C29	C30	117.9(7)
C13	N3	Ru1	128.0(3)	C28	C29	C30A	118.6(7)
C13	N3	C24	117.4(3)	O5	C29	C28	122.7(5)
C24	N3	Ru1	114.6(3)	O5	C29	C30	118.8(7)
C22	N4	Ru1	127.2(3)	O5	C29	C30A	118.2(8)
C22	N4	C23	117.9(4)	C29	C30	C31	116.9(10)
C23	N4	Ru1	114.9(3)	O6	C30	C29	120.1(17)
C25	N5	Ru1	126.9(3)	O6	C30	C31	122.3(18)
C25	N5	C36	117.8(4)	C32	C31	C30	122.6(7)
C36	N5	Ru1	115.1(3)	C32	C31	C30A	118.2(11)
C34	N6	Ru1	127.4(3)	C35	C31	C30	117.5(7)
C34	N6	C35	118.1(3)	C35	C31	C32	119.1(4)
C35	N6	Ru1	114.5(3)	C35	C31	C30A	122.2(10)
N1	C1	C2	122.5(4)	C33	C32	C31	119.1(4)
C3	C2	C1	119.2(4)	C32	C33	C34	119.0(4)
C2	C3	C4	119.1(4)	N6	C34	C33	122.6(4)
C3	C4	C5	122.1(4)	N6	C35	C31	122.0(4)
C3	C4	C12	118.5(4)	N6	C35	C36	116.1(4)
C12	C4	C5	119.4(4)	C31	C35	C36	121.8(4)
O1	C5	C4	122.4(4)	N5	C36	C28	122.4(4)
O1	C5	C6	119.6(5)	N5	C36	C35	115.2(4)
C4	C5	C6	117.9(4)	C28	C36	C35	122.5(4)
O2	C6	C5	118.5(4)	N7	C37	C38	178.6(6)
O2	C6	C7	123.1(4)	N8	C39	C40	178.8(8)
C7	C6	C5	118.4(4)	O11	Cl2	O14	101.8(7)
C8	C7	C6	121.1(4)	O12	Cl2	O11	112.6(7)
C11	C7	C6	119.6(4)	O12	Cl2	O13	119.5(8)
C11	C7	C8	119.3(4)	O12	Cl2	O14	99.4(7)
C9	C8	C7	118.5(4)	O13	Cl2	O11	114.1(7)
C8	C9	C10	119.2(4)	O13	Cl2	O14	106.2(7)
N2	C10	C9	122.9(4)	O15	Cl3	O18	113.0(11)
N2	C11	C7	122.4(4)	O16	Cl3	O15	96.7(10)
N2	C11	C12	115.3(4)	O16	Cl3	O17	112.1(10)
C7	C11	C12	122.3(4)	O16	Cl3	O18	100.9(9)

N1	C12	C4	122.4(3)	O17	Cl3	O15	117.6(11)
N1	C12	C11	115.5(4)	O17	Cl3	O18	113.8(9)
C4	C12	C11	122.0(4)	N9	C41	C42	173(2)
N3	C13	C14	123.0(4)	C31	C30A	C29	115.0(13)
C15	C14	C13	118.9(4)	O6A	C30A	C29	119.8(19)
C16	C15	C14	119.2(4)	O6A	C30A	C31	124(2)
C15	C16	C17	121.6(4)				

Table A3.6. Torsion Angles for stahl194.

A	B	C	D	Angle/°	A	B	C	D	Angle/°
Ru1	N1	C1	C2	-178.2(3)	C17	C16	C24	N3	-177.7(4)
Ru1	N1	C12	C4	175.8(3)	C17	C16	C24	C23	2.4(6)
Ru1	N1	C12	C11	-7.3(5)	C17	C18	C19	C20	174.3(4)
Ru1	N2	C10	C9	171.1(3)	C17	C18	C19	C23	-6.5(6)
Ru1	N2	C11	C7	-171.5(3)	C18	C19	C20	C21	-178.1(4)
Ru1	N2	C11	C12	9.8(5)	C18	C19	C23	N4	-179.5(4)
Ru1	N3	C13	C14	-179.6(3)	C18	C19	C23	C24	-1.3(6)
Ru1	N3	C24	C16	178.1(3)	C19	C20	C21	C22	-3.0(6)
Ru1	N3	C24	C23	-2.0(4)	C19	C23	C24	N3	-176.2(4)
Ru1	N4	C22	C21	-177.3(3)	C19	C23	C24	C16	3.7(6)
Ru1	N4	C23	C19	177.1(3)	C20	C19	C23	N4	-0.3(6)
Ru1	N4	C23	C24	-1.2(4)	C20	C19	C23	C24	177.9(4)
Ru1	N5	C25	C26	176.6(3)	C20	C21	C22	N4	0.9(6)
Ru1	N5	C36	C28	-176.4(3)	C22	N4	C23	C19	-1.8(6)
Ru1	N5	C36	C35	3.6(4)	C22	N4	C23	C24	179.9(4)
Ru1	N6	C34	C33	179.7(3)	C23	N4	C22	C21	1.5(6)
Ru1	N6	C35	C31	-179.8(4)	C23	C19	C20	C21	2.7(6)
Ru1	N6	C35	C36	-0.2(4)	C24	N3	C13	C14	0.4(6)
O1	C5	C6	O2	2.5(8)	C24	C16	C17	O3	169.5(4)
O1	C5	C6	C7	-177.6(4)	C24	C16	C17	C18	-10.1(6)
O2	C6	C7	C8	3.0(7)	C25	N5	C36	C28	-0.3(6)
O2	C6	C7	C11	-177.4(4)	C25	N5	C36	C35	179.6(4)
O3	C17	C18	O4	10.1(7)	C25	C26	C27	C28	-0.1(7)
O3	C17	C18	C19	-167.4(4)	C26	C27	C28	C29	179.9(4)
O4	C18	C19	C20	-3.2(7)	C26	C27	C28	C36	0.8(7)
O4	C18	C19	C23	176.0(4)	C27	C28	C29	O5	5.6(7)

N1	C1	C2	C3	1.9(6)	C27	C28	C29	C30	-165.4(13)
N2	C11	C12	N1	-1.8(6)	C27	C28	C29	C30A	177.4(15)
N2	C11	C12	C4	175.1(4)	C27	C28	C36	N5	-0.7(6)
N3	C13	C14	C15	1.2(7)	C27	C28	C36	C35	179.4(4)
N4	C23	C24	N3	2.1(5)	C28	C29	C30	O6	164.9(12)
N4	C23	C24	C16	-178.0(4)	C28	C29	C30	C31	-25(2)
N5	C25	C26	C27	-0.8(7)	C28	C29	C30A	C31	9(3)
N6	C35	C36	N5	-2.2(5)	C28	C29	C30A	O6A	178.4(18)
N6	C35	C36	C28	177.7(4)	C29	C28	C36	N5	-179.7(4)
C1	N1	C12	C4	-4.0(6)	C29	C28	C36	C35	0.4(6)
C1	N1	C12	C11	172.9(4)	C29	C30	C31	C32	-168.0(12)
C1	C2	C3	C4	-3.0(6)	C29	C30	C31	C35	22(2)
C2	C3	C4	C5	179.4(4)	C29	C30	C31	C30A	-89(6)
C2	C3	C4	C12	0.7(6)	O5	C29	C30	O6	-6.4(18)
C3	C4	C5	O1	-6.1(7)	O5	C29	C30	C31	163.9(13)
C3	C4	C5	C6	175.1(4)	O5	C29	C30A	C31	-179.0(15)
C3	C4	C12	N1	2.9(6)	O5	C29	C30A	O6A	-9(2)
C3	C4	C12	C11	-173.8(4)	C30	C29	C30A	C31	-83(5)
C4	C5	C6	O2	-178.7(4)	C30	C29	C30A	O6A	87(4)
C4	C5	C6	C7	1.2(7)	C30	C31	C32	C33	-169.6(14)
C5	C4	C12	N1	-175.9(4)	C30	C31	C35	N6	170.6(13)
C5	C4	C12	C11	7.4(7)	C30	C31	C35	C36	-8.9(14)
C5	C6	C7	C8	-177.0(4)	C30	C31	C30A	C29	66(6)
C5	C6	C7	C11	2.7(7)	C30	C31	C30A	O6A	-103(6)
C6	C7	C8	C9	179.2(4)	O6	C30	C31	C32	2(2)
C6	C7	C11	N2	179.7(4)	O6	C30	C31	C35	-167.5(13)
C6	C7	C11	C12	-1.8(7)	O6	C30	C31	C30A	81(5)
C7	C8	C9	C10	1.0(7)	C31	C32	C33	C34	0.3(7)
C7	C11	C12	N1	179.6(4)	C31	C35	C36	N5	177.3(4)
C7	C11	C12	C4	-3.5(7)	C31	C35	C36	C28	-2.8(6)
C8	C7	C11	N2	-0.7(6)	C32	C31	C35	N6	0.5(7)
C8	C7	C11	C12	177.9(4)	C32	C31	C35	C36	-179.0(4)
C8	C9	C10	N2	-0.6(7)	C32	C31	C30A	C29	176.4(13)
C10	N2	C11	C7	1.1(6)	C32	C31	C30A	O6A	7(2)
C10	N2	C11	C12	-177.6(4)	C32	C33	C34	N6	-0.9(7)
C11	N2	C10	C9	-0.5(6)	C34	N6	C35	C31	-1.1(6)
C11	C7	C8	C9	-0.4(6)	C34	N6	C35	C36	178.4(4)

C12	N1	C1	C2	1.5(6)	C35	N6	C34	C33	1.3(6)
C12	C4	C5	O1	172.6(4)	C35	C31	C32	C33	-0.1(8)
C12	C4	C5	C6	-6.2(7)	C35	C31	C30A	C29	-12(3)
C13	N3	C24	C16	-1.9(6)	C35	C31	C30A	O6A	179.5(18)
C13	N3	C24	C23	178.0(3)	C36	N5	C25	C26	1.0(6)
C13	C14	C15	C16	-1.3(7)	C36	C28	C29	O5	-175.4(4)
C14	C15	C16	C17	179.4(4)	C36	C28	C29	C30	13.6(14)
C14	C15	C16	C24	0.0(7)	C36	C28	C29	C30A	-3.5(15)
C15	C16	C17	O3	-10.0(7)	C30A	C29	C30	O6	-98(5)
C15	C16	C17	C18	170.5(4)	C30A	C29	C30	C31	72(4)
C15	C16	C24	N3	1.7(6)	C30A	C31	C32	C33	172.3(17)
C15	C16	C24	C23	-178.2(4)	C30A	C31	C35	N6	-171.5(18)
C16	C17	C18	O4	-170.3(4)	C30A	C31	C35	C36	9.0(19)
C16	C17	C18	C19	12.1(6)					

Table A3.7 Hydrogen Atom Coordinates (Å×10^4) and Isotropic Displacement Parameters (Å^2×10^3) for stahl194.

Atom	***x***	***y***	***z***	**U(eq)**
H1	7164	2907	5934	21
H2	6732	1908	6786	22
H3	5990	2556	7708	23
H8	5888	7379	7830	22
H9	6608	8160	6944	24
H10	7161	7271	6071	20
H13	8890	5637	6534	22
H14	10519	5214	6620	27
H15	11188	4143	5869	29
H20	8009	2186	3750	27
H21	6444	2840	3758	28
H22	6055	4010	4510	23
H25	8789	6252	4939	23
H26	8915	7374	4112	29
H27	7496	7923	3598	29
H32	3268	6150	4728	36
H33	3390	5018	5555	31
H34	4918	4587	5940	23

H38A	6842	10254	5486	67
H38B	7062	9478	6035	67
H38C	6083	10095	6064	67
H40A	8572	1104	7040	94
H40B	8945	2172	7150	94
H40C	9711	1315	7106	94
H42A	8720	7485	7558	115
H42B	8524	8374	8026	115
H42C	9603	8157	7775	115

Appendix 4

NMR Spectra for Chapter 6

This work has been published:

Wendlandt, A. E.; Stahl, S. S. *Org. Biomol. Chem.* **2012,** *10,* 3866-3870.

^{1}H and ^{13}C NMR Spectra of Substrates

(E)-**1**:

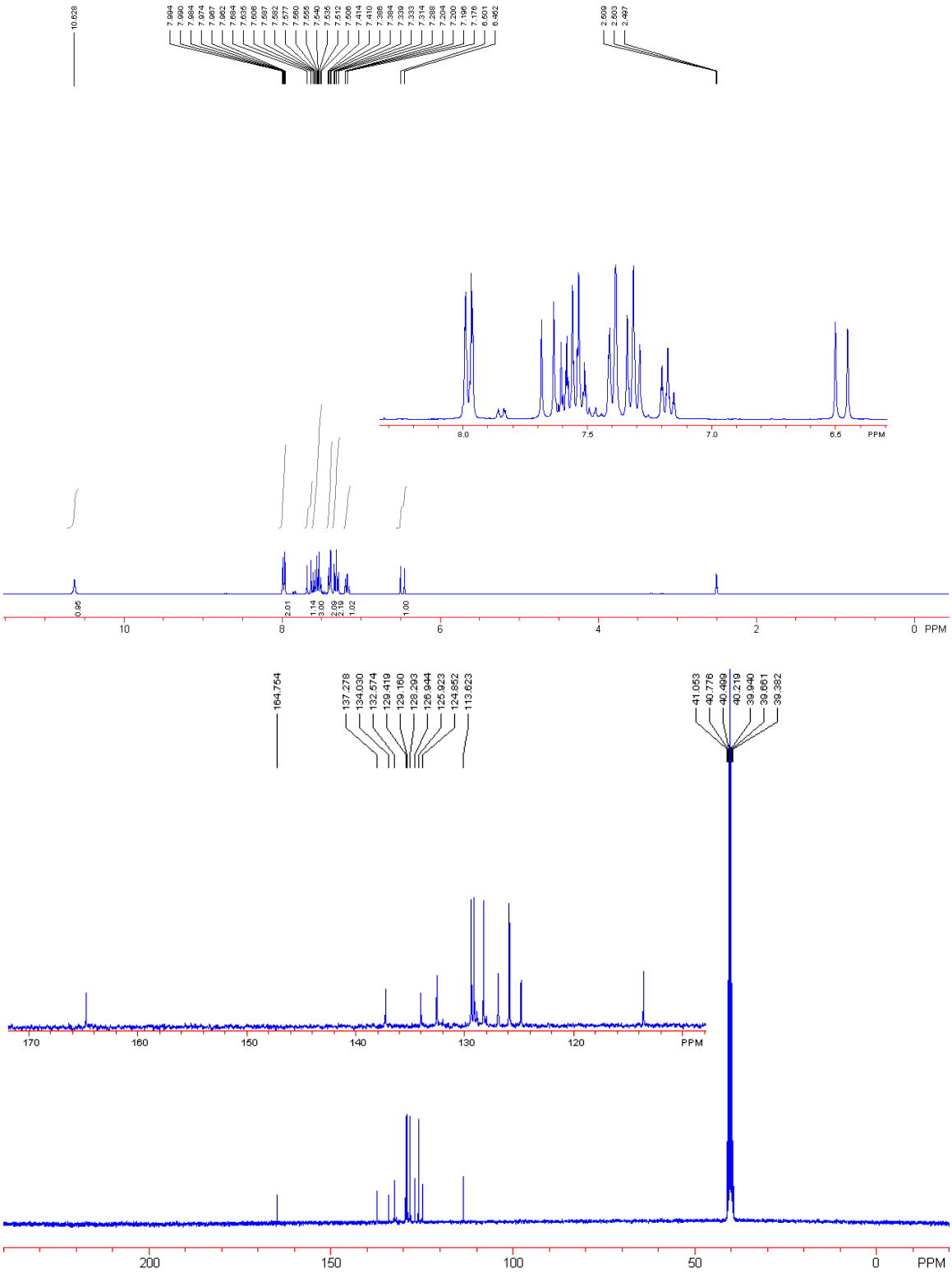

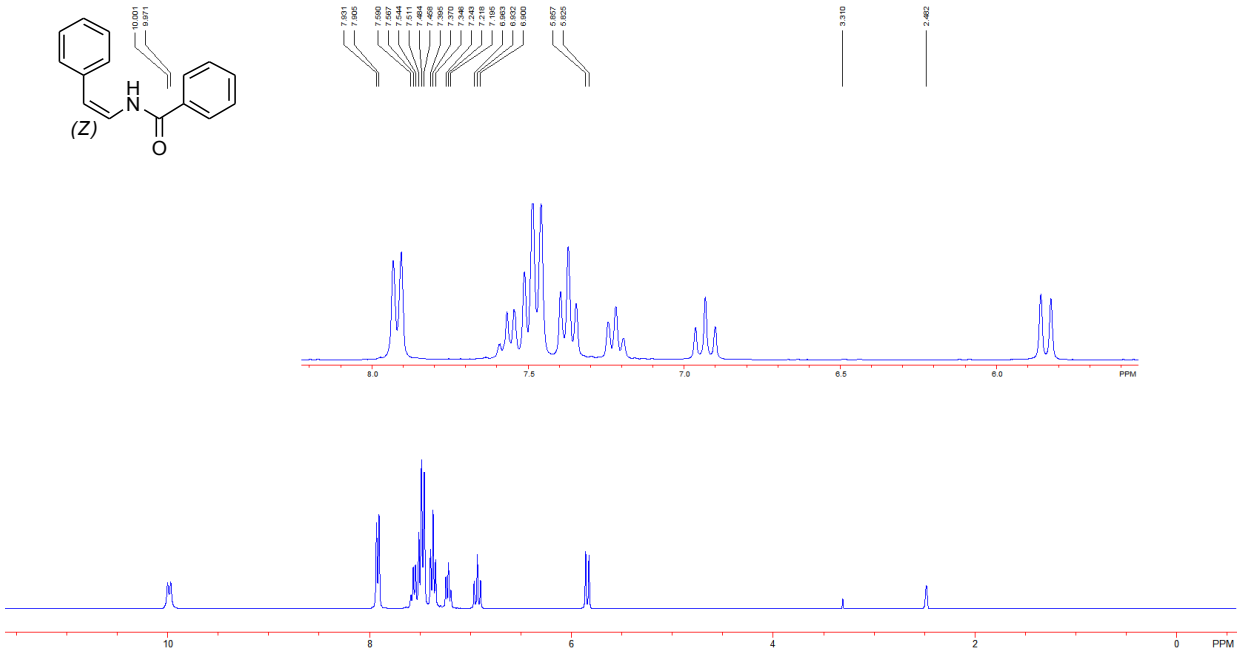
10.001
9.971
H
N
O
(Z)
7.931
7.905
7.590
7.567
7.544
7.511
7.464
7.459
7.395
7.370
7.348
7.243
7.218
7.195
6.955
6.932
6.900
5.857
5.825
3.310
2.462
8.0
7.5
7.0
6.5
6.0
PPM
10
8
6
4
2
0
PPM

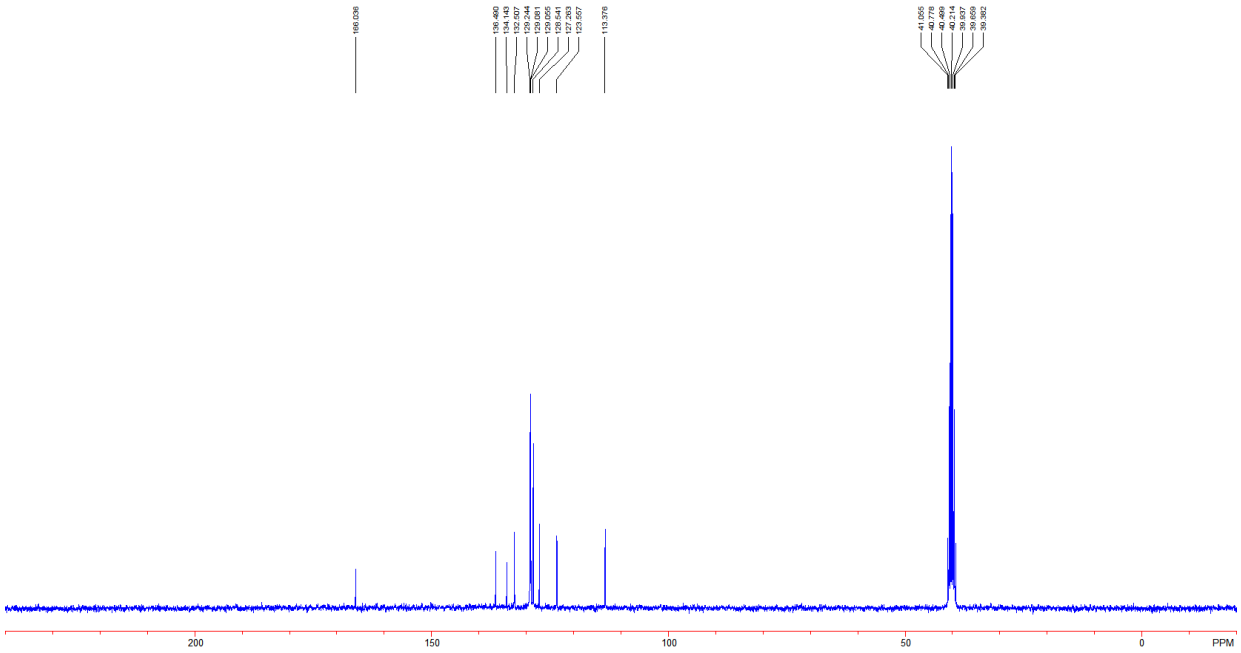
166.038
136.490
134.143
132.027
129.244
129.081
128.955
128.541
127.283
123.557
113.376
41.055
40.778
40.499
40.214
39.937
39.659
39.352
200
150
100
50
0
PPM

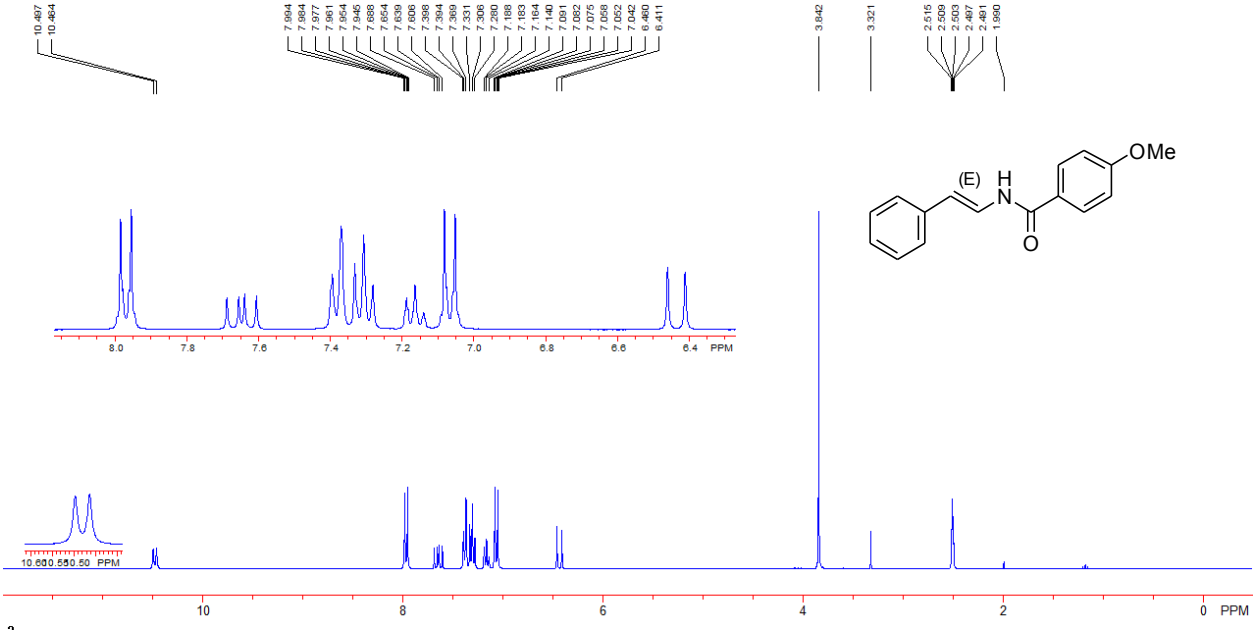
10.497
10.484
7.994
7.984
7.977
7.961
7.954
7.946
7.936
7.654
7.639
7.606
7.396
7.394
7.369
7.331
7.306
7.280
7.188
7.183
7.164
7.140
7.091
7.082
7.075
7.058
7.052
7.042
6.490
6.411
3.842
3.321
2.515
2.509
2.503
2.497
2.491
1.990
(E)
H
N
O
OMe
8.0
7.8
7.6
7.4
7.2
7.0
6.8
6.6
6.4
PPM
10.500.550.50 PPM
10
8
6
4
2
0
PPM

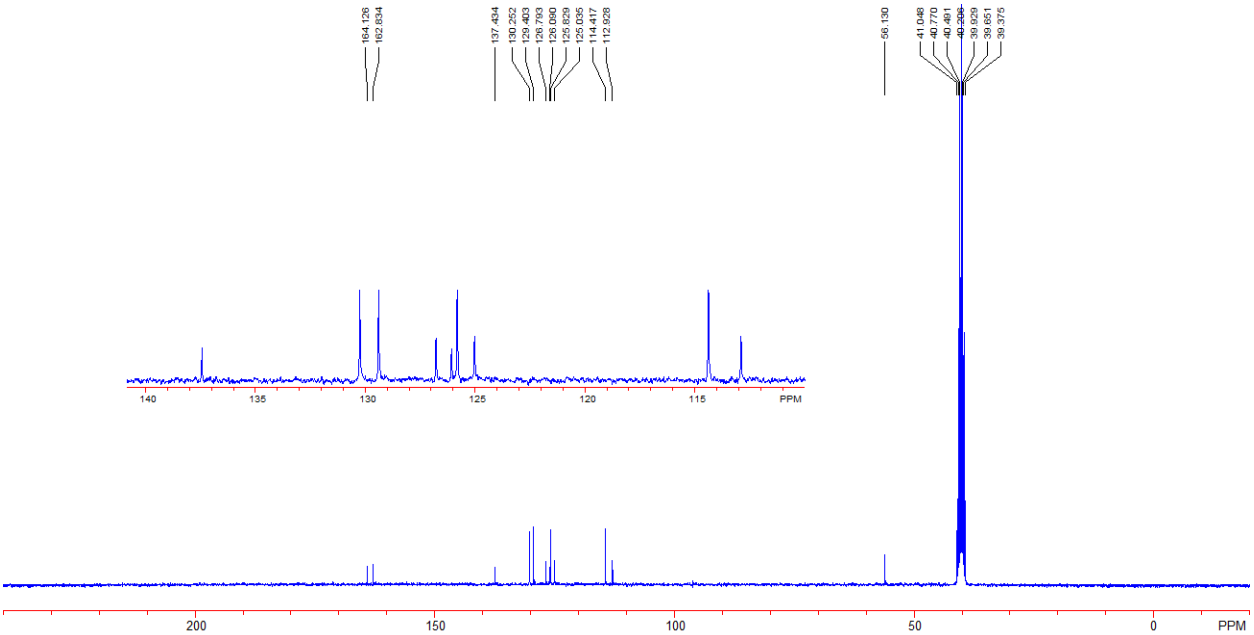
164.126
162.834
137.434
130.252
129.403
128.793
128.080
126.829
125.056
114.417
112.928
56.130
41.048
40.770
40.491
40.212
39.929
39.651
39.375
140
135
130
125
120
115
PPM
200
150
100
50
0
PPM

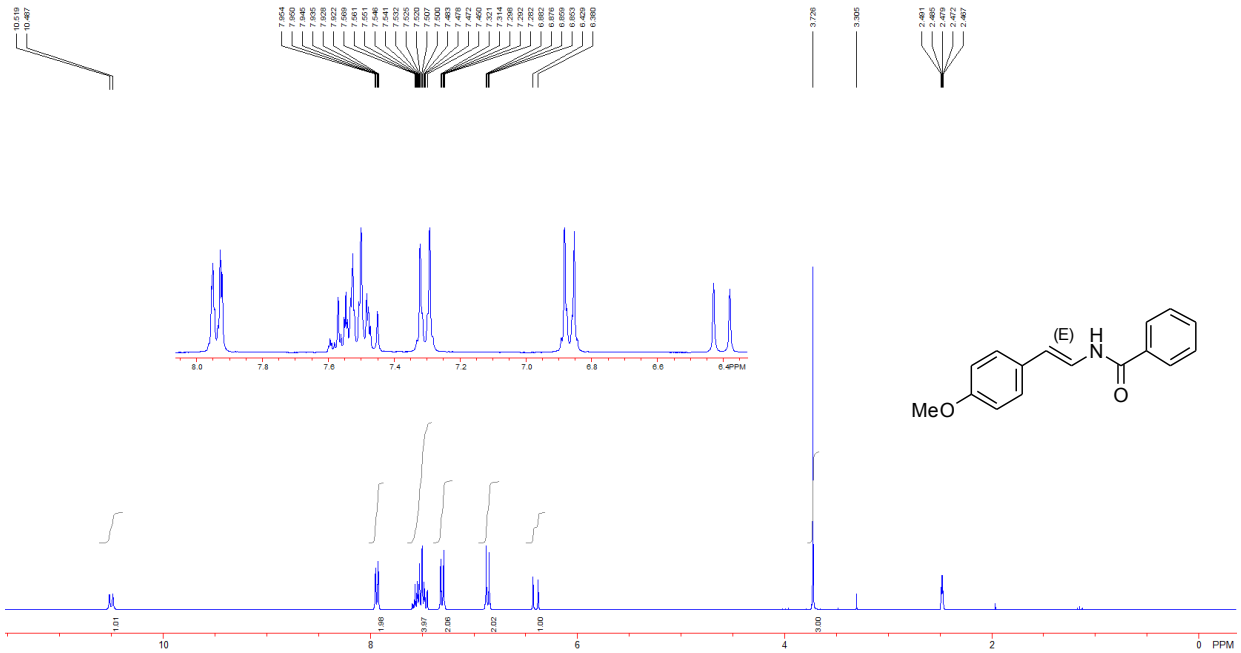
(E)
H
N
O
MeO
PPM

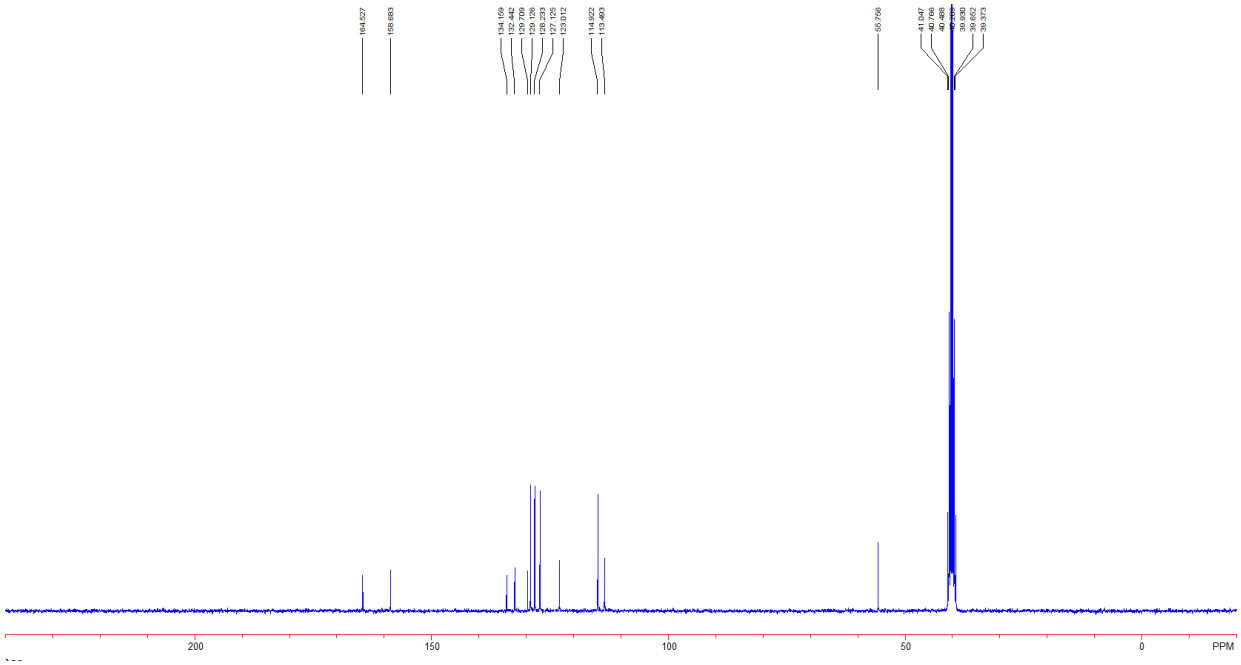
PPM

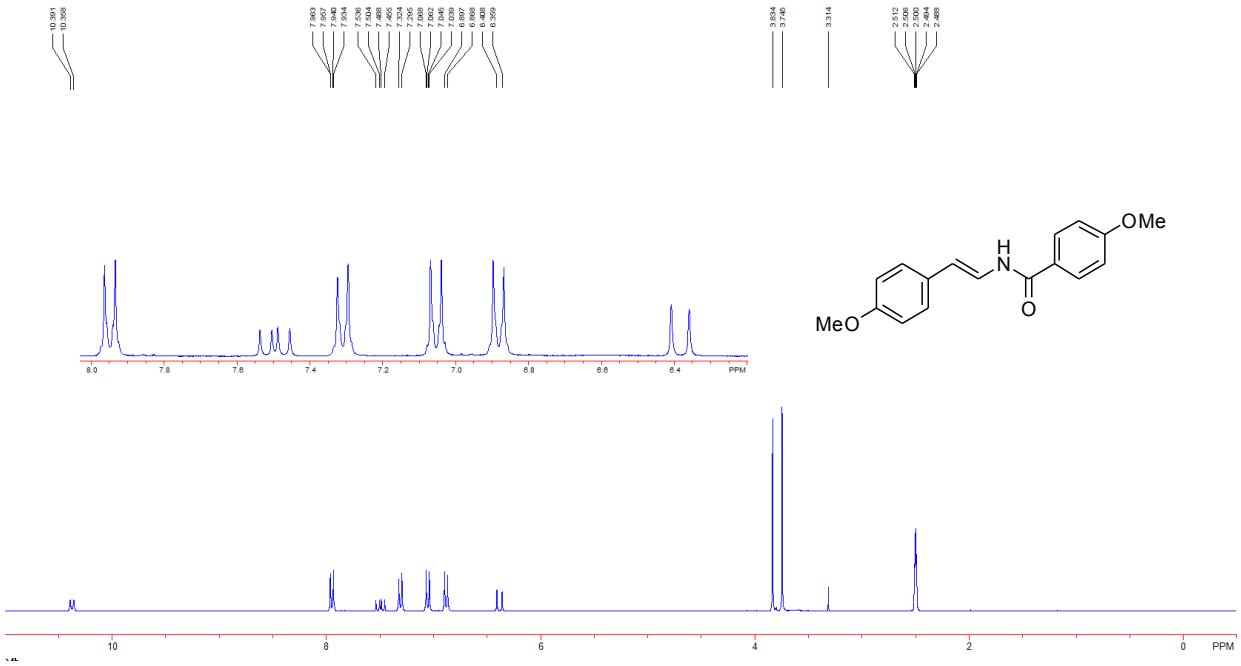
10.391
10.359
7.963
7.957
7.940
7.934
7.536
7.504
7.496
7.465
7.324
7.295
7.289
7.062
7.045
7.039
6.997
6.988
6.409
6.359
3.834
3.746
3.314
2.512
2.506
2.500
2.494
2.488
OMe
H
N
O
MeO
8.0
7.8
7.6
7.4
7.2
7.0
6.8
6.6
6.4
PPM
10
8
6
4
2
0
PPM

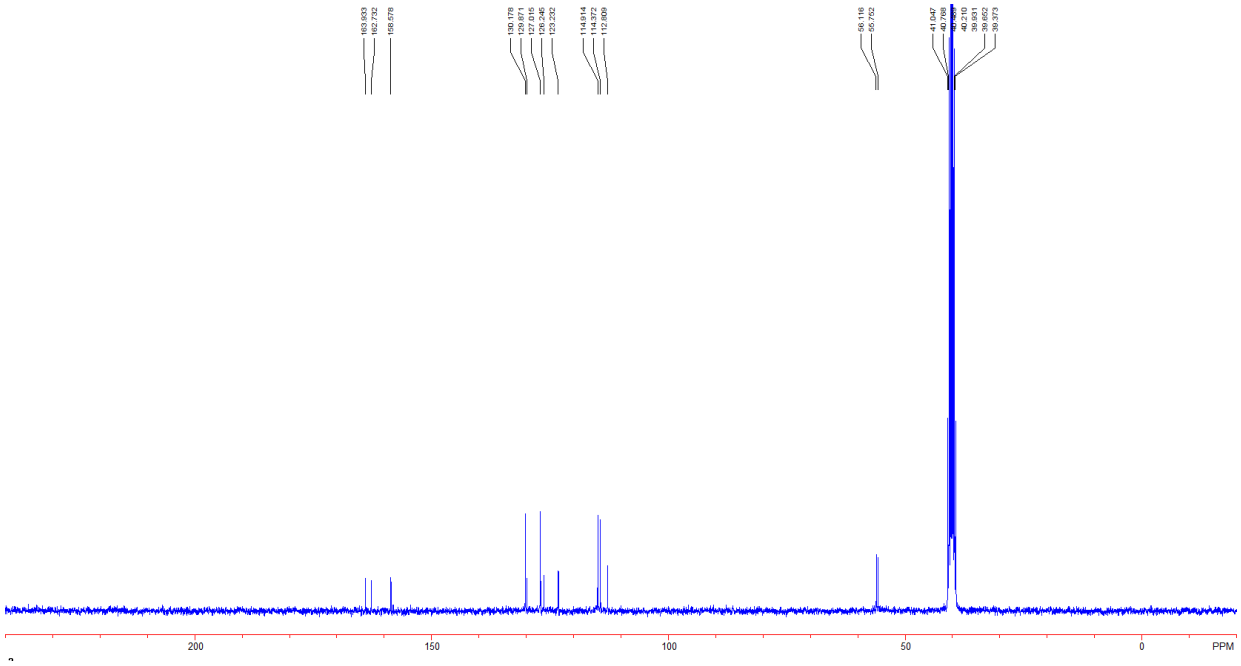
163.933
162.732
155.578
130.178
129.871
127.015
126.246
123.232
114.914
114.372
112.609
55.116
55.752
41.047
40.768
40.218
39.931
39.652
39.373
200
150
100
50
0
PPM

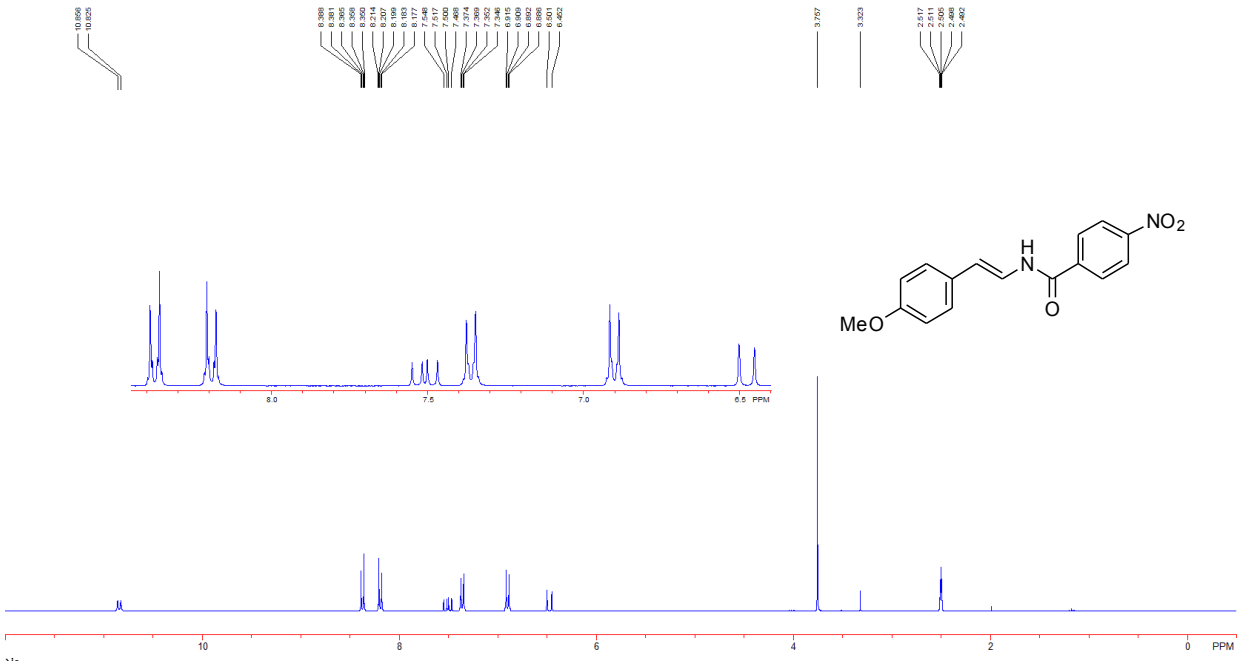
10.956
10.825
8.398
8.381
8.365
8.356
8.254
8.214
8.207
8.199
8.193
8.177
7.548
7.537
7.517
7.500
7.469
7.374
7.369
7.352
7.346
6.915
6.899
6.892
6.889
6.501
6.482
3.757
3.323
2.517
2.511
2.505
2.499
2.492
NO2
H
N
O
MeO
8.0
7.5
7.0
6.5 PPM
10
8
6
4
2
0 PPM

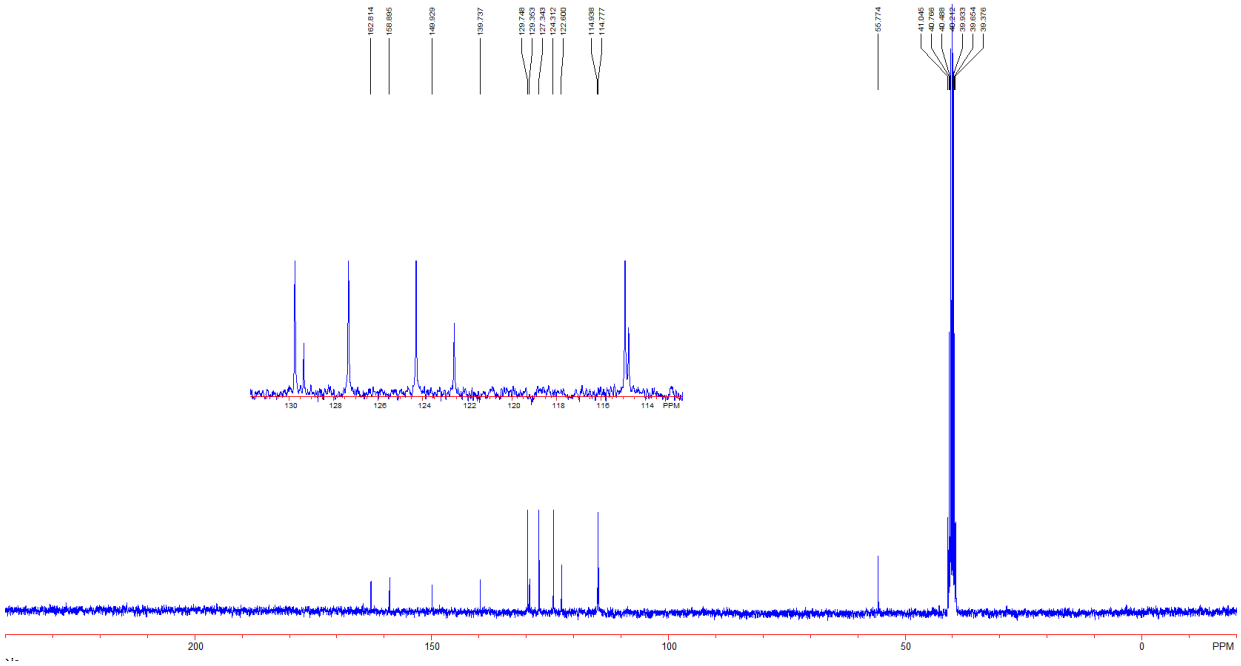
162.814
158.895
146.929
139.737
129.748
129.253
127.343
124.312
122.600
114.539
114.277
55.774
41.045
40.766
40.488
40.209
39.933
39.654
39.376
130
128
126
124
122
120
118
116
114 PPM
200
150
100
50
0 PPM

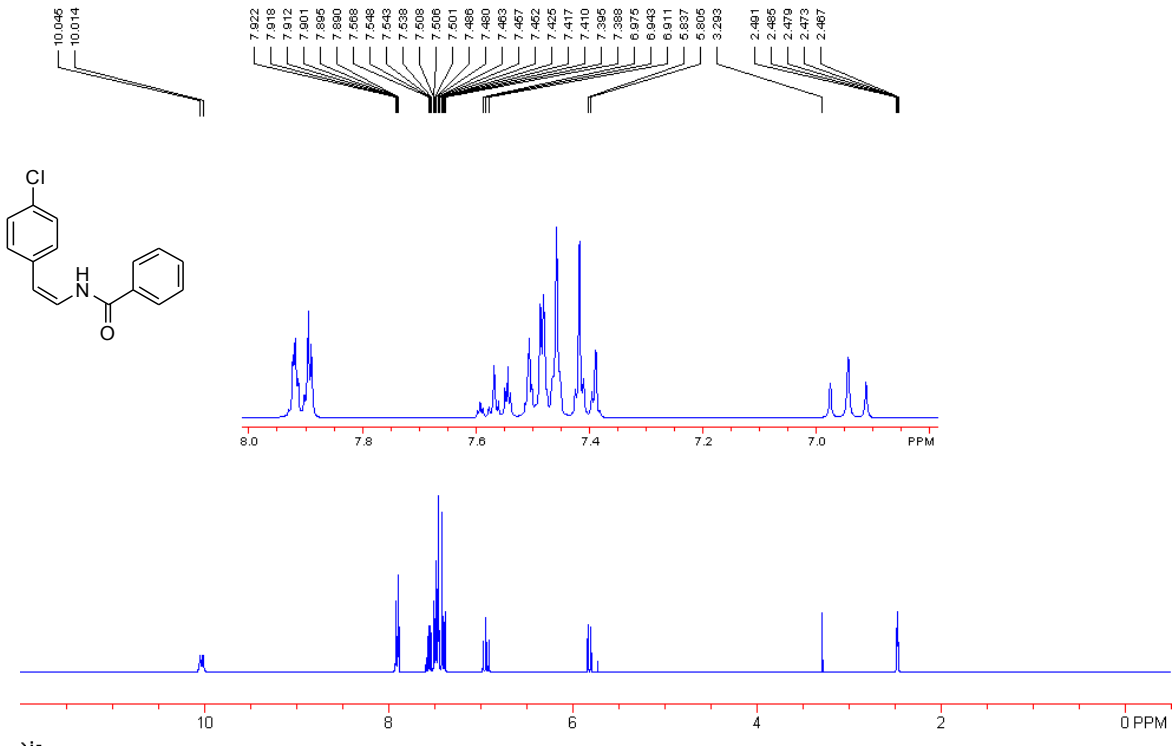
10.045
10.014
7.922
7.918
7.912
7.901
7.895
7.890
7.568
7.548
7.543
7.538
7.508
7.506
7.501
7.486
7.480
7.463
7.457
7.452
7.425
7.417
7.410
7.395
7.388
6.975
6.943
6.911
5.837
5.805
3.293
2.491
2.485
2.479
2.473
2.467
Cl
H
N
O
8.0
7.8
7.6
7.4
7.2
7.0
PPM
10
8
6
4
2
0 PPM

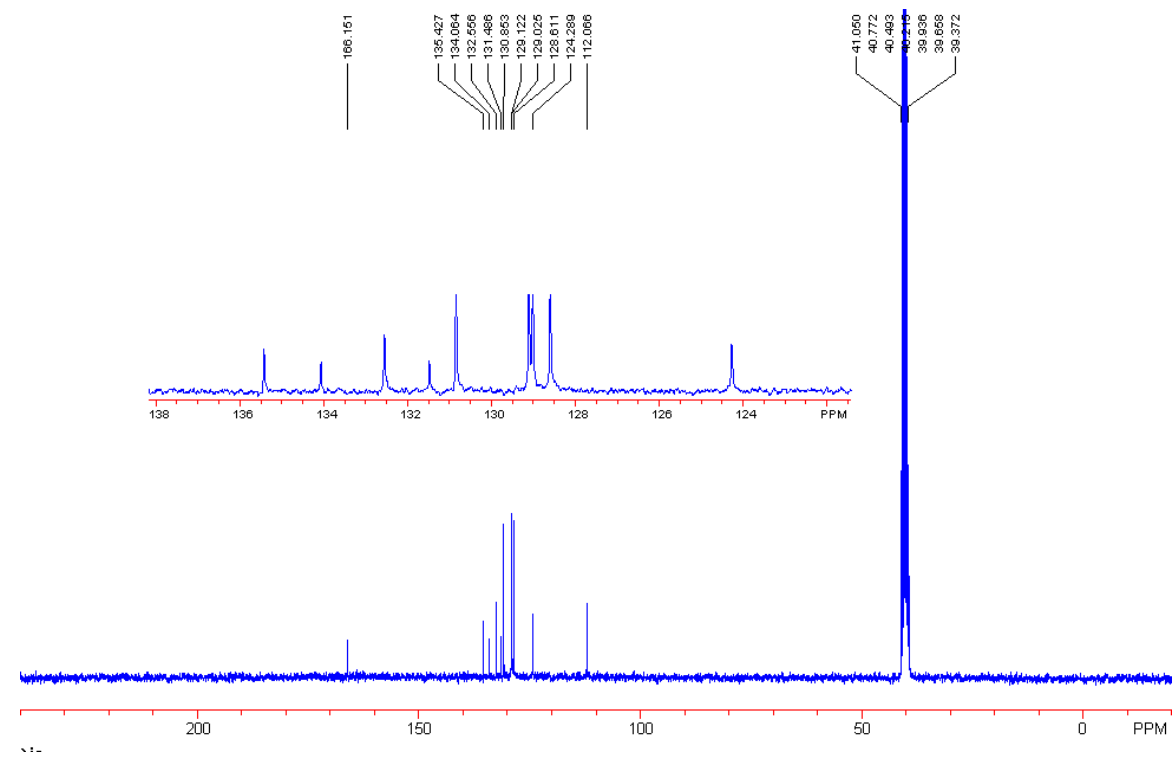
166.151
135.427
134.064
132.556
131.486
130.853
129.122
129.025
128.611
124.289
112.066
41.050
40.772
40.493
39.936
39.658
39.372
138
136
134
132
130
128
126
124
PPM
200
150
100
50
0
PPM

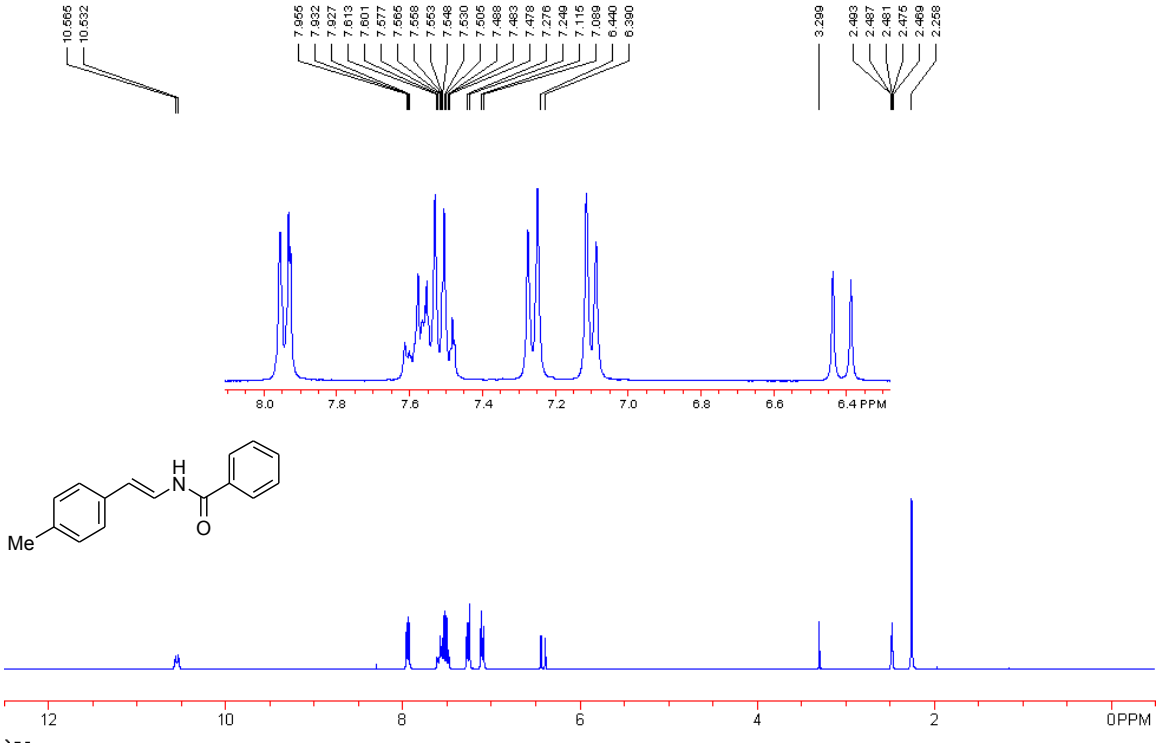
10.565
10.532
7.955
7.932
7.927
7.613
7.601
7.577
7.565
7.558
7.553
7.548
7.530
7.505
7.488
7.483
7.478
7.276
7.249
7.115
7.089
6.440
6.390
3.299
2.493
2.487
2.481
2.475
2.469
2.258
8.0
7.8
7.6
7.4
7.2
7.0
6.8
6.6
6.4 PPM
H
N
O
Me
12
10
8
6
4
2
0PPM

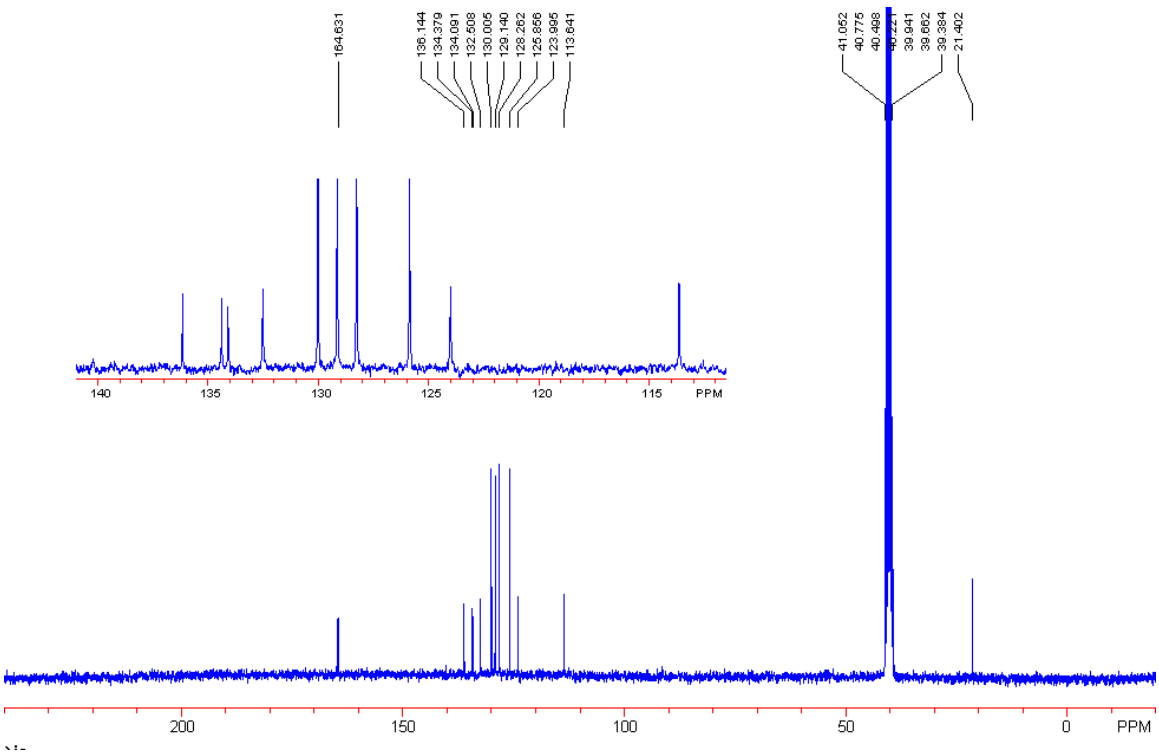
164.631
136.144
134.379
134.091
132.508
130.005
129.140
128.282
125.856
123.995
113.641
41.052
40.775
40.498
40.221
39.941
39.662
39.384
21.402
140
135
130
125
120
115
PPM
200
150
100
50
0
PPM

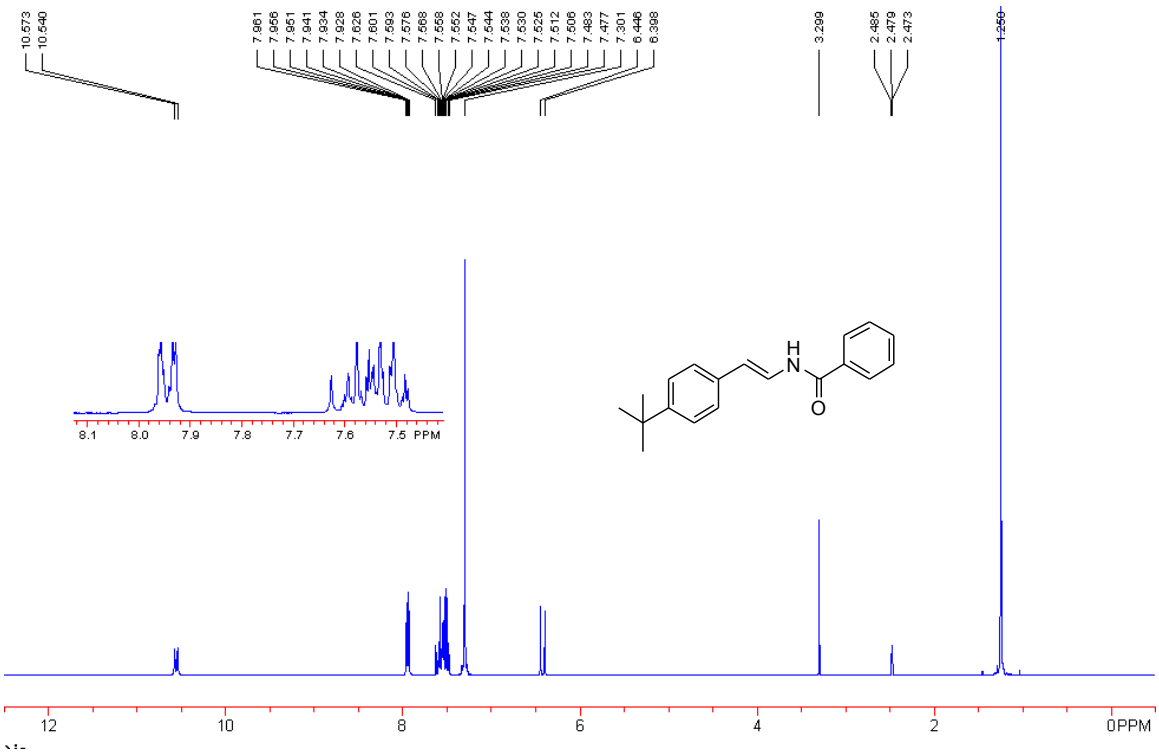
10.573
10.540
7.961
7.956
7.951
7.941
7.934
7.928
7.626
7.601
7.593
7.576
7.568
7.558
7.552
7.547
7.544
7.538
7.530
7.525
7.512
7.506
7.483
7.477
7.301
6.446
6.398
3.299
2.485
2.479
2.473
1.259
8.1 8.0 7.9 7.8 7.7 7.6 7.5 PPM
H
N
O
12 10 8 6 4 2 0PPM

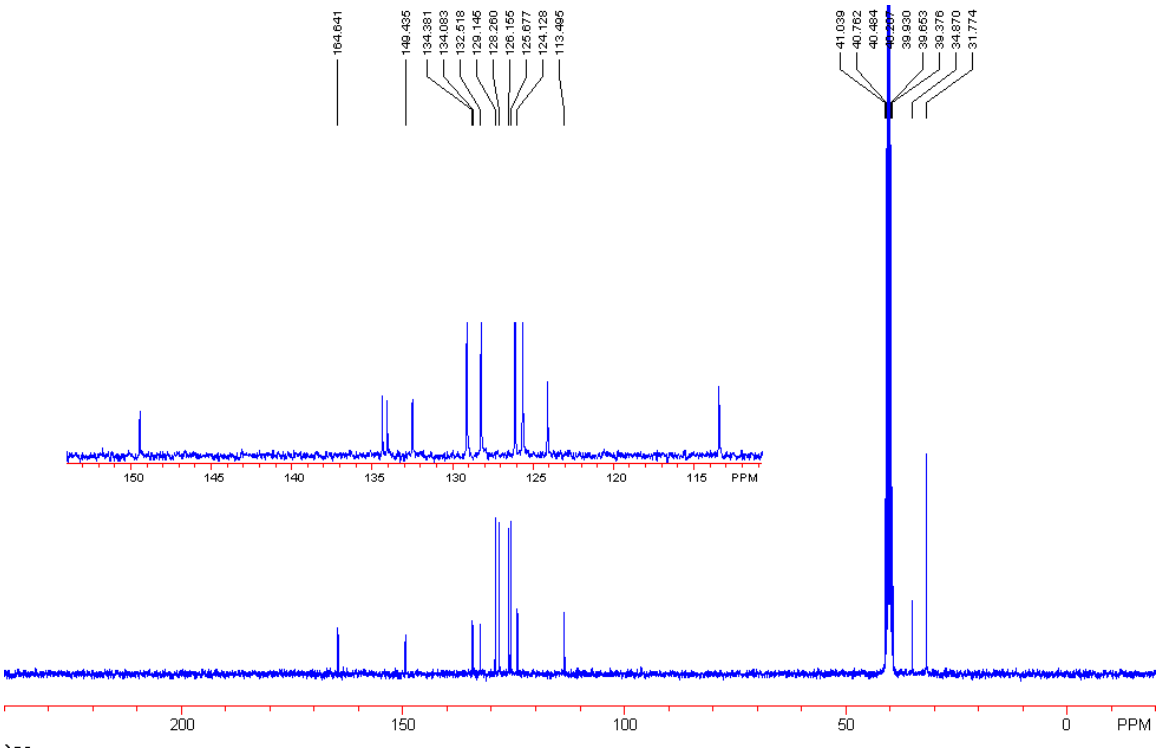
164.641
149.435
134.381
134.083
132.518
129.145
128.260
126.155
125.677
124.128
113.495
41.039
40.762
40.484
40.207
39.930
39.653
39.376
34.870
31.774
150 145 140 135 130 125 120 115 PPM
200 150 100 50 0 PPM

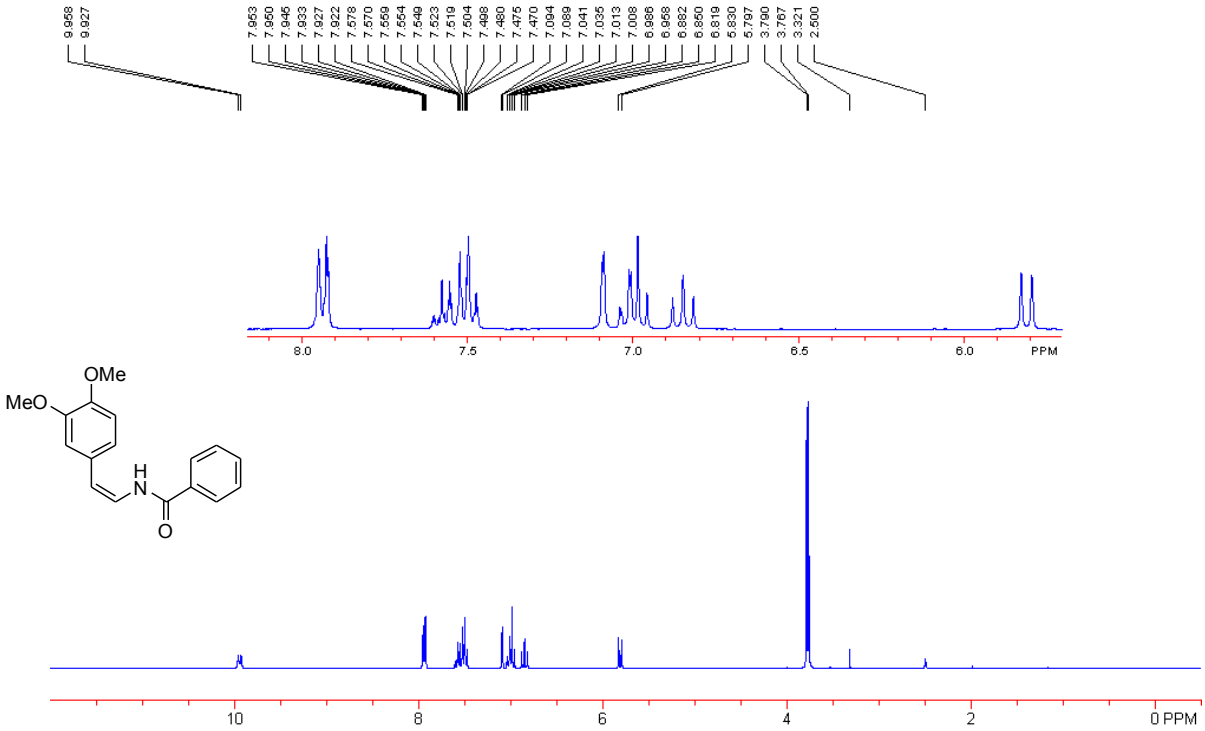
9.958
9.927
7.953
7.950
7.946
7.933
7.927
7.922
7.578
7.570
7.559
7.554
7.549
7.523
7.519
7.504
7.498
7.480
7.475
7.470
7.094
7.089
7.041
7.035
7.013
7.008
6.986
6.958
6.882
6.850
6.819
5.830
5.797
3.790
3.767
3.321
2.500
8.0
7.5
7.0
6.5
6.0
PPM
OMe
MeO
H
N
O
10
8
6
4
2
0 PPM

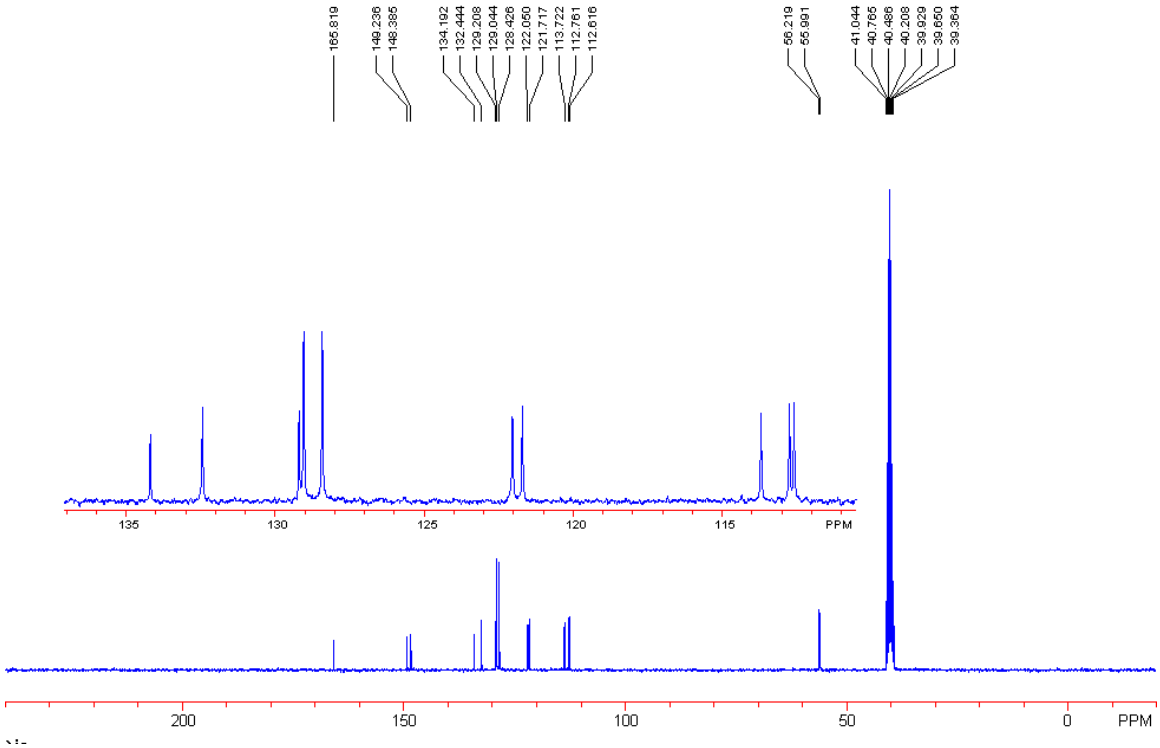
165.819
149.236
148.386
134.192
132.444
129.208
129.044
128.426
122.050
121.717
113.722
112.761
112.616
56.219
55.991
41.044
40.765
40.486
40.208
39.929
39.650
39.364
135
130
125
120
115
PPM
200
150
100
50
0
PPM

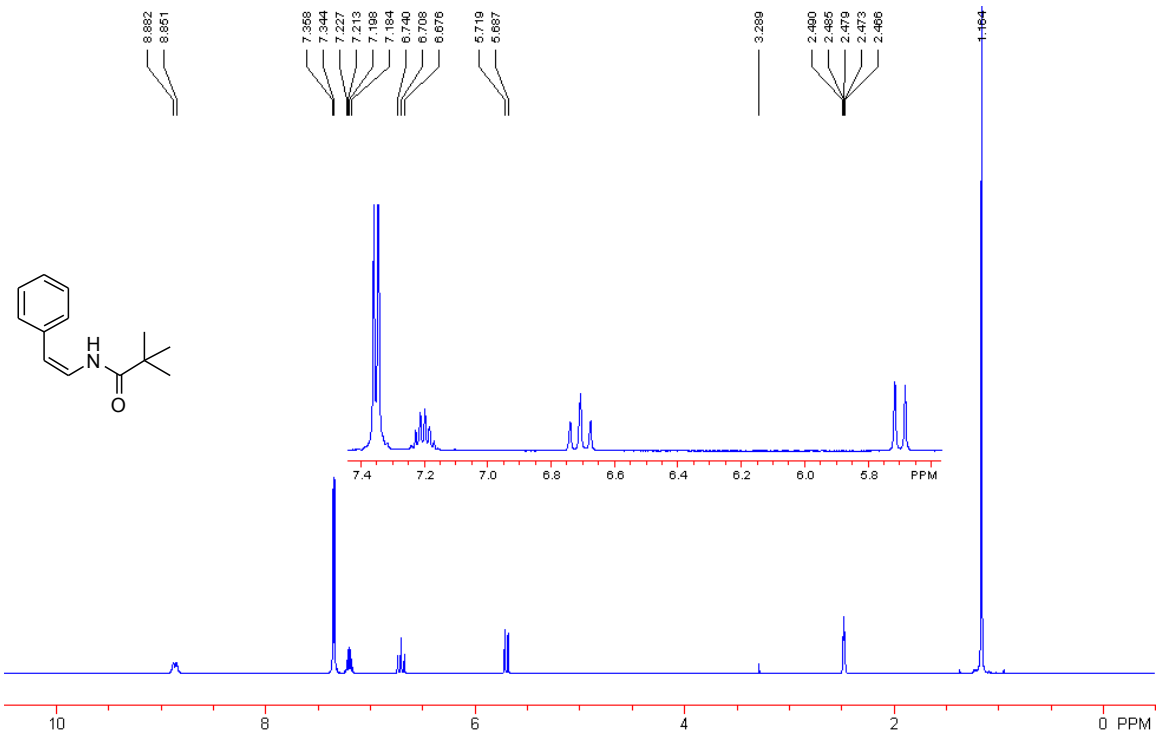
8.882
8.851
7.358
7.344
7.227
7.213
7.198
7.184
6.740
6.708
6.676
5.719
5.687
3.289
2.490
2.485
2.479
2.473
2.466
1.164
H
N
O
7.4
7.2
7.0
6.8
6.6
6.4
6.2
6.0
5.8
PPM
10
8
6
4
2
0 PPM

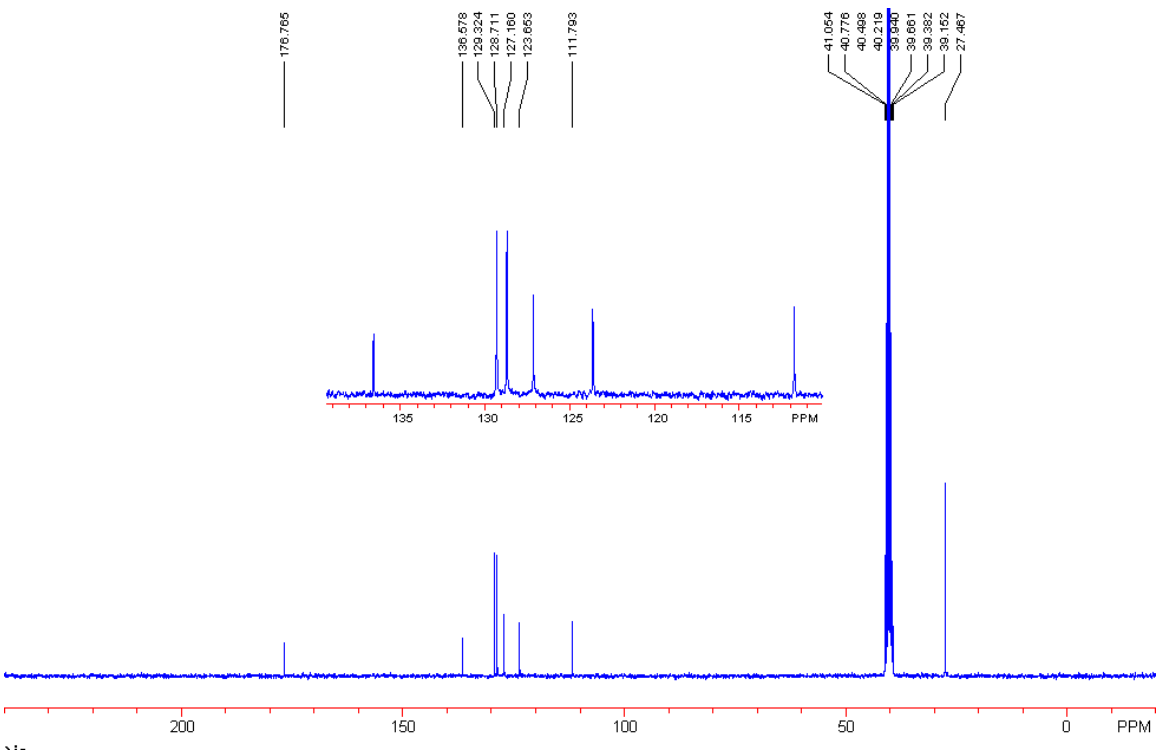
176.785
138.578
129.324
128.711
127.160
123.653
111.793
41.054
40.776
40.498
40.219
39.940
39.661
39.382
39.152
27.467
135
130
125
120
115
PPM
200
150
100
50
0
PPM

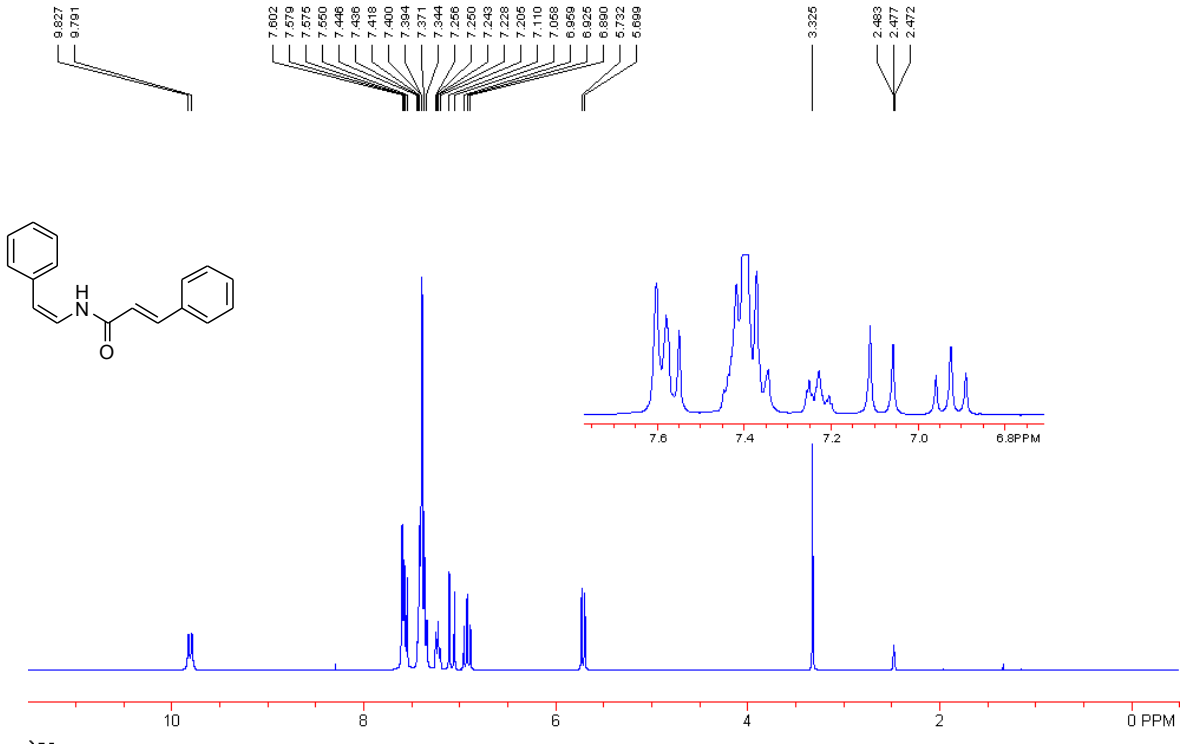
9.827
9.791
7.602
7.579
7.575
7.550
7.446
7.436
7.418
7.400
7.394
7.371
7.344
7.256
7.250
7.243
7.228
7.205
7.110
7.068
6.969
6.925
6.890
5.732
5.699
3.325
2.483
2.477
2.472
H
N
O
7.6
7.4
7.2
7.0
6.8PPM
10
8
6
4
2
0 PPM

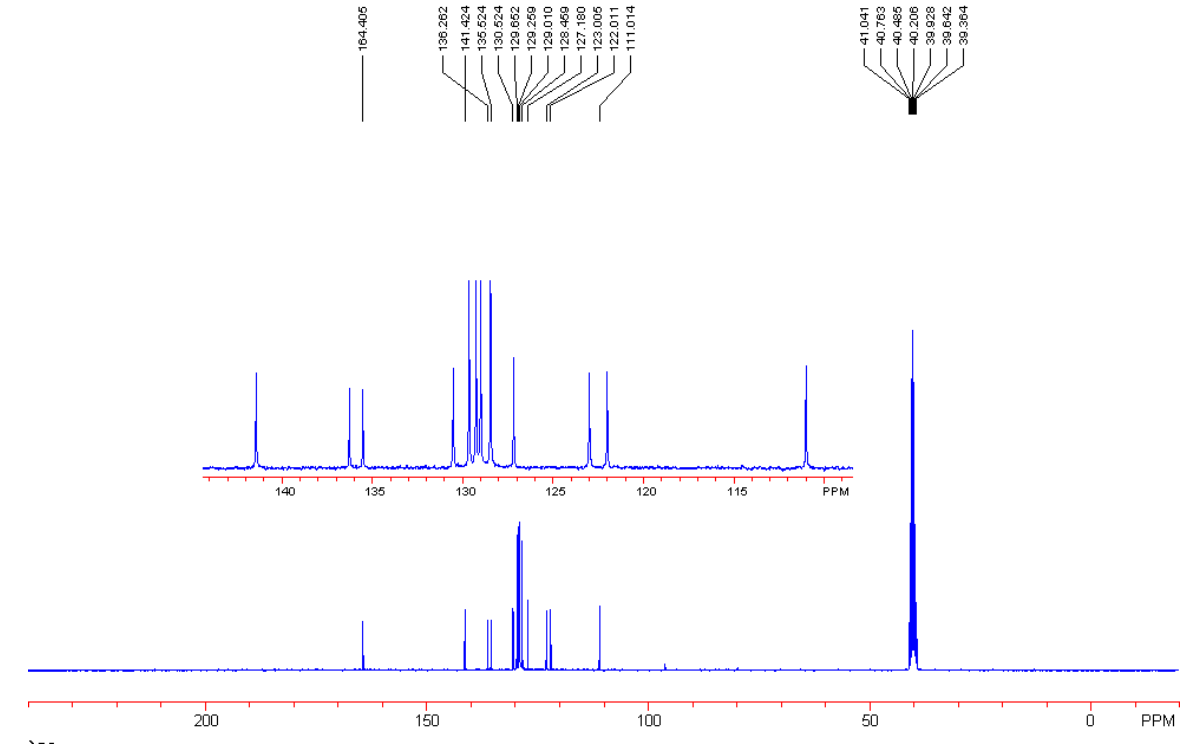
164.405
136.262
141.424
135.524
130.524
129.652
129.259
129.010
128.469
127.180
123.005
122.011
111.014
41.041
40.763
40.485
40.206
39.928
39.642
39.364
140
135
130
125
120
115
PPM
200
150
100
50
0
PPM

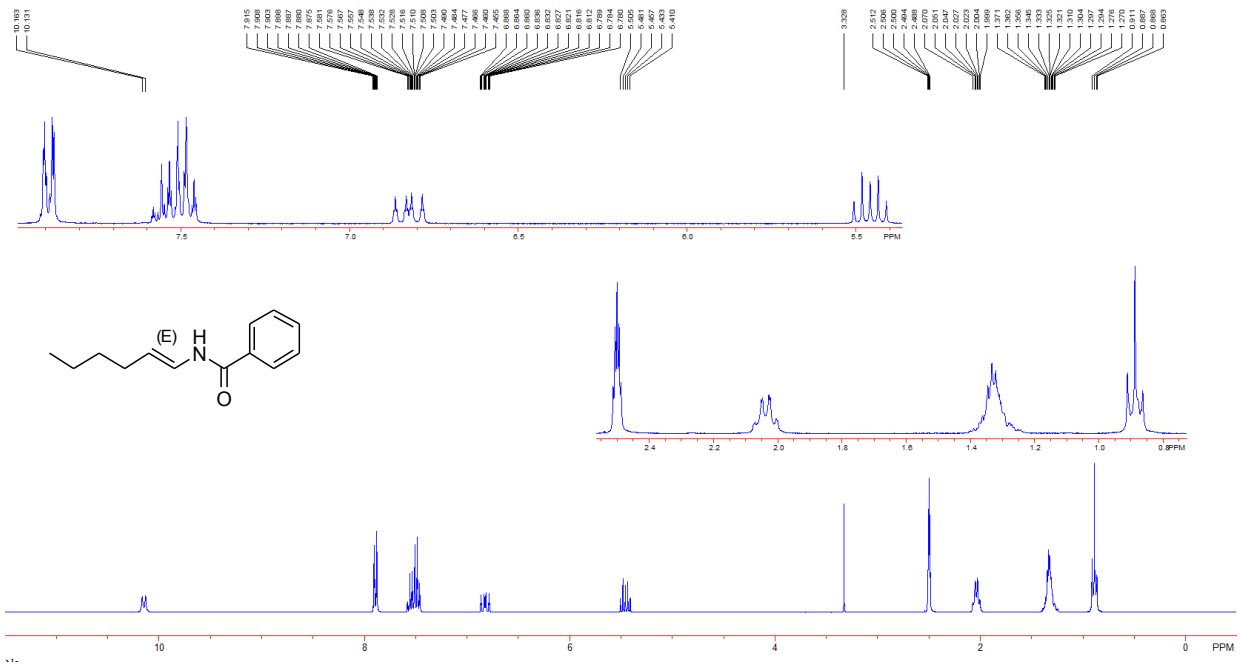
(E)
H
N
O
PPM

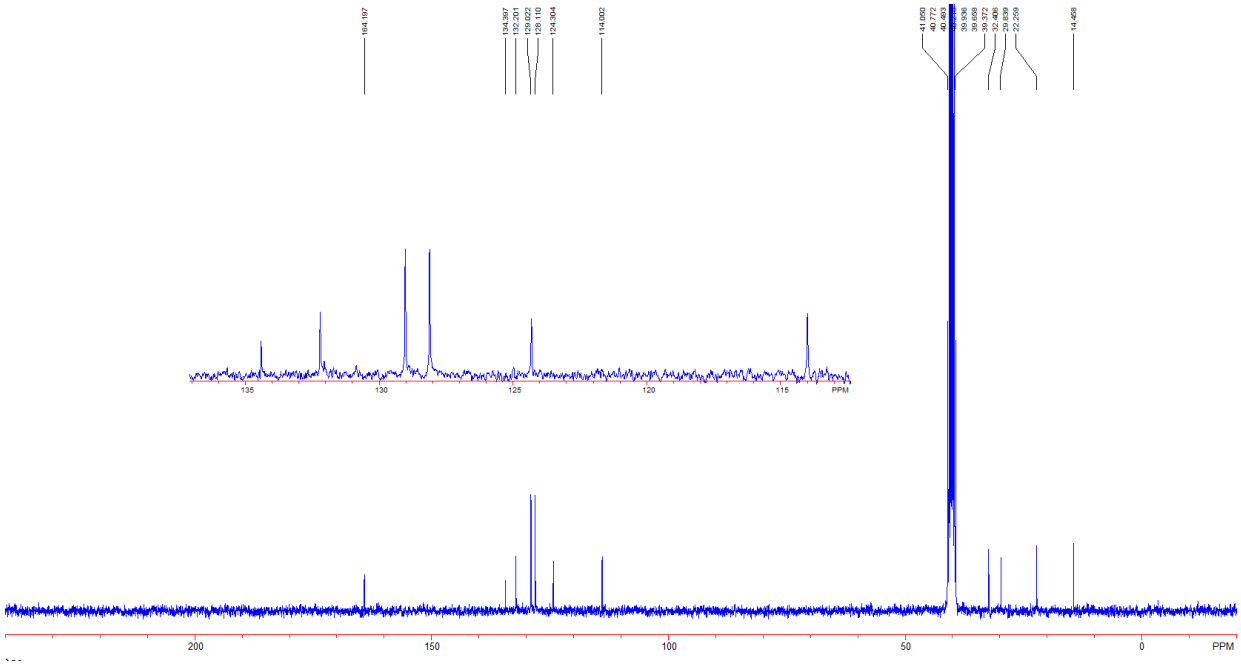
164.197
134.307
132.201
129.022
128.110
124.304
114.002
41.050
40.772
40.493
39.936
39.658
39.372
32.499
29.839
22.259
14.468
PPM

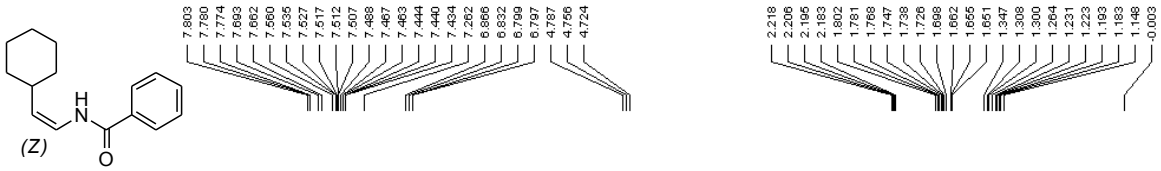
(Z)
H
N
O
7.803
7.780
7.774
7.693
7.662
7.560
7.535
7.527
7.517
7.512
7.507
7.488
7.467
7.463
7.444
7.440
7.434
7.262
6.886
6.832
6.799
6.797
4.787
4.756
4.724
2.218
2.206
2.195
2.183
1.802
1.781
1.768
1.747
1.738
1.726
1.698
1.662
1.655
1.651
1.347
1.308
1.300
1.264
1.231
1.223
1.193
1.183
1.148
-0.003

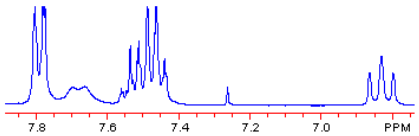
7.8
7.6
7.4
7.2
7.0
PPM

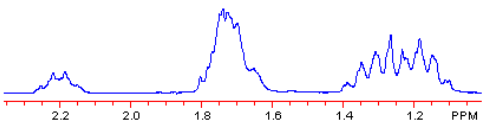
2.2
2.0
1.8
1.6
1.4
1.2
PPM

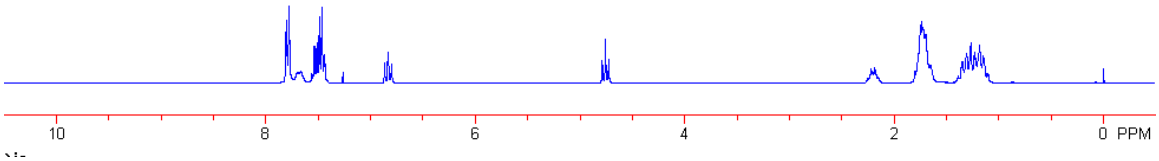
10
8
6
4
2
0 PPM

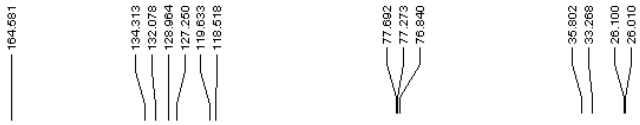
164.581
134.313
132.078
128.964
127.250
119.633
118.518
77.692
77.273
76.840
35.802
33.268
26.100
26.010

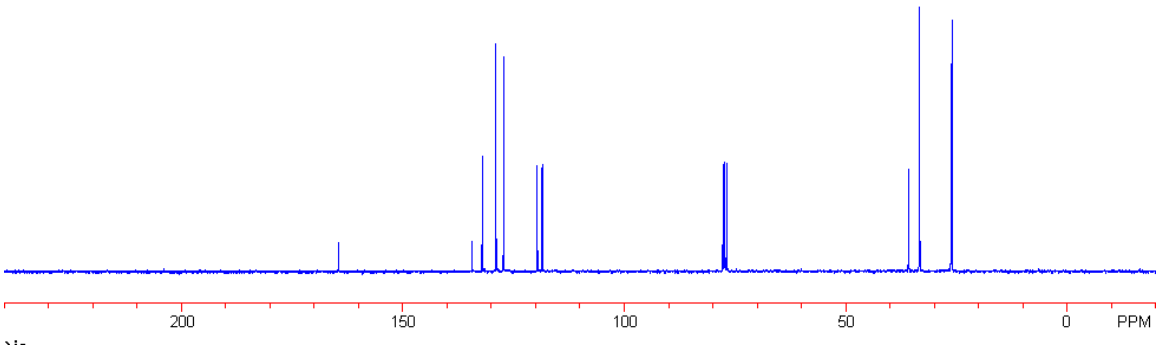
200
150
100
50
0
PPM

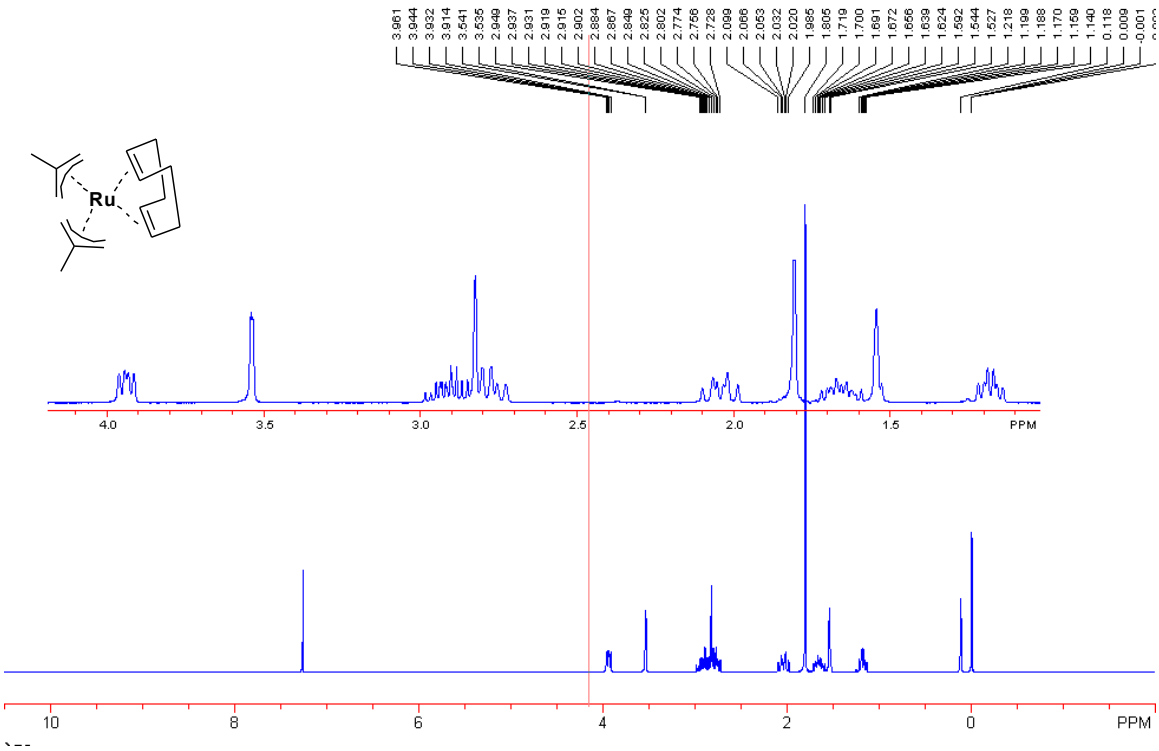
3.961
3.944
3.932
3.914
3.541
3.535
2.949
2.937
2.931
2.919
2.915
2.902
2.884
2.867
2.849
2.825
2.802
2.774
2.756
2.728
2.099
2.066
2.053
2.032
2.020
1.985
1.805
1.719
1.700
1.691
1.672
1.656
1.639
1.624
1.592
1.544
1.527
1.218
1.199
1.188
1.170
1.159
1.140
0.118
0.009
-0.001
Ru
4.0
3.5
3.0
2.5
2.0
1.5
PPM
10
8
6
4
2
0
PPM

^{1}H and ^{13}CNMR Spectra of Products

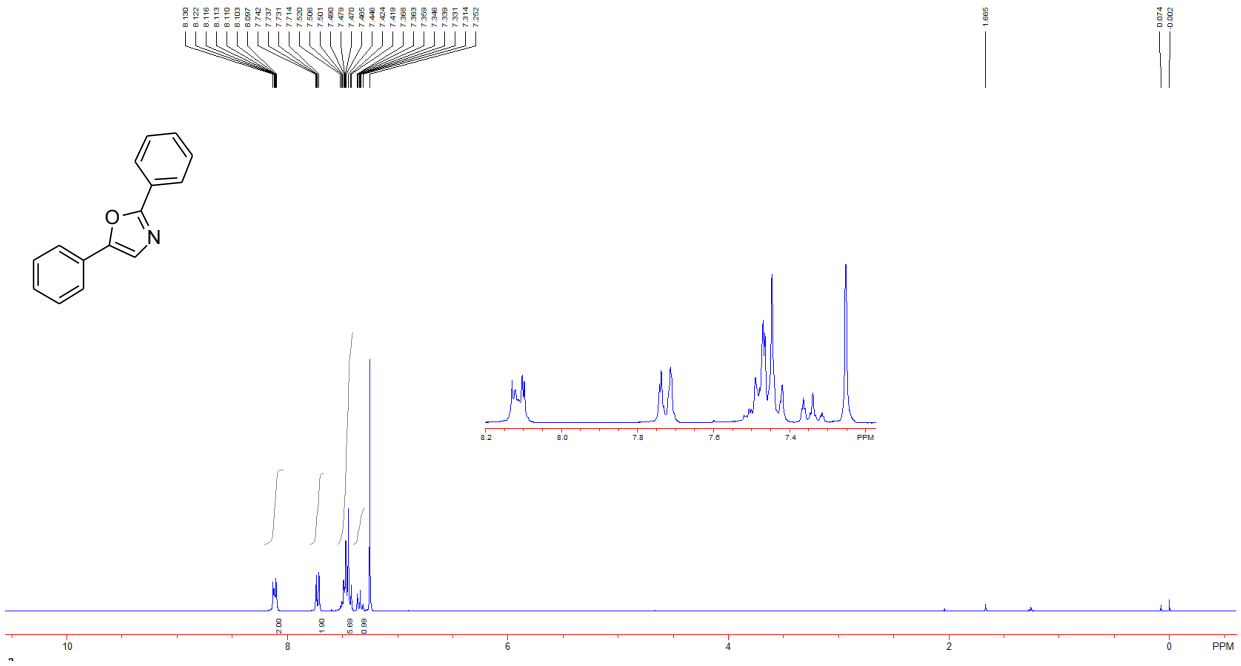

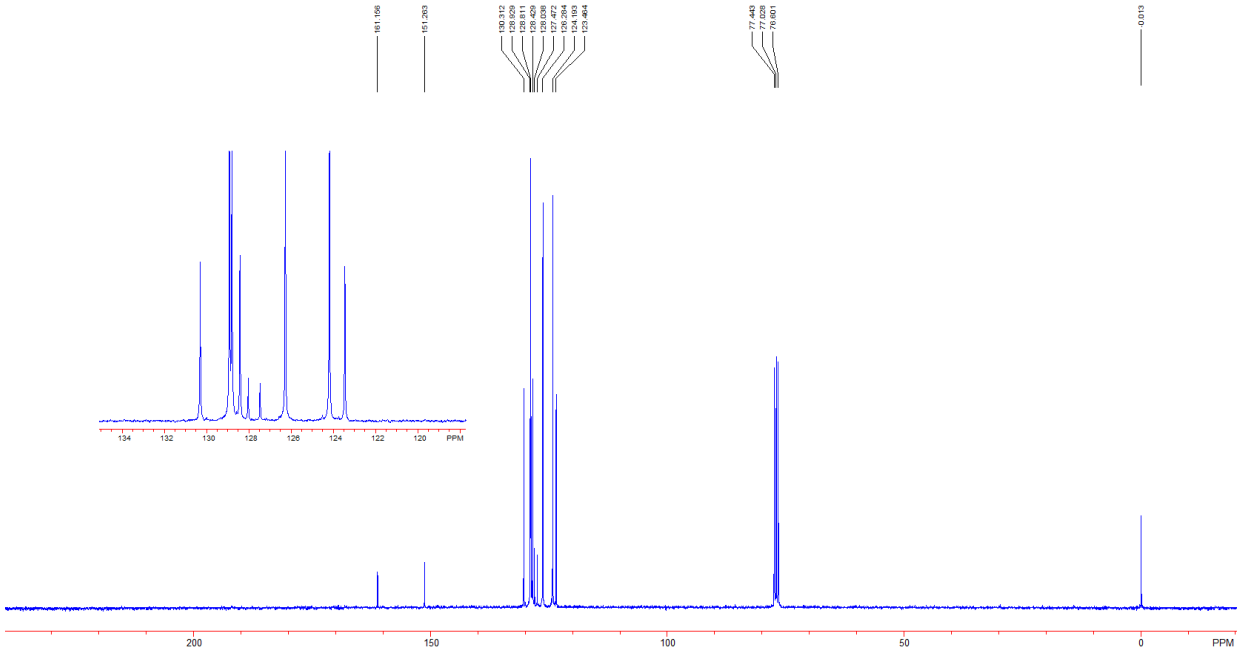

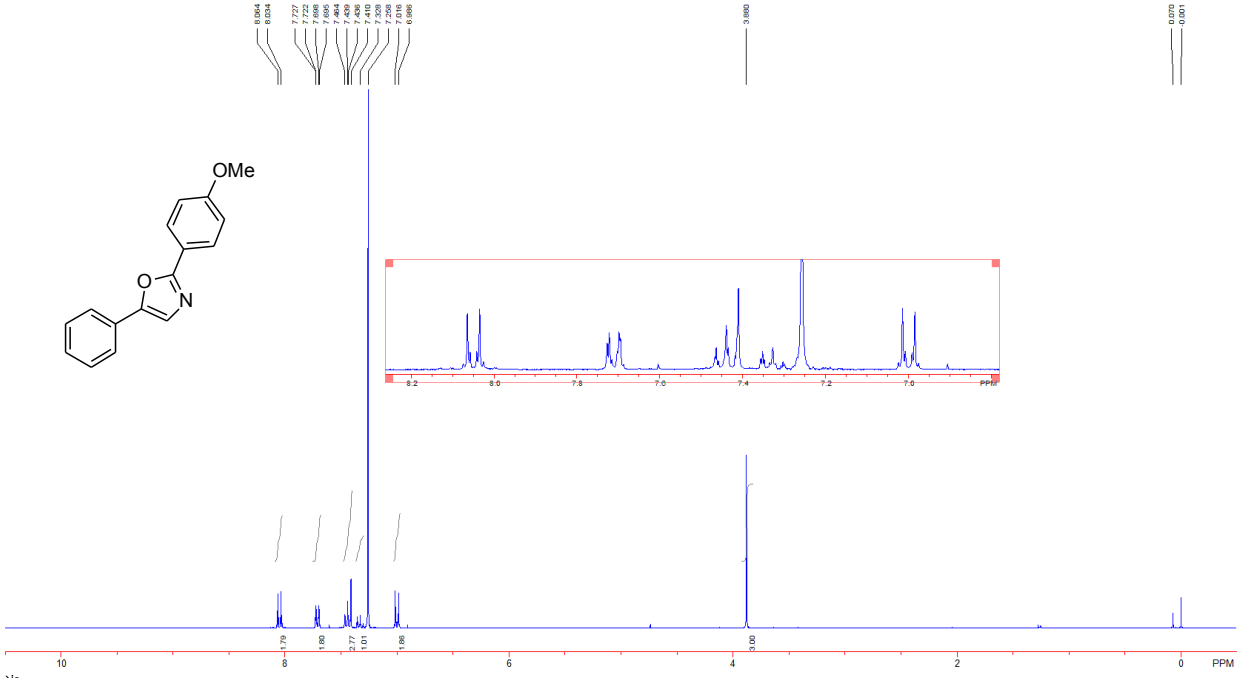
OMe
O
N
8.054
8.034
7.727
7.722
7.698
7.695
7.464
7.464
7.439
7.436
7.410
7.409
7.358
7.358
7.016
6.986
3.880
0.070
-0.001
1.79
1.80
2.77
1.01
1.88
3.00
10
8
6
4
2
0
PPM

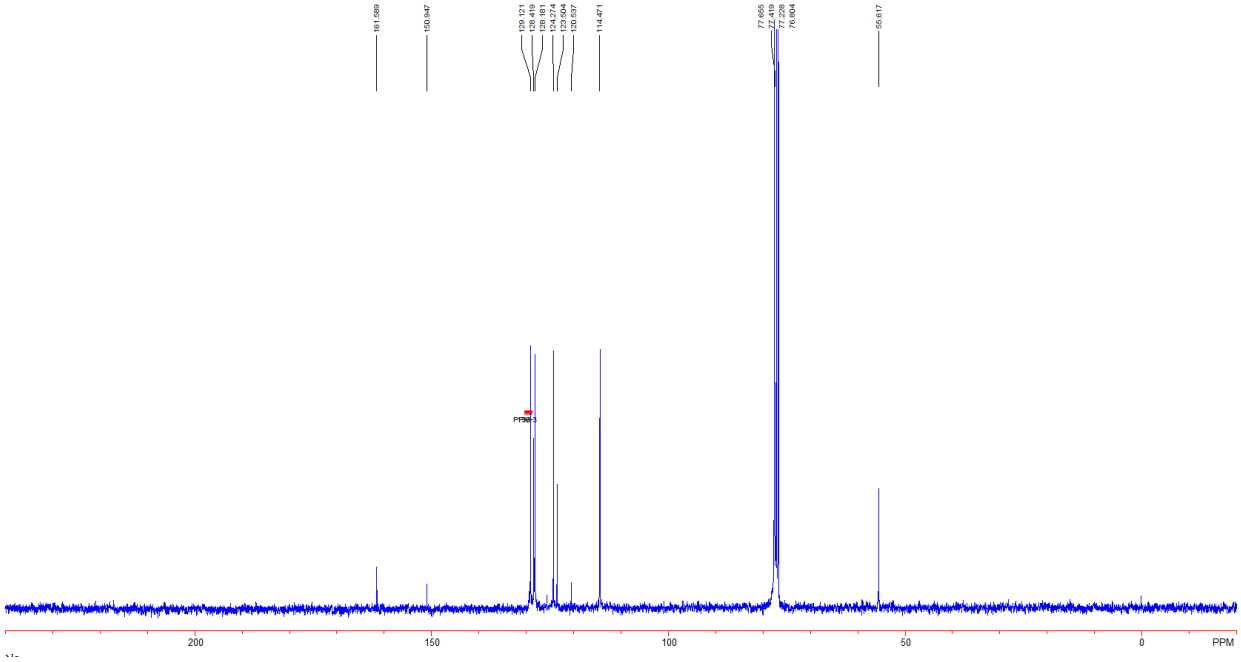
161.589
150.947
129.121
128.849
128.181
124.274
123.504
120.307
114.471
77.655
77.439
77.228
76.804
55.617
PPM: 3
200
150
100
50
0
PPM

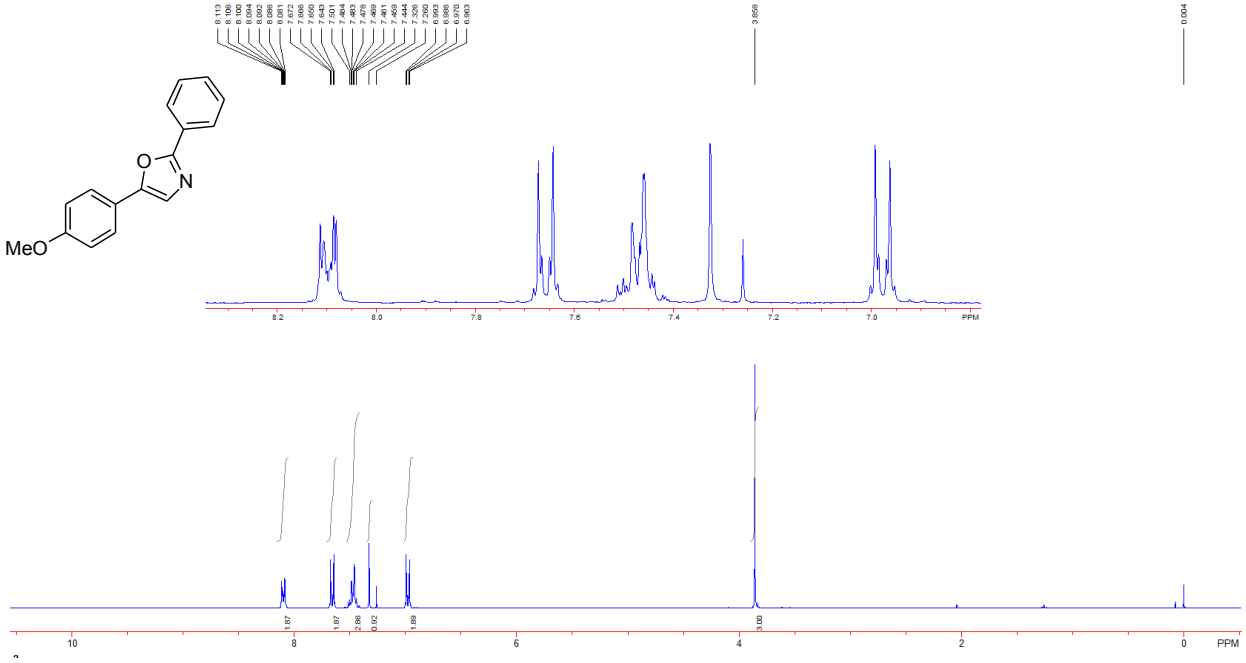
MeO
O
N
8.113
8.106
8.100
8.094
8.092
8.088
8.081
7.672
7.666
7.660
7.543
7.501
7.464
7.463
7.478
7.469
7.461
7.460
7.444
7.326
7.309
7.293
6.993
6.988
6.970
6.963
3.859
0.004
8.2
8.0
7.8
7.6
7.4
7.2
7.0
PPM
1.87
1.87
2.88
0.92
1.89
3.00
10
8
6
4
2
0
PPM

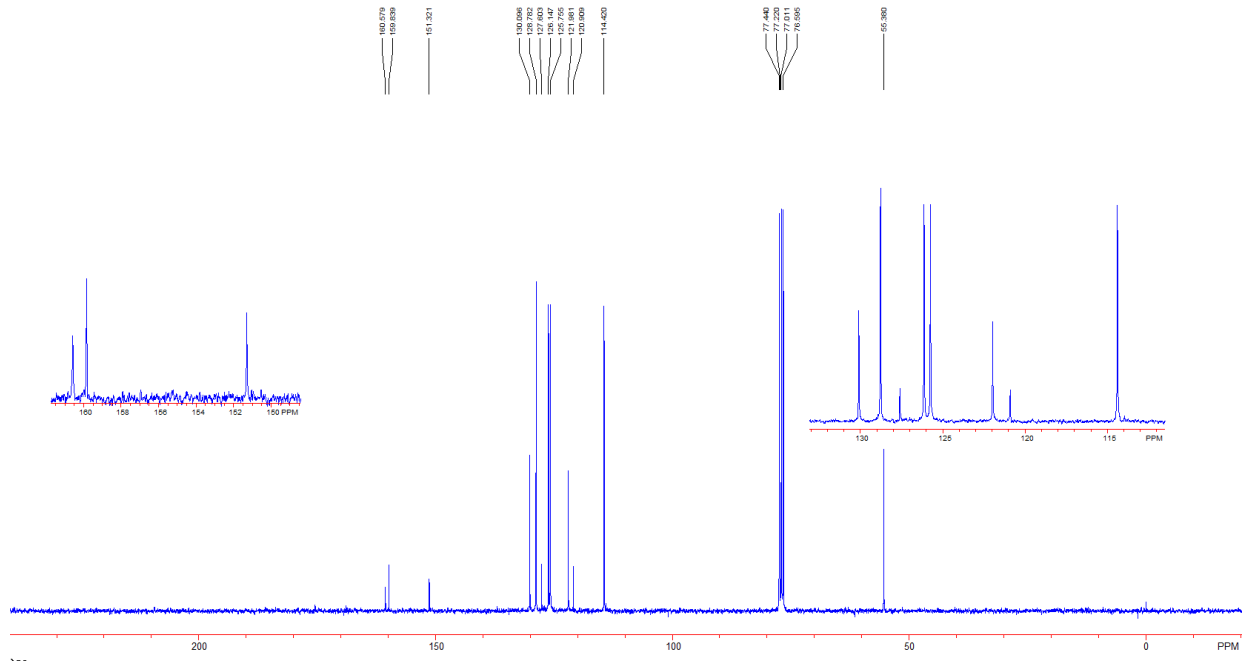
160.579
159.839
151.321
130.096
129.782
127.603
126.947
125.755
121.981
120.909
114.420
77.440
77.229
77.013
76.595
55.380
160
158
156
154
152
150 PPM
130
125
120
115
PPM
200
150
100
50
0
PPM

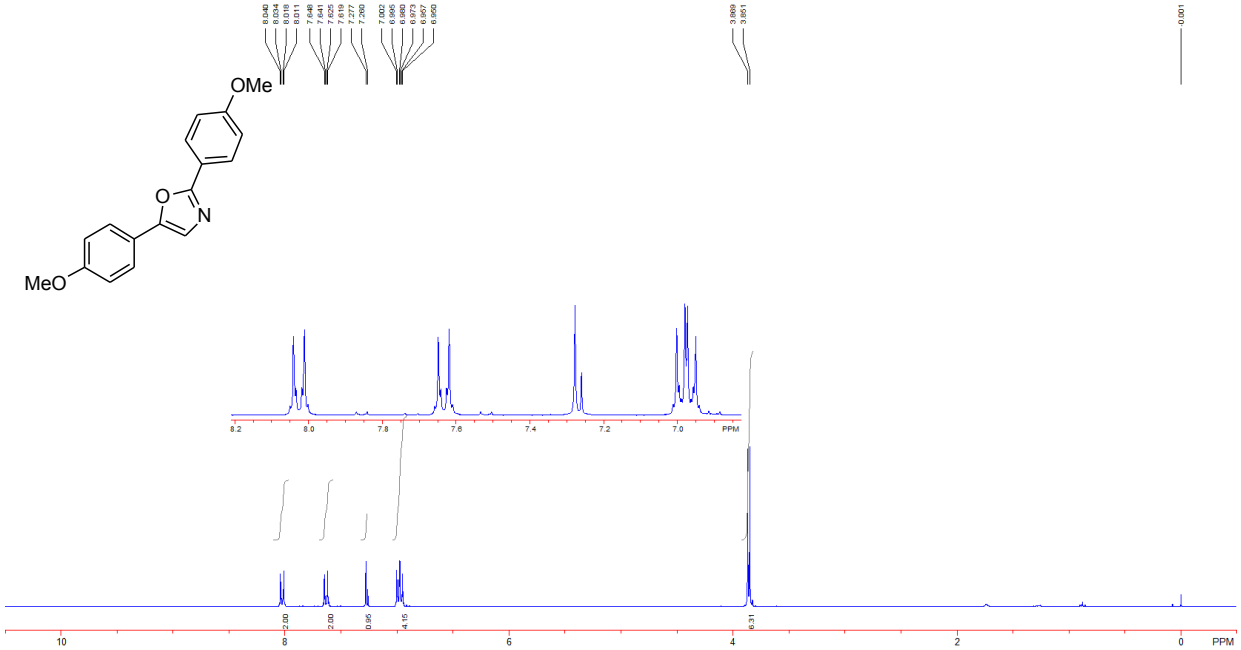
OMe
O
N
MeO
8.040
8.034
8.019
8.011
7.648
7.641
7.625
7.619
7.277
7.260
7.002
6.995
6.980
6.973
6.957
6.950
3.869
3.851
0.001
2.00
2.00
0.95
4.15
6.31
PPM

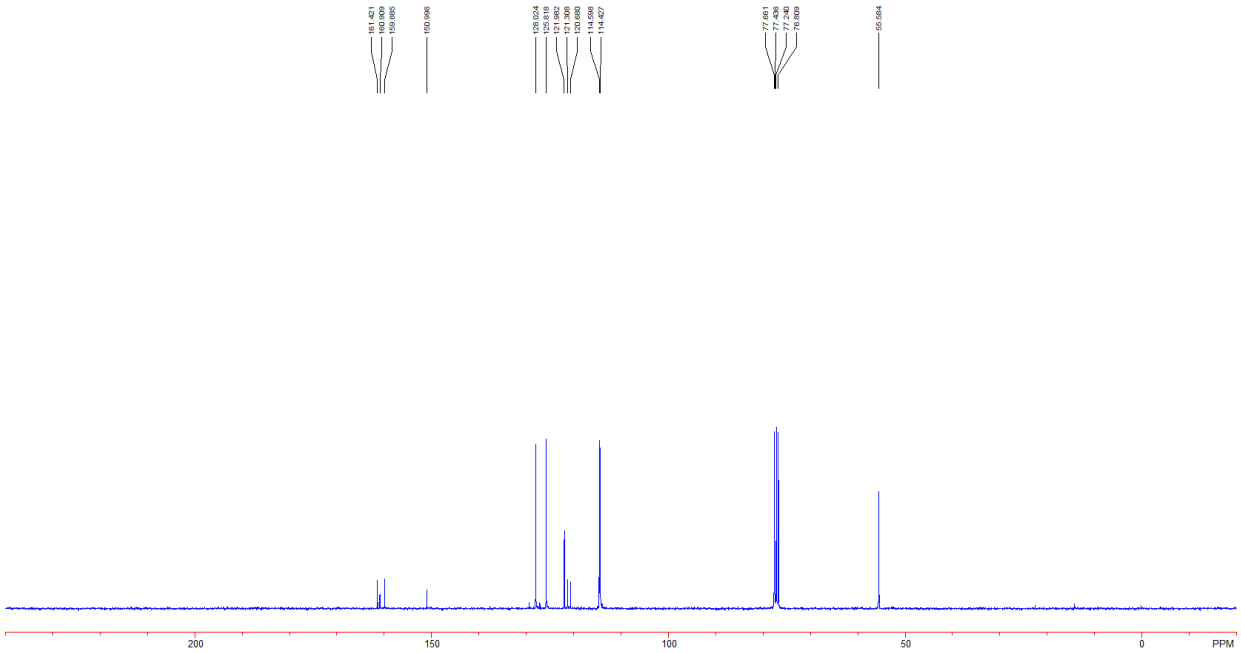
161.421
160.909
159.985
150.998
128.624
125.918
121.982
121.309
120.980
114.399
114.427
77.661
77.439
77.240
76.819
55.994
PPM

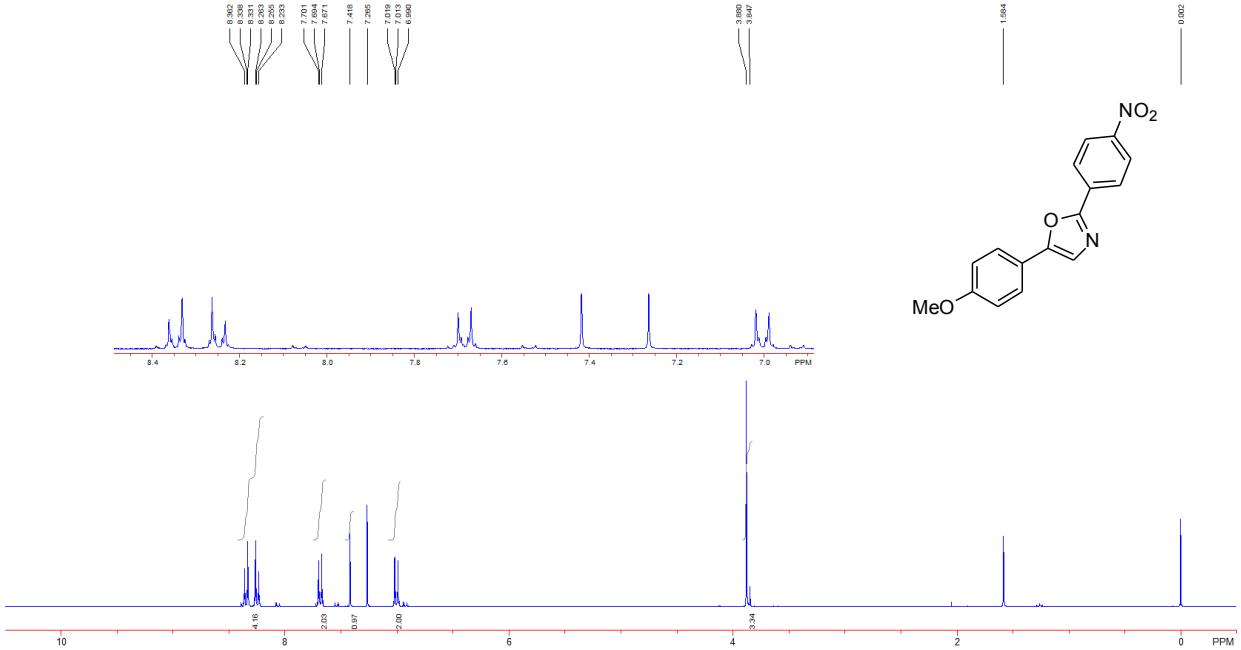
8.362
8.338
8.321
8.303
8.255
8.233
7.701
7.684
7.671
7.418
7.265
7.019
7.013
6.960
3.980
3.947
1.984
0.002
NO2
O
N
MeO
8.4
8.2
8.0
7.8
7.6
7.4
7.2
7.0
PPM
4.16
2.03
0.97
2.00
3.34
10
8
6
4
2
0
PPM

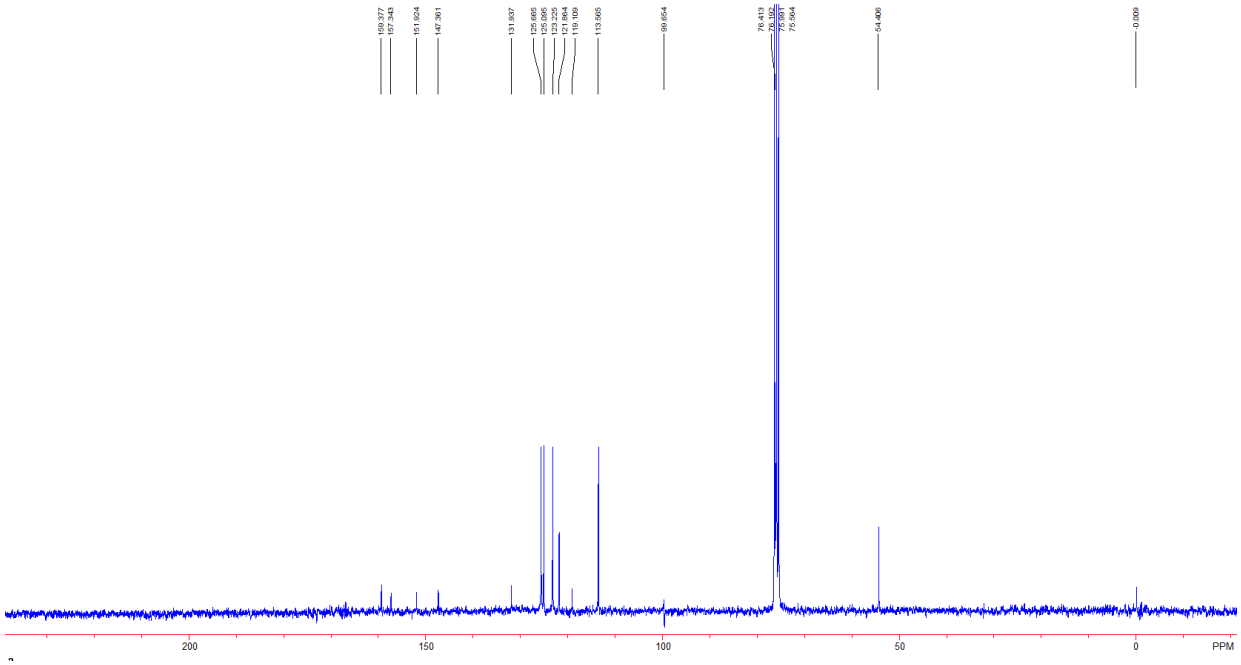
159.377
157.348
151.924
147.361
131.937
125.995
125.995
123.225
121.984
119.109
113.965
99.954
76.413
76.102
75.895
75.564
54.409
0.009
200
150
100
50
0
PPM

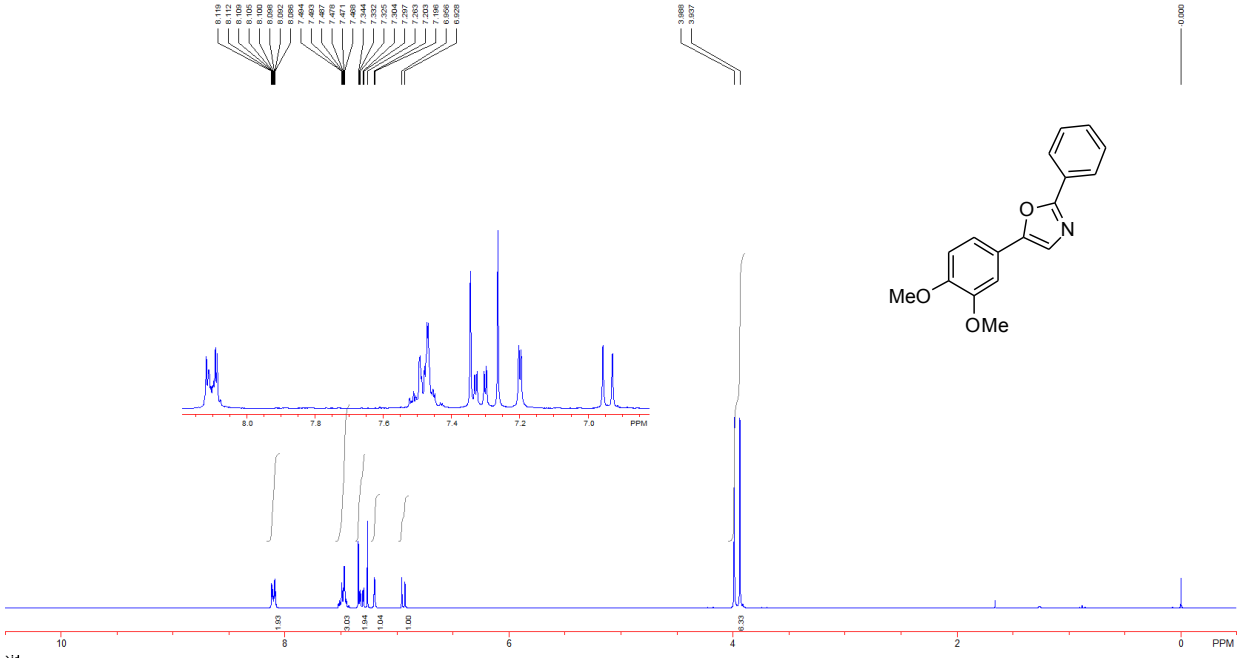
8.119
8.112
8.109
8.105
8.100
8.098
8.092
8.088
7.484
7.483
7.467
7.479
7.471
7.468
7.444
7.332
7.325
7.304
7.297
7.293
7.203
7.196
6.956
6.928
3.988
3.937
0.000
O
N
MeO
OMe
8.0
7.8
7.6
7.4
7.2
7.0
PPM
1.93
3.03
1.94
1.04
1.00
8.33
10
8
6
4
2
0
PPM

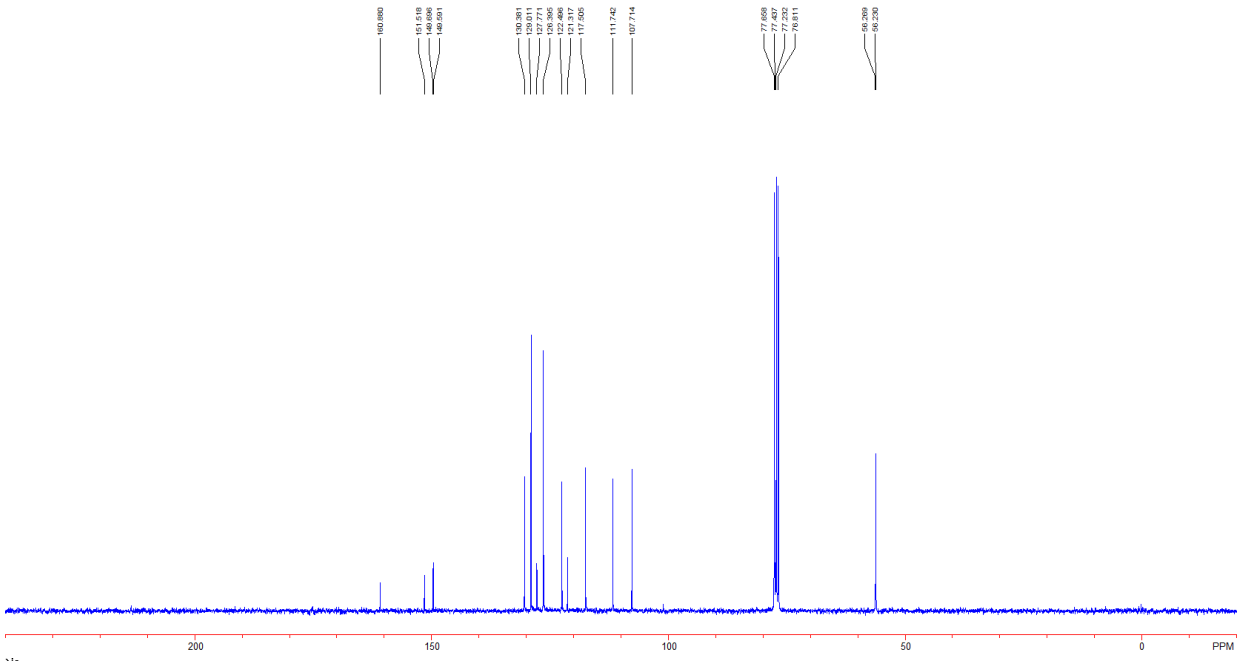
160.880
151.518
149.696
149.591
130.361
129.011
127.771
126.595
124.496
121.317
117.505
111.742
107.714
77.658
77.437
77.220
76.811
56.269
56.230
200
150
100
50
0
PPM

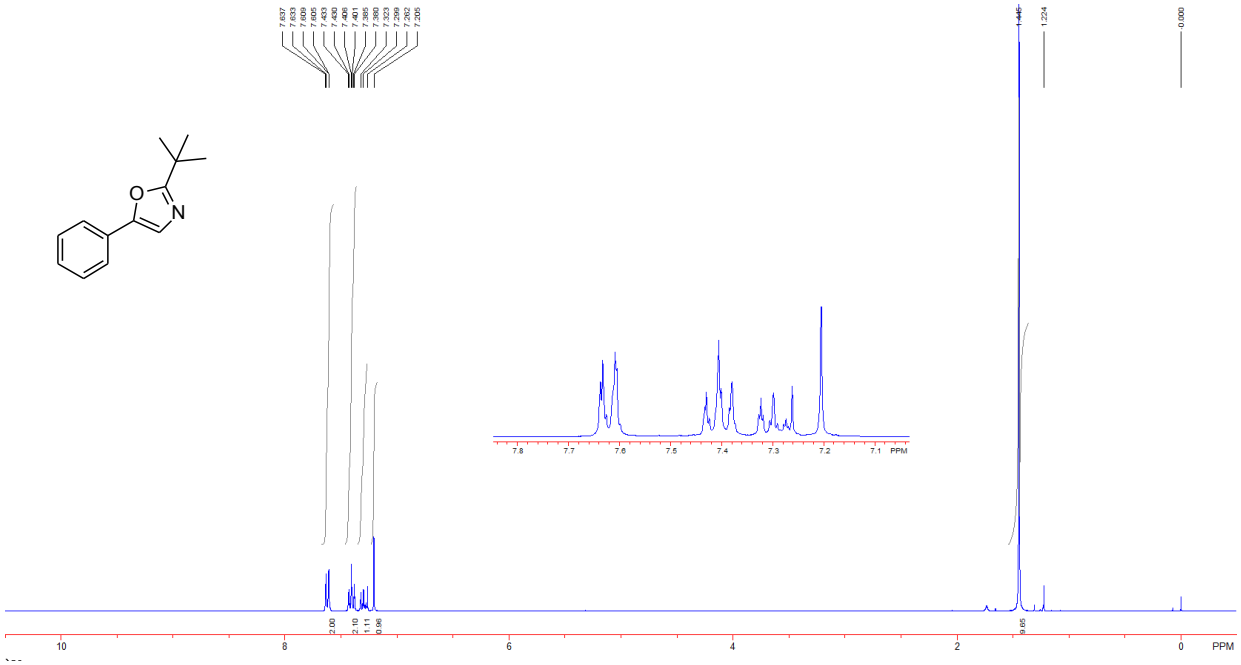
7.637
7.633
7.609
7.605
7.433
7.429
7.406
7.401
7.396
7.380
7.323
7.299
7.292
7.205
1.445
1.224
0.000
O
N
2.00
2.10
1.11
0.96
9.85
10
8
6
4
2
0
PPM
7.8
7.7
7.6
7.5
7.4
7.3
7.2
7.1
PPM

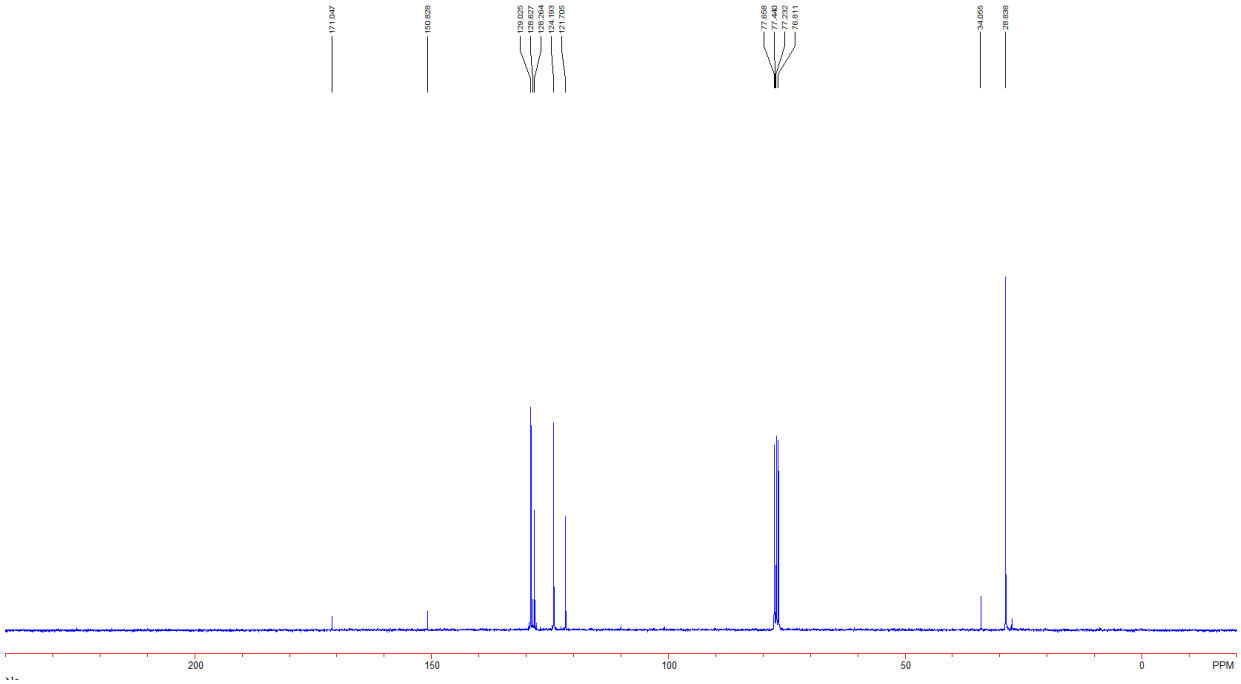
171.047
160.628
129.825
128.627
128.204
124.193
121.705
77.658
77.440
77.223
76.811
34.055
28.838
200
150
100
50
0
PPM

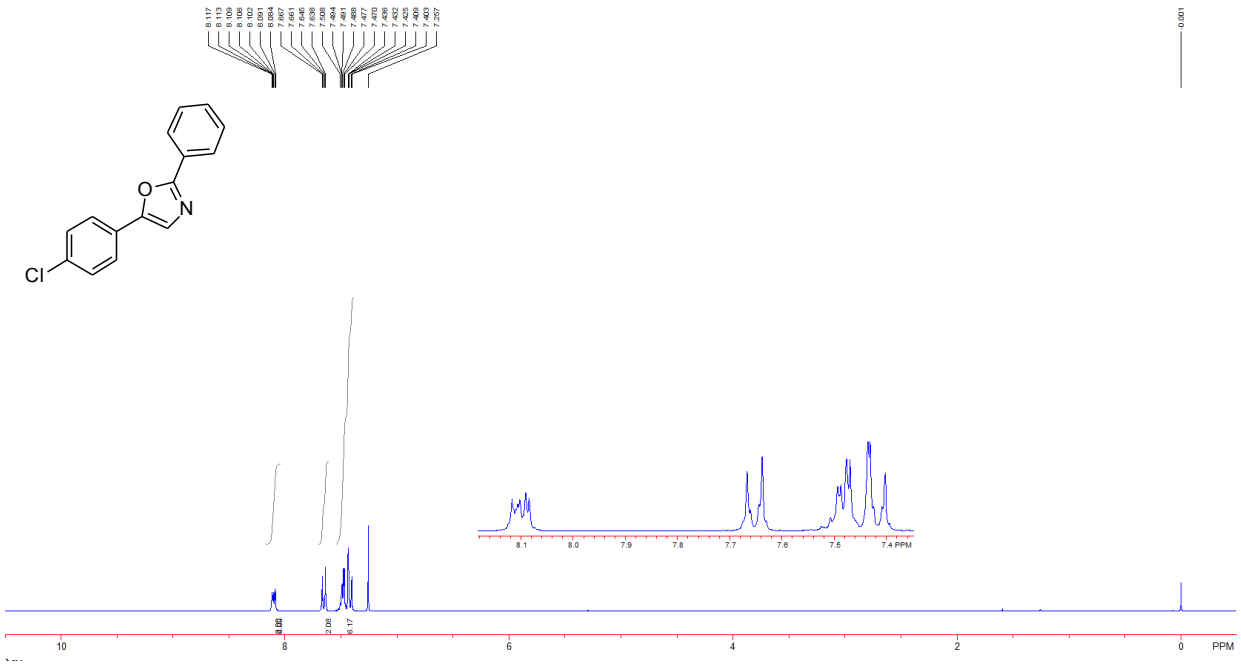
8.117
8.113
8.109
8.106
8.102
8.091
8.084
7.697
7.691
7.645
7.638
7.635
7.464
7.461
7.459
7.457
7.455
7.453
7.436
7.432
7.429
7.409
7.403
7.257
0.001
O
N
Cl
8.17
10
8
6
4
2
0
PPM
8.1
8.0
7.9
7.8
7.7
7.6
7.5
7.4 PPM

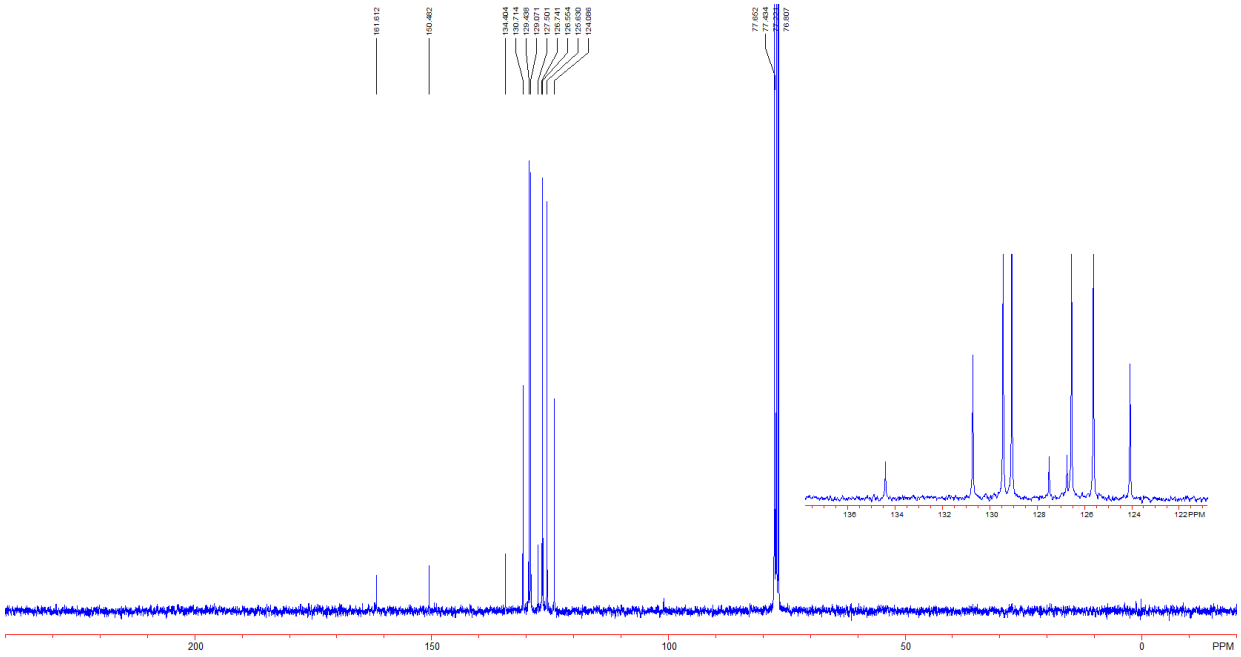
161.612
150.492
134.404
130.714
129.438
129.071
127.091
126.741
126.554
125.630
124.066
77.652
77.434
76.607
200
150
100
50
0
PPM
136
134
132
130
128
126
124
122PPM

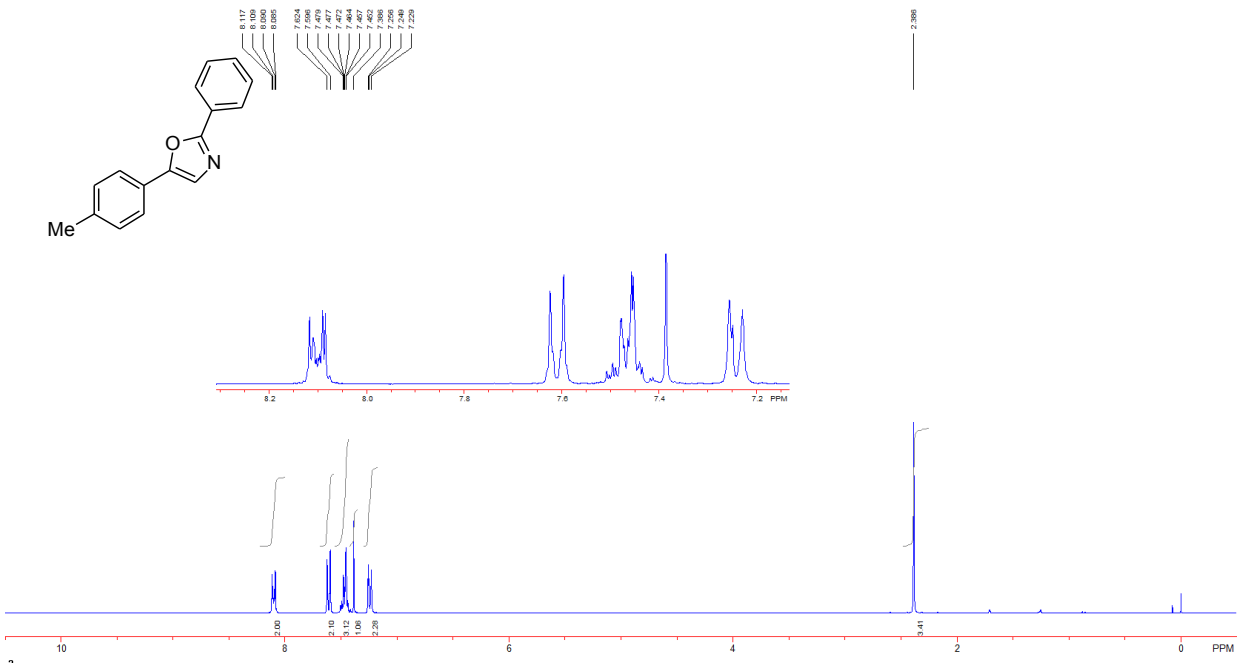
8.117
8.109
8.090
8.085
7.624
7.496
7.479
7.477
7.473
7.464
7.457
7.462
7.386
7.356
7.249
7.229
2.388
O
N
Me
8.2
8.0
7.8
7.6
7.4
7.2 PPM
2.00
2.10
3.12
1.00
2.29
3.41
10
8
6
4
2
0 PPM

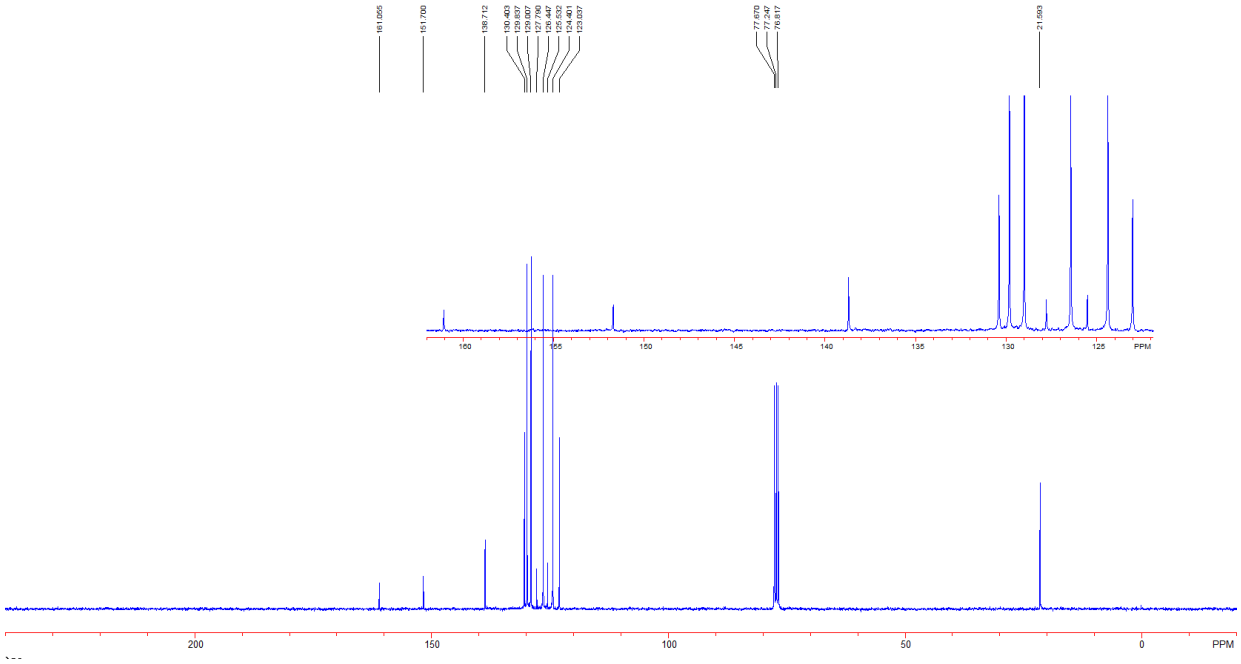
161.055
151.700
136.712
130.403
129.877
129.007
127.790
126.447
125.652
124.401
123.037
77.670
77.247
76.817
21.593
160
155
150
145
140
135
130
125 PPM
200
150
100
50
0 PPM

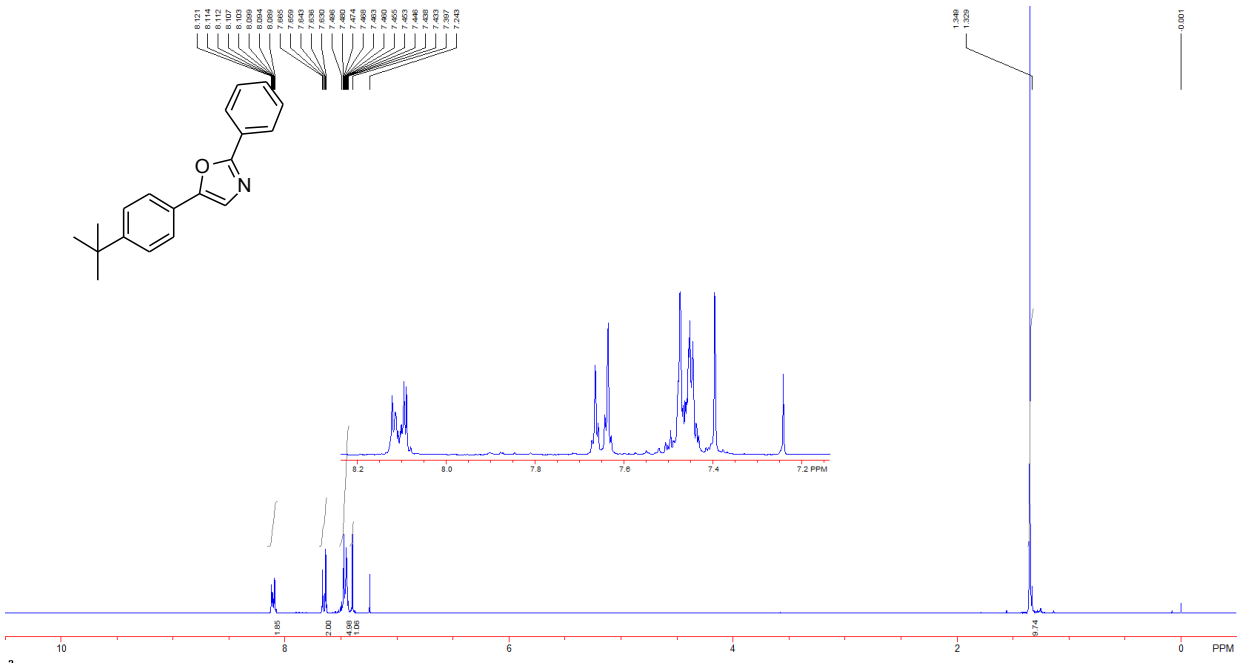
8.121
8.114
8.112
8.107
8.099
8.099
8.094
8.089
7.666
7.659
7.543
7.536
7.528
7.486
7.480
7.474
7.466
7.463
7.460
7.455
7.450
7.446
7.439
7.437
7.397
7.243
1.348
1.329
0.001
O
N
1.85
2.00
4.98
9.74
10
8
6
4
2
0
PPM
8.2
8.0
7.8
7.6
7.4
7.2 PPM

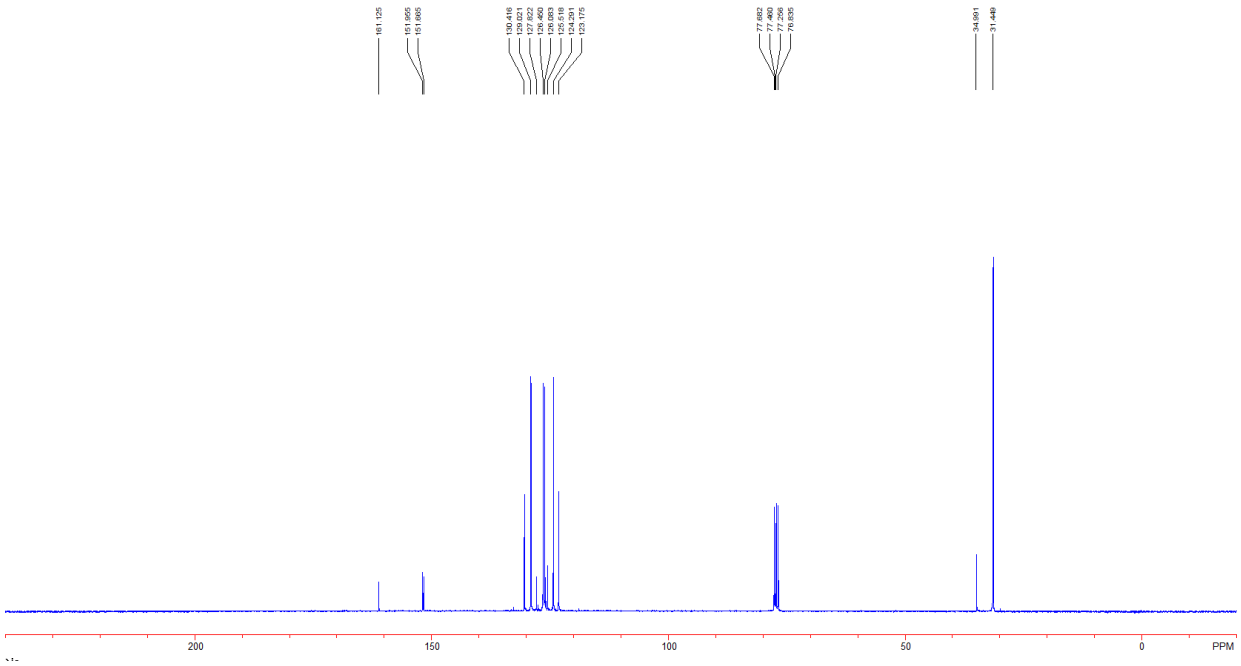
161.125
151.955
151.895
130.416
129.221
127.822
126.450
126.083
125.618
124.291
123.175
77.682
77.460
77.256
76.835
34.891
31.449
200
150
100
50
0
PPM

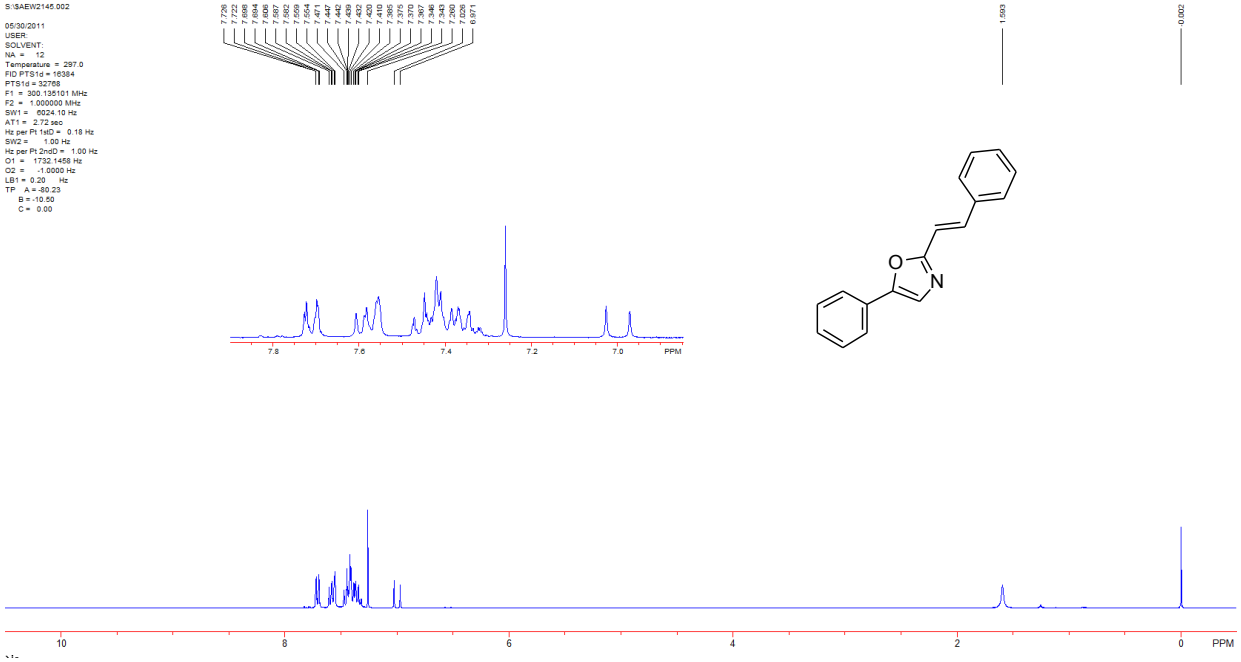
S:\SAEW2145.002
05/30/2011
USER:
SOLVENT:
NA = 12
Temperature = 297.0
FID PTS1d = 16384
PTS1d = 32768
F1 = 300.135101 MHz
F2 = 1.000000 MHz
SW1 = 6024.10 Hz
AT1 = 2.72 sec
Hz per Pt 1stD = 0.18 Hz
SW2 = 1.00 Hz
Hz per Pt 2ndD = 1.00 Hz
O1 = 1732.1458 Hz
O2 = -1.0000 Hz
LB1 = 0.20 Hz
TP A = -80.23
B = -10.50
C = 0.00
7.728
7.722
7.698
7.684
7.666
7.657
7.652
7.639
7.564
7.471
7.447
7.442
7.439
7.432
7.420
7.410
7.395
7.375
7.370
7.367
7.346
7.343
7.290
7.285
6.971
1.593
0.002
O
N
7.8
7.6
7.4
7.2
7.0
PPM
10
8
6
4
2
0
PPM

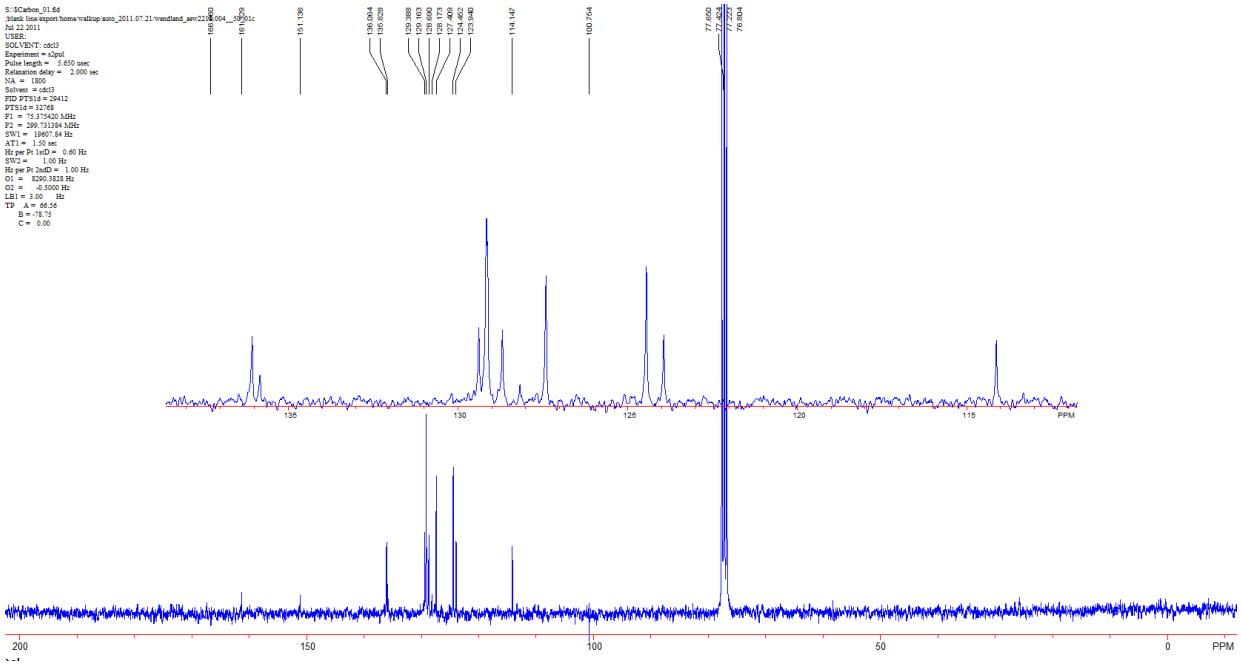
S:\$Carbon_01.fid
:blank line/export/home/walkup/auto_2011.07.21/wendland_aev2218.004__5d_01c
Jul 22 2011
USER:
SOLVENT: cdcl3
Experiment = s2pul
Pulse length = 5.650 usec
Relaxation delay = 2.000 sec
NA = 1800
Solvent = cdcl3
FID PTS1d = 29412
PTS1d = 32768
F1 = 75.375420 MHz
F2 = 299.731384 MHz
SW1 = 19607.84 Hz
AT1 = 1.50 sec
Hz per Pt 1stD = 0.60 Hz
SW2 = 1.00 Hz
Hz per Pt 2ndD = 1.00 Hz
O1 = 8290.3828 Hz
O2 = -0.5000 Hz
LB1 = 3.00 Hz
TP A = -66.56
B = -78.75
C = 0.00
160.960
161.929
151.136
136.064
135.628
129.988
129.303
128.890
128.173
127.429
124.402
123.940
114.147
100.754
77.650
77.424
77.197
76.804
135
130
125
120
115
PPM
200
150
100
50
0
PPM

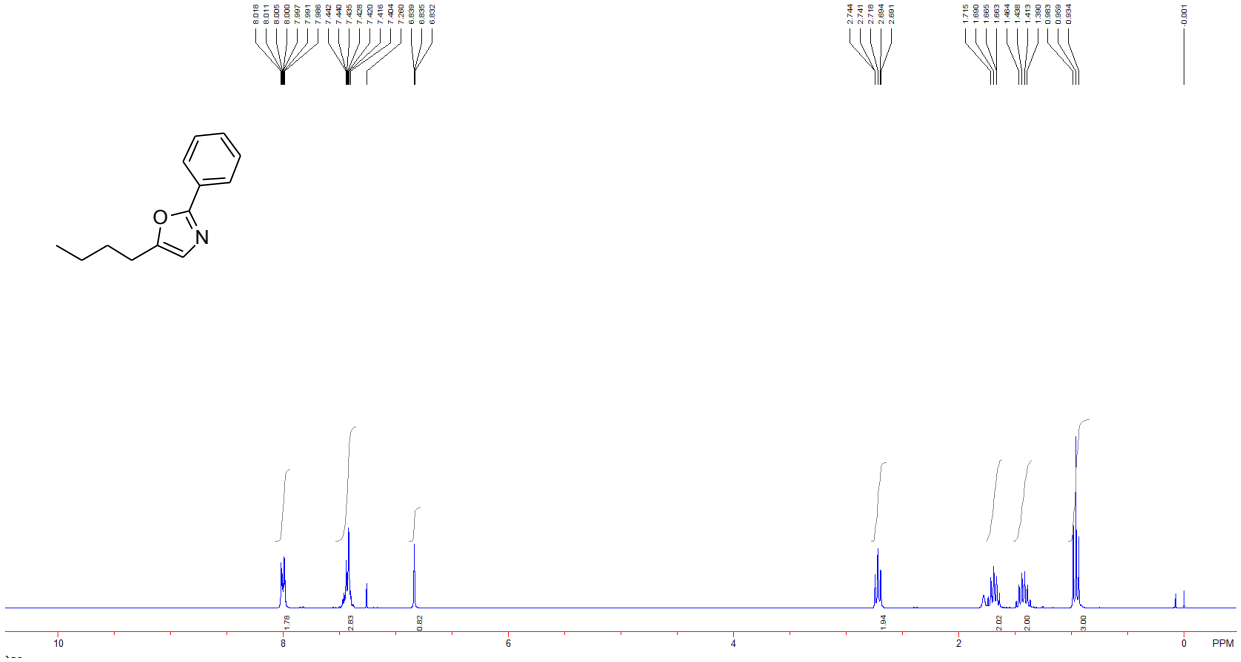
8.018
8.011
8.005
8.000
7.997
7.991
7.988
7.442
7.440
7.435
7.428
7.420
7.416
7.414
7.260
6.839
6.835
6.832
2.744
2.741
2.718
2.694
2.691
1.715
1.690
1.665
1.653
1.464
1.438
1.413
1.390
1.365
0.959
0.934
0.001
O
N
1.78
2.83
0.82
1.94
2.02
2.00
3.00
10
8
6
4
2
0
PPM

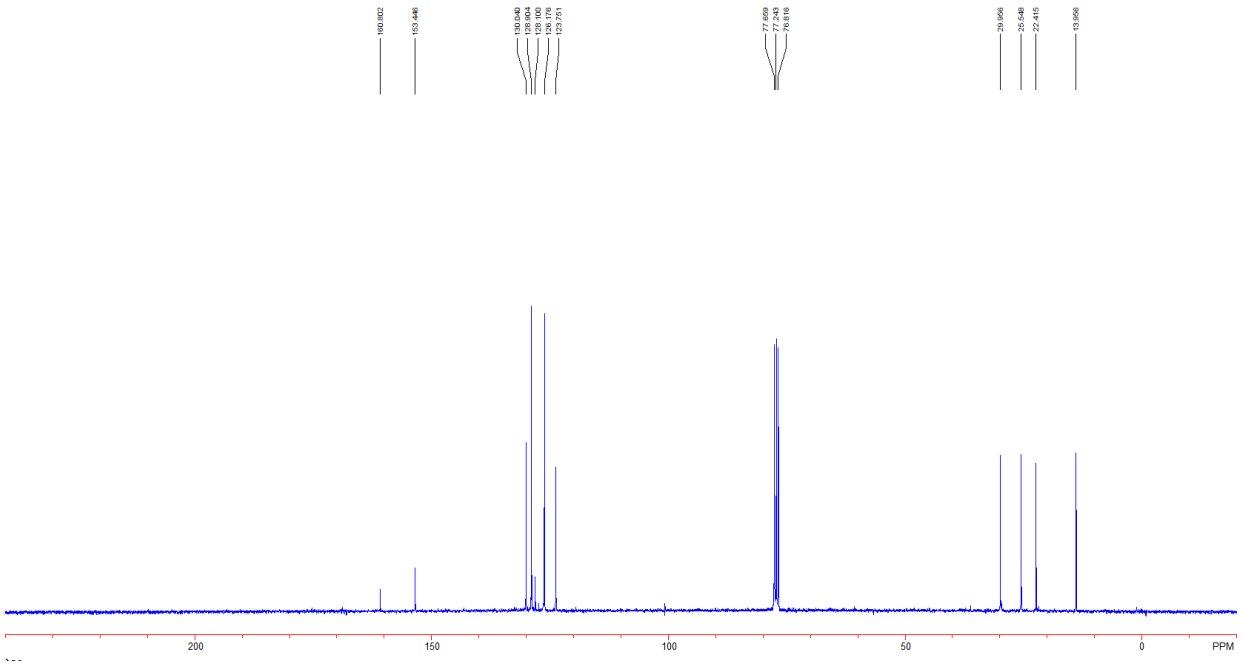
160.602
153.446
130.040
128.804
128.100
126.176
125.771
77.659
77.243
76.816
29.956
25.548
22.415
13.956
200
150
100
50
0
PPM

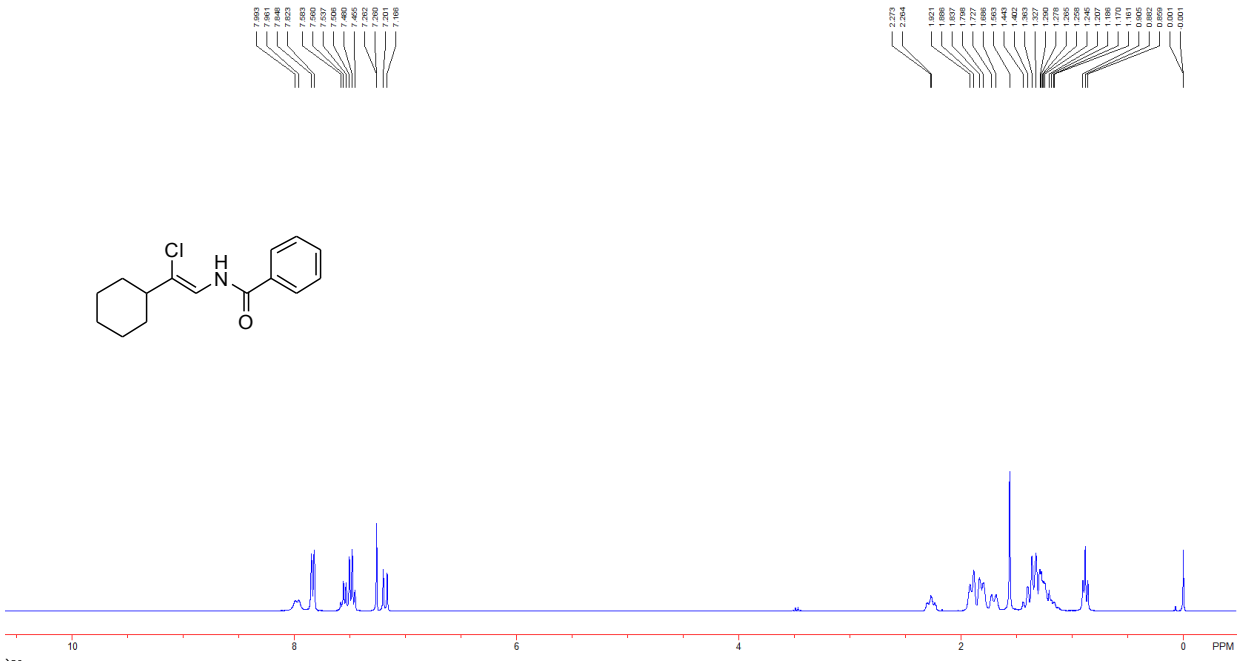
7.993
7.991
7.848
7.823
7.583
7.560
7.537
7.506
7.480
7.455
7.292
7.290
7.301
7.166
2.273
2.264
1.921
1.889
1.857
1.798
1.727
1.688
1.655
1.443
1.402
1.363
1.327
1.322
1.290
1.278
1.266
1.256
1.245
1.207
1.176
1.166
1.151
0.905
0.892
0.859
0.001
0.001
Cl
H
N
O
10
8
6
4
2
0
PPM

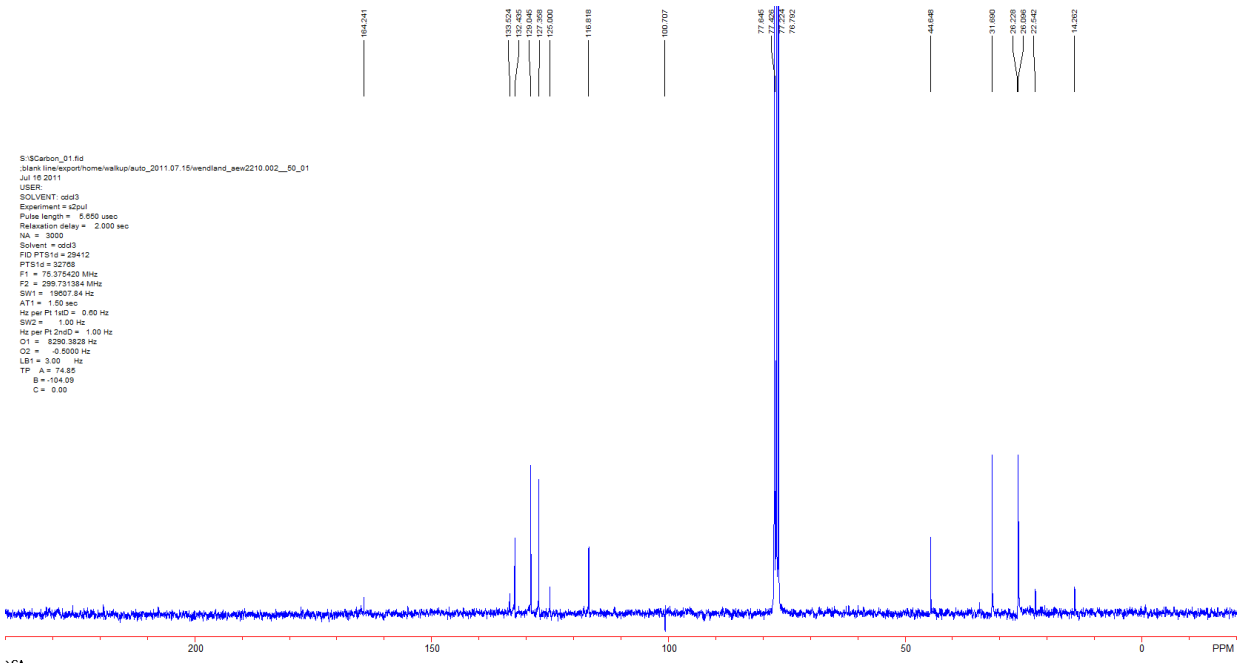
164.241
133.534
132.495
129.045
127.358
125.000
116.818
100.707
77.646
77.334
77.024
76.702
44.648
31.690
26.228
25.946
22.542
14.262
S:\$Carbon_01.fid
.blank line/export/home/walkup/auto_2011.07.15/wendland_aew2210.002__50_01
Jul 16 2011
USER:
SOLVENT: cdcl3
Experiment = s2pul
Pulse length = 5.650 usec
Relaxation delay = 2.000 sec
NA = 3000
Solvent = cdcl3
FID PTS1d = 29412
PTS1d = 32768
F1 = 75.375420 MHz
F2 = 299.731384 MHz
SW1 = 19607.84 Hz
AT1 = 1.50 sec
Hz per Pt 1stD = 0.60 Hz
SW2 = 1.00 Hz
Hz per Pt 2ndD = 1.00 Hz
O1 = 8290.3828 Hz
O2 = -0.5000 Hz
LB1 = 3.00 Hz
TP A = 74.85
B = -104.09
C = 0.00
200
150
100
50
0
PPM